



EPA's Composite Model for Leachate Migration with Transformation Products (EPACMTP)

Technical Background Document

**Office of Solid Waste (5305W)
Washington, DC 20460
EPA530-R-03-006
April 2003
www.epa.gov/osw**

EPA's Composite Model for Leachate Migration with Transformation Products (EPACMTP) Technical Background Document

Work Assignment Manager
and Technical Direction:

David Cozzie
U.S. Environmental Protection Agency
Office of Solid Waste
Washington, DC 20460

Prepared by:

HydroGeoLogic, Inc.
1155 Herndon Parkway, Suite 900
Herndon, VA 20170

Under Subcontract No.: RMC-B-00-021

and

Resource Management Concepts, Inc.
46970 Bradley Blvd., Suite B
Lexington Park, MD 20653

Under Contract No.: 68-W-01-004

U.S. Environmental Protection Agency
Office of Solid Waste
Washington, DC 20460

April 2003

This page intentionally left blank.

TABLE OF CONTENTS

| Section | Page |
|--|-------------|
| LIST OF ACRONYMS | ix |
| LIST OF SYMBOLS | xi |
| ACKNOWLEDGMENTS | xxv |
| EXECUTIVE SUMMARY | xxvii |
| | |
| 1.0 INTRODUCTION | 1-1 |
| 1.1 DEVELOPMENT HISTORY OF EPACMTP | 1-1 |
| 1.2 WHAT IS THE EPACMTP MODEL? | 1-2 |
| 1.2.1 Source-Term Module | 1-5 |
| 1.2.2 Unsaturated-Zone Module | 1-6 |
| 1.2.3 Saturated-Zone Module | 1-7 |
| 1.2.4 Monte-Carlo Module | 1-8 |
| 1.3 EPACMTP ASSUMPTIONS AND LIMITATIONS | 1-9 |
| | |
| 2.0 SOURCE-TERM MODULE | 2-1 |
| 2.1 PURPOSE OF THE SOURCE-TERM MODULE | 2-1 |
| 2.1.1 Continuous Source | 2-2 |
| 2.1.2 Finite Source | 2-2 |
| 2.2 IMPLEMENTATION FOR DIFFERENT WASTE UNITS | 2-4 |
| 2.2.1 Landfills | 2-4 |
| 2.2.1.1 Assumptions for the Landfill Source Module | 2-4 |
| 2.2.1.2 List of Parameters for the Landfill Source Module | 2-6 |
| 2.2.1.2.1 Landfill Area | 2-6 |
| 2.2.1.2.2 Landfill Depth | 2-6 |
| 2.2.1.2.3 Depth Below Grade | 2-8 |
| 2.2.1.2.4 Waste Fraction | 2-8 |
| 2.2.1.2.5 Waste Density | 2-8 |
| 2.2.1.2.6 Areal Recharge and Infiltration Rates | 2-8 |
| 2.2.1.2.7 Leachate Concentration | 2-9 |
| 2.2.1.2.8 Waste Concentration | 2-9 |
| 2.2.1.2.9 Waste-Concentration-to- Leachate-Concentration Ratio | 2-10 |
| 2.2.1.2.10 Source Leaching Duration | 2-10 |
| 2.2.1.2.11 Waste Volume | 2-10 |
| 2.2.1.3 Mathematical Formulation of the Landfill Source Module | 2-11 |
| 2.2.1.3.1 Continuous Source Scenario | 2-11 |
| 2.2.1.3.2 Pulse Source Scenario | 2-11 |
| 2.2.1.3.3 Depleting Source Scenario | 2-14 |
| 2.2.2 Surface Impoundments | 2-17 |
| 2.2.2.1 Assumptions for the Surface Impoundment Source-Term Module | 2-17 |
| 2.2.2.2 List of Parameters for the Surface Impoundment Source-Term Module | 2-18 |
| 2.2.2.2.1 Surface Impoundment Area | 2-19 |
| 2.2.2.2.2 Areal Recharge Rate | 2-19 |

TABLE OF CONTENTS

| Section | Page |
|------------|--|
| 2.2.2.2.3 | Areal Infiltration Rate 2-20 |
| 2.2.2.2.4 | Depth Below Grade 2-20 |
| 2.2.2.2.5 | Operating Depth and Ponding Depth 2-20 |
| 2.2.2.2.6 | Total Thickness of Sediment 2-21 |
| 2.2.2.2.7 | Distance to the Nearest Surface Water Body 2-21 |
| 2.2.2.2.8 | Leachate Concentration 2-21 |
| 2.2.2.2.9 | Source Leaching Duration 2-21 |
| 2.2.2.2.10 | Liner Thickness 2-22 |
| 2.2.2.2.11 | Liner Hydraulic Conductivity 2-22 |
| 2.2.2.2.12 | Unsaturated-zone Thickness 2-22 |
| 2.2.2.2.13 | Leak Density 2-22 |
| 2.2.2.3 | Mathematical Formulation of the Surface Impoundment Source-Term Module . . 2-22 |
| 2.2.2.3.1 | Surface Impoundment Leakage (Infiltration) Rate 2-22 |
| 2.2.2.3.2 | Calculation of the Surface Impoundment Infiltration Rate 2-28 |
| 2.2.3 | Waste Piles 2-31 |
| 2.2.3.1 | Assumptions for the Waste Pile Source- Term Module 2-31 |
| 2.2.3.2 | List of Parameters for the Waste Pile Source- Term Module 2-31 |
| 2.2.3.2.1 | Waste Pile Area 2-31 |
| 2.2.3.2.2 | Areal Infiltration and Recharge Rates 2-32 |
| 2.2.3.2.3 | Leachate Concentration 2-33 |
| 2.2.3.2.4 | Source Leaching Duration 2-33 |
| 2.2.3.2.5 | Depth Below Grade 2-33 |
| 2.2.3.3 | Mathematical Formulation of the Waste Pile Source-Term Module 2-33 |
| 2.2.4 | Land Application Units 2-35 |
| 2.2.4.1 | Assumptions for the Land Application Unit Source-Term Module 2-35 |
| 2.2.4.2 | List of Parameters for the Land Application Unit Source-Term Module 2-35 |
| 2.2.4.2.1 | Land Application Unit Area 2-35 |
| 2.2.4.2.2 | Infiltration and Recharge Rates . . . 2-35 |
| 2.2.4.2.3 | Leachate Concentration 2-36 |
| 2.2.4.2.4 | Source Leaching Duration 2-37 |
| 2.2.4.3 | Mathematical Formulation of the Land Application Unit Source-Term Module 2-37 |
| 2.2.5 | Limitations on Maximum Infiltration Rate 2-39 |
| 3.0 | UNSATURATED-ZONE MODULE 3-1 |
| 3.1 | PURPOSE OF THE UNSATURATED-ZONE MODULE 3-1 |
| 3.2 | UNSATURATED-ZONE FLOW SUBMODULE 3-3 |

TABLE OF CONTENTS

| Section | Page |
|----------|--|
| 3.2.1 | Description of the Unsaturated-zone Flow Submodule 3-3 |
| 3.2.2 | Assumptions Underlying the Unsaturated-zone Flow Submodule 3-3 |
| 3.2.3 | List of the Parameters for the Unsaturated-zone Flow Submodule 3-4 |
| 3.2.3.1 | Soil Characteristic Curve Parameters 3-5 |
| 3.2.3.2 | Thickness of the Unsaturated Zone 3-6 |
| 3.2.3.3 | Saturated Hydraulic Conductivity 3-7 |
| 3.2.4 | Mathematical Formulation of the Unsaturated-zone Flow Submodule 3-7 |
| 3.2.5 | Solution Method for Flow in the Unsaturated Zone 3-7 |
| 3.3 | UNSATURATED-ZONE SOLUTE TRANSPORT SUBMODULE 3-10 |
| 3.3.1 | Description of the Unsaturated-zone Transport Submodule 3-10 |
| 3.3.2 | Assumptions Underlying the Unsaturated-zone Transport Submodule 3-10 |
| 3.3.3 | List of Parameters for the Unsaturated-zone Transport Submodule 3-12 |
| 3.3.3.1 | Longitudinal Dispersivity 3-13 |
| 3.3.3.2 | Percent Organic Matter 3-14 |
| 3.3.3.3 | Soil Bulk Density (ρ_{bu}) 3-15 |
| 3.3.3.4 | Freundlich Sorption Coefficient (Distribution Coefficient) 3-15 |
| 3.3.3.5 | Freundlich Isotherm Exponent 3-15 |
| 3.3.3.6 | Sorption Coefficient for Metals 3-15 |
| 3.3.3.7 | Chemical and Biological Transformation Coefficients 3-16 |
| 3.3.3.8 | Molecular Diffusion Coefficient 3-17 |
| 3.3.3.9 | Molecular Weight 3-17 |
| 3.3.3.10 | Ground-water Temperature 3-17 |
| 3.3.3.11 | Ground-water pH 3-17 |
| 3.3.4 | Mathematical Formulation of the Unsaturated-zone Transport Submodule 3-17 |
| 3.3.5 | Solution Methods for Transport in the Unsaturated Zone 3-23 |
| 3.3.5.1 | Steady-state, Single Species Analytical Solution 3-23 |
| 3.3.5.2 | Transient, Decay Chain Semi- analytical Solution 3-25 |
| 3.3.5.3 | Semi-analytical Solution for Metals with Non- linear Sorption 3-25 |
| 4.0 | SATURATED ZONE (AQUIFER) MODULE 4-1 |
| 4.1 | PURPOSE OF THE SATURATED-ZONE MODULE 4-1 |
| 4.2 | LINKING THE UNSATURATED-ZONE AND SATURATED- ZONE MODULES 4-1 |
| 4.3 | SATURATED-ZONE FLOW SUBMODULE 4-2 |

TABLE OF CONTENTS

| Section | Page |
|----------|---|
| 4.3.1 | Description of the Flow Submodule 4-2 |
| 4.3.2 | Assumptions Underlying the Flow Submodule 4-2 |
| 4.3.3 | List of Parameters for the Flow Submodule 4-3 |
| 4.3.3.1 | Particle Diameter 4-3 |
| 4.3.3.2 | Porosity 4-5 |
| 4.3.3.3 | Bulk Density 4-6 |
| 4.3.3.4 | Saturated-zone Thickness 4-6 |
| 4.3.3.5 | Hydraulic Conductivity 4-6 |
| 4.3.3.6 | Anisotropy Ratio 4-7 |
| 4.3.3.7 | Hydraulic Gradient 4-7 |
| 4.3.3.8 | Seepage Velocity 4-8 |
| 4.3.4 | Mathematical Formulation of the Saturated-Zone Flow Submodule 4-8 |
| 4.3.5 | Solution Methods for Flow in the Saturated Zone 4-8 |
| 4.3.5.1 | One-dimensional Flow Solution 4-9 |
| 4.3.5.2 | Two-dimensional Flow Solutions 4-12 |
| 4.3.5.3 | Three-dimensional Flow Solution 4-13 |
| 4.3.6 | Parameter Screening For Infeasible Ground-water Flow Conditions 4-16 |
| 4.4 | SATURATED-ZONE SOLUTE TRANSPORT SUBMODULE 4-20 |
| 4.4.1 | Description of the Solute Transport Submodule 4-20 |
| 4.4.2 | Assumptions Underlying the Saturated-zone Transport Submodule 4-21 |
| 4.4.3 | List of Parameters for the Solute Transport Submodule . . 4-21 |
| 4.4.3.1 | Retardation Factor 4-23 |
| 4.4.3.2 | Dispersivity 4-24 |
| 4.4.3.3 | Ground-water Temperature 4-26 |
| 4.4.3.4 | Ground-water pH 4-26 |
| 4.4.3.5 | Fractional Organic Carbon Content 4-26 |
| 4.4.3.6 | Receptor Well Location and Depth 4-26 |
| | 4.4.3.6.1 Horizontal Well Location 4-27 |
| | 4.4.3.6.2 Vertical Well Location 4-32 |
| 4.4.3.7 | Freundlich Isotherm Coefficient 4-34 |
| 4.4.3.8 | Freundlich Isotherm Exponent 4-34 |
| 4.4.3.9 | Sorption Coefficient for Metals 4-34 |
| 4.4.3.10 | Chemical & Biological Transformation Coefficients 4-35 |
| 4.4.3.11 | Molecular Diffusion Coefficient 4-35 |
| 4.4.3.12 | Molecular Weight 4-35 |
| 4.4.4 | Mathematical Formulation of the Saturated-zone Solute Transport Submodule 4-35 |
| 4.4.4.1 | Dispersion Coefficients 4-36 |
| 4.4.4.2 | Retardation Factor 4-37 |
| 4.4.4.3 | Coefficient Q_0 4-38 |
| 4.4.4.4 | Degradation Products Terms 4-39 |
| 4.4.4.5 | Initial Condition 4-39 |
| 4.4.4.6 | Boundary Conditions 4-40 |
| 4.4.4.7 | Source Concentration 4-41 |

TABLE OF CONTENTS

| Section | Page |
|-----------|--|
| 4.4.4.8 | Treatment of Nonlinear Isotherms 4-43 |
| 4.4.5 | Solution Methods for the Solute Transport Submodule . . 4-44 |
| 4.4.5.1 | Aquifer Discretization and Solution Method Selection 4-44 |
| 4.4.5.1.1 | Determination of Model Domain Dimensions 4-44 |
| 4.4.5.1.2 | Discretization of Model Domain . . . 4-47 |
| 4.4.5.1.3 | Solution Method Selection 4-48 |
| 4.4.5.2 | Three-dimensional Transport Solutions 4-49 |
| 4.4.5.2.1 | Laplace Transform Galerkin Solution 4-49 |
| 4.4.5.2.2 | Solution for Steady-state and Nonlinear Transport 4-55 |
| 4.4.5.2.3 | Analytical Solution 4-56 |
| 4.4.5.3 | Two-dimensional Transport Solutions 4-59 |
| 4.4.5.3.1 | Two-dimensional Cross- sectional Transport Solution 4-59 |
| 4.4.5.3.2 | Two-dimensional Areal Transport Solution 4-62 |
| 4.4.5.3.3 | Criterion for selecting Two- dimensional Solutions 4-62 |
| 4.4.5.4 | Pseudo-3D Transport Solution 4-63 |
| 4.4.6 | Determining the Exposure Concentration at the Receptor Well 4-82 |
| 4.4.6.1 | Time-Averaged Concentration 4-83 |
| 4.4.6.2 | Peak Concentration 4-84 |
| 4.4.6.3 | Time-to-Arrival of the Peak Concentration 4-84 |
| 4.4.7 | Determining the Contaminant Mass Flux from Ground- water into a Surface Water Body 4-85 |
| 5.0 | MONTE-CARLO MODULE 5-1 |
| 5.1 | PURPOSE OF THE MONTE-CARLO MODULE 5-1 |
| 5.1.1 | Treatment of Uncertainty and Variability 5-2 |
| 5.2 | MONTE-CARLO MODULE OPERATION 5-3 |
| 5.3 | ENSURING INTERNALLY CONSISTENT DATA SETS 5-4 |
| 5.3.1 | Upper and Lower Limits 5-6 |
| 5.3.2 | Screening Procedures 5-6 |
| 5.3.3 | Regional Site-Based Approach 5-7 |
| 5.4 | METHODOLOGY FOR GENERATING INPUT VALUES ACCORDING TO SPECIFIED DISTRIBUTIONS 5-8 |
| 5.4.1 | Constant 5-8 |
| 5.4.2 | Normal Distribution 5-9 |
| 5.4.3 | Lognormal Distribution 5-10 |
| 5.4.4 | Exponential Distribution 5-10 |
| 5.4.5 | Uniform Distribution 5-10 |
| 5.4.6 | Log ₁₀ Uniform Distribution 5-11 |
| 5.4.7 | Empirical Distribution 5-11 |
| 5.4.8 | Johnson SB Distribution 5-13 |

TABLE OF CONTENTS

| Section | Page |
|----------------|---|
| 5.4.9 | Special Distributions 5-13 |
| 5.4.9.1 | Gelhar Distribution for Aquifer Dispersivity 5-13 |
| 5.4.9.2 | Vertical Well Intake Point Depth 5-14 |
| 5.4.10 | Derived Parameters 5-15 |
| 5.4.11 | Parameter Upper and Lower Bounds 5-15 |
| 5.5 | MONTE-CARLO METHODOLOGY FOR REGIONAL SITE-BASED, CORRELATED DISTRIBUTIONS 5-15 |
| 5.5.1 | Description of Regional Site-Based Approach 5-16 |
| 5.5.2 | Regional Site-Based Monte-Carlo Procedure 5-18 |
| 5.5.3 | Methodology for Generating Missing Data Values 5-19 |
| 5.6 | INTERPRETING A MONTE-CARLO MODELING ANALYSIS . . . 5-22 |
| 5.7 | REQUIRED NUMBER OF MONTE-CARLO REALIZATIONS . . . 5-26 |
| 6.0 | REFERENCES 6-1 |

APPENDIX A: EPACMTP CODE STRUCTURE

APPENDIX B.1: ANALYTICAL SOLUTION FOR ONE-DIMENSIONAL
TRANSPORT OF A STRAIGHT AND BRANCHING CHAIN OF
DECAYING SOLUTES

APPENDIX B.2: ANALYTICAL SOLUTION FOR ONE-DIMENSIONAL
TRANSPORT OF A SOLUTE WITH NON-LINEAR SORPTION

APPENDIX C: ANALYTICAL SOLUTION FOR THREE-DIMENSIONAL
STEADY-STATE GROUNDWATER FLOW IN A CONSTANT
THICKNESS AQUIFER

APPENDIX D: VERIFICATION AND VALIDATION OF THE EPA'S COMPOSITE
MODEL FOR TRANSFORMATION PRODUCTS

APPENDIX E: PARAMETER SCREENING

APPENDIX F: GROUND-WATER-TO-SURFACE-WATER MASS FLUX

APPENDIX G: MINTEQA2-BASED METAL ISOTHERMS

LIST OF TABLES

| | Page |
|-----------|--|
| Table 2.1 | Source-Specific Variables for Landfills 2-7 |
| Table 2.2 | Source-Specific Variables for Surface Impoundments 2-18 |
| Table 2.3 | Source-Specific Variables for Waste Piles 2-32 |
| Table 2.4 | Source-Specific Variables for Land Application Units 2-36 |
| Table 3.1 | Parameters for the Unsaturated Zone Flow Submodule 3-4 |
| Table 3.2 | Parameters for the Unsaturated Zone Transport Submodule . . 3-12 |
| Table 4.1 | Aquifer-Specific Variables for the Flow Module 4-4 |
| Table 4.2 | Ratio Between Effective and Total Porosities as a Function of Particle Diameter (after McWorter and Sunada, 1977) 4-6 |
| Table 4.3 | Aquifer-Specific Variables for the Saturated-Zone Transport Submodule 4-22 |
| Table 5.1 | Probability distributions and their associated codes available for use in Monte-Carlo module of EPACMTP 5-9 |
| Table 5.2 | Example Empirical Distribution 5-12 |
| Table 5.3 | Relationship between confidence interval and number of Monte-Carlo realizations 5-27 |

LIST OF FIGURES

| | | Page |
|-------------|---|-------------|
| Figure 1.1 | Conceptual Cross-Section View of the Subsurface System Simulated by EPACMTP | 1-3 |
| Figure 1.2 | (a) Leachate Concentration, and (b) Ground-water Exposure Concentration | 1-4 |
| Figure 2.1 | Leachate Concentration Versus Time for Pulse Source and Depleting Source Conditions | 2-3 |
| Figure 2.2 | WMU Types Modeled in EPACMTP | 2-5 |
| Figure 2.3 | Schematic Cross-Section View of SI Unit | 2-23 |
| Figure 2.4 | Flowchart Describing the Infiltration Screening Procedure | 2-41 |
| Figure 2.5 | Infiltration Screening Criteria | 2-42 |
| Figure 3.1 | Cross-sectional View of the Unsaturated Zone Considered by EPACMTP | 3-2 |
| Figure 3.2 | Typical Saturation Profile for a Homogenous Soil under Steady Infiltration Conditions. The Water Table Is Located at $Z_u = 10$ m | 3-11 |
| Figure 4.1 | Schematic Illustration of the Saturated Three-dimensional Ground-water Flow System Simulated by the Model | 4-3 |
| Figure 4.2 | Three-dimensional Brick Element Used in Numerical Flow and Transport Model Showing Local Node Numbering Convention | 4-15 |
| Figure 4.3 | Flowchart Describing the Infiltration Screening Procedure | 4-18 |
| Figure 4.4 | Infiltration Screening Criteria | 4-19 |
| Figure 4.5 | Schematic View of the Two Possible Zones for Receptor Well Location | 4-29 |
| Figure 4.6 | Schematic Cross-sectional View of the Aquifer Showing the Contributing Components of the Ground-water Flow Field | 4-33 |
| Figure 4.7 | Schematic Cross-sectional View of the Aquifer, Illustrating the Procedure for Determining the X-Dimension of the Model Domain | 4-45 |
| Figure 4.8 | Difference $(C_{\text{analytical}} - C_{\text{numerical}})/C_0$ Between Analytical and Numerical Transport Solutions as a Function of (ratio of regional flux to near-source flux). C_0 Is the Source Concentration | 4-50 |
| Figure 4.9 | Schematic View of the Time-varying Receptor Well Concentration (Break Through Curve) and Illustration of the Procedure for Determining r_w | 4-86 |
| Figure 4.10 | Schematic Illustration of the Effect of Increasing Pulse Duration, T_p , on the Receptor Well Break Through Curve | 4-87 |
| Figure 5.1 | Flow chart of EPACMTP for a Monte-Carlo Problem | 5-5 |
| Figure 5.2 | Frequency distribution of normalized receptor well concentrations | 5-25 |
| Figure 5.3 | Cumulative Distribution Function of Normalized Receptor Well Concentration | 5-25 |
| Figure 5.4 | Relative Monte-Carlo Prediction Error | 5-28 |

LIST OF ACRONYMS

| | |
|-----------|---|
| 1-D | One-dimensional |
| 3-D | Three-dimensional |
| API | American Petroleum Institute |
| CANSAZ-3D | Combined Analytical-Numerical in Saturated Zone in 3 Dimensions |
| CDF | Cumulative Distribution Function |
| DAF | Dilution-Attenuation Factor |
| EPA | Environmental Protection Agency |
| EPACML | EPA's Composite Model for Landfills |
| EPACMS | EPA's Composite Model for Surface impoundments |
| EPACMTP | EPA's Composite Model for Leachate Migration with Transformation Products |
| EPA | Environmental Protection Agency |
| EPRI | Electric Power Research Institute |
| FECTUZ | Finite Element Contaminant Transport in the Unsaturated Zone |
| HBN | Health-based Number |
| HELP | Hydrologic Evaluation of Landfill Performance |
| HWIR | Hazardous Waste Identification Rule |
| IWEM | Industrial Waste Management Evaluation Model |
| LAU | Land Application Unit |
| LF | Landfill |
| LTG | Laplace Transform Galerkin |
| LTU | Land Treatment Unit |
| MCL | Maximum Contaminant Level |
| MINTEQA2 | EPA's Geochemical Equilibrium Speciation Model for Dilute Aqueous Systems |
| NOAA | National Oceanic and Atmospheric Administration |
| ORTHOMIN | EPACMTP's matrix solver |

LIST OF ACRONYMS (continued)

| | |
|--------|--|
| OSW | Office of Solid Waste |
| OSWER | Office of Solid Waste and Emergency Response |
| RCRA | Resource Conservation and Recovery Act |
| RGC | Reference Groundwater Concentration |
| SAB | Science Advisory Board |
| SI | Surface Impoundment |
| SPLP | Synthetic Precipitation Leaching Procedure |
| STORET | EPA's STORage and RETrieval database of water quality, biological, and physical data |
| TC | Toxicity Characteristics |
| TCLP | Toxicity Characteristic Leaching Procedure |
| USEPA | United States Environmental Protection Agency |
| VADOFT | EPA's numerical unsaturated zone simulator, VADose Zone Flow and Transport code |
| VHS | Vertical and Horizontal Spread Model |
| WMU | Waste Management Unit |
| WP | Waste Pile |

LIST OF SYMBOLS

| Symbol | Definition | Equation in which the symbol first appears |
|---------------|---|--|
| A | empirical constant (dimensionless) | 2.14 |
| A'' | $\log_{10}(A_{LU})$ | 5.6 |
| A_{cp} | parent compound A_{cp} | 4.37 |
| a_{gh} | area of hole in the geomembrane (m^2) | 2.24c |
| A_r | anisotropy ratio = K_x/K_z | 4.5 |
| a_v | compressibility of the sediment ($m \cdot s^2/kg$) | 2.15 |
| A_w | area of WMU footprint (m^2) | 2.3 |
| A_{YJ} | lower bound for Y_{JSB} | 5.8 |
| A_{YLU} | lower bound for Y_{LU} | 5.6 |
| A_{YU} | lower bound for Y_U | 5.5 |
| | | |
| b | empirical constant ($1/\log(m/s)$) | 2.14 |
| B | thickness of the saturated zone (m) | 2.31 |
| B' | estimated plume depth (m) | 4.71 |
| B'' | $\log_{10}(B_{LU})$ | 5.6 |
| B_{cp} | degradation product B_{cp} | 4.37 |
| B_{LU} | upper bound for Y_{LU} | 5.6 |
| B^* | matrix of square root of $V_{1,2}$ | 5.11b |
| B_{YJ} | upper bound for Y_{JSB} | 5.8 |
| B_{YU} | upper bound for Y_U | 5.5 |
| $\{b\}$ | vector containing the known transformed natural boundary conditions, as well as contributions from decaying parents | 4.50 |
| | | |
| c | aqueous concentration of the constituent of interest (mg/L) | 3.25a |
| $c(0, t)$ | aqueous concentration at $z_u^1 = 0$ (mg/L) | 3.26 |
| $c(z_u)$ | aqueous concentration of the constituent of interest at z_u (mg/L) | 3.27 |
| \bar{c} | Laplace transformed concentration (y-mg/L) | 4.61 |
| \tilde{c}_i | initial aqueous concentration of species i in the source (mg/L) | 3.24 |
| C_1 | constant (dimensionless) | 2.19 |
| C_2 | constant (1/m) | 2.20 |
| C_A | average groundwater concentration over a specified exposure period (mg/L) | 4.58 |
| C_c | compression index (dimensionless) | 2.16 |
| C_{cp} | degradation product C_{cp} | 4.37 |

LIST OF SYMBOLS (continued)

| Symbol | Definition | Equation in which the symbol first appears |
|------------------|---|---|
| C_E | parameter value whose cumulative probability is F_3 | 5.7b |
| C_{fact} | clogging factor | 2.23 |
| c_i | aqueous concentration of species i (mg/L) | 3.14 |
| $c_i(0, t)$ | aqueous concentration of species i at $z_u = 0$ (mg/L) | 3.22 |
| $c_i(l_u, t)$ | aqueous concentration of species i at time t at the bottom of the saturated zone (mg/L) | 3.23a |
| $c_i(z_u, 0)$ | initial aqueous concentration of species i at depth z_u (mg/L) | 3.20 |
| $c_i(\infty, t)$ | aqueous concentration at infinity (mg/L) | 3.23b |
| $c_j(t)$ | concentration at node j of the finite element grid at time t (mg/L) | 4.51 |
| \bar{c}_j | Laplace-transformed concentration (y-mg/L) | 4.51 |
| c_k | aqueous concentration of species k (mg/L) | 4.72 |
| C_L | leachate concentration (mg/L) | 2.1 |
| c_ℓ | aqueous concentration of the ℓ -th component in the decay chain (mg/L) | 4.31 |
| \bar{c}_ℓ | Laplace-transformed concentration of species ℓ (y-mg/L) | 4.49 |
| c_m | aqueous concentration of parent m (mg/L) | 3.14 |
| \bar{c}_m | Laplace-transformed concentration of parent m (y-mg/L) | 4.49 |
| \bar{C}_r | relative concentration at receptor well (dimensionless) | 5.12 |
| C_{RW} | instantaneous receptor well concentration | 4.108 |
| C_{rwell} | constituent concentration at receptor well (mg/L) (instantaneous or time-averaged) | 5.12 |
| \bar{C}_{RW} | time-averaged receptor well concentration (mg/L) | 4.108 |
| C_w | constituent concentration in the waste (mg/kg) | 2.3 |
| c_i^{in} | initial aqueous concentration of species i in the unsaturated zone (mg/L) | 3.20 |
| C_L^{max} | maximum allowable leachate concentration (mg/L) | 5.14 |
| c^o | source concentration of constituent of interest (mg/L) | 3.26 |
| $c^o(t)$ | source concentration of constituent of interest at time t (mg/L) | 4.55 |
| c_i^o | leachate concentration of species i emanating from the source (mg/L) | 3.21 |
| $c_i^o(t)$ | leachate concentration of species i emanating from the source at time t (mg/L) | 3.22 |
| C_{iave}^o | average concentration value during the time interval $[t_i^{on}, t_i^{off}]$ (mg/L) | 4.55 |
| c_k^o | source concentration for species k (mg/L) | 4.74b |
| C_L^o | initial leachate concentration at the time of landfill closure (mg/L) | 2.1 |

LIST OF SYMBOLS (continued)

| Symbol | Definition | Equation in which the symbol first appears |
|------------------|---|---|
| c_e^o | source concentration of the ℓ -th component species in the decay chain (mg/L) | 4.39b |
| c_e^i | initial source concentration of the ℓ -th species in the decay chain (mg/L) | 4.40b |
| c_e^o | Laplace - transformed source concentration of species ℓ (y-mg/L) | 4.41 |
| $\bar{c}_e^o(p)$ | Laplace transform of the source function (y-mg/L) | 4.49 |
| c_m^o | leachate concentration of parent m emanating from the source (mg/L) | 3.24a |
| c_m^o | Laplace - transformed concentration of parent m (y-mg/L) | 4.41 |
| C_w^o | initial constituent concentration in the waste at the time of landfill closure (mg/kg) | 2.9 |
| $c_k^s(t)$ | equivalent aqueous concentration of species k on the vertical plane at the downgradient edge of the source (mg/L) | 4.88 |
| $\{\bar{c}\}$ | Laplace-transformed concentration vector | 4.50 |
| | | |
| d | mean particle diameter (cm) | 4.1 |
| d_{BG} | depth below grade of WMU (m) | 2.24b |
| d_c | distance from a point at the water table underneath the patch source to the downgradient location x_c (m) | 4.66a |
| D_E | parameter value whose cumulative probability is F_4 | 5.7b |
| D_{fc} | thickness of consolidated sediment layer (m) | 2.16 |
| D_i | molecular diffusion coefficient in free water for species i (m^2/y) | 3.15 |
| D_{ij} | dispersion coefficient tensor (m^2/y) | 4.31 |
| D_{LF} | landfill depth (m) | 2.3 |
| D_{lin} | liner thickness (m) | 2.24b |
| D_{Lu} | apparent dispersion coefficient (m^2/y) | 3.14 |
| D_R | average penetration depth due to recharge between the downgradient edge of the source and the observation point (m) | 4.82 |
| D_{soil} | thickness of unaffected native soil underneath the WMU (m) | 2.24a |
| D_u | total depth of the unsaturated zone (m) | 2.24b |
| D_{uc} | thickness of unconsolidated sediment (m) | 2.17 |
| D_{xx} | longitudinal dispersion coefficient (m^2/y) | 4.32a |
| D_{xy} | off-diagonal dispersion coefficient for the x-y plane (m^2/y) | 4.32d |
| D_{xz} | off-diagonal dispersion coefficient for the x-z plane (m^2/y) | 4.32e |
| D_{yy} | horizontal transverse dispersion coefficient (m^2/y) | 4.32b |
| D_{yz} | off-diagonal dispersion coefficient for the y-z plane (m^2/y) | 4.32f |

LIST OF SYMBOLS (continued)

| Symbol | Definition | Equation in which the symbol first appears |
|---------------|--|---|
| D_{zz} | vertical dispersion coefficient (m^2/y) | 4.32c |
| D_{dui}^* | effective molecular diffusion coefficient (m^2/yr) | 3.15 |
| D_{soil}^* | thickness of clogged soil layer underneath the WMU (m) | 2.24a |
| D^* | diagonal matrix consisting of the square root of the eigenvalues of $V_{1,2}$ | 5.11a |
| D^{S*} | effective molecular diffusion coefficient for species of interest (m^2/y) | 4.29 |
| D_k^{S*} | effective molecular diffusion coefficient for species k in the saturated zone (m^2/y) | 4.107 |
| D_ℓ^{S*} | effective molecular diffusion coefficient for species ℓ (m^2/y) | 4.32a |
| DAF | Dilution-Attenuation Factor (dimensionless) | 5.13 |
| DAF_{10} | 10th percentile value of DAF (which corresponds to the 90 th percentile of relative concentration) | 5.14 |
| | | |
| e | void ratio (dimensionless) | 2.14 |
| E | an error term arising because the Fourier coefficients are approximations obtained from \bar{c}_i rather than $c_i(t)$ and because the series is truncated after $2N$ terms (mg/L) | 4.51 |
| e_0 | initial void ratio at no-stress condition (dimensionless) | 2.15 |
| | | |
| f | fraction of the source that migrates downgradient in the event that a water table crest occurs within the source area (dimensionless) | 4.84 |
| $f(x^*)$ | probability density function of x^* | 5.1 |
| $f(c)$ | nonlinear function representing the adsorption isotherm (mg/kg) | 3.32 |
| $F(\psi)$ | a function of ψ | 3.7 |
| $f'c$ | derivative of $f(c)$ (dimensionless) | 3.31 |
| F_3 | a cumulative probability value | 5.7b |
| F_4 | a cumulative probability value | 5.7b |
| F_c | concentration ratio (dimensionless) | 4.89 |
| F_h | volume fraction of the waste in the landfill at time of closure (m^3/m^3) | 2.3 |
| f_i | slope of the adsorption isotherm for species i (L/kg) | 3.16 |
| f_{oc} | fractional organic carbon content (dimensionless) | 3.10 |
| f_{ocw} | fraction of organic carbon in the soil layer in which the waste is mixed (dimensionless) | 2.26 |
| f_{oc}^s | fractional organic carbon content of the aquifer material (dimensionless) | 4.30 |

LIST OF SYMBOLS (continued)

| Symbol | Definition | Equation in which the symbol first appears |
|----------------|--|--|
| | | |
| g | gravitational acceleration (m/s ²) | 2.17 |
| G_q | q -th coefficient (l/m) | 4.65a |
| | | |
| H | hydraulic head (m) | 4.7 |
| $H(x)$ | hydraulic head at distance x (m) | 4.12a |
| $H(0,z)$ | hydraulic head at $x = 0$ (m) | 4.9a |
| $H(x_L, z)$ | hydraulic head at $x = x_L$ (m) | 4.9b |
| H_1 | prescribed hydraulic head at the upgradient boundary (m) | 4.9a |
| H_2 | prescribed hydraulic head at the downgradient boundary (m) | 4.9b |
| H_P | SI ponding depth (m) | 2.17 |
| H_T | SI operating (total) depth (m) | 2.24c |
| $H_V(\bullet)$ | Heaviside step function (dimensionless) | 4.55 |
| $\{H\}$ | vector of unknown nodal head values (m) | 4.15 |
| HBN | health-based number, which is a ground-water exposure concentration corresponding to a defined risk level (mg/L) | 5.14 |
| | | |
| I | annual infiltration rate through the source (m/y) | 2.6 |
| I_{EFF} | effective infiltration rate through the strip source area (m/y) | 4.9c |
| Im | imaginary part of the complex \bar{c}_j values (y-mg/L) | 4.51 |
| I_{Max} | maximum allowable infiltration rate (m/y) | 2.31 |
| I_r | effective recharge rate outside the strip source area (m/y) or recharge rate outside the source area (m/y) | 4.9c |
| | | |
| K | hydraulic conductivity (cm/s) | 4.4 |
| k_1 | nonlinear Freundlich parameter for the unsaturated zone (mg constituent/kg dry soil) (mg/L) ⁻ⁿ | 4.34 |
| k_{1i} | nonlinear Freundlich parameter for species i in the unsaturated zone (dimensionless) | 3.18 |
| K_d | distribution (solid-aqueous phase) coefficient in the unsaturated zone (cm ³ /g) | 3.11 |
| K_d^s | solid-liquid distribution coefficient of the aquifer (cm ³ /g) | 4.18 |
| K_{dw} | waste partition coefficient (cm ³ /g) | 2.25 |
| K_{fc} | averaged saturated hydraulic conductivity of the consolidated sediment (m/y) | 2.21 |
| K_{lin} | saturated hydraulic conductivity of liner (m/y) | 2.24b |
| k_{oc} | constituent-specific organic carbon partition coefficient (cm ³ /g) | 2.26 |

LIST OF SYMBOLS (continued)

| Symbol | Definition | Equation in which the symbol first appears |
|------------------------|---|---|
| k_{oc} | normalized organic carbon distribution coefficient [cm^3/g] | 3.11 |
| k_{rw} | relative permeability of the native soil in the unsaturated zone (dimensionless) | 2.24a |
| k_{rw}^* | relative permeability of the clogged soil in the unsaturated zone (dimensionless) | 2.24a |
| k_{rwlin} | relative permeability of the liner (dimensionless) | 2.24b |
| K_s | saturated hydraulic conductivity of the native soil (m/y) | 2.23 |
| K_s^* | saturated hydraulic conductivity of clogged unsaturated-zone soil (m/y) | 2.23 |
| K_{Sed} | hydraulic conductivity of consolidated sediment (m/s) | 2.14 |
| K_u | soil hydraulic conductivity at pressure ψ (m/y) | 3.7 |
| K_w | waste-concentration-to-leachate-concentration ratio (L/kg) | 2.8 |
| K_x | hydraulic conductivity of the saturated zone in the longitudinal (x) direction (m/y) | 2.31 |
| K_y | hydraulic conductivity in the saturated zone in the horizontal transverse (y) direction (m/y) | 4.7 |
| K_z | hydraulic conductivity in the saturated zone in the vertical (z) direction (m/y) | 4.5 |
| | | |
| L | overall length of the model domain in the x-direction (m) | 4.43 |
| $\mathcal{L}(\bullet)$ | Laplace transformation operator (dimensionless) | 4.48 |
| l_u | bottom of the unsaturated zone (m) | 3.23a |
| L^* | ($p \times p$) matrix of the eigenvectors of $V_{1,2}$ | 5.11a |
| l^i | the thickness of layer i | 3.27 |
| | | |
| M | number of parent species | 3.14 |
| \mathbf{m} | sample mean vector of missing and observed values | 5.9 |
| \mathbf{m}_1 | sample mean vector of missing values | 5.9 |
| $\mathbf{m}_{1,2}$ | mean vector of Y_1 conditioned by Y_2 | 5.10a |
| \mathbf{m}_2 | sample mean vector of observed values | 5.9 |
| M_c | total constituent mass in the landfill (mg) | 2.3 |
| \mathbf{m}_{cL} | annual constituent mass lost by leaching (mg/y) | 2.6 |
| M_{LWP} | total mass of constituent leached from a waste pile | 2.27 |
| M_s | contaminant mass flux ($\text{mg}/\text{m}^2 \cdot \text{y}$) which is applied over the rectangular source area | 4.62 |
| \mathbf{m}_w | annual waste loading during active life (kg/y) | 4.37 |
| MW_ℓ | molecular weight of species ℓ | 2.4 |
| | | |

LIST OF SYMBOLS (continued)

| Symbol | Definition | Equation in which the symbol first appears |
|---------------|---|---|
| $N[0, 1]$ | normally distributed value with mean of zero and standard deviation of one | 5.2 |
| n_c | number of component species in the decay chain (dimensionless) | 4.31 |
| $N_n()$ | n - variate normal distribution with mean vector \bar{m} and covariance matrix V | 5.9 |
| N_s | number of steps into which $c^o(t)$ is discretized (dimensionless) | 4.55 |
| | | |
| $\%OM$ | percent organic matter (dimensionless) | 3.10 |
| | | |
| p | Laplace-transform parameter (1/y) | 4.41 |
| p_k | k -th term of the parameter in the Laplace inversion series (1/y) | 4.51 |
| p_{rw} | probability that the receptor well will be located in Zone 2 (dimensionless) | 4.27 |
| p^o | a real constant for the inversion of Laplace transform (1/yr) | 4.51 |
| $[P]$ | advective-dispersive transport matrix, including the decay term λ | 4.50 |
| | | |
| Q_i | coefficient to incorporate decay in the sorbed phase for species i (dimensionless) | 3.14 |
| Q_m | coefficient to incorporate decay in the sorbed-phase of parent m (dimensionless) | 3.14 |
| \bar{q}_x | average Darcy velocity in the x direction between the downgradient edge of the source and the point of interest along the x direction (m/y) | 4.78 |
| Q_1^F | background groundwater flux (m ² /y) | 4.29 |
| Q_2^F | recharge flux upgradient of the source (m ² /y) | 4.29 |
| Q_3^F | infiltration flux through the source (m ² /y) | 4.29 |
| Q_4^F | recharge flux downgradient of the source (m ² /y) | 4.29 |
| Q_r^F | ratio of the background groundwater flux to that near the source (dimensionless) | 4.47 |
| $\{Q\}$ | vector of nodal boundary flux values (m ³ /y) | 4.15 |
| | | |
| r | regional hydraulic gradient (m/m) | 4.6 |
| R_n | generated random number which corresponds to the cumulative probability of Y | 5.7a |
| R_0 | Equivalent source radius (m) | 2.31 |

LIST OF SYMBOLS (continued)

| Symbol | Definition | Equation in which the symbol first appears |
|---------------|---|---|
| R_i | retardation factor for species i (dimensionless) | 3.14 |
| R_{rw} | radial distance between waste management unit and well (m) | 4.21 |
| R_∞ | distance between the center of the source and the nearest downgradient boundary where the boundary location has no perceptible effects on the heads near the source (m) | 2.31 |
| r_ϕ | ratio between effective and total porosities | 4.2b |
| R^s | retardation factor (dimensionless) | 4.62 |
| R_ℓ^s | saturated zone retardation factor of species ℓ (dimensionless) | 4.18 |
| Re | real part of the complex $\bar{c}_i(t)$ values (y-mg/L) | 4.51 |
| $[R]$ | conductance matrix (m^2/y) | 4.15 |
| | | |
| s | sorbed concentration for constituent of interest (mg constituent/kg dry soil) | 3.29 |
| S_e | effective saturation (dimensionless) | 3.2 |
| s_i | sorbed concentration for species i (mg constituent/kg dry soil) | 3.17 |
| s_k | sorbed concentration of species k (mg constituent/kg dry soil) | 4.72 |
| $[S]$ | Laplace-transformed mass matrix | 4.50 |
| | | |
| t | time (y) | 2.1 |
| t' | travel time from x_u to x_c (yr) | 4.66b |
| t_1 | beginning of the time interval of interest (y) | 4.58 |
| t_2 | end of the time interval of interest (y) | 4.58 |
| t_A | WMU active life (y) | 2.4 |
| t_d | exposure time interval of interest (y) | 4.108 |
| t_{max} | maximum simulation time (y) | 4.52 |
| t_p | pulse duration (y) | 2.2 |
| t_{peak} | time value at which the receptor well concentration reaches its peak (y) | 4.108 |
| τ_t | time integration variable (y) | 4.65a |
| t_i^{off} | end of the time interval of interest (y) | 4.55 |
| t_i^{on} | beginning of the time interval of interest (y) | 4.55 |
| | | |
| u | vector of independent and identically distributed standard normal random variables | 5.11a |

LIST OF SYMBOLS (continued)

| Symbol | Definition | Equation in which the symbol first appears |
|------------------|--|---|
| U | seepage (pore-water) velocity (m/y) | 3.29 |
| $U(0, 1)$ | uniform random number varying between 0 and 1 | 4.25b |
| u^i | retarded seepage velocity in layer i (m/y) | 3.25a |
| u^k | retarded seepage velocity in layer k (m/y) | 3.27 |
| | | |
| V | sample covariance matrix | 5.9 |
| $ V $ | absolute value of the Darcy velocity (m/yr) | 4.32a |
| V_{11} | upper left partition of V | 5.10c |
| V_{12} | upper right partition of V | 5.10b |
| $V_{1,2}$ | covariance matrix of Y_1 conditioned by Y_2 | 5.10c |
| V_{21} | lower left partition of V | 5.10c |
| V_{22} | lower right partition of V | 5.10b |
| V_ℓ | Darcy velocity in the ℓ -th direction (m/y) | 4.16 |
| V_u | Darcy velocity obtained from solution of the flow equation (m/y) | 3.14 |
| V_u^i | Darcy velocity in the i -th layer (m/y) | 3.25b |
| V_x | longitudinal groundwater velocity (in the x-direction) (m/y) | 4.6 |
| \overline{V}_x | average Darcy velocity in the x direction between the downgradient edge of the source and the point of interest along the x direction (m/y) | 4.66b |
| V_y | horizontal transverse Darcy velocity (m/y) | 4.32a |
| V_z | vertical Darcy velocity (m/y) | 4.32a |
| | | |
| x | principal Cartesian coordinate along the regional flow direction (m) | 4.7 |
| x' | transformed x-coordinate (m) | 4.94g |
| x_1 | x- coordinate (m) | 4.31 |
| x_2 | y- coordinate (m) | 4.31 |
| x_3 | z- coordinate (m) | 4.31 |
| x_c | downgradient location at which dispersion is calculated (m) | 4.66 |
| x_{crest} | x-coordinate of the crest of the water table (m) | 4.85 |
| x_d | downgradient coordinates of the strip source area (m) | 4.9c |
| x_i | Cartesian coordinates in the i -th direction (the 1 st , 2 nd , and 3 rd directions correspond to the x, y, and z directions, respectively) (m) | 4.31 |
| X_e | x-direction component of the solution for species e | 4.92 |
| x_L | length of the aquifer system, or x-coordinate at the downgradient end of the domain (m) | 4.9b |

LIST OF SYMBOLS (continued)

| Symbol | Definition | Equation in which the symbol first appears |
|----------------|--|---|
| x_p | length of the model domain downgradient of the source (m) | 4.43 |
| x_{rw} | distance from the downgradient boundary of the WMU to the receptor well (m) | 4.20 |
| x_s | distance between the upgradient domain boundary and the upgradient edge of the source (m) | 4.42a |
| x_t | average travel distance in the x direction (m) | 4.19 |
| x_u | upgradient coordinates of the strip source area (m) | 4.9c |
| x_w | length of the WMU in the x-direction (parallel to groundwater flow) (m) | 4.20 |
| x^* | random variable | 5.1 |
| x_{rw}^{max} | distance from the downgradient boundary of the WMU to the receptor well (m) | 4.43 |
| x_s^{max} | maximum allowable distance between the upgradient domain boundary and the upgradient edge of the source (m) | 4.42a |
| | | |
| y | principal Cartesian coordinate normal to the flow direction, or distance from the plume centerline (m) | 4.7 |
| y' | transformed y-coordinate (m) | 4.94g |
| y_0 | source half-width ($y_D/2$) (m) | 4.62 |
| Y_1 | vector of missing values | 5.10a |
| Y_2 | vector of observed values | 5.10a |
| $Y_{1,2}$ | prediction of the missing vector Y_1 | 5.11a |
| y_D | source width along the y-axis (m) | 4.10 |
| Y_E | random variable with empirical distribution | 5.7b |
| Y_{EXP} | exponentially distributed random variable | 5.4 |
| Y_{JSB} | random variable with Johnson SB distribution | 5.8 |
| Y_e | y-direction component of the solution for species e | 4.92 |
| y_L | length of the model domain in the y-direction (see Figure 4.1) | 4.10 |
| Y_{LN} | lognormally distributed random variable | 5.3 |
| Y_{LU} | \log_{10} uniform random variable | 5.6 |
| y_{rw} | Cartesian coordinate of the receptor well in the y-direction (m) | 4.22 |
| y_S | equivalent source width in the direction normal to the regional flow direction on the vertical plane at the downgradient edge of the waste (m) | 4.81 |
| Y_U | uniform random variable | 5.5 |
| y_{rw}^{max} | farthest horizontal distance between the receptor well and the plume centerline (m) | 4.45a |

LIST OF SYMBOLS (continued)

| Symbol | Definition | Equation in which the symbol first appears |
|----------------------|---|---|
| y_S^{New} | y_s adjusted to account for z_S^{new} (m) | 4.91 |
| y^{plume} | transverse extent of the plume (m) | 4.45a |
| | | |
| z | principal Cartesian coordinate in the vertical direction (m) | 4.7 |
| Z_e | z-direction component of the solution for species e | 4.92 |
| z_S | equivalent source depth in the vertical direction on the vertical plane at the downgradient edge of the waste management unit (m) | 4.82 |
| Z_{Sed} | vertically downward distance from the top of the consolidated sediment (m) | 2.16 |
| z_u | depth coordinate measured from the bottom of the base of a waste management unit (m) | 3.4 |
| z' | transformed z-coordinate (m) | 4.94g |
| z'_1 | transformed well depth in image 1 (m) | 4.105 |
| z'_2 | transformed well depth in image 2 (m) | 4.105 |
| Z'_e | a component of Z_e | 4.102 |
| z_{rw}^* | z-coordinate of the receptor well positive downward from the water table(m) | 4.29 |
| z_{rw}^{*i} | transformed well depth (m) | 4.106 |
| z_{rwmax}^* | maximum allowable z-coordinate of the receptor well (m) | 4.29 |
| z_u^i | local depth coordinate measured from the tip of layer i (m) | 3.25a |
| z_S^{New} | z_s adjusted to account for the presence of recharge depth D_R (m) | 4.90 |
| GREEK SYMBOLS | | |
| α | van Genuchten soil-specific shape parameter (1/m) | 3.1 |
| α_L | longitudinal dispersivity of the aquifer (m) | 4.19 |
| α_{Lu} | longitudinal dispersivity in the unsaturated zone [m] | 3.9 |
| α_{Ref} | reference longitudinal dispersivity, as determined from the probabilistic distribution (m) | 4.19 |
| α_T | horizontal transverse dispersivity (m) | 4.28 |
| α_V | vertical transverse dispersivity (m) | 4.29 |
| α_{Lu}^i | longitudinal dispersivity for the i-th layer (m) | 3.25a |
| | | |
| β | van Genuchten soil-specific shape parameter (dimensionless) | 3.1 |
| | | |
| γ | van Genuchten soil-specific shape parameter (dimensionless) | 3.1 |

LIST OF SYMBOLS (continued)

| Symbol | Definition | Equation in which the symbol first appears |
|-------------------|---|---|
| γ_i | first-order decay rate for species i (1/y) | 3.24a |
| γ_m | first order decay rate for parent m (1/y) | 3.24a |
| | | |
| $\delta(\bullet)$ | Dirac Delta function | 4.62 |
| δ_{adj} | empirical adjustment factor (dimensionless) | 4.71 |
| Δs | magnitude of nodal spacing (m) | 4.46 |
| Δz_u | grid size in the z_u direction (m) | 3.7 |
| | | |
| ζ | distance along a principal Cartesian coordinate direction (m) | 4.16 |
| | | |
| η_i | non-linear Freundlich exponent for species i for the unsaturated zone (dimensionless) | 3.18 |
| η^s | Freundlich exponent for the saturated zone (dimensionless) | 4.34 |
| | | |
| θ | soil water content (dimensionless) | 3.1 |
| θ_r | residual soil water content (dimensionless) | 3.1 |
| θ_{nw} | angle measured counter-clockwise from the plume centerline (degrees) | 4.21 |
| θ_s | saturated soil water content (dimensionless) | 3.1 |
| θ_w | water content of the waste (dimensionless) | 2.25 |
| θ^i | water content of the i -th layer (dimensionless) | 3.25b |
| | | |
| λ_1 | hydrolysis constant for dissolved phase (1/y) | 3.13 |
| λ_2 | hydrolysis constant for sorbed phase (1/y) | 3.13 |
| λ_{bu} | transformation coefficient due to biological transformation (1/y) | 3.12 |
| λ_{cu} | transformation coefficient due to chemical transformation (1/y) | 3.12 |
| λ_i | first-order decay constant for species i (1/y) | 3.14 |
| λ_m | first-order decay constant of parent m (1/y) | 3.14 |
| λ_u | overall decay coefficient (first-order transformation) (1/y) | 3.12 |
| λ^i | first order decay constant for layer i (1/y) | 3.25a |
| λ^s | first-order decay constant (1/y) | 4.62 |
| λ_ℓ^s | first-order decay coefficient for species ℓ in the saturated zone (1/y) | 4.31 |
| λ_m^s | first-order decay coefficient for parent m in the saturated zone (1/y) | 4.31 |
| | | |

LIST OF SYMBOLS (continued)

| Symbol | Definition | Equation in which the symbol first appears |
|---------------|---|---|
| μ | dynamic viscosity of water (N-s/m ²) | 4.4 |
| μ_N | mean of normal distribution | 5.1 |
| | | |
| ξ_{im} | stoichiometric fraction of parent m that degrades into daughter i (dimensionless) | 3.14 |
| | | |
| ρ | density of water (kg/m ³) | 2.17 |
| ρ_b | bulk density of the aquifer (g/cm ³) | 3.13 |
| ρ_{bu} | soil bulk density of the unsaturated zone (g/cm ³) | 3.16 |
| ρ_{bw} | dry bulk density of the waste (g/cm ³) | 2.25 |
| ρ_{hw} | waste density (g/cm ³) | 2.3 |
| ρ_{leak} | leak density (number of pinholes/m ²) | 2.24c |
| ρ_s | bulk density of the solid phase (g/cm ³) | 4.72 |
| ρ_{Sed} | sediment grain density (kg/m ³) | 2.17 |
| | | |
| σ_N | standard deviation of normal distribution | 5.1 |
| σ_{vf} | vertical effective stress in the consolidated sediment layer (kg/m-s ²) | 2.15 |
| | | |
| ϕ | total porosity (dimensionless) | 4.1 |
| ϕ_e | effective porosity of the saturated zone (dimensionless) | 4.2b |
| ϕ_{eu} | effective porosity of the unsaturated zone (dimensionless) | 3.15 |
| ϕ_{Sed} | consolidated sediment porosity (dimensionless) | 2.14 |
| | | |
| ψ | soil pressure head (m) | 3.1 |
| ψ_l | pressure head at the water table located at distance l from the bottom of a waste management unit (m) | 3.5 |
| ψ_q | q -th constant (1/m) | 4.65a |
| ψ_{zu} | pressure head at z_u (m) | 3.7 |
| Ψ | effective pressure head between z and $z_u - \Delta z_u$ (m) | 3.7 |
| | | |
| ω | weighting factor, $0 \leq w \leq 1$ (dimensionless) | 3.8 |

This page intentionally left blank.

ACKNOWLEDGMENTS

A number of individuals have been involved with this work. Ms. Ann Johnson and Mr. David Cozzie of the U.S. EPA, Office of Solid Waste (EPA/OSW) provided overall project coordination and review and guidance throughout this work. The report was prepared by the staffs of Resource Management Concepts, Inc. (RMC) and HydroGeoLogic, Inc. (HGL) under EPA Contract Number 68-W-01-004.

This page intentionally left blank.

EXECUTIVE SUMMARY

EPACMTP version 2.0 is a subsurface fate and transport model used by the U.S. Environmental Protection Agency (EPA) to simulate the impact of the release of constituents present in waste that is managed in land disposal units. Figure ES.1 shows a conceptual, cross-sectional view of the aquifer system modeled by EPACMTP.

EPACMTP simulates fate and transport in both the unsaturated zone and the saturated zone (ground water) using the advective-dispersive equation with terms to account for equilibrium sorption and first-order transformation. The source of constituents is a waste management unit (WMU) located at the ground surface overlying an unconfined aquifer. The base of the WMU can be below the actual ground surface. Waste constituents leach from the base of the WMU into the underlying soil. They migrate vertically downward until they reach the water table. As the leachate enters the ground water, it will mix with ambient ground water (which is assumed to be free of pollutants) and a ground-water plume, which extends in the direction of downgradient ground-water flow, will develop. EPACMTP accounts for the spreading of the plume in all three dimensions.

Leachate generation is driven by the infiltration of precipitation that has percolated through the waste unit, from the base of the WMU into the soil. Different liner designs control the rate of infiltration that can occur. EPACMTP models flow in both the unsaturated and saturated zones as steady-state processes, that is, representing long-term average conditions.

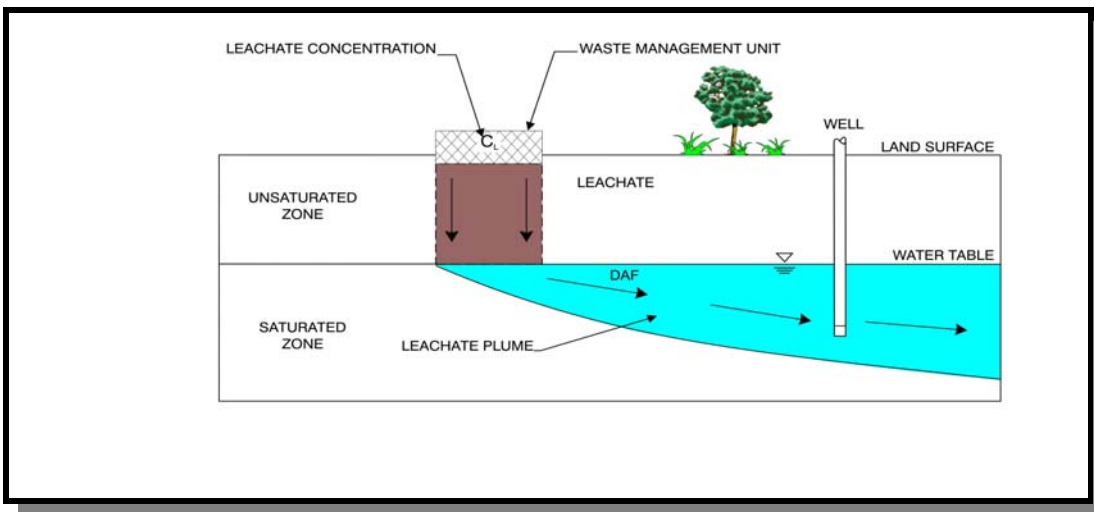


Figure ES.1 Conceptual Cross-Section View of the Subsurface System Simulated by EPACMTP.

In addition to dilution of the constituent concentration caused by the mixing of the leachate with ground water, EPACMTP accounts for attenuation due to sorption of waste constituents in the leachate onto soil and aquifer solids, and for bio-chemical transformation (degradation) processes in the unsaturated and saturated zone.

For organic constituents, EPACMTP models sorption between the constituents and the organic matter in the soil or aquifer, based on constituent-specific organic carbon partition coefficients, and a site-specific organic carbon fraction in the soil and aquifer. In the case of metals, EPACMTP accounts for more complex geochemical reactions by using effective sorption isotherms for a range of aquifer geochemical conditions, generated using EPA's geochemical equilibrium speciation model for dilute aqueous systems (MINTEQA2).

Four types of WMUs with the following key characteristics are simulated by EPACMTP:

- **Landfill (LF).** EPACMTP considers LFs closed with an earthen cover. The release of waste constituents into the soil and ground water underneath the LF is caused by dissolution and leaching of the constituents due to precipitation that percolates through the LF.
- **Surface Impoundment (SI).** In EPACMTP, SIs are ground level or below-ground level, flow-through units. Release of leachate is driven by the ponding of water in the impoundment, which creates a hydraulic head gradient with the ground water underneath the unit.
- **Waste Pile (WP).** WPs are typically used as temporary storage units for solid wastes. Due to their temporary nature, EPACMTP does not consider them to be covered.
- **Land Application Unit (LAU).** LAUs are areas of land which receive regular applications of waste that can be either tilled or sprayed directly onto the soil and subsequently mixed with the soil. EPACMTP simulated the leaching of wastes after tilling with soil. Losses due to volatilization during or after waste application are not accounted for by EPACMTP.

The output from EPACMTP is the predicted maximum ground-water exposure concentration, measured at a well located down-gradient from a WMU.

EPACMTP uses a regional site-based Monte-Carlo simulation approach to determine the probability distribution of predicted ground-water concentrations, as a function of the variability of modeling input parameters. The Monte-Carlo technique is based on the repeated random sampling of input parameters from their respective frequency distribution, executing the EPACMTP fate and transport model for each realization of input parameter values. The regional site-based approach is incorporated into the EPACMTP model to reduce the likelihood that a physically infeasible set of

environmental data will be generated. The results of EPACMTP Monte-Carlo simulations are used to generate probability distributions of constituent concentrations at receptor wells and associated ground-water dilution and attenuation factors (DAFs).

EPACMTP has been peer-reviewed, verified, and enhanced extensively during the past decade. It has also been validated using actual site data from four different sites.

EPACMTP has been applied to support the development of regulations for management and disposal of hazardous wastes. Examples of regulations based on EPACMTP analysis include: Toxicity Characteristic (TC) Rule, Hazardous Waste Identification Rule (HWIR), and Petroleum Refining Process Wastes Listing Determination.

This page intentionally left blank.

1.0 INTRODUCTION

This document provides technical background for **EPA's Composite Model for Leachate Migration with Transformation Products (EPACMTP)**. EPACMTP is a subsurface fate and transport model used by EPA to simulate the impact of the release of constituents present in waste that is managed in land disposal units. This document describes the science and assumptions underlying the EPACMTP. EPA has also developed a complementary document, the *EPACMTP Parameters/Data Background Document* (U.S. EPA, 2003), which describes the EPACMTP input parameters, data sources and default parameter values and distributions which EPA has assembled for its use of EPACMTP as a ground-water assessment tool.

This document is organized as follows. The remainder of this section introduces the main components and features of EPACMTP, and also presents the primary assumptions and limitations of the model. The purpose of this section is to provide the user with an overall understanding of the model and its capabilities. Subsequent sections of this document describe the components, or modules, of EPACMTP in detail:

- Section 2 describes the source-term module;
- Section 3 describes the unsaturated-zone module;
- Section 4 describes the saturated-zone module; and
- Section 5 describes the Monte-Carlo module.

Several appendices provide detailed mathematical formulations, and testing and verification of the unsaturated zone and saturated zone flow and transport solutions incorporated into EPACMTP.

1.1 DEVELOPMENT HISTORY OF EPACMTP

The U.S. Environmental Protection Agency (EPA), Office of Solid Waste (OSW) has been using and improving mathematical models since the early 1980s when the Vertical Horizontal Spread (VHS) model (Domenico and Palciauskas, 1982) was used. In the late 1980s, the model was replaced by the EPA's Composite Model for Landfills [EPACML] (U.S. EPA, 1990). EPACML simulates the movement of contaminants leaching from a landfill through the unsaturated and saturated zones. The composite model consists of a steady-state, one-dimensional numerical module that simulates flow and transport in the unsaturated zone. The contaminant flux at the water table is used to define the Gaussian-source boundary conditions for the transient, semi-analytical, saturated-zone transport module. The latter includes one-dimensional uniform flow, three-dimensional dispersion, linear adsorption, lumped first-order decay, and dilution due to direct infiltration into the ground-water plume.

EPACML accounts for first-order decay and linear equilibrium sorption of chemicals, but disregards the formation and transport of transformation products (also known as degradation products). The analytical ground-water transport solution technique employed in EPACML further imposes certain restrictive assumptions; specifically, the solution can handle only uniform, unidirectional ground-water flow and thereby

ignores the effects of ground-water mounding on contaminant migration and ground-water flow. To address the limitations of EPACML, the modeling approach has been enhanced and implemented in EPACMTP. The EPACMTP modeling approach incorporates greater flexibility and versatility in the simulation capability; i.e., the model explicitly can take into consideration:

- a) chain transformation reactions and transport of degradation products,
- b) effects of water-table mounding on ground-water flow and contaminant migration,
- c) finite source, as well as continuous source, scenarios, and
- d) metals transport by linking EPACMTP with outputs from the MINTEQA2 metals speciation model (U.S. EPA, 1999).

EPACMTP contains an unsaturated-zone module called Finite Element Contaminant Transport in the Unsaturated Zone (FECTUZ) (U.S. EPA, 1989), a saturated-zone module called Combined Alytical-Numerical Saturated Zone in 3-Dimensions (CANSAZ-3D) (Sudicky et al., 1990) and a Monte-Carlo module for nationwide uncertainty analysis. The FECTUZ model and the CANSAZ model were reviewed by the Science Advisory Board (SAB) in 1988, and 1990 (SAB, 1988; 1990), respectively. In March 1994, the SAB provided a consultation on an earlier version of EPACMTP. Based on recommendations for the SAB, EPACMTP was further enhanced and improved. The code received a favorable review by the SAB in 1995 for its intended use in RCRA/Superfund regulations (SAB, 1995).

EPACMTP and its predecessors (EPACML, CANSAZ-3D, and FECTUZ) have been peer-reviewed, verified and enhanced extensively during the past decade at each of the developmental stages. The model has been verified, in numerous cases, by comparing the simulation results against both analytical and numerical solutions. Additionally, EPACMTP and its predecessors have been validated using actual site data from four different sites. Details of verification and validation history and results are presented in Appendix D of this document.

EPACMTP has been applied to support the development of regulations for management and disposal of hazardous wastes. Examples of regulations based on EPACMTP analysis include: Toxicity Characteristic (TC) Rule, and Petroleum Refining Process Wastes Listing Determination. The Agency has implemented a version control procedure over the development of EPACMTP to ensure repeatability of simulation results. The current version of EPACMTP is 2.0.

1.2 WHAT IS THE EPACMTP MODEL?

Figure 1.1 depicts a cross-sectional view of the subsurface system simulated by EPACMTP. EPACMTP treats the subsurface aquifer system as a composite domain, consisting of an unsaturated (vadose) zone and an underlying saturated zone. The demarcation between the two zones is the water table. EPACMTP simulates one-dimensional, vertically downward flow and transport of constituents in the unsaturated zone beneath a waste disposal unit as well as ground-water flow and three-dimensional constituent transport in the underlying saturated zone. The

unsaturated-zone and saturated-zone modules are computationally linked through continuity of flow and constituent concentration across the water table directly underneath the waste management unit (WMU). The model accounts for the following processes affecting constituent fate and transport as the constituent migrates from the bottom of a WMU through the unsaturated and saturated zones: advection, hydrodynamic dispersion and molecular diffusion, linear or nonlinear equilibrium sorption, first-order decay and zero-order production reactions (to account for transformation breakdown products), and dilution due to recharge in the saturated zone.

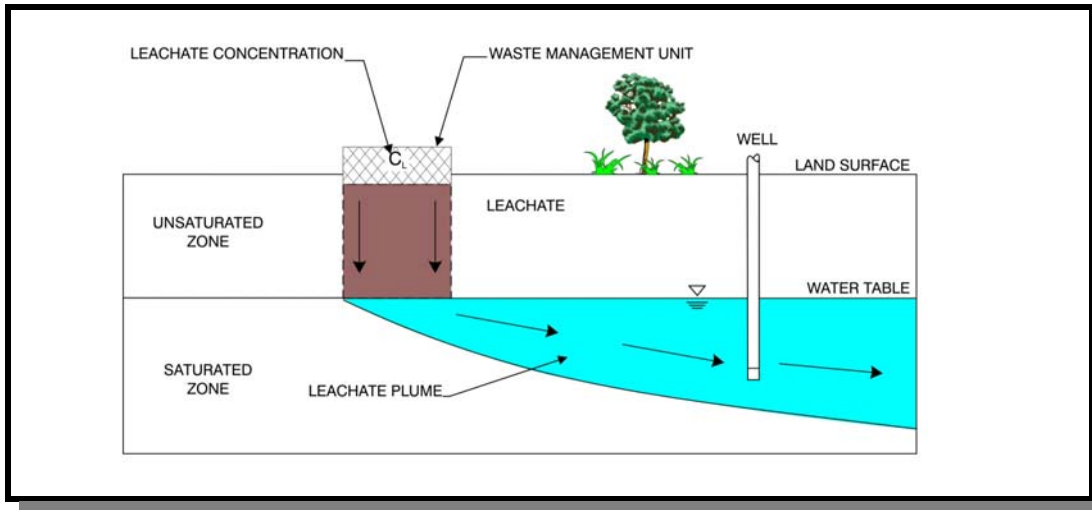
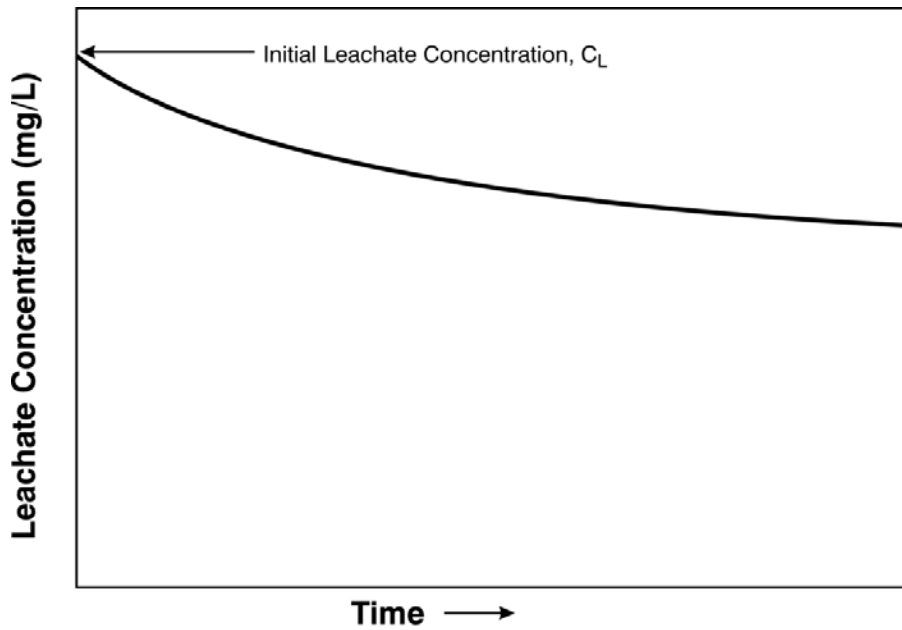


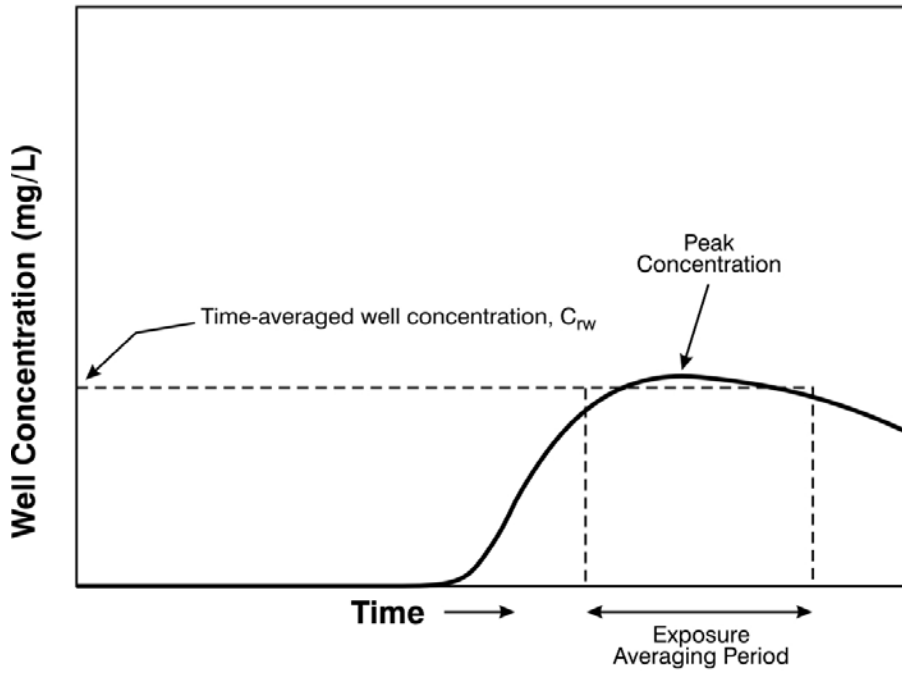
Figure 1.1 Conceptual Cross-Section View of the Subsurface System Simulated by EPACMTP.

The primary input to the model is the rate and the concentration of constituent release (leaching) from a WMU. The output from EPACMTP is a prediction of the constituent concentration arriving at a downgradient well. This can be either a steady-state concentration value, corresponding to a continuous-source scenario, or a time-dependent concentration, corresponding to a finite-source scenario. In the latter case, the model can calculate the peak concentration arriving at the well or a time-averaged concentration corresponding to a specified exposure duration (for example a 30-year average exposure time).

The relationship between the constituent concentration leaching from a WMU and the resulting ground-water exposure at a well located down-gradient from the WMU is depicted in Figure 1.2. This figure shows the time history of the leachate concentration emanating from a landfill-type WMU, and the corresponding time history (also called a *breakthrough curve*) of the concentration in ground water at a well, located downgradient from the WMU. The figure shows how the leachate concentration emanating from the landfill unit gradually diminishes over time as a result of depletion of the waste mass in the WMU. The constituent does not arrive at the well until some time after the leaching begins. The ground-water concentration



(a) Leachate Concentration Versus Time



(b) Groundwater Well Concentration Versus Time

Figure 1.2 (a) Leachate Concentration, and (b) Ground-water Exposure Concentration.

will reach a peak value at the well, and will eventually begin to diminish again because the leaching from the waste unit occurs only over a finite period of time. The maximum constituent concentration at the well will generally be lower than the original leachate concentration as a result of various dilution and attenuation processes which occur during its transport through the unsaturated and saturated zones. For risk assessment purposes, the concentration measure of interest is the magnitude of the ground-water concentration, averaged over some defined exposure period. EPACMTP has the capability to calculate the maximum average ground-water concentration, as depicted by the horizontal dashed line in Figure 1.2. C_{rw} in this figure represents the time-averaged well concentration that is used in risk evaluations.

EPACMTP consists of four major components:

- A source-term module that simulates the rate and concentration of leachate exiting from beneath a WMU and entering the unsaturated zone;
- An unsaturated-zone module which simulates one-dimensional vertical flow of water and dissolved constituent transport in the unsaturated zone;
- A saturated-zone module which simulates ground-water flow and dissolved constituent transport in the saturated zone.
- A Monte-Carlo module for randomly selecting input parameter values to account for variations in the model input, and determining the probability distributions of predicted ground-water concentrations.

1.2.1 Source-Term Module

In an EPACMTP ground-water flow and transport analysis, the source term describes the rate of leaching and the constituent concentration in the leachate as a function of time. The leachate concentration used in the model directly represents the concentration of the leachate released from the base of the WMU as a boundary condition for the fate and transport model.

The source term as conceptualized and modeled in EPACMTP contains a number of simplifications. The model does not attempt to account explicitly for the multitude of physical and biochemical processes inside the WMU that may control the release of waste constituents to the subsurface. Instead, the net result of these processes are used as inputs to the model. For instance, EPA uses the Hydrologic Evaluation of Landfill Performance (HELP) model (Schroeder et al., 1994a and 1994b) to determine infiltration rates for unlined, single lined, and composite-lined units externally to EPACMTP. The HELP-calculated infiltration rates are used as inputs to EPACMTP. Likewise, the model does not explicitly account for the complex physical, biological, and geochemical processes in the WMU that determines the resultant leachate concentration used as an input to EPACMTP. These processes

are typically estimated outside the EPACMTP model using geochemical modeling software, equilibrium partitioning models, or analytical procedures such as the Toxicity Characteristic Leaching Procedure (TCLP) or the Synthetic Precipitation Leaching Procedure (SPLP) test. Given the broad range of EPACMTP model applications, making these source-specific calculations outside the model maintains flexibility, and computational efficiency, as well as allows the EPACMTP analyses to be tailored to the requirements of a specific application.

The constituent source term for the EPACMTP fate and transport model is defined in terms of four primary parameters:

- 1) Area of the waste unit,
- 2) Leachate flux rate emanating from the waste unit (infiltration rate),
- 3) Constituent-specific leachate concentration, and
- 4) Leaching duration.

Leachate flux rate and leaching duration depend on both the design and operational characteristics of the WMU and the waste stream characteristics (waste quantities and waste constituent concentrations).

EPACMTP represents the leaching process in one of two ways: 1) The WMU is modeled as a depleting source; or 2) The WMU is modeled as a pulse source. In the depleting-source scenario, the WMU is considered permanent and leaching continues until all waste that is originally present has been depleted. In the pulse-source scenario, leaching occurs at a constant leachate concentration for a fixed period of time, after which leaching stops¹. EPACMTP uses the pulse source scenario to model temporary WMUs; usually the leaching period represents the operational life of the unit. Under clean closure conditions, the leaching stops when the unit is closed.

1.2.2 Unsaturated-Zone Module

The unsaturated-zone module of EPACMTP simulates vertical water flow and solute transport through the unsaturated zone between the base of the WMU and the water table of an unconfined aquifer. Constituents migrate downward from the disposal unit through the unsaturated zone to the water table. The general simulation scenario for which the module was designed is depicted schematically in Figure 1.1. This figure shows a vertical cross-section through the unsaturated zone underlying a WMU.

EPACMTP models flow in the unsaturated zone as a one-dimensional, vertically downward process. EPACMTP assumes the flow rate is steady-state, that is, it does not change with time. The flow rate is determined by the long-term average infiltration rate from the WMU.

¹ If the leaching period is set to a very large value, EPACMTP will simulate **continuous source** conditions.

Constituent transport in the unsaturated zone is assumed to occur by advection and dispersion². Advection refers to transport along with ground-water flow. Hydrodynamic dispersion is caused by local variations in ground-water flow and acts as a mixing mechanism, which causes the constituent plume to spread, but also be diluted.

The unsaturated zone is assumed to be initially constituent-free and constituents migrate vertically downward from the WMU. EPACMTP can simulate both steady-state and transient contaminant transport in the unsaturated zone with single-species or multiple-species chain decay reactions. Steady-state refers to situations in which the release of constituents from a WMU occurs at a constant rate for a very long period of time, so that eventually constituent concentrations in the subsurface reach a constant level. In a transient (or time-dependent) analysis, the constituent concentration in the subsurface may not reach steady-state and therefore, the constituent fate and transport processes are simulated as a function of time.

1.2.3 Saturated-Zone Module

The saturated-zone module of EPACMTP is designed to simulate flow and transport in an idealized aquifer with uniform saturated thickness (see Figure 1.1). The module simulates regional flow in a horizontal direction with recharge and infiltration from the overlying unsaturated zone and WMU. The lower boundary of the aquifer is assumed to be impermeable. The aquifer is assumed to be initially constituent-free, and constituents enter the saturated zone only from the overlying unsaturated zone directly underneath the waste disposal facility.

EPACMTP assumes that flow in the saturated zone is steady-state. In other words, EPACMTP models long-term average flow conditions. EPACMTP accounts for different recharge rates beneath and outside the source area. Ground-water mounding beneath the source is represented in the flow system by increased head values at the top of the aquifer. It is important to realize that while EPACMTP calculates the degree of ground-water mounding that may occur underneath a WMU due to high infiltration rates, and will restrict the allowable infiltration rate to prevent physically unrealistic input parameter combinations, the actual saturated-zone flow and transport modules in EPACMTP are based on the assumption of a constant saturated thickness. That is, the water table position is assumed to be fixed, and the only direct effect of ground-water mounding is to increase simulated ground-water velocities.

EPACMTP simulates the transport of dissolved constituents in the saturated zone using the advection-dispersion equation. Advection refers to transport along with ground-water flow. Dispersion encompasses the effects of both hydrodynamic dispersion and molecular diffusion. Both act as mixing mechanisms which cause a

² In the case of metals which are subject to nonlinear sorption, EPACMTP uses a method-of-characteristics solution method that does not include dispersion. In these case, transport is dominated by the nonlinear sorption behavior and dispersion effects are considered minor.

constituent plume to spread, but also be diluted. Hydrodynamic dispersion is caused by local variations in ground-water flow and is usually a significant plume-spreading mechanism in the saturated zone. Molecular diffusion on the other hand is usually a very minor mechanism, except when ground-water flow rates are very low. The saturated-zone transport simulation also accounts for first-order transformation reactions in both the aqueous and sorbed phases, and retardation due to linear equilibrium sorption of constituents onto aquifer particles.

1.2.4 Monte-Carlo Module

The final component of EPACMTP is a Monte-Carlo module which allows the model to perform probabilistic analyses of constituent fate and transport in the subsurface. Monte-Carlo simulation is a statistical technique by which a quantity is calculated repeatedly, using randomly selected model input parameter values for each calculation. The results approximate the full range of possible outcomes, and the likelihood of each. In particular, EPA uses Monte-Carlo simulation to determine the likelihood, or probability, that the concentration of a constituent at the receptor well, and hence exposure and risk, will be either above or below a certain value.

EPACMTP requires values for the various source-specific, chemical-specific, unsaturated-zone-specific and saturated-zone-specific model parameters to determine well concentrations. For many assessments it is not appropriate to assign single values to all of these parameters. Rather, the values are represented as a probability distribution, reflecting both the range of variation that may be encountered at different waste sites, as well as the uncertainty about site-specific conditions. Thus, the fate and transport simulation modules in EPACMTP are linked to a Monte-Carlo module to allow quantitative estimation of the probability that the receptor well concentration will be below a threshold value, due to variability and uncertainty in the model input parameters.

Variability describes parameters whose values are not constant, but which we can measure and characterize with relative precision in terms of a frequency distribution. Uncertainty pertains to parameters whose values or distributions we know only approximately. An example of variability is a distribution of body weights of the human population across the nation. Body weight data are abundant and measurement errors are considered insignificant. The distribution of body weights based on a large volume of data may be regarded as variable but not uncertain. A distribution of hydraulic conductivity values for a heterogenous aquifer may be regarded as variable and uncertain. Variability is due to the fact that hydraulic conductivity values are spatially varied. Uncertainty of the distribution may be attributed to, at least, measurement and analysis errors, and sampling errors. In practice, we normally use probability distributions to describe variability which may also be associated with uncertainty. In the EPACMTP Monte-Carlo module, parameter distributions include both variability and uncertainty of parameter data. The combined entities are not separated nor distinguished by the module.

The Monte-Carlo module requires that for each input parameter, except constant parameters, a probability distribution be provided. The method involves the repeated

generation of pseudo-random values of the input variables (drawn from the known distribution and within the range of any imposed bounds). The EPACMTP model is executed for each set of randomly generated model parameters and the corresponding ground-water well exposure concentration is computed and stored. Each simulation of a site by the model based on a set of input parameter values is termed a **realization**. The simulation process is repeated by generating additional realizations.

At the conclusion of the Monte-Carlo simulation, the realizations are statistically analyzed to yield a cumulative distribution function (CDF), a probability distribution of the ground-water well exposure concentration. The construction of the CDF simply involves sorting the ground-water well concentration values calculated in each of the individual Monte-Carlo realizations from low to high. The well concentration values simulated in the EPACMTP Monte-Carlo process range from very low values to values that approach the original leachate concentration. By examining how many of the total number of Monte-Carlo realizations resulted in a high value of the predicted ground-water concentration, it is possible to assign a probability to these high-end events, or conversely determine what is the expected ground-water concentration level corresponding to a specific probability of occurrence.

1.3 EPACMTP ASSUMPTIONS AND LIMITATIONS

EPA designed EPACMTP to be used for regulatory assessments in a probabilistic framework. The simulation algorithms that are incorporated into the model are intended to meet the following requirements:

- Account for the primary physical and chemical processes that affect constituent fate and transport in the unsaturated and saturated zones;
- Be useable with relatively little site input data; and
- Be computationally efficient for Monte-Carlo analyses.

This section discusses the primary assumptions and limitations of EPACMTP that EPA made in developing the model to balance the competing requirements. EPACMTP may not be suitable for all sites, and the user should understand the capabilities and limitations of the model to ensure it is used appropriately.

Source-Term Module

The EPACMTP source-term module provides a relatively simple representation of different types of WMUs. EPACMTP does not simulate the fate and transport of chemical constituents within a WMU. WMUs are represented in terms of a source area, and a defined rate and duration of leaching. EPACMTP only accounts for the release of leachate through the base of the WMU, and assumes that the only mechanism of constituent release is through dissolution of waste constituents in the water that percolates through the WMU. In the case of surface impoundments EPACMTP assumes that the leachate concentration is the same as the constituent

concentration in the waste water in the surface impoundment. EPACMTP does not account for the presence of non-aqueous free-phase liquids, such as an oily phase that might provide an additional release mechanism into the subsurface. EPACMTP does not account for releases from the WMU via other environmental pathways, such as volatilization or surface run-off. EPACMTP assumes that the rate of infiltration through the WMU is constant, representing long-term average conditions. EPACMTP does not account for fluctuations in rainfall rate, or degradation of liner systems that may cause the rate of infiltration and release of leachate to vary over time.

Unsaturated-Zone and Saturated-Zone Modules

EPACMTP simulates the unsaturated zone and saturated zone as separate domains that are connected at the water table. Both the unsaturated zone and the saturated zone are assumed to be uniform porous media. The thickness of the saturated zone is uniform in space and constant in time. EPACMTP does not account for the presence of macro-pores, fractures, solution features, faults or other heterogeneities in the soil or aquifer that may provide pathways for rapid or retarded movement of constituents. EPACMTP may not be appropriate for sites overlying fractured or very heterogeneous aquifers.

EPACMTP is designed for relatively simple ground-water flow systems in which flow is predominantly horizontal along the regional gradient direction. Flow in the saturated zone is assumed to be driven by long-term average infiltration and recharge; EPACMTP treats flow in the unsaturated zone as steady-state and does not account for fluctuations in the infiltration or recharge rate. The rate of ambient recharge outside of the WMU is assumed to be uniform and constant over time. With this assumption, EPACMTP is appropriate for the simulation of long-term flow and transport at sites where the general flow direction does not change over time, and where the long-term average saturated thickness is relatively constant. EPACMTP does not account for the presence of major ground-water sources or sinks such as surface water bodies or large municipal pumping or injection wells. Therefore, use of EPACMTP may not be appropriate at sites with these or any other features which significantly modify regional flow fields, or at sites where the recharge varies locally.

EPACMTP models ground-water flow based on the assumption that the contribution of recharge and infiltration from the unsaturated zone are small relative to the regional ground-water flow, and that the rise of water table elevation due to infiltration and recharge is small compared with the initial saturated thickness. The implication is that the saturated zone can be modeled as having a thickness unaffected by infiltration and recharge and constant in time, with mounding underneath the WMU represented by an increased head distribution along the water table. The foregoing assumption allows EPACMTP to approximate an unconfined aquifer by an equivalent confined aquifer with constant and uniform thickness. The major benefit of this approximation is that the flow equation becomes linear and the computational effort for its solution is significantly less (by a factor of 10 or 20) than that for the truly unconfined scenario. With this approximation, the general flow

characteristics are preserved in terms of general flow direction and velocity distribution. However, as stated earlier, with the confined approximation, EPACMTP does not account for the actual physical increase in saturated thickness, thereby tending to overestimate ground-water velocities at downgradient locations. The overestimation of velocity usually results in conservative estimates of constituents' arrival times and peak concentrations. The assumption of constant and uniform saturated-zone thickness means that EPACMTP may not be suitable at sites with a highly variable thickness of the water-bearing zone. Similar to the source module, the unsaturated-zone and saturated-zone modules do not account for free-phase flow conditions of an oily, non-aqueous phase liquid, and vapor-phase transport of volatile organic chemicals.

The unsaturated-zone and saturated-zone modules of EPACMTP account for constituent fate and transport by advection, hydrodynamic dispersion, molecular diffusion, sorption and first-order transformation. However, EPACMTP does not account for matrix-diffusion processes, which may occur when the aquifer formation comprises zones with large contrasts in permeability. In these situations, transport occurs primarily in the more permeable zones, but constituents can move into and out of the low permeability zones by diffusion. Lateral diffusion is assumed very small, compared with advection and hydrodynamic dispersion.

Leachate constituents can be subject to complex biological and geochemical interactions in soil and ground water. EPACMTP treats these interactions as equilibrium sorption and first-order degradation processes. In the case of sorption processes, the equilibrium assumption means that the sorption process occurs instantaneously, or at least very quickly relative to the time-scale of constituent transport. Although sorption, or the attachment of leachate constituents to solid soil or aquifer particles may result from multiple chemical processes, EPACMTP lumps these processes together into an effective soil-water partition coefficient.

For organic constituents, EPACMTP assumes that the partition coefficient is constant, and equal to the product of the mass fraction of organic carbon in the soil or aquifer, and a constituent-specific organic carbon partition coefficient. This relationship should be used when the mass fraction of organic carbon is greater than 0.001, otherwise sorption of the organic constituents on non-organic solids can become significant. A majority of soils and aquifer materials across the U. S. have a mass fraction of organic carbon larger than 0.001 (Carsel et al., 1988). In addition, the partition coefficient of a constituent remains relatively constant when the aqueous concentration of the constituent remains below one half of its solubility limit (de Marsily, 1986).

For metals, EPACMTP allows the partition coefficient to vary as a function of a number of primary geochemical parameters, including pH, leachate organic matter, soil organic matter, and the fraction of iron-oxide in the soil or aquifer (see Section 3.3.3.2 in The EPACMTP Parameters/Data Background Document (U.S. EPA, 2003)). EPACMTP uses a set of effective sorption isotherms which were developed by EPA by running the MINTEQA2 geochemical speciation model for each metal and combination of geochemical parameters. In modeling metals transport in the unsaturated zone, EPACMTP uses the complete, nonlinear sorption isotherms. In

modeling metals transport in the saturated zone, EPACMTP uses linearized MINTEQA2 isotherms, based on the assumption that after dilution of the leachate plume in ground water, concentration values of metals will typically be in a range where the isotherm is approximately linear. This assumption may not be valid when metals concentrations in the leachate are high. Although EPACMTP is able to account for the effect of the geochemical environment at a site on the mobility of metals, the model assumes that the geochemical environment at a site is constant and not affected by the presence of the leachate plume. In reality, the presence of a leachate plume may alter the ambient geochemical environment locally.

EPACMTP does not account for colloidal transport or other forms of facilitated transport. For metals and other constituents that tend to strongly sorb to soil particles, and which EPACMTP will simulate as relatively immobile, movement as colloidal particles can be a significant transport mechanism. It is possible to approximate the effect of these transport processes by using a lower value of the partition coefficient as a user-input.

EPACMTP accounts for biological and chemical transformation processes as first-order degradation reactions. That is, it assumes that the transformation process can be described in terms of a constituent-specific half-life. EPACMTP allows the degradation rate to have different values in the unsaturated zone and the saturated zone, but the model assumes that the value is uniform throughout each zone for each constituent. EPA's ground-water modeling database includes constituent-specific hydrolysis rate coefficients for constituents that are subject to hydrolysis transformation reactions; for these constituents, EPACMTP simulates transformation reactions subject to site-specific values of pH and soil and ground-water temperature, but other types of transformation processes are not explicitly simulated in EPACMTP.

For many organic constituents, biodegradation can be an important fate mechanism, but EPACMTP has only limited ability to account for this process. The user must provide an appropriate value for the effective first-order degradation rate. In an actual leachate plume, biodegradation rates may be different in different regions in the plume; for instance in portions of the plume that are anaerobic some constituents may biodegrade more readily, while other constituents will biodegrade only in the aerobic fringe of the plume. EPACMTP does not account for these processes that may cause a constituent's rate of transformation to vary in space and time.

Monte-Carlo Module

The Monte-Carlo module of EPACMTP allows you to take into account the effects of parameter distributions on predicted ground-water concentrations. The validity of the resulting probability distribution of outcomes is based on assumptions that the models of the flow and transport processes can accurately capture the salient flow and transport characteristics in the field and that the distributions of parameters are accurate. The resulting probability distribution is also subject to uncertainties associated with sampling errors (due to the fact that a small sample is used to

represent the whole data population), model errors (because the flow and transport models are approximations of the actual flow and transport processes), measurement errors of parameters, and possible misspecification of parameter distributions. Because the Monte-Carlo module in EPACMTP Version 2 is based on a single-stage Monte-Carlo methodology, the confidence interval of a given percentile of the resulting probability distributions cannot be ascertained.

In addition, EPACMTP can account only for intersite variability of flow and transport properties. Intrasite variability of properties (heterogeneity within the site) is not included as part of the analysis. As a result, EPACMTP does not account for uncertainty arising from treating each site as a homogeneous site with uniform flow and transport properties.

This page was intentionally left blank.

2.0 SOURCE-TERM MODULE

The source-term module simulates the rate of water leakage from a waste management unit (WMU) into the underlying unsaturated (or vadose) zone, and the concentration(s) of dissolved constituent(s) in the leachate. In EPACMTP, the rate of water leakage is called the *infiltration rate*, and the concentration of a constituent in the infiltrating water is called the *leachate* concentration.

The EPACMTP source-term module can simulate various types of WMUs. The module is not designed to model the multitude of physical and bio-chemical processes that result in leachate generation inside a WMU in detail. Rather, this module is designed to capture significant and salient physical and biochemical processes within a WMU. However, if processes not included in the current source-term module are required, the simulation of the source-term processes should be carried out externally to EPACMTP. The EPACMTP source-term module can accommodate output from external process models to represent relevant processes in more detail. An example of such an external model is the HELP model (Hydraulic Evaluation of Landfill Performance; Schroeder et al., 1994a and 1994b) which predicts infiltration through landfill units as a function of unit design and climate characteristics.

This section is organized as follows:

- Section 2.1 discusses the purpose of the source-term module and describes the difference between a continuous and finite source;
- Section 2.2 discusses how the source-term module is implemented for four different types of WMUs - landfills, surface impoundments, land application units, and waste piles.

2.1 PURPOSE OF THE SOURCE-TERM MODULE

The release of contaminants into the subsurface constitutes the source term for the ground-water fate and transport model. In an EPACMTP modeling analysis, the source term can be characterized as either a continuous source or a finite source. A continuous source simply means that leachate is generated at a constant rate and with constant leachate concentration, without a cut-off time. A continuous source scenario conceptually represents an inexhaustible supply of leachate. The continuous source is the simplest and the most protective, but may not be realistic in many cases. For this reason, the finite source option is available. In the finite source scenario, release of leachate occurs over only a finite period of time, as controlled by the operational life of a WMU or the gradual depletion of the waste constituent mass in the WMU.

EPACMTP defines the source term for the subsurface fate and transport model in terms of four primary parameters:

- (1) Area of the waste unit,
- (2) Leachate flux rate emanating from the waste unit (infiltration rate),

- (3) Constituent-specific leachate concentration, and
- (4) Duration of the constituent leaching.

The infiltration rate and leaching duration are a function of both the design and operational characteristics of the waste management unit and the waste stream characteristics (waste quantities and waste constituent concentrations). EPACMTP assumes that the leachate concentration is a characteristic of a particular waste and constituent. The source-term module does not account for constituent losses from the WMU via processes other than leaching. Such other loss mechanisms can include volatilization, surface run-off, and bio-chemical transformation reactions. Not accounting for these processes means that the modeled leaching will generally maximize leaching concentrations.

2.1.1 Continuous Source

In the continuous source scenario, the constituent concentration in the leachate remains constant over time. Under these conditions, the ground-water concentration at the modeled receptor well location will also eventually reach a constant value. We refer to this well concentration as the steady-state concentration level. The steady-state concentration value is the theoretical maximum ground-water well concentration that can be achieved for a given value of the leachate concentration.

While true steady-state conditions are unlikely to be achieved at actual waste sites, a WMU which releases leachate at a more or less constant rate and concentration over a long period of time, may cause the ground-water well concentrations to approach or reach this steady-state level. For a given waste management scenario, EPACMTP can calculate the steady-state ground-water well concentration much more quickly than it can calculate the ground-water concentration values for finite source conditions.

The continuous source scenario in EPACMTP is therefore useful for screening purposes and to ensure a protective analysis. If the ground-water concentrations predicted by EPACMTP under continuous source (steady-state) conditions remain below appropriate regulatory or health-based levels, the user has assurance that these levels will not be exceeded under more realistic finite source conditions. A continuous source analysis may also be appropriate when it is desirable to ensure a protective evaluation of potential ground-water exposures.

2.1.2 Finite Source

In EPACMTP, the finite source scenario refers to the situation in which a constituent's leachate concentration is a function of time. Specifically, under finite-source conditions the constituent is present in the leachate for a finite period of time. EPACMTP version 2.0 can model two basic types of finite source conditions. The first is a pulse source in which the leachate concentration is constant over a prescribed period of time (t_p) and then goes to zero. The second scenario is in which the leachate concentration diminishes gradually to reflect depletion of the contaminant mass in the waste unit. The two scenarios are depicted graphically in Figure 2.1.

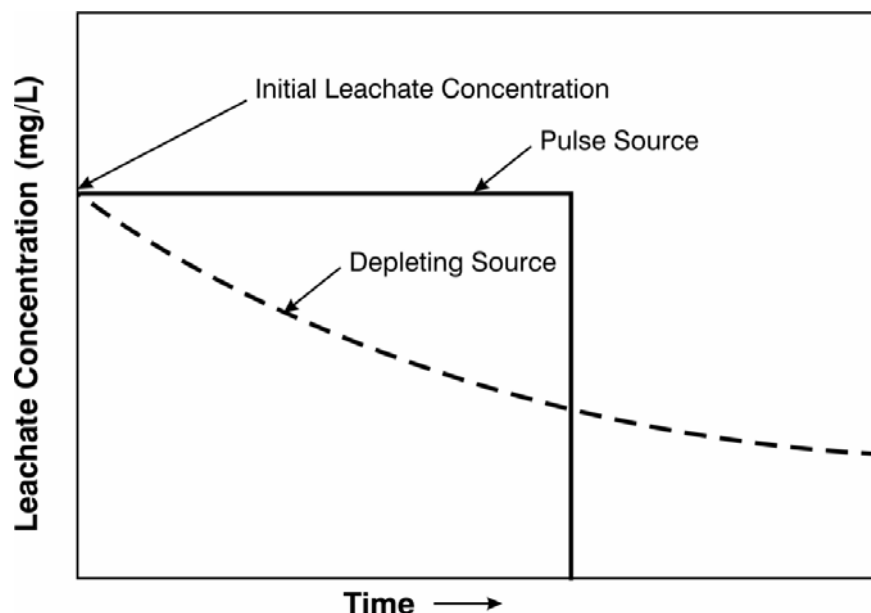


Figure 2.1 Leachate Concentration Versus Time for Pulse Source and Depleting Source Conditions.

The pulse source scenario is most appropriate for WMUs which operate for a prescribed period of time, followed by clean closure. Examples include waste piles, surface impoundments and land application units where the leaching occurs during the active life of the unit. During this period, continual addition of “fresh” waste will serve to keep the leachate concentration at a more or less constant value. If the user specifies a very long value for the pulse duration, t_p , then the pulse source scenario becomes equivalent to a continuous source.

The depleting source scenario is most appropriate for a landfill waste management scenario, where the waste accumulates during the active life of the unit, but leaching may continue for a long period of time after the unit is closed.

The finite source module in EPACMTP version 2.0 has the following restrictions:

- The module does not account for situations in which the leachate concentration increases with time; it can only handle scenarios with a constant concentration pulse or scenarios with a depleting source.
- The depleting source option for landfills cannot be used to model metals that have non-linear sorption isotherms; for these constituents, the pulse source must be used. In other words, the depleting source option for landfills can only be used for organic constituents. To model a metal constituent, the depletion of the source is approximated or linearized using a linear sorption isotherm, or a single value of K_w (waste-concentration-to-leachate-concentration ratio).

2.2 IMPLEMENTATION FOR DIFFERENT WASTE UNITS

EPACMTP can perform Monte-Carlo or deterministic analyses for four different types of waste management units:

- Landfills,
- Surface impoundments,
- Waste piles, and
- Land application units.

Figure 2.2 shows a schematic, cross-sectional view of the four types of waste units. In EPACMTP, each type of waste management unit is described by a relatively small number of parameters. The differences between waste units are generally represented by different values or frequency distributions of these source-specific parameters. Source-specific parameters that are used by EPACMTP include:

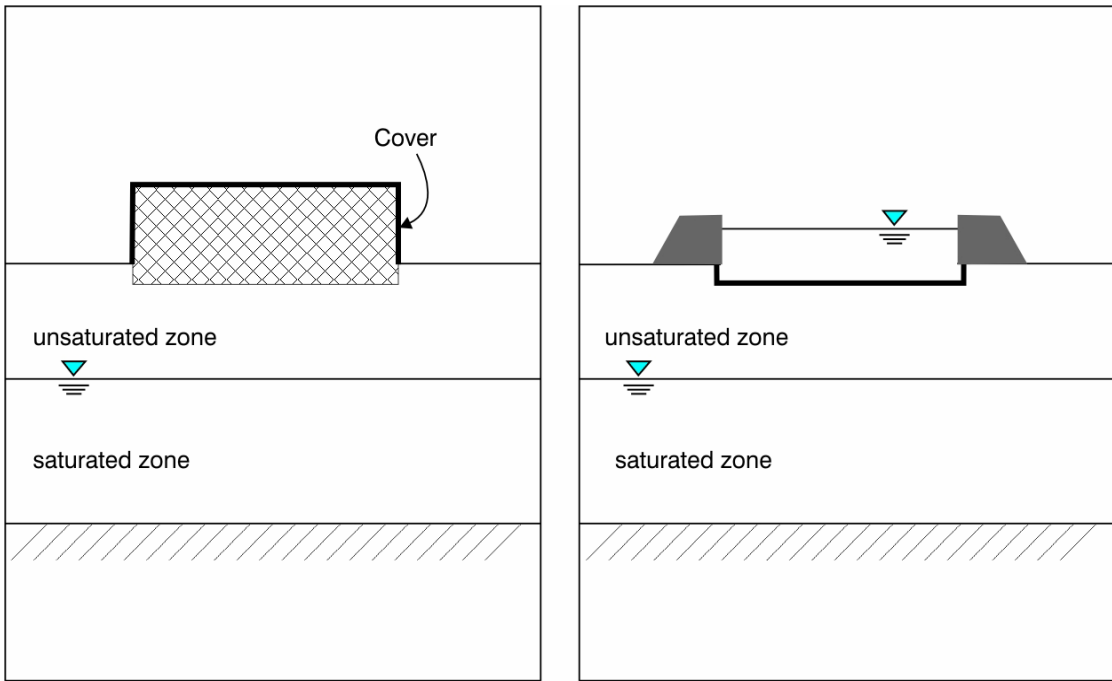
- Dimensions of the waste unit, i.e., area and depth, as well as depth of the base of the unit below grade;
- Amount of waste in the WMU, as given by an average annual waste addition rate and number of years of operation, or fraction of the WMU that is dedicated to a particular waste;
- Infiltration (or leakage rate) of water through the unit;
- Type of source condition (continuous, or finite source)
- If finite source, constituent concentration in the leachate when leaching begins, and either duration of the leachate pulse, or amount of waste in the unit when leaching begins, density of the waste, and concentration of the chemical constituent in the waste.

The four types of waste management units and the source-specific input parameters used to conceptualize and model each type of unit are discussed in the following sections.

2.2.1 Landfills

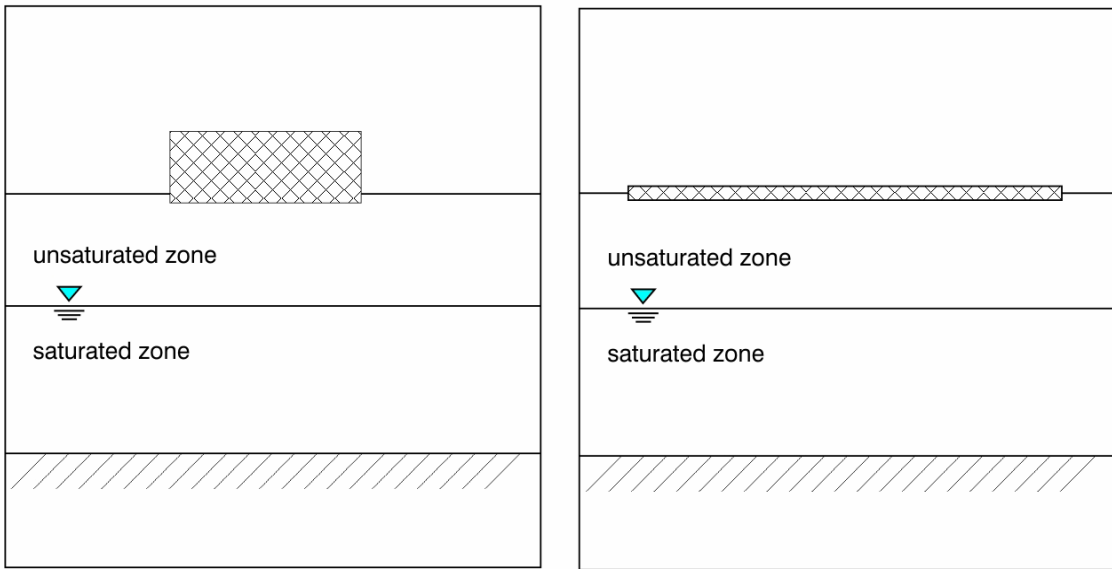
2.2.1.1 Assumptions for the Landfill Source Module

The landfill is modeled as a permanent waste management unit, with a rectangular footprint and a uniform depth. In EPACMTP version 2.0, only square footprints are allowed. The landfill is filled with waste during the unit's operational life. Upon closure of the landfill, the waste is left in place, and a final soil cover is installed. The starting point for the EPACMTP simulation is at the time when the landfill is closed, i.e., the unit is at its maximum capacity. EPACMTP does not implicitly simulate any loss process that may occur during the unit's active life, e.g., due to leaching, volatilization, runoff on erosion, or biochemical degradation. If these losses are considered to be significant they can be taken into account by subtracting the



(A) LANDFILL

(B) IMPOUNDMENT



(C) WASTE PILE

(D) LAND APPLICATION UNIT

Figure 2.2 WMU Types Modeled in EPACMTP.

cumulative amount of contaminant mass loss that occurred during the unit's active life, from the amount of contaminant mass that is present at the time of landfill closure.

Leaching of contaminant(s) from the landfill into the subsurface is the result of dissolution as partitioning of constituent(s) from the waste into water that percolates (infiltrates) downward through the landfill unit. EPACMTP assumes that this process is driven by natural precipitation. Because of the long term nature of the ground-water pathway analysis, EPACMTP assumes a steady-state infiltration rate which is equal to the long-term average annual rate. The value of the infiltration rate is a user-input. However, EPACMTP provides a database of nationwide infiltration rates generated with the HELP model (Hydrologic Evaluation of Landfill Performance), using climatic data from climate stations throughout the United States (see the *EPACMTP Parameters/Data Background Document*, U.S. EPA, 2003). The HELP-generated infiltration rates are based on an assumption that each landfill is covered by 2 feet of soil, and does not have a liner or leachate collection system.

2.2.1.2 List of Parameters for the Landfill Source Module

The source-specific input parameters for the landfill scenario include parameters to determine the amount of waste disposed in the landfill, the infiltration and recharge rates, the initial waste and leachate concentrations, and the source leaching duration. Together these parameters are used to determine how much contaminant mass enters the subsurface and over what time period. The source-specific parameters for the landfill scenario are presented in Table 2.1 and are described in the following sections.

EPACMTP allows the user to specify the amount of waste that is placed in the landfill in two different ways. The first is to specify the duration of the unit's active life and the average annual quantity of waste. The second is to provide the dimensions (area and depth) of the landfill and the fraction of the landfill volume that is occupied by the waste of concern. EPACMTP then calculates the actual amount of waste. In the former case, EPACMTP will check that the cumulative waste amount, as determined by multiplying the number of years of operation by the average annual waste quantity, does not exceed the capacity of the landfill.

2.2.1.2.1 *Landfill Area*

The landfill area is defined as the square footprint of the landfill. The length and width of the landfill are each calculated as the square root of the area. The landfill area is used to determine the area over which the infiltration rate is applied and is one of several parameters used to calculate the contaminant mass within the landfill for the landfill depleting source option.

2.2.1.2.2 *Landfill Depth*

The landfill depth is defined as the average depth of the landfill, from top to bottom; the thickness of the cover soil is assumed to be insignificant. The landfill depth is measured from the top to the base of the unit, irrespective of where the ground

Table 2.1 Source-Specific Variables for Landfills

| Parameter | Symbol | Units | Section in EPACMTP Parameters/Data Background Document |
|--|-------------|---|--|
| Waste Site Area: the footprint of the square landfill (Section 2.2.1.2.1) | A_w | m ² | 2.3.1 |
| Landfill Depth: the average depth of the landfill, from top to bottom (Section 2.2.1.2.2) | D_{LF} | m | 2.3.2 |
| Depth Below Grade: the depth of the bottom of the landfill below the surrounding ground surface (Section 2.2.1.2.3) | d_{BG} | m | 2.3.3 |
| Waste Fraction: the fraction of the landfill volume that is occupied by the waste of concern when the landfill is closed (Section 2.2.1.2.4) | F_h | unitless | 2.3.4 |
| Waste Density: the average bulk density of the waste of concern (Section 2.2.1.2.5) | ρ_{hw} | g/cm ³ | 3.2.1 |
| Areal Recharge Rate: water percolating through the soil to the aquifer outside of the footprint of the WMU (Section 2.2.1.2.6) | I_R | m ³ /m ² /y or m/y | 4.4 |
| Areal Infiltration Rate: water percolating through a WMU to the underlying soil (Section 2.2.1.2.6) | I | m ³ /m ² /y or m/y | 4.3.1 |
| Leachate Concentration: the concentration of a constituent in the leachate emanating from the base of the waste management unit (Section 2.2.1.2.7) | C_L | mg/L | 3.2.3 |
| Waste Concentration: the total concentration of constituent in the waste which may eventually leach out (Section 2.2.1.2.8) | C_w | mg/kg | 3.2.2 |
| Waste-Concentration-to-Leachate Concentration Ratio: the ratio of the waste concentration (C_w) to the leachate concentration (C_L) (Section 2.2.1.2.9) | K_w | L/kg | 3.2.2 and 3.2.3 |
| Source Leaching Duration: the duration of the leachate release period (Section 2.2.1.2.10) | t_p | y | 2.3.6 |

Note: A_w and D_{LF} are used to calculate landfill capacity. However, if the landfill is not used to its capacity, other methods of calculating waste volume must be employed. See Section 2.2.1.3.2.

surface is. The landfill depth is one of several parameters used to calculate the contaminant mass within the landfill for the landfill depleting source option.

2.2.1.2.3 Depth Below Grade

The depth below grade is defined as the depth of the bottom of the landfill below the surrounding ground surface. If a non-zero value is entered for this input, then the thickness of the unsaturated zone beneath the landfill is adjusted accordingly.

2.2.1.2.4 Waste Fraction

The waste fraction is defined as the volume fraction of the landfill that is occupied by the waste of concern when the landfill is closed. This value can range from a very small value to 1.0; the value of 1.0 is the most conservative value and means that the entire landfill is filled with leachate forming waste. In most applications of EPACMTP, the analysis is performed for specific waste. The situation of a waste fraction equal to 1.0, is therefore equivalent to a monofill scenario. The waste fraction is one of several parameters used to calculate the contaminant mass within the landfill; the contaminant mass is an important input for the landfill depleting source option.

2.2.1.2.5 Waste Density

The waste density is defined as the average bulk density of the waste, i.e., mass of waste per unit volume (kg/L or g/cm³) containing the constituent(s) of concern and should be measured on the waste as disposed, as opposed to a dry bulk density. The waste density is used to convert the waste volume to an equivalent mass of waste or vice-versa.

2.2.1.2.6 Areal Recharge and Infiltration Rates

The EPACMTP model requires input of the net areal rate of vertical downward percolation of water and leachate through the unsaturated zone to the water table. Infiltration is defined as water percolating through a WMU to the underlying soil, while recharge is water percolating through the soil to the aquifer outside of the footprint of the WMU. The model allows the infiltration rate to be different from the regional recharge rate. The landfill infiltration rate can be different from the recharge rate for a variety of reasons, including the engineering design of the landfill (for instance, a soil tighter than the local soil being used for the final cover), topography, land use, and vegetation. The recharge rate is determined by regional climatic conditions, such as precipitation, evapotranspiration, and surface run-off, and regional soil type.

Infiltration and recharge rates for selected soil types at cities around the country have been estimated using the HELP water-balance model and are incorporated into a database included in one of the EPACMTP input files. Further details about how these rates were determined and other options for determining recharge and infiltration rates outside of the EPACMTP model can be found in Section 4.0 of the *EPACMTP Parameters/Data Background Document* (U.S. EPA, 2003).

2.2.1.2.7 Leachate Concentration

The leachate concentration (C_L , mg/L) used in the model represents the concentration of the leachate emanating from the base of the waste management unit. This parameter provides the boundary condition for the EPACMTP simulation of constituent fate and transport through the unsaturated and saturated zones. Consistent with the continuous and finite source options of EPACMTP, the model will treat the leachate concentration as either a constant value, or as a parameter that can change with time.

In the finite source option, the simplest and generally most protective case is to assign the leachate concentration a constant value until all of the initially present contaminant mass has leached out of the disposal unit. After this time, the leachate concentration is zero. This case is referred to as the pulse source scenario. The boundary condition for the fate and transport model then becomes a constant concentration pulse, with defined duration. Alternatively, EPACMTP can simulate conditions in which the value of the leachate concentration diminishes gradually over time. In other words, as the waste in the landfill is depleted, the value of the leachate concentration also goes down. When using this depleting source option, the user specifies the initial leaching concentration, and the model automatically adjusts this rate over time as explained below in Section 2.2.1.3.3. As stated in Section 2.1.2, for constituents with non-linear isotherms, the depleting source scenario is applicable only when the isotherms are linearized by making the distribution coefficient (K_d) constant.

2.2.1.2.8 Waste Concentration

The waste concentration (C_w , mg/kg), represents the total mass fraction of constituent in the waste which may eventually leach out. Therefore, in the context of the finite source methodology, C_w is the total leachable waste concentration. From a practical perspective it is important to know how this property will be measured for actual waste samples. There are established procedures to measure the leachate concentration C_L , but these methods may not measure the “leachable” waste concentration very precisely. Thus, C_w may be interpreted to represent the total waste concentration and measured accordingly. This approach will be protective because the measured total waste concentration should always be at least as high as the potentially more difficult to quantify “leachable” waste concentration.

The waste concentration used by EPACMTP reflects the average concentration of the constituent(s) of concern in the waste in the landfill at the time of closure. Contaminant losses that may occur during the WMU's active life are not explicitly modeled in EPACMTP. If such losses are significant, it may be appropriate to adjust the waste concentration value that is entered into EPACMTP, to represent the constituent concentration that remains, and is available for leaching. Ignoring these other loss pathways will be protective for the ground-water pathway analysis.

2.2.1.2.9 Waste-Concentration-to-Leachate-Concentration Ratio

For the landfill waste management scenario in which leaching continues until the source is depleted (depleting source option), the duration of the leaching period is dependent on both the waste concentration (C_w) and the leachate concentration (C_L). The EPACMTP model uses these concentrations in terms of the ratio of waste concentration to leachate concentration, or C_w/C_L .

The waste-to-leachate ratio can be thought of as a type of partition coefficient or as a measure of the relative leachability of waste constituents. In general, a relatively high value of this parameter means that the waste leaches slowly from the unit, resulting in a source with a long duration. Conversely, a relatively low value means that the waste can be rapidly leached to the subsurface.

In applications that involve back-calculating threshold waste and/or leachate concentrations that satisfy regulatory or risk-based ground-water thresholds, it is convenient for the user to provide the EPACMTP input in terms of a ratio of waste-to-leachate concentrations rather than as individual waste concentration and leachate concentration values.

2.2.1.2.10 Source Leaching Duration

In finite source analyses with a pulse-type source, the user must specify the duration of the leaching period (t_p) in years. If leaching is modeled with the depleting source option, EPACMTP will internally calculate the leachate concentration as a function of time, as well as the leaching period.

2.2.1.2.11 Waste Volume

The waste volume is defined as the volume of the waste of interest (at landfill closure) contributed to the landfill. EPACMTP uses the waste volume to calculate the contaminant mass within the landfill for the landfill depleting source option (see Section 2.2.1.3.3).

For waste-stream-specific applications of EPACMTP, the total waste volume to be input to EPACMTP can be calculated by multiplying the annual waste volume by the number of years of landfill operation. If the annual waste amount is given as a mass value (e.g., tons/year), it should be divided by the waste density in order to yield the value as a volume (m^3). The user should ensure that the modeled waste volume does not exceed the total landfill capacity.

For nationwide risk assessments, a distribution of values can be used for the waste volume by entering the waste volume as a fraction of the entire landfill volume (see Section 2.2.1.2.4). If the landfill volume and the waste volume are treated as random parameters, specifying the waste volume in terms of a waste fraction ensures that the modeled waste volume can never exceed the modeled landfill capacity.

2.2.1.3 Mathematical Formulation of the Landfill Source Module

The mathematical formulation of the landfill source module is presented below.

2.2.1.3.1 *Continuous Source Scenario*

In the continuous (infinite) source scenario, the leachate concentration is simply set to a constant value with no time cut-off. The continuous source scenario represents the most protective leaching assumption, namely that there is an infinite supply of waste in the landfill. In this case, the leachate concentration at any time t is given by

$$C_L(t) = C_L^0 \quad (2.1)$$

where

| | | |
|---------|---|---|
| C_L | = | leachate concentration (mg/L) |
| t | = | time since leaching began at landfill closure (y) |
| C_L^0 | = | initial leachate concentration at the time of landfill closure (mg/L) |

2.2.1.3.2 *Pulse Source Scenario*

In the pulse source scenario the leachate concentration is constant over a prescribed period, t_p , and then goes to zero:

$$C_L = C_L^0 \quad t \leq t_p \quad (2.2)$$

$$C_L = 0 \quad t > t_p$$

where

| | | |
|---------|---|---|
| C_L | = | leachate concentration (mg/L) |
| C_L^0 | = | initial leachate concentration at the time of landfill closure (mg/L) |
| t | = | time since leaching began at landfill closure (y) |
| t_p | = | pulse duration (y) |

Although it is possible to set t_p to any value, the duration of the leachate pulse is usually derived from mass balance principles. The total mass of constituent which is present in the landfill at the time that leaching is assumed to start (i.e., at the time of landfill closure) is given by

$$M_c = C_w \times A_w \times D_{LF} \times F_h \times \rho_{hw} \times 1000 \quad (2.3)$$

where

| | | |
|-------------|---|---|
| M_c | = | total constituent mass in the landfill (mg) |
| C_w | = | constituent concentration in the waste (mg/kg) |
| A_w | = | area of the landfill footprint (m ²) |
| D_{LF} | = | landfill depth (m) |
| F_h | = | volume fraction of the waste in the landfill at time of closure (m ³ /m ³) |
| ρ_{hw} | = | waste density (g/cm ³) |
| 1000 | = | conversion factor used to convert volume from m ³ to liters |

Equation (2.3) states that the total constituent mass is equal to the waste concentration times the volume of the landfill dedicated to the waste ($A_w \cdot D_{LF} \cdot F_h$) multiplied by the density of the waste (ρ_{hw}). The latter converts the waste volume to waste mass.

In many practical situations, the waste loading into the landfill may be specified in terms of an annual waste amount and duration at the landfill active life, or:

$$M_c = C_w \times \dot{m}_w \times t_A \quad (2.4)$$

where

| | | |
|-------------|---|--|
| M_c | = | total constituent mass in the landfill (mg) |
| C_w | = | constituent concentration in the waste (mg/kg) |
| \dot{m}_w | = | annual waste loading during active life (kg/y) |
| t_A | = | WMU active life (y) |

If the landfill is characterized in terms of annual waste loading, the parameters in Equation (2.3) which are needed in EPACMTP can be easily calculated by simply combining the two equations to yield:

$$F_h = \frac{(\dot{m}_w \times t_A)}{(A_w \times D_{LF} \times \rho_{hw} \times 1000)} \quad (2.5)$$

where

| | | |
|-------------|---|---|
| F_h | = | volume fraction of the waste in the landfill at time of closure (dimensionless) |
| \dot{m}_w | = | annual waste loading during active life (kg/y) |
| t_A | = | WMU active life (y) |
| A_w | = | area of the landfill footprint (m ²) |
| D_{LF} | = | landfill depth (m) |

$$\begin{aligned}\rho_{hw} &= \text{waste density (g/cm}^3\text{)} \\ 1000 &= \text{conversion factor used to convert volume from m}^3\text{ to liters}\end{aligned}$$

When the waste density is unknown, a default value of $\rho_{hw} = 1.0$ can be used. In that case the calculated waste fraction, F_h , may be different from the actual waste fraction in the landfill, but mathematically, the model will still simulate the correct waste amount in the landfill.

During the period the landfill is generating leachate, the annual mass of constituent which is lost by leaching is equal to:

$$\dot{m}_{cL} = C_L(t) \times A_w \times I \times 1000 \quad (2.6)$$

where

$$\begin{aligned}\dot{m}_{cL} &= \text{annual constituent mass lost by leaching (mg/y)} \\ C_L &= \text{leachate concentration (mg/L)} \\ t &= \text{time since leaching began at landfill closure (y)} \\ A_w &= \text{area of the landfill (m}^2\text{)} \\ I &= \text{annual areal infiltration rate (m/y)} \\ 1000 &= \text{conversion factor used to convert volume from liters to m}^3\end{aligned}$$

From basic mass balance considerations, leaching from the landfill will stop when all of the constituent mass M_c has leached from the landfill. For the constant concentration pulse source condition, the pulse duration, t_p , is then simply given by

$$\dot{m}_{cL} \times t_p = M_c \quad (2.7a)$$

or

$$t_p = \frac{M_c}{\dot{m}_{cL}} \quad (2.7b)$$

$$t_p = \frac{C_w \times A_w \times D_{LF} \times F_h \times \rho_{hw} \times 1000}{C_L \times A_w \times I \times 1000} \quad (2.7c)$$

$$t_p = \frac{C_w \times D_{LF} \times F_h \times \rho_{hw}}{C_L \times I} \quad (2.7d)$$

where

| | | |
|----------------|---|---|
| \dot{m}_{cL} | = | annual constituent mass lost by leaching (mg/y) |
| t_p | = | pulse duration (y) |
| M_c | = | total constituent mass in the landfill (mg) |
| C_w | = | constituent concentration in the waste (mg/kg) |
| A_w | = | area of the landfill footprint (m ²) |
| D_{LF} | = | landfill depth (m) |
| F_h | = | volume fraction of the waste in the landfill at time of closure (dimensionless) |
| ρ_{hw} | = | waste density (g/cm ³) |
| 1000 | = | conversion factor used to convert volume from m ³ to liters |
| C_L | = | leachate concentration (mg/L) |
| I | = | annual areal infiltration rate (m/y) |
| 1000 | = | conversion factor used to convert volume from liters to m ³ |

2.2.1.3.3 Depleting Source Scenario

In the pulse source scenario described above, the leachate concentration is constant until all of the constituent mass which is present in the waste has leached out. This approximation may be valid when the leachate concentration is controlled by solubility of the constituent(s) of concern. More generally, however, it is expected that the leachate concentration emanating from a landfill will gradually diminish with time, as the amount of constituent that remains in the WMU gets depleted.

The EPACMTP depleting source option assumes that the leachate concentration at any time (t) since the beginning of the leaching process, i.e., $C_L(t)$, is a linear function of the remaining constituent concentration in the waste, $C_w(t)$, or:

where

$$C_L(t) = K_w C_w(t) \quad (2.8)$$

| | | |
|-------|---|--|
| C_L | = | leachate concentration (mg/L) |
| t | = | time since leaching began at landfill closure (y) |
| K_w | = | waste-concentration-to-leachate-concentration ratio (L/kg) |
| C_w | = | constituent concentration in the waste (mg/kg) |

The waste-concentration-to-leachate concentration ratio, K_w , in this equation can be thought of as a partition coefficient between the concentrations in the waste itself and the concentration dissolved in the leachate. In general, K_w may depend on both the chemical composition of the waste and leachate, as well as the physical waste form.

The general mass balance for the WMU source term is that the difference between the initial constituent mass in the WMU and the mass remaining at time t is equal to the amount that has leached out up to that time, which can be written as:

$$A_w \times D_{LF} \times F_h \times \rho_{hw} \times (C_w^0 - C_w(t)) = A_w \times I \int_0^t C_L(t) dt \quad (2.9)$$

where

| | | |
|-------------|---|---|
| A_w | = | area of the landfill footprint (m ²) |
| D_{LF} | = | landfill depth (m) |
| F_h | = | volume fraction of the waste in the landfill at time of closure (dimensionless) |
| ρ_{hw} | = | waste density (g/cm ³) |
| C_w^0 | = | initial constituent concentration in the waste at the time of landfill closure (mg/L) |
| C_w | = | constituent concentration in the waste (mg/kg) |
| t | = | time since leaching began at landfill closure (y) |
| I | = | annual areal infiltration rate (m/y) |
| C_L | = | leachate concentration (mg/kg) |

The left-hand side of the equation represents the difference in the mass of constituent in the landfill, from the initial amount (represented by C_w^0) to the amount remaining at time t (represented by $C_w(t)$). The right-hand side represents the cumulative amount of mass lost via leaching. Equation (2.9) can alternatively be written as

$$A_w \times D_{LF} \times F_h \times \rho_{hw} \frac{dC_w}{dt} = A_w \times I \times C_L(t) \quad (2.10)$$

where

| | | |
|-------------|---|---|
| A_w | = | area of the landfill footprint (m ²) |
| D_{LF} | = | landfill depth (m) |
| F_h | = | volume fraction of the waste in the landfill at time of closure (dimensionless) |
| ρ_{hw} | = | waste density (g/cm ³) |
| C_w | = | constituent concentration in the waste (mg/kg) |
| t | = | time since leaching began at landfill closure (y) |

| | | |
|-------|---|--------------------------------------|
| I | = | annual areal infiltration rate (m/y) |
| C_L | = | leachate concentration (mg/L) |

Using Equation (2.8) in Equation (2.10) and rearranging the resulting equation yields

$$\frac{dC_L}{dt} = \frac{-I}{D_{LF} \times F_h \times \rho_{hw} \times K_w} C_L \quad (2.11)$$

where

| | | |
|-------------|---|---|
| C_L | = | leachate concentration (mg/L) |
| t | = | time since leaching began at landfill closure (y) |
| I | = | annual areal infiltration rate (m/y) |
| D_{LF} | = | landfill depth (m) |
| F_h | = | volume fraction of the waste in the landfill at time of closure (dimensionless) |
| ρ_{hw} | = | waste density (g/cm ³) |
| K_w | = | waste-concentration-to-leachate-concentration ratio (L/kg) |

Integration of Equation (2.11) gives

$$C_L(t) = C_L^0 \exp \left\{ \left(\frac{-I}{D_{LF} \times F_h \times \rho_{hw} \times K_w} \right) t \right\} \quad (2.12)$$

where

| | | |
|-----------------|---|---|
| C_L | = | leachate concentration (mg/L) |
| t | = | time since leaching began at landfill closure (y) |
| C_L^0 | = | initial leachate concentration at the time of landfill closure (mg/L) |
| $\exp(\bullet)$ | = | exponential operator |
| I | = | annual areal infiltration rate (m/y) |
| D_{LF} | = | landfill depth (m) |
| F_h | = | volume fraction of the waste in the landfill at time of closure (dimensionless) |
| ρ_{hw} | = | waste density (g/cm ³) |
| K_w | = | waste-concentration-to-leachate-concentration ratio (L/kg) |

The depleting landfill source option of EPACMTP uses both the waste concentration, C_w , and the leachate concentration C_L . In EPACMTP version 2.0, the user must provide as inputs, the initial leachate concentration of the waste stream entering the landfill, and the waste-to-leachate concentration ratio, K_w . The latter input parameter can be calculated by the user from waste characterization data as

$$K_w = \frac{C_w^0}{C_L^0} \quad (2.13)$$

where

$$\begin{aligned} K_w &= \text{waste-to-leachate-concentration ratio (L/kg)} \\ C_w^0 &= \text{waste concentration of the waste stream entering the landfill} \\ &\quad \text{(mg/kg)} \\ C_L^0 &= \text{initial leachate concentration at the time of landfill closure} \\ &\quad \text{(mg/L)} \end{aligned}$$

The superscript 0 is used to denote that these concentrations reflect the initial waste characteristic, prior to any depletion.

2.2.2 Surface Impoundments

2.2.2.1 Assumptions for the Surface Impoundment Source-Term Module

The surface impoundment is modeled as a temporary waste management unit with a prescribed operational life. Clean closure is assumed, that is, at the end of the unit's operational life, the model assumes there is no further release of waste constituents to the ground water.

Following the unit's closure; however, it is further assumed that the contaminated liquid and sediment compartments are replaced by contaminant-free liquid and sediment compartments with identical configurations and properties. The remaining contaminants in the unsaturated zone are allowed to continue to migrate towards the water table with the same infiltration rate. This assumption allows the infiltration through the surface impoundment unit to be treated as a single steady-state flow regime throughout the simulation period. A decrease of infiltration rate due to the closure of the surface impoundment unit requires that the flow be treated as a transient flow regime, otherwise the mass of contaminants within the unsaturated zone cannot be conserved. Because of the non-linearity of the flow equation, a great deal of computational effort is required per Monte-Carlo realization, thereby making the transient solution for the infiltration rate after the unit's closure computationally impractical. In addition, by maintaining the same infiltration rate, the flow and transport in the unsaturated and saturated zones are considered conservative because the ground-water velocity at any downgradient location does not decrease with time, thus causing the contaminant to reach receptor wells sooner. In the case of degradable contaminants, their concentrations tend to be larger at receptor wells due to less degradational time available.

The surface impoundment is modeled as a unit with a square foot print, with a constant ponding depth during its operational life (see Figure 2.2B). By default, EPACMTP assumes an unlined impoundment. The model assumes that while the impoundment is in operation, a consolidated layer of sediment accumulates at the

bottom of the impoundment; the leakage (infiltration) rate through the impoundment is a function of the ponding depth in the impoundment, and the thickness and effective permeability of the consolidated sediment layer at the bottom of the impoundment.

The rate of leakage is constrained to ensure there is not a physically unrealistic high rate of leakage which would cause ground-water mounding beneath the unit to rise above the ground surface. Underlying the assumption of a constant ponding depth, EPACMTP assumes that the waste water in the impoundment is continually being replenished while the impoundment is in operation. It is also assumed that the sediment is always in equilibrium with the waste water since the onset of the unit's operation so that the presence of sediment does not alter the concentration of leachate. Accordingly, EPACMTP also assumes that the leachate concentration is constant during the impoundment operational life, and typically it is equal to the concentration in the waste water entering the impoundment.

2.2.2.2 List of Parameters for the Surface Impoundment Source-Term Module

The source-specific input parameters for the surface impoundment scenario include parameters to determine the unit dimensions; ponding depth; infiltration rate; the ambient recharge rate; the leachate concentration; and the leachate concentration and leaching duration. Together these parameters are used to determine how much contaminant mass enters the subsurface and over what time period.

The source-specific parameters for the surface impoundment scenario are presented in Table 2.2 and are described in the following sections.

Table 2.2 Source-Specific Variables for Surface Impoundments

| Parameter | Symbol | Units | Section in EPACMTP Parameters/Data Background Document |
|---|----------|--|--|
| Surface Impoundment Area: the footprint of the impoundment (Section 2.2.2.2.1) | A_w | m ² | 2.4.1 |
| Areal Recharge Rate: water percolating through the soil to the aquifer outside of the footprint of the waste management unit (Section 2.2.2.2.2) | I_r | m ³ /m ² /y or m/y | 4.4 |
| Areal Infiltration Rate: water percolating through a WMU to the underlying soil (Section 2.2.2.2.3) | I | m ³ /m ² /y or m/y | 4.3.4 |
| Depth Below Grade: the depth of the bottom of the impoundment below the surrounding ground surface. (Section 2.2.2.2.4) | d_{BG} | m | 2.4.6 |
| Operating Depth: total average depth of the impoundment, including both water and sediment (Section 2.2.2.2.5) | H_T | m | 2.4.2 |
| Ponding Depth: the average total depth of waste water in the impoundment above the consolidated sediment (Section 2.2.2.2.5) | H_p | m | 2.4.2 |

Table 2.2 Source-Specific Variables for Surface Impoundments (continued)

| Parameter | Symbol | Units | Section in EPACMTP Parameters/Data Background Document |
|--|---------------|----------------------|--|
| Total Sediment Thickness: thickness of sediment, including both the consolidated and non-consolidated sediments (Section 2.2.2.2.6) | D_s | m | 2.4.3 |
| Consolidated Sediment Thickness: Thickness of consolidated sediment at base of impoundment (Section 2.2.2.2.6) | D_{fc} | m | 2.4.3 |
| Unconsolidated Sediment Thickness: Thickness of loose sediment layer at base of impoundment (Section 2.2.2.2.6) | D_{uc} | m | 2.4.3 |
| Distance to Surface Water Body: provides a boundary condition in screening the calculated surface impoundment infiltration rate against physically unrealistic values (Section 2.2.2.2.7) | R_w | m | 2.4.8 |
| Leachate Concentration: the concentration of a constituent in the leachate emanating from the base of the impoundment (Section 2.2.2.2.8) | C_L | mg/L | 3.2.3 |
| Source Leaching Duration: the duration of the leachate release period (Section 2.2.2.2.9) | t_p | y | 2.4.9 |
| Liner Thickness: the thickness of a single liner underlying the SI unit (Section 2.2.2.2.10) | D_{lin} | m | 2.4.4 |
| Liner Hydraulic Conductivity: The saturated hydraulic conductivity of a single liner underlying the SI unit (Section 2.2.2.2.11) | K_{lin} | m/y | 2.4.5 |
| Unsaturated-zone Thickness: The total thickness of the unsaturated zone at the SI site (Section 2.2.2.2.12) | D_u | m | 5.2.1 |
| Leak Density: number of holes per unit area (Section 2.2.2.2.13) | ρ_{leak} | holes/m ² | 2.4.7 |

2.2.2.2.1 Surface Impoundment Area

The surface impoundment area is defined as the footprint of the impoundment. In EPACMTP, the impoundment is assumed to be square. The impoundment area is used to determine the area over which the infiltration rate is applied.

2.2.2.2.2 Areal Recharge Rate

Recharge is water percolating through the soil to the aquifer from outside of the footprint of the WMU. The recharge rate is determined by the regional climatic conditions and regional soil type. Recharge is specified as areal rates, with the units of cubic meters of fluid (water or leachate) per square meter per year (m³/m²/y). Thus, the units for recharge simplify to meters per year (m/y).

For surface impoundments, recharge rates for selected soil types at cities around the country have been estimated using the HELP water-balance model and are

incorporated into a database included in one of the EPACMTP input files. Further details about how these rates were determined and other options for determining recharge rates outside of the EPACMTP model can be found in Section 4.0 of the *EPACMTP Parameters/Data Background Document* (U.S. EPA, 2003).

2.2.2.2.3 Areal Infiltration Rate

For the surface impoundment scenario, the leachate flux (infiltration) rate is typically computed internally by EPACMTP, as a function of the ponding depth in the impoundment and other characteristics. In essence, the leachate flux rate is calculated by applying Darcy's law as a function of:

- Impoundment depth,
- Thickness of an engineered liner or sediment layer at the base of the impoundment, and
- Hydraulic conductivity of this liner or sediment layer and the underlying soil material.

The algorithm is more fully described below in Section 2.2.2.3. However, you can also determine the infiltration rate outside the EPACMTP model (for example, by using the HELP model or variably unsaturated flow simulation models) and provide it as an input value or a distribution of values in the input file.

The surface impoundment source-term module in the EPACMTP model cannot accommodate a time-varying infiltration rate; the infiltration rate that is derived or specified in the input file is applied over the area of the impoundment for the entire modeling period even after the unit has been closed. The contaminant mass, however, only enters the subsurface during the period of the leaching duration. Consistent with the assumption of clean closure in Section 2.2.2.1, it is assumed that all the contaminants within the source (contaminants in the liquid and sediment compartments) are removed at the end of the operational period. However, the remaining contaminants in the unsaturated zone are allowed to continue to migrate toward the water table.

2.2.2.2.4 Depth Below Grade

The depth below grade is defined as the depth of the bottom of the impoundment below the surrounding ground surface. If a non-zero value is entered for this input, then the thickness of the unsaturated zone beneath the impoundment is adjusted accordingly.

2.2.2.2.5 Operating Depth and Ponding Depth

The operating depth is defined as the average total depth of waste water in the impoundment, measured from the base of the impoundment, that is, it is not just the depth of free standing water above any sediment layer that may have accumulated in the impoundment. The operating depth includes the sediment layer. Seasonal

differences and differences due to non-uniform bottom elevation should be averaged out into a long-term average value or distribution of values. The ponding depth is defined as the average depth of water above the consolidated sediment, including the depth of unconsolidated sediment.

2.2.2.2.6 Total Thickness of Sediment

By default, EPACMTP models unlined, surface impoundments with a layer of “sludge” or sediment above the base of the unit. The sediment layer is divided into two sublayers: the upper sublayer with loose sediment, and the lower sublayer with sediment consolidated by the weight of overlying waste water and the loose sediment. The consolidated sediment has relatively low hydraulic conductivity and acts to impede flow. The calculated infiltration rate is inversely related to the thickness of the consolidated sediment sublayer. Smaller consolidated sediment thickness will result in a higher infiltration rate, and greater rate of constituent loss from the impoundment. If the impoundment is periodically dredged, using the minimum consolidated sediment thickness is recommended.

2.2.2.2.7 Distance to the Nearest Surface Water Body

In the case of deep unlined impoundments, EPACMTP may calculate very high surface impoundment infiltration rates. EPACMTP checks against the occurrence of excessively high rates by calculating the estimated height of ground-water mounding underneath the WMU, and if necessary reduces the infiltration rate to ensure the predicted water table does not rise above the ground surface. This screening procedure requires as input the distance to the nearest point at which the water table elevation is kept at a fixed value. Operationally, this is taken to be the distance to the nearest surface water body.

2.2.2.2.8 Leachate Concentration

The fate and transport model requires stipulation of the leachate concentration as a function of time, $C_L(t)$. The leachate concentration, $C_L(t)$, used in the model directly represents the concentration of the leachate emanating from the base of the waste management unit, as a boundary condition for the fate and transport model. For the surface impoundment scenario, the EPACMTP model accounts for this boundary condition as a constant concentration pulse condition. The boundary condition for the fate and transport model then becomes a constant concentration pulse, with a defined duration. When there are no contaminant losses in the impoundment, the leachate concentration value can be assumed equal to the incoming waste water concentration. EPACMTP version 2.0 does not account for losses (e.g., volatilization, biochemical degradation) in surface impoundments.

2.2.2.2.9 Source Leaching Duration

The duration of the leaching period may be assigned a constant value or an appropriate frequency distribution in EPACMTP. For surface impoundments, the addition and removal of waste during the operational life period are more or less balanced, without significant net accumulation of waste. In the finite source

implementation for surface impoundments, the duration of the leaching period is, for practical purposes, assumed to be the same as the operational life of the surface impoundment.

2.2.2.2.10 Liner Thickness

In the event that the SI is underlain by a single liner, the thickness of the liner must be provided. The liner thickness is defined as the average thickness of the single liner by which the SI unit is underlain. Examples of single liner include compacted clay liners, and synthetic clay liners. This parameter is required for the calculation of infiltration rate.

2.2.2.2.11 Liner Hydraulic Conductivity

The liner hydraulic conductivity is defined as the average hydraulic conductivity of the liner mentioned in Section 2.2.2.2.10. Hydraulic conductivity is the volume of fluid that is allowed to traverse a liner of unit thickness and unit hydraulic head difference in a given unit time over a unit area.

2.2.2.2.12 Unsaturated-zone Thickness

The unsaturated-zone thickness is defined as the average height of natural soil surface above the local water table elevation.

2.2.2.2.13 Leak Density

EPACMTP can also account for infiltration through composite liners. The infiltration is assumed to result from defects (pin holes) in the geomembrane. The pin holes are assumed to have a circular shapes and to be uniform in size. The leak density is defined as the average number of circular pin holes per square meter.

2.2.2.3 Mathematical Formulation of the Surface Impoundment Source-Term Module

2.2.2.3.1 Surface Impoundment Leakage (Infiltration) Rate

Figure 2.3 illustrates a compartmentalized surface impoundment with stratified sediment. Shown in the figure are: the liquid compartment, the sediment compartment (with loose and consolidated sediments), and the unsaturated zone (with clogged and unaffected native materials). The model assumes that all sediment layer thicknesses remain unchanged throughout the life of the unit.

EPACMTP calculates infiltration through the accumulated sediment at the bottom of an impoundment, accounting for clogging of the native soil materials underlying the impoundment and mounding due to infiltration. No leachate collection system is assumed to exist beneath the unit.

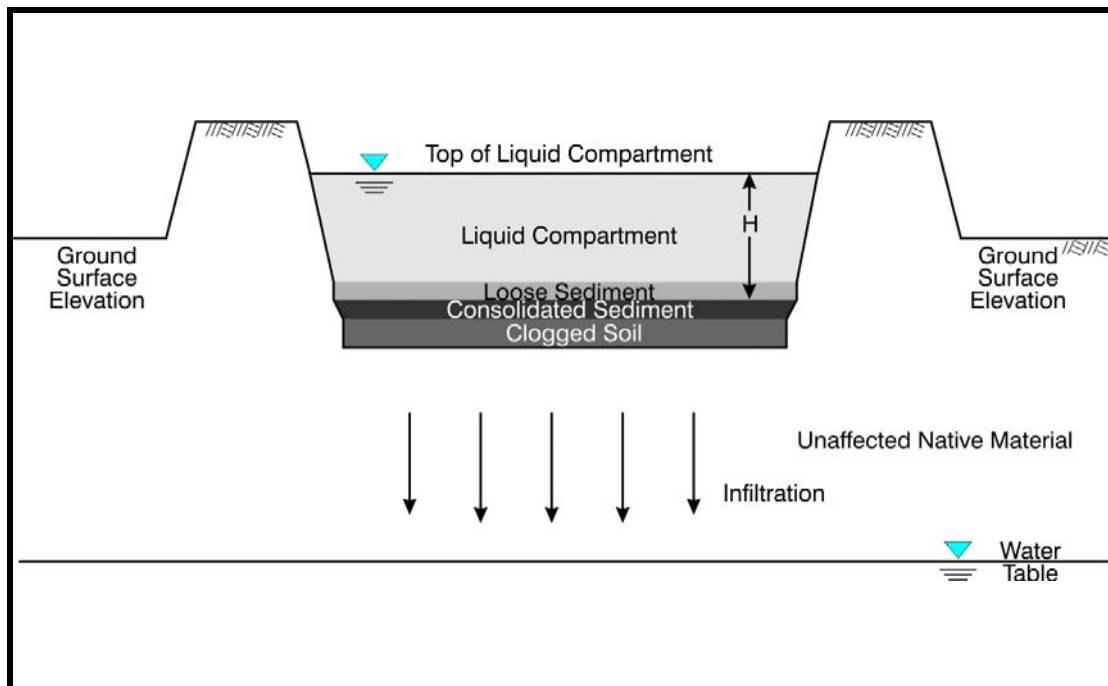


Figure 2.3 Schematic Cross-Section View of SI Unit.

The modeled infiltration is governed by the following:

- **Effective hydraulic conductivity of consolidated sediment layer.** As sediment accumulates at the base of the impoundment, the weight of the liquid and upper sediments tends to compress (or consolidate) the lower sediments. The consolidation process reduces the hydraulic conductivity of the sediment layer, and the layer of consolidated sediment will act as a restricting layer for flow out of the impoundment. This consolidated sediment acts as a filter cake, and its hydraulic conductivity may be much lower than the nonconsolidated sediment. The layer of loose, unconsolidated sediment which is part of the conceptual model for SI units, and which overlies the consolidated sediment layer, is not explicitly considered in the SI flow module. Instead, EPACMTP assumes that the permeability of this loose material is so large that it does not restrict the flow rate.
- **Effective hydraulic conductivity of clogged native material.** As liquids infiltrate soils underlying the impoundment, suspended particulate matter accumulates in the soil pore spaces, reducing hydraulic conductivity and lowering infiltration rates.
- **Limitations on maximum infiltration rate from mounding.** If the calculated infiltration rate exceeds the rate at which the saturated zone can transport the ground water, the ground-water level will rise

into the unsaturated zone and the assumption of zero pressure head at the base of the unsaturated zone is violated. This ground-water “mounding” will reduce the effective infiltration rate so that the maximum infiltration rate is estimated as the rate that does not cause the ground-water mound to rise to the bottom elevation of the SI unit.

The following sections describe the algorithms used in this model to calculate the infiltration rate through the consolidated sediment at the bottom of the impoundment. A detailed discussion of the maximum allowable infiltration rate based on the ground-water mounding condition is presented in Section 2.2.5.

Effective Hydraulic Conductivity of Consolidated Sediment Layer. EPACMTP estimates the effective hydraulic conductivity of the consolidated sediment layer using principles of soil mechanics. From a number of tests on soil samples as reported by Lambe and Whitman (1969), the following empirical relationship between the hydraulic conductivity and void ratio of a layer of consolidated granular material was derived:

$$K_{sed} = \left(\frac{e}{A} \right)^{\frac{1}{b}} \quad (2.14)$$

where

$$\begin{aligned} K_{sed} &= \text{hydraulic conductivity of the consolidated sediment (m/s)} \\ e &= \text{void ratio (dimensionless)} \\ &= \frac{\phi_{sed}}{(1 - \phi_{sed})}, \text{ with} \\ \phi_{sed} &= \text{porosity of the consolidated sediment (dimensionless)} \\ A &= \text{empirical constant (119) (dimensionless)} \\ b &= \text{empirical constant (0.206 1/log (m/s))} \end{aligned}$$

The values of the empirical constants A and b are 119 and 0.206, respectively. The void ratio, e , is a function of the initial void ratio of the sediment (before consolidation) and the stress that results from the combined weight of the waste water in the impoundment and the overlying loose sediment deposits, or:

$$e = e_0 - a_v \Delta \sigma_{vf} \quad (2.15)$$

where

$$\begin{aligned} e &= \text{void ratio (dimensionless)} \\ e_0 &= \text{initial void ratio at no-stress condition (dimensionless)} \\ a_v &= \text{compressibility of the sediment (m-s}^2\text{/kg)} \\ \sigma_{vf} &= \text{vertical effective stress in the consolidated sediment layer (kg/m-s}^2\text{)} \end{aligned}$$

The compressibility, a_v , is given by:

$$a_v = \frac{0.435C_c}{\frac{1}{2}\sigma_{vf} \text{ (at } z_{sed} = \frac{1}{2}D_{fc})} \quad (2.16)$$

where

| | | |
|---------------|---|---|
| a_v | = | compressibility of the sediment (m-s ² /kg) |
| C_c | = | compression index (0.55) (dimensionless) |
| σ_{vf} | = | vertical effective stress in the consolidated sediment layer (kg/m-s ²) |
| z_{sed} | = | vertically downward distance from the top of the consolidated sediment (m) |
| D_{fc} | = | thickness of consolidated sediment layer (m) |

The value assigned to the compression index, C_c , is 0.55; this value is an average of values presented in Lambe and Whitman (1969). The vertical effective stress in the sediment layer, σ_{vf} , is a function of the depth of water in the SI unit, and the thickness and density of the sediment layer, and is given by:

$$\begin{aligned} \sigma_{vf} = & (H_p - D_{uc} - D_{fc})\rho g + (1 - \phi_{sed})\rho_{sed}gD_{uc} + \phi_{sed}\rho gD_{uc} \\ & + (1 - \phi_{sed})\rho_{sed}gz_{sed} + \phi_{sed}\rho gz_{sed} - [(H_p - D_{fc})\rho g - \frac{z_{sed}}{D_{fc}}(H_p - D_{fc})\rho g] \end{aligned} \quad (2.17)$$

where

| | | |
|---------------|---|---|
| σ_{vf} | = | vertical effective stress in the consolidated sediment layer (kg/m-s ²) |
| H_p | = | SI ponding depth (m) |
| D_{uc} | = | thickness of unconsolidated sediment (m) |
| D_{fc} | = | thickness of consolidated sediment layer (m) |
| ρ | = | water density (1,000 kg/m ³) |
| g | = | gravitational acceleration (9.81 m/s ²) |
| ϕ_{sed} | = | porosity of the consolidated sediment (dimensionless) |
| ρ_{sed} | = | sediment grain density (2,650 kg/m ³) |
| z_{sed} | = | vertically downward distance from the top of the consolidated sediment (m) |

The values of 1,000 kg/m³, 9.81 m/s², and 2,650 kg/m³ are assigned for the water density, the gravitational acceleration, and the sediment grain density, respectively.

In EPACMTP, Equations (2.14) to (2.17) are combined to provide the following relationship between the thickness of the consolidated sediment and the hydraulic conductivity of the consolidated sediment layer:

$$K_{sed} = (C_1 + C_2 z_{sed})^{\frac{1}{b}} \quad (2.18)$$

where

| | | |
|-----------|---|--|
| K_{sed} | = | hydraulic conductivity of the consolidated sediment (m/s) |
| C_1 | = | constant defined in Equation (2.19) (dimensionless) |
| C_2 | = | constant defined in Equation (2.20) (1/m) |
| z_{sed} | = | vertically downward distance from the top of the consolidated sediment (m) |
| b | = | empirical constant (= 0.206) (1/log (m/s)) |

The constants C_1 and C_2 are given by:

$$C_1 = e_0 - \frac{a_v}{A} [(\phi_{sed} D_{uc} - D_{fc}) \rho g + (1 - \phi_{sed}) D_{uc} \rho_{sed} g] \quad (2.19)$$

$$C_2 = -\frac{a_v}{A} [(1 - \phi_{sed}) \rho_{sed} g + \phi_{sed} \rho g + \frac{1}{D_{fc}} (H_p - D_{fc}) \rho g] \quad (2.20)$$

where

| | | |
|--------------|---|---|
| C_1 | = | constant defined by Equation (2.19) (dimensionless) |
| e_0 | = | initial void ratio at no-stress condition (dimensionless) |
| a_v | = | compressibility of the sediment (m-s ² /kg) |
| A | = | empirical constant (119) (dimensionless) |
| ϕ_{sed} | = | porosity of the consolidated sediment (dimensionless) |
| D_{uc} | = | thickness of unconsolidated sediment (m) |
| D_{fc} | = | thickness of consolidated sediment layer (m) |
| ρ | = | water density (1,000 kg/m ³) |
| g | = | gravitational acceleration (9.81 m/s ²) |
| ρ_{sed} | = | sediment grain density (2,650 kg/m ³) |
| C_2 | = | constant defined by Equation (2.20) (1/m) |
| H_p | = | SI ponding depth (m) |

Equation (2.18) indicates that the hydraulic conductivity of the consolidated sediment layer is not uniform, but varies across the layer. The effective hydraulic conductivity of this layer is given by averaging across the thickness D_{fc} according to:

$$\frac{1}{K_{fc}} = \frac{1}{D_{fc}} \int_0^{D_{fc}} \frac{1}{(C_1 + C_2 z_{sed})^{\frac{1}{b}}} dz_{sed} \quad (2.21)$$

where

| | | |
|-----------|---|--|
| K_{fc} | = | averaged saturated hydraulic conductivity of the consolidated sediment (m/y) |
| D_{fc} | = | thickness of consolidated sediment layer (m) |
| C_1 | = | constant defined in Equation (2.19) (dimensionless) |
| C_2 | = | constant defined in Equation (2.20) (1/m) |
| z_{sed} | = | vertically downward distance from the top of the consolidated sediment (m) |
| b | = | empirical constant (0.206 1/log (m/s)) |

EPACMTP determines the final value of the hydraulic conductivity of the consolidated sediment layer by integrating Equation (2.21), which results in:

$$K_{fc} = \left[\frac{(C_1 + C_2 D_{fc})^{1 - \frac{1}{b}} - (C_1)^{1 - \frac{1}{b}}}{D_{fc} (1 - \frac{1}{b}) C_2} \right]^{-1} \quad (2.22)$$

where

| | | |
|----------|---|--|
| K_{fc} | = | averaged saturated hydraulic conductivity of the consolidated sediment (m/y) |
| C_1 | = | constant defined in Equation (2.19) (dimensionless) |
| C_2 | = | constant defined in Equation (2.20) (1/m) |
| D_{fc} | = | thickness of consolidated sediment layer (m) |
| b | = | empirical constant (0.206 1/log (m/s)) |

EPACMTP requires values for the thickness of the consolidated and unconsolidated sediment that has accumulated at the base of an impoundment unit. The actual range of values in unlined impoundments across the United States is not well characterized. In developing the EPACMTP SI module, EPA therefore assigned the following values: the total sediment thickness is set to 20 centimeters (0.2 meters), and it is assumed that the upper half (0.1 meters) consists of unconsolidated material, while the lower half (0.1 meters) consists of consolidated deposits. In other words: $D_{uc} = D_{fc} = 0.1$ meters. The void ratio of the sediment before consolidation is assigned a value of $e_0 = 2.7$, which corresponds to an initial porosity of 0.73. This value represents the mean initial void ratio of data presented by Lambe and Whitman (1969) and Bear (1972).

The hydraulic conductivity calculated in Equation (2.22) has units of m/s. EPACMTP converts this value to m/y by multiplying by 31,536,000.

In EPACMTP, the unconsolidated or loose sediment is not included as part of the calculation of infiltration. It is assumed that the loose material is so conductive that the hydraulic gradient across the material is negligible. As a result, it does not exert significant resistance to the flow.

Effective Hydraulic Conductivity of Clogged Native Soil

EPACMTP determines the reduction in hydraulic conductivity of the upper part of the soil by assigning a 'clogging' factor. The value of saturated hydraulic conductivity of the clogged zone is lower than that of the native soil at the site according to, or

$$K_s^* = C_{fact} K_s \quad (2.23)$$

where

| | | |
|------------|---|---|
| K_s^* | = | saturated hydraulic conductivity of the clogged unsaturated-zone soil (m/y) |
| C_{fact} | = | clogging factor (= 0.1) (dimensionless) |
| K_s | = | saturated hydraulic conductivity of the native unsaturated-zone soil (m/y) |

The assigned value of the clogging factor of 0.1 is based upon technical judgment. The depth of the clogged layer is set to a value of 0.5 meters in EPACMTP.

2.2.2.3.2 Calculation of the Surface Impoundment Infiltration Rate

EPACMTP uses the unsaturated-zone flow module to calculate the infiltration rate out of the bottom of the impoundment. This module, which is described in detail in Section 3 of this document, is designed to simulate steady-state downward flow through the unsaturated zone consisting of one or more soil layers. Steady-state means that the rate of flow does not change with time.

In the case of flow out of a surface impoundment, the module simulates flow through a three-layer system, consisting of:

- Consolidated sediment layer;
- Clogged soil layer; and
- Native unsaturated-zone soil.

The native unsaturated-zone soil extends downward to the water table. The steady-state infiltration rate out of the surface impoundment is driven by the head gradient between the water ponded in the impoundment and the head at the water table. The pressure head at the top of the consolidated sediment layer is equal to the water depth in the impoundment plus the thickness of the unconsolidated sediment.

The pressure head at the water table is zero by definition. The rate of infiltration is then given by:

$$I = \frac{(H_p + D_{fc} + D_{soil}^* + D_{soil})}{\frac{D_{fc}}{K_{fc}} + \frac{D_{soil}^*}{K_s^* k_{rw}} + \frac{D_{soil}}{K_s k_{rw}}} \quad (2.24a)$$

where

| | | |
|--------------|---|---|
| I | = | areal infiltration rate (m/y) |
| H_p | = | ponding depth of waste water in the SI unit (m) |
| D_{fc} | = | thickness of consolidated sediment layer (m) |
| D_{soil}^* | = | thickness of clogged soil layer (= 0.5 m) |
| D_{soil} | = | thickness of remaining unaffected native soil underneath the WMU from below the clogged soil layer to the water table (m) |
| K_{fc} | = | saturated hydraulic conductivity of the consolidated sediment (m/y) |
| K_s^* | = | saturated hydraulic conductivity of clogged soil (= 0.1 K_s) (m/y) |
| k_{rw}^* | = | relative permeability of the clogged soil (dimensionless) |
| K_s | = | saturated hydraulic conductivity of native soil (m/y) |
| k_{rw} | = | relative permeability of the native soil (dimensionless) |

The relative permeability of each soil layer is a dimensionless factor that represents the reduction in the hydraulic conductivity of the layer once it becomes unsaturated. Under these conditions, the actual hydraulic conductivity of the layer is less than its saturated value. EPACMTP assumes that the consolidated sediment layer is always fully saturated, hence its relative permeability is always 1.0 and this term is omitted from Equation (2.24a). In general, if a more permeable layer lies underneath a less permeable layer, the higher permeability layer may become partially unsaturated. For instance, the upper part of the unaffected soil underneath an impoundment unit may become unsaturated because of the reduced permeability of the clogged layer above it. Moving downward through the soil, the soil will become fully saturated again at the watertable and the capillary fringe just above the water table. The relative permeabilities in Equation (2.24a) represent effective, average, values for each soil layer. EPACMTP assumes that the relative permeability – pressure head relation for the clogged soil is the same as for the unaffected soil. The latter is determined by the values of the soil characteristic parameters that are provided as EPACMTP inputs (see Section 3.0).

EPACMTP solves Equation (2.24a) in an iterative manner. The equation cannot be solved directly because the infiltration rate, I , and the relative permeabilities, k_{rw} , in the soil layers are mutually dependent. The calculation begins with an estimate of infiltration rate based upon a combination of bounding conditions in which (a) all layers are saturated, and (b) the clogged native material is the primary flow restriction. Using the initial estimate of I , EPACMTP calculates the vertical pressure head distribution throughout the sediment-soil system, and adjusts the value for I as necessary, until the calculated pressure head at the water table is equal to zero, within a convergence tolerance of 0.001 meters.

In the event that the SI unit is underlain by a single liner, the rate of infiltration is then given by:

$$I = \frac{(H_p + D_{fc} + D_{lin} + D_u - d_{BG})}{\frac{D_{fc}}{K_{fc}} + \frac{D_{lin}}{K_{lin} k_{rwin}} + \frac{(D_u - d_{BG})}{K_s k_{rw}}} \quad (2.24b)$$

where

| | | |
|------------|---|---|
| I | = | areal infiltration rate (m/y) |
| H_p | = | ponding depth of waste water in the SI unit (m) |
| D_{fc} | = | thickness of consolidated sediment layer (m) |
| D_{lin} | = | thickness of clogged soil layer (= 0.5 m) |
| D_u | = | thickness of initially unaffected native soil underneath the WMU from below the base of the SI to the water table (m) |
| d_{BG} | = | depth below grade of the SI unit (m) |
| K_{fc} | = | saturated hydraulic conductivity of the consolidated sediment (m/y) |
| K_{lin} | = | saturated hydraulic conductivity of the liner (m/y) |
| k_{rwin} | = | relative permeability of the liner (dimensionless) |
| K_s | = | saturated hydraulic conductivity of native soil (m/y) |
| k_{rw} | = | relative permeability of the native soil (dimensionless) |

In the event that the SI unit is underlain by a composite liner (a geomembrane underlain by a low permeability liner such as either a compacted clay liner or a geosynthetic clay liner), the following modified equation of Bonaparte et al. (1989) is used to calculate the infiltration rate:

$$I = 0.21 a_{gh}^{0.1} H_T^{0.9} K_{lin}^{0.74} (31,536,000) \rho_{leak} \quad (2.24c)$$

where

| | | |
|---------------|---|---|
| I | = | areal infiltration rate (m/y) |
| 0.21 | = | empirical constant ($m^{1.16}/s^{0.26}$) |
| a_{gh} | = | average area of a hole in the geomembrane = $6 \times 10^{-6} m^2$ |
| H_T | = | head of liquid on top of geomembrane (m) |
| K_{lin} | = | hydraulic conductivity of the low-permeability liner (e.g., compacted clay) underlying the geomembrane = $1 \times 10^{-9} m/s$ |
| 31,536,000 | = | conversion factor, from year to seconds |
| ρ_{leak} | = | leak density (holes/ m^2) |

This equation is applicable to cases where there is good contact between the geomembrane and the underlying compacted clay liner.

In EPACMTP, a uniform leak size of 6 millimeters squared (mm^2) is assumed. This leak size is the middle of a range of hole sizes reported by Rollin et al. (1999), who found that 25 percent of holes were less than 2 mm^2 , 50 percent of holes were 2 to 10 mm^2 , and 25 percent of holes were greater than 10 mm^2 . Equation (2.24c) also assumes that the hydraulic conductivity of the underlying compacted clay liner is always $1 \times 10^{-7} \text{ cm/s}$ (or $1 \times 10^{-9} \text{ m/s}$).

2.2.3 Waste Piles

2.2.3.1 Assumptions for the Waste Pile Source-Term Module

The waste pile management scenario is conceptually similar to that of the landfill, but differs in a number of key aspects. In contrast to landfills which represent a long-term waste management scenario, waste piles represent a more temporary management scenario. During the operational life of the waste pile, it may be regarded as an uncovered landfill. Typically at the end of the active life of a waste pile, the waste material is either removed for land filling, or the waste pile is covered and left in place. If the waste is removed, there is no longer a source of potential contamination. If a waste pile is covered and left in place, it then becomes equivalent to a landfill. In this case, it should be treated as a landfill in EPACMTP. However, the treatment of a covered waste pile as a landfill is valid only when the operational period is very short compared with the total leaching period.

2.2.3.2 List of Parameters for the Waste Pile Source-Term Module

The source-specific input parameters for the waste pile scenario include the area of the waste pile, the infiltration rate; the ambient recharge rate, the leachate concentration, and the source leaching duration. Together these parameters are used to determine how much contaminant mass enters the subsurface and the time period over which this occurs.

The source-specific parameters for the waste pile scenario are presented in Table 2.3 and are described in the following sections.

2.2.3.2.1 Waste Pile Area

The waste pile area is defined as the footprint of the unit. In EPACMTP, the waste pile is assumed to be square. The length and width of the waste pile are each calculated as the square root of the area. The waste pile area is used to determine the area over which the infiltration rate is applied.

Table 2.3 Source-Specific Variables for Waste Piles

| Parameter | Symbol | Units | Section in EPACMTP Parameters/Data Background Document |
|--|----------|--|--|
| Waste Pile Area: the square footprint of the waste pile (Section 2.2.3.2.1) | A_w | m ² | 2.5.1 |
| Areal Recharge Rate: water percolating through the soil to the aquifer outside of the footprint of the waste pile (Section 2.2.3.2.2) | I_r | m ³ /m ² /y or m/y | 4.4 |
| Areal Infiltration Rate: water percolating through the waste pile to the underlying soil (Section 2.2.3.2.2) | I | m ³ /m ² /y or m/y | 4.3.2 |
| Leachate Concentration: the concentration of the leachate emanating from the base of the waste pile (Section 2.2.3.2.3) | C_L | mg/L | 3.2.3 |
| Source Leaching Duration: the duration of the leachate release period (Section 2.2.3.2.4) | t_p | y | 2.5.2 |
| Depth Below Grade: the depth of the bottom of the waste pile below the surrounding ground surface (Section 2.2.3.2.5) | d_{BG} | m | 2.5.3 |

2.2.3.2.2 Areal Infiltration and Recharge Rates

The EPACMTP model requires input of the net areal rate of vertical downward percolation of water and leachate through the unsaturated zone to the water table. Infiltration is defined as water percolating through a WMU to the underlying soil, while recharge is water percolating through the soil to the aquifer outside of the footprint of the WMU. The model allows the infiltration rate to be different from the ambient regional recharge rate. The waste pile infiltration rate can be different from the ambient recharge rate for a variety of reasons, including the engineering design of the waste pile (for instance, waste with a conductivity much lower than that of the regional soil type), topography, land use, and vegetation. The recharge rate is determined by the regional climatic conditions, such as precipitation, evapotranspiration, surface run-off, and regional soil type.

Both infiltration and recharge are specified as areal rates, with the units of cubic meters of fluid (water or leachate) per square meter per year (m³/m²/y or m/y).

Infiltration and recharge rates for selected soil types at cities around the country have been estimated using the HELP water-balance model and are incorporated into a database included in one of the EPACMTP input files. Further details about how these rates were determined and other options for determining recharge and infiltration rates outside of the EPACMTP model can be found in Section 4.0 of the *EPACMTP Parameters/Data Background Document* (U.S. EPA, 2003).

2.2.3.2.3 Leachate Concentration

The leachate concentration (C_L , mg/L) is the concentration of dissolved constituent in the leachate that enters the subsurface from the base of the WMU. For the waste pile scenario, the EPACMTP model assumes a constant concentration pulse condition. This parameter is a user-input parameter. Alternatively, EPACMTP can estimate it from the waste concentration using Equation (2.25).

2.2.3.2.4 Source Leaching Duration

Waste piles are a temporary management scenario in which the addition and removal of waste during the operational life period are more or less balanced, without significant net accumulation of waste. Typically at the end of the active life of a waste pile, the waste material is either removed for land filling, or the waste pile is covered and left in place. If the waste is removed, there is no longer a source of potential contamination. Consequently, the finite source implementation that is most appropriate for waste piles is the pulse (or non-depleting) source scenario. The boundary condition for the fate and transport model then becomes a constant concentration pulse, with a defined duration that is equal to the operational life of the waste pile. When conducting a Monte-Carlo modeling simulation of a waste pile in EPACMTP using a pulse source, the duration of the leaching period may be assigned a constant value or an appropriate frequency distribution, based on the available data. Alternatively, if a waste pile is covered and left in place, it then becomes equivalent to a landfill and should be simulated as a landfill (that is, using the depleting source option of the finite source scenario). However, this approach is valid only when the operational life of the waste pile is much shorter than the subsequent leaching period.

2.2.3.2.5 Depth Below Grade

The depth below grade is defined as the depth of the bottom of the waste pile below the surrounding ground surface. If a non-zero value is entered for this input, then the thickness of the unsaturated zone beneath the impoundment is adjusted accordingly.

2.2.3.3 Mathematical Formulation of the Waste Pile Source-Term Module

The waste pile source module assumes a constant leachate concentration applied uniformly over the area of the waste pile unit for a period of time equal to the unit's operating life. EPACMTP requires the user to specify the duration of the leachate pulse, and the leachate concentration of constituents of concern. If available, the leachate concentration value can be set equal to measured concentration values from appropriate leaching tests such as the TCLP or SPLP tests.

Alternatively, the leachate concentration emanating from the waste pile can be estimated from the total waste concentrations as:

$$C_L = \frac{C_w}{K_w + \frac{\theta_w}{\rho_{hw}}} \quad (2.25)$$

where

| | | |
|-------------|---|---|
| C_L | = | leachate concentration (mg/L) |
| C_w | = | total waste concentration (mg/kg) |
| K_w | = | waste partition coefficient (cm ³ /g) |
| θ_w | = | volumetric water content of the waste (dimensionless) |
| ρ_{hw} | = | waste density (g/cm ³) |

For organic constituents, the partition coefficient, K_w , in the above equation can be determined from the constituent-specific organic carbon partition coefficient and the fraction organic carbon in the waste.

$$K_w = f_{ocw} \times k_{oc} \quad (2.26)$$

where

| | | |
|-----------|---|--|
| K_w | = | waste partition coefficient (cm ³ /g) |
| f_{ocw} | = | fraction organic carbon in the waste (g/g) |
| k_{oc} | = | constituent-specific organic carbon partition coefficient (cm ³ /g) |

Under conditions of a constant leachate concentration and defined leaching period, t_p , the total mass lost from the waste pile by leaching is

$$M_{LWP} = t_p \times I \times A_w \times C_L \times 1000 \quad (2.27)$$

where

| | | |
|-----------|---|--|
| M_{LWP} | = | total mass of constituent leached from a waste pile (mg) |
| t_p | = | duration of leaching period (y) |
| I | = | areal infiltration rate (m/y) |
| A_w | = | area of the waste pile footprint (m ²) |
| C_L | = | leachate concentration (mg/L) |
| 1000 | = | conversion factor used to convert volume from m ³ to liters |

2.2.4 Land Application Units

2.2.4.1 Assumptions for the Land Application Unit Source-Term Module

EPACMTP models land application units (LAUs) as temporary management units in which waste is spread on the soil on a periodic basis. EPACMTP assumes the LAU has no liner or leachate collection system, and that the rate of leachate generation from the unit is driven primarily by ambient climate conditions. EPACMTP assumes the water contained in the land applied waste is insignificant relative to the ambient regional recharge rate.

The annual waste amount applied to land application units is typically constrained by the capacity of the site to absorb waste (e.g., remove through biodegradation and/or plant uptake) without significant accumulation of potentially hazardous constituents. While there may be significant leaching to ground water occurring during the operational life of a land application unit, the leaching will diminish quickly after waste application ceases.

2.2.4.2 List of Parameters for the Land Application Unit Source-Term Module

The source-specific input parameters for the land application unit (LAU) scenario include the WMU area, infiltration rate; the ambient recharge rate, the leachate concentration, and the source leaching duration. Together these parameters are used to determine how much contaminant mass enters the subsurface and over what time period.

The source-specific parameters for the LAU scenario are presented in Table 2.4 and are described in the following sections.

2.2.4.2.1 Land Application Unit Area

The land application unit (LAU) area is defined as the footprint of the unit. In EPACMTP, the LAU is modeled as being square, i.e., equal length and width. Thus, the length and width of the LAU are each calculated as the square root of the area. The LAU area is used to determine the area over which the infiltration rate is applied.

2.2.4.2.2 Infiltration and Recharge Rates

The EPACMTP model requires input of the net areal rate of vertical downward percolation of water and leachate through the unsaturated zone to the water table. Infiltration is defined as water percolating through a WMU to the underlying soil, while recharge is water percolating through the soil to the aquifer outside of the footprint of the WMU. The model allows the infiltration rate to be different from the ambient regional recharge rate. The LAU infiltration rate can be different from the ambient recharge rate for a variety of reasons, including the engineering design of the LAU (for instance, a high water content in the land applied sludge), topography, land use, and vegetation. The recharge rate is determined by the regional climatic

Table 2.4 Source-Specific Variables for Land Application Units

| Parameter | Symbol | Units | Section in EPACMTP Parameters/Data Background Document |
|--|---------------|--|---|
| Waste Site Area: the footprint of the LAU (Section 2.2.4.2.1) | A_w | m ² | 2.6.1 |
| Areal Recharge Rate: water percolating through the soil to the aquifer outside of the footprint of the LAU (Section 2.2.4.2.2) | I_r | m ³ /m ² /y or m/y | 4.4 |
| Areal Infiltration Rate: water percolating through the LAU to the underlying soil (Section 2.2.4.2.2) | I | m ³ /m ² /y or m/y | 4.3.3 |
| Leachate Concentration: the concentration of a constituent in the leachate emanating from the base of the LAU (Section 2.2.4.2.3) | C_L | mg/L | 3.2.3 |
| Source Leaching Duration: the duration of the leachate release period (Section 2.2.4.2.4) | t_p | y | 2.6.2 |

conditions, such as precipitation, evapotranspiration, and surface run-off, and regional soil type.

Both infiltration and recharge are specified as areal rates, with the units of cubic meters of fluid (water or leachate) per square meter per year (m³/m²/y or m/y).

Default infiltration and recharge rates for selected soil types at 102 climate stations around the country have been estimated using the HELP water-balance model and are incorporated into a database included in the EPACMTP input files. The default infiltration rate is based on an assumption that 6 inches of waste sludge with 80 percent water is applied on a yearly basis. Further details about how these rates were determined and other options for determining recharge and infiltration rates outside of the EPACMTP model can be found in Section 4.0 of the *EPACMTP Parameters/Data Background Document* (U.S. EPA, 2003).

2.2.4.2.3 Leachate Concentration

The fate and transport model requires stipulation of the leachate concentration as a function of time, $C_L(t)$. The leachate concentration $C_L(t)$ used in the model directly represents the concentration of the leachate emanating from the base of the waste management unit, as a boundary condition for the fate and transport model. For the LAU scenario, the EPACMTP model accounts for this time variation as a constant concentration pulse condition, but it does not attempt to account explicitly for the multitude of physical and biochemical processes inside the waste unit that may control the release of waste constituents. Given the difficulty of accurately predicting

leachate concentration over time as a function of both chemical and waste properties and the intended use of EPACMTP for generic application to a wide range of site conditions and chemical constituents, the parameterization of the source term, and the leachate concentration in particular, is simplified. However, other models can be used to simulate processes not included in EPACMTP (such as biodegradation of organic constituents within the LAU), but considered significant in some land application scenarios. The results of these models can be used as input to the EPACMTP model.

2.2.4.2.4 Source Leaching Duration

The finite source option that is most appropriate for the LAU scenario is the pulse (or non-depleting) source scenario. The boundary condition for the fate and transport model then becomes a constant concentration pulse, with a defined duration. For land application units, the addition and removal of waste (via leaching, biodegradation, etc.) during the operational life usually are more or less balanced, without significant net accumulation of waste. Once waste application ceases at the end of the operational life of the LAU, the leachable waste is expected to be rapidly depleted. Consequently, in the finite source implementation for LAUs, the duration of the leaching period will, in most cases be the same as the operational life of the LAU. The duration of the leaching period may be assigned a constant value or an appropriate frequency distribution.

2.2.4.3 Mathematical Formulation of the Land Application Unit Source-Term Module

By default, the LAU source-term module assumes a constant leachate concentration applied uniformly over the area of the LAU waste unit for a period of time equal to the unit's operating life. EPACMTP requires the user to specify the duration of the leachate pulse, and the leachate concentration of contaminants of concern. The duration of the leachate pulse is equal to or shorter than the unit's operating life.

If not given by a measured value such as the TCLP or SPLP leaching test, the leachate concentration in LAU applied wastes can be estimated from the total waste concentration as:

$$C_L = \frac{C_w}{\left(K_w + \frac{\theta_w}{\rho_{hw}}\right)} \quad (2.28)$$

where

| | | |
|-------------|---|--|
| C_L | = | leachate concentration (mg/L) |
| C_w | = | total waste concentration (mg/kg) |
| K_w | = | waste partition coefficient (cm ³ /g) |
| θ_w | = | water content of the waste (dimensionless) |
| ρ_{hw} | = | density of the waste (g/cm ³) |

For organic constituents, the partition coefficient K_w in the above equation can be determined from the constituent specific organic carbon partition coefficients and the fraction organic carbon in the LAU waste-soil mixing layer:

$$K_w = f_{ocw} \times k_{oc} \quad (2.29)$$

where

| | | |
|-----------|---|--|
| K_w | = | waste partition coefficient (cm ³ /g) |
| f_{ocw} | = | fraction of organic carbon in the soil layer in which the waste is mixed (dimensionless) |
| k_{oc} | = | constituent-specific organic carbon partition coefficient (cm ³ /g) |

A key purpose of many LAU waste management units is to promote degradation of waste constituents by spreading and mixing them with soil, so that most of the constituent mass is consumed between waste application intervals. EPACMTP does not explicitly simulate the resulting variations in leachate concentration, but rather approximates the source as a constant concentration pulse, with duration equal to the WMU's operational life. This approximation may not be protective for constituents (such as metals) which tend to accumulate in the LAU treatment zone, because the residual constituent mass which remains after the end of the units' operational life may continue to act as a source of leachate. In these situations, the effective leachate pulse duration can be determined from mass-balance analysis as:

$$t_p = \frac{t_A \times \dot{m}_w \times C_w}{C_L \times I \times A_w \times 1000} \quad (2.30)$$

where

| | | |
|-------------|---|--|
| t_p | = | duration of leaching period (y) |
| t_A | = | WMU active life (y) |
| \dot{m}_w | = | annual waste mass loading during active life (kg/y) |
| C_w | = | constituent concentration in waste (mg/kg) |
| C_L | = | leachate concentration (mg/L) |
| I | = | infiltration rate (m/y) |
| A_w | = | area of WMU footprint (m ²) |
| 1000 | = | conversion factor used to convert volume from m ³ to liters |

In Equation (2.30), the leachate concentration, C_L , as well as all other variables in the equation are assumed to be unchanged throughout the leaching period. The use of the total applied waste mass in Equation (2.30) assumes no losses other than through leaching which may conservatively overestimate the magnitude of potential exposure of the ground-water pathway.

2.2.5 Limitations on Maximum Infiltration Rate

The EPACMTP source-term module incorporates several checks to ensure that WMU infiltration rate does not result in an unrealistic degree of ground-water mounding. This screening procedure is especially important when EPACMTP is used in Monte-Carlo mode (see Section 5), to provide a safeguard that parameter values drawn randomly from their individual probability distributions, do not result in physically infeasible situations. One such situation can occur when the infiltration rate from the WMU unit is high, and the aquifer underlying the site has a low transmissivity. This could result in an excessive degree of simulated ground-water mounding. Specifically, the EPACMTP source module checks the following conditions:

- Infiltration and recharge so high they cause the water table to rise above the ground surface;
- The top of the water level in an SI unit below the water table, causing flow into the SI; and
- Infiltration rate from an SI exceeds the saturated hydraulic conductivity of the soil underneath.

The logic diagram for the infiltration screening procedure is presented in Figure 2.4; Figure 2.5 provides a graphical illustration of the screening criteria. The numbered criteria checks in Figure 2.4 correspond to the numbered diagrams in Figure 2.5. High infiltration rates are most likely with surface impoundments. Therefore, the screening procedure is the most involved for surface impoundment WMUs.

Figure 2.4(a) depicts the screening procedures for landfills, waste piles, and land application units. For these units, after the WMU infiltration rate, as well as regional recharge rate and values for the primary hydrogeologic parameters (depth to water table, aquifer saturated thickness, aquifer hydraulic conductivity, and regional gradient), have been assigned, either as user input values, or generated by the EPACMTP Monte-Carlo module, EPACMTP calculates the estimated water table mounding that would result from the selected combination of parameter values. The combination of parameters is accepted if the calculated maximum water table elevation (the ground-water 'mound') remains below the ground surface elevation at the site. If the criterion is not satisfied, the selected parameters for the realization are rejected. If the model is used in Monte-Carlo mode, a new set of parameter values is generated, otherwise EPACMTP generates an error message.

For surface impoundments, there are two additional screening steps, as depicted in Figure 2.4(b). EPACMTP first determines whether the base of the impoundment is in direct hydraulic contact with the water table. If the base of the surface impoundment is below the water table, the surface impoundment unit is said to be hydraulically connected to the water table (see Figure 2.5, Criterion 1). The realization is rejected and a new set of hydrogeologic parameters is regenerated if the hydraulically connected surface impoundment is an in seeping type (see Figure 2.5, Criterion 1(b)). As long as the elevation of the waste water surface in the impoundment is

above the water table, and the surface impoundment is an outseeping source (see Figure 2.5, Criterion 1 (a)), the first criterion is passed.

If the base of the unit is located above the water table, the unit is said to be hydraulically separated from the water table (see Figure 2.5, Criterion 2). However, in this case, it is necessary to ensure that the calculated infiltration rate does not exceed the maximum feasible infiltration rate. The maximum feasible infiltration rate is the maximum infiltration that allows the water table to be hydraulically separated from the surface impoundment. In other words, it is the rate that does not allow the crest of the local ground-water mound to be higher than the base of the surface impoundment. This limitation allows EPACMTP to determine a conservative infiltration rate that is based on the free-drainage condition at the base of the surface impoundment. If the water table is allowed to be in hydraulic contact with the base of the surface impoundment, the hydraulic gradient across the bottom of the surface will decrease thereby causing the infiltration rate to decrease accordingly.

EPACMTP calculates the maximum allowable infiltration rate as:

$$I_{Max} \leq \frac{2K_x B(D_u - d_{BG})}{R_0^2 \ln \frac{R_\infty}{R_0}} \quad (2.31)$$

where

| | | |
|------------|---|--|
| I_{Max} | = | maximum allowable infiltration rate (m/y) |
| K_x | = | longitudinal hydraulic conductivity of the saturated zone (m/y) |
| B | = | thickness of the saturated zone (m) |
| D_u | = | thickness of the unsaturated zone (m) |
| d_{BG} | = | depth below grade of the surface impoundment (m) |
| R_0 | = | equivalent source radius (m) |
| R_∞ | = | distance between the center of the source and the nearest downgradient boundary where the boundary location has no perceptible effects on the heads near the source (m). |

Equation (2.31) is based on the Thiem equation for steady-state water level rise in a uniform aquifer with constant infiltration within the equivalent source area (radius = R_0) (see, for instance, Todd, 1959). The equivalent source radius, R_0 , is based on a circular infiltration source. For a rectangular WMU with area A (m^2), EPACMTP calculates the equivalent source radius as:

$$R_0 = \sqrt{\frac{A_w}{\pi}} \quad (2.32)$$

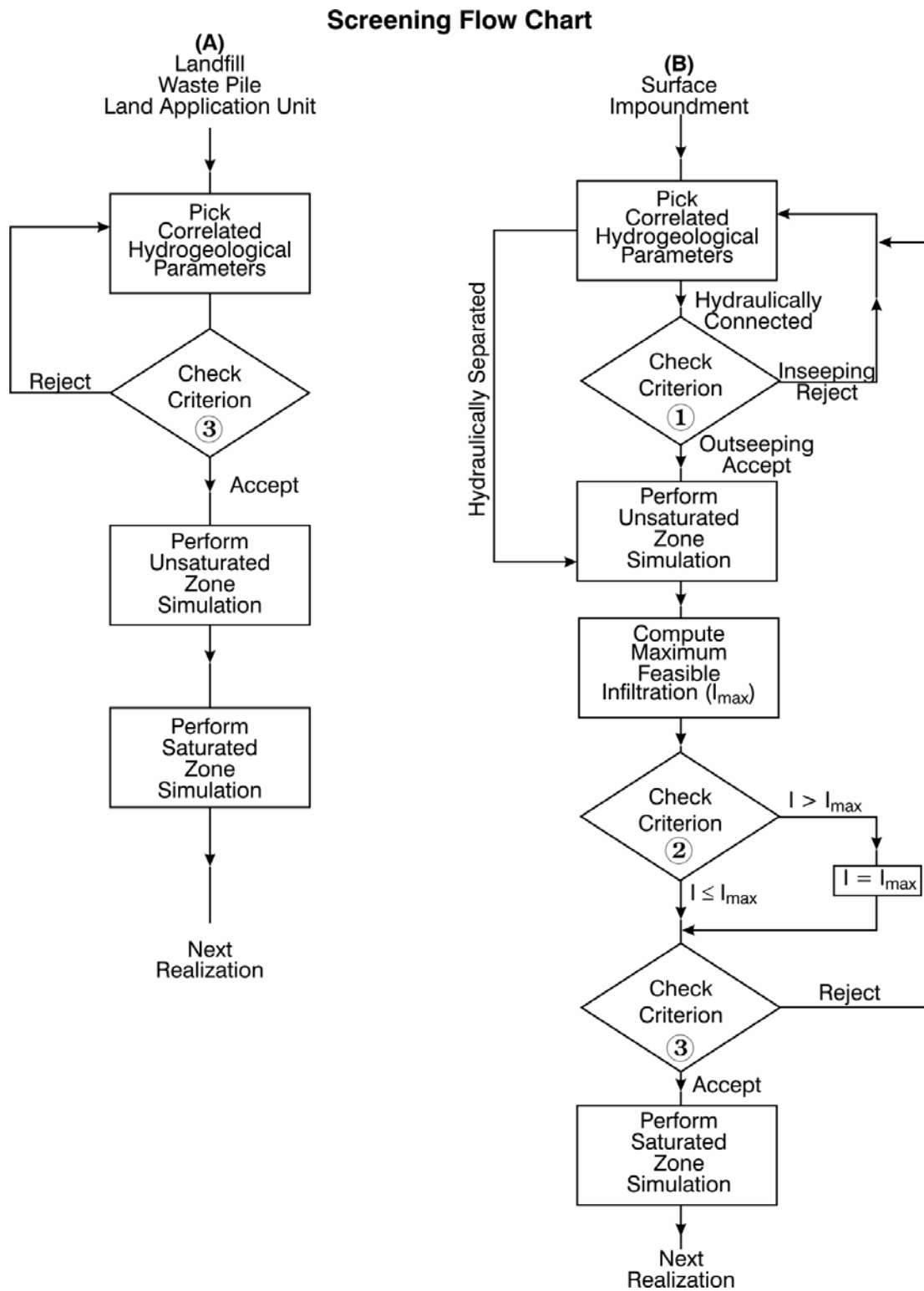
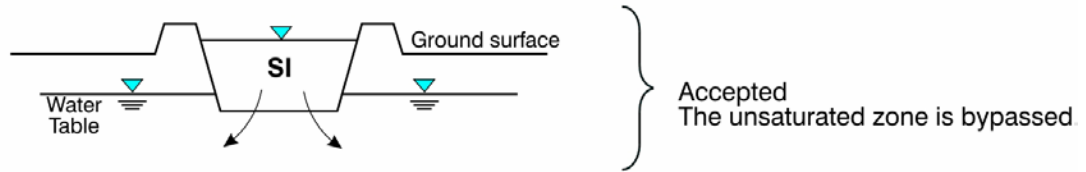


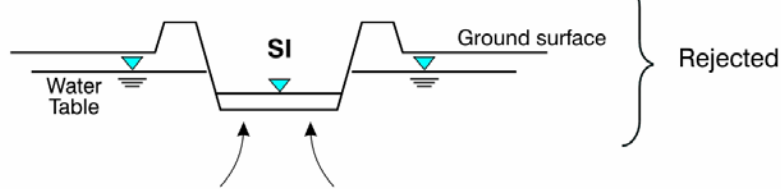
Figure 2.4 Flowchart Describing the Infiltration Screening Procedure.

① Surface impoundment initially hydraulically connected with the saturated zone.

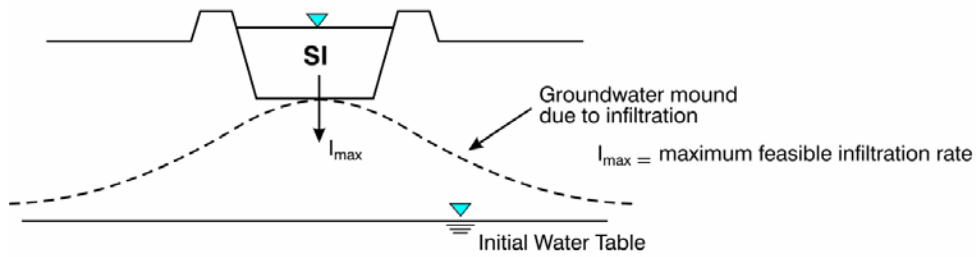
1.a Outseeping SI Unit



1.b Inseeping SI Unit



② Surface impoundment initially hydraulically separated from the saturated zone.



③ Feasible criterion for all WMU types.

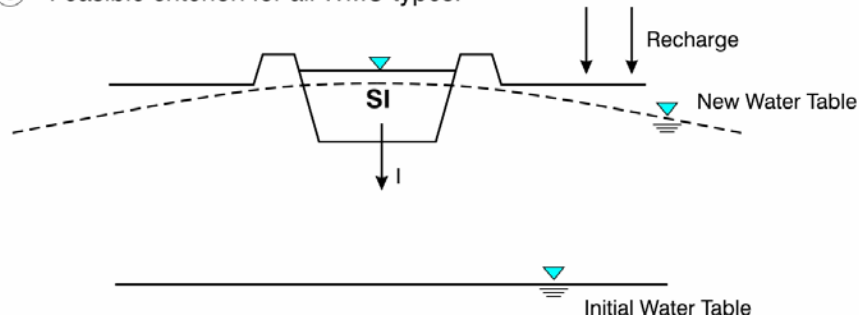


Figure 2.5 Infiltration Screening Criteria.

where

$$\begin{aligned} R_o &= \text{equivalent source radius (m)} \\ A_w &= \text{area of WMU footprint (m}^2\text{)} \end{aligned}$$

The distance to the nearest downgradient boundary location, R_{∞} , is normally the nearest surface water body located along one of the streamlines traversing WMU. The implied assumption is that the water level in this surface water body is in hydraulic equilibrium with the ground-water level, and the surface water body is not affected by the infiltration of water from the WMU.

For surface impoundments, Criterion 2 is used to cap the infiltration rate at I_{\max} .

Once Criteria 1 and 2 are passed, the combination of infiltration rate, recharge rate, and primary hydrogeologic parameters is used to estimate water table mounding elevation. As for LFs, LAUs, and WPs, Criterion 3 is passed if the calculated maximum ground-water elevation is below the ground surface elevation at the site.

This page was intentionally left blank.

3.0 UNSATURATED-ZONE MODULE

3.1 PURPOSE OF THE UNSATURATED-ZONE MODULE

The unsaturated-zone module simulates vertical water flow and solute transport through the unsaturated zone above an unconfined aquifer. Since one of the primary intended uses of the module is for Monte-Carlo uncertainty analysis, the flow and transport routines in this module are designed for optimal computational efficiency.

The unsaturated zone is based on the Finite-Element Contaminant Transport in the Unsaturated Zone (FECTUZ) code (U.S. EPA, 1989). The FECTUZ code is designed to simulate vertically downward steady-flow and contaminant transport through the unsaturated zone above an unconfined aquifer. FECTUZ is based on the EPA's numerical unsaturated-zone simulator, VADOse zone Flow and Transport code (VADOFT) (Huyakorn and Buckley, 1987), but with extensions and enhancements to optimize the computational efficiency for Monte-Carlo analyses (McGrath and Irving, 1973) and to handle multi-species decay chains. The FECTUZ code was reviewed by the EPA's Science Advisory Board in 1988 (SAB, 1988).

The module consists of a number of solution schemes which solve the flow and transport equations governing fate and transport of contaminants in the unsaturated zone. The general simulation scenario for which the module was designed is depicted schematically in Figure 3.1. This figure shows a vertical cross-section through the unsaturated zone underlying a waste management unit (WMU; e.g., landfill, surface impoundment, waste pile, or land application unit). Contaminants migrate downward from the WMU, through the unsaturated zone to an unconfined aquifer with a water table present at some depth. The module simulates the unsaturated zone in between the base of the WMU and the water table. Inputs are the rate of water and contaminant leakage from the WMU, as well as soil and contaminant properties. The primary output is the contaminant concentration entering the saturated zone at the water table, either as a function of time (transient simulation) or at steady-state. The transient or steady-state contaminant concentration at the water table provides the source term for the saturated-zone module.

The assumptions used in deriving the flow and transport solutions are detailed in Sections 3.2.2 and 3.3.2, but the most important assumptions are summarized below.

- Flow and transport are one-dimensional, in the downward vertical direction.
- Flow and transport are driven by seepage from a WMU, which is assumed to occur at a constant rate.

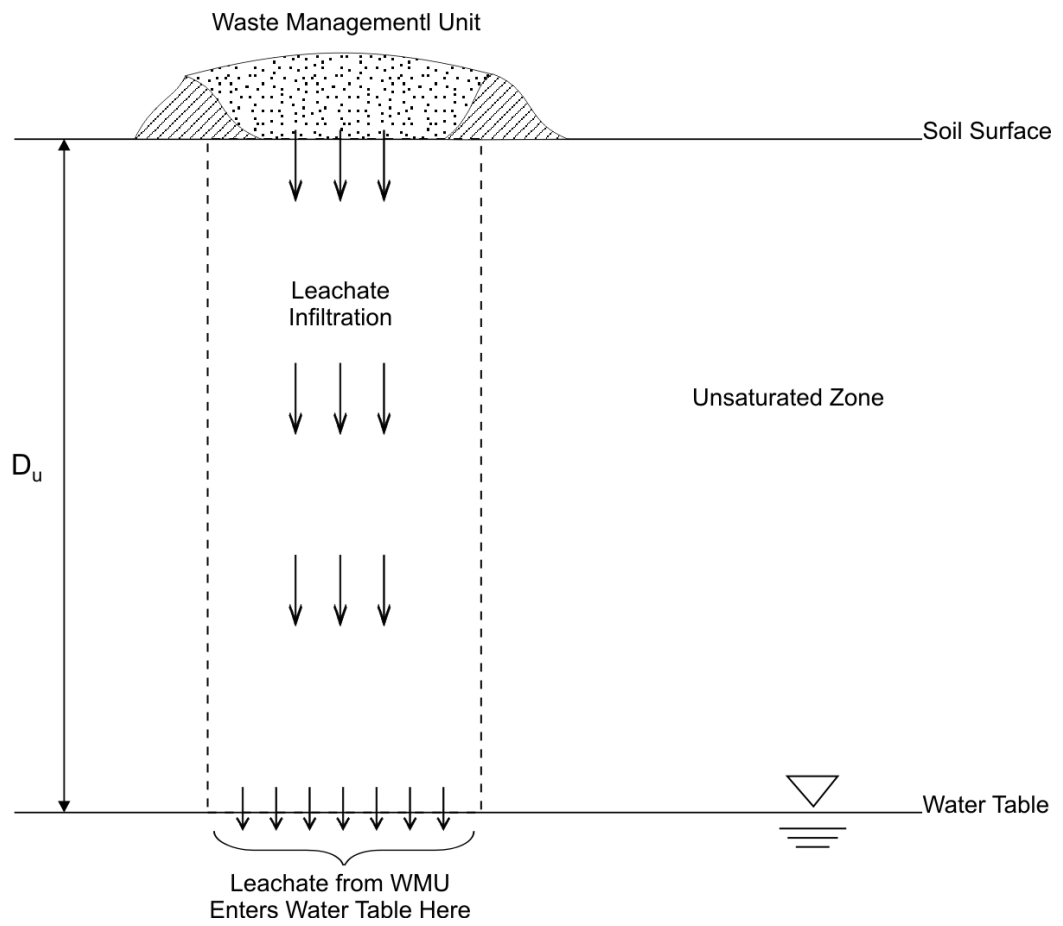


Figure 3.1 Cross-sectional View of the Unsaturated Zone Considered by EPACMTP.

-
- Flow is always at steady state, while either transient or steady-state solute transport simulations can be performed.
 - The unsaturated zone comprises a soil with a single uniform layer.

3.2 UNSATURATED-ZONE FLOW SUBMODULE

3.2.1 Description of the Unsaturated-zone Flow Submodule

A schematic view of the one-dimensional system simulated by the unsaturated-zone module is provided in Figure 3.1. In order to simulate flow in the unsaturated zone between the base of the waste management facility and water table, the following data are required:

- Thickness of the unsaturated zone (depth to water table from base of WMU).
- Soil hydraulic parameters. If these parameters are not available, but the soil type is known, the parameter values from the database of Carsel and Parrish (1988) are suggested. Parametric distributions based on these databases are incorporated into the EPACMTP model; however, site-specific values can be used, if available.
- The water flow rate (infiltration rate) through the WMU. The user can assign infiltration rates for landfills, waste piles, and land application units from the long term net percolation rate (precipitation minus runoff minus evapotranspiration). However, infiltration rates for selected soil types at cities around the country estimated using the HELP water-balance model are incorporated into the nationwide databases for these WMUs that are distributed with EPACMTP (see Sections 2.2.1.2.6, 2.2.2.3.2, 2.2.3.2.2, and 2.2.4.2.2). For surface impoundments, the code is capable of estimating the infiltration rate from the characteristics of the impoundment and the soil column, D_u , as shown in Figure 3.1 (see also Section 2.2.2.3.1).

3.2.2 Assumptions Underlying the Unsaturated-zone Flow Submodule

The most important assumptions and limitations incorporated in the unsaturated-zone flow model are described below:

- Flow of the fluid phase is one-dimensional, isothermal and governed by Darcy's law.
- The air phase is assumed to be immobile, and no volatilization occurs.
- The fluid considered is slightly compressible and homogeneous.
- Flow of water is always steady.

- Effects of hysteresis in soil constitutive relations (relations between water content and pressure head, and between water content and relative permeability) are negligible.
- The soil is an incompressible porous medium which does not contain fractures or macro pores. The module in EPACMTP assumes only one layer in the unsaturated zone for LFs, LAUs, and WPs. For surface impoundment units, a layer of consolidated sediment at the base of the impoundment on top of the unsaturated zone may be modeled. Underneath the consolidated sediment layer, a layer of the unsaturated-zone soil with decreased hydraulic conductivity due to clogging by the invading suspended solids may also be modeled.
- Flow of water is not affected by the presence of dissolved chemicals.

3.2.3 List of the Parameters for the Unsaturated-zone Flow Submodule

The unsaturated-zone-specific input parameters for the ground-water flow module include parameters to characterize the flow regime in the unsaturated zone in the vicinity of the waste management unit. These unsaturated-zone flow parameters, together with the transport parameters described in Section 3.3.3, are used to determine the advective-dispersive transport (in the vertical direction) of dissolved contaminants through the soil to the water table. These unsaturated-zone-specific parameters for the ground-water flow module are presented below in Table 3.1.

Table 3.1 Parameters for the Unsaturated-zone Flow Submodule

| Parameter | Symbol | Units | Section in EPACMTP Parameters/ Data Background Document |
|--|------------|--|---|
| Saturated hydraulic conductivity: a measure of the soil's ability to transmit water under fully saturated conditions (Section 3.2.3.3) | K_s | cm/hr in input file; m/y in output file | 5.2.3.1 |
| Residual water content: the water content at which no additional water will flow (Section 3.2.3.1) | θ_r | unitless | 5.2.3.4 |
| Saturated water content: the fraction of the total volume of the soil that is occupied by water contained in the soil (Section 3.2.3.1) | θ_s | unitless | 5.2.3.5 |
| van Genuchten parameter (α): soil-specific shape parameter that is obtained from an empirical relationship between pressure head and volumetric water content (Section 3.2.3.1) | α | 1/cm in input file; 1/m in output file | 5.2.3.2 |

Table 3.1 Parameters for the Unsaturated-zone Flow Submodule (continued)

| Parameter | Symbol | Units | Section in EPACMTP Parameters/ Data Background Document |
|---|---------|----------|---|
| van Genuchten parameter (β): soil-specific shape parameter that is obtained from an empirical relationship between pressure head and volumetric water content (Section 3.2.3.1) | β | unitless | 5.2.3.3 |
| Unsaturated-zone thickness: regional average depth to the water table (Section 3.2.3.2) | D_u | m | 5.2.1 |

3.2.3.1 Soil Characteristic Curve Parameters

In unsaturated flow, the pore water is under a negative pressure head caused by capillary pressure within the pore space. The relationship between pressure head and water content for a particular soil is known as a soil-water characteristic curve, the other characteristic curve needed to solve unsaturated-zone flow is the relationship between hydraulic conductivity and water saturation.

The van Genuchten (1980) model is used for modeling soil-water content as a function of pressure head.

According to the van Genuchten model, the water content-pressure head relation is given by

$$\theta = \theta_r + (\theta_s - \theta_r) [1 + (-\alpha\psi)^\beta]^{-\gamma} \quad \begin{matrix} \psi < 0 \\ \theta = \theta_s \end{matrix} \quad \psi \geq 0 \quad (3.1)$$

or

$$S_e = \frac{\theta - \theta_r}{\theta_s - \theta_r} = [1 + (-\alpha\psi)^\beta]^{-\gamma} \quad \begin{matrix} \psi < 0 \\ \psi \geq 0 \end{matrix} \quad (3.2)$$

where

- θ = soil water moisture content (dimensionless)
- θ_r = residual soil water content (dimensionless)
- θ_s = saturated soil water content (dimensionless)
- α = van Genuchten soil-specific shape parameter (1/m)

| | | |
|----------|---|---|
| ψ | = | soil pressure head (m) |
| β | = | van Genuchten soil-specific shape parameter (dimensionless) |
| γ | = | a β -dependent soil-specific shape parameter = $1-1/\beta$ (dimensionless) |
| S_e | = | effective saturation (dimensionless) |

Parameters β and γ in Equation (3.1) are related through $\gamma = 1-1/\beta$, and in practice only the parameters α and β are specified.

At atmospheric pressure head ($\psi = 0$), the soil is saturated, with the water content equal to θ_s . The saturated water content (θ_s) represents the maximum fraction of the total volume of soil that is occupied by the water contained in the soil. The soil will remain saturated as the pressure head is gradually decreased. Eventually, the pressure head will become sufficiently negative to where water can drain from the soil. This pressure head is known as the bubbling pressure. The moisture content will continue to decline as the pressure head is lowered, until it reaches some irreducible residual water content (θ_r). Should the pressure head be further reduced, the soil would not lose any additional moisture.

The unsaturated hydraulic conductivity is indirectly determined using the relative permeability which, for water, is defined as the ratio of unsaturated soil hydraulic conductivity over saturated hydraulic conductivity of the same soil. The relative permeability as a function of the effective saturation is given by the Mualem-van Genuchten model (van Genuchten, 1980):

$$k_{rw} = S_e^2 \left[1 - \left(1 - S_e^{\frac{1}{\alpha}} \right)^\gamma \right]^2 \quad (3.3)$$

where

| | | |
|----------|---|---|
| k_{rw} | = | relative permeability (dimensionless) |
| S_e | = | effective saturation (dimensionless) |
| α | = | van Genuchten soil-specific shape parameter (1/m) |
| β | = | van Genuchten soil-specific shape parameter (dimensionless) |
| γ | = | a β -dependent soil-specific shape parameter = $1-1/\beta$ (dimensionless) |

Relative permeabilities depend on the characteristics of the soil, the wettability characteristics, and the surface tension of the wetting fluid (in this case, water).

3.2.3.2 Thickness of the Unsaturated Zone

The unsaturated-zone thickness, or depth to the water table, for each waste site can be specified as a single value or distribution of values or it can be obtained from the regional hydrogeologic data base. In the latter case, based on a site's geographic location, the corresponding hydrogeologic region is selected. In a Monte-Carlo simulation, the unsaturated-zone thickness is selected randomly from data available for that hydrogeologic region.

3.2.3.3 Saturated Hydraulic Conductivity

The hydraulic conductivity of the soil is a measure of the soil's ability to transmit water under fully saturated conditions. It is used as an input to the unsaturated zone flow module and is used to calculate the moisture content in the soil under a given rate of leachate infiltration from the WMU. Details relating to the available data for this parameter are presented in U.S. EPA (2003).

3.2.4 Mathematical Formulation of the Unsaturated-zone Flow Submodule

The steady-state flow module of EPACMTP simulates steady downward flow to a water table. The governing equation is given by Darcy's law below (Bear, 1972):

$$I = -K_s k_{rw} \left(\frac{d\psi}{dz_u} - 1 \right) \quad (3.4)$$

where

| | | |
|----------|---|--|
| I | = | infiltration rate (m/y) |
| K_s | = | saturated hydraulic conductivity (m/y) |
| k_{rw} | = | relative permeability (dimensionless) |
| ψ | = | soil pressure head (m) |
| z_u | = | depth coordinate which is taken positive downward from the base of a WMU (m) |

The boundary condition at the water table is

$$\psi_\ell = 0 \quad (3.5)$$

where

| | | |
|-------------|---|--|
| ψ_ℓ | = | pressure head at the water table located at distance ℓ from the bottom of a waste management unit (m) |
|-------------|---|--|

Solution of Equation (3.4) requires stipulation of the relationships between relative permeability and water content and between water content and pressure head. The permeability-water content relation $k_{rw}(\theta)$ is assumed to follow the Mualem-van Genuchten model described above.

3.2.5 Solution Method for Flow in the Unsaturated Zone

As a first step in the solution of Equation (3.4), the soil constitutive relations in Equations (3.1, 3.2, and 3.3) are combined, leading to the following expression for the $k_{rw}(\psi)$ relation

$$k_{rw} = \begin{cases} 1 & \psi \geq 0 \\ \frac{1 - (-\alpha\psi)^{\beta-1} [1 + (-\alpha\psi)^{\beta}]^{-\gamma}}{[1 + (-\alpha\psi)^{\beta}]^{\frac{\gamma}{2}}} & \psi < 0 \end{cases} \quad (3.6)$$

where

| | | |
|----------|---|--|
| k_{rw} | = | relative permeability (dimensionless) |
| α | = | van Genuchten soil-specific shape parameters (1/m) |
| ψ | = | the soil pressure head (m) |
| β | = | van Genuchten soil-specific shape parameter (dimensionless) |
| γ | = | a β -dependent soil-specific shape parameter = $1 - 1/\beta$ (dimensionless) |

Next, Equation (3.6) is substituted into Equation (3.4) and the derivative replaced by a backward finite-difference approximation (Huyakorn and Pinder, 1983). This results, after some rearranging, in

$$F(\psi) = \begin{cases} \frac{K_u}{l} \left\{ \frac{\psi_{z_u - \Delta z_u} - \psi_{z_u}}{\Delta z_u} + 1 \right\} - 1 = 0 & \bar{\psi} \geq 0 \\ \frac{K_s}{l} \left\{ \frac{1 - (-\alpha\bar{\psi})^{\beta-1} [1 + (-\alpha\bar{\psi})^{\beta}]^{-\gamma}}{[1 + (-\alpha\bar{\psi})^{\beta}]^{\frac{\gamma}{2}}} \left\{ \frac{\psi_{z_u - \Delta z_u} - \psi_{z_u}}{\Delta z_u} \right\} + 1 \right\} - 1 = 0 & \bar{\psi} < 0 \end{cases} \quad (3.7)$$

where

| | | |
|--------------|---|---|
| $F(\psi)$ | = | function F of ψ |
| K_u | = | soil hydraulic conductivity of pressure ψ (m/y) |
| | = | $K_s \cdot k_{rw}$ |
| K_s | = | saturated hydraulic conductivity (m/y) |
| k_{rw} | = | relative permeability (dimensionless) |
| l | = | infiltration rate (m/y) |
| z_u | = | depth coordinate which is taken positive downward from the base of a WMU (m) |
| ψ_{z_u} | = | soil pressure head (m) at z_u |
| Δz_u | = | grid size along the z_u direction (m) |
| $\bar{\psi}$ | = | effective pressure head for the soil layer between z and $z_u - \Delta z_u$ (m) |
| α | = | van Genuchten soil-specific shape parameter (1/m) |
| β | = | van Genuchten soil-specific shape parameter (dimensionless) |
| γ | = | $1 - 1/\beta$ (dimensionless) |

The parameter $\bar{\psi}$ can be written as a weighted average of ψ_{z_u} and $\psi_{z_u - \Delta z_u}$.

$$\bar{\psi} = \omega \psi_{z_u - \Delta z_u} + (1 - \omega) \psi_{z_u} \quad (3.8)$$

where

| | | |
|--------------|---|---|
| $\bar{\psi}$ | = | effective pressure head for the soil layer between z and $z_u - \Delta z_u$ (m) |
| ω | = | weighting factor, $0 \leq \omega \leq 1$ (dimensionless) |
| ψ | = | soil pressure head (m) |
| ψ_{z_u} | = | soil pressure head (m) at z_u |
| Δz_u | = | grid size in the z_u direction (m) |

Analysis of a number of example problems showed that optimal results, in terms of accuracy and rate of convergence, are achieved when ω , which corresponds to an upstream-weighted approximation, is set to 1.0.

Using Equations (3.7 and 3.8) together with the lower boundary condition (Equation (3.5)), allows $\psi_{z_u - \Delta z_u}$ to be solved. This value for $\psi_{z_u - \Delta z_u}$ is then used in the place of ψ_{z_u} in Equations (3.7 and 3.8) and the equation is solved for the pressure head at the next desired distance upward from the water table in this sequential manner, the pressure head at any depth in the unsaturated zone can be computed. A combined Newton-Raphson and bi-section method is used to solve the nonlinear root-finding problem (Equation (3.7)).

After the pressure head distribution in the unsaturated zone has been found, the corresponding water content distribution $\theta(z_u)$, is computed using Equation (3.1). In principle, the saturation distribution can be found without first solving for $\psi(z_u)$ by substituting Equation (3.3) rather than Equation (3.6) into Equation (3.8). The disadvantage of this approach is that it becomes more difficult to accommodate layered soils. Whereas the ψ -profile is continuous in the unsaturated zone, the θ -profile is discontinuous at the interface of soil layers with contrasting hydraulic properties. A θ -based solution also cannot handle saturated or partially saturated conditions.

Unsaturated-zone Discretization. Solution of the steady-state flow equation requires discretization of the unsaturated zone into a number of one-dimensional segments of finite thickness. These segments are similar to elements in the finite element method. Optimized for computational efficiency, the unsaturated-zone module will perform the discretization automatically in a manner which ensures a fine discretization in regions where the water content changes rapidly with depth and a coarser discretization in regions with constant water content. A typical steady-state saturation profile for a homogeneous soil is shown in Figure 3.2. This figure shows that the saturation is essentially constant throughout much of the unsaturated zone, and varies significantly only in a relatively narrow zone above the water table. To accurately but efficiently represent this saturation profile, a fine discretization is required only close to the water table (or close to layer interfaces for layered soils). Previous verification work of the unsaturated-zone module (U.S. EPA, 1996b)

suggests that for single-layer soils, an accurate discretization requires no more than 5 to 6 points. The discretization algorithm used in the semi-analytical flow module is based on this principle.

3.3 UNSATURATED-ZONE SOLUTE TRANSPORT SUBMODULE

3.3.1 Description of the Unsaturated-zone Transport Submodule

A schematic view of the one-dimensional system simulated by the unsaturated-zone module is provided in Figure 3.1. In order to simulate contaminant transport in the unsaturated zone between the base of the WMU and water table, the following data are required:

- Soil transport parameters. If not available, the dispersivity can be estimated from the unsaturated-zone thickness, and, for organics, the retardation and decay coefficients can be estimated from the soil bulk density, fraction of organic matter and chemical-specific properties.
- The leachate concentration emanating from the base of the waste site. If a finite source is being simulated, the duration of the pulse must be specified (or internally derived in the case of landfills).
- The number of component species and decay reaction stoichiometry, in the case of chain decay reactions.
- Organic carbon partition coefficient (k_{oc}) for organic chemicals and the effective distribution coefficient (K_d), as a function of concentration, in the case of metals with nonlinear sorption.

The transport submodule can simulate the effects of both linear and nonlinear sorption reactions, as well as first-order decay reactions. When decay reactions involve the formation of hazardous degradation products, it has the capability to perform a multi-species transport simulation of a decay chain consisting of up to seven members. Decay reaction paths can be represented by either straight or branched decay chains.

3.3.2 Assumptions Underlying the Unsaturated-zone Transport Submodule

The most important assumptions and limitations incorporated in the unsaturated-zone transport model are described below:

- Only the transport of chemicals in the aqueous phase is considered.
- Advection and dispersion are one-dimensional.
- Fluid properties are independent of concentrations of contaminants.

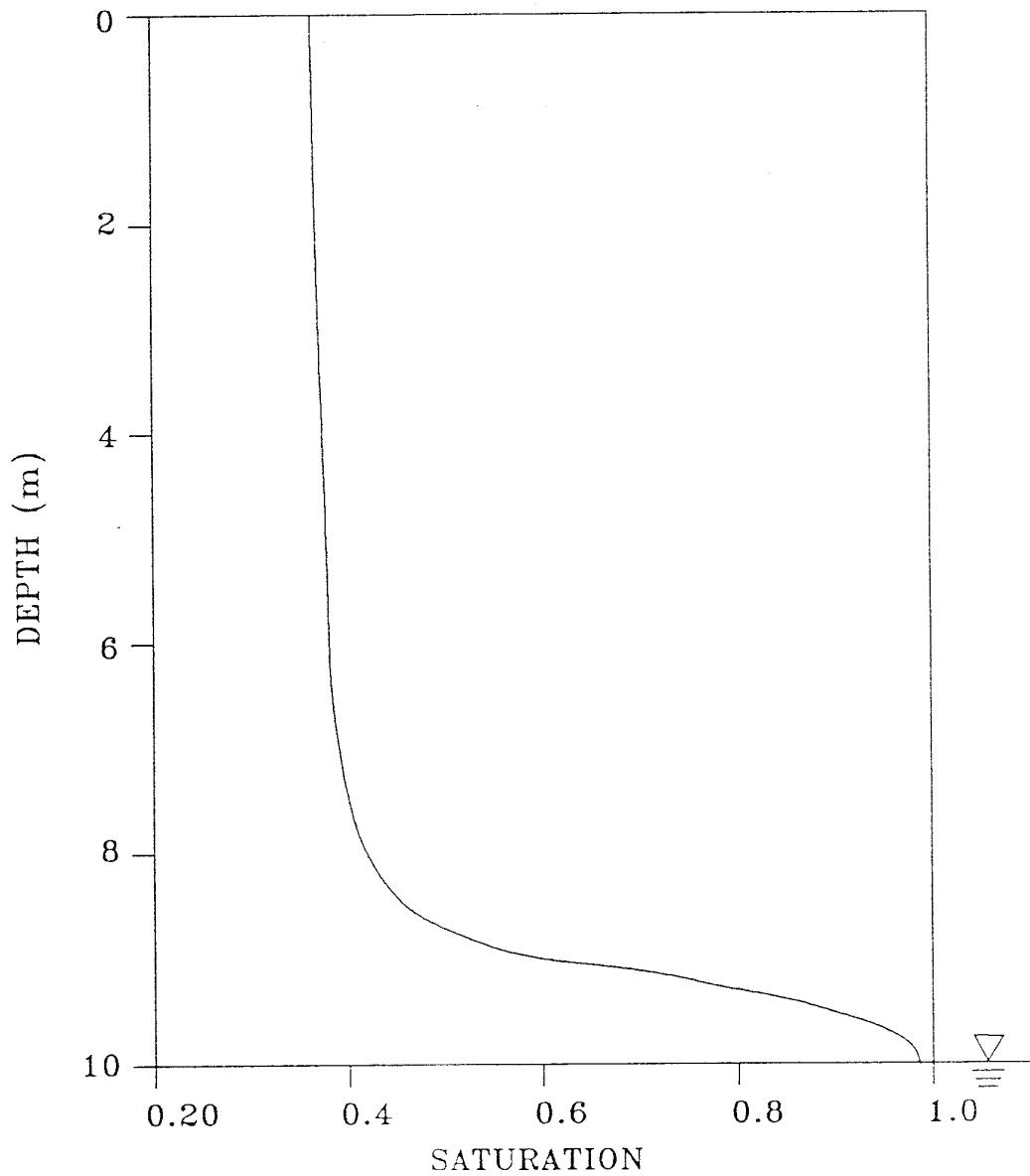


Figure 3.2 Typical Saturation Profile for a Homogeneous Soil under Steady Infiltration Conditions. The Water Table Is Located at $Z_u = 10$ m.

- Diffusive/dispersive transport in the porous medium system is governed by Fick’s law. The hydrodynamic dispersion coefficient is defined as the sum of the coefficients of mechanical dispersion and molecular diffusion.
- Sorption reactions can be described by a linear or non-linear Freundlich equilibrium isotherm.
- The effects of biological and chemical decay can be described by first-order degradation and zero-order production reactions.
- The soil can be modeled as a layered uniform porous medium.

3.3.3 List of Parameters for the Unsaturated-zone Transport Submodule

The unsaturated-zone-specific input parameters for the transport module include parameters to characterize ground-water transport in the unsaturated zone in the vicinity of the waste management unit. These unsaturated-zone transport parameters, together with the ground-water flow parameters described in Section 3.2.3, are used to determine the advective-dispersive transport (in the vertical direction) of dissolved contaminants through the soil to the water table. These unsaturated-zone-specific parameters for the ground-water transport module are presented below and summarized in Table 3.2.

The ground-water temperature and pH for the unsaturated zone are not inputs to the EPACMTP model. The model assumes that these values are the same as those input or generated for the saturated zone. The assumed temperature and pH for the unsaturated zone are used to calculate the overall hydrolysis rate for organics from the temperature- and pH-dependent hydrolysis rate constants.

Table 3.2 Parameters for the Unsaturated-zone Transport Submodule

| Parameter | Symbol | Units | Section in EPACMTP Parameters/Data Background Document |
|---|---------------|--------------------|--|
| Longitudinal dispersivity: The characteristic length of longitudinal dispersion (Section 3.3.3.1) | α_{Lu} | m | 5.2.4 |
| Percent organic matter: The percent organic matter in the soil (Section 3.3.3.2) | %OM | unitless | 5.2.3.7 |
| Soil bulk density: The ratio of the mass of the solid soil to its total volume (Section 3.3.3.3) | ρ_{bu} | g/cm ³ | 5.2.3.6 |
| Freundlich Sorption Coefficient: A constant used with the aqueous concentration to determine the adsorption isotherm according to the Freundlich model (Section 3.3.3.4) | K_d | cm ³ /g | 5.2.5.1 |

Table 3.2 Parameters for the Unsaturated-zone Transport Submodule
(continued)

| Parameter | Symbol | Units | Section in EPACMTP Parameters/Data Background Document |
|--|----------------|--------------------|--|
| Freundlich Isotherm Exponent: the exponent to which the aqueous concentration is raised in the determination of the adsorption isotherm according to the Freundlich model; when the adsorption isotherm is linear, this exponent is one (Section 3.3.3.5) | η | unitless | 5.2.5.2 |
| Metals Sorption Coefficient: The non-linear, non-Freundlich type sorption isotherm for metals (Section 3.3.3.6) | K_d | cm ³ /g | 3.3.3 and 5.2.5.1 |
| Chemical transformation coefficient: EPACMTP accounts for biochemical transformation processes using a lumped first-order decay coefficient (Section 3.3.3.7) | λ_{cu} | 1/y | 5.2.6 |
| Biological transformation coefficient: EPACMTP accounts for biological transformation processes using a lumped first-order decay coefficient (Section 3.3.3.7) | λ_{bu} | 1/y | 5.2.7 |
| Molecular diffusion coefficient: EPACMTP accounts for chemical-specific molecular diffusion (Section 3.3.3.8) | D_i | m ² /y | 3.3.1.1 |
| Molecular Weight: EPACMTP accounts for concentrations of degradation products using stoichiometry (Section 3.3.3.9) | MW | g | 3.3.1.3 |
| Ground-water Temperature: average temperature of the unsaturated zone, used to derive hydrolysis rates for degrading organic constituents (Section 3.3.3.10) | T | °C | 5.2.8 |
| Ground-water pH: average regional ground-water pH, assuming that pH is not influenced by the addition of leachate from the WMU or changes in temperature, used to derive hydrolysis rates for degrading organic constituents and can be used to calculate sorption of metals (Section 3.3.3.11) | pH | std. units | 5.2.9 |

3.3.3.1 Longitudinal Dispersivity

Dispersion is caused by contaminants encountering heterogeneities in the soil, resulting in differing travel distances. These differing travel distances in turn cause some of the contaminants to arrive sooner and some to arrive later at the water table

than would occur by advection alone. Dispersion along the flow direction is characterized by a characteristic length called longitudinal dispersivity.

The longitudinal dispersivity of the soil (measured in the direction of flow, that is, vertically downward) can be input as a distribution or it may be derived by EPACMTP. If derived, it is computed as a linear function of the total depth of the unsaturated zone using

$$\alpha_{Lu} = 0.02 + 0.022 D_u \quad (3.9)$$

where

$$\begin{aligned} \alpha_{Lu} &= \text{longitudinal dispersivity for the unsaturated zone (m)} \\ D_u &= \text{total depth of the unsaturated zone (m)} \end{aligned}$$

Equation (3.9) is based on a regression analysis of data presented by Gelhar et al. (1985).

3.3.3.2 Percent Organic Matter

EPACMTP uses the average percent organic matter in the soil to determine the retardation of organic constituents. The percent organic matter is converted internally by EPACMTP to fractional organic carbon content through the following equation (Enfield et al., 1982):

$$f_{oc} = \frac{\%OM}{174} \quad (3.10)$$

where

$$\begin{aligned} f_{oc} &= \text{fractional organic carbon content (dimensionless)} \\ \%OM &= \text{percent organic matter (dimensionless)} \end{aligned}$$

Once the fractional organic carbon content is obtained, the linear distribution coefficient can be found using:

$$K_d = k_{oc} f_{oc} \quad (3.11)$$

where

$$\begin{aligned} K_d &= \text{distribution coefficient (cm}^3\text{/g)} \\ k_{oc} &= \text{normalized organic carbon partition coefficient (cm}^3\text{/g)} \\ f_{oc} &= \text{fractional organic carbon content (dimensionless)} \end{aligned}$$

Equation (3.11) is based on the assumption that hydrophobic binding dominates the sorption process (Karickhoff, 1985).

3.3.3.3 Soil Bulk Density (ρ_{bu})

The dry soil bulk density (mass of soil per unit volume) is used to calculate the retardation coefficient of organic constituent and convert soil mass to volume.

3.3.3.4 Freundlich Sorption Coefficient (Distribution Coefficient)

For organic constituents, EPACMTP version 2.0 only allows using a linear Freundlich isotherm to describe the constituent's sorption behavior. In this case, the leading Freundlich coefficient is known as the solid-liquid phase distribution coefficient (K_d). The distribution coefficient may be specified directly or as a derived parameter. In the latter case, it is computed through Equation (3.11) from the fraction organic carbon (f_{oc}) and the organic carbon partition coefficient (k_{oc}). Additionally, if K_d is derived, f_{oc} is internally calculated from the percent organic matter specified in the unsaturated-zone-specific input group according to Equation (3.10), and the k_{oc} is specified in the chemical-specific input group.

For metals that are modeled using MINTEQA2-derived isotherms or pH-dependent empirical isotherms, the K_d data is either read in from an auxiliary input file or internally calculated based on the ground-water pH. In both cases, the Freundlich isotherm coefficient is not used; see Section 3.3.3.6 below. Alternatively, metals can be modeled using an empirical distribution of distribution coefficients (e.g., based on reported K_d values in the scientific literature).

3.3.3.5 Freundlich Isotherm Exponent

For organic constituents, EPACMTP version 2.0 only allows using a linear Freundlich isotherm to describe the constituent's sorption behavior. That is, the Freundlich isotherm exponent (n) must be set equal to 1.0. If this parameter is omitted from the input data file, it is assigned a default value of 1.0, which is equivalent to specifying a linear sorption isotherm.

For metals that are modeled using MINTEQA2-derived isotherms or pH-dependent empirical isotherms, the K_d data is either read in from an auxiliary input file or internally calculated based on the ground-water pH. In both cases, the Freundlich isotherm exponent is not used; see Section 3.3.3.6 below.. Alternatively, metals can be modeled using an empirical distribution of distribution coefficients (e.g., based on reported K_d values in the scientific literature); in this case, the Freundlich isotherm exponent should be set to its default value of 1.0.

3.3.3.6 Sorption Coefficient for Metals

In the subsurface, metal constituents may undergo reactions with ligands in the pore water and with surface sites on the soil or aquifer matrix material. Reactions in which the metal is bound to the solid matrix are referred to as sorption reactions. In EPACMTP, users can specify a metal sorption coefficient (K_d) as:

- a constant value (a linear isotherm) from an empirical distribution, or
- a pH-dependent linear isotherm, or
- a non-linear isotherm.

pH-dependent linear isotherms can be determined from metal-specific pH-based empirical relationships. Non-linear isotherms were generated using a metal speciation model, MINTEQA2, as functions of five primary geochemical variables: pH, hydrous ferric oxide absorbent content, natural organic matter content, leachate organic acid concentration, and carbonate level in the ambient ground water. These non-linear isotherm functions are typically available in a tabulated form read in from an external data file.

Further details of metals sorption coefficients can be found in Section 3.3.3 of the *EPACMTP Parameters/Data Background Document* (U.S. EPA, 2003).

3.3.3.7 Chemical and Biological Transformation Coefficients

EPACMTP accounts for biochemical transformation processes using a lumped first-order decay coefficient. The overall decay coefficient is the sum of the chemical and biological transformation coefficients.

$$\lambda_u = \lambda_{cu} + \lambda_{bu} \quad (3.12)$$

where

| | | |
|----------------|---|---|
| λ_u | = | overall decay coefficient (first-order transformation) (1/y) |
| λ_{cu} | = | transformation coefficient due to chemical transformation (1/y) |
| λ_{bu} | = | transformation coefficient due to biological transformation (1/y) |

The coefficients λ_{cu} and λ_{bu} are specified in the EPACMTP data input file, either as constants or as a distribution. By default, λ_{bu} is set to zero and λ_{cu} is a derived parameter, in which case it is calculated from the chemical-specific hydrolysis constants:

$$\lambda_{cu} = \frac{\lambda_1 \theta + \lambda_2 \rho_b K_d}{\theta + \rho_b K_d} \quad (3.13)$$

where

| | | |
|----------------|---|--|
| λ_{cu} | = | transformation coefficient due to chemical transformation (1/y) |
| λ_1 | = | hydrolysis constant for dissolved phase (1/y) |
| θ | = | soil water content (dimensionless) |
| λ_2 | = | hydrolysis constant for sorbed phase (1/y) |
| ρ_b | = | bulk density of the porous media (g/cm ³) |
| K_d | = | liquid-solid phase distribution coefficient (cm ³ /g) |

The hydrolysis constants (λ_1 and λ_2) may be temperature and pH dependent. In EPACMTP, the unsaturated-zone module uses the same ground-water temperature and pH values as those generated for the saturated zone.

3.3.3.8 Molecular Diffusion Coefficient

EPACMTP accounts for molecular diffusion as part of hydrodynamic dispersion. For a given solute species i , its free-water molecular diffusion coefficient D_i along with tortuosity given by Millington and Quirk (1961) are used to determine the constituent's effective molecular diffusion coefficient in the unsaturated zone (see Equation (3.15)).

3.3.3.9 Molecular Weight

EPACMTP accounts for concentrations of degradation products via stoichiometry. A degradation-product concentration is determined by converting its concentration from moles/L to mg/L using its molecular weight.

3.3.3.10 Ground-water Temperature

In a typical Monte-Carlo analysis using EPACMTP, the ground-water temperature is assigned as a regional site-based parameter based on the location of the waste management unit. The EPACMTP model uses the temperature of the ground water in the aquifer as the temperature of the ground water within the unsaturated zone. For further details, see Section 4.4.3.3.

3.3.3.11 Ground-water pH

A nationwide ground-water pH distribution was derived from STORET, the EPA's STORage and RETrieval database of water quality, biological, and physical data. The EPACMTP model uses the pH of the ground water in the aquifer as the pH of the ground water within the unsaturated zone. For further details see Section 4.4.3.4.

3.3.4 **Mathematical Formulation of the Unsaturated-zone Transport Submodule**

One-dimensional transport of solute species is modeled using the following advection-dispersion equation:

$$\frac{\partial}{\partial z_u} \left(D_{Lu} \frac{\partial c_i}{\partial z_u} \right) - V_u \frac{\partial c_i}{\partial z_u} = \theta R_i \frac{\partial c_i}{\partial t} + \theta Q \lambda_i c_i - \sum_{m=1}^M \theta \xi_{im} Q_m \lambda_m c_m \quad (3.14)$$

where

$$\begin{aligned} z_u &= \text{depth coordinate from the base of a WMU (m)} \\ D_{Lu} &= \text{apparent dispersion coefficient (m}^2\text{/y)} \end{aligned}$$

| | | |
|-------------|---|--|
| c_i | = | aqueous concentration of species i (mg/L) |
| V_u | = | Darcy velocity obtained from solution of the flow equation (m/y) |
| θ | = | soil water content (dimensionless) |
| R_i | = | retardation factor for species i (dimensionless) |
| t | = | time (y) |
| Q_i | = | coefficient to incorporate decay in the sorbed phase of species i (defined by Equation (3.19)) (dimensionless) |
| λ_i | = | first-order decay constant for species i (1/y) |
| ξ_{im} | = | stoichiometric fraction of parent m that degrades into degradation product i (dimensionless) |
| Q_m | = | coefficient to incorporate decay in the sorbed-phase of parent m (dimensionless) |
| λ_m | = | first-order decay constant of parent m (1/y) |
| c_m | = | aqueous concentration of parent m (mg/L) |

The summation term on the right-hand side of Equation (3.14) represents the production due to decay of parent species, where:

| | | |
|-----|---|------------------------------|
| M | = | total number of parents; and |
| m | = | parent species index. |

The parameters Q_m , and λ_m pertain to parent species m . The coefficient ξ_{im} is a constant related to the decay reaction stoichiometry. It expresses the fraction of a parent species that decays to each degradation species. For instance consider the following hydrolysis reaction whereby parent constituent A produces degradation product B:



In the above reaction, parent species A is species 1 and degradation product B is species 2. The speciation factor for degradation product B, ξ_{21} is equal to $3/2 = 1.5$. The speciation factor depends also on the units used to express concentration, e.g., mg/L versus Molar concentration will result in different values for ξ_{im} . This is because ξ_{im} relates to the number of molecules reacting not the masses.

The dispersion coefficient D_{Lu} in Equation (3.14) is defined as:

$$D_{Lu} = \alpha_{Lu} V_u + \theta D_{dwi}^* \quad (3.15)$$

where

| | | |
|---------------|---|---|
| D_{Lu} | = | apparent dispersion coefficient (m ² /y) |
| α_{Lu} | = | longitudinal (along the vertical flow direction) dispersivity in the unsaturated zone defined by Equation (3.9) (m) |
| V_u | = | Darcy velocity obtained from solution of the flow equation (m/y) |

| | | |
|-------------|---|---|
| θ | = | soil water content (dimensionless) |
| D_{dij}^* | = | effective molecular diffusion coefficient (m ² /y) |

The effective molecular diffusion coefficient is determined from

$$D_{dij}^* = \frac{\theta^{\frac{7}{3}}}{\phi_{eu}^2} D_i$$

where:

| | | |
|-------------|---|---|
| D_{dij}^* | = | effective molecular diffusion coefficient (m ² /y) |
| θ | = | soil moisture content (dimensionless) |
| D_i | = | molecular diffusion coefficient in free water for species i (m ² /y) |
| ϕ_{eu} | = | effective porosity for the unsaturated zone (dimensionless) |

The first expression on the right hand side of the above equation is referred to as tortuosity and is derived by Millington and Quirk (1961).

The effect of equilibrium sorption is expressed through the retardation coefficient R_i :

$$R_i = 1 + \frac{\rho_{bu}}{\theta} f_i \quad (3.16)$$

$$f_i = \frac{ds_i}{dc_i} \quad (3.17)$$

where

| | | |
|-------------|---|---|
| R_i | = | retardation factor for species i (dimensionless) |
| ρ_{bu} | = | soil bulk density of the unsaturated zone (g/cm ³) |
| θ | = | soil water content (dimensionless) |
| f_i | = | slope of the adsorption isotherm for species i (L/kg) |
| s_i | = | sorbed constituent concentration for species i (mg constituent/kg dry soil) |
| c_i | = | aqueous concentration of species i (mg/L) |

When the adsorption isotherm expressed in Equation (3.17) is linear, f_i is equal to the solid-liquid phase distribution coefficient, K_d . Alternatively, EPACMTP allows the use of a nonlinear Freundlich adsorption isotherm

$$\begin{aligned} s_i &= k_{1i} c_i^{\eta_i} \\ \frac{ds_i}{dc_i} &= k_{1i} \eta_i c_i^{\eta_i - 1} \end{aligned} \quad (3.18)$$

where

| | | |
|----------|---|--|
| s_i | = | sorbed concentration of species i (mg constituent/kg dry soil) |
| k_{1i} | = | nonlinear Freundlich parameter for species i (mg/kg) |
| c_i | = | aqueous concentration of species i (mg/L) |
| η_i | = | nonlinear Freundlich exponent for species i (dimensionless) |

In the special case of a linear Freundlich isotherm (that is, when the exponent $\eta = 1.0$), the parameter k_{1i} is the same as the distribution coefficient K_d .

For nonlinear metals transport, the model accommodates tabular isotherm data from external sources. The existing database in EPACMTP was generated using the MINTEQA2 speciation model. Further details of the derivation and use of distribution coefficients for metals can be found in Section 3.3.3 of the *EPACMTP Parameters/Data Background Document* (U.S. EPA, 2003).

EPACMTP accounts for biochemical transformation processes using a lumped first order decay coefficient derived from the hydrolysis constants of the sorbed and dissolved phases.

To account for degradation in both the dissolved and sorbed phase, the lumped degradation coefficient λ_i is multiplied by the coefficient Q_i , which is given by

$$Q_i = 1 + \frac{\rho_{bu}}{\theta} k_{1i} c_i^{\eta_i - 1} \quad (3.19)$$

where

| | | |
|-------------|---|--|
| Q_i | = | coefficient to incorporate decay in the sorbed phase for species i (dimensionless) |
| ρ_{bu} | = | soil bulk density for the unsaturated zone (g/cm ³) |
| θ | = | soil water or moisture content (dimensionless) |
| k_{1i} | = | nonlinear Freundlich parameter for species i (mg/kg) |
| c_i | = | aqueous concentration of species i (mg/L) |
| η_i | = | non-linear Freundlich exponent for species i (dimensionless) |

When sorption is linear, Q_i is the same as the retardation coefficient, R_i .

The initial and boundary conditions of the one-dimensional transport problem may be expressed as:

$$c_i(z_u, 0) = c_i^{in} \quad (3.20)$$

where

- $c_i(z_u, 0)$ = initial aqueous concentration of species i at depth z_u (mg/L)
 z_u = depth coordinate which is taken positive downward from the base of a waste management unit (m)
 c_i^{in} = initial concentration in the soil column (mg/L) (In EPACMTP, it is assumed that the unsaturated zone is initially contaminant-free, and so this parameter is set to zero).

and either a prescribed source flux condition, assuming a perfectly mixed influent

$$-D_{Lu} \frac{\partial c_i}{\partial z_u}(0,t) = V_u(c_i^0(t) - c_i) \quad (3.21)$$

where

- D_{Lu} = apparent dispersion coefficient (m²/y)
 c_i = aqueous concentration of species i (mg/L)
 z_u = depth coordinate which is taken positive downward from the base of a waste management unit (m)
 t = time (y)
 V_u = Darcy velocity (m/y)
 c_i^0 = aqueous concentration of species i at the source (mg/L)

or a prescribed source concentration condition

$$c_i(0,t) = c_i^0(t) \quad (3.22)$$

where

- $c_i(0,t)$ = aqueous concentration of species i at $z_u = 0$ (mg/L)
 $c_i^0(t)$ = leachate concentration of species i emanating from the WMU (mg/L)

and a zero concentration gradient condition at the bottom of the unsaturated zone ($z_u=l_u$)

$$\frac{\partial c_i(l_u,t)}{\partial z_u} = 0 \quad (3.23a)$$

where

- $c_i(l_u, t)$ = aqueous concentration of species i at time t at the bottom of the saturated zone (mg/L)
 z_u = depth coordinate which is taken positive downward from the base of a waste management unit (m)

$$\begin{aligned} l_u &= \text{bottom of the unsaturated zone (m)} \\ t &= \text{time (y)} \end{aligned}$$

Analytical or semi-analytical solutions for the transport equation for the unsaturated zone are based on an assumption that the flow and transport domain is semi-infinite. In other words, the flow and transport domain along the positive z_u direction is extended to infinity. However, concentration of species i at the water table is still determined as $z_u = l_u$. When either the analytical steady-state transport or semi-analytical multi-species transport solutions are used (see Section 3.3.5), the boundary condition shown in Equation (3.23a) is prescribed at the new extreme end of the flow and transport domain instead of at $z_u = l_u$, i.e.,

$$\frac{\partial c_i(\infty, t)}{\partial z_u} = 0 \quad (3.23b)$$

where

$$\begin{aligned} c_i(\infty, t) &= \text{aqueous concentration of species } i \text{ at } z_u \rightarrow \infty \text{ (mg/L)} \\ z_u &= \text{depth coordinate which is taken positive downward from the} \\ &\quad \text{base of a waste management unit (m)} \\ t &= \text{time (y)} \end{aligned}$$

The source concentration $c_i^0(t)$ can be either constant in time, or may represent a decaying source. In the latter case, the source concentration of the i -th species is given by Bateman's equation:

$$\frac{\partial c_i^0}{\partial t} = -\gamma_i c_i^0 + \sum_{m=1}^M \xi_{im} \gamma_m c_m^0 \quad (3.24a)$$

where

$$\begin{aligned} c_i^0 &= \text{aqueous concentration of species } i \text{ in the source (mg/L)} \\ t &= \text{time (y)} \\ \gamma_i &= \text{first-order decay rate for species } i \text{ in the source (1/y)} \\ m &= \text{index of the parent species (dimensionless)} \\ M &= \text{total number of parent species (dimensionless)} \\ \xi_{im} &= \text{stoichiometric fraction of parent } m \text{ that degrades into} \\ &\quad \text{degradation product } i \text{ (dimensionless)} \\ \gamma_m &= \text{first-order decay rate for parent } m \text{ (1/y)} \\ c_m^0 &= \text{aqueous concentration of parent } m \text{ (mg/L)} \end{aligned}$$

Subject to

$$c_i^0(t=0) = \tilde{c}_i \quad (3.24b)$$

where

$$\begin{aligned} c_i^0 &= \text{aqueous concentration of species } i \text{ (mg/L)} \\ t &= \text{time (y)} \\ \tilde{c}_i &= \text{initial aqueous concentration of species } i \text{ in the source (mg/L)} \end{aligned}$$

3.3.5 Solution Methods for Transport in the Unsaturated Zone

The transport module incorporates three solution options for the transport equation. An analytical solution is used for steady-state, single species simulations involving a linear adsorption isotherm. A semi-analytical solution is used for transient or steady-state decay chain simulations with linear sorption. A semi-analytical solution is used for all cases involving metals that have nonlinear sorption. The three solution methods are discussed below.

3.3.5.1 Steady-state, Single Species Analytical Solution

The analytical solution considers the unsaturated zone as a layered system with constant seepage velocity and uniform saturation in each layer. These layers correspond to the segments used in the steady-state flow solution. Each segment or layer is assigned an average water content. The governing equation for steady-state transport in the i -th layer is

$$\alpha_{Lu}^i \frac{\partial^2 c}{\partial z_u^2} - u^i \frac{\partial c}{\partial z_u} - \lambda^i c = 0 \quad (3.25a)$$

where

$$\begin{aligned} \alpha_{Lu}^i &= \text{longitudinal dispersivity for the } i\text{-th layer (m)} \\ c &= \text{aqueous concentration of the constituent of interest (mg/L)} \\ z_u^i &= \text{local depth coordinate measured from the top of the } i\text{-th layer} \\ &\quad \text{(m)} \\ u^i &= \text{retarded seepage velocity in the } i\text{-th layer (m/y)} \\ \lambda^i &= \text{first order decay constant (1/y)} \end{aligned}$$

The retarded seepage velocity of the constituent of interest, u^i , is given by

$$u^i = \frac{V_u^i}{\theta^i R^i} \quad (3.25b)$$

where

$$\begin{aligned}
 u^i &= \text{retarded seepage velocity in the } i\text{-th layer (m/y)} \\
 V_u^i &= \text{ground-water velocity in the } i\text{-th layer (m/y)} \\
 \theta^i &= \text{water content in the } i\text{-th layer (dimensionless)} \\
 R^i &= \text{retardation factor in } i\text{-th layer (dimensionless)}
 \end{aligned}$$

The source boundary condition for the uppermost layer is given by

$$c(0,t) = c^0 \quad (3.26)$$

where

$$\begin{aligned}
 c(0,t) &= \text{aqueous-phase concentration at } z_u^1 = 0 \text{ (mg/L)} \\
 c^0 &= \text{aqueous-phase source concentration (mg/L)}
 \end{aligned}$$

Using the bottom layer boundary condition (Equation (3.23)) and continuity of concentration between layers, the analytical steady-state transport solution for the multi-layered system is

$$c(z_u) = c^0 \exp \left[\sum_{i=1}^{k-1} \left\{ \frac{l^i}{\alpha_{Lu}^i} - \frac{l^i}{2\alpha_{Lu}^i} \sqrt{1 + \alpha_{Lu}^i \frac{\lambda^i}{u^i}} \right\} + \left\{ \frac{z_u^k}{\alpha_{Lu}^k} - \frac{z_u^k}{\alpha_{Lu}^k} \sqrt{1 + 4\alpha_{Lu}^k \frac{\lambda^k}{u^k}} \right\} \right] \quad (3.27)$$

$$z_u = \sum_{i=1}^{k-1} (l^i) + z_u^k$$

where

$$\begin{aligned}
 c(z_u) &= \text{aqueous concentration of the constituent of interest at } z_u \text{ (mg/L)} \\
 c^0 &= \text{aqueous concentration at the source (mg/L)} \\
 k &= \text{index of the layer of interest (dimensionless)} \\
 i &= \text{index of a layer from the top layer to the layer immediately above the layer of interest (dimensionless)} \\
 l^i &= \text{thickness of layer } i \text{ (m)} \\
 \alpha_{Lu}^i &= \text{longitudinal dispersivity for the } i\text{-th layer (m)} \\
 \lambda^i &= \text{first order decay constant (1/y)} \\
 u^i &= \text{retarded seepage velocity in the } i\text{-th layer (m/y)} \\
 \lambda^k &= \text{first order decay constant in the } k\text{-th layer (1/y)} \\
 u^k &= \text{retarded seepage velocity in the } k\text{-th layer (m/y)}
 \end{aligned}$$

-
- z_u = depth coordinate which is taken positive downward from the base of a waste management unit, in this case it corresponds to a location within the k -th layer (m)
 z_u^k = local depth coordinate measured from the top of the k -th layer (m) (m)

If the effect of either dispersion or decay is very small, i.e., $\alpha_i \lambda^i / u_i \ll 1$, Equation (3.27) reduces to the steady-state solution for purely advective transport where

$$c(z_u) = c^0 \exp \left[- \sum_{i=1}^{k-1} \left(\frac{\lambda^i l^i}{u^i} \right) - \frac{\lambda^k z_u^k}{u^k} \right] \quad (3.28)$$

where

- $c(z_u)$ = aqueous concentration of the constituent of interest (mg/L)
 c^0 = aqueous concentration at the source (mg/L)
 k = index of the layer of interest (dimensionless)
 i = index of a layer from the top layer to the layer immediately above the layer of interest (dimensionless)
 λ^i = first order decay constant (1/y)
 l^i = thickness of layer i (m)
 u^i = retarded seepage velocity in the i -th layer (m/y)
 λ^k = first order decay constant (1/y)
 z_u^k = local depth coordinate measured from the top of the k -th layer (m) (m)
 u^k = retarded seepage velocity in the k -th layer (m/y)

3.3.5.2 Transient, Decay Chain Semi-analytical Solution

A semi-analytical transport solution is used for steady-state or transient problems involving multi-species chained decay reactions, but linear sorption. The Laplace transformation is applied to the governing transport equation. The resulting ordinary differential equation in the spatial coordinate is solved analytically, followed by numerical inversion of the Laplace transformed solution using the de Hoog algorithm (de Hoog et al., 1982). Transient boundary conditions reflecting pulse input of contaminants are accommodated using the superposition method. The semi-analytical solution for chain-decay transport is given in Appendix B.1 of this report.

3.3.5.3 Semi-analytical Solution for Metals with Non-linear Sorption

The general advection-dispersion solute transport equation can be written as:

$$\frac{\partial c}{\partial t} + \frac{\rho_{bu}}{\theta} \frac{\partial s}{\partial t} + U \frac{\partial c}{\partial z_u} = \frac{\partial}{\partial z_u} \left(D_{Lu} \frac{\partial c}{\partial z_u} \right) \quad (3.29)$$

where

| | | |
|-------------|---|--|
| c | = | aqueous phase concentration of the constituent of interest (mg/L) |
| t | = | time (y) |
| ρ_{bu} | = | soil bulk density for the unsaturated zone (g/cm ³) |
| θ | = | moisture content (dimensionless) |
| s | = | sorbed phase concentration of the constituent of interest (mg/kg) |
| U | = | seepage velocity (m/y) |
| z_u | = | depth coordinate which is taken positive downward from the base of a waste management unit (m) |
| D_{Lu} | = | dispersion coefficient (m ² /y) |

Assuming equilibrium and reversible sorption, the sorbed phase and dissolved phase concentrations are related through:

$$s = K_d c \quad (3.30)$$

where

| | | |
|-------|---|------------------------------------|
| s | = | sorbed phase concentration (mg/kg) |
| K_d | = | distribution coefficient (L/kg) |
| c | = | aqueous phase concentration (mg/L) |

When K_d is a function of c , as in the metals case, the governing equation (Equation (3.29)) becomes nonlinear. An exact analytical solution to Equation (3.29) in general form is intractable because of the nonlinear adsorption term. In order to solve the problem, some approximations are required. If the solute transport is advection-dominated, we may ignore the dispersion term in Equation (3.29). In that case, the transport equation (Equation (3.29)) can be written as

$$U \frac{\partial c}{\partial z_u} + [1 + f'(c)] \frac{\partial c}{\partial t} = 0 \quad (3.31)$$

$$f'(c) = \frac{\partial f(c)}{\partial s} \quad (3.32)$$

where

| | | |
|-------|---|--|
| U | = | seepage velocity (m/y) |
| c | = | aqueous phase concentration (mg/L) |
| z_u | = | depth coordinate which is taken positive downward from the base of a waste management unit (m) |

| | | |
|--------|---|---|
| $f(c)$ | = | nonlinear function representing the adsorption isotherm (mg/kg) |
| $f'c$ | = | derivative of $f(c)$ with respect to s (dimensionless) |
| t | = | time (y) |
| s | = | sorbed phase concentration (mg/kg) |

The semi-analytical solution for metals transport is given in Appendix B.2 of this report. In addition, the solution of Equation (3.32) requires that K_d be a monotonic function of c . Details relating to the monotonicity treatment of K_d are given in Appendix B.2.

This page was intentionally left blank.

4.0 SATURATED ZONE (AQUIFER) MODULE

4.1 PURPOSE OF THE SATURATED-ZONE MODULE

This section of the background document describes the module of EPACMTP used for the simulation of saturated-zone flow and transport of leachate from waste disposal facilities. This module consists of a numerical simulator for three-dimensional steady-state ground-water flow, coupled with both an analytical and a numerical three-dimensional (3D) contaminant transport simulator. Since EPACMTP is intended to be used for Monte-Carlo uncertainty analysis, much emphasis has been placed on numerical robustness and computational efficiency during the development of the saturated-zone module.

The module has three simulation options:

Option 1: Three-dimensional steady-state ground-water flow and advective-dispersive transport in an aquifer with constant saturated thickness and non-uniform recharge across the upper aquifer boundary;

Option 2: Quasi-three dimensional ground-water flow and advective-dispersive transport, through a combination of 2D areal and cross-sectional solutions; and

Option 3: One-dimensional ground-water flow and pseudo-three-dimensional advective-dispersive transport through a combination of hybrid one-dimensional numerical and two-dimensional analytical solutions.

The three simulation options are listed in descending order of accuracy and in ascending order of computational efficiency. Option 3 is normally preferred because of its acceptable accuracy (see Appendix D) and relatively high computational efficiency. It is several times faster than Options 1 and 2.

4.2 LINKING THE UNSATURATED-ZONE AND SATURATED-ZONE MODULES

The unsaturated-zone and saturated-zone modules of EPACMTP are linked at the water table. The unsaturated-zone module calculates the constituent concentration arriving at the water table as a function of time, that is, the breakthrough curve. This information is stored in an interval table of constituent concentrations versus time. When EPACMTP simulates a decay chain, the concentration values for both the parent constituent and its degradation products are stored. In the subsequent saturated-zone transport simulation, this record of concentration versus time is used to specify the time-varying water table boundary condition. The continuously varying contaminant mass flux entering the saturated zone at the water table is treated as a series of stepwise changes in mass flux. Experience shows that discretizing the time dependent boundary condition into approximately 50 steps yields an accurate approximation. The stepwise treatment of the boundary condition also lends itself readily to incorporation in the Laplace Transform Galerkin (LTG) scheme used in the

saturated-zone transport module. Details of this scheme are provided in Section 4.4.5.2.1. Because linearized sorption isotherms for all constituents, including metals, are used in the saturated zone, the LTG scheme is applicable. The unsaturated-zone simulation is run for a sufficiently long time to ensure that the entire breakthrough curve at the water table is captured. As a practical criterion, the unsaturated-zone transport simulation is terminated when the concentrations of all species in the decay chain arriving at the water table have been reduced to below their respective health-based ground-water concentration limits. The corollary is that for strongly sorbing metals and constituents that degrade via chemical hydrolysis to form non-toxic compounds, when even the maximum concentration at the peak of the water table breakthrough curve remains below the drinking water standard, there is no need to run the saturated transport simulation, because that particular case will not result in an exceedance of the drinking water standard. For constituents with degradation products that may be toxic, the saturated transport simulation is not necessary when the peak concentrations of the parent constituent and its degradation products are below their respective drinking water standards. The drinking water standard for each constituent is an input parameter that must be specified by the user.

4.3 SATURATED-ZONE FLOW SUBMODULE

4.3.1 Description of the Flow Submodule

Ground-water flow in the saturated zone is simulated using a steady-state solution for predicting hydraulic head and Darcy velocities in a uniform ground-water system of constant thickness subject to recharge along the top of the aquifer, and a regional gradient defined by upgradient and downgradient head boundary conditions. A generalized three-dimensional flow system is depicted schematically in Figure 4.1. As shown in this figure, the source is centered about the y-origin. Since the aquifer is taken to be homogeneous, we can therefore take advantage of symmetry and simulate only half of the system along the positive y-axis.

4.3.2 Assumptions Underlying the Flow Submodule

The ground-water flow simulation is based on the following simplifying assumptions:

- The contribution of recharge and infiltration from the unsaturated zone is small relative to the regional flow in the aquifer, and the initial saturated aquifer is large relative to the rise of water table due to recharge and infiltration;
- The aquifer is homogeneous.;
- Ground-water flow is steady-state;
- Flow is single phase, isothermal, and governed by Darcy's Law;
- The fluid is homogeneous and slightly compressible; and

Table 4.1 Aquifer-Specific Variables for the Flow Module

| Parameter | Symbol | Units | Section in EPACMTP Parameters/Data Background Document |
|--|-----------------------|-------------------|--|
| Particle diameter (input): mean particle diameter of the aquifer material (Section 4.3.3.1) | d | cm | 5.3.1 |
| Porosity (derived or input): by default, it is derived and represents the effective porosity of the aquifer material; if input, it may represent the total porosity (Section 4.3.3.2) | ϕ_e (or ϕ) | dimensionless | 5.3.2 |
| Bulk Density (derived): bulk density of the aquifer material (Section 4.3.3.3) | ρ_b | g/cm ³ | 5.3.3 |
| Saturated-zone Thickness (input): saturated thickness of the regional, unconfined aquifer (Section 4.3.3.4) | B | m | 5.3.4.3 |
| Hydraulic Conductivity (input): a measure of the ability of the aquifer to transmit water (Section 4.3.3.5) | K | m/y | 5.3.4.4 |
| Anisotropy Ratio (input): a factor used to specify the relationship between the horizontal and vertical aquifer hydraulic conductivities (Section 4.3.3.6) | A_r | dimensionless | 5.3.6 |
| Hydraulic Gradient (input): regional average hydraulic gradient (Section 4.3.3.7) | r | dimensionless | 5.3.4.5 |
| Seepage Velocity (derived): regional average ground-water seepage velocity (Section 4.3.3.8) | V | m/y | 5.3.5 |

it as a derived parameter. In the latter case, EPACMTP will calculate the value for the parameter.

Default data for this parameter are provided in Section 5.3.1 of the *EPACMTP Parameters/Data Background Document* (U.S. EPA, 2003).

Alternatively, if the particle diameter is treated as a derived parameter, then its value is calculated using the value of porosity (which may be constant or randomly generated from a probability distribution) using an empirical relationship based on data reported by Davis (1969):

$$d = \exp [(0.261 - \phi)/0.0385] \quad (4.1)$$

where

| | | |
|---------------|---|--------------------------------|
| d | = | mean particle diameter (cm) |
| $\exp(\cdot)$ | = | exponential operator |
| ϕ | = | total porosity (dimensionless) |

4.3.3.2 Porosity

In the absence of a user-specified distribution for porosity, it can be calculated from the particle diameter by rewriting the equation above as:

$$\phi = 0.261 - 0.0385 \ln(d) \quad (4.2a)$$

where

| | | |
|--------|---|--------------------------------|
| ϕ | = | total porosity (dimensionless) |
| d | = | mean particle diameter (cm) |

This approximation yields the total porosity of the aquifer. For contaminant transport assessments, it is generally more appropriate to use effective porosity, ϕ_e , than total porosity. The effective porosity can be significantly smaller than the total porosity, although an exact relationship cannot be established. McWorter and Sunada (1977) present data on total and effective porosity for a range of aquifer materials. EPA used their data to establish ranges for the ratio between effective and total porosity as a function of grain size (see Table 4.2). For Monte-Carlo assessments, EPACMTP assumes that the actual ratio varies uniformly between the upper and lower value for ϕ_e/ϕ in each particle-size class for a given value of the mean aquifer grain size class. For a given value of the mean aquifer grain size, that total porosity can thus be converted into effective porosity using the following relationship:

$$\phi_e = r_\phi \phi \quad (4.2b)$$

where

| | | |
|----------|---|---|
| ϕ_e | = | effective porosity (dimensionless) |
| r_ϕ | = | ratio between effective and total porosities (dimensionless) given in Table 4.2 |
| ϕ | = | total porosity (dimensionless) |

It should be noted that the default setting for this parameter in EPACMTP is as a derived parameter (calculated from grain size); only in this case will the model automatically make the conversion from total to effective porosity. In all other cases, no conversion is performed, and the user must specify the actual porosity data to be used by the model by specifying a constant value or a distribution of values for either total porosity or effective porosity in the EPACMTP input file.

Table 4.2 Ratio Between Effective and Total Porosities as a Function of Particle Diameter (after McWorter and Sunada, 1977)

| Mean Particle Diameter (cm) | Range of Ratio ϕ_e/ϕ |
|---|------------------------------|
| $\leq 6.25 \times 10^{-3}$ | 0.03 to 0.77 |
| 6.25×10^{-3} to 2.5×10^{-2} | 0.04 to 0.87 |
| 2.5×10^{-2} to 5.0×10^{-2} | 0.31 to 0.91 |
| 5.0×10^{-2} to 1.0×10^{-1} | 0.58 to 0.94 |
| $> 1.0 \times 10^{-1}$ | 0.52 to 0.95 |

4.3.3.3 Bulk Density

Bulk density is defined as the mass of aquifer solid material per unit volume of the aquifer, in g/cm^3 or mg/L . Bulk density takes into account the fraction of the volume that is taken up by pore space.

The aquifer bulk density directly influences the retardation of solutes and is related to aquifer porosity. An exact relationship between porosity, particle density, and the bulk density can be derived (Freeze and Cherry, 1979). Assuming the particle density to be $2.65 \text{ g}/\text{cm}^3$, this relationship can be expressed as:

$$\rho_b = 2.65 (1 - \phi) \quad (4.3)$$

where

$$\begin{aligned} \rho_b &= \text{bulk density of the soil (g/cm}^3\text{)} \\ \phi &= \text{total porosity of the aquifer material (dimensionless)} \end{aligned}$$

The bulk density is one of several parameters used to calculate the degree to which contaminant velocities are retarded (that is, the retardation factor for the given chemical species).

4.3.3.4 Saturated-zone Thickness

Saturated-zone thickness is the vertical distance from the water table to the base of the saturated zone.

In a typical Monte-Carlo analysis using EPACMTP, the aquifer saturated thickness is assigned as a regional site-based parameter. Information about the regional, site-based methodology is provided in Section 5.5. The aquifer thickness impacts the dilution rates in the saturated zone.

4.3.3.5 Hydraulic Conductivity

Hydraulic conductivity (K) is a measure of the ability to transmit water.

By default, the aquifer hydraulic conductivity is assigned as a regional site-based parameter using the procedure detailed in Section 5.5.2.

Alternatively, the hydraulic conductivity can be specified as a derived parameter. In this case, K is calculated directly from the particle diameter using the Kozeny-Carman (Bear, 1979) equation

$$K = \frac{\rho g}{\mu} \frac{\phi^3}{(1 - \phi)^2} \frac{d^2}{1.8} \quad (4.4)$$

where

- K = hydraulic conductivity (cm/s)
- ρ = density of water (kg/m³)
- g = acceleration due to gravity (m/s²)
- μ = dynamic viscosity of water (N-s/m²)
- ϕ = total porosity of the aquifer material (dimensionless)
- d = mean particle diameter (m)

In Equation (4.4) shown above, the constant 1.8 is a unit conversion factor to yield K in units of cm/s. Both the density and the dynamic viscosity of water are functions of temperature and are computed using the regression equations presented in *The Handbook of Chemistry and Physics* (CRC, 1981).

4.3.3.6 Anisotropy Ratio

The anisotropy ratio is a factor used to specify the relationship between the horizontal and vertical aquifer hydraulic conductivities:

$$A_r = \frac{K_x}{K_z} \quad (4.5)$$

where

- A_r = anisotropy ratio = K_x/K_z .
- K_x = hydraulic conductivity in the x direction (m/y)
- K_z = hydraulic conductivity in the z direction (m/y)

The default value of A_r is 1, which indicates an isotropic system. In EPACMTP, the horizontal transverse hydraulic conductivity is by default set equal to the horizontal longitudinal conductivity, that is, $K_y = K_x$.

4.3.3.7 Hydraulic Gradient

Hydraulic gradient measures the head difference between two points as a function of their distance. The hydraulic gradient provides the driving force for ground-water flow.

In a typical Monte-Carlo analysis using EPACMTP, the hydraulic gradient is assigned as a regional, site-based parameter. More information about the regional, site-based methodology is provided in Section 5.5.

4.3.3.8 Seepage Velocity

The seepage velocity is related to the aquifer properties through Darcy's law. The regional seepage velocity may be input directly or it may be a derived parameter (default). In the latter case, it is computed as

$$V_x = \frac{K_x}{\phi_e} r \quad (4.6)$$

where

- V_x = longitudinal ground-water seepage velocity (in the x-direction) (m/y)
- K_x = longitudinal hydraulic conductivity (in the x-direction) (m/y)
- ϕ_e = effective porosity (dimensionless)
- r = regional hydraulic gradient (dimensionless)

Default lower and upper bounds for the seepage velocity are 0.1 and 1.1×10^4 m/y, respectively. This range of seepage velocity values is based on survey data reported by Newell et al (1990).

4.3.4 Mathematical Formulation of the Saturated-Zone Flow Submodule

The governing equation for steady-state flow in three dimensions is:

$$K_x \frac{\partial^2 H}{\partial x^2} + K_y \frac{\partial^2 H}{\partial y^2} + K_z \frac{\partial^2 H}{\partial z^2} = 0 \quad (4.7)$$

where

- K_x = hydraulic conductivity in the longitudinal (x) direction (m/y)
- H = hydraulic head (m)
- x = principal Cartesian coordinate along the regional flow direction (m)
- K_y = hydraulic conductivity in the horizontal transverse (y) direction (m/y)
- y = principal Cartesian coordinate normal to the flow direction (m)
- K_z = hydraulic conductivity in the vertical (z) direction (m/y)
- z = principal Cartesian coordinate in the vertical direction (m)

4.3.5 Solution Methods for Flow in the Saturated Zone

As stated in Section 4.1, three simulation options are available in EPACMTP.

Option 1: Three-dimensional steady-state ground-water flow and advective-dispersive transport in an aquifer with constant saturated thickness and non-uniform recharge across the upper aquifer boundary;

Option 2: Quasi-three dimensional ground-water flow and advective-dispersive transport, through a combination of 2D areal and cross-sectional solutions; and

Option 3: One-dimensional ground-water flow and pseudo-three-dimensional advective-dispersive transport through a combination of hybrid one-dimensional numerical and two-dimensional analytical solutions.

Details of the flow component of each of the three simulation options are presented below.

4.3.5.1 One-dimensional Flow Solution

The steady-state flow equation in a vertical (x-z) plane may be written as:

$$K_x \frac{\partial^2 H}{\partial x^2} + K_z \frac{\partial^2 H}{\partial z^2} = 0 \quad (4.8)$$

where

- K_x = hydraulic conductivity in the longitudinal (x) direction (m/y)
- H = hydraulic head (m)
- x = principal Cartesian coordinate along the regional flow direction (m)
- K_z = hydraulic conductivity in the vertical (z) direction (m/y)
- z = principal Cartesian coordinate in the vertical direction (m)

Equation (4.8) is solved subject to the following boundary conditions:

(i) Upgradient boundary

$$H(0, z) = H_1 \quad (4.9a)$$

(ii) Downgradient boundary

$$H(x_L, z) = H_2 \quad (4.9b)$$

(iii) Top boundary

$$\begin{aligned}
 -K_z \frac{\partial H}{\partial z}(x, B) &= I_{EFF}, & x_u \leq x \leq x_d \\
 &= I_r & \text{elsewhere}
 \end{aligned}
 \tag{4.9c}$$

(iv) Bottom boundary

$$-K_z \frac{\partial H}{\partial z}(x, 0) = 0 \tag{4.9d}$$

where

| | | |
|-------------|---|--|
| $H(0, z)$ | = | hydraulic head at $x = 0$ (m) |
| H_1 | = | prescribed hydraulic head at the upgradient boundary (m) |
| $H(x_L, z)$ | = | hydraulic head at $x = x_L$ (m) |
| x_L | = | length of the aquifer system (m) |
| H_2 | = | prescribed hydraulic head at the downgradient boundary (m) |
| K_z | = | hydraulic conductivity in the vertical (z) direction (m/y) |
| H | = | hydraulic head (m) |
| z | = | principal Cartesian coordinate in the vertical direction (m) |
| x | = | principal Cartesian coordinate along the regional flow direction (m) |
| B | = | saturated thickness of the system (m) |
| I_{EFF} | = | effective infiltration rate through the strip source area (m/y) |
| x_u | = | upgradient coordinate of the strip source area (m) |
| x_d | = | downgradient coordinate of the strip source area (m) |
| I_r | = | effective recharge rate outside the strip source area (m/y) |

I_{EFF} represents the laterally-averaged vertical water flux in the source area as defined by

$$I_{EFF} = \frac{I y_D + I_r (y_L - y_D)}{y_L} \tag{4.10}$$

where

| | | |
|-----------|---|---|
| I_{EFF} | = | effective infiltration rate through the strip source area (m/y) |
| I | = | infiltration rate through the rectangular source area (m/y) |
| y_D | = | source width along the y -axis (m) |
| I_r | = | recharge rate (m/y) |
| y_L | = | length of the domain in the y -direction (m) (see Figure 4.1) |

By vertically integrating Equation (4.8) and incorporating Equations (4.9c and 4.9d), and invoking the Dupuit-Forchheimer assumption (Bear, 1972), one obtains:

$$-K_x B \frac{\partial^2 H}{\partial x^2} = I_{EFF} \quad (4.11)$$

where

$$\begin{aligned} K_x &= \text{hydraulic conductivity in the longitudinal (x) direction (m/y)} \\ B &= \text{saturated thickness of the system (m)} \\ H &= \text{hydraulic head (m)} \\ x &= \text{principal Cartesian coordinate along the regional flow direction (m)} \\ I_{EFF} &= \text{effective infiltration rate through the strip source area (m/y)} \end{aligned}$$

It is possible that the Dupuit-Forchheimer assumption may be violated underneath the source where the vertical velocity component is significant. However, the assumption should remain approximately true for the rest of the flow domain. To circumvent potential limitations due to the violation of the Dupuit-Forchheimer assumption, the source dimensions on the vertical plane normal to the flow direction immediately downgradient from the WMU are determined from the condition of local mass conservation. The determination of source dimensions is discussed later in Section 4.4.5.4.

Solving Equation (4.11) subject to boundary conditions in Equations (4.9a and 4.9b), one obtains:

For $0 \leq x \leq x_u$

$$H(x) = \frac{-I_r}{2K_x B} x^2 + \left[\frac{I_r - I}{2K_x B} \left(\frac{x_d^2 - x_u^2}{x_L} \right) + \frac{I_r - I_{EFF}}{K_x B} (x_u - x_d) + \frac{I_r}{2K_x B} x_L + \frac{H_2 - H_1}{x_L} \right] x + H_1 \quad (4.12a)$$

For $x_u \leq x \leq x_d$

$$H(x) = \frac{-I_{EFF}}{2K_x B} x^2 + \left[\frac{I_r - I}{2K_x B} \left(\frac{x_d^2 - x_u^2}{x_L} \right) - \frac{I_r - I_{EFF}}{K_x B} x_d + \frac{I_r}{2K_x B} x_L + \frac{H_2 - H_1}{x_L} \right] x + \frac{I_r - I_{EFF}}{2K_x B} x_u^2 + H_1 \quad (4.12b)$$

For $x_d \leq x \leq x_L$

$$H(x) = \frac{-I_r}{2K_x B} x^2 + \left[\frac{I_r - I_{EFF}}{2K_x B} \left(\frac{x_d^2 - x_u^2}{x_L} \right) + \frac{I_r}{2K_x B} x_L + \frac{H_2 - H_1}{x_L} \right] x - \frac{I_r - I_{EFF}}{2K_x B} (x_d^2 - x_u^2) + H_1 \quad (4.12c)$$

where

| | | |
|-----------|---|--|
| x | = | principal Cartesian coordinate along the regional flow direction (m) |
| x_u | = | upgradient coordinate of the strip source area (m) |
| $H(x)$ | = | hydraulic head at distance x (m) |
| I_r | = | effective recharge rate outside the strip source area (m/y) |
| K_x | = | hydraulic conductivity in the longitudinal (x) direction (m/y) |
| B | = | saturated thickness of the system (m) |
| I_{EFF} | = | effective infiltration rate through the strip source area (m/y) |
| x_d | = | downgradient coordinate of the strip source area (m) |
| x_L | = | length of the aquifer system (m) |
| H_2 | = | prescribed hydraulic head at the downgradient boundary (m) |
| H_1 | = | prescribed hydraulic head at the upgradient boundary (m) |

4.3.5.2 Two-dimensional Flow Solutions

As an alternative, the flow submodule can also simulate two-dimensional (2D) steady-state ground-water flow in either the vertical (x - z) cross-section, or the areal (x - y) plane. These two options are combined with corresponding transport solutions. The 2D cross-sectional solution is appropriate for cases in which flow in the horizontal transverse (y -) direction is of minor significance. An example would be a situation in which the rate of infiltration through the patch source at the water table is relatively low compared to the regional ground-water flow rate, and the lateral extent of the source is large. Conversely, a 2D areal solution is appropriate when the contaminant mass flux into the saturated zone is relatively large and the saturated zone is relatively thin. In this case, ground-water flow in the horizontal transverse direction may be significant. In addition, the contaminant plume would be expected to quickly occupy the entire saturated aquifer thickness, allowing a 2D areal treatment.

Strictly speaking, the second condition may cause the first assumption in Section 4.3.2 to be violated because of the rise of water table due to infiltration may be significant compared with the initial aquifer saturated thickness. However, as discussed in Section 1.3, the violation of the water-table-rise assumption leads to conservative arrival times and peak concentrations of chemical constituents at receptor well locations.

Both of the 2D solutions are obtained as special cases of the general three-dimensional solution (see Section 4.3.5.3). For the vertical cross-sectional model, the horizontal transverse hydraulic conductivity, K_y , is set to zero and a computational grid is generated which is only one grid block wide and spans exactly the half-width of the source.

$$\frac{1}{2}y_L = \frac{1}{2}y_D \quad (4.13)$$

where

$$\begin{aligned} y_L &= \text{length of the model domain in the y-direction (m)} \\ y_D &= \text{length of the source in the y-direction (m)} \end{aligned}$$

For the 2D areal solution, the vertical conductivity, K_z , is set to zero, and a one grid block thick, planar grid is generated.

The benefit of using a 2D approximation is the substantial savings in computational effort as compared to a fully 3D solution, both in terms of memory requirements and in terms of execution speed. This is especially of benefit when performing Monte-Carlo simulations. The implementation of the 2D flow and transport solutions for Monte-Carlo simulations in EPACMTP incorporates an automatic criterion for switching between cross-sectional and areal solutions based on the importance of vertical versus areal plume movement. Details of this procedure are presented later in Section 4.4.5.3.3.

4.3.5.3 Three-dimensional Flow Solution

The governing equation for steady-state flow in three dimensions is given in Equation (4.7). This equation is solved subject to the following boundary conditions:

$$H(0, y, z) = H_1 \quad (4.14a)$$

$$H(x_L, y, z) = H_2 \quad (4.14b)$$

$$-K_z \frac{\partial H}{\partial z}(x, y, B) = \begin{cases} I & x_u \leq x \leq x_d, -\frac{1}{2}y_D \leq y \leq \frac{1}{2}y_D \\ r & \text{elsewhere} \end{cases} \quad (4.14c)$$

$$\frac{\partial H}{\partial y}(x, 0, z) = 0 \quad (4.14d)$$

$$\frac{\partial H}{\partial y}(x, \pm \frac{1}{2}y_L, z) = 0 \quad (4.14e)$$

and

$$\frac{\partial H}{\partial z}(x, y, 0) = 0 \quad (4.14f)$$

where

| | | |
|----------------|---|---|
| $H(0, y, z)$ | = | hydraulic head at $x = 0$ (m) |
| H_1 | = | prescribed hydraulic head at the upgradient boundary (m) |
| $H(x_L, y, z)$ | = | hydraulic head at $x = x_L$ (m) |
| H_2 | = | prescribed hydraulic head at the downgradient boundary (m) |
| K_z | = | hydraulic conductivity in the vertical (z) direction (m/y) |
| H | = | hydraulic head (m) |
| z | = | principal Cartesian coordinate in the vertical direction (m) |
| x | = | principal Cartesian coordinate along the regional flow direction (m) |
| y | = | principal Cartesian coordinate normal to the flow direction (m) |
| B | = | thickness of the aquifer system (m) |
| I | = | infiltration rate (m/y) through the rectangular source area ($x_u \leq x \leq x_d, -\frac{1}{2} y_D \leq y \leq \frac{1}{2} y_D$) |
| x_u | = | upgradient coordinate of the strip source area (m) |
| x_d | = | downgradient coordinate of the strip source area (m) |
| y_D | = | width of the source in the y-direction (m) |
| I_r | = | recharge rate at the water table outside the rectangular source area (m/y) |

The solution to the three-dimensional flow equation (Equation (4.7)), subject to Equations (4.14a through 4.14f), is obtained numerically using either a mesh-centered finite difference approximation with 7-point nodal connectivity, or a 27-point Galerkin finite element approximation. With the latter method, the element integrations are performed using the influence coefficient method (Huyakorn et al., 1986), which yields a very efficient solution.

The aquifer region of interest is first discretized into a grid consisting of hexahedral (brick) elements, as shown in Figure 4.2. This figure shows the local numbering of nodes associated with the element and the element dimensions represented by Δx , Δy , and Δz . The grid is the same as that used in the subsequent transport analysis and is generated internally by the saturated-zone module, based on the overall dimensions of the modeled aquifer region and location and size of the source. Nodal spacings in the latter case are automatically assigned based on the Peclet number criterion using the dispersivity values specified for the solute transport problem. The generated grid will be finest near the source, with wider nodal spacings away from the source. Details of this procedure which is automatically implemented in EPACMTP are provided in Section 4.4.5.1.

Spatial discretization by either finite differences or finite elements leads to a final matrix equation of the form:

$$[R] \{\tilde{H}\} = \{Q\} \quad (4.15)$$

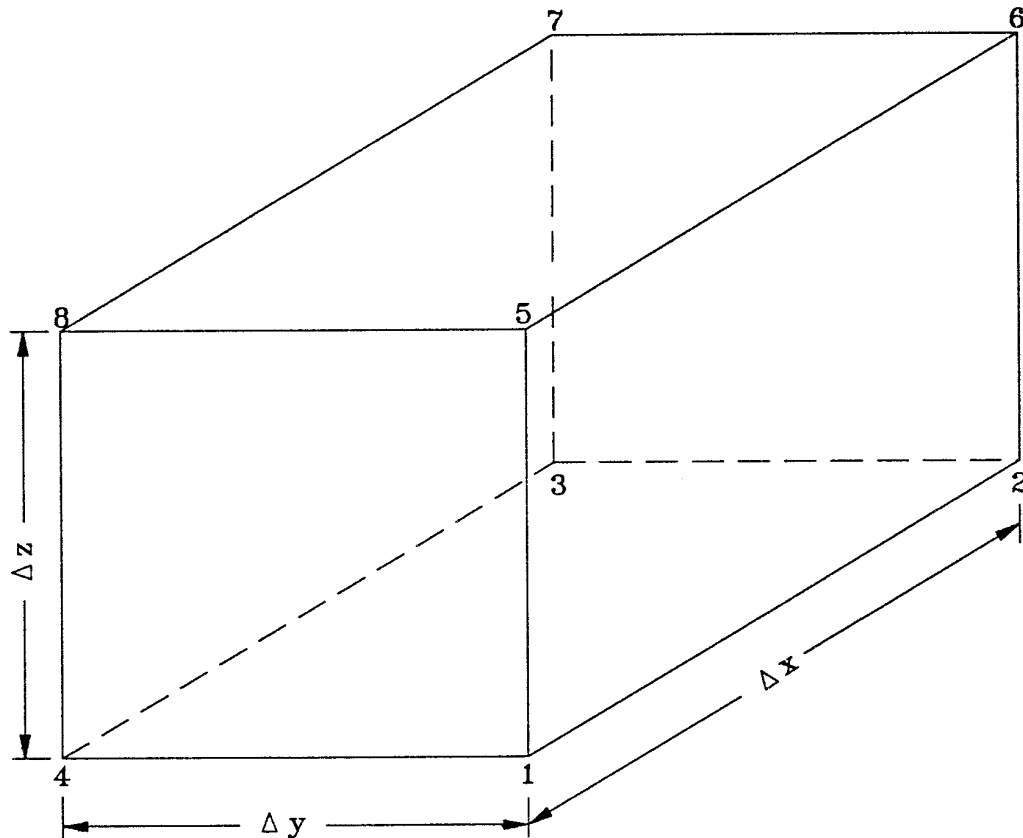


Figure 4.2 Three-dimensional Brick Element Used in Numerical Flow and Transport Model Showing Local Node Numbering Convention.

where

- $[R]$ = conductance matrix (m^2/y)
- $\{H\}$ = vector of unknown nodal head values (m)
- $\{Q\}$ = vector of nodal boundary flux values (m^3/y)

The solution of Equation (4.15) is obtained using an efficient iterative matrix solver with ORTHOMIN acceleration. The solution scheme is described by Sudicky and McLaren (1991).

After the nodal head values have been obtained, the Darcy velocity values at the centroid of each element which are required for the solute transport analysis are computed from Darcy's Law as

$$V_z = -K_z \frac{dH}{dz} \quad (4.16)$$

where

- V_{ζ} = Darcy velocity in the ζ^{th} direction (m/y)
- K_{ζ} = hydraulic conductivity in the ζ^{th} direction (m/yr)
- H = hydraulic head (m)
- ζ = distance along a principal Cartesian coordinate direction (m)

The head derivative at the element centroid is approximated as

$$\left. \frac{dH}{d\zeta} \right|_{\zeta + \frac{1}{2}\Delta\zeta} \cong \frac{1}{4\Delta\zeta} \left[\sum_{i=1}^4 H_{\zeta + \Delta\zeta}^i - \sum_{i=1}^4 H_{\zeta}^i \right] \quad (4.17)$$

where

- H = hydraulic head (m)
- ζ = distance along a principal Cartesian coordinate direction (m)
- i = nodal index (dimensionless)
- $\Delta\zeta$ = element dimension in the direction of ζ (m)
- $H_{\zeta + \Delta\zeta}^i$ = hydraulic head at node i at distance $\zeta + \Delta\zeta$ (m)
- H_{ζ}^i = hydraulic head at node i at distance ζ (m)

and where the summations are performed over the element nodes with common coordinates in the ζ^{th} direction, that is, for each 8-noded element, four nodes will have a coordinate value of ζ and four nodes will have a coordinate value of $\zeta + \Delta\zeta$.

4.3.6 Parameter Screening For Infeasible Ground-water Flow Conditions

Inherent in the Monte-Carlo process is that parameter values are drawn from multiple data sources, and then combined in each realization of the modeling process. Because the parameter values are drawn randomly from their individual probability distributions, it is possible that, in some instances, parameters are combined in ways that may be physically infeasible and may violate the validity of the EPACMTP flow model. A number of checks are implemented to eliminate or reduce these occurrences as much as possible. As a relatively simple measure, upper and lower limits are specified on individual parameter values to ensure that their randomly generated values are within physically realistic limits. Where possible, we use data sources that contain multiple parameters, and implement these in the Monte-Carlo process in a way that preserves the existing correlations among the parameters. For example, we use the HGDB database of hydrogeologic parameters (see Section 5.5.1 and Section 5.3.4 of the *EPACMTP Parameters/Data Background Document* (U.S. EPA, 2003)) in combination with knowledge of the hydrogeologic environments at each waste site location in our WMU parameter database to assign the most appropriate combinations of hydrogeological parameters to each site. Likewise, we assign climate-related parameters based on each site's proximity to an infiltration modeling database of 102 climate stations, as summarized in Section 5.5 of this

document and explained fully in Section 4.2 of the *EPACMTP Parameters/Data Background Document* (U.S. EPA, 2003).

In EPACMTP, we also specify upper and lower limits on secondary parameters whose values are calculated (derived) internally in the Monte-Carlo module as functions of the primary EPACMTP input parameters (see the *EPACMTP Parameters/Data Background Document* (U.S. EPA, 2003)) and implement a set of screening procedures to ensure that infiltration rates and the resulting predicted ground-water mounding remain physically plausible. Specifically, we screen the parameter values generated in each Monte-Carlo realization for the following conditions:

- Infiltration and recharge so high that they cause the water table to rise above the ground surface;
- Liquid level in an SI unit below the water table, causing ground water to flow into the SI; and
- Infiltration rate from an SI that exceeds the saturated hydraulic conductivity of the soil underneath.

These screening procedures are discussed in more detail below, and the mathematical algorithms for implementing the screening are presented in Appendix E. The logic diagram for the infiltration screening procedure is presented in Figure 4.3; Figure 4.4 provides a graphical illustration of the screening criteria. The numbered criteria checks in Figure 4.3 correspond to the numbered diagrams in Figure 4.4. Because high infiltration rates are most likely to occur with unlined surface impoundments, the screening procedure is the most involved for this type of WMU.

Figure 4.3(a) depicts the infiltration screening procedures for landfills, waste piles, and land application units. For these units, after the four correlated hydrogeologic parameters (depth to water table, aquifer saturated thickness, aquifer hydraulic conductivity, and regional gradient), recharge associated with the selected soil type and the nearest climate center, and source infiltration have been generated for each Monte-Carlo realization, the EPACMTP model calculates the estimated water table mounding that would result from the selected combination of parameter values. The combination of parameters is accepted if the calculated maximum water table elevation (the ground-water 'mound') remains below the ground surface elevation at the site. If the criterion is not satisfied, the selected parameters for the realization are rejected and a new data set is selected.

For surface impoundments, there are two additional screening steps, as depicted in Figure 4.3(b). At each Monte-Carlo realization, a surface impoundment unit is selected from the surface impoundment WMU data base. Unit-specific parameters, including ponding depth and base depth below ground surface, are retrieved from the data base. The four correlated hydrogeologic parameters are then selected from

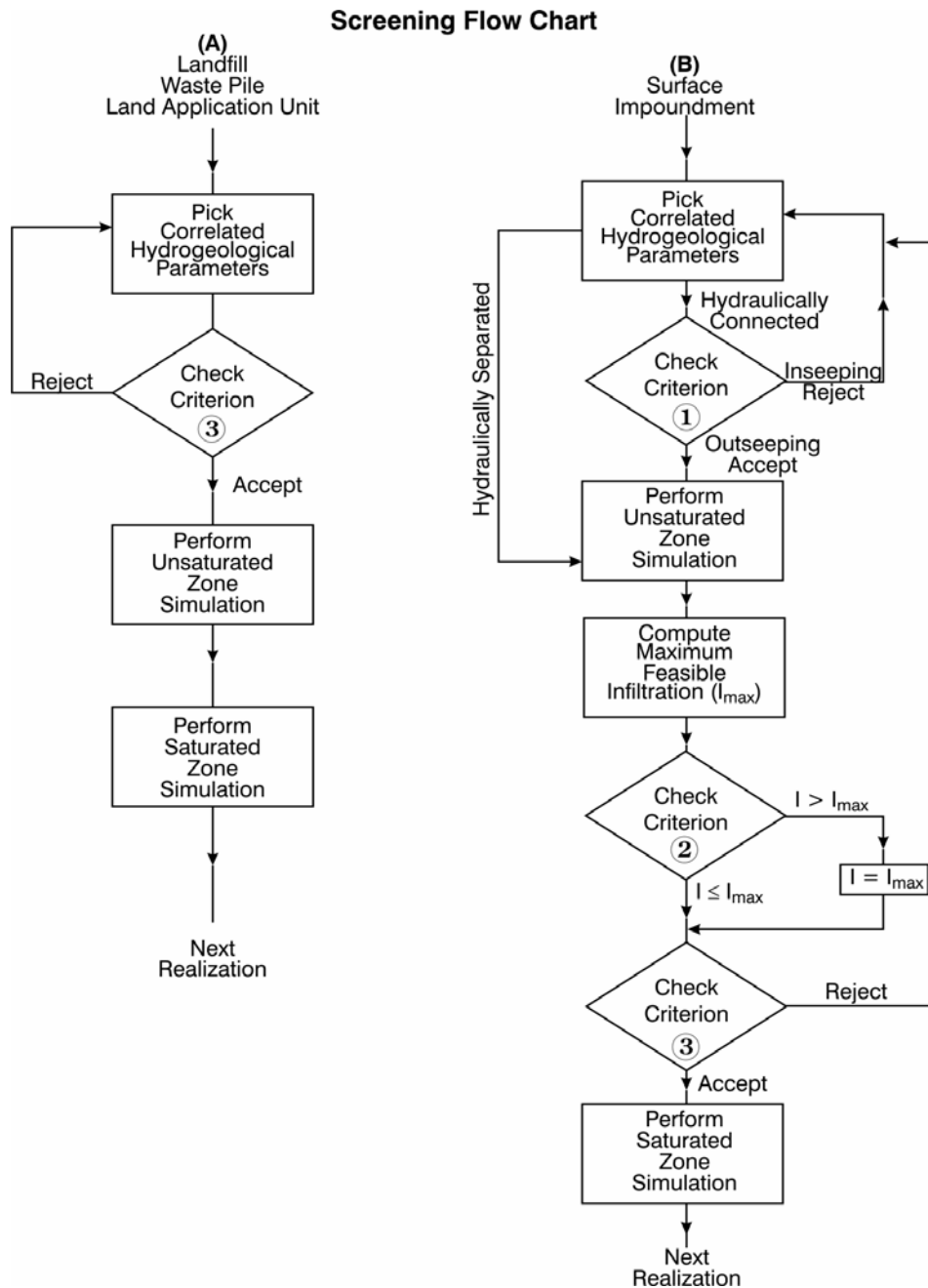
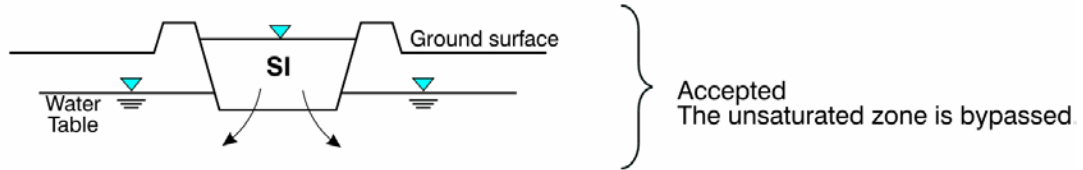


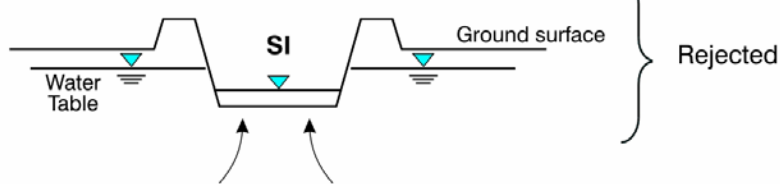
Figure 4.3 Flowchart Describing the Infiltration Screening Procedure.

① Surface impoundment initially hydraulically connected with the saturated zone.

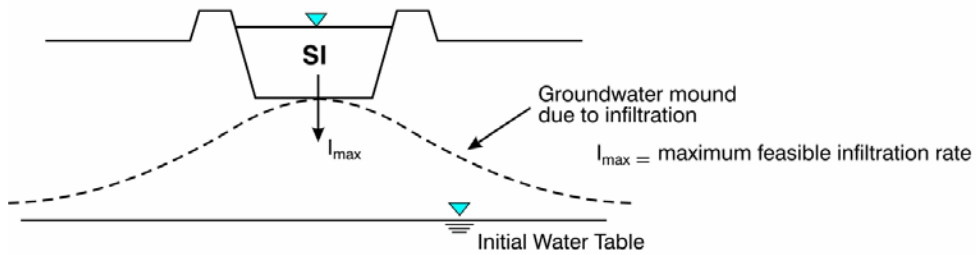
1.a Outseeping SI Unit



1.b Inseeping SI Unit



② Surface impoundment initially hydraulically separated from the saturated zone.



③ Feasible criterion for all WMU types.

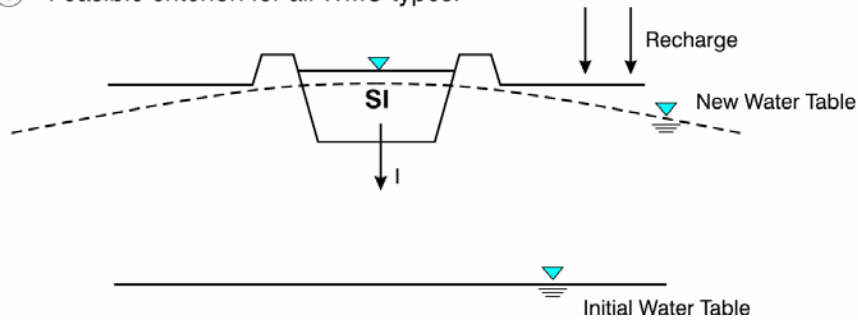


Figure 4.4 Infiltration Screening Criteria.

the hydrogeologic data base, based on the hydrogeologic environment at that WMU location. Using the information on the base depth and water table elevations, we can determine whether the surface impoundment unit is hydraulically connected to the water table. If the base of the surface impoundment is below the water table, the surface impoundment unit is said to be hydraulically connected to the water table (see Figure 4.4, Criterion 1). If the hydraulically connected surface impoundment is an inseeping type (see Figure 4.4, Criterion 1(b)), the realization is rejected, and the set of hydrogeologic parameters is regenerated. An inseeping type of surface impoundment (the elevation of the waste water surface in the impoundment is below the water table) means that ground-water transport would tend to be from the aquifer into the impoundment rather than from the impoundment into the aquifer; the model rejects this type of scenario because it is unlikely that an impoundment like this would be constructed to manage waste water. However, as long as the elevation of the waste water surface in the impoundment is **above** the water table, the first criterion is passed (Figure 4.4, Criterion 1(a)).

If the base of the unit is located above the water table, the unit is said to be hydraulically separated from the water table (see Figure 4.4, Criterion 2). However, in this case, it is necessary to ensure that the calculated infiltration rate does not exceed the maximum feasible infiltration rate. The maximum feasible infiltration rate is the maximum infiltration that allows the water table to remain hydraulically separated from the surface impoundment. In other words, it is the rate that does not allow the crest of the local ground-water mound to be higher than the base of the surface impoundment. This limitation allows us to determine a maximum infiltration rate that is based on the free-drainage condition at the base of the surface impoundment. The infiltration rate tends to decrease thereby reducing the contaminant flux if the water table is allowed to be in hydraulic contact with the base of the surface impoundment. If the maximum feasible infiltration rate (I_{max}) is exceeded, the EPACMTP model will set the infiltration rate to this maximum value.

Once the infiltration limit has been imposed, the third criterion is checked to ensure that any ground-water mounding does not result in a rise of the water table mound above the ground surface, in the same manner as done for other types of WMUs.

4.4 SATURATED-ZONE SOLUTE TRANSPORT SUBMODULE

4.4.1 Description of the Solute Transport Submodule

The saturated-zone transport submodule simulates the advective-dispersive transport of dissolved contaminants in a three-dimensional, constant thickness aquifer (Figure 4.1). The modeled region is the same as that used for flow modeling, that is, only the half of the system along the positive y-axis is actually simulated. Ambient ground-water flow is in the direction of the positive x-axis. The initial concentration of a chemical constituent in the aquifer is taken to be zero. The constituent concentration along the upgradient system boundary is held at zero throughout the simulation. The concentration gradient along the downgradient boundary is zero, and the lower aquifer boundary is assumed to be impermeable. Contaminants enter the saturated zone through a rectangular patch source of either prescribed concentration or prescribed mass flux on the upper aquifer boundary.

Recharge of contaminant-free infiltration water occurs along the upper aquifer boundary outside the patch source. Transport mechanisms considered are advection, longitudinal, vertical and transverse hydrodynamic dispersion, linear or nonlinear equilibrium sorption, zero-order production and first-order decay.

The transport submodule consists of analytical and numerical three-dimensional contaminant transport simulators. The transport submodule has the following transport options:

- Three-dimensional advective-dispersive transport in an aquifer with a steady-state flow field and a patch source of contaminants at the water table.
- Quasi-three dimensional advective-dispersive transport, through a combination of 2D areal and cross-sectional solutions.
- Pseudo-three-dimensional advective-dispersive transport through a combination of hybrid one-dimensional numerical and two-dimensional analytical solutions.

4.4.2 Assumptions Underlying the Saturated-zone Transport Submodule

The major assumptions underlying the solution of the saturated-zone transport equation are:

- (1) The flow field is single phase and at steady state;
- (2) The aquifer is homogeneous and initially contaminant free;
- (3) Adsorption onto the solid phase is described by the Freundlich equilibrium isotherm;
- (4) Chemical and/or biochemical degradation of the contaminant can be described as a first-order process;
- (5) The chemical is dilute and is present only in the solution or adsorbed onto the soil matrix;
- (6) Hydrodynamic dispersion can be described as a Fickian process; and
- (7) The saturated zone is a chemically buffered system with constant and uniform geochemical characteristics.

4.4.3 List of Parameters for the Solute Transport Submodule

The aquifer-specific input parameters for the saturated-zone transport submodule include parameters to characterize ground-water transport in the vicinity of the waste management unit. These ground-water transport parameters, together with the ground-water flow parameters described in Section 4.3.3, are used to determine the

advective-dispersive transport of dissolved contaminants in a three-dimensional, constant thickness aquifer. The aquifer-specific parameters for the saturated-zone transport submodule are presented below and summarized in Table 4.3.

Table 4.3 Aquifer-Specific Variables for the Saturated-Zone Transport Submodule

| Parameter | Symbol | Units | Section in EPACMTP Parameters/Data Background Document |
|---|---|--------------------|--|
| Retardation Factor: a number that describes the speed of a constituent's travel through the subsurface relative to that of the bulk mass of ground water (1.0 = no sorption) (See Section 4.4.3.1) | R^s | dimensionless | 5.3.7 |
| Dispersivities: characteristic lengths that define spatial extent of dispersion of contaminants, along the flow direction, horizontally normal to the flow direction, and vertically normal to the flow direction (Section 4.4.3.2) | α_L α_T α_V | m | 5.3.8 |
| Ground-water Temperature: average regional ground-water temperature, used to derive hydrolysis rates for degrading organic constituents (Section 4.4.3.3) | T | °C | 5.3.9 |
| Ground-water pH: average regional ground-water pH, assuming that pH is not influenced by the addition of leachate from the WMU or changes in temperature, used to derive hydrolysis rates for degrading organic constituents and can be used to calculate sorption of metals (Section 4.4.3.4) | pH | std. units | 5.3.10 |
| Fractional Organic Carbon Content: the fraction of organic carbon in the aquifer material (Section 4.4.3.5) | f_{oc}^s | unitless | 5.3.11 |
| Receptor Well Parameters: <ul style="list-style-type: none"> • angle of well off plume centerline • radial distance to well • distance to well in x direction • distance to well in y direction • depth of well below water table (Section 4.4.3.6) | θ_{rw} R_{rw} x_{rw} y_{rw} z_{rw} | m | 6.2 through 6.6 |
| Freundlich Sorption Coefficient: a constant used with the aqueous concentration to determine the adsorption isotherm according to the Freundlich model (Section 4.4.3.7) | k_1^s or K_d^s | cm ³ /g | 5.3.12 |
| Freundlich Sorption Exponent: the exponent to which the aqueous concentration is raised in the determination of the adsorption isotherm according to the Freundlich model; when the adsorption isotherm is linear, this exponent is one (Section 4.4.3.8) | n^s | dimensionless | 5.3.13 |

Table 4.3 Aquifer-Specific Variables for the Saturated-Zone Transport Submodule (continued)

| Parameter | Symbol | Units | Section in EPACMTP Parameters/Data Background Document |
|--|---------------|--------------------|--|
| Metals Sorption Coefficient: the non-linear, non-Freundlich type adsorption isotherm for metals (Section 4.4.3.9) | K_d^s | cm ³ /g | 3.3.3 |
| Chemical Degradation Rate Coefficient: first order decay rate that accounts for chemical transformation only (Section 4.4.3.10) | λ_c^s | 1/y | 5.3.14 |
| Biodegradation Rate Coefficient: first order decay rate that accounts for biodegradation only; the default value is zero (Section 4.4.3.10) | λ_b^s | 1/y | 5.3.15 |
| Molecular diffusion coefficient: a constituent-specific parameter that accounts for the effects of molecular diffusion in free water (Section 4.4.3.11) | D_i | m ² /y | 3.3.1.1 |
| Molecular weight: the amount of mass in one mole of molecules of a constituent as determined by summing the atomic weights of the elements in that constituent, multiplied by their stoichiometric factors (Section 4.4.3.12) | MW_i | g/mole | 3.3.1.3 |

4.4.3.1 Retardation Factor

The retardation factor is defined for a linear adsorption isotherm by

$$R_l^s = 1 + \frac{\rho_b K_d^s}{\phi_e} \quad (4.18)$$

where

- R_l^s = saturated-zone retardation factor of component species l (dimensionless)
- ρ_b = bulk density of the aquifer (g/cm³)
- K_d^s = distribution coefficient of the aquifer (cm³/g)
- ϕ_e = effective porosity of the aquifer (dimensionless)

When the sorption isotherm is nonlinear, R_l^s is no longer constant but depends on concentration. In this case, R_l^s must be given as a derived variable and the K_d -concentration relation must be specified by the user in terms of two the parameters: the Freundlich coefficient (k_f) and the Freundlich exponent (n) (see Equation (3.16)).

For the modeling of metals, the EPACMTP user has three options for specifying the relationship between dissolved and adsorbed concentrations: 1) MINTEQA2-derived

non-linear isotherms, 2) pH-dependent empirical isotherms, or 3) an empirical distribution of values. In the case of the first option, the non-linear isotherm is only used in the unsaturated zone; a linear sorption isotherm (that is, an effective K_d value) is used for the saturated zone. This effective K_d value is determined from the maximum contaminant concentration at the water table and values of the five environmental master variables (pH, iron-oxide, leachate organic matter, natural organic matter in the aquifer, and ground-water environment type (carbonate or non-carbonate)), following the procedure described in Appendix G.

The aquifer-specific input parameters for the saturated-zone transport submodule include parameters to characterize ground-water transport in the vicinity of the waste management unit. These ground-water transport parameters, together with the ground-water flow parameters described in Section 4.3.3, are used to determine the advective-dispersive transport of dissolved contaminants in a three-dimensional, constant thickness aquifer.

4.4.3.2 Dispersivity

The spreading and dilution of the contaminant plume in the saturated zone is controlled by two mechanisms: advection and dispersion. EPACMTP allows for non-uniform ground-water flow due to vertical recharge and infiltration from the waste site. The model simulates actual spreading mechanisms occurring in the field. For non-degrading chemical constituents, the dilution caused by dispersive mixing is a controlling factor in determining the constituent concentration observed at a receptor well. In Monte-Carlo analyses, transport is a relatively insensitive to dispersion. The reason for this is that low dispersivities lead to a compact, concentrated plume. If the plume is relatively small, the likelihood that the receptor well will intercept the plume is reduced, but the concentration in the well, if it does, will be relatively high. High dispersivities will lead to a more dilute plume which occupies a greater volume, thereby increasing the likelihood that a receptor well will intercept the plume. Concentrations in the plume however, are likely to be lower than in the first case. In the case of a full Monte-Carlo analysis, the resultant distribution will tend not to be sensitive to dispersivity.

The model computes the longitudinal, lateral, and vertical dispersion coefficients as the product of the seepage velocity and longitudinal (α_L), transverse (α_T) and vertical (α_V) dispersivities. A literature review indicated the absence of a generally accepted theory to describe dispersivities, although a strong dependence on scale has been noted (Gelhar et al., 1985; Gelhar et al., 1992).

In the absence of user-specified values or distributions, the default probabilistic distribution (see Section 5.4.9.1 of this document and Section 5.3.8 of the *EPACMTP Parameters/Data Background Document* (U.S. EPA, 2003)) is used. Within each of the discrete intervals of the probabilistic distribution, the longitudinal dispersivity is assumed to be uniform. The values of longitudinal dispersivity in each interval are based on a receptor well distance of 152.4 m. For distances other than 152.4 m, the following equations are used to adjust the sampled value of dispersivity:

$$\alpha_L(x_t) = \alpha_{Ref} \left(\frac{x_t}{152.4} \right)^{\frac{1}{2}} \quad (4.19)$$

$$x_t = \frac{1}{2}x_w + x_{rw} \quad (4.20)$$

where

- α_L = longitudinal dispersivity (m)
- x_t = average travel distance in the x direction (m)
- α_{Ref} = reference longitudinal dispersivity, as determined from the probabilistic distribution (m)
- x_w = length of the WMU in the x-direction (parallel to ground-water flow) (m)
- x_{rw} = distance from the downgradient boundary of the WMU to the receptor well (m)

In other words, the travel distance x_t is equal to the distance of the receptor well (x_{rw}) from the downgradient facility boundary, plus one-half of the facility dimension. The average distance for all of the contaminants to migrate to the edge of the waste management unit is equal to one half the length of the unit or $\frac{1}{2} x_w$. Within the EPACMTP model, the minimum allowed value of α_L is 0.01 m.

By default, the transverse (α_T) and vertical (α_V) dispersivities are calculated by the EPACMTP model as a fraction of the longitudinal dispersivity. The default values for the ratio of the longitudinal to the transverse dispersivity, α_L/α_T , and the ratio of the longitudinal to the vertical dispersivity, α_L/α_V , are 8 and 160, respectively. The rationale for these values is presented below.

The dispersivity relationship described above has been derived based on a review of available data. More recently, Gelhar et al. (1992) have compiled and documented results from a large number of studies in which dispersivity values have been reported. These studies represent a wide range of spatial scales, from a few meters to over ten-thousand meters. The data as presented by Gelhar et al. (1992) show a clear correlation between scale and apparent dispersivity. The dispersivity relationship used in EPACMTP describes the observed data reasonably well. The field data suggest a somewhat steeper slope of the distance-dispersivity relation on a log-log scale than is used in the modeling analyses. A sensitivity analysis performed using EPACMTP has shown that the model results are virtually identical when the slope is varied from 0.5 to 1.5. For this reason the original relationship as shown above has been retained. The data presented by Gelhar et al. (1992) also show that the ratios between longitudinal, and horizontal and vertical transverse dispersivities used in the nationwide modeling, are consistent with published data.

4.4.3.3 Ground-water Temperature

In a typical Monte-Carlo analysis using EPACMTP, the ground-water temperature is assigned as a regional site-based parameter based on the location of the waste management unit. The map shown in Figure 4.2 of the *EPACMTP Parameters/Data Background Document* (U.S. EPA, 2003) was used to assign the ground-water temperature to each facility in the database of waste sites. For each waste site, the assigned temperature is obtained from averaging the upper and lower temperatures within the appropriate region. You can find more information about the regional, site-based methodology in Section 5.5. Additionally, the EPACMTP model uses the temperature of the ground water in the aquifer as the temperature of the ground water within the unsaturated zone.

4.4.3.4 Ground-water pH

A nationwide ground-water pH distribution was derived from EPA's STORET data base. The model assumes that the ground water is sufficiently buffered such that pH is not influenced by the input of contaminants from the waste management unit located above or changes in temperature. The default distribution for ground-water pH is an empirical distribution with a median value of 6.8 and lower and upper bounds of 3.2 and 9.7, respectively. The complete distribution is presented in Table 5.6 of the *EPACMTP Parameters/Data Background Document* (U.S. EPA, 2003). Additionally, the EPACMTP model uses the pH of the ground water in the aquifer as the pH of the ground water within the unsaturated zone.

4.4.3.5 Fractional Organic Carbon Content

The organic carbon content, f_{oc}^s , is used to determine the linear distribution coefficient, K_d^s . This approach is valid for organic contaminants containing hydrophobic groups. These chemicals will tend to sorb preferentially on non-polar natural organic compounds in the soil or aquifer. Unfortunately, few if any comprehensive subsurface characterizations of organic carbon content exist. In general, the reported values are low, typically less than 0.01. A low range for f_{oc}^s was assumed and the distribution shape was based on the distribution of measured dissolved organic carbon recorded as entries to EPA's STORET data base. The default distribution for fractional organic carbon content is a Johnson SB distribution with a mean and standard deviation in arithmetic space of 4.32×10^{-4} and 0.0456, respectively and upper and lower limits of 0.064 and 0.0, respectively. The complete distribution is presented in Table 5.6 of the *EPACMTP Parameters/Data Background Document* (U.S. EPA, 2003). In the case of metals, the sorption is controlled by complex geochemical interactions which are simulated using MINTEQA2 (U.S. EPA, 1996c).

4.4.3.6 Receptor Well Location and Depth

A receptor well is a drinking water well (actual or hypothetical) that is located downgradient of the waste management unit in consideration. It represents the location at which the potential exposure to the ground water is measured. In a typical Monte-Carlo simulation performed with EPACMTP, the primary model output

for each realization is the exposure concentration at a receptor well located downgradient from the waste site. When site-specific data on the receptor well location are not available, the EPA typically uses a default database of downgradient distances to the nearest receptor well obtained from the OSW landfill survey (see the *EPACMTP Parameters/Data Background Document* (U.S. EPA, 2003)). At most waste sites included in this survey, the direction of ambient ground-water flow was not known exactly; therefore, it cannot be ascertained that the nearest receptor well is located directly along the plume centerline (where the highest concentrations would be expected). Therefore, when site-specific data are not available, the modeled well can be positioned a variable x-distance from the downgradient edge of the waste management unit and at a variable y-distance from the plume centerline to reflect uncertainties and variations in the location of the receptor well in relation to the direction of ambient ground-water flow. In the Monte-Carlo model, a realization is associated with a single receptor well. Multiple receptor wells are not allowed.

The EPACMTP model requires that the receptor well location be specified in the x-, y-, and z*-directions as follows:

| | | |
|------------|---|---|
| x_{rw} | = | distance from the waste unit (m) |
| y_{rw} | = | perpendicular distance from the plume centerline (m) |
| z_{rw}^* | = | well depth within the saturated zone, measured vertically downward from the water table (m) |

A receptor well can be located horizontally 1) anywhere downgradient of the waste management unit (by using default settings for radial distance R_{rw} and angle θ_{rw} , for example), 2) within the areal extent of the contaminant plume, or 3) along the contaminant plume centerline (by setting the angle θ_{rw} to zero, as described below). The vertical position of the receptor well can be anywhere within the saturated zone or restricted to lie within the vertical extent of the contaminant plume; additionally, there are several options within EPACMTP that can be used to specify the well depth. Details of the various well-location options are presented below.

4.4.3.6.1 Horizontal Well Location

EPACMTP incorporates two Well-Location Options for determining the x- and y-coordinates of the receptor well: 1) Well-Location Option 1: specifying the well location as a function of radial distance and angle off the plume centerline or 2) Well-Location Option 2: specifying it directly so that the resulting distribution of locations is varied according to a particular type of distribution between the plume centerline and the areal plume boundary (a uniform distribution is the default type for this option). These two options are further explained below.

Well-Location Option 1

When using Well-Location Option (1) (specifying R_{rw} and θ_{rw}), the user has a choice about how the point along the downgradient edge of the waste unit (from which the radial distance to the well is measured) is determined. This point can either be constrained to always lie at the center of the downgradient edge of the WMU or it can vary along this downgradient edge according to the relationship between the

magnitude of R_{rw} and width of the WMU. That is, in Well-Location Option (1a), the radial distance to the well is always measured from the center of the downgradient edge of the WMU; in Well-Location Option (1b), the radial distance to the well is measured from a randomly varying point somewhere between the upper corner and the center of the downgradient edge of the WMU. These two options for measuring R_{rw} have been included as a means of reducing the bias introduced by large WMUs. When R_{rw} is always measured from the center of the downgradient edge of the WMU, receptor well locations are more likely to lay inside the areal extent of the contaminant plume as the size of the WMU increases, biasing exposure concentrations upward.

Well-Location Option (1a) involves determining the x- and y-coordinates of the receptor well as a function of its radial distance, R_{rw} , from the center of the downgradient edge of the waste unit, and the angle off-center, θ_{rw} . In this case the x- and y-coordinate values must be specified in the data input file as derived variables and are computed as

$$x_{rw} = R_{rw} \cos \theta_{rw} \quad (4.21)$$

$$y_{rw} = R_{rw} \sin \theta_{rw} \quad (4.22)$$

where

- x_{rw} = distance from the waste unit (m)
- R_{rw} = radial distance between waste management unit and well measured from the center of the downgradient edge of waste management unit (m)
- θ_{rw} = angle measured counter-clockwise from the plume centerline (degrees)
- y_{rw} = perpendicular distance from the plume centerline (m)

The default setting is to consider any well located downgradient of the waste unit; in this case, the angle θ_{rw} is taken to be uniformly distributed between 0 and 90°

($\frac{\pi}{2}$ radians). However, if the user wishes to constrain the receptor well to the plume centerline, the angle θ_{rw} should be set to zero.

In Well-Location Option 1b; the receptor well may be located in one of two zones, as shown in Figure 4.5.

Zone 1 is defined by

$$0 \leq x_{rw} \leq \infty \quad (4.23a)$$

$$0 \leq y_{rw} \leq \frac{1}{2}y_D \quad (4.23b)$$

where

- x_{rw} = distance from the waste unit (m)
 y_D = width of the WMU normal to the flow direction (m)
 y_{rw} = perpendicular distance from the plume centerline (m)

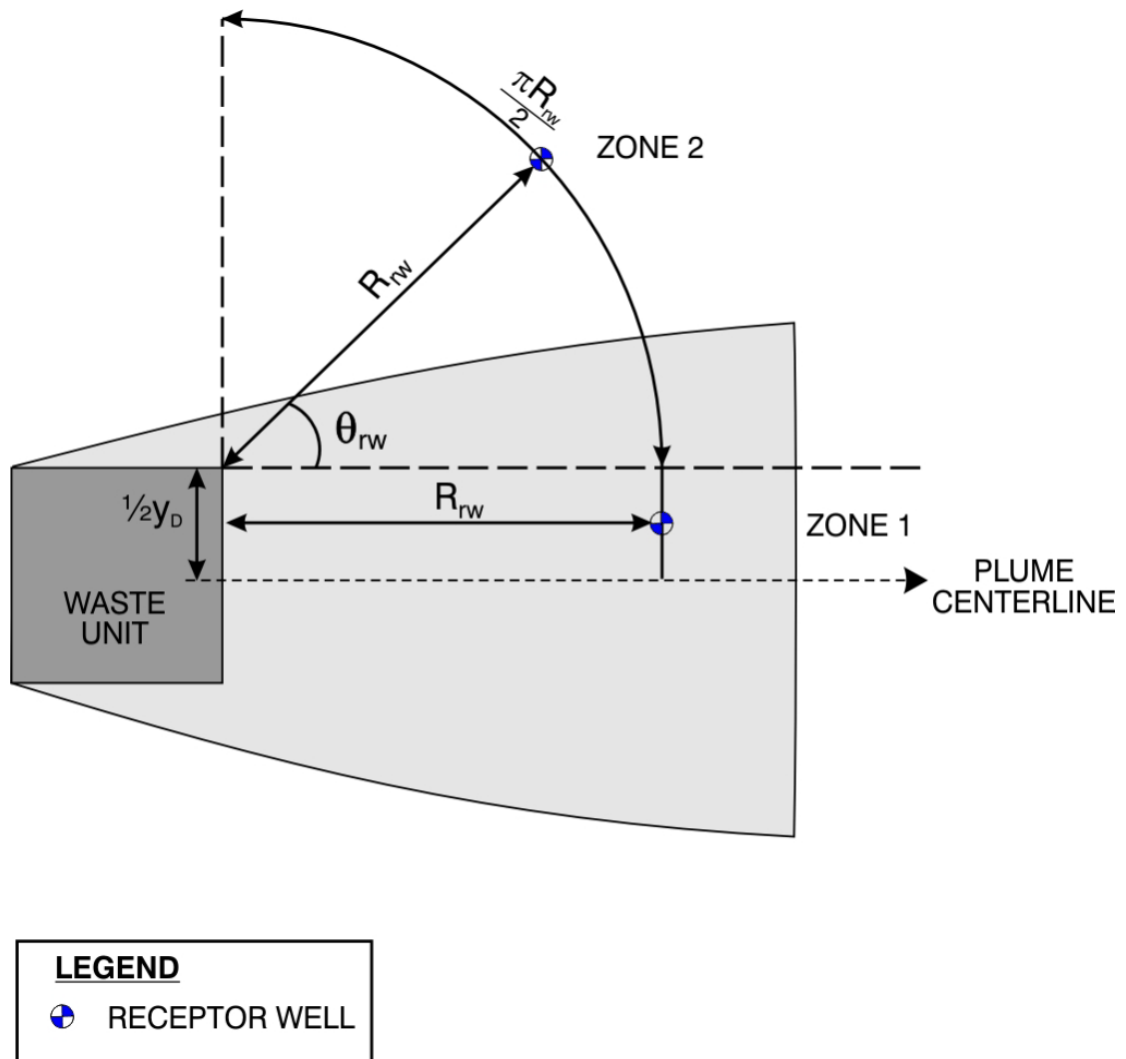


Figure 4.5 Schematic View of the Two Possible Zones for Receptor Well Location.

Zone 2 is defined by

$$0 \leq x_{rw} \leq \infty \quad (4.24a)$$

$$\frac{1}{2} y_D \leq y_{rw} \leq \infty \quad (4.24b)$$

where

- x_{rw} = distance from the waste unit (m)
- y_D = width of the WMU normal to the flow direction (m)
- y_{rw} = perpendicular distance from the plume centerline (m)

In Zone 1, the well location coordinates (x_{rw} , y_{rw}), measured in the (x , y) coordinates defined above, are given by:

$$x_{rw} = R_{rw} \quad (4.25a)$$

$$y_{rw} = \frac{1}{2} y_D U(0,1) \quad (4.25b)$$

where

- x_{rw} = distance from the waste unit (m)
- R_{rw} = radial distance between waste management unit and well (m)
- y_{rw} = perpendicular distance from the plume centerline (m)
- y_D = width of the WMU normal to the flow direction (m)
- $U(0, 1)$ = uniform random number varying between 0 and 1 (dimensionless)

Similarly, in Zone 2, the well location coordinates are defined by:

$$\theta_{rw} = \frac{\pi}{2} U(0,1) \quad (4.26a)$$

$$x_{rw} = R_{rw} \cos(\theta_{rw}) \quad (4.26b)$$

$$y_{rw} = \frac{1}{2} y_D + R_{rw} \cdot \sin(\theta_{rw}) \quad (4.26c)$$

where

- θ_{rw} = angle measured counter-clockwise from the plume centerline (degrees)
- $U(0, 1)$ = uniform random number varying between 0 and 1 (dimensionless)
- x_{rw} = distance from the waste unit (m)
- R_{rw} = radial distance between waste management unit and well (m)
- y_{rw} = perpendicular distance from the plume centerline (m)
- y_D = width of the WMU normal to the flow direction (m)

Based on the above description, it can be readily seen that:

- In Zone 1, the well is located at the distance of R_{rw} , along the x direction, from the down-gradient edge of the WMU; and
- In Zone 2, the well is located at the radial distance of R_{rw} from a down-gradient corner of the WMU within a quadrant defined by two lines that traverse the corner along (in the x direction) and normal to (in the y direction) the flow direction.

When using Well-Location Option (1b), the probabilities of a receptor well being located in Zones 1 and 2 are: $1 - p_{rw}$, and p_{rw} , respectively, where the probability, p_r , is defined as:

$$p_{rw} = \frac{\frac{\pi R_{rw}}{2}}{\frac{1}{2} y_D + \frac{\pi R_{rw}}{2}} \quad (4.27)$$

where

- p_{rw} = probability that the receptor well will be located in Zone 2 (dimensionless) (see Figure 4.5)
- R_{rw} = radial distance between waste management unit and well (m)
- y_D = width of the WMU normal to the flow direction (m)

In addition, when using Well-Location Options (1a) and (1b), the y-coordinate of the well can be optionally constrained to lie within the areal extent of the main contaminant plume as defined by

$$y_{rw} \leq \frac{1}{2} y_D + 3[2\alpha_T(x_w + x_{rw})]^{1/2} \quad (4.28)$$

where

- y_{rw} = perpendicular distance from the plume centerline (m)
- y_D = width of the WMU normal to the flow direction (m)
- α_T = horizontal transverse dispersivity (m)
- x_w = length of WMU in the x-direction (parallel to ground-water flow) (m)
- x_{rw} = distance from the waste unit (m)

This approximation for the lateral extent of the contaminant plume is based on the assumption that plume spreading in the horizontal-transverse direction is caused by dispersive mixing, which results in a Gaussian profile as the edge of the plume cross-section. The limit of y_{rw} in Equation (4.28) above implies that at least 99.7% of the contaminant mass will be present inside the transverse plume limit.

When using Well-location Option (2) to determine the receptor well location, the well position is generated directly for each model realization so that at the conclusion of the Monte-Carlo analysis, the resulting distribution of locations is varied according to a particular type of distribution between the plume centerline and the areal plume boundary, for any given x-distance. A uniform distribution is the default type for this option. For Well-location Option (2), an x-distance is typically generated from the empirical distribution presented in Table 6.2 of the *EPACMTP Parameters/Data Background Document* (U.S. EPA, 2003), and the y-coordinate of the well is typically generated from a uniform distribution with a minimum value of zero and a maximum value given by Equation (4.26c).

4.4.3.6.2 Vertical Well Location

In addition to Well-Location Options (1) and (2) which are used to determine the x- and y-coordinates of the receptor well, three well depth options (described below) are available for specifying the vertical position of the well intake point below the water table.

Well-depth Option (1) is the default and is used to specify that the vertical position of the well be uniformly distributed between the water table ($z^* = 0$) and the saturated aquifer thickness. This option is selected by specifying the z^* -position as a uniformly distributed relative depth below water table (EPACMTP distribution type code 0; see Table 5.1 and Section 5.4.1) with lower and upper limits of 0.0 and 1.0. EPACMTP will multiply this uniformly generated value by the saturated-zone thickness to yield the actual receptor well depth below the water table for each Monte-Carlo iteration.

In Well-depth Option (2), data on the depth of receptor wells obtained from Agency surveys can be used directly in the model as an empirical distribution (EPACMTP distribution type code 6; see Table 5.1 and Section 5.4.7). The data values range from 15 ft (4.5 m) to 301 ft (90.9 m), and the complete distribution is presented in Table 6.2 of the *EPACMTP Parameters/Data Background Document* (U.S. EPA, 2003). When the generated value for the vertical position of the receptor well intake point is either above the top or below the bottom of the aquifer (physically impossible conditions), a new well position is generated to ensure that the well depth is always located within the aquifer.

In Well-depth Option (3), the receptor well depth can be specified as a constant absolute depth below the water table (that is, not a relative depth as in Well-depth Option (1) above). In this case, one of the special distribution types in EPACMTP – the vertical well position distribution (EPACMTP distribution type code 12; see Table 5.1 and Section 5.4.9.2) – should be used and the well depth below the water table should be entered in meters.

For Well-depth Options (1) and (2) listed above, the vertical position of the observation well can also be optionally constrained to lie within the approximate vertical penetration depth of the contaminant plume emanating from the waste unit, with the z^* -coordinate of the receptor well (z_{rw}^*) constrained to lie within the approximate vertical extent of the contaminant plume as defined by:

$$z_{rw}^* \leq 2.5 \left\{ \frac{Q_3^F + Q_4^F}{Q_1^F} B + \left[\alpha_v (x_w + x_{rw}) + \alpha_L \left(\frac{Q_3^F + Q_4^F}{Q_1^F} B \right) + \phi_e D^{s*} \right] \frac{1}{2} \right\} = z_{rwmax}^*$$

(4.29)

where

- z_{rw}^* = z^* -coordinate of the receptor well, positive downward from the water table (m)
 $Q_1^F - Q_4^F$ = components of fluxes in the ground-water flow field (m^2/y) (see Figure 4.6)
 B = saturated-zone thickness (m)
 α_v = vertical dispersivity (m)
 x_w = length of WMU in the x-direction (parallel to ground-water flow) (m)
 x_{rw} = distance from the waste unit (m)
 α_L = longitudinal dispersivity (m)
 ϕ_e = effective porosity of the aquifer (dimensionless)
 D^{s*} = effective molecular diffusion coefficient in the aquifer (m^2/y)
 z_{rwmax}^* = maximum allowable z^* -coordinate of the receptor well; that is, the approximate vertical penetration depth of the contaminant plume (m)

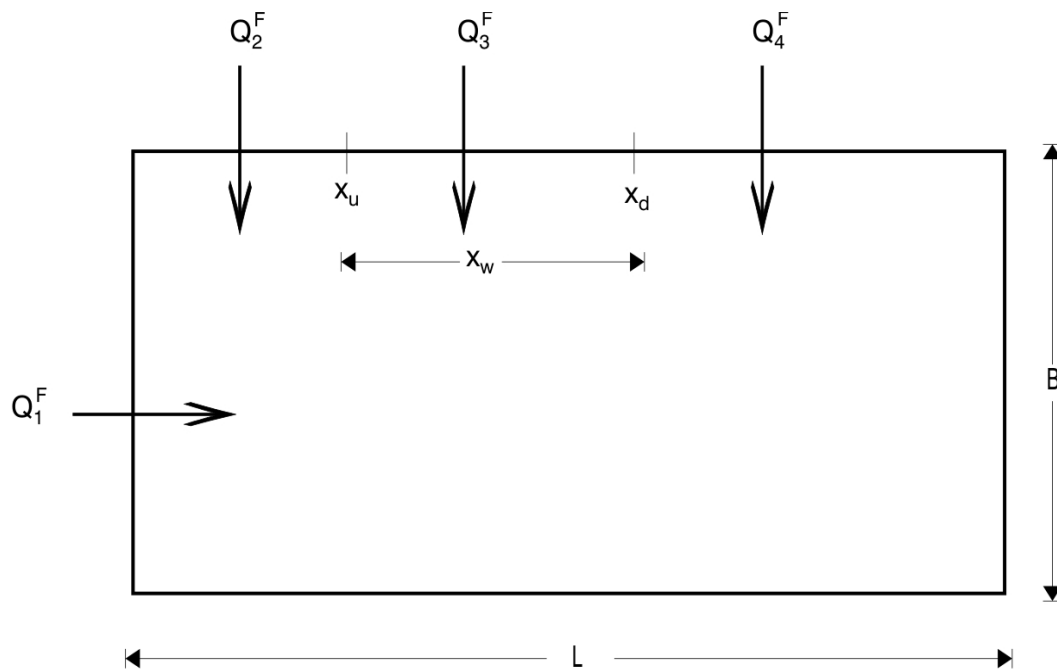


Figure 4.6 Schematic Cross-sectional View of the Aquifer Showing the Contributing Components of the Ground-water Flow Field.

4.4.3.7 Freundlich Isotherm Coefficient

For organic constituents, EPACMTP version 2.0 only allows using a linear Freundlich isotherm to describe the constituent's sorption behavior. In this case, the leading Freundlich coefficient is known as the solid-liquid phase distribution coefficient (K_d). The distribution coefficient may be specified directly or as a derived parameter. In the latter case, it is computed according to the following relationship:

$$K_d^s = k_{oc} f_{oc}^s \quad (4.30)$$

where

| | | |
|------------|---|--|
| K_d^s | = | solid-liquid phase distribution coefficient (cm ³ /g) |
| k_{oc} | = | distribution coefficient with respect to organic carbon (cm ³ /g) |
| f_{oc}^s | = | fractional organic carbon content of the aquifer material (dimensionless) |

The above relationship does not apply to simulations of metals transport. For metals that are modeled using MINTEQA2-derived isotherms or pH-dependent empirical isotherms, the K_d data is either read in from an auxiliary input file or internally calculated based on the ground-water pH. In both cases, the Freundlich isotherm coefficient is not used; see Section 4.4.3.9 below. Alternatively, metals can be modeled using an empirical distribution of distribution coefficients (e.g., based on reported K_d values in the scientific literature).

4.4.3.8 Freundlich Isotherm Exponent

For organic constituents, EPACMTP version 2.0 only allows using a linear Freundlich isotherm to describe the constituent's sorption behavior. That is, the Freundlich isotherm exponent (n) must be set equal to 1.0. If this parameter is omitted from the input data file, it is assigned a default value of 1.0, which is equivalent to specifying a linear sorption isotherm.

For metals that are modeled using MINTEQA2-derived isotherms or pH-dependent empirical isotherms, the K_d data is either read in from an auxiliary input file or internally calculated based on the ground-water pH. In both cases, the Freundlich isotherm exponent is not used; see Section 4.4.3.9 below.. Alternatively, metals can be modeled using an empirical distribution of distribution coefficients (e.g., based on reported K_d values in the scientific literature); in this case, the Freundlich isotherm exponent should be set to its default value of 1.0.

4.4.3.9 Sorption Coefficient for Metals

In general, there are three options available within EPACMTP for modeling metals transport: 1) use non-linear isotherms generated by the MINTEQA2 geochemical model, 2) use pH-dependent empirical isotherms, and 3) use an empirical distribution of values for K_d^s . For Options (1) and (2), the Freundlich isotherm coefficient and exponent are not used. However, for metals that are modeled using

an empirical distribution of values for the saturated-zone K_d^s , the Freundlich isotherm exponent should be specified as 1.0.

For Options (1) and (2), the K_d^s is either provided in tabular form as a function of the concentration value or calculated as a function of pH, respectively. For Option (3), the saturated-zone K_d^s should be specified using an empirical distribution (EPACMTP distribution type code 6; see Table 5.1 and Section 5.4.7)) and this distribution should be appended to the end of the input file.

Further details of metals sorption coefficients can be found in Section 3.3.3 of the *EPACMTP Parameters/Data Background Document* (U.S. EPA, 2003).

4.4.3.10 Chemical & Biological Transformation Coefficients

The overall decay coefficient (the sum of the chemical and biological transformation coefficients) can be expressed as a distribution of values or as a constant value. The saturated-zone derivation of the overall decay is calculated in the same manner as that for the unsaturated zone (see Section 3.3.3.7). Although the temperature and pH values are assumed not to vary between the saturated and unsaturated zones, the porosity and bulk density values may differ, leading to a difference in the decay coefficients for the two zones.

4.4.3.11 Molecular Diffusion Coefficient

EPACMTP accounts for molecular diffusion in the saturated zone as part of hydrodynamic dispersion. Further details of molecular diffusion in the saturated-zone hydrodynamic dispersion can be found in Section 4.4.4.1.

4.4.3.12 Molecular Weight

EPACMTP accounts for concentrations of degradation products via stoichiometry. A degradation-product concentration is determined by converting its concentration from moles/L to mg/L using its molecular weight.

4.4.4 **Mathematical Formulation of the Saturated-zone Solute Transport Submodule**

The governing equation for 3D transport is:

$$\frac{\partial}{\partial x_i} \left(D_{ij} \frac{\partial c_\ell}{\partial x_j} \right) - V_i \frac{\partial c_\ell}{\partial x_i} = \phi_o Q_\ell \lambda_\ell^s c_\ell + \phi_o R_\ell^s \frac{\partial c_\ell}{\partial t} - \phi_o \sum_{m=1}^M \xi_{\ell m} Q_m \lambda_m^s c_m, \quad \begin{matrix} \ell = 1, n_c \\ i, j = 1, 2, 3 \end{matrix} \quad (4.31)$$

where

$$\begin{aligned} x_i, x_j &= \text{Cartesian coordinates with} \\ x_1 &= \text{x coordinate (m)} \\ x_2 &= \text{y coordinate (m)} \\ x_3 &= \text{z coordinate (m)} \end{aligned}$$

-
- i, j = directional indices (dimensionless) ($i, j = 1, 2, 3$)
 ℓ = component species being evaluated (dimensionless)
 n_c = number of component species in the decay chain (dimensionless)
 D_{ij} = dispersion coefficient tensor (m^2/y)
 c_ℓ = aqueous concentration of the ℓ^{th} component species in the decay chain (mg/L)
 V_i = Darcy velocity in the i^{th} direction (m/y)
 ϕ_e = effective porosity of the aquifer (dimensionless)
 Q_ℓ = coefficient to incorporate decay of sorbed phase species ℓ (dimensionless)
 λ_ℓ^s = first-order decay coefficient for species ℓ (1/y)
 R_ℓ^s = saturated-zone retardation factor for species ℓ (dimensionless)
 t = time (y)
 m = immediate parent of the component species being evaluated (dimensionless)
 M = number of parent species (dimensionless)
 $\xi_{m,\ell}$ = stoichiometric fraction of parent m that degrades into degradation product ℓ (dimensionless)
 Q_m = coefficient to incorporate sorbed phase decay of parent m (dimensionless)
 λ_m^s = first-order decay coefficient for parent m (1/y)
 c_m = concentration of parent m (mg/L)

Parameters, and initial and boundary conditions for Equation (4.31) are described below.

4.4.4.1 Dispersion Coefficients

For computation of the longitudinal, horizontal transverse, and vertical dispersion coefficients (D_{11} , D_{22} ; and D_{33} which can be written as D_{xx} , D_{yy} , and D_{zz}), the conventional dispersion tensor for isotropic porous media is modified to allow the use of different horizontal transverse and vertical dispersivities (Burnett and Frind, 1987). The dispersion coefficients are given by:

$$D_{xx} = \alpha_L \frac{V_x^2}{|V|} + \alpha_T \frac{V_y^2}{|V|} + \alpha_V \frac{V_z^2}{|V|} + \phi_e D_\ell^{s*} \quad (4.32a)$$

$$D_{yy} = \alpha_L \frac{V_y^2}{|V|} + \alpha_T \frac{V_x^2}{|V|} + \alpha_V \frac{V_z^2}{|V|} + \phi_e D_\ell^{s*} \quad (4.32b)$$

$$D_{zz} = \alpha_L \frac{V_z^2}{|V|} + \alpha_V \frac{V_y^2}{|V|} + \alpha_V \frac{V_x^2}{|V|} + \phi_e D_\ell^{s*} \quad (4.32c)$$

$$D_{xy} = D_{yx} = (\alpha_L - \alpha_T) V_x V_y / |V| \quad (4.32d)$$

$$D_{xz} = D_{zx} = (\alpha_L - \alpha_v) V_x V_z / |V| \quad (4.32e)$$

$$D_{yz} = D_{zy} = (\alpha_L - \alpha_v) V_y V_z / |V| \quad (4.32f)$$

$$D_\ell^{s*} = \phi_e^{1/2} D_\ell \quad (4.32g)$$

where

| | | |
|------------------|---|--|
| D_{xx} | = | longitudinal dispersion coefficient (m ² /y) |
| α_L | = | longitudinal dispersivity (m) |
| V_x | = | longitudinal Darcy velocity (m/y) |
| $ V $ | = | absolute value of the Darcy velocity (m/y) |
| α_T | = | horizontal transverse dispersivity (m) |
| V_y | = | horizontal transverse Darcy velocity (m/y) |
| α_v | = | vertical dispersivity (m) |
| V_z | = | vertical Darcy velocity (m/y) |
| ϕ_e | = | effective porosity (dimensionless) |
| D_ℓ^{s*} | = | effective molecular diffusion for species ℓ (m ² /y) |
| D_{yy} | = | horizontal transverse dispersion coefficient (m ² /y) |
| D_{zz} | = | vertical dispersion coefficient (m ² /y) |
| D_{xy}, D_{yx} | = | off-diagonal dispersion coefficients for the x-y plane (m ² /y) |
| D_{xz}, D_{zx} | = | off-diagonal dispersion coefficients for the x-z plane (m ² /y) |
| D_{yz}, D_{zy} | = | off-diagonal dispersion coefficients for the y-z plane (m ² /y) |

The effects of molecular diffusion are incorporated into hydrodynamic dispersion using the last terms of Equations (4.32a), (4.32b), and (4.32c). Equation (4.32g) is adapted from Equation (3.15) with water saturation equal to unity.

4.4.4.2 Retardation Factor

The saturated-zone retardation factor for each of the member species (R^s) is given by

$$R_\ell^s = 1 + \frac{\rho_b ds_\ell}{\phi_e dc_\ell} \quad (4.33)$$

where

| | | |
|------------|---|--|
| R_ℓ^s | = | saturated-zone retardation factor for species ℓ (dimensionless) |
| ρ_b | = | bulk density of the aquifer (g/cm ³) |

| | | |
|----------|---|--|
| s_ℓ | = | adsorbed concentration of the ℓ^{th} component species (mg/kg) |
| ϕ_e | = | effective porosity of the aquifer (dimensionless) |
| c_ℓ | = | aqueous concentration of the ℓ^{th} component species (mg/L) |

Assuming the adsorption isotherm follows the equilibrium Freundlich equation:

$$s_\ell = k_1 c_\ell^{\eta^s} \quad (4.34)$$

where

| | | |
|----------|---|--|
| s_ℓ | = | adsorbed concentration of the ℓ^{th} component species (mg/kg) |
| k_1^s | = | Freundlich coefficient (dimensionless) |
| c_ℓ | = | aqueous concentration of the ℓ^{th} component species (mg/L) |
| η^s | = | Freundlich exponent (dimensionless) |

Then the retardation factor can be written as:

$$R_\ell^s = 1 + \frac{\rho_b}{\phi_e} k_1^s \eta^s c_\ell^{\eta^s - 1} \quad (4.35)$$

where

| | | |
|------------|---|--|
| R_ℓ^s | = | saturated-zone retardation factor for species ℓ (dimensionless) |
| ρ_b | = | bulk density of the aquifer (g/cm^3) |
| ϕ_e | = | effective porosity (dimensionless) |
| k_1^s | = | Freundlich coefficient (dimensionless) |
| η^s | = | Freundlich exponent (dimensionless) |
| c_ℓ | = | aqueous concentration of the ℓ^{th} component species (mg/L) |

4.4.4.3 Coefficient Q_ℓ

The coefficient Q_ℓ is given by

$$Q_\ell = 1 + \frac{\rho_b}{\phi_e} k_1^s c_\ell^{\eta^s - 1} \quad (4.36)$$

where

| | | |
|----------|---|---|
| Q_ℓ | = | coefficient to incorporate decay of sorbed phase species ℓ (dimensionless) |
| ρ_b | = | bulk density of the porous media (aquifer material) (g/cm^3) |
| ϕ_e | = | effective porosity (dimensionless) |
| k_1^s | = | Freundlich coefficient (dimensionless) |
| c_ℓ | = | aqueous concentration of the ℓ^{th} component species (mg/L) |
| η^s | = | Freundlich exponent (dimensionless) |

In general, the retardation factor is a nonlinear function of concentration. The Freundlich isotherm becomes linear when the exponent $n^s = 1.0$. The Freundlich coefficient k_1^s in this case is the same as the familiar solid-liquid phase partition coefficient, K_d^s . When sorption is linear, the coefficients R_ℓ^s and Q_ℓ also become identical.

4.4.4.4 Degradation Products Terms

The summation term on the right-hand side of Equation (4.31) represents the production of species ℓ due to decay (U.S. EPA 1996a) of its immediate parents, c_m , with m varying from 1 to M . The coefficient $\xi_{m\ell}$ is called the stoichiometric fraction which expresses how many units of species ℓ are produced in the decay of each unit of parent m . The value of the stoichiometric fraction is thus determined by the reaction stoichiometry, as well as the units used to express concentration. For instance, consider the following hydrolysis reaction in which 2 moles of degradation product B_{cp} and 1 mole of degradation product C_{cp} are formed from the hydrolysis of 3 moles of parent A_{cp} :



where

| | | |
|----------|---|------------------------------|
| A_{cp} | = | parent compound A_{cp} |
| H_2O | = | water molecule |
| B_{cp} | = | degradation product B_{cp} |
| C_{cp} | = | degradation product C_{cp} |
| $(OH)^-$ | = | hydroxide ion |
| H^+ | = | hydrogen ion |

In this example, ξ_{BA} is equal to $\frac{2 MW_B}{3 MW_A}$ and ξ_{CA} is equal to $\frac{1 MW_C}{3 MW_A}$

where

| | | |
|------------|---|--|
| MW_ℓ | = | molecular weight of species ℓ |
| ξ_{BA} | = | speciation factor between parent A_{cp} and degradation product B_{cp} |
| ξ_{CA} | = | speciation factor between parent A_{cp} and degradation product C_{cp} |

4.4.4.5 Initial Condition

The saturated zone is taken to be initially contaminant free

$$c_\ell(x, y, z, t=0) = 0 \quad (4.38)$$

where

| | | |
|----------|---|---|
| c_ℓ | = | ground-water (aqueous) concentration of the ℓ^{th} component species (mg/L) |
|----------|---|---|

| | | |
|-----|---|---|
| x | = | x coordinate (m) |
| y | = | y coordinate (m) |
| z | = | z coordinate (m) |
| t | = | time – a value of zero indicates the beginning of the leaching duration (y) |

4.4.4.6 Boundary Conditions

Boundary conditions are as follows (see Figure 4.1 for references axes):

(i) Upgradient boundary

$$c_t = 0 \quad \begin{array}{l} x = 0 \\ -\frac{1}{2}y_L \leq y \leq \frac{1}{2}y_L \\ 0 \leq z \leq B \end{array} \quad (4.39a)$$

(ii) Top boundary

$$c_t(x, y, B, t) = c_t^o(t), \quad \begin{array}{l} x_u \leq x \leq x_d \\ -\frac{1}{2}y_D \leq y \leq \frac{1}{2}y_D \end{array} \quad (4.39b)$$

or

$$\left[-D_{zz} \frac{\partial c_t}{\partial z} + V_z c_t \right]_{z=B} = c_t^o(t)I, \quad \begin{array}{l} x_u \leq x \leq x_d \\ -\frac{1}{2}y_D \leq y \leq \frac{1}{2}y_D \end{array} \quad (4.39c)$$

The second boundary condition in Equation (4.39c), is more general as it reflects the preservation of mass flux at the water table. Equation (4.39c) is implemented in EPACMTP.

$$\left[-D_{zz} \frac{\partial c_t}{\partial z} + V_z c_t \right]_{z=B} = 0, \quad \begin{array}{l} x < x_u, x > x_d \\ \text{and} \\ y < -\frac{1}{2}y_D, y > \frac{1}{2}y_D \end{array} \quad (4.39d)$$

and

(iii) Downgradient boundary

$$\frac{\partial c_t}{\partial x} = 0, \quad x = x_L, \quad -\frac{1}{2}y_L \leq y \leq \frac{1}{2}y_L, \quad 0 \leq z \leq B \quad (4.39e)$$

(iv) Left boundary

$$\frac{\partial c_t}{\partial y} = 0, \quad 0 \leq x \leq x_L, \quad y = -\frac{1}{2}y_L, \quad 0 \leq z \leq B \quad (4.39f)$$

(v) Right boundary

$$\frac{\partial c_\ell}{\partial y} = 0, \quad 0 \leq x \leq x_L, \quad y = +\frac{1}{2}y_L, \quad 0 \leq z \leq B \quad (4.39g)$$

(vi) Bottom boundary

$$\frac{\partial c_\ell}{\partial z} = 0, \quad 0 < x \leq x_L, \quad -\frac{1}{2}y_L \leq y \leq \frac{1}{2}y_L, \quad z = 0 \quad (4.39h)$$

where

| | | |
|------------|---|--|
| c_ℓ | = | aqueous concentration of the ℓ^{th} component species (mg/L) |
| x | = | x coordinate (m) |
| y_L | = | length of the aquifer system in the y-direction (m) |
| B | = | thickness of the aquifer system (m) |
| t | = | time (y) |
| c_ℓ^o | = | source concentration (mg/L) |
| x_u | = | upgradient coordinates of the patch source (m) |
| x_d | = | downgradient coordinates of the patch source (m) |
| y_D | = | width of the source in the y-direction (m) |
| D_{zz} | = | vertical dispersion coefficient (m^2/y) |
| z | = | z coordinate (m) |
| V_z | = | vertical ground-water velocity (m/y) |
| I | = | infiltration rate of water through the source (m/y) |
| x_L | = | length of the aquifer system in the x-direction (m) |
| y | = | y coordinate (m) |

Equation (4.39a) describes a zero-concentration condition at the upgradient boundary of the model domain. This condition ensures that no contaminant enters the model through this boundary. However, in cases representing high infiltration from the waste source, the ground-water flow direction in the vicinity of the source may be opposite to the regional ground-water flow direction, with outflow rather than inflow across the upgradient boundary. Setting the concentration to be zero in this case means that the boundary acts as a sink, resulting in excessive loss of contaminant mass from the system. Therefore, when the local flow direction at the upgradient boundary is outward from the domain, condition Equation (4.39a) is replaced by a zero concentration gradient condition to minimize the loss of contaminant mass. Boundary conditions Equation (4.39b) and Equation (4.39c) correspond to a prescribed source concentration and prescribed source contaminant mass flux, respectively.

4.4.4.7 Source Concentration

The source concentration, c_ℓ^o , in Equations (4.39b and 4.39c) is generally time-dependent to reflect possible decay or other concentration variations at the source. The source concentration component of the saturated-zone module provides source

concentration directly to the water table. For a multi-species decay chain, the source concentration at time t is determined by the Bateman equation:

$$\frac{dc_\ell^o}{dt} = -\lambda_\ell^s c_\ell^o + \sum_{m=1}^M \xi_{\ell m} \lambda_m^s c_m^o \quad (4.40a)$$

subject to

$$c_\ell^o(t=0) = \hat{c}_\ell^o \quad (4.40b)$$

where

| | | |
|------------------|---|---|
| c_ℓ^o | = | source concentration of the ℓ^{th} component species in the decay chain (mg/L) |
| t | = | time (y) |
| λ_ℓ^s | = | first-order decay coefficient for species ℓ (1/y) |
| m | = | immediate parent of the ℓ^{th} component species (dimensionless) |
| M | = | number of parent species (dimensionless) |
| $\xi_{\ell m}$ | = | stoichiometric fraction, expressing how many units of species ℓ are produced in the decay of each unit of parent m (dimensionless) |
| λ_m^s | = | first-order decay coefficient for parent m (1/y) |
| c_m^o | = | source concentration of parent species m (mg/L) |
| \hat{c}_ℓ^o | = | initial source concentration of the ℓ^{th} component species in the decay chain (mg/L) |

For a decay chain having n_c members (with ℓ varying from 1 to n_c), the solution of Equation (4.40a) subject to Equation (4.40b) is obtained most conveniently by applying the Laplace transform (see below) to Equation (4.40a). The Laplace-transformed solution takes the simple form:

$$\bar{c}_\ell^o(\rho) = \frac{1}{\rho + \lambda_\ell^s} \left[\hat{c}_\ell^o + \sum_{m=1}^M \xi_{\ell m} \lambda_m^s \bar{c}_m^o(\rho) \right] \quad (4.41)$$

where

| | | |
|------------------|---|--|
| \bar{c}_ℓ^o | = | Laplace-transformed source concentration of species ℓ (y-mg/L) |
| ρ | = | Laplace transform parameter (1/y) |
| λ_ℓ^s | = | first-order decay coefficient for species ℓ (1/y) |
| \hat{c}_ℓ^o | = | initial source concentration of the ℓ^{th} species in the decay chain (mg/L) |

| | | |
|---------------------------|---|---|
| m | = | immediate parent of the ℓ^{th} component species (dimensionless) |
| M | = | number of parent species (dimensionless) |
| $\xi_{m\ell}$ | = | stoichiometric fraction, expressing how many units of species ℓ are produced in the decay of each unit of parent m (dimensionless) |
| λ_m^s | = | first-order decay coefficient for parent m (1/y) |
| $\frac{\lambda_m^s}{C_m}$ | = | Laplace-transformed concentration of parent species m (y-mg/L) |

The desired concentration $c_\ell^o(t)$ is subsequently obtained by numerically inverting Equation (4.41) using the de Hoog algorithm (de Hoog et al., 1982).

4.4.4.8 Treatment of Nonlinear Isotherms

Although EPACMTP can be run using nonlinear adsorption in both the unsaturated and saturated zones in the deterministic case (in other words, for a single set of hydrogeological parameters), the computer processing time required for a Monte-Carlo analysis that includes nonlinear adsorption in both zones is prohibitive. For that reason, a technique was developed that calculates a single value of K_d^s from a nonlinear isotherm. This "linearized" single K_d^s value can then be used as a linear partition coefficient in the model, which decreases computer processing time dramatically (from tens of hours to a few seconds per realization). Obviously, when the original nonlinear isotherm from which the linear K_d^s is calculated is almost linear to begin with, the impact of reducing it to a linear K_d^s is small. Conversely, the error associated with using a linear approximation is increased for highly nonlinear isotherms. The linearization in EPACMTP is such that errors are minimized or conservative results are obtained.

In EPACMTP, two methods are provided for approximating a linear isotherm from a nonlinear isotherm. In the first method, a concentration-interval weighted approach is used to compute a single K_d^s from the nonlinear K_d^s versus dissolved (aqueous) concentration curve. In effect, the technique simply calculates an average K_d^s over the range of dissolved metal concentrations represented by the isotherm. Concentration-interval weighting is used to account for the fact that the dissolved concentration values are not evenly spaced on the isotherm. This method is an option for the EPACMTP model in the unsaturated zone. In the second method (that EPACMTP uses in the saturated zone), the K_d^s corresponding to the peak water table metal concentration is used for linear partitioning. The procedure involves the following steps: First, a saturated-zone isotherm is specified by Monte-Carlo selection of values for the five geochemical master variables. Then, the peak dissolved metal concentration at the water table is determined, and the K_d^s corresponding to this dissolved concentration is obtained from the isotherm by searching for the minimum K_d^s on the isotherm between the minimum concentration and the peak dissolved metal concentration at the water table. This search is conducted to ensure that conservative results are always obtained, even though the isotherm is monotonically increasing with dissolved metal concentration.

4.4.5 Solution Methods for the Solute Transport Submodule

As stated in Section 4.1, three simulation options are available in EPACMTP for modeling ground-water fate and transport in the saturated zone. The saturated-zone transport submodule of EPACMTP contains numerical and analytical solution options for: (i) three-dimensional transport; (ii) numerical solutions for quasi three-dimensional and two-dimensional areal solute transport; and (iii) a hybrid numerical-analytical solution for pseudo-three-dimensional transport.

The three options above are ranked in descending order for accuracy and in ascending order for computational efforts required. In general, the third option (the pseudo three-dimensional solution) is preferred due to its acceptable accuracy (see verification results in Appendix D) and relatively low computational efforts required. It is several times faster than the first two solution options.

4.4.5.1 Aquifer Discretization and Solution Method Selection

For most model applications, no matter what solution method is used for saturated-zone transport, it will be convenient to use the option to automatically discretize the model domain; this option generates the computational grid without requiring detailed user input on node numbers and element sizes. The procedure involves two main steps. The first involves determination of the overall dimensions, that is, length, width, and height of the aquifer region to be modeled. The second step involves generating a computational grid representing the model domain.

4.4.5.1.1 *Determination of Model Domain Dimensions*

The model domain is determined based upon the length and width of the contaminant source, location(s) of receptor well(s), and the aquifer saturated thickness. The length of the model domain is determined to be sufficiently long that the source itself and any receptor wells are included. In addition, the boundaries are placed far enough upgradient of the source, and downgradient of the farthest receptor well, to minimize boundary effects in the flow field and simulated contaminant plume. Particular care is given to the distance between the upgradient model boundary and the source. It is desirable to place this boundary far enough away from the source to be outside the influence of a ground-water mound resulting from the locally higher infiltration through the source area. This involves determining the location of the stagnation point along the x-axis upgradient of the source, that is, the point at which the hydraulic head gradient vanishes. An analytical flow solution (see Appendix C) for areal recharge in a finite domain is used to evaluate the head gradient. The Newton-Raphson method is used to locate the x-coordinate at which the gradient becomes zero. The upgradient boundary in the model domain is then placed at a distance equal to three times the upgradient distance of the stagnation point, away from the source.

The factor of three is an empirically chosen safety factor to ensure that the boundary location is well away from the region of influence of the source. To ensure that the upgradient boundary is not located either too far from the source which might lead to an excessively large computational grid, or too close to the source, the distance, x_s ,

(see Figure 4.7) between the upgradient domain boundary and the upgradient edge of the source is always constrained to fall within the following upper and lower bounds:

$$x_s^{\max} \geq x_s \geq 0.5 x_s^{\max} \quad (4.42a)$$

$$x_s^{\max} = \min(20\alpha_L, 2x_w) \quad (4.42b)$$

where

- x_s^{\max} = maximum allowable distance between the upgradient domain boundary and the upgradient edge of the source (m)
- x_s = distance between the upgradient domain boundary and the upgradient edge of the source (m)
- α_L = longitudinal dispersivity (m)
- x_w = length of the source in the x-direction (m) (see Figure 4.7)

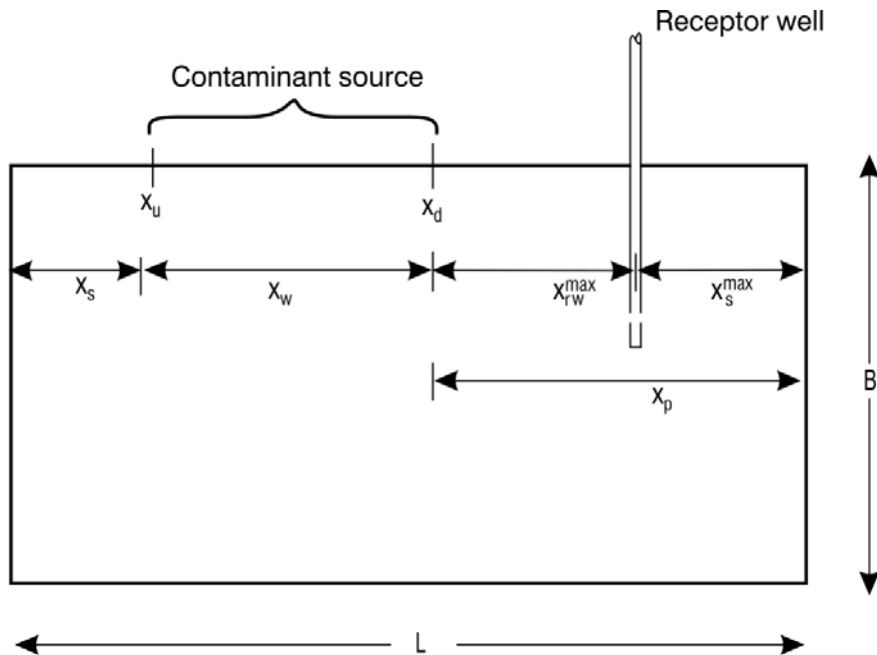


Figure 4.7 Schematic Cross-sectional View of the Aquifer, Illustrating the Procedure for Determining the X-Dimension of the Model Domain.

The parameter x_s^{\max} is determined as a function of the longitudinal dispersivity (α_L) to reflect the dependence of nodal spacings in the computational grid on the Peclet number ($\Delta s/\alpha_L$, where Δs is the grid dimension (m), and α_L the longitudinal dispersivity (m)). Small dispersivity values will lead to a closer spacing of nodal

points. In this case, Equation (4.42b) will have the effect of reducing the length of the domain upgradient of the source to ensure that the number of elements required to discretize this portion of the domain does not become too large. The opposite is true when the dispersivity is large, in which case a greater distance to the upgradient boundary is allowed since the code will use a coarser grid.

The length of the model domain downgradient of the source, x_p , is determined from the position of the receptor well located farthest away from the source, as

$$x_p = x_{rw}^{\max} + x_s^{\max} \quad (4.43)$$

where

| | | |
|-----------------|---|---|
| x_p | = | length of the model domain downgradient of the source (m) |
| x_{rw}^{\max} | = | farthest horizontal distance between the receptor well and the downgradient edge of the source area (m) |
| x_s^{\max} | = | maximum allowable distance between the upgradient domain boundary and the upgradient edge of the source (m) |

The overall length of the model domain in the x-direction is thus equal to

$$L = x_s + x_w + x_p \quad (4.44)$$

where

| | | |
|-------|---|---|
| L | = | overall length of the model domain in the x-direction (m) |
| x_s | = | distance between the upgradient domain boundary and the upgradient edge of the source (m) |
| x_w | = | length of the source in the x-direction (m) (see Figure 4.7) |
| x_p | = | length of the model domain downgradient of the source (m) |

The dimension of the domain in the y-direction is determined as

$$y_L = \max(y_{rw}^{\max}, y_{plume}) \quad (4.45a)$$

where

| | | |
|-----------------|---|---|
| y_L | = | length of the model domain in the y-direction (m) |
| y_{rw}^{\max} | = | farthest horizontal distance between the receptor well and the plume centerline (m) |
| y^{plume} | = | transverse extent of the plume (m) |

And the transverse extent of the plume is approximated by

$$y_{plume} = \frac{1}{2} y_D + 3 \sqrt{2 \alpha_T (x_{rw}^{\max} + x_w)} \quad (4.45b)$$

where

- y^{plume} = transverse extent of the plume (m)
- y_D = source width (m)
- α_T = horizontal transverse dispersivity (m)
- x_{rw}^{max} = farthest horizontal distance between the receptor well and the downgradient edge of the source area (m)
- x_w = length of the source in the x-direction (m) (see Figure 4.7)

The last term on the right-hand side of Equation (4.45b) represents the transverse plume spreading due to dispersive mixing.

The dimension of the model domain in the y-direction, y_L , is determined based on the assumption that the infiltration rate is small relative to the lateral ambient ground-water flux. However, in the event that the infiltration rate is large, the model results will be conservative. In this case, the width of the model domain will be underestimated and the predicted ground-water velocity will be overestimated, thereby causing the modeled contaminants to arrive at receptors sooner and with greater peak concentrations (due to less dilution and less degradation).

The vertical dimension of the model domain is equal to the saturated aquifer thickness, B , except in cases involving very thick saturated zones and shallow contaminant plumes. In these cases, only the upper portion of the saturated zone is actually included in the model domain, based on the approximate vertical extent of the contaminant plume. The vertical extent of the model domain below the water table is determined using Equation (4.71) (see Section 4.4.5.3.3), with the adjustment factor, $\bar{\delta}_{ad}$, set equal to 7.5. A relatively large value for $\bar{\delta}_{ad}$ is used to minimize boundary influence on the modeling results. The final vertical dimension of the model domain is taken to be the lesser of the value obtained using Equation (4.71) (see Section 4.4.5.3.3) and the physical thickness of the saturated zone.

4.4.5.1.2 Discretization of Model Domain

Following determination of the model dimensions, the domain is discretized. Since simple hexagonal (brick) elements are used, the discretization step involves determining the spacings of the grid lines, which is done sequentially for the x-, y-, and z-directions. The nodal spacings are smallest near the source and increase with distance away from the source. The magnitude of nodal spacing, Δs , is controlled by the dispersivity with

$$2.5\alpha_L \leq \Delta s \leq 7.5\alpha_L \quad (4.46)$$

where

- α_L = longitudinal dispersivity (m)
- Δs = magnitude of nodal spacing (m)

This results in grid Peclet numbers varying between 2.5 and 7.5.

The transport equation can be solved numerically using spatial discretization schemes based on either 7-point or 27-point nodal connectivity. The 7-point scheme is equivalent to a typical finite difference method, while the 27-point scheme is usually encountered in finite element schemes. The 7-point finite difference scheme leads to a reduced matrix bandwidth and thus less memory requirements, as well as reduced computational effort during the matrix assembly stage. The option to use either a 7-point finite difference or a 27-point finite element spatial discretization is selected by the user. The use of the 7-point scheme results in an approximately four-fold savings in CPU time and matrix storage requirements as compared to the 27-point scheme. Since the loss in accuracy in the solution is relatively small, in many cases, this is an attractive option to use.

4.4.5.1.3 Solution Method Selection

The applicability and appropriateness of using each of the transport solution options (fully 3D, quasi-3D a combination of (cross-sectional and areal solutions), pseudo-3D (hybrid analytical and numerical solution), and analytical solution options) depends on the problem considered.

Using the quasi three-dimensional option instead of the fully three-dimensional option, will result in a greater savings of CPU time and memory requirements. For Monte-Carlo uses of the code, as in the composite EPACMTP model, the appropriate 2D areal or cross-sectional solution can be selected automatically using the criterion discussed in Section 4.4.5.3.3. The pseudo-3D solution is the most computationally efficient of the four solutions available.

Use of the analytical solution is restricted to situations when the criteria for using the analytical solution are satisfied, that is, single species transport with regional ground-water flow only in the horizontal direction. In this case, the influences of infiltration and recharge are negligibly small. Moreover, use of the analytical solution is attractive only when the number of observation points (n_{obs}) and observation times (n_t) is relatively small, that is, $n_{obs} \times n_t \leq 20$. When these conditions are satisfied, the analytical solution is much faster than the numerical one.

A practical criterion for determining whether the assumption of one-dimensional regional ground-water flow is satisfied is given by the ratio of infiltration and recharge flux to the regional, longitudinal ground-water flux. Shown in Figure 4.7 is a schematic vertical cross-section of an aquifer system, identifying the various contributing components of the ground-water flow field. Q_1^F represents the "background" ground-water flux. Q_2^F and Q_4^F are recharge fluxes and Q_3^F is the infiltration flux through the source. Each of these components is obtained by multiplying the Darcy flow rate by the length of the appropriate boundary segment, that is, Q_3^F is the infiltration rate times the length of the source. Next, Q_r^F is defined as the ratio

$$Q_r^F = \frac{Q_2^F \frac{x_u}{L} + Q_3^F \frac{x_d - x_u}{L} + Q_4^F \frac{L - x_d}{L}}{Q_1^F} \quad (4.47)$$

where

| | | |
|---------|---|---|
| Q_r^F | = | ratio of the background ground-water flux to that near the source (dimensionless) |
| Q_2^F | = | recharge flux upgradient of the source (m^2/y) |
| x_u | = | upgradient coordinates of the source (m) |
| L | = | overall length of the model domain in the x-direction (m) |
| x_d | = | downgradient coordinates of the source (m) |
| Q_3^F | = | infiltration flux through the source (m^2/y) |
| Q_4^F | = | recharge flux downgradient of the source (m^2/y) |
| Q_1^F | = | background ground-water flux (m^2/y) |

Shown in Figure 4.8 is the difference between the results of the analytical and numerical solutions in a randomly located downgradient well as a function of Q_r^F . In this figure, the difference is calculated as the relative concentration difference, $(C_{\text{analytical}} - C_{\text{numerical}})/C_0$, where C_0 is the source concentration. This figure was obtained by performing a hundred simulations with both the analytical and numerical solutions. In these simulations, the well location, source and aquifer parameters were varied randomly according to probability distributions for Subtitle D surface impoundments. The figure clearly illustrates that as the value of Q_r^F decreases (as the ground-water flow field becomes one-dimensional), the analytical and numerical solutions converge. For most practical purposes, a value of $Q_r^F = 0.02$ is a good upper limit for using the analytical solution. The upper limit for Q_r^F , Q_{max}^F , is a user-specified variable. For every problem, the code evaluates Q_r^F using Equation (4.47). If this value is less than the specified Q_{max}^F , the analytical transport solution is used, otherwise, the numerical solution is used.

4.4.5.2 Three-dimensional Transport Solutions

4.4.5.2.1 Laplace Transform Galerkin Solution

For time-dependent simulations with linear adsorption ($r^s = 1.0$, see Equation (4.35)), the governing Equation (4.31) with initial and boundary conditions Equation (4.36) through Equation (4.40) is solved using the Laplace Transform Galerkin (LTG) technique. The method is described in detail by Sudicky (1989), and only the most important steps are given here. The Laplace transform, $\bar{f}(p)$, of a function $f(t)$ is defined as

$$\mathcal{L}[f(t)] = \bar{f}(p) = \int_0^{\infty} f(t) \exp(-pt) dt \quad (4.48)$$

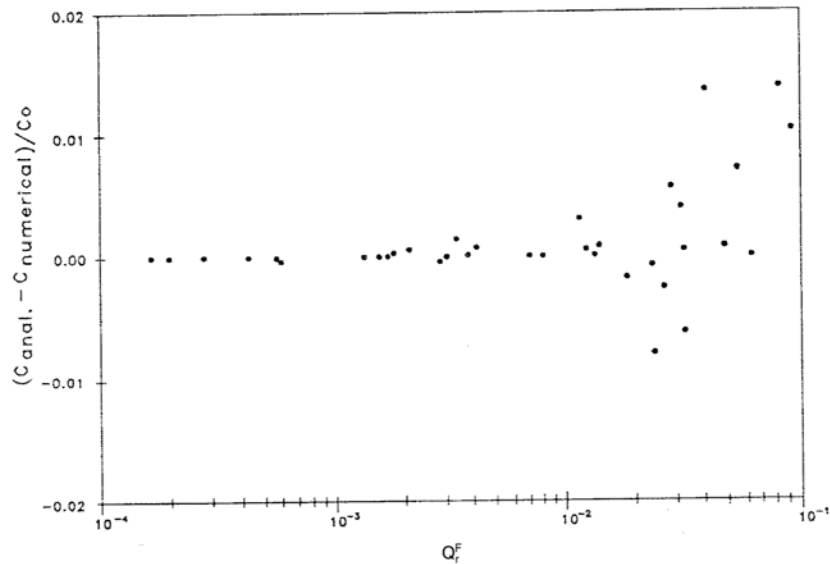


Figure 4.8 Difference $(C_{\text{analytical}} - C_{\text{numerical}})/C_0$ Between Analytical and Numerical Transport Solutions as a Function of Q_r^F (ratio of regional flux to near-source flux). C_0 is the Source Concentration.

where

| | | |
|----------------------|---|--|
| $\mathcal{L}(\cdot)$ | = | Laplace transform operator (dimensionless) |
| $f(p)$ | = | Laplace transformed function (original dimension $\cdot y$) |
| p | = | Laplace transform variable ($1/y$) |
| t | = | time (y) |

Application of the Laplace transformation to the governing transport equation leads to

$$\frac{\partial}{\partial x_i} \left(D_{ij} \frac{\partial \bar{c}_l}{\partial x_j} \right) - V_i \frac{\partial \bar{c}_l}{\partial x_i} = \phi_\theta Q_l \lambda_l^s \bar{c}_l + \phi_\theta R_{\theta l}^s p \bar{c}_l - \phi_\theta \sum_{m=1}^M \xi_m \lambda_m^s Q_m \bar{c}_m \quad (4.49)$$

where

| | | |
|-------------|---|---|
| i, j | = | directional indices for x, y, and z (dimensionless) |
| x_i | = | spatial coordinate in the i^{th} direction (m) |
| x_j | = | spatial coordinate in the j^{th} direction (m) |
| | | $x_1 = x$ coordinate (m) |
| | | $x_2 = y$ coordinate (m) |
| | | $x_3 = z$ coordinate (m) |
| D_{ij} | = | dispersion coefficient tensor (m^2/y) |
| \bar{c}_l | = | $\bar{c}_l(x, y, z, p)$, Laplace-transformed concentration of species l (y-mg/L) |
| V_i | = | Darcy velocity in the i^{th} direction (m/y) |

- ϕ_e = effective porosity of the aquifer (dimensionless)
 Q_ℓ = coefficient to incorporate sorbed phase decay of species ℓ (dimensionless)
 λ_ℓ^s = first-order decay coefficient for species ℓ (1/y)
 R_ℓ^s = saturated-zone retardation factor for species ℓ (dimensionless)
 p = Laplace transform variable (1/y)
 m = immediate parent of the ℓ^{th} component species (dimensionless)
 M = number of parent species (dimensionless)
 ξ_m = stoichiometric fraction, expressing how many units of species ℓ are produced in the decay of each unit of parent m (dimensionless)
 λ_m^s = first-order decay coefficient for parent m (1/y)
 Q_m = coefficient to incorporate sorbed phase decay of parent m (dimensionless)
 \bar{c}_m = Laplace-transformed concentration of parent species m (y-mg/L)

Equation (4.49) together with the transformed boundary conditions is solved employing either 7-point finite difference or 27-point finite element spatial discretization schemes. In both cases, a rectangular, three-dimensional grid is employed. This grid is the same as that used for the steady-state ground-water flow solution. It yields a final matrix equation of the form

$$([P] + p[S]) \{\bar{c}\} - \{b\} = 0 \quad (4.50)$$

where

- $[P]$ = advective-dispersive transport matrix, including the decay term λ
 $[S]$ = Laplace-transformed mass matrix
 p = Laplace transform variable (1/y)
 $\{\bar{c}\}$ = Laplace-transformed concentration vector
 $\{b\}$ = a vector containing the known transformed natural boundary conditions, as well as contributions from decaying parents

The species index, ℓ , has been dropped to simplify the notation.

The solution of Equation (4.50) is obtained using the iterative ORTHOMIN matrix solver also employed for the ground-water flow solution. This solution yields the transformed concentration $\bar{c}(x,y,z,p)$. The last step in the solution process is inversion of the transformed concentration. The inverse Laplace transformation is carried out numerically using the de Hoog algorithm (de Hoog et al., 1982). The concentration at node j of the finite element grid, $c_j(t)$, is found from \bar{c}_j using the Fourier series approximation

$$c_j(t) = \frac{1}{T} \exp(p^o t) \left[\frac{1}{2} \bar{c}_j(p^o) + \sum_{k=0}^{\infty} \left(\text{Re}\{\bar{c}_j(p_k)\} \cos(k\pi t/T) - \text{Im}\{\bar{c}_j(p_k)\} \sin(k\pi t/T) \right) \right] + E \quad (4.51)$$

where

| | | |
|-------------|---|---|
| $c_j(t)$ | = | concentration at node j of the finite element grid at time t (mg/L) |
| T | = | one-half of the fundamental period of the Fourier series approximating the inverse function on the interval $[0, 2T]$ (y) |
| p° | = | real constant for the inversion of Laplace transform (1/y) |
| t | = | time (y) |
| \bar{c}_j | = | Laplace-transformed concentration (y-mg/L) |
| N | = | number of terms in the series (dimensionless) |
| k | = | index of the series (dimensionless) |
| Re | = | real part of the complex \bar{c}_j values (y-mg/L) |
| p_k | = | k^{th} term of the parameter in the Laplace inversion series (1/y) |
| Im | = | imaginary part of the complex \bar{c}_j values (y-mg/L) |
| E | = | error term arising because the Fourier coefficients are approximations obtained from \bar{c}_j rather than $c_j(t)$ and because the series is truncated after $2N$ terms (mg/L) |

The parameter p° is evaluated as:

$$p^\circ = \frac{-\ln E}{1.6 t_{\max}} \quad (4.52)$$

where

| | | |
|------------|---|---|
| p° | = | real constant for the inversion of Laplace transform (1/y) |
| E | = | error term arising because the Fourier coefficients are approximations obtained from \bar{c}_j rather than $c_j(t)$ and because the series is truncated after $2N$ terms (mg/L) |
| t_{\max} | = | maximum simulation time (y) |

The k discrete values of the Laplace variable p_k are related to the parameter p° according to the relationship

$$p_k = p^\circ + \frac{k\pi i}{T} \quad (4.53)$$

where

| | | |
|-----------|---|---|
| p_k | = | k^{th} term of the parameter in the Laplace inversion series (1/y) |
| p° | = | real constant for the inversion of Laplace transform (1/y) |
| k | = | index of the series (dimensionless) |
| i | = | an imaginary number equal to $\sqrt{-1}$ |
| T | = | one-half of the fundamental period of the Fourier series approximating the inverse function on the interval $[0, 2T]$ (y) |

The truncation error in Equation (4.51) is reduced, and, therefore, convergence is accelerated by applying a quotient difference acceleration scheme algorithm (MacDonald, 1964).

Application of the Laplace transform method requires that the boundary conditions be transformed along with the transport equation itself (Equation (4.31)). In the case of a constant source concentration, $c_i^o(t) = C_i^o$, the transformed boundary condition is simply

$$\bar{c}_i^o(p) = \frac{1}{p} C_i^o \quad (4.54)$$

where

$$\begin{aligned} \bar{c}_i^o(p) &= \text{Laplace transform of the source function (y-mg/L)} \\ p &= \text{Laplace transform variable (1/y)} \\ C_i^o &= \text{constant source concentration (mg/L)} \end{aligned}$$

When the source concentration is described by the Bateman equation (Equation (4.40a)), the transformed boundary condition is given by Equation (4.41). EPACMTP furthermore allows the source concentration $c_i^o(t)$ to vary as an arbitrary function of time. To make this case amenable to solution by the Laplace transform method, the source function $c_i^o(t)$ is approximated as a sequence of Heaviside step functions. Dropping the species subscript i to simplify the notation, this can be expressed as

$$c^o(t) \approx \sum_{i=1}^{N_s} C_{iave}^o [H_v(t - t_i^{on}) - H_v(t - t_i^{off})] \quad (4.55)$$

where

$$\begin{aligned} c^o(t) &= \text{source concentration at time } t \text{ (mg/L)} \\ i &= \text{step index (dimensionless)} \\ N_s &= \text{number of steps into which } c^o(t) \text{ is discretized (dimensionless)} \\ C_{iave}^o &= \text{average concentration value during the time interval } [t_i^{on}, t_i^{off}] \text{ (mg/L)} \\ H_v &= \text{Heaviside step function (dimensionless) (see Equation 4.56)} \\ t &= \text{time (y)} \\ t_i^{on} &= \text{beginning of the time interval of step } i \text{ (y)} \\ t_i^{off} &= \text{end of the time interval of step } i \text{ (y)} \\ \exp(\cdot) &= \text{exponential operator (dimensionless)} \end{aligned}$$

The Heaviside step function is defined as

$$H_v(t - t_i^{on}) = \begin{cases} 0, & t < t_i^{on} \\ 1, & t \geq t_i^{on} \end{cases}, \quad (4.56)$$

where

$$\begin{aligned} H_V &= \text{Heaviside step function (dimensionless)} \\ t &= \text{time (y)} \\ t_i^{on} &= \text{beginning of the time interval of step } i \text{ (y)} \end{aligned}$$

The Laplace transform of the source function, $\bar{c}^o(p)$, then becomes

$$\bar{c}^o(p) = \frac{1}{p} \sum_{i=1}^{N_s} C_{iave}^o [\exp(-pt_i^{on}) - \exp(-pt_i^{off})] \quad (4.57)$$

where

$$\begin{aligned} \bar{c}^o(p) &= \text{Laplace transform of the source function (y-mg/L)} \\ p &= \text{Laplace transform variable (1/y)} \\ i &= \text{step index} \\ N_s &= \text{number of steps into which } c^o(t) \text{ is discretized (dimensionless)} \\ C_{iave}^o &= \text{average concentration during time interval } [t_i^{on}, t_i] \text{ (mg/L)} \\ t_i^{on} &= \text{beginning of the time interval of interest (y)} \\ t_i^{off} &= \text{end of the time interval of interest (y)} \end{aligned}$$

The LTG solution scheme offers additional advantages when it is desired to compute ground-water concentration values that represent temporal averages rather than instantaneous values. For instance, for risk assessment purposes, exposure is often defined as the average concentration over a specified exposure period, that is,

$$C_A = \frac{1}{t_2 - t_1} \int_0^{t_2} c(x,y,z,t) dt. \quad (4.58)$$

where

$$\begin{aligned} C_A &= \text{average ground-water concentration over a specified exposure period (mg/L)} \\ t_1 &= \text{beginning of the time interval of interest (y)} \\ t_2 &= \text{end of the time interval of interest (y)} \\ c(x,y,z,t) &= \text{concentration at x,y,z at time t (mg/L)} \\ t &= \text{time (y)} \end{aligned}$$

Noting the Laplace transform property

$$\mathcal{L} \left[\int_0^t f(t) dt \right] = \frac{1}{p} \bar{f}(p), \quad (4.59)$$

where

| | | |
|----------------------|---|--|
| $\mathcal{L}(\cdot)$ | = | Laplace transformation operator (dimensionless) |
| t | = | time (y) |
| p | = | Laplace transform variable (1/y) |
| $f(p)$ | = | Laplace-transformed function (original unit · y) |

the desired time-averaged concentration can be conveniently obtained as

$$C_A = \frac{1}{t_2 - t_1} \left[\int_0^{t_2} c(x,y,z,t) dt - \int_0^{t_1} c(x,y,z,t) dt \right] \quad (4.60)$$

$$= \frac{1}{t_2 - t_1} \left\{ \mathcal{L}^{-1} \left[\frac{1}{p} \bar{c}(x,y,z,p) \right]_{t_2} - \mathcal{L}^{-1} \left[\frac{1}{p} \bar{c}(x,y,z,p) \right]_{t_1} \right\} \quad (4.61)$$

where

| | | |
|----------------------|---|--|
| C_A | = | average ground-water concentration over a specified exposure period (mg/L) |
| t_2 | = | end of the time interval of interest (y) |
| t_1 | = | beginning of the time interval of interest (y) |
| $c(x,y,z,t)$ | = | concentration at x,y,z at time t (mg/L) |
| x | = | x coordinate (m) |
| y | = | y coordinate (m) |
| z | = | z coordinate (m) |
| t | = | time (y) |
| $\mathcal{L}(\cdot)$ | = | Laplace transformation operator (dimensionless) |
| p | = | Laplace transform variable (1/y) |
| $\bar{c}(x,y,z,t)$ | = | Laplace-transformed concentration at x, y, z at time t (y-mg/L) |

4.4.5.2.2 Solution for Steady-state and Nonlinear Transport

A major advantage of the LTG method for linear transport problems compared with conventional time marching numerical approaches is that in order to obtain the solution for any arbitrary time value, the governing equation (Equation (4.49)) needs to be solved only $2N+1$ times where N is typically 5 or 7. When the solution is required for multiple time values, only the inversion of the Laplace transformed solution needs to be repeated. This advantage disappears when only the steady-state solution is desired. In this situation the solution, using conventional time discretization, can be obtained in a single step by setting the time derivative to zero, whereas the LTG method still requires $2N+1$ steps. Moreover, the LTG method cannot be used for problems with nonlinear adsorption isotherms. For this purpose, EPACMTP contains a separate standard Galerkin finite element numerical solution (Huyakorn and Pinder, 1983) for the steady-state or nonlinear transient transport equation. Compared to the Laplace Transform method, standard numerical transport solution schemes are more susceptible to oscillatory behavior in the

computed concentration profiles when the grid Peclet number $\Delta s/\alpha_L$, where Δs is the grid dimension, increases. Upgradient weighting (Huyakorn and Nilkuha, 1979) is therefore used to reduce numerical oscillations in the predicted concentrations. In the case of nonlinear sorption, a central difference time stepping solution is used with Picard iteration (Huyakorn and Pinder, 1983) to resolve the non-linearity.

4.4.5.2.3 Analytical Solution

In situations where the vertical and transverse components of ground-water flow are negligibly small, and sorption is linear, the ground-water transport problem may be solved analytically. The analytical solution is reserved for single component simulations. The species subscript will therefore be omitted in the remainder of this section. When ground-water flow is in the longitudinal direction only, and considering only the half of the system along the positive y-axis, the governing three-dimensional transport equation can be written as

$$D_{xx} \frac{\partial^2 c}{\partial x^2} + D_{yy} \frac{\partial^2 c}{\partial y^2} + D_{zz} \frac{\partial^2 c}{\partial z^2} - V_x \frac{\partial c}{\partial x} + M_s [\{H_v(x-x_u) - H_v(x-x_d)\} \{H_v(y+y_0) - H_v(y-y_0)\} \delta(z-B)] = \phi_e R^s \left(\frac{\partial c}{\partial t} + \lambda^s c \right) \quad (4.62)$$

where

| | | |
|-------------------|---|--|
| D_{xx} | = | longitudinal dispersion coefficient (m ² /y) |
| c | = | contaminant concentration in the aqueous phase (mg/L) |
| x | = | x coordinate (m) |
| D_{yy} | = | horizontal transverse dispersion coefficient (m ² /y) |
| y | = | y coordinate (m) |
| D_{zz} | = | vertical transverse dispersion coefficient (m ² /y) |
| z | = | z coordinate (m) |
| V_x | = | Darcy velocity in the x-direction (m/y) |
| M_s | = | contaminant mass flux (mg/m ² ·y) which is applied over the rectangular area given by $x_u \leq x \leq x_d$ and $0 \leq y \leq y_0$ |
| $H_v(\bullet)$ | = | Heaviside step function (dimensionless) |
| x_u | = | upgradient coordinates of the source (m) |
| x_d | = | downgradient coordinates of the source (m) |
| y_0 | = | one-half the source width (Y_D) (m) |
| $\delta(\bullet)$ | = | Dirac Delta function (dimensionless) |
| B | = | aquifer thickness (m) |
| ϕ_e | = | effective porosity (dimensionless) |
| R^s | = | retardation factor for the saturated zone (dimensionless) |
| t | = | time (y) |
| λ^s | = | first-order decay constant (1/y) |

Equation (4.62) is solved analytically for a zero concentration initial condition

$$c(x, y, z, 0) = 0 \quad (4.63a)$$

where

$$c(x, y, z, 0) = \text{concentration at } x, y, z \text{ at time } 0 \text{ (mg/L)}$$

and boundary conditions

$$\frac{\partial c}{\partial x} = 0 \quad y = \pm \infty \quad (4.63b)$$

$$\frac{\partial c}{\partial y} = 0 \quad y = 0, y = \infty \quad (4.63c)$$

$$\frac{\partial c}{\partial z} = 0 \quad z = 0, z = B \quad (4.63d)$$

where

| | | |
|-----|---|---|
| c | = | contaminant concentration in the aqueous phase (mg/L) |
| x | = | x coordinate (m) |
| y | = | y coordinate (m) |
| z | = | z coordinate (m) |
| B | = | aquifer thickness (m) |

Since flow in the saturated zone is taken to be in the longitudinal direction only, the components of the dispersion tensor now become

$$D_{xx} = \alpha_L V_x + \phi_e D_l^{s*} \quad (4.64a)$$

$$D_{yy} = \alpha_T V_x + \phi_e D_l^{s*} \quad (4.64b)$$

$$D_{zz} = \alpha_V V_x + \phi_e D_l^{s*} \quad (4.64c)$$

where

| | | |
|------------|---|---|
| D_{xx} | = | longitudinal dispersion coefficient (m ² /y) |
| α_L | = | longitudinal dispersivity (m) |
| V_x | = | longitudinal ground-water velocity (m/y) |
| ϕ_e | = | effective porosity (dimensionless) |

| | | |
|---------------|---|--|
| D_ℓ^{s*} | = | effective molecular diffusion coefficient for species ℓ (m^2/y) |
| D_{yy} | = | horizontal transverse dispersion coefficient (m^2/y) |
| α_T | = | horizontal transverse dispersivity (m) |
| D_{zz} | = | vertical transverse dispersion coefficient (m^2/y) |
| α_V | = | vertical transverse dispersivity (m) |

The solution of Equations (4.62 through 4.64) is given by

$$c(x, y, z, t) = \frac{M_s}{4R^s} \sum_{q=0}^{\infty} G_q \int_0^t \exp\left(-\frac{\psi_q^2 D_{zz}}{R^s} - \lambda^s\right) \tau_t \cdot \quad (4.65a)$$

$$\left\{ -\operatorname{erfc}\left[\frac{(x_d - x)}{4D_{xx}\tau_t}\right]^{1/2} + V_x \left(\frac{\tau_t}{4D_{xx}R^s}\right)^{1/2}\right\} + \operatorname{erfc}\left[\frac{(x_u - x)}{4D_{xx}\tau_t}\right]^{1/2} + V_x \left(\frac{\tau_t}{4D_{xx}R^s}\right)^{1/2}\right\} \\ \cdot \left\{ \operatorname{erfc}\left[\frac{(y - y_0)}{4D_{yy}\tau_t}\right]^{1/2} - \operatorname{erfc}\left[\frac{(y + y_0)}{4D_{yy}\tau_t}\right]^{1/2}\right\} d\tau_t$$

with

$$\psi_q = \pi q/B \quad q = 0, 1, \dots \quad (4.65b)$$

$$G_q = \begin{cases} 1/B & q = 0 \\ \frac{2\cos(\psi_q z)}{B} & q = 1, 2, \dots \end{cases} \quad (4.65c)$$

where

| | | |
|-----------------|---|---|
| $c(x, y, z, t)$ | = | concentration at x, y, z at time t (mg/L) |
| M_s | = | contaminant mass flux ($\text{mg}/\text{m}^2\text{-y}$) which is applied over the rectangular area given by $x_u \leq x \leq x_d$ and $0 \leq y \leq y_0$ |
| R^s | = | retardation factor for the saturated zone (dimensionless) |
| q | = | index of the series (dimensionless) |
| G_q | = | m^{th} coefficient described by Equation (4.65c) (1/m) |
| ψ_q | = | constant described by Equation (4.65b) (1/m) |
| D_{zz} | = | vertical transverse dispersion coefficient (m^2/y) |
| R^s | = | retardation factor (dimensionless) |
| λ^s | = | first-order decay coefficient (1/y) |
| τ_t | = | time integration variable (y) |

| | | |
|----------|---|--|
| x_d | = | downgradient coordinates of the source (m) |
| x | = | x coordinate (m) |
| D_{xx} | = | longitudinal dispersion coefficient (m ² /y) |
| V_x | = | longitudinal ground-water velocity (m/y) |
| x_u | = | upgradient coordinates of the source (m) |
| y | = | y coordinate (m) |
| y_0 | = | half-source width (m) |
| | = | one-half the source width (Y_D) (m) |
| D_{yy} | = | horizontal transverse dispersion coefficient (m ² /y) |
| B | = | saturated thickness of the aquifer (m) |
| q | = | index of terms in the summation (dimensionless) |
| z | = | z coordinate (m) |

The solution presented in Equation (4.65a) is a transient solution. The analytical steady-state solution is obtained by using a large t value in Equation (4.65a).

4.4.5.3 Two-dimensional Transport Solutions

Consistent with the 2D cross-sectional and 2D areal ground-water flow options of the model (see Section 4.3.5.2), the transport module includes options to ignore horizontal transverse advection and vertical advection, respectively.

4.4.5.3.1 Two-dimensional Cross-sectional Transport Solution

For the case in which 2D cross-sectional flow is considered, EPACMTP contains a corresponding transport solution which does not consider advection in the horizontal transverse (y-direction). The solution, however, does take into account dispersion in the y-direction, thus yielding a quasi three-dimensional contaminant transport approximation. The governing transport Equation (4.31) is rigorously solved in the two-dimensional, cross-sectional (x-z) plane, using either the Laplace transform or standard Galerkin numerical schemes. The same one grid block-wide grid employed for the two-dimensional, cross-sectional ground-water flow equation is used. Since the transverse ground-water flow rate, V_y , obtained from the flow solution is zero and the grid spans exactly the half source width, a two-dimensional transport solution is obtained. To account for dispersion in the y-direction, the analytical method of Domenico and Robbins (1985) is used. The computation of horizontal transverse dispersion from a point in the x-z plane ($x_c, 0, z_c$) involves the use of the travel time t' which is defined as the time required for a particle of water to travel a distance d_c from a point at the water table underneath the patch source to the downgradient location x_c . The distance d_c is defined as

$$d_c = \max(0, x_c - x_u) \quad (4.66a)$$

$$t' = \frac{d_c}{V_x} \quad (4.66b)$$

where

- d_c = distance from a point at the water table underneath the patch source to the downgradient location x_c (m)
 x_c = downgradient location at which dispersion is calculated (m)
 x_u = upgradient location underneath the patch source (m)
 t' = travel time from x_u to x_c (y)
 \overline{V}_x = average longitudinal ground-water velocity (m/y)

The governing equation for one-dimensional dispersive transport in the horizontal transverse direction is

$$D_{yy} \frac{\partial^2 c_\ell}{\partial y^2} = R_\ell^s \frac{\partial c_\ell}{\partial t'} \quad (4.67)$$

where

- D_{yy} = horizontal transverse dispersion coefficient (m^2/y)
 c_ℓ = aqueous concentration of the species ℓ (mg/L)
 y = y coordinate (m)
 R_ℓ^s = retardation factor for the saturated zone of the species ℓ (dimensionless)
 t' = travel time from x_u to x_c (y)

with the initial condition

$$c_\ell(y, t = 0) = 0 \quad (4.68a)$$

where

- $c_\ell(y, t = 0)$ = initial aqueous concentration of the species ℓ at y at the beginning of the leaching duration ($t = 0$) (mg/L)

and boundary conditions

$$c_\ell(y, t) |_{x,z} = c_\ell(x, z, t) \quad 0 \leq y \leq y_o \quad (4.68b)$$

$$\frac{\partial c_\ell}{\partial y} = 0 \quad y \rightarrow \infty \quad (4.68c)$$

where

- $c_\ell(y, t = 0)$ = aqueous concentration of the species ℓ at y at the beginning of the leaching duration ($t = 0$) (mg/L)
 x = x coordinate (m)
 z = z coordinate (m)

| | | |
|-------------------|---|--|
| $c_\ell(x, z, t)$ | = | aqueous concentration of the species ℓ at x, z at time t (mg/L) |
| y | = | y coordinate (m) |
| y_o | = | one-half the source width (y_o) (m) |
| c_ℓ | = | aqueous concentration of the species ℓ (mg/L) |

The one-dimensional transverse and two-dimensional cross-sectional transport solutions are coupled through the boundary condition presented in Equation (4.68b). The transverse dispersion coefficient D_{yy} is given by

$$D_{yy} = \alpha_T \bar{V}_x + \phi_e D_\ell^{s*} \quad (4.69)$$

where

| | | |
|---------------|---|---|
| D_{yy} | = | horizontal transverse dispersion coefficient (m^2/y) |
| α_T | = | horizontal transverse dispersivity (m) |
| \bar{V}_x | = | average longitudinal ground-water velocity (m/y) |
| ϕ_e | = | effective porosity (dimensionless) |
| D_ℓ^{s*} | = | effective molecular diffusion coefficient of species ℓ (m^2/y) |

The final three-dimensional solution is obtained by multiplication of the two-dimensional and one-dimensional solutions

$$c_\ell(x, y, z, t) = c_\ell(x, z, t) \frac{1}{2} \left[\operatorname{erfc} \left\{ \frac{y - y_o}{2 \left(\frac{D_{yy} t'}{R_\ell^s} \right)^{1/2}} \right\} - \operatorname{erfc} \left\{ \frac{y + y_o}{2 \left(\frac{D_{yy} t'}{R_\ell^s} \right)^{1/2}} \right\} \right] \quad (4.70)$$

where

| | | |
|----------------------|---|---|
| $c_\ell(x, y, z, t)$ | = | aqueous concentration of the species ℓ at x, y, z at time t (mg/L) |
| $c_\ell(x, z, t)$ | = | aqueous concentration of the species ℓ at x, z at time t on a vertical plane with $y = 0$ (mg/L) |
| x | = | x coordinate (m) |
| y | = | y coordinate (m) |
| z | = | z coordinate (m) |
| y_o | = | one-half the source width (y_D) (m) |
| D_{yy} | = | horizontal transverse dispersion coefficient (m^2/y) |
| t' | = | travel time from x_u to x_c (y) |
| R_ℓ^s | = | retardation factor for the saturated zone of the species ℓ (dimensionless) |

The contaminant decay constant λ_ℓ does not appear explicitly in Equation (4.70). The effects of degradation are implicitly accounted for through the linking term, $c_\ell(x, z, t)$, with the two-dimensional solution.

4.4.5.3.2 Two-dimensional Areal Transport Solution

For the case in which ground-water flow in the vertical direction is ignored, the module contains a two-dimensional areal transport solution. This solution yields a vertically averaged concentration distribution, representing the case in which the contaminant plume occupies the entire saturated aquifer thickness with complete vertical mixing. This solution employs the 2D areal grid used in the two-dimensional areal flow solution. This grid is one grid block deep with a thickness equal to the saturated aquifer thickness. The source mass flux is apportioned equally to the upper and lower plane of the grid, with each receiving one-half of the total mass flux. This ensures a correct mass balance and yields a vertically averaged solution.

4.4.5.3.3 Criterion for selecting Two-dimensional Solutions

As mentioned before, it is expected that the 2D cross-sectional flow and transport solutions will be most accurate in situations involving a large waste facility overlying a deep saturated zone, while the 2D areal approximation is expected to be most accurate in cases with a thin saturated zone. For Monte-Carlo applications of the model, the 2D approximations will result in substantial savings of computational effort as compared to the fully 3D solution. In order to implement these options for Monte-Carlo applications, a suitable criterion for selecting either a 2D vertical or a 2D areal solution is required.

The criterion for automatic switching between the cross-sectional and areal solutions is based on the penetration depth of the contaminant plume in the quasi-3D saturated zone. If the plume has reached the base of the saturated zone when it reaches the nearest observation well, the areal solution is used. In other cases, the cross-sectional approximation is used. The approximation for the plume depth, B' , takes into account both advective and dispersive movement of the contaminant, and takes the form where

B' = estimated plume depth (m)
 δ_{ad} = empirical adjustment factor (dimensionless)

$$B' = \delta_{ad} \left\{ \frac{Q_3^F + Q_4^F}{Q_1^F} B + \left[\alpha_v (x_w + x_{rw}) + \alpha_L \left(\frac{Q_3^F + Q_4^F}{Q_1^F} B \right) \right]^{\frac{1}{2}} \right\} \quad (4.71)$$

Q_1^F = background ground-water flux (m^2/y)
 Q_3^F = infiltration flux through the source (m^2/y)
 Q_4^F = recharge flux downgradient of the source (m^2/y)
 α_v = transverse vertical dispersivity (m)
 x_w = length of the source along the flow direction (m)

- x_{rw} = horizontal distance between the source and receptor well (m)
 α_L = longitudinal dispersivity (m)
 B = saturated thickness of the aquifer (m)

Each of the Q^F terms is obtained by multiplying the areal flux by the length of the corresponding boundary segment; for example, Q_1^F equals the ambient ground-water flow rate times the saturated aquifer thickness. The first term in the right-hand side of Equation (4.71) includes the ratio of vertical to horizontal ground-water flow components. It approximates the extent of vertical plume movement due to advection. The second term in Equation (4.71) describes the downward plume movement due to dispersive action. The adjustment factor, δ_{ad} , is introduced to account for the approximate nature of Equation (4.71). Its value is determined such that differences between the fully 3D and quasi-3D transport solutions are minimized. A value of $\delta_{ad} = 0.65$ was determined by evaluating 1,000 randomly generated aquifer realizations, and comparing the differences in predicted plume concentration values at a randomly located receptor well between the fully 3D and quasi-3D solutions, as a function of δ_{ad} . The simulation was conducted using the Monte-Carlo procedure implemented in the composite EPACMTP code and representative landfill parameter distributions.

The approximation for the vertical plume extent is useful also to determine whether an observation well lies within the plume at all, or lies underneath the plume and samples only pristine ground water. The latter case would obviate the need to perform the transport simulation at all. In this case, a conservative approach to determining whether a receptor well lies outside of the plume is adopted. This is achieved by setting the adjustment factor in Equation (4.71) to $\delta_{ad} = 2.5$. This value was determined also by simulating 1,000 randomly generated aquifer realizations. By using a value of $\delta_{ad} = 2.5$, virtually all cases with a non-zero receptor well concentration were accounted for. Out of 1,000 random realizations, the highest normalized observation well concentration value that was missed was 5×10^{-6} mg/L. This value is smaller than the numerical accuracy of the transport solution.

4.4.5.4 Pseudo-3D Transport Solution

Assuming that equilibrium exists between the solid and aqueous phases and that the dimension in the y direction is infinite, the transport in the saturated zone may be described as :

$$\begin{aligned}
 & \frac{\partial}{\partial t} [c_t (\phi_\theta + (1 - \phi_\theta) \rho_s \frac{\partial s_t}{\partial c_t})] + \frac{\partial}{\partial x_j} [V_j c_t - D_{ij} \frac{\partial c_t}{\partial x_j}] \\
 & + \lambda_t^s [c_t \phi_\theta + (1 - \phi_\theta) \rho_s s_t] \\
 & - \sum_{m=1}^M \lambda_m^s [c_m \phi_\theta + (1 - \phi_\theta) \rho_s s_m] \xi_{jm} = 0
 \end{aligned} \tag{4.72}$$

$i, j = 1, 2, 3.$

where

| | | |
|------------------|---|---|
| t | = | time (y) |
| c_ℓ | = | concentration of species ℓ in the aqueous phase (mg/L) |
| ϕ_e | = | effective porosity (dimensionless) |
| ρ_s | = | density of the solid phase (g/cm ³) |
| s_ℓ | = | concentration of species ℓ in the solid (adsorbed) phase (mg/kg) |
| x_i | = | Cartesian coordinates in the i^{th} direction (the 1 st , 2 nd , and 3 rd directions correspond to the x, y, and z directions, respectively) (m) |
| V_i | = | ground-water velocity in the i^{th} direction (aqueous phase) (m/y) |
| D_{ij} | = | dispersion coefficient tensor (aqueous phase) (m ² /y) |
| x_j | = | Cartesian coordinates in the j^{th} direction (the 1 st , 2 nd , and 3 rd directions correspond to the x, y, and z directions, respectively) (m) |
| λ_ℓ^s | = | degradation constant for the ℓ^{th} species (1/y) |
| m | = | immediate parent of the component species being evaluated (dimensionless) |
| M | = | total number of parent chemicals (dimensionless) |
| λ_m^s | = | degradation constant for parent m (1/y) |
| c_m | = | concentration of parent species m in the aqueous phase (mg/L) |
| s_m | = | concentration of parent species m in the solid (adsorbed) phase (mg/kg) |
| $\xi_{\ell m}$ | = | constant related to decay reaction stoichiometry of the m^{th} parent chemical and the ℓ^{th} chemical which is a degradation product of the m^{th} parent chemical (dimensionless) |

Boundary and Initial Conditions

The saturated zone is taken to be initially contaminant free, that is,

$$c_\ell (x, y, z, 0) = 0 \quad (4.73)$$

where

$$c_\ell (x, y, z, 0) = \text{initial concentration of species } \ell \text{ at } x, y, z \text{ (mg/L)}$$

Boundary conditions are as follows:

(i) Upgradient boundary

$$c_\ell = 0 \quad \begin{array}{l} x = 0 \\ -\infty \leq y \leq +\infty \\ 0 \leq z \leq B \end{array} \quad (4.74a)$$

(ii) Top boundary

$$c_t(x, y, B, t) = c_t^o(t), \quad \begin{array}{l} x_u \leq x \leq x_d, \\ -\frac{y_D}{2} \leq y \leq \frac{y_D}{2} \end{array} \quad (4.74b)$$

or

$$\left[-D_{zz} \frac{\partial c_t}{\partial z} + V_z c_t \right]_{z=B} = c_t^o(t) I, \quad \begin{array}{l} x_u \leq x \leq x_d, \\ -\frac{y_D}{2} \leq y \leq \frac{y_D}{2} \end{array} \quad (4.74c)$$

and

$$\left[-D_{zz} \frac{\partial c_t}{\partial z} + V_z c_t \right]_{z=B} = 0, \quad \begin{array}{l} x < x_u, \ x > x_d, \text{ or} \\ y < -\frac{y_D}{2}, \ y > \frac{y_D}{2} \end{array} \quad (4.74d)$$

(iii) Downgradient boundary

$$\frac{\partial c_t}{\partial x} = 0, \quad x = x_L, \quad -\infty \leq y \leq +\infty, \quad 0 \leq z \leq B \quad (4.74e)$$

(iv) Left and right boundaries

$$c_t \rightarrow 0, \quad 0 \leq x \leq x_L, \quad y \rightarrow \pm\infty, \quad 0 \leq z \leq B \quad (4.74f)$$

or, alternatively,

$$\frac{\partial c_t}{\partial y} \rightarrow 0, \quad 0 \leq x \leq x_L, \quad y \rightarrow \pm\infty, \quad 0 \leq z \leq B \quad (4.74g)$$

(v) Bottom boundary

$$\frac{\partial c_\ell}{\partial z} = 0, \quad 0 < x \leq x_L, \quad -\infty \leq y \leq +\infty, \quad z = 0 \quad (4.74h)$$

where

- c_ℓ = aqueous concentration of species ℓ (mg/L)
- x = x coordinate (m)
- y = y coordinate (m)
- z = z coordinate (m)
- B = aquifer thickness (m)
- c_ℓ^o = source concentration for species ℓ (mg/L)
- x_u = upgradient coordinate of the source (m)
- x_d = downgradient coordinate of the source (m)
- y_D = source dimension in the y direction (m)
- D_{zz} = vertical transverse dispersion coefficient (m²/y)
- V_z = vertical ground-water velocity (m/y)
- I = infiltration rate through the source (see Figure 4.1) (m/y)
- x_L = downgradient coordinate of the transport domain (m)

The boundary condition in Equation (4.74d) indicates the finiteness of the source in the y direction, and the boundary conditions in Equations (4.74b and 4.74c) correspond to a prescribed source concentration and prescribed source contaminant mass flux, respectively.

In order to obtain a computationally efficient solution for Equation (4.72), the following assumptions are adopted:

- Ground-water velocity in the x direction is uniform.
- Ground-water flow in the lateral and vertical directions is negligible compared with the flow along the x direction.
- Contaminant mass entering the saturated zone at the water table within the source area is instantaneously transported to a vertical plane that is coplanar with the downgradient boundary of the strip source. All the fluid particles entering the water table at the same time are assumed to arrive simultaneously at the vertical plane.
- The source may be represented by an equivalent source on the plane described in the previous assumption. The dimension of the source on this plane is such that the mass conservation principle is not violated.

Utilizing the first and second assumptions, Equation (4.72) becomes

$$\begin{aligned} \phi_e R_\ell^s \frac{\partial c_\ell}{\partial t} + \bar{V}_x \frac{\partial c_\ell}{\partial x} - D_{xx} \frac{\partial^2 c_\ell}{\partial x^2} - D_{yy} \frac{\partial^2 c_\ell}{\partial y^2} - D_{zz} \frac{\partial^2 c_\ell}{\partial z^2} \\ + \lambda_\ell^s c_\ell \phi_e Q_\ell - \sum_{m=1}^M \lambda_m^s c_m \phi_e Q_m \xi_{\ell m} = 0 \end{aligned} \quad (4.75)$$

where

$$R_\ell^s = 1 + \frac{(1 - \phi_e) \rho_s \partial s_\ell}{\phi_e \partial c_\ell} \quad (4.76)$$

$$Q_\ell = 1 + \frac{(1 - \phi_e) \rho_s s_\ell}{\phi_e c_\ell} \quad (4.77)$$

and

$$\bar{q}_x = \frac{\int_{x_d}^x -K_x \frac{\partial H}{\partial x} dx}{x - x_d}, \quad x > x_d \quad (4.78)$$

where

| | | |
|------------------|---|---|
| ϕ_e | = | effective porosity (dimensionless) |
| R_ℓ^s | = | retardation factor of species ℓ (dimensionless) |
| c_ℓ | = | aqueous concentration of species ℓ (mg/L) |
| t | = | time (y) |
| \bar{V}_x | = | average Darcy velocity in the x direction between the downgradient edge of the source and the point of interest along the x direction (m/y) |
| x | = | x coordinate (m) |
| D_{xx} | = | longitudinal dispersion coefficient (m ² /y) |
| D_{yy} | = | horizontal transverse dispersion coefficient (m ² /y) |
| y | = | y coordinate (m) |
| D_{zz} | = | vertical dispersion coefficient (m ² /y) |
| z | = | z coordinate (m) |
| λ_ℓ^s | = | degradation constant for the ℓ^{th} species (1/y) |
| Q_ℓ | = | coefficient to incorporate sorbed phase decay of species ℓ (dimensionless) |

| | | |
|---------------|---|---|
| m | = | immediate parent of the component species being evaluated (dimensionless) |
| M | = | total number of parent chemicals (dimensionless) |
| λ_m^s | = | degradation constant for parent m (1/y) |
| c_m | = | concentration of parent species m in the aqueous phase (mg/L) |
| Q_m | = | coefficient to incorporate sorbed phase decay of species m (dimensionless) |
| $\xi_{m\ell}$ | = | constant related to decay reaction stoichiometry of the m^{th} parent chemical and the ℓ^{th} chemical which is a degradation product of the m^{th} parent chemical (dimensionless) |
| ρ_s | = | density of the solid phase (g/cm ³) |
| s_ℓ | = | concentration of species ℓ in the solid (adsorbed) phase (mg/kg) |
| \bar{q}_x | = | average Darcy velocity in the x direction between the downgradient edge of the source and the point of interest along the x direction (m/y) |
| K_x | = | hydraulic conductivity in the x direction (m/y) |
| H | = | hydraulic head (m) |
| x_d | = | downgradient coordinate of the source (m) |

According to the third and fourth assumptions, the vertical plane that is coplanar with the downgradient edge of the source area is defined by:

$$\mathbf{x} = \mathbf{x}_d; \quad -\infty \leq \mathbf{y} \leq +\infty; \quad 0 \leq \mathbf{z} \leq B \quad (4.79)$$

where

| | | |
|-------|---|---|
| x | = | x coordinate (m) |
| x_d | = | downgradient coordinate of the source (m) |
| y | = | y coordinate (m) |
| z | = | z coordinate (m) |
| B | = | aquifer thickness (m) |

The dimension of the source on this plane is defined by the following conditions:

$$c_\ell(x_d, y, z, t) = c_\ell^o(t) \quad (4.80)$$

$$-\frac{1}{2}y_s \leq y \leq \frac{1}{2}y_s \quad (4.81)$$

$$B - z_s - D_R \leq z \leq B - D_R \quad (4.82)$$

where

| | | |
|------------------------|---|---|
| $c_\ell(x_d, y, z, t)$ | = | aqueous concentration of species ℓ at x_d, y, z at time t (mg/L) |
| c_ℓ^o | = | source concentration for species ℓ (mg/L) |
| t | = | time (y) |
| y_S | = | width of the source on the source plane in the y direction (m) |
| y | = | y coordinate (m) |
| B | = | aquifer thickness (m) |
| z_S | = | width of the source on the source plane in the z direction (m) |
| D_R | = | average penetration depth due to recharge between the downgradient edge of the source and the observation point (m) |
| z | = | z coordinate (m) |

Outside the source area on the source plane, the source concentration is absent.

The average penetration depth due to recharge may be determined from:

$$D_R = \int_{x_d}^{x_d + \frac{x - x_d}{2}} \frac{I_r}{q_x} dx \quad (4.83)$$

where

| | | |
|-------|---|---|
| D_R | = | average penetration depth due to recharge between the downgradient edge of the source and the observation point (m) |
| x_d | = | downgradient coordinate of the source (m) |
| x | = | x coordinate (m) |
| I_r | = | recharge rate outside the source area (m/y) |
| q_x | = | average Darcy velocity in the x direction between the downgradient edge of the source and the point of interest along the x direction (m/y) |

The average penetration depth is used to replace the boundary condition between the downgradient edge of the source and the point of interest (typically the location of an observation well; presented as Equation (4.74c)). It represents the influx of recharge and the average vertical displacement of the bulk of the plume between the source plane and the point of interest.

As a first approximation, the width of the source on the vertical source plane, y_S , is determined as the width resulting from a particle advected from the most upgradient location ($x_u \leq x \leq \max(x_{crest}, x_d)$) (see Equation (4.84)) along the side of the source (where $y = \frac{1}{2} y_D$) to the vertical plane at $x = x_d$. The particle is advected within the horizontal plane using a two-dimensional flow field described by a two-dimensional

analytical solution presented in Appendix C. The source half width is assumed to be equal to the distance from $y = 0$ to the point where the advected particle transverses the vertical plane at $x = x_d$. The source half width is not allowed to be smaller than $\frac{1}{2}y_D$. The vertical source dimension is approximated by the following expression (U.S. EPA, 1990):

$$z_S = \sqrt{2\alpha_v f(x_d - x_u)} + B \left[1 - \exp\left(\frac{-f(x_d - x_u)l}{B\bar{q}_x}\right) \right] \quad (4.84)$$

where

| | | |
|-------------|---|---|
| z_S | = | width of the source on the source plane in the z direction (m) |
| α_v | = | vertical transverse dispersivity (m) |
| f | = | fraction of the source that migrates downgradient in the event that a water table crest occurs within the source area (dimensionless) |
| x_d | = | downgradient coordinate of the source (m) |
| x_u | = | upgradient coordinate of the source (m) |
| B | = | aquifer thickness (m) |
| l | = | areal infiltration rate (m/y) |
| \bar{q}_x | = | average Darcy velocity in the x direction between the downgradient edge of the source and the point of interest along the x direction (m/y) |

The first term on the right hand side of Equation (4.84) accounts for potential mixing due to transverse dispersion in the vertical direction, while the second term accounts for vertical displacement due to infiltration in the source area.

In Equation (4.84), the fraction, f , indicates the fraction of the source that migrates downgradient in the event that a water table crest occurs within the source area. The water table crest within the source area occurs when the hydraulic gradient in that area vanishes. The location of the water table crest is determined by differentiating Equation (4.84) with respect to x and equating the resulting derivative to zero, so that:

$$x_{crest} = \frac{K_x B}{l} \left[\frac{l_r - l}{2K_x B} \left(\frac{x_d^2 - x_u^2}{x_L} \right) - \frac{l_r - l}{K_x B} x_d + \frac{l_r}{2K_x B} x_L + \frac{H_2 - H_1}{x_L} \right] \quad (4.85)$$

where

| | | |
|-------------|---|--|
| x_{crest} | = | x-coordinate of the crest of the water table (m) |
| K_x | = | longitudinal hydraulic conductivity along the flow direction (m/y) |
| B | = | aquifer thickness (m) |
| l | = | infiltration rate (m/y) |

| | | |
|-------|---|--|
| I_r | = | recharge rate (m/y) |
| x_d | = | downgradient coordinate of the source (m) |
| x_u | = | upgradient coordinate of the source (m) |
| x_L | = | x-coordinate at the downgradient end of the domain (m) |
| H_2 | = | hydraulic head at the downgradient end of the domain (m) |
| H_1 | = | hydraulic head at the upgradient end of the domain (m) |

The fraction of the source, f , is then determined from the following expression:

$$f = \frac{x_d - x_{crest}}{x_d - x_u} \quad (4.86)$$

where

| | | |
|-------------|---|---|
| f | = | fraction of the source that migrates downgradient in the event that a water table crest occurs within the source area (dimensionless) |
| x_d | = | downgradient coordinate of the source (m) |
| x_{crest} | = | x-coordinate of the crest of the water table (m) |
| x_u | = | upgradient coordinate of the source (m) |

One can readily see that if f is negative, the crest occurs at $x > x_d$ from the source area and all the contaminant mass migrates towards the origin of the x-axis. Similarly, if f is greater than unity, the crest occurs at $x < x_u$, and all the contaminant mass migrates downgradient. In the event that f is negative, the solution is trivial, and the contaminant concentration at each observation well location is set to zero. In the determination of the source dimension, the fraction f is limited to the following range:

$$0 \leq f \leq 1 \quad (4.87)$$

where

| | | |
|-----|---|---|
| f | = | fraction of the source that migrates downgradient in the event that a water table crest occurs within the source area (dimensionless) |
|-----|---|---|

In the event that f is greater than unity, the source will not be partitioned, and f is set to unity in Equation (4.87) as well as in the procedure shown below. The release location of the advected particle is also determined by the location of the water table crest. If $x_u \leq x_{crest} \leq x_d$, the release location is $(x_{crest}, \frac{1}{2}y_D)$. If $x_{crest} < x_u$, the release location is $(x_u, \frac{1}{2}y_D)$.

To account for source partitioning, the boundary condition described by Equation (4.80) must be adjusted to reflect the change in source location and dimension. Letting $c_k^s(t)$ represent the adjusted boundary condition, the following statement results from the principle of mass conservation:

$$c_k^o(t) \text{ If } x_w y_D = c_k^s(t) \bar{V}_x z_s y_s \quad (4.88)$$

where

- $c_k^o(t)$ = aqueous concentration of species k within the source (mg/L)
 l = infiltration rate (m/y)
 f = fraction of the source that migrates downgradient in the event that a water table crest occurs within the source area (dimensionless)
 x_w = length of the source along the flow direction ($x_w = x_d - x_u$) (m)
 y_D = source dimension in the y direction (m)
 $c_k^s(t)$ = equivalent aqueous concentration of species k on the vertical plane at the downgradient edge of the source (mg/L)
 \bar{V}_x = average Darcy velocity in the x direction between the downgradient edge of the source and the point of interest along the x direction (m/y)
 z_s = equivalent source dimension in the vertical direction on the vertical plane at the downgradient edge of the waste management unit (m)
 y_s = equivalent source dimension in the direction normal to the regional flow direction on the vertical plane at the downgradient edge of the waste (m)

Rearranging Equation (4.88), we get a concentration ratio, F_c , which can be applied to the contaminant concentration within the waste management unit:

$$\frac{c_k^s(t)}{c_k^o(t)} = \frac{\text{If } x_w y_D}{\bar{V}_x z_s y_s} = F_c \quad (4.89)$$

where

- $c_k^s(t)$ = equivalent aqueous concentration of species k on the vertical plane at the downgradient edge of the source (mg/L)
 $c_k^o(t)$ = aqueous concentration of species k within the source (mg/L)
 l = infiltration rate (m/y)
 f = fraction of the source that migrates downgradient in the event that a water table crest occurs within the source area (dimensionless)
 x_w = length of the source along the flow direction ($x_w = x_d - x_u$) (m)
 y_D = source dimension in the y direction (m)
 \bar{V}_x = average Darcy velocity in the x direction between the downgradient edge of the source and the point of interest along the x direction (m/y)
 z_s = equivalent source dimension in the vertical direction on the vertical plane at the downgradient edge of the waste management unit (m)
 y_s = equivalent source dimension in the direction normal to the regional flow direction on the vertical plane at the downgradient edge of the waste (m)
 F_c = concentration ratio (dimensionless)

If the source dimension in the vertical direction, determined using Equation (4.85), is such that $z_S + D_R > B$, then the vertical source dimension is set to

$$z_S^{new} = B - D_R \quad (4.90)$$

where

$$\begin{aligned} z_S^{new} &= \text{vertical source dimension on the vertical source plane,} \\ &\text{adjusted to account for the presence of recharge depth } D_R \text{ (m)} \\ B &= \text{aquifer thickness (m)} \\ D_R &= \text{average penetration depth due to recharge between the} \\ &\text{downgradient edge of the source and the observation point} \\ &\text{(m)} \end{aligned}$$

and the horizontal source dimension is set to

$$y_S^{new} = \frac{y_S z_S}{z_S^{new}} \quad (4.91)$$

where

$$\begin{aligned} y_S^{new} &= \text{horizontal source dimension on the vertical source plane,} \\ &\text{adjusted to account for } z_S^{new} \text{ (m)} \\ y_S &= \text{equivalent source dimension in the direction normal to the} \\ &\text{regional flow direction on the vertical plane at the} \\ &\text{downgradient edge of the waste (m)} \\ z_S &= \text{equivalent source dimension in the vertical direction on the} \\ &\text{vertical plane at the downgradient edge of the waste} \\ &\text{management unit (m)} \\ z_S^{new} &= z_S \text{ adjusted to account for the presence of recharge depth } D_R \\ &\text{(m)} \end{aligned}$$

Solution Method

A solution to Equation (4.75) and boundary and initial conditions in Equations (4.73 through 4.74) is sought in the form of a product solution (Carslaw and Jaeger, 1959). Assuming that the solution to Equation (4.72) may be obtained in the following product form:

$$c_i(x, y, z, t) = X_i(x, t) Y_i(x, y) Z_i(x, z) \quad (4.92)$$

where

$$\begin{aligned} c_i(x, y, z, t) &= \text{aqueous concentration of species } i \text{ at } x, y, z \text{ at time } t \text{ (mg/L)} \\ t &= \text{time (y)} \\ X_i &= \text{x-direction component of the solution for species } i \end{aligned}$$

- x = x coordinate (m)
 Y_ℓ = y-direction component of the solution for species ℓ
 y = y coordinate (m)
 Z_ℓ = z-direction component of the solution for species ℓ
 z = z coordinate (m)

so that Equation (4.75) can be recast as

$$\begin{aligned}
 & \phi_e R_\ell^s \frac{\partial}{\partial t} X_\ell Y_\ell Z_\ell + \bar{V}_x \frac{\partial}{\partial x} [X_\ell Y_\ell Z_\ell] - D_{xx} \frac{\partial^2}{\partial x^2} [X_\ell Y_\ell Z_\ell] \\
 & - D_{yy} \frac{\partial^2}{\partial y^2} [X_\ell Y_\ell Z_\ell] - D_{zz} \frac{\partial^2}{\partial z^2} [X_\ell Y_\ell Z_\ell] \\
 & + \lambda_\ell^s X_\ell Y_\ell Z_\ell \phi_e Q_\ell - \sum_{m=1}^M \lambda_m^s X_m Y_m Z_m \phi_e Q_m \epsilon_{lm} = 0 \quad (4.93)
 \end{aligned}$$

where

- ϕ_e = effective porosity (dimensionless)
 R_ℓ^s = retardation factor (dimensionless)
 t = time (y)
 X_ℓ = x-direction component of the solution for species ℓ
 Y_ℓ = y-direction component of the solution for species ℓ
 Z_ℓ = z-direction component of the solution for species ℓ
 \bar{V}_x = average Darcy velocity in the x direction between the downgradient edge of the source and the point of interest along the x direction (m/y)
 x = x coordinate (m)
 D_{xx} = longitudinal dispersion coefficient (m²/y)
 D_{yy} = horizontal transverse dispersion coefficient (m²/y)
 y = y coordinate (m)
 D_{zz} = vertical transverse dispersion coefficient (m²/y)
 z = z coordinate (m)
 λ_ℓ^s = degradation constant for the ℓ^{th} species (1/y)
 Q_ℓ = coefficient to incorporate sorbed phase decay of species ℓ (dimensionless)
 m = immediate parent of the component species being evaluated (dimensionless)
 M = total number of parent chemicals (dimensionless)
 λ_m^s = degradation constant for parent m (1/y)
 X_m = x-direction component of the solution for species m
 Y_m = y-direction component of the solution for species m
 Z_m = z-direction component of the solution for species m
 Q_m = coefficient to incorporate sorbed phase decay of species m (dimensionless)

ξ_m = constant related to decay reaction stoichiometry of the m^{th} parent chemical and the l^{th} chemical which is a degradation product of the m^{th} parent chemical (dimensionless)

Equation (4.93) is subject to the following boundary conditions:

On the source plane coplanar with the downgradient edge of the WMU

$$X_l Y_l Z_l = c_k^0(t) F_c ; x = x_d , -\frac{y_s}{2} \leq y \leq +\frac{y_s}{2}, B - z_s - D_R \leq z \leq B - D_R \quad (4.94a)$$

= 0, *elsewhere.*

Along the top and bottom boundaries

$$D_{zz} \frac{\partial}{\partial z} X_l Y_l Z_l = 0, \quad z = 0, z = B \quad (4.94b)$$

The boundary conditions of Equation (4.93) are used to replace the boundary conditions of Equations (4.74d and 4.74h).

Along the left and right boundaries

$$X_l Y_l Z_l \rightarrow 0, \quad y \rightarrow \pm\infty \quad (4.94c)$$

and, as a corollary:

$$D_{yy} \frac{\partial}{\partial y} X_l Y_l Z_l \rightarrow 0, \quad y \rightarrow \pm\infty \quad (4.94d)$$

Downgradient boundary

$$X_l Y_l Z_l \rightarrow 0, \quad x \rightarrow +\infty \quad (4.94e)$$

(In order to simplify the equation, the downgradient dimension of the domain is extended to infinity.)

Initial condition

From the condition stated by Equation (4.73),

$$X_l(t=0) Y_l Z_l = 0, \quad \text{throughout the saturated zone} \quad (4.94f)$$

In order to further simplify the equations, the x, y, and z coordinates are transformed as follows:

$$\begin{aligned}
 x' &= x - x_d \\
 y' &= y \\
 z' &= B - z - \frac{z_s}{2} - D_R
 \end{aligned}
 \tag{4.94g}$$

where

- X_ℓ = x-direction component of the solution for species ℓ
- Y_ℓ = y-direction component of the solution for species ℓ
- Z_ℓ = z-direction component of the solution for species ℓ
- $c_\ell^o(t)$ = aqueous concentration of species ℓ within the source (mg/L)
- F_c = concentration ratio (dimensionless)
- x = x coordinate (m)
- x_d = downgradient coordinate of the source (m)
- y_s = equivalent source dimension in the direction normal to the regional flow direction on the vertical plane at the downgradient edge of the waste (m)
- y = y coordinate (m)
- B = aquifer thickness (m)
- z_s = equivalent source dimension in the vertical direction on the vertical plane at the downgradient edge of the waste management unit (m)
- Y_s = equivalent source dimension in the vertical direction on the vertical plane at the downgradient edge of the waste management unit (m)
- D_R = average penetration depth due to recharge between the downgradient edge of the source and the observation point (m)
- z = z coordinate (m)
- D_{zz} = vertical transverse dispersion coefficient (m²/y)
- D_{yy} = horizontal transverse dispersion coefficient (m²/y)
- t = time (y)
- x' = transformed x-coordinate (m)
- y' = transformed y-coordinate (m)
- z' = transformed z-coordinate (m)

Since the boundary and initial conditions may be expressed as products of the three basic functions, X_ρ , Y_ρ , and Z_ρ , the simplified transport equation may be separated into the following three single-unknown equations, which can be individually solved for X_ρ , Y_ρ , and Z_ρ .

$$\phi_\theta R_\ell^s \frac{\partial X_\ell}{\partial t} + \bar{V}_x \frac{\partial X_\ell}{\partial x'} - D_{xx} \frac{\partial^2 X_\ell}{\partial x'^2}$$

$$+ \lambda_{\ell}^s \phi_e X_{\ell} Q_{\ell} - \sum_{m=1}^M \lambda_m^s \phi_e X_m Q_m \xi_{\ell m} = 0 \quad (4.95)$$

$$\bar{V}_x \frac{\partial Y_{\ell}}{\partial x'} - D_{yy} \frac{\partial^2 Y_{\ell}}{\partial y'^2} = 0 \quad (4.96)$$

$$\bar{V}_x \frac{\partial Z_{\ell}}{\partial x'} - D_{zz} \frac{\partial^2 Z_{\ell}}{\partial z'^2} = 0 \quad (4.97)$$

where

- ϕ_e = effective porosity (dimensionless)
- R_{ℓ}^s = retardation factor of species ℓ (dimensionless)
- t = time (y)
- X_{ℓ} = x-direction component of the solution for species ℓ
- \bar{V}_x = average Darcy velocity in the x direction between the downgradient edge of the source and the point of interest along the x direction (m/y)
- x' = transformed x-coordinate (m)
- D_{xx}^s = longitudinal dispersion coefficient (m²/y)
- λ_{ℓ}^s = degradation constant for the ℓ^{th} species (1/y)
- Q_{ℓ} = coefficient to incorporate sorbed phase decay of species ℓ (dimensionless)
- m = immediate parent of the component species being evaluated (dimensionless)
- M = total number of parent chemicals (dimensionless)
- λ_m^s = degradation constant for parent m (1/y)
- X_m = x-direction component of the solution for species m
- Q_m = coefficient to incorporate sorbed phase decay of species m (dimensionless)
- $\xi_{\ell m}$ = constant related to decay reaction stoichiometry of the m^{th} parent chemical and the ℓ^{th} chemical which is a degradation product of the m^{th} parent chemical (dimensionless)
- Y_{ℓ} = y-direction component of the solution for species ℓ
- D_{yy} = horizontal transverse dispersion coefficient (m²/y)
- y' = transformed y-coordinate (m)
- Z_{ℓ} = z-direction component of the solution for species ℓ
- D_{zz} = vertical dispersion coefficient (m²/y)
- z' = transformed z-coordinate (m)

Upon simplification, Equations (4.96 to 4.97) require the following assumptions:

$$\left| Y_\ell Z_\ell D_{xx} \frac{\partial^2 X_\ell}{\partial x'^2} \right| \gg \left| 2D_{xx} \frac{\partial Y_\ell Z_\ell}{\partial x'} \frac{\partial X_\ell}{\partial x'} \right| \quad (4.98a)$$

$$\left| \bar{V}_x \frac{\partial Y_\ell Z_\ell}{\partial x'} \right| \gg \left| D_{xx} \frac{\partial^2 Y_\ell Z_\ell}{\partial x'^2} \right| \quad (4.98b)$$

and

$$X_\ell Y_\ell \approx X_m Y_m \quad (4.98c)$$

where

- Y_ℓ = y-direction component of the solution for species ℓ
- Z_ℓ = z-direction component of the solution for species ℓ
- D_{xx} = longitudinal dispersion coefficient (m²/y)
- X_ℓ = x-direction component of the solution for species ℓ
- x' = transformed x-coordinate (m)
- \bar{V}_x = average Darcy velocity in the x direction between the downgradient edge of the source and the point of interest along the x direction (m/y)
- X_m = x-direction component of the solution for species m
- Y_m = y-direction component of the solution for species m

The proviso in Equation (4.98b) is used by Harleman and Rumer (1963) in their steady-state solution for transversal dispersion. It is approximately true in the event that the plume is extended to infinity so that the transversal dispersive flux relatively close to the source is much greater than the longitudinal dispersive flux. Equation (4.98a) is approximately true when the variation of $Y_\ell Z_\ell$ in the x-direction is negligibly small. The steady-state solutions of Equations (4.96 and 4.97) are based on an assumption that x is extended to infinity (see the explanation below of the solution for X_ℓ and Y_ℓ). Equation (4.98c) is predicated upon the condition that molecular diffusion coefficients are approximately the same for all chemicals.

Solution for X_ℓ

Equation (4.95) corresponds to the three-dimensional multi-species aqueous phase transport equation for the saturated zone in the EPACMTP code (U.S. EPA, 1996c), with uniform ground-water velocity in the x-direction and unit cross-sectional area in the y-z plane. With appropriate boundary conditions and parameters, the existing solution procedure in EPACMTP may be used to obtain X_ℓ .

Solution for Y_ℓ

Equation (4.96) is restated below:

$$\bar{V}_x \frac{\partial Y_\ell}{\partial x'} - D_{yy} \frac{\partial^2 Y_\ell}{\partial y'^2} = 0 \quad (4.99)$$

where

- \bar{V}_x = average Darcy velocity in the x direction between the downgradient edge of the source and the point of interest along the x direction (m/y)
 Y_ℓ = y-direction component of the solution for species ℓ
 x' = transformed x-coordinate (m)
 D_{yy} = horizontal transverse dispersion coefficient (m²/y)
 y' = transformed y-coordinate (m)

which is subject to the following boundary conditions:

$$\frac{\partial}{\partial y'} Y_\ell \rightarrow 0, \quad y' \rightarrow \pm\infty \quad (4.100a)$$

$$Y_\ell \text{ bounded}, \quad x \rightarrow \infty \quad (4.100b)$$

$$\begin{aligned} Y_\ell(x'=0) &= 1, \text{ with } -0.5y_s \leq y' \leq 0.5y_s, \\ &= 0, \text{ } y' \leq -0.5y_s, \text{ and } y' \geq 0.5y_s, \end{aligned} \quad (4.100c)$$

where

- y' = transformed y-coordinate (m)
 Y_ℓ = y-direction component of the solution for species ℓ
 x = x-coordinate (m)
 x' = transformed x-coordinate (m)
 y_s = equivalent source dimension in the direction normal to the regional flow direction on the vertical plane at the downgradient edge of the waste (m)

A solution to Equations (4.99 and 4.100) is given by (Carslaw and Jaeger, 1959)

$$Y_\ell = \frac{1}{2} \left(\operatorname{erf} \frac{0.5y_s - y'}{\sqrt{2D_{yy} \frac{x}{\bar{V}_x}}} + \operatorname{erf} \frac{0.5y_s + y'}{\sqrt{2D_{yy} \frac{x}{\bar{V}_x}}} \right) \quad (4.101)$$

where

- Y_ℓ = y-direction component of the solution for species ℓ
 y_s = equivalent source dimension in the direction normal to the regional flow direction on the vertical plane at the downgradient edge of the waste (m)
 y' = transformed y-coordinate (m)
 D_{yy} = horizontal transverse dispersion coefficient (m²/y)
 x = x-coordinate (m)
 \bar{V}_x = average Darcy velocity in the x direction between the downgradient edge of the source and the point of interest along the x direction (m/y)
 $\text{erf}(\cdot)$ = error function

Solution for Z_k

Equation (4.97) is restated below:

$$\bar{V}_x \frac{\partial Z'_\ell}{\partial x'} - D_{zz} \frac{\partial^2 Z'_\ell}{\partial z'^2} = 0 \quad (4.102)$$

which is subject to the following boundary conditions:

$$\frac{\partial Z'_\ell}{\partial z'} \rightarrow 0, \quad z' \rightarrow \pm\infty \quad (4.103a)$$

$$Z'_\ell \text{ bounded}, \quad z' \rightarrow \infty \quad (4.103b)$$

$$\begin{aligned} Z'_\ell(x' = 0) &= 1, \text{ with } -0.5z_s \leq z' \leq 0.5z_s, \\ &= 0, \text{ with } z' \leq -0.5z_s, \quad z' \geq 0.5z_s, \end{aligned} \quad (4.103c)$$

where

- \bar{V}_x = average Darcy velocity in the x direction between the downgradient edge of the source and the point of interest along the x direction (m/y)
 Z'_ℓ = a component of the solution for species ℓ
 x' = transformed x-coordinate (m)
 D_{zz} = vertical dispersion coefficient (m²/y)
 z' = transformed z-coordinate (m)
 z_s = equivalent source dimension in the vertical direction on the vertical plane at the downgradient edge of the waste management unit (m)

The boundary conditions in Equations (4.103a and 4.103b) are used as intermediate boundary conditions from which the intermediate solution, Z'_ℓ may be derived. The

boundary conditions in Equation (4.93) at the top and bottom of the saturated zone are imposed through the use of the method of images (Bear, 1972).

A solution to Equations (4.102 and 4.103) is given by (Carslaw and Jaeger, 1959).

$$Z'_\ell = \frac{1}{2} \left(\operatorname{erf} \frac{0.5z_s - z'}{2\sqrt{D_{zz}\frac{x}{V_x}}} + \operatorname{erf} \frac{0.5z_s + z'}{2\sqrt{D_{zz}\frac{x}{V_x}}} \right) \quad (4.104)$$

where

- Z'_ℓ = a component of the solution for species ℓ
- z_s = equivalent source dimension in the vertical direction on the vertical plane at the downgradient edge of the waste management unit (m)
- z' = transformed z-coordinate (m)
- D_{zz} = vertical dispersion coefficient (m²/y)
- x = x-coordinate (m)
- $\frac{x}{V_x}$ = average Darcy velocity in the x direction between the downgradient edge of the source and the point of interest along the x direction (m/y)
- $\operatorname{erf}(\cdot)$ = error function

The boundary conditions at the top and bottom of the saturated zone are imposed by using one image on either side. In general, it is found that multiple images are not necessary and only one image per side is adequate. The final solution for Z'_ℓ at the well depth, z_{rw}^* , may be obtained by:

$$Z'_\ell(x', z_{rw}^{*'}) = Z'_\ell(x', z_{rw}^{*'}) + Z'_\ell(x', z_1') + Z'_\ell(x', z_2') \quad (4.105)$$

where

$$\begin{aligned} z_{rw}^{*'} &= z_{rw}^* - \frac{z_s}{2} - D_R \\ z_1' &= 2B - \frac{z_s}{2} - D_R - z_{rw}^* \\ z_2' &= z_{rw}^* + \frac{z_s}{2} + D_R \end{aligned} \quad (4.106)$$

where

- Z'_ℓ = z-direction component of the solution for species ℓ
- x' = transformed x-coordinate (m)

| | | |
|---------------------|---|---|
| Z_{RW}^{*} | = | transformed well depth (m) |
| Z_{ℓ}^{\prime} | = | a component or an image of Z_{ℓ} |
| Z_1^{\prime} | = | transformed well depth in image 1 (m) |
| Z_2^{\prime} | = | transformed well depth in image 2 (m) |
| Z_{RW}^{*} | = | well depth (m) |
| Z_s | = | equivalent source dimension in the vertical direction on the vertical plane at the downgradient edge of the waste management unit (m) |
| D_R | = | average penetration depth due to recharge between the downgradient edge of the source and the observation point (m) |
| B | = | aquifer thickness (m) |

Determination of D_{ij}

From Equations (4.32a to 4.32c), dispersion coefficients for the saturated zone may be written as follows:

$$\begin{aligned}
 D_{xx} &= \alpha_L \bar{V}_x + \phi_e D_k^{s*} \\
 D_{yy} &= \alpha_T \bar{V}_x + \phi_e D_k^{s*} \\
 D_{zz} &= \alpha_V \bar{V}_x + \phi_e D_k^{s*}
 \end{aligned}
 \tag{4.107}$$

where

| | | |
|-------------|---|---|
| D_{xx} | = | longitudinal dispersion coefficient (m ² /y) |
| α_L | = | longitudinal dispersivity (m) |
| \bar{V}_x | = | average Darcy velocity in the x direction between the downgradient edge of the source and the point of interest along the x direction (m/y) |
| ϕ_e | = | effective porosity (dimensionless) |
| D_k^{s*} | = | effective molecular diffusion coefficient for species k (m ² /y) |
| D_{yy} | = | horizontal transverse dispersion coefficient (m ² /y) |
| α_T | = | lateral dispersivity in the horizontal direction (m) |
| D_{zz} | = | vertical dispersion coefficient (m ² /y) |
| α_V | = | lateral dispersivity in the vertical direction (m) |

4.4.6 Determining the Exposure Concentration at the Receptor Well

The finite source methodology involves evaluation of the temporally averaged receptor well concentration, C_{RW} . Two options have been implemented. The first is based on determining the average receptor well concentration over a specified time interval, for instance a 30 years average residence time (U.S. EPA, 1991). In order to ensure that a protective result is obtained, the exposure period is always selected to be centered about the time at which the receptor well concentration reaches its maximum value (see Figure 4.9). The second option is to forego the time-averaging and set C_{RW} equal to the peak receptor well concentration value, C_{RW}^{\max} . The second option will yield higher values for the receptor well concentration, C_{RW} , and therefore will be more conservative with regard to health risks. As mentioned before, as the pulse duration, t_p , increases, the receptor well breakthrough curve will exhibit a

plateau with maximum concentration equal to the steady-state concentration, and eventually the time-averaged concentration will be the same as the peak concentration value (Figure 4.10).

4.4.6.1 Time-Averaged Concentration

When time-averaged receptor well concentrations are required, a two-step procedure is used. The first step is again to determine the time value at which the receptor well concentration reaches its peak, as described below in Section 4.4.6.2. Denoting this time value as t_{max} and denoting the exposure time interval of interest as t_d , the time-averaged receptor well concentration C_{RW} is computed as (Figure 4.9):

$$\bar{C}_{RW} = \frac{1}{t_d} \int_{t_{peak} - \frac{1}{2}t_d}^{t_{peak} + \frac{1}{2}t_d} C_{RW}(t) dt \quad (4.108)$$

$$\bar{C}_{RW} = \frac{1}{t_d} \left\{ \int_0^{t_{peak} + \frac{1}{2}t_d} C_{RW}(t) dt - \int_0^{t_{peak} - \frac{1}{2}t_d} C_{RW}(t) dt \right\} \quad (4.109)$$

where

| | | |
|----------------|---|--|
| \bar{C}_{RW} | = | time-averaged receptor well concentration (mg/L) |
| t_d | = | exposure time interval of interest (y) |
| t_{peak} | = | time value at which the receptor well concentration reaches its peak (y) |
| C_{RW} | = | instantaneous receptor well concentration (mg/L) |
| t | = | time (y) |

Equation (4.109) is used because the Laplace Transform Galerkin (LTG) formulation in EPACMTP makes it very straightforward to directly evaluate the time-integrated concentration at any location (U.S. EPA, 1996b).

Strictly speaking, use of Equation (4.109) may not always ensure that \bar{C}_{RW} is indeed the highest possible average exposure concentration. Use of Equation (4.108) will yield the maximum average exposure concentration provided the receptor well breakthrough curve is symmetrical. If the breakthrough curve is not symmetrical, the time period of the maximum average receptor well concentration may be shifted relative to the time of the peak concentration. Using Equation (4.109) has a considerable computational advantage because, after t_{peak} has been found, it requires only two quick Laplace inversions to determine \bar{C}_{RW} . Using a search procedure to find the maximum average receptor well concentration, versus using Equation (4.109) has been evaluated for a range of different constituents and modeling scenarios. The two approaches were found to yield almost the same

averaged exposure concentrations, but using Equation (4.109) in a Monte-Carlo simulation required only about half the CPU time of a direct search procedure.

For the pseudo three-dimensional transport equation, t_{peak} for a given receptor well is found directly from the well's breakthrough curve. Equation (4.108) is then applied to determine C_{RW} .

In EPACMTP, up to 10 values of exposure duration of interest (t_e) may be specified, and multiple exposure duration values may be used with any of the transport solutions (fully 3D transport, pseudo-3D transport, and 2D transport).

4.4.6.2 Peak Concentration

The procedure for locating the receptor well concentration peak and the time-averaged concentration value is as follows. The time value at which the receptor well concentration reaches its maximum is estimated based on the distance to the receptor well and the average solute travel velocity. An empirical search procedure is then employed to locate the exact position of the peak. The search procedure is a one-dimensional search algorithm to determine the maximum concentration that occurs within a predetermined time period. The algorithm, which is similar to the Fibonacci search algorithm, attempts to decrease the time period with the maximum concentration through successive searches. The search is terminated when two successive time periods and maximum concentrations are approximately the same (or differ within a predetermined tolerance). If the analysis is based on the peak concentration value itself, this value is stored for later post-processing. For a degrading compound with degradation products that may be toxic, the peak concentrations for each member of the species may occur at different times. The searching procedure is therefore repeated for all member species.

For the pseudo three-dimensional transport solution, a complete breakthrough curve (concentration versus time) is determined for each receptor well in each model realization. The peak concentration at a given receptor well is found by performing a direct search for the maximum value of concentration in the breakthrough curve.

4.4.6.3 Time-to-Arrival of the Peak Concentration

For the pseudo three-dimensional transport equation, the time-to-arrival of the peak concentration at a given receptor well is determined by searching the well's breakthrough curve. For other solutions, the empirical search algorithm described in Section 4.4.6.2 is used.

4.4.7 Determining the Contaminant Mass Flux from Ground-water into a Surface Water Body

A ground water to surface water pathway can be included in an EPACMTP modeling analysis, however, these calculations are not incorporated into the EPACMTP model and must be done separately as a post-processing step. Determining the contaminant mass flux from the ground water into a surface water body is done by calculating the total contaminant mass flux at a given downgradient location selected to represent the intersection of the contaminant plume with a surface water body. It is assumed that the surface water body fully penetrates the aquifer and the plume fully intersects the water body. The total contaminant mass flux (in mg/y) is then calculated by multiplying the ground-water flux with the net contaminant mass across the entire plume cross section. The details of this calculation are presented in Appendix F.

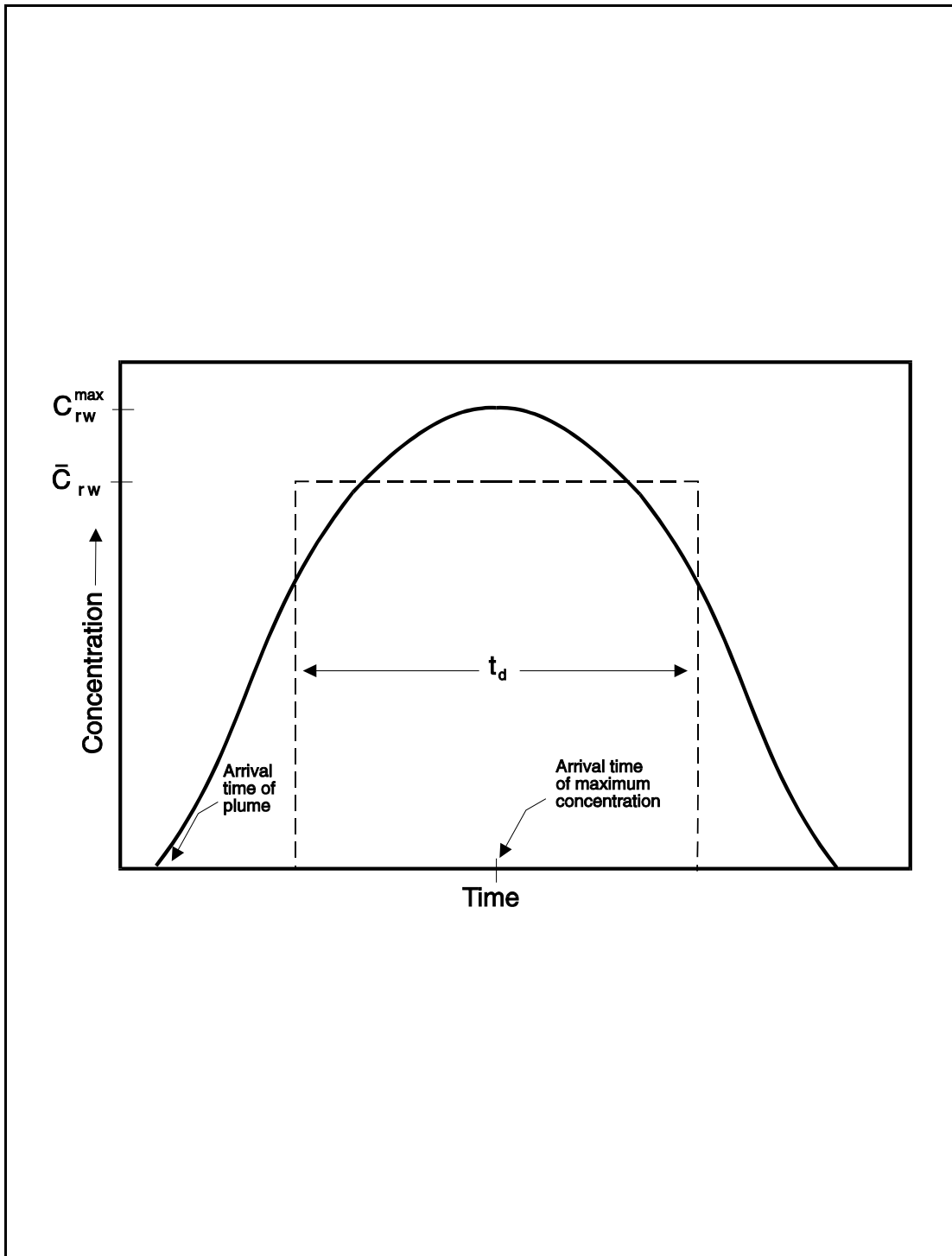


Figure 4.9 Schematic View of the Time-varying Receptor Well Concentration (Break Through Curve) and Illustration of the Procedure for Determining \bar{C}_{rw} .

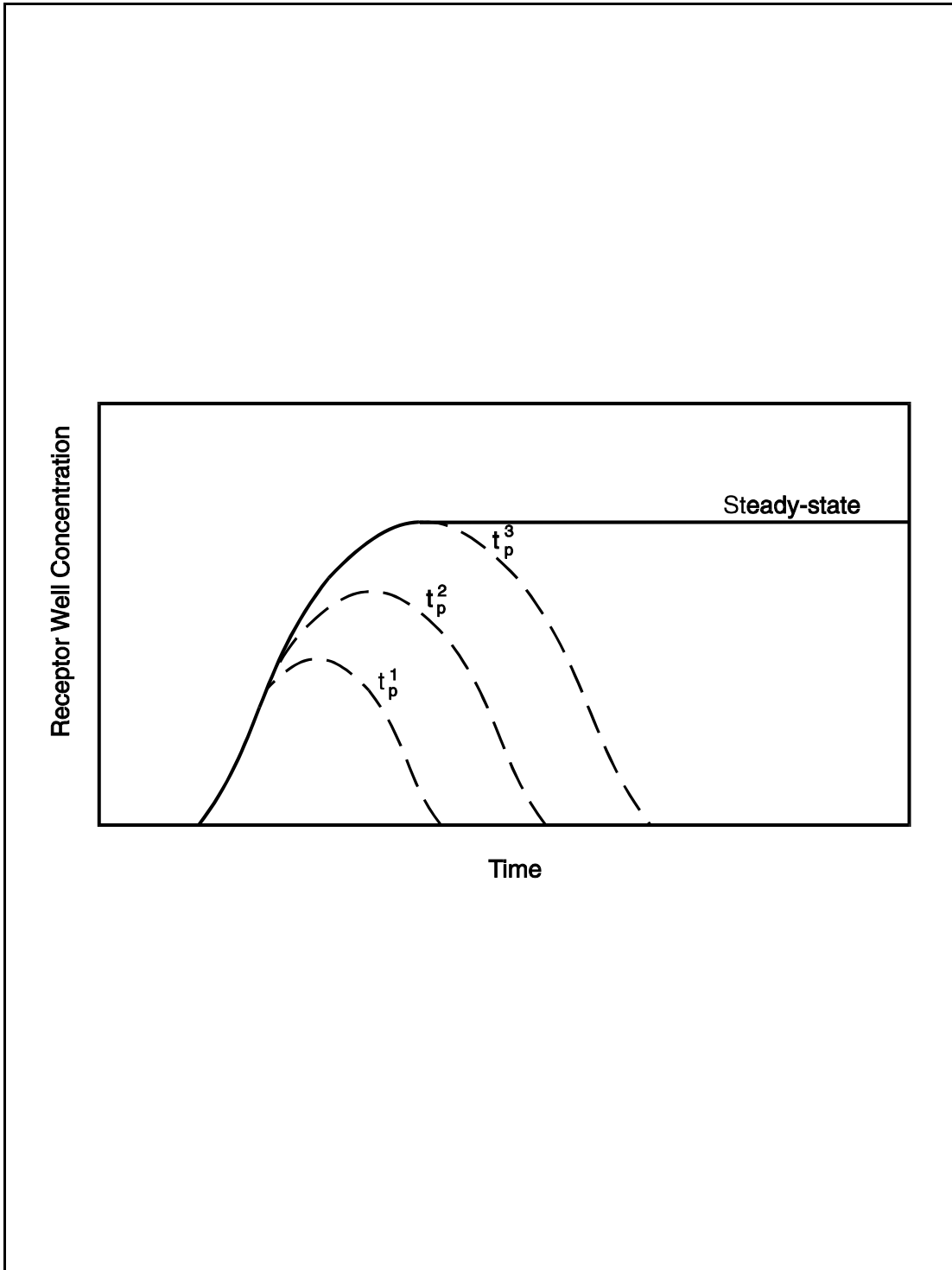


Figure 4.10 Schematic Illustration of the Effect of Increasing Pulse Duration, T_p , on the Receptor Well Break Through Curve.

This page was intentionally left blank.

5.0 MONTE-CARLO MODULE

Monte-Carlo simulation is a statistical technique by which a quantity is calculated repeatedly, as many as thousands of times, using randomly selected parameter values for each calculation. The results approximate the full range of possible outcomes, and the likelihood of each. When Monte-Carlo simulation is applied to risk assessment, risk appears as a frequency distribution.

The Monte-Carlo simulation technique was developed during World War II and is named after the casinos in Monte Carlo, Monaco, where the primary attractions are games of chance. The random behavior in games of chance is similar to how Monte-Carlo simulation selects variable values at random to simulate a particular modeling scenario. When we roll a die, we know that either a 1, 2, 3, 4, 5, or 6 will come up, but we do not know *a priori* which value it will be for any particular roll. It is the same with the variables that have a known range of values but an uncertain value for any particular time or event.

This section presents the Monte-Carlo module of the EPACMTP model and describes how this probabilistic module is implemented for ground-water fate and transport analyses. The purpose of the Monte-Carlo module and a description of its operation are presented in Sections 5.1 and 5.2, respectively. The methods used to ensure that each model realization uses an internally consistent set of data are summarized in Section 5.3. Section 5.4 describes each of the distribution types that can be selected for each of the EPACMTP input parameters. Section 5.5 explains in detail how the regional, site-based Monte-Carlo methodology is implemented in EPACMTP; and Section 5.6 describes how to interpret the results of a Monte-Carlo modeling analysis. Finally, Section 5.7 summarizes the results of an analysis performed by EPA to determine the appropriate number of Monte-Carlo computer runs needed to achieve reliable results.

5.1 PURPOSE OF THE MONTE-CARLO MODULE

Application of the EPACMTP model for determining receptor well concentrations requires values for the various source-specific, chemical-specific, unsaturated-zone-specific and saturated-zone-specific model parameters. For many assessment purposes it is not appropriate to assign single values to all of these parameters. Rather, their values represent a probability distribution, reflecting both the range of variation that may be encountered at different waste sites around the country, as well as our uncertainty about the specific conditions at each site.

The Monte-Carlo module in EPACMTP makes it possible to incorporate uncertainty and variability in the values of parameters into the subsurface pathway modeling analysis, and to quantify the impact of parameter variability and uncertainty on expected receptor well concentrations. In particular, we use Monte-Carlo simulation to determine the likelihood, or probability, that the concentration of a constituent at the receptor well, and hence exposure and risk, will be above or below a certain value.

5.1.1 Treatment of Uncertainty and Variability

Variability arises from true heterogeneity in characteristics, such as rainfall at different locations in the United States. **Uncertainty** represents lack of knowledge about factors and processes, such as the effective hydraulic conductivity of the aquifer at a given waste management unit site or the nature of degradation mechanisms, that affect constituent fate and transport.

EPA classifies the major areas of uncertainty in risk assessments as parameter uncertainty, scenario uncertainty, and model uncertainty. Parameter uncertainty is the “uncertainty regarding some parameter” of the analysis. Scenario uncertainty is “uncertainty regarding missing or incomplete information needed to fully define exposure and dose.” Model uncertainty is “uncertainty regarding gaps in scientific theory required to make predictions on the basis of causal inferences” (U.S. EPA, 1992).

The sources of parameter uncertainty are measurement errors, sampling errors, variability, and use of generic or surrogate data (U.S. EPA, 1992). In other words, many of the input parameters used to quantify contaminant fate and transport cannot be measured precisely and/or accurately.

The sources of scenario uncertainty include: estimation errors of operational periods, approximations of operational conditions, and disposal history of constituents in waste management units. Many of the operational conditions are so complex that the respective simplified approximations may not describe the true conditions precisely. In addition, the amount of data relating to operational conditions may not be adequate or may be subject to high degree of uncertainty.

The sources of model uncertainty are relationship errors and modeling errors (U.S. EPA, 1992). Models and their mathematical expressions are simplifications of reality that are used to approximate real-world conditions and processes and their relationships. Models do not include all parameters or equations necessary to express reality because of the inherent complexity of the natural environment and the lack of sufficient data to fully describe it. Consequently, models are based on various assumptions and simplifications and reflect an incomplete understanding of natural processes.

In the remainder of Section 5, we will use the term ‘uncertainty’ to cover both parameter variability and uncertainty. As explained above, strictly speaking, variability and uncertainty are different concepts. Variability describes parameters whose values are not constant in space and/or time; however, at least in principle, these parameter values can be measured or estimated and specified as a frequency distribution in the modeling input file. Uncertainty pertains to parameters, processes and relationships that we know or can model only approximately. In practice, we use probability distributions to describe both variability and uncertainty, and for the purpose of the EPACMTP Monte-Carlo module, we treat variability and uncertainty as equivalent.

The EPACMTP model accounts for the variability and uncertainty in environmental setting through the use of several linked databases: 1) a nationwide database of waste management unit sites and the environmental setting for each, 2) a database of the characteristics of each type of environmental setting (e.g. aquifer thickness and hydraulic conductivity), and 3) databases of climatic parameters (e.g., ground-water temperature, infiltration rate, and regional recharge rate). That is, through the use of these linked databases the EPACMTP model accounts for both the nationwide variability in environmental conditions and the uncertainty about these conditions at any given site. A fundamental underlying assumption in EPA's implementation of the EPACMTP Monte-Carlo module is that uncertainty in local conditions can be approximated using data that characterize the variability of sites across the United States.

In planning a Monte-Carlo modeling analysis, it is desirable to specifically address as much of the parameter variability and uncertainty as possible, either directly in the Monte-Carlo modeling process or through disaggregation of the data into discrete elements of the analysis. The use of a distribution of distances to the nearest downgradient receptor well accounts for spatial variability in concentrations around a WMU and uncertainty in receptor locations and is an example of doing this directly in the modeling process. The WMU site databases are an example of how disaggregation of the data can be used to address parameter uncertainty and variability. For a typical nationwide analysis conducted for regulatory purposes, a given waste stream may be disposed in a number of WMUs located all across the country. In modeling this scenario with EPACMTP, we account for the variability of WMU characteristics (such as area, depth, and operational life) by using large WMU site databases that were created by surveying a representative sample of the existing WMUs. Each record in the database represents one possible WMU site, and one record (or one set of correlated data representing an individual WMU) is selected for each model realization, such that at the end of the Monte-Carlo analysis the modeling results reflect the range of possible WMU characteristics.

5.2 MONTE-CARLO MODULE OPERATION

The Monte-Carlo method requires that for each input parameter, except constant and derived parameters, a probability distribution be provided. The method involves the repeated generation of pseudo-random values of the uncertain input variable(s) (drawn from the known distribution and within the range of any imposed bounds). The EPACMTP model is executed for each set of randomly generated model parameters and the corresponding receptor well exposure concentration is computed and stored. Each set of input values and corresponding receptor well concentration is termed a **realization**.

A typical Monte-Carlo simulation can involve thousands of realizations. At the conclusion of the Monte-Carlo simulation, the realizations are statistically analyzed to yield a cumulative probability distribution of the receptor well exposure concentration. The various steps involved in the application of the Monte-Carlo simulation technique are:

- (1) Select representative probability distribution functions for the relevant input variables.
- (2) Generate random values from the distributions selected in (1). These values represent a possible set of values (a *realization*) for the input variables.
- (3) Run EPACMTP with these input values. Store the resulting receptor well exposure concentration.
- (4) Repeat Steps (2) and (3) for a specified number of times.
- (5) Statistically analyze the computed receptor well concentrations to develop a cumulative probability distribution of either the receptor well concentration or a *Dilution Attenuation Factor* (DAF); the DAF is defined as the ratio of the initial leachate concentration to the receptor well concentration. In other words, it represents the reduction in constituent concentration that occurs before the leachate reaches the well.

The EPACMTP user performs Step 1 during the creation of the modeling input file(s), and the Monte-Carlo module of EPACMTP performs Steps 2 through 4. Step 5 is typically performed as a post-processing step using a spreadsheet or a utility program.

A simplified flow chart that illustrates the linking of the Monte-Carlo module to the simulation modules of the EPACMTP composite model is presented in Figure 5.1. The model input data are read first, followed by the generation of the random numbers. The generated random and/or derived parameter values are then assigned to the model variables. Following this, the contaminant transport fate and transport simulation is performed. The result is given in terms of the predicted contaminant concentration in a downgradient ground-water receptor well. The generation of random parameter values and fate and transport simulation is repeated as many times as necessary to accurately determine the probability distribution of receptor well concentrations.

5.3 ENSURING INTERNALLY CONSISTENT DATA SETS

As discussed in Section 5.1, a ground-water modeler needs input values for many waste, chemical, and subsurface parameters in order to perform a ground-water pathway analysis using the EPACMTP model.

Inherent in the Monte-Carlo process is that parameter values are drawn from multiple data sources, and then combined in each realization of the modeling process. Because the parameter values are drawn randomly from their individual probability distributions, it is possible that parameters are combined in ways that are physically infeasible and that violate the validity of the EPACMTP flow and transport model. The Monte-Carlo module of EPACMTP incorporates three main methods to eliminate or reduce these occurrences as much as possible:

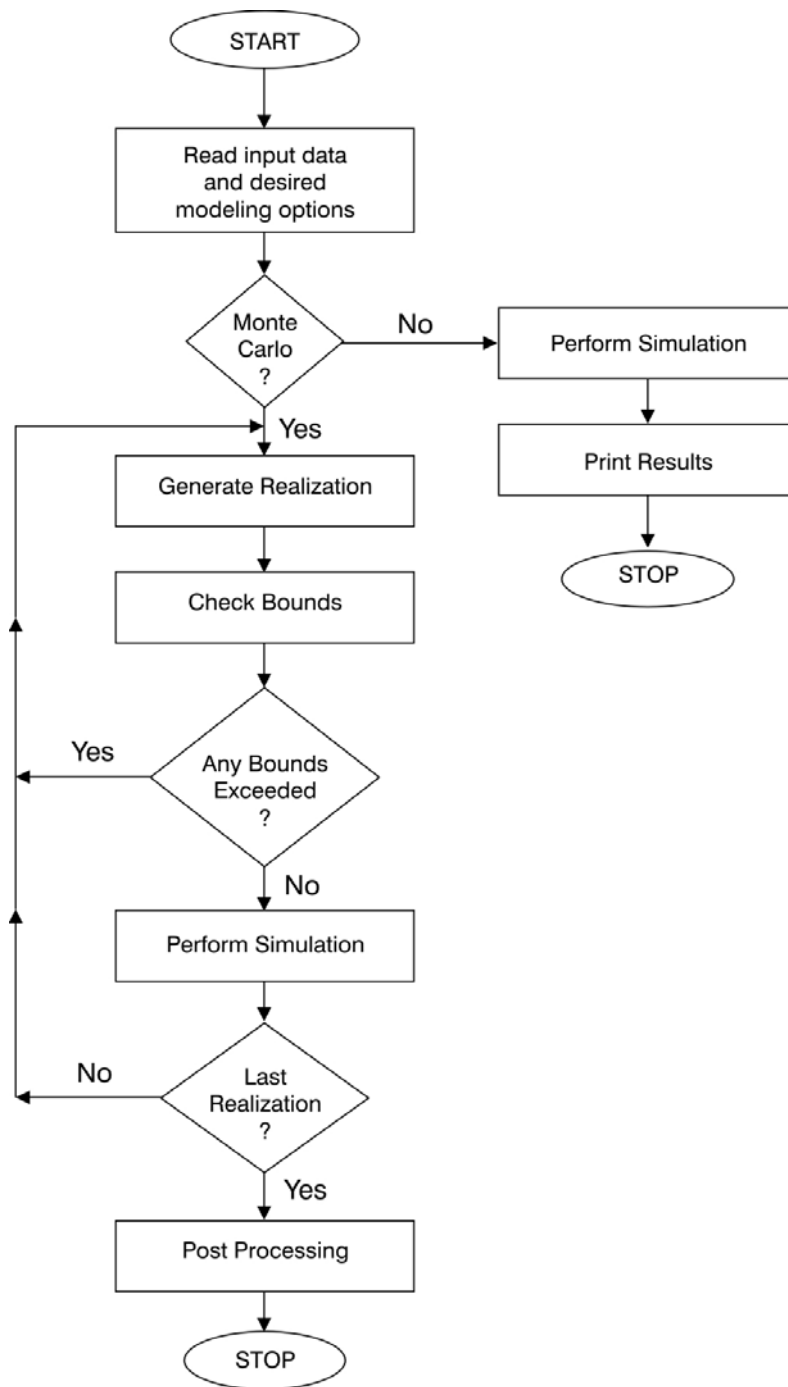


Figure 5.1 Flow chart of EPACMTP for a Monte-Carlo Problem.

-
- Impose upper and lower limits on parameters that are randomly chosen from defined distributions or internally calculated by the model (see Sections 5.3.1 and 5.4.11);
 - Perform a ground-water table elevation screening procedure to ensure that the generated parameter values for a given Monte-Carlo realization do not result in a physically implausible scenario with respect to the elevation of the ground surface, the water table, and/or the top of an impoundment (see Sections 4.3.6 and 5.3.2); and
 - Use of the regional site-based methodology which links together several correlated data sets (see Sections 5.3.3 and 5.5).

5.3.1 Upper and Lower Limits

As a relatively simple measure, upper or lower limits are specified on the values of individual Monte-Carlo parameters to ensure that their randomly generated values are within physically realistic limits. We also specified upper and lower limits on secondary parameters whose values are calculated (derived) internally in the Monte-Carlo module as functions of the primary EPACMTP input parameters, (see the *EPACMTP Parameters/Data Background Document* (U.S. EPA, 2003)).

5.3.2 Screening Procedures

In addition to the enforcement of upper and lower limits for randomly generated and derived input values, EPACMTP also automatically performs a set of screening procedures to ensure that the conceptual model remains physically plausible. These screening procedures are summarized below; additional details, mathematical formulations, and flow charts of the screening process are presented Section 4.3.6.

The ground-water elevation screening procedure is used to ensure that the generated parameter values for a given Monte-Carlo realization do not result in a physically implausible scenario with respect to the elevation of the ground surface, the water table, and/or the top of an impoundment. Physically, a rise of the water table above the ground surface would indicate the WMU is located in a swamp. The reason for implementing this type of screening is that the EPACMTP Monte-Carlo module may generate unrealistically high values for infiltration and recharge at a site with shallow depth to ground water and low hydraulic conductivity of the aquifer. And a rise in the water table above the height of the waste water in a surface impoundment would mean that ground-water transport would tend to be from the aquifer into the impoundment rather than from the impoundment into the aquifer; it is unlikely that an impoundment like this would be constructed to manage waste water.

For a given Monte-Carlo realization for landfills, waste piles, and land application units, the four correlated hydrogeological parameters, infiltration rate through the WMU, and ambient regional recharge rate are generated. Then the EPACMTP model calculates the estimated water table mounding that would result from the selected combination of parameter values. The combination of parameters is accepted if the calculated maximum water table elevation (the ground-water 'mound')

remains below the ground surface elevation at the site. If the criterion is not satisfied, the selected parameter values for the realization are rejected and a new data set is selected from the appropriate distributions.

For surface impoundments, there are two additional considerations in the screening process. In a typical Monte-Carlo modeling analysis for a surface impoundment, a site is selected from the surface impoundment WMU data base for each realization. The unit-specific parameters, including ponding depth and base depth below ground surface, are retrieved from the data base. The four correlated hydrogeologic parameters are then selected from the hydrogeologic data base, based on the hydrogeologic environment at that WMU location. The EPACMTP model then executes the probabilistic screener using these values for the base depth and water table elevation. If the elevation of the waste water surface in the impoundment is below the water table, that set of parameter values fails the screening process. In this case, the selected parameter values for that realization will be rejected and a new data set selected from the appropriate distributions.

If the base of the unit is located above the water table, the unit is said to be hydraulically separated from the water table. However, in this case, it is necessary to ensure that the calculated infiltration rate does not exceed the maximum feasible infiltration rate; that is, the maximum rate that does not cause the crest of the local ground-water mound to be higher than the base of the surface impoundment. This limitation allows us to determine a conservative infiltration rate that is based on the free-drainage condition at the base of the surface impoundment. If the maximum feasible infiltration rate (I_{\max}) is exceeded, the EPACMTP model will set the infiltration rate to this maximum value.

For a surface impoundment, once these limits on the derived infiltration have been imposed, a check to ensure that any ground-water mounding does not result in a rise of the water table above the ground surface is performed in the same manner as for other types of WMUs.

5.3.3 Regional Site-Based Approach

The regional site-based approach is the third method incorporated into the EPACMTP model to reduce the likelihood that a physically infeasible set of environmental data will be generated. This modeling approach and the correlated data sets are summarized below, and additional details are presented Section 5.5.

The main advantage of this regional site-based approach over a strictly nationwide methodology is that it is based on correlated data sets compiled at actual waste sites around the country that are linked to databases of climatic and hydrogeologic parameters through the use of climate and hydrogeologic indices. Using these correlated and linked databases, the regional site-based approach can, for each Monte-Carlo realization, generate a random, yet internally consistent, set of the required site-specific values without requiring the exhaustive sampling that would be required to actually gather these data from waste sites around the country.

Fundamentally, the approach used for a site-based Monte-Carlo analysis consists of conducting the modeling analysis for the waste sites in the Subtitle D survey on the assumption that these sites are an adequate representation of the universe of possible waste sites in the U.S. For each Monte-Carlo realization, EPACMTP selects a site, at random, from the Subtitle D survey data set. The corresponding climatic and hydrogeologic indices and the generated soil type are then used by the model to generate random, but internally consistent, sets of values for the climatic, soil and aquifer parameters. Thus, the use of the regional site-based methodology which links together several correlated data sets serves to reduce the probability that the generated data set contains a physically infeasible, unrealistic, or highly unlikely set of parameter values. Additional details about the data sources and implementation of the regional site-based modeling method are presented in Section 5.5.

5.4 METHODOLOGY FOR GENERATING INPUT VALUES ACCORDING TO SPECIFIED DISTRIBUTIONS

Variables that are treated as random must be assigned one of the thirteen probability distribution types that are available in EPACMTP. The distribution types and their corresponding EPACMTP distribution type codes are listed in Table 5.1. The default distribution type for each Monte-Carlo variable is discussed in the *EPACMTP Parameters/Data Background Document* (U.S. EPA, 2003).

The first step in generating a parameter value from a specified distribution involves generating a uniformly distributed random number between zero and one, designated as $U[0,1]$ (hereafter referred to as a uniform random number). The Monte-Carlo module uses standard FORTRAN pseudo-random number generation routines (provided in the FORTRAN compiler software) to generate this uniform random number. This uniform random number generator is initialized using a seed value. EPACMTP uses a constant seed value which means that when a EPACMTP Monte-Carlo simulation is repeated with the same data input file, the model will reproduce exactly the same results.

The second step consists of using this uniform random number in conjunction with the probability distribution specified in the input file to generate an appropriate value for the given EPACMTP input parameter; this process is referred to as a transformation and is more fully explained for each distribution type in Sections 5.4.2 through 5.4.9. More specifically, the Monte-Carlo module of EPACMTP uses FORTRAN software routines (documented by McGrath and Irving, 1973) to perform these parameter transformations – that is, to generate a random value from a specified distribution using a uniform random number.

These two steps are then repeated for each input parameter specified in the input file as a distribution of values until a complete set of modeling data is generated.

5.4.1 Constant

Constant parameters are set to a fixed value during the Monte-Carlo simulation.

Table 5.1 Probability distributions and their associated codes available for use in Monte-Carlo module of EPACMTP.

| Distribution Type | EPACMTP Distribution Type Code |
|-------------------------------------|--------------------------------|
| Constant | 0 |
| Normal | 1 |
| Lognormal | 2 |
| Exponential | 3 |
| Uniform | 4 |
| Log 10 Uniform | 5 |
| Empirical | 6 |
| Johnson SB | 7 |
| Gelhar Empirical ^a | 8 |
| Area Transformation ^b | 9 |
| Vertical Well Position ^c | 12 |
| Site-based ^d | 99 |
| Derived Variable | -1 |

^aGelhar’s distribution applies only to saturated-zone dispersivities (Gelhar et al., 1992).

^bThis distribution applies to municipal Subtitle D landfill areas only.

^cThis distribution applies to the vertical position of the receptor well below the water table only; it is used to specify that the receptor well is located at a fixed depth below the water table.

^dThis distribution applies to parameters that are read directly from an ancillary data file that contains waste locations, volume and area, and corresponding regional climatic and hydrogeological parameters for the site-based Monte-Carlo analysis.

5.4.2 Normal Distribution

The normal, or Gaussian, distribution is given by:

$$f(x^*) = \frac{1}{\sigma_N \sqrt{2\pi}} \exp\left[-0.5 \left(\frac{x^* - \mu_N}{\sigma_N}\right)^2\right] \tag{5.1}$$

where

- x^* = random variable (normally distributed)
- $f(x^*)$ = probability density function of x^*
- σ_N = standard deviation of normal distribution, and
- μ_N = mean of normal distribution

Normally distributed random variables are generated from U[0,1] values using the ANRMRN function in McGrath and Irving (1973). This function transforms a U[0,1] random value into a normally distributed value with mean of zero and unit standard deviation N[0,1]. The random parameter value for a normal distribution with mean μ and standard deviation σ is then given by

$$x^* = \sigma_N N[0,1] + \mu_N \quad (5.2)$$

where

| | | |
|------------|---|--|
| x^* | = | random variable (normally distributed) |
| σ_N | = | standard deviation of normal distribution |
| $N[0,1]$ | = | normally distributed value with mean of zero and standard deviation of one |
| μ_N | = | mean of normal distribution |

5.4.3 Lognormal Distribution

A variable has a lognormal distribution if it is converted to a normal distribution by taking the natural log of its value(s). The lognormal distribution is given by:

$$Y_{LN} = \exp(x^*) \quad (5.3)$$

where

| | | |
|----------|---|---|
| Y_{LN} | = | lognormally distributed random variable |
| x^* | = | normally distributed random variable |

5.4.4 Exponential Distribution

A variable has a exponential distribution if it is converted to a normal distribution by taking the exponential of its value(s). The exponential distribution is given by:

$$Y_{exp} = \ln(x^*) \quad (5.4)$$

where

| | | |
|-----------|---|---|
| Y_{exp} | = | exponentially distributed random variable |
| x^* | = | normally distributed random variable |

5.4.5 Uniform Distribution

In a uniform distribution, each value has an equal (uniform) probability of occurrence. The user must specify the upper and lower bounds for the distribution. Uniformly distributed variables are generated from:

$$Y_u = A_{YU} + (B_{YU} - A_{YU}) U[0,1] \quad (5.5)$$

where

| | | |
|----------|---|--|
| Y_u | = | uniform random variable |
| A_{YU} | = | lower bound for Y_u |
| B_{YU} | = | upper bound for Y_u |
| $U[0,1]$ | = | uniform random number between zero and one |

5.4.6 Log₁₀ Uniform Distribution

A variable has a log₁₀ uniform distribution if it is converted to a uniform distribution by taking the logarithm to the base 10 of its value(s). The user must specify upper and lower bounds for the distribution. The upper and lower bounds are specified in the same units as the actual EPACMTP variable of interest, but the bounds are internally converted to log₁₀ values. The log₁₀ uniform distribution is given by:

$$Y_{LU} = 10^{(A'' + (B'' - A'')U[0,1])} \quad (5.6)$$

where

| | | |
|-----------|---|--|
| Y_{LU} | = | log ₁₀ uniform random variable |
| A'' | = | $\text{Log}_{10}(A_{YLU})$ |
| A_{YLU} | = | lower bound for Y_{LU} |
| B'' | = | $\text{Log}_{10}(B_{YLU})$ |
| B_{YLU} | = | upper bound for Y_{LU} |
| $U[0,1]$ | = | uniform random number between zero and one |

5.4.7 Empirical Distribution

The empirical distribution is the most flexible probability distribution allowed in EPACMTP. Whereas other distributions assume that the probability of the actual modeling parameter of interest can be described by a particular type of mathematical equation, the empirical distribution does not make any assumptions about the underlying probability distribution of the data. The empirical distribution is simply a tabulation of parameter values and their corresponding frequency of occurrence. The empirical distribution is therefore well suited to empirically measured data, especially when there are relatively few measured data points. For empirical distributions, the user must provide a table of (measured) data values and their corresponding cumulative frequency of occurrence. The frequency is normalized from zero to one. EPACMTP generates random values for an empirical distribution as follows: First, it generates a uniform random number, $U[0,1]$, representing the normalized cumulative frequency for the empirical parameter of interest. Next, it reads the corresponding parameter value off the table of data values and their frequency. Linear interpolation between the next lowest and next highest data values is used when the randomly generated probability value does not exactly match any of the tabulated frequency values.

For example, let us consider a simple empirical distribution with 4 data points, listed in increasing order as shown below in Table 5.2.

Table 5.2 Example Empirical Distribution

| Relative Cumulative Frequency | Value |
|-------------------------------|-------|
| F_1 | A_E |
| F_2 | B_E |
| F_3 | C_E |
| F_4 | D_E |

By definition, the relative cumulative frequency for the lowest value in the table (A_E) is zero ($F_1 = 0$); for the highest value in the table (D_E), it is one ($F_4 = 1.0$). To generate a random value for the parameter, EPACMTP first generates a random probability, R_n :

$$R_n = U[0,1] \tag{5.7a}$$

where

- R_n = generated random number which corresponds to the cumulative probability of Y
- $U[0,1]$ = a uniform random number between zero and one

The code then performs a table look-up to find the next lower and next higher value in the frequency column of the table, and calculates the corresponding value for the parameter of interest by linear interpolation. Assume for the current example that the probability, R_n , lies in between F_3 and F_4 . The corresponding parameter value is then calculated as:

$$Y_E = \left(1 - \frac{R_n - F_3}{F_4 - F_3}\right)C_E + \left(\frac{F_4 - R_n}{F_4 - F_3}\right)D_E \tag{5.7b}$$

where

- Y_E = the random variable with empirical distribution
- R_n = generated random number which corresponds to the cumulative probability of Y_E
- F_3, F_4 = cumulative probabilities for C_E and D_E , respectively
- C_E = parameter value whose cumulative probability is F_3
- D_E = parameter value whose cumulative probability is F_4

5.4.8 Johnson SB Distribution

The Johnson SB distribution (McGrath and Irving, 1973) represents a special transformation applied to a random variable such that the transformed variable is normally distributed. The Johnson SB distribution is given by:

$$Y_{JSB} = \frac{(A_{YJ} + B_{YJ}e^{x^*})}{(1 + e^{x^*})} \quad (5.8)$$

where

| | | |
|-----------|---|--|
| Y_{JSB} | = | random variable with Johnson SB distribution |
| A_{YJ} | = | lower bound for Y_{JSB} |
| B_{YJ} | = | upper bound for Y_{JSB} |
| x^* | = | normally distributed random variable |

5.4.9 Special Distributions

In addition to the general distributions that can be used for any EPACMTP input parameter, the model handles a number of special distributions, each of which is unique to a particular EPACMTP model parameter. These special distributions are presented in this section.

5.4.9.1 Gelhar Distribution for Aquifer Dispersivity

The transport of the contaminant plume in the saturated zone is controlled by two mechanisms: advection and dispersion; the EPACMTP saturated-zone flow module simulates both of these mechanisms. Dispersion is the phenomenon by which a contaminant plume in flowing ground water is mixed with uncontaminated water and becomes reduced in concentration at the perimeter of the plume. Not all of a contaminant plume is traveling at the same velocity due to differences in pore size and flow path length and friction along pore walls, resulting in mixing along the flow path which decreases solute concentrations.

The model computes the longitudinal (along the flow path, or in the x-direction), horizontal transverse (perpendicular to the flow path, or in the y-direction), and vertical (in the z-direction) dispersion coefficients as the product of the seepage velocity and longitudinal (α_L), transverse (α_T) and vertical (α_V) dispersivities. A literature review indicated the absence of a generally accepted theory to describe dispersivities, although a strong dependence on scale has been noted (Gelhar et al., 1985; Gelhar et al., 1992). In a typical Monte-Carlo modeling analysis performed with EPACMTP, the longitudinal dispersivity is represented through a probabilistic formulation and the horizontal transverse and vertical dispersivities are then calculated from the longitudinal dispersivity, as summarized below; further details are given in Section 5.3.8 of the *EPACMTP Parameters/Data Background Document* (U.S. EPA, 2003).

In the absence of user-specified values or distributions, the longitudinal dispersivity is represented through a probabilistic formulation that is scaled based on well distance (Gelhar, 1986, personal communication), and the horizontal transverse and vertical dispersivities are then calculated from the longitudinal dispersivity. By default, the transverse (α_T) and vertical (α_V) dispersivities are calculated as a fraction of the longitudinal dispersivity. The default values of the ratio of the longitudinal to the transverse dispersivity, α_L/α_T , and the ratio of the longitudinal to the vertical dispersivity, α_L/α_V , are 8 and 160, respectively. The rationale for these default values are presented in Section 4.4.3.2.

5.4.9.2 Vertical Well Intake Point Depth

The depth of the intake point below the water table is the depth at which the model calculates the resulting ground-water concentration. Unlike most wells in the real world that have a screened interval of several feet or more, the simulated receptor well in EPACMTP has an intake that is a single point in space, as if the well consisted of a solid casing that was open at the bottom. In this case, the intake point would be the same as the depth of the well (or ZWELL). This depth is measured from the water table, not from the ground surface. For a Monte-Carlo analysis, there are several options for determining the depth of the well intake point that are implemented through the use of different EPACMTP distribution type codes.

The default option is to model the vertical position of the well as being uniformly distributed between the water table ($z_{rw}^* = 0$) and the saturated aquifer thickness ($z_{rw}^* = B$). This option is selected by specifying the z_{rw}^* -position as a uniform distribution (EPACMTP distribution type code 4, Table 5.1) with lower and upper limits of 0.0 and 1.0. EPACMTP will multiply this uniformly generated value by the saturated-zone thickness to yield the actual receptor well depth below the water table for each Monte-Carlo iteration.

Alternatively, if the upper limit is greater than 1, the vertical position of the receptor well is modeled as being uniformly distributed between these two limits. If the computed depth is greater than the saturated thickness, a new well position and/or a new depth are generated.

As a second option, data on the depth of receptor wells obtained from Agency surveys can be used directly in the model as an empirical distribution. The data values range from 15 ft (4.5 m) to 301 ft (90.9 m). If the generated value for the vertical position of the receptor well intake point exceeds the saturated thickness of the aquifer or if it is less than the depth to the saturated zone, a new well position is generated.

As a third option, the well position may be fixed at a constant depth. In this case, a EPACMTP distribution type code of either 12 or 0 (see Table 5.1) can be used in the input file. Each of these codes refers to a constant depth (measured in meters) for the well intake.

For the first two options, the vertical position of the receptor well can also be constrained to lie within the approximate vertical penetration depth of the

contaminant plume emanating from the waste unit, as defined by Equation (6.14) in Section 6 of the *EPACMTP Parameters/Data Background Document* (U.S. EPA, 2003).

5.4.10 Derived Parameters

In EPACMTP, a derived parameter is the one whose value is calculated directly from one or more other EPACMTP variables. Usually one or more of these variables has a probability distribution, so that the value of the derived variable also follows a frequency distribution. The relationships that are used to calculate values for derived variables represent direct physical relationships. An example is the relationship between aquifer porosity and bulk density. If we know porosity, it is possible to estimate bulk density and vice versa.

The individual parameters that are treated as derived parameters in EPACMTP, and their dependence on other EPACMTP variables are presented in the *EPACMTP Parameters/Data Background Document* (U.S. EPA, 2003).

5.4.11 Parameter Upper and Lower Bounds

Upper and lower bounds can be specified for each of the EPACMTP Monte-Carlo parameters. A number of the probability distributions in EPACMTP, including the uniform, Log_{10} uniform, empirical and the Johnson SB distribution already incorporate upper and lower bound values in the algorithm itself, so that the generated values for these distributions always fall within the allowable range. In the case of the normal and lognormal distribution, EPACMTP first generates a random value, compares it to the upper and lower bounds that are specified for that parameter, and if necessary regenerates new values until an acceptable value is obtained. EPACMTP follows a modified procedure for derived parameters. Because derived parameters reflect physical dependencies on other EPACMTP model parameters, it is not appropriate to simply modify the value of a derived parameter. Derived parameters may depend on more than one other EPACMTP parameter, which in turn may be related to more than one derived parameter. To deal with these multiple dependencies, EPACMTP regenerates the entire set of Monte-Carlo parameters in that realization until all parameter bounds are satisfied.

5.5 MONTE-CARLO METHODOLOGY FOR REGIONAL SITE-BASED, CORRELATED DISTRIBUTIONS

In reality, many of the site characteristics that control contaminant fate and transport are correlated with one another. For instance, climatic characteristics that drive infiltration and recharge, as well as soil and aquifer properties, are a function of a site's location. Except for derived parameters, the Monte-Carlo methodology and EPACMTP distribution types described in Section 5.4 treat each model parameter as independent. Parameter upper and lower bounds ensure that the value of each parameter is within a reasonable range, but they do not guarantee that the combination of parameter values that is randomly generated necessarily represents realistic site conditions. For instance, many of the Monte-Carlo input distributions that have been developed for EPACMTP (see the *Parameters/Data Background*

Document (U.S. EPA, 2003)) reflect nationwide variability. Random sampling from these individual distributions may result, for instance, in combining recharge rates from the arid southwestern United States, with ground-water depths that are typical of Florida. For situations in which the appropriately correlated parameter data sets are available, EPACMTP's regional, site-based, Monte-Carlo capability overcomes the above-mentioned limitation.

5.5.1 Description of Regional Site-Based Approach

The Monte-Carlo methodology implemented in EPACMTP is called 'regional site-based' because waste site databases are linked by each site's geographic location and underlying aquifer type to regional databases of climatic and subsurface parameters, respectively. In this way, the regional site-based approach attempts to approximate the ideal situation where we have a complete set of the site-specific input data required to run the EPACMTP model for each waste site in a statistically valid subset of the universe of waste management units in the United States.

In order to implement this site-based approach, the Agency has assembled a regional, site-based modeling database for each of the four types of waste management units that are typically modeled with EPACMTP (landfill, waste pile, surface impoundment, and land application unit). Additional details about the data included in these databases (and the corresponding data sources) are provided in the *EPACMTP Parameters/Data Background Document* (U.S. EPA, 2003). The remainder of this section briefly explains how the regional, site-based modeling approach is implemented.

The regional, site-based modeling procedure is based on an empirical distribution of waste sites, which can be envisioned as a list of sites; each record in the list corresponds to an actual waste site located somewhere in the U.S. For each record in the list, the site-related characteristics corresponding to that site are provided, and the value for each characteristic is specified as either as a single value or as a distribution or range of values. For instance, EPACMTP can handle either a specific value for the depth to ground water or a distribution of values, in case the specific value at that waste site is uncertain. However, in the site-based procedure, not all of the EPACMTP input parameters need to be specified as site-related. When inputs are not specified as site-related, the parameters are specified as one of the probability distribution types presented in Section 5.4. As an example, the receptor well location is often a non-site-related input parameter. Even if data on specific receptor well locations downgradient from waste sites are available, these locations may change in the future, thus, the user may want to consider a range or probability distribution of receptor well locations in conducting a risk assessment.

The data sources for the regional site-based methodology that are typically used to conduct a Monte-Carlo modeling analysis with EPACMTP include: 1) the Hydrogeologic DataBase for Modeling (HGDB) (Newell et al., 1989; U.S. EPA, 1997), developed from a survey of hydrogeologic parameters for actual hazardous waste sites in the United States; 2) the infiltration and recharge analysis performed for 102 U.S. climatic centers using the HELP model (U.S. EPA, 1997, 2003); 3) the Industrial Subtitle D Facility Study (also called the Subtitle D survey), conducted by

the U.S. EPA OSW which provides a statistically valid set of site-specific areas, volumes and locations for industrial Subtitle D landfills, waste piles, and land application units around the country; and 4) the EPA's recent 5-year nationwide study of nonhazardous (subtitle D) industrial surface impoundments (the SI Study) which provides a statistically valid set of site-specific impoundment characteristics, including impoundment location, area, ponding depth, and operational life.

The HGDB, developed by Rice University for American Petroleum Institute in 1989, provides site specific data on ground-water parameters (aquifer thickness, depth to ground water, hydraulic gradient and hydraulic conductivity) collected by independent investigators for approximately 400 hazardous waste sites throughout the U.S. These site-specific data were then regrouped into 13 hydrogeologic environments, based on the USGS classification of aquifer regions (Heath, 1984). The result is a database of aquifer types, with each aquifer type consisting of an empirical distribution of values for each of the four aquifer parameters.

Infiltration and recharge rates for use in EPACMTP modeling applications have been estimated for selected soil types at cities around the country through the use of the HELP water-balance model. Using the Soil Conservation Service's (SCS) county-by-county soil mapping database, three soil textures were defined: coarse-; medium-; and fine-grained soils. Using National Oceanic and Atmospheric Administration (NOAA) data on precipitation and evaporation rates in the United States, 102 cities were selected as climatic centers for the HELP model. For each selected city, historical climatic data were used to develop an ambient regional recharge rate as a function of site location and soil type; likewise, infiltration rates were developed for each type of WMU, as a function of site location, liner type (if any) and soil type.

We have tabulated the results of the Industrial Subtitle D Facility Study (U.S. EPA, 1986) into a nationwide database of waste management unit sites for use in probabilistic EPACMTP modeling analyses of landfills, waste piles and land application units. The original survey provides a set of observations of site-specific areas, volumes and locations for Industrial Subtitle D landfill, waste pile, and land application facilities across the U.S. Although surface impoundments were included in the Industrial Subtitle D Facility Study, EPA has adopted the results of the more recent Surface Impoundment (SI) Study as the data source for the database of surface impoundment sites. The SI Study provided data on impoundment locations, area, operating depths (depth of ponding in the impoundment), depth of the SI base below the ground surface, operational life of the impoundment, and proximity of the impoundment to a surface water body. Since the Subtitle D survey and the SI Study include only facility-specific data, linkages to the other two data sources (HGDB and the HELP-modeled climatic database) are used to generate the additional input parameters required to perform the ground-water fate and transport modeling for each site. That is, for use in EPACMTP modeling analyses, the modelers classified each site in the Subtitle D survey and the SI Study databases according to the type of aquifer underlying the site and the closest climate center used in the HELP modeling in order to provide links to the hydrogeologic and climatic databases. Details of the analysis and screening of SI facilities and units are presented in the EPA SI Study report (U.S. EPA, 2001). Data on various types of waste management

units for use in EPACMTP are provided in the *EPACMTP Parameters/Data Background Document* (U.S. EPA, 2003).

5.5.2 Regional Site-Based Monte-Carlo Procedure

Fundamentally, the approach used for a site-based Monte-Carlo analysis consists of conducting the modeling analysis for the sites in a waste site database (either the Subtitle D survey or the SI Study) on the assumption that these sites are an adequate representation of the universe of possible waste sites in the U.S. The actual procedure of the Monte-Carlo simulation is summarized in a number of steps below. These steps describe the general procedure used at the time of preparation of this document and reflect the currently available databases commonly used by EPA. Some of the specifics may vary for individual projects as EPA updates its databases, but the steps below will still illustrate the essence of the methodology:

STEP 1: Select a Waste Site

The first step involves selecting a site, at random, from the list of waste sites. The data set is treated as an empirical distribution. In most instances, each site will have an equal probability of occurrence, although it is possible to vary the probability so that some sites have a greater likelihood of being selected than others. When the model selects a site, the data read into EPACMTP include the appropriate characteristics for that site, including unit area, unit depth, an index that specifies the nearest climate center, and an index that specifies the underlying aquifer type.

STEP 2: Generate Recharge and Infiltration for the Selected Waste Site

The soil type at the chosen waste site (and cover type for landfills) and the specified liner scenario (no liner/in-situ soil, single clay liner, or composite liner) are then used along with the climate center index to determine the appropriate values for recharge and infiltration at the site by querying the database of HELP-modeled recharge and infiltration rates. The specific soil (and landfill cover type) can be specified individually for each waste unit or as a probability distribution.

STEP 3: Generate Hydrogeologic Variables for Selected Site in the Industrial Subtitle D Facility Study

As explained above, given the resolution of available hydrogeological databases and acknowledging the uncertainty in the effective local values of hydrogeological site characteristics, the regional site-base approach is generally implemented by using the aquifer type assigned to the chosen site in the WMU database. The input values for the hydrogeologic parameters for the chosen site are then determined from the probability distributions that define the corresponding aquifer type. That is, a correlated set of hydrogeologic parameter values is randomly chosen from among those available in the hydrogeologic database for the chosen aquifer type. If the selected ground-water parameter set is missing any values, a joint distribution of the parameters (derived for each environment) is used to fill in the missing values. The details of this procedure are presented in Section 5.5.3.

STEP 4: Generate Remaining Parameters for the Selected Waste Site

The remaining parameters for the waste site that are not assigned as site-related (e.g., x, y, and z coordinates of the receptor well) are generated by using one of the probability distributions described in Section 5.4. Any derived parameters are calculated as described in Section 5.4.10.

STEP 5: Calculate the Predicted Receptor Well Concentration Value for the Selected Waste Site

Given the complete set of input parameter values generated in the previous four steps, and the chemical-specific characteristics (e.g., leachate concentration, adsorption coefficient and exponent, and degradation rate), the EPACMTP flow and transport modules are executed to compute the receptor well concentration value for this Monte-Carlo realization.

STEP 6: Repeat Steps 1 Through 5 a Specified Number of Times, and Estimate the National Distribution of Receptor Well Concentrations

After Step 5, the receptor well concentration value for a specific realization is obtained. The process is then repeated as many times as is specified by the user. The result of the Monte-Carlo modeling analysis is a receptor well concentration for each model realization; these results represent the nationwide distribution of drinking water exposure concentrations. In most cases, the number of Monte-Carlo realizations will be much greater than the number of sites used in the regional, site-based analysis, and because the selection of sites as described in Step 1 above is random, each site is expected to be picked more than once. However, because there is an additional random component to the process of assigning values to all of the EPACMTP parameters (e.g., well location), repeated selection of the same waste site in the Monte-Carlo process generally will not result in the same predicted receptor well exposure concentration.

5.5.3 Methodology for Generating Missing Data Values

Below is a step-by-step presentation of the methodology used, within the framework of the site-based Monte-Carlo approach, to generate missing parameter values, based on the statistical correlation between parameters with missing values and model input parameters whose values are known.

For each parameter of interest, for example, hydraulic conductivity, we have a set of known (observed) values, but also a number of missing values. For the known values we also have corresponding values of related parameters, e.g., hydraulic gradient and saturated thickness. From this information we constructed a covariance matrix that expresses the statistical relationships among all parameters. Given this covariance matrix and values for one or more parameters it is possible to estimate missing values for the parameter of interest. For instance, we can estimate the value of hydraulic conductivity given values for hydraulic gradient and/or saturated thickness. The methodology described here is applicable to parameters with multi-variate normal (Gaussian) distributions. Consequently, if the actual

parameters have non-Gaussian distributions, each must first be transformed to a normal distribution. If applicable, any statistically generated values must also be back-transformed to obtain the parameter value in the original, untransformed space. The parameter covariance matrix is required also. The covariance matrix is calculated from the transformed variables.

The algorithm to generate missing values is described using vector notation. In the notation below, the superscript \top denotes the transpose operator, i.e. switching of rows and columns, and superscript $^{-1}$ denotes an inverse matrix.

1. The process begins with a set of parameters transformed to a normal distribution if necessary. The set can be expressed as a data vector, X :

$$X = (n \times 1) \text{ data vector of normally distributed, correlated parameters}$$

$$= (X_1, \dots, X_n)^T$$
2. The second step is to create a vector Y by partitioning the data vector x so that the first p elements of Y correspond to the missing values of X , and the remaining q elements correspond to the observed values of X :

$$Y = (Y_1, Y_2)^T$$

$$Y_1 = (p \times 1) \text{ vector of missing values of } X$$

$$Y_2 = (q \times 1) \text{ vector of observed values of } X$$

3. As stated above, Y consists of normally distributed parameters and known correlations (covariance) among parameters. The parameter vector Y can therefore be expressed statistically in terms of a multivariate normal distribution characterized by a vector of mean values, m , and a covariance matrix V :

$$Y \sim N_n(\bar{m}, V) \quad (5.9)$$

where

$N_n()$ = n-variate normal distribution with mean vector m and covariance matrix V

$$\bar{m} = (m_1, m_2)^T$$

$$n = p + q$$

$$m_1 = (p \times 1) \text{ mean vector of missing values}$$

$$m_2 = (q \times 1) \text{ mean vector of observed values}$$

$$V = (n \times n) \text{ covariance matrix}$$

Given that Y is composed of unknown (Y_1) and known (Y_2) values, its multivariate statistical representation can also be partitioned accordingly. Given Y_2 , the conditional distribution of Y_1 which is a multivariate normal distribution with $(p \times 1)$ mean vector $m_{1,2}$ and $(p \times p)$ covariance matrix $V_{1,2}$ is:

$$Y_1 | Y_2 \sim N_n(m_{1.2}, V_{1.2}) \quad (5.10a)$$

$$m_{1.2} = m_1 + V_{12} V_{22}^{-1} (Y_2 - m_2) \quad (5.10b)$$

$$V_{1.2} = V_{11} - V_{12} V_{22}^{-1} V_{21} \quad (5.10c)$$

where

- Y_1 = vector of missing values
- Y_2 = vector of observed values
- N_n = n-variate normal distribution with mean vector m and covariance matrix V
- $m_{1.2}$ = $(p \times 1)$ mean vector of Y_1 conditioned by Y_2
- $V_{1.2}$ = $(p \times p)$ covariance matrix of Y_1 , conditioned by Y_2
- m_1 = vector of means of missing values
- V_{22}^{-1} = inverse of V_{22}
- m_2 = vector of means of observed values
- V_{11} = $(p \times p)$ upper left partition of V
- V_{12} = $(p \times q)$ upper right partition of V
- V_{21} = $(q \times p)$ lower left partition of V
- V_{22} = $(q \times q)$ lower right partition of V

4. The steps above now lead to the following equation for estimating unknown values of Y_1 . Given the observed vector Y_2 , a prediction of the missing vector $Y_{1.2}$, is generated by:

$$Y_{1.2} = m_{1.2} + L^* (D^*)^{1/2} u \quad (5.11a)$$

where

- $Y_{1.2}$ = prediction of the missing vector Y_1
- $m_{1.2}$ = $(p \times 1)$ mean vector of Y_1 conditioned by Y_2
- L^* = $(p \times p)$ matrix of the eigenvectors of $V_{1.2}$

- u = ($p \times 1$) vector of independent and identically distributed standard normal random variables
 D^* = ($p \times p$) diagonal matrix consisting of the square root of the eigenvalues of $V_{1,2}$, so that

$$V_{1,2} = B^* B^{*T} \quad (5.11b)$$

where

- $V_{1,2}$ = ($p \times q$) upper right partition of V
 B^* = ($p \times p$) matrix of square root of $V_{1,2} = L^* (D^*)^{1/2}$
 B^{*T} = transpose of B^*

An inspection of equation (5.11 a) shows that missing values are estimated from their mean, $m_{1,2}$, plus a contribution from the covariance with other parameters, expressed by $L^* (D^*)^{1/2}$. This contribution also includes a random factor, u . If the correlation between the parameter whose value is unknown and related parameters is weak, then the second term on the right-hand side of (5.11 a) will tend to be close to zero, and the estimated value will be close to the mean. Conversely, a strong correlation means that $L^* (D^*)^{1/2}$ will have a higher value and this will allow the estimated value for Y to be more different from the mean. The incorporation of u means that there always is a random component to the estimate, except in the case of zero correlation when $L^* (D^*)^{1/2}$ is exactly zero.

5.6 INTERPRETING A MONTE-CARLO MODELING ANALYSIS

The result of a Monte-Carlo simulation is a sequence of receptor well concentration values. Each value corresponds to one Monte-Carlo realization. Collectively, they represent the range of possible outcomes for the EPACMTP modeling scenario of interest based on the probability distributions assigned to each of the EPACMTP input parameters. The Monte-Carlo outputs are best analyzed and interpreted in terms of probability. For ease of interpretation, it is often convenient to normalize the computed receptor well concentrations to the (initial) value of the leachate concentration infiltrating to the subsurface from the base of the waste unit:

$$\bar{C}_r = \frac{C_{rwell}}{C_L} \quad (5.12)$$

where

- \bar{C}_r = relative concentration at receptor well (dimensionless)
 C_{rwell} = constituent concentration at receptor well (mg/L)
 (instantaneous or time-averaged)
 C_L = leachate concentration (mg/L)

If the modeling scenario includes a time-varying leachate concentration, as in the case of a depleting landfill, the value of the initial leachate concentration is used in Equation 5.12. \bar{C}_r is a dimensionless quantity, with a value between zero and one. It is called the normalized or relative concentration. The reduction in concentration between the leachate concentration which enters the subsurface and the eventual concentration predicted to occur at the receptor well is a result of dilution and attenuation processes which occur during the transport of the constituent through soil and ground water. A convenient way to express the aggregate effects of all fate and transport processes simulated by EPACMTP is in terms of the Dilution-Attenuation Factor (DAF) which is defined as:

$$DAF = \frac{C_L}{C_{rwell}} = \frac{1}{\bar{C}_r} \quad (5.13)$$

where

DAF = dilution-attenuation factor

The DAF is a dimensionless quantity, the value of which can vary from one (1) to infinity. A DAF value of 1 corresponds to a relative receptor well concentration of one. This situation means that the exposure concentration at the receptor well is the same as the leachate concentration that enters the subsurface from the modeled waste management unit, and no dilution or attenuation occurs along the subsurface pathway. Conversely, if the contaminant plume does not reach the receptor well at all, the receptor well concentration will be zero and the corresponding DAF will approach infinity.

For organic constituents, the fate and transport equations solved by EPACMTP are linear, which means that the magnitude of the predicted ground-water well concentration is linearly proportional to the value of the leachate concentration. In other words, for organics, a doubling of the EPACMTP input value of leachate concentration would result in a doubling of the predicted ground-water well concentration, as long as all other model parameters stay the same. Equation 5.13 is applicable to chemicals with both linear and non-linear sorption isotherms. For chemicals with linear sorption isotherms, their DAFs are not dependent on leachate concentrations. In other words, once the DAF for a chemical with a linear isotherm has been determined, it can be used to determine C_{rwell} regardless of the value of C_L . On the other hand, DAFs for constituents whose geochemical behavior is characterized by nonlinear sorption isotherms (i.e., metals) are C_L -specific, and C_{rwell} is not linearly related to C_L . For this reason, the DAF is a less useful concept for describing the transport behavior of metals.

Conceptually, each Monte-Carlo realization represents one possible real-world outcome, and each realization has an equal probability of occurrence. A Monte-Carlo simulation will result in a distribution of predicted receptor well concentrations, and through a post-processing step the EPACMTP user can obtain the probability distribution of the expected receptor well exposure concentrations – or DAFs – by

constructing a simple frequency histogram of the Monte-Carlo modeling results. An example is shown in Figure 5.2.

Figure 5.2 shows the frequency distribution of the normalized receptor well concentrations obtained in a EPACMTP Monte-Carlo analysis. Frequency is expressed on a normalized scale from 0 to 100. Although this is a fictitious example, it does illustrate a number of typical features of a Monte-Carlo simulation. One of these key features is that many of the Monte-Carlo realizations result in very low concentrations at the receptor well. In the example shown, the receptor well concentration is $1/50^{\text{th}}$ or less of the leachate concentration in more than 80% of the cases. Correspondingly, there are relatively few occurrences of high normalized concentration values. In showing these features, Figure 5.2 also illustrates that a regular frequency histogram is not the most convenient way to present the results. A more useful way to do this is to present the Monte-Carlo results in the form of a cumulative frequency graph, otherwise known as a Cumulative Distribution Function (CDF). Figure 5.3 presents the data from Figure 5.2 as a CDF.

Figure 5.3 shows the cumulative frequency expressed as a percentile. EPA often summarizes a Monte-Carlo analysis in terms of specific percentile values of the CDF of the normalized receptor well concentration, or its corollary, the DAF. In the example shown in Figure 5.3, the 90th percentile of the concentration CDF corresponds to a normalized receptor well concentration of about 0.1. This means that in 90% of the cases, the receptor well concentration is one-tenth or less of the leachate concentration at the waste management unit. An equivalent statement is that the 10th percentile of DAF is 10 (the reciprocal of a normalized receptor well concentration value of 0.1)

There are several ways to summarize the results of the Monte-Carlo analysis process. For instance, the resulting distribution of receptor well concentrations can be analyzed to identify the percentage of realizations that produce a receptor well concentration above or below a specified ground-water reference concentration (such as a Maximum Contaminant Level (MCL)). Alternatively, using the DAF, the input leachate concentration can be scaled to calculate the leachate concentration threshold value – that is, the maximum allowable leachate concentration that results in a predicted receptor well concentration being less than the ground-water reference concentration (such as an MCL) in a defined percentage of the model realizations. Assuming that the Monte Carlo modeling process indeed captures the range of variability and uncertainty encountered at actual waste sites across the United States, the Monte-Carlo results indicate the fraction of sites for which expected receptor well concentrations are less (or DAFs higher) than a particular threshold value. This, in turn, provides the basis for developing regulatory leachate and/or waste concentration threshold values and determining appropriate waste management requirements to ensure compliance with risk-based or other ground-water quality criteria.

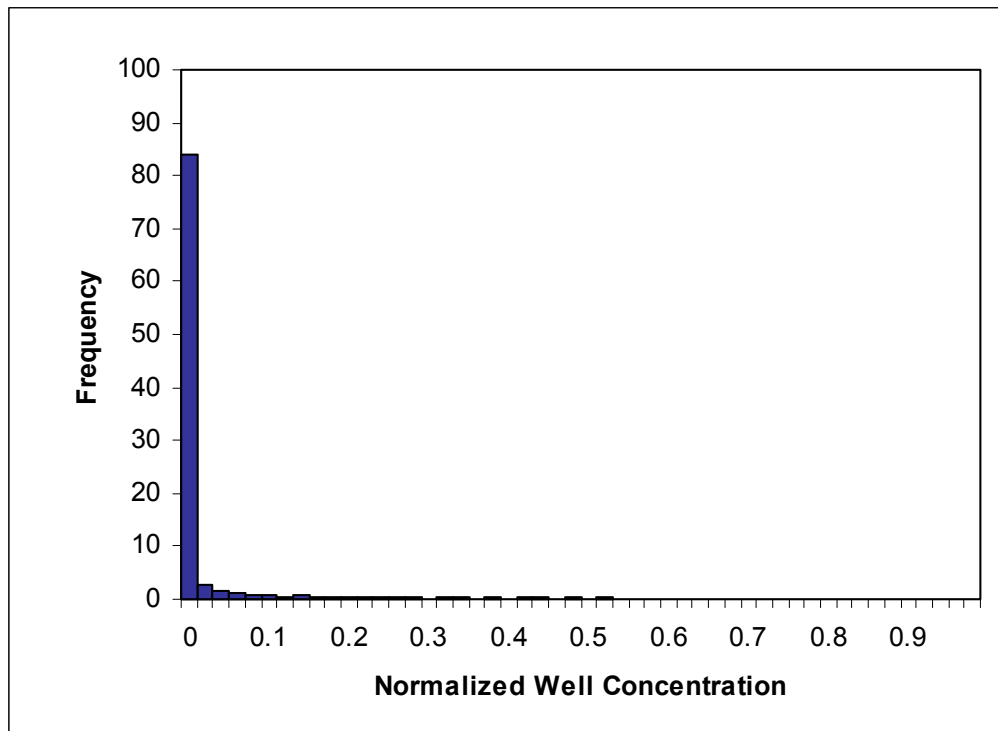


Figure 5.2 Frequency distribution of normalized receptor well concentrations.

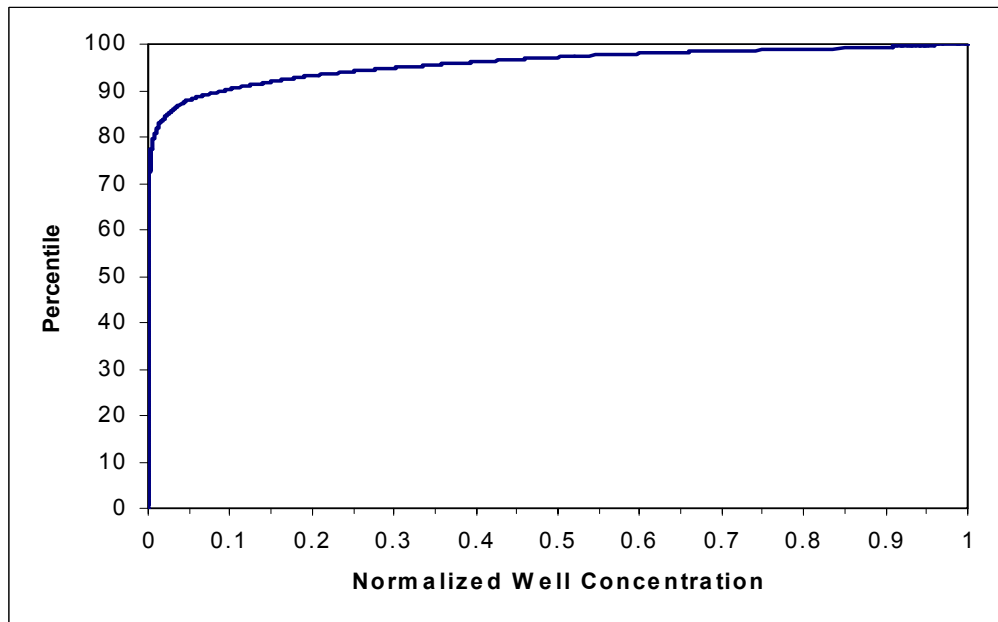


Figure 5.3 Cumulative Distribution Function of Normalized Receptor Well Concentration.

For instance, consider the following question: “What is the maximum allowable leachate concentration for chemical x in this waste stream that is protective of human health in at least 90% of the cases ?” This question can be answered in the following manner. For exposure to ground water, the human health standard (also called the Reference Ground-water Concentration or RGC) can be expressed in terms of a ground-water exposure concentration value (e.g., health-based number (HBN) or maximum contaminant level (MCL)) at a well intake point, corresponding to an acceptable risk level, say 10^{-6} cancer risk. The corresponding maximum allowable leachate concentration can then be back-calculated using the Monte-Carlo modeling results as:

$$C_L^{\max} = DAF_{10} \times HBN \quad (5.14)$$

where

| | | |
|--------------|---|---|
| C_L^{\max} | = | maximum allowable leachate concentration (mg/L) |
| DAF_{10} | = | 10th percentile value of DAF (which corresponds to the 90th percentile of relative concentration) (dimensionless) |
| HBN | = | Health-Based Number, which is a ground-water exposure concentration corresponding to a defined risk level (mg/L) |

Using the DAF values from the example presented in this section and a protection level of 90%, the maximum allowable leachate concentration would be 10 times the health-based ground-water concentration threshold, reflecting the fact that we expect the dilution and attenuation during ground-water transport to be a factor of 10 or greater in at least 90% of the modeled cases.

5.7 REQUIRED NUMBER OF MONTE-CARLO REALIZATIONS

It is inherent in the random sampling approach of a Monte-Carlo analysis that the modeling outcome depends on the number of realizations. For instance, the estimate of the 90th percentile predicted ground-water concentration will likely be different if we calculate it from 100 realizations, as compared to 1,000 realizations. In using a Monte-Carlo modeling approach, a higher number of realizations usually leads to a more convergent and reliable result. Results are said to be converged if the estimate of a particular percentile value does not change significantly if additional Monte-Carlo simulations are performed. However, it is not generally possible to determine beforehand how many realizations are needed to achieve a specified degree of convergence since the value can be highly dependent on parameter distributions.

EPA conducted a bootstrap analysis for the EPACMTP model to evaluate how convergence improves with increasing number of realizations. A bootstrap analysis is a technique of replicated re-sampling (usually by a computer) of an original data set for estimating standard errors, biases, confidence intervals, or other measures of statistical accuracy. Bootstrap analysis can automatically produce accuracy estimates in almost any situation without requiring subjective statistical assumptions

about the original distribution. The EPACMTP modeling scenario represented in EPA’s bootstrap analysis was that of a continuous source, landfill disposal scenario in which the “true” 10th percentile DAF was 10. The results of the bootstrap analysis are summarized in Table 5.3. These results show that, with 10,000 realizations, the expected value of the 10th percentile DAF was 10 with a 95 percent confidence interval of 10 ± 0.7 . Decreasing the number of realizations to 5,000 increased the confidence interval to 10 ± 1.0 .

Table 5.3 Relationship between confidence interval and number of Monte-Carlo realizations.

| Number of Realizations | 97.5 Percent Confidence Interval | |
|------------------------|----------------------------------|----------------------------------|
| | Lower Limit of DAF ₁₀ | Upper Limit of DAF ₁₀ |
| 1,000 | 7.52 | 12.74 |
| 2,000 | 8.36 | 11.60 |
| 5,000 | 9.02 | 11.06 |
| 10,000 | 9.31 | 10.74 |
| 20,000 | 9.51 | 10.46 |
| 30,000 | 9.63 | 10.40 |

This bootstrap analysis illustrates the relatively slow decrease in the prediction error as the number of Monte-Carlo realizations is increased.

EPA has adopted 10,000 model realizations in recent EPACMTP modeling applications. The actual number of realizations adopted for regulatory analyses by EPA is a balance between the desire for optimal convergence and practical constraints of resources and time needed to perform large numbers of computer analyses, as well as considering the relative benefit of increasing the number of Monte-Carlo realizations against other inherent sources of uncertainty. The diminishing benefit of increasing the number of Monte-Carlo realizations is illustrated in Figure 5.4 in this figure. The relative prediction error from the bootstrap analysis is plotted against the number of realizations. The relative error here is defined as 95 percent confidence interval (difference between upper and lower confidence limits in Table 5.3), divided by the number of Monte-Carlo realizations. The results in the figure are multiplied by a scaling factor of 1,000 for presentation purposes. This figure illustrates that when the number of Monte-Carlo realizations is fairly small, that is on the order of 1,000, increasing this number can significantly reduce the prediction error. However, this benefit diminishes when the number of realizations is already on the order of 10,000 or greater.

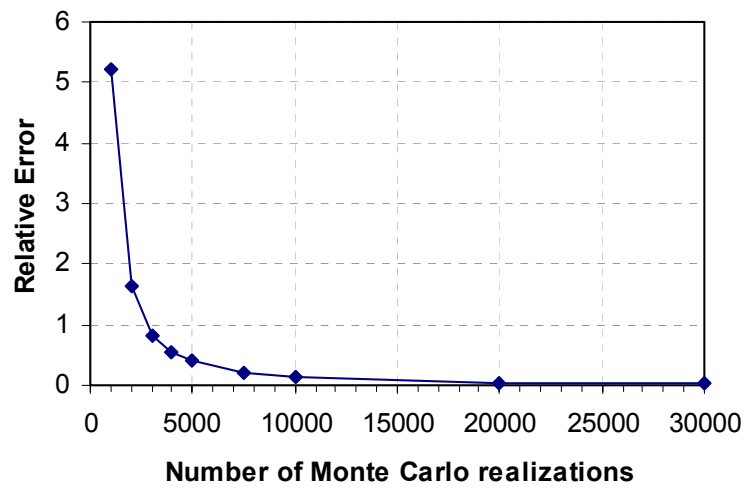


Figure 5.4 Relative Monte-Carlo Prediction Error.

6.0 REFERENCES

- Bear, J., 1972. *Dynamics of Fluids in Porous Media*. American Elsevier, New York, NY.
- Bear, J., 1979. *Hydraulics of Groundwater*. McGraw Hill, New York, NY.
- Bonaparte, R., J.P. Giroud, and B.A. Cross, 1989. Rates of Leakage through Landfill liners. *Geosynthetics 1989 Conference*, San Diego, California.
- Burnett, R.D. and E.O. Frind, 1987. Simulation of contaminant transport in three dimensions. 2. Dimensionality effects. *Water Resources Research* 23(4): 695-705.
- Carsel, Robert F., and R.S. Parrish, 1988. A method for developing joint probability distributions of soil-water retention characteristics. *Water Resources Research* 5: 755-700.
- Carsel, Robert F., Rudolph S. Parrish, Russell L. Jones, James L. Hansen, and Richard L. Lamb, 1988. Characterizing the uncertainty of pesticide leaching in agricultural soils. *Journal of Contaminant Hydrology* 2: 111-124.
- Carlsaw, H.S., and Jaeger, J.C., 1959. *Conduction of Heat in Solids*. 2nd Ed., Oxford University Press.
- CRC, 1981. *Handbook of Chemistry and Physics*. 62nd Ed. CRC Press.
- Davis, S.N., 1969. Porosity and permeability of natural materials. In: *Flow Through Porous Media*, R.J.M. de Wiest, Editor, Academic Press, NY.
- de Hoog, F.R., J.H. Knight, and A.N. Stokes, 1982. An improved method for numerical inversion of Laplace transforms. *SIAM J. Sci. Stat. Comput.* 3(3): 357-366.
- de Marsily, G., 1986. *Quantitative Hydrology*, Academic Press, Orlando, FL.
- Domenico, P.A. and V.V Palciauskas., 1982. Alternative boundaries in solid waste management, *Ground Water* 20: 301-311.
- Domenico, P.A., and G.A. Robbins, 1985. A new method for contaminant plume analysis, *Ground Water* 25(6): 733-739.
- Enfield, C.G. et al., 1982. Approximating pollutant transport to groundwater. *Ground Water* 10(6): 711-722.
- Freeze, R. Allen and John A. Cherry, 1979. *Groundwater*. Prentice-Hall, Englewood Cliffs, NJ.

-
- Gelhar, L.W., A. Mantoglou, C. Weltey, and K. R. Rehfeldt, 1985. *A review of field-scale physical solute transport processes in saturated and unsaturated porous media*, Electric Power Research Institute Report EA-4190, Project 2485-5, Palo Alto, CA, 1985.
- Gelhar, L.W., 1986. Personal communication
- Gelhar, L.W., C. Welty, K.R. Rehfeldt, 1992. A critical review of data on field-scale dispersion in aquifers. *Water Resources Research* 28(7): 1955-1974.
- Harleman, D.R.F., and R.R. Rumer, 1963. Longitudinal and Lateral Dispersion in Isotropic Porous Medium, *J. Fluid Mech.* 16(3): 385-394.
- Heath, R.C., 1984. National Water Summary 1984. Section entitled *State Summaries of Groundwater Resources*. USGS Water-Supply Paper 2275.
- Huyakorn, P.S., and K. Nilkuha, 1979. Solution of Transient Transport Equation Using an Upstream Finite Element Scheme. *Appl. Math. Modelling* 3: 7-17.
- Huyakorn, P.S., and G.F. Pinder, 1983. *Computational Methods in Subsurface Flow*, Academic Press.
- Huyakorn, P.S., B.G. Jones, and P.F. Andersen, 1986. Finite Element Algorithms for Simulating Three-Dimensional Groundwater Flow and Solute Transport in Multilayer Systems. *Water Resources Research* 22(3):361-374.
- Huyakorn, P.S., and J.E. Buckley, 1987. *VADOFT: Finite Element Code for Simulating One-Dimensional Flow and Solute Transport in the Vadose-zone*. Technical Report Prepared for the U.S. Environmental Protection Agency, Athens, GA.
- Karickhoff, S.W., 1985. *Sorption protocol for evaluation of OSW chemicals*. U.S. EPA, Athens Environmental Research laboratory, Athens, GA.
- Lambe, T.W., and Whitman, R.V., 1969. *Soil Mechanics*. John Wiley and Sons.
- MacDonald, J.R., 1964. Accelerated Convergence, Divergence, Iteration, Extrapolation, and Curve Fitting. *J. Appl. Phys.* 10: 3034-3041.
- McGrath, E.J. and D.C. Irving, 1973. *Techniques for Efficient Monte Carlo Simulation*. Technical report prepared for Department of the Navy, Office of Naval Research, Arlington, VA.
- McWorter, D.B., and D.K. Sunada, 1977. *Groundwater Hydrology and Hydraulics*. Water Resources Publications, Fort Collins, CO.
- Millington, R.J. and J.P. Quirk, 1961. Permeability of porous solids, *Trans. Faraday Soc.* 57: 1200-1207.
-

-
- Newell, Charles J., Loren P. Hopkins, and Philip B. Bedient, 1989. *Hydrogeologic Database for Ground Water Modeling*. API Publication No. 4476, American Petroleum Institute, Washington, DC.
- Newell, Charles J., Loren P. Hopkins, and Philip B. Bedient, 1990. Hydrogeologic Database for Ground Water Modeling. *Ground Water* 28(5): 703 - 714.
- Rollin, A.L., M. Marcotte, T. Jacquelin, and L. Chaput, 1999. Leak Location in Exposed Geomembrane Liners using an Electrical Leak Detection Technique. *GeoSynthetics '99: Specifying Geosynthetics and Developing Design Details 2*: 615-626.
- Schroeder, Paul, Cheryl Lloyd, Paul Zappi, and Nadim Aziz, 1994a. *The Hydrologic Evaluation of Landfill Performance (HELP) Model: User's Guide for Version 3*. EPA/600/R-94/168a. U.S. EPA Risk Reduction Engineering Laboratory, Cincinnati, OH.
- Schroeder, Paul, Cheryl Lloyd, Paul Zappi, and Nadim Aziz, 1994b. *The Hydrologic Evaluation of Landfill Performance (HELP) Model: Engineering Documentation for Version 3*. EPA/600/R-94/168b. U.S. EPA Risk Reduction Engineering Laboratory, Cincinnati, OH.
- Science Advisory Board, 1988. *Review of the Unsaturated Zone Code for the OSW Fate and Transport Model*. Report of the Unsaturated Zone Code Subcommittee. SAB-EEC-88-030. June, 1988.
- Science Advisory Board, 1990. *Review of the CANSAZ Flow and Transport Model for Use in EPACMS*. Report of the Saturated Zone Model Subcommittee. EPA-SAB-EEC-90-009. March, 1990.
- Science Advisory Board, 1995. An SAB Report: *Review of EPA's Composite Model for Leachate Migration with Transformation Product-EPACMTP*. EPA-SAB-EEC-95-110. August, 1998.
- Sudicky, E.A., 1989. The Laplace Transform Galerkin Technique: A Time-Continuous finite Element theory and Application to Mass Transport in Groundwater. *Water Resources Research* 25 (8): 1833-1846.
- Sudicky, E.A., J.B. Kool and P.S. Huyakorn, 1990. *CANSAZ: Combined Analytical-Numerical Model for Simulating Flow and Contaminant Transport in the Saturated Zone. Version 2.0 with Nonlinear Adsorption and Chain Decay Reactions*. Technical Report Prepared for U.S. EPA, Office of Solid Waste, Washington, DC, 20460.
- Sudicky, E.A., and R.G. McLaren, 1992. The Laplace Transform Galerkin Technique for Large-Scale Simulation of Mass Transport in discretely-Fractured Porous Formations. *Water Resources Research* 28 (2): 499-514.
-

-
- Todd, D.K., 1959. *Ground Water Hydrology*. John Wiley, New York.
- U.S. EPA, 1986. Industrial Subtitle D Facility Study (Telephone Survey), U.S. Environmental Protection Agency, October 20, 1986.
- U.S. EPA, 1989. *Unsaturated Zone Flow and Transport Module: Version 2.0 with Nonlinear Sorption and Chain Decay Reactions*. U.S. Environmental Protection Agency, Office of Solid Waste, Washington, DC, 20460.
- U.S. EPA, 1990. *Background Document for EPA's Composite Model for Landfills (EPACML)*. U.S. Environmental Protection Agency, Office of Solid Waste, Washington, D.C. 20460.
- U.S. EPA, 1991. *Standard Default Exposure Factors*, OSWER Directive 9285.6-03, U.S. Environmental Protection Agency Office of Emergency and Remedial Response, Washington, DC.
- U.S. EPA, 1992. *Guidelines for Exposure Assessment*. EPA-600Z-92-001. Office of Research and Development, Risk Assessment Forum, Washington, DC. May.
- U.S. EPA, 1996a. *EPA's Composite Model for Leachate Migration with Transformation Products: (EPACMTP) Technical Background Document*. U.S. Environmental Protection Agency, Office of Solid Waste, Washington, D.C. 20460.
- U.S. EPA, 1996b. *EPA's Composite Model for Leachate Migration with Transformation Products: (EPACMTP) Background Document for Finite Source Methodology for Chemicals with Transformation Products*. U.S. Environmental Protection Agency, Office of Solid Waste, Washington, D.C. 20460.
- U.S. EPA, 1996c. *EPACMTP Sensitivity Analyses*. U.S. Environmental Protection Agency, Washington, D.C. 20460.
- U.S. EPA, 1997. *Analysis of EPA's Industrial Subtitle D Databases used in Groundwater Pathway Analysis of the Hazardous Waste Identification Rule (HWIR)*. U.S. Environmental Protection Agency, Office of Solid Waste, Washington, DC.
- U.S. EPA, 1999. *EPA's Composite Model for Leachate Migration with Transformation Products, Background Document for EPACMTP: Metals Transport in the Subsurface, Volume 1: Methodology*. U.S. Environmental Protection Agency, Office of Solid Waste, Washington, D.C. 20460.
- U.S. EPA, 2001. *Industrial Surface Impoundments in the United States*. U.S. Environmental Protection Agency, Office of Solid Waste, Washington, DC 20460. U.S. EPA 530-R-01-005.
-

U.S. EPA, 2003. *EPA's Composite Model for Leachate Migration with Transformation Products (EPACMTP): Parameters/Data Background Document*. U.S. Environmental Protection Agency, Office of Solid Waste, Washington, D.C. 20460. U.S. EPA 530-R-03-003.

van Genuchten, M.Th., 1980. A closed-form equation for predicting the hydraulic conductivity of unsaturated soils, *Soil Sci. Soc. J.* 44: 892-898.

This page was intentionally left blank.

APPENDIX A

EPACMTP CODE STRUCTURE

This page intentionally left blank.

LIST OF FIGURE

Figure A.1 Flowchart

This page intentionally left blank.

APPENDIX A

EPACMTP CODE STRUCTURE

A flowchart of the general structure of EPACMTP is shown in Figure A.1. In the figure, a self-explanatory logical sequence of the main functions of the code is presented. The flowchart is presented in a general stochastic mode. A deterministic mode is achieved by setting the number of Monte-Carlo realizations to unity. In the deterministic mode, the generation of values of random and derived variables is disabled by the code and the user-defined parameter values are used.

Each simulation may be conducted in either a steady-state or transient mode. In the transient mode, the source terms for landfills and non-landfills are different. The leachate concentration for a non-landfill in a realization is constant for the operation period; however, the leachate concentration for a landfill may diminish with time as the source is allowed to leach out over time.

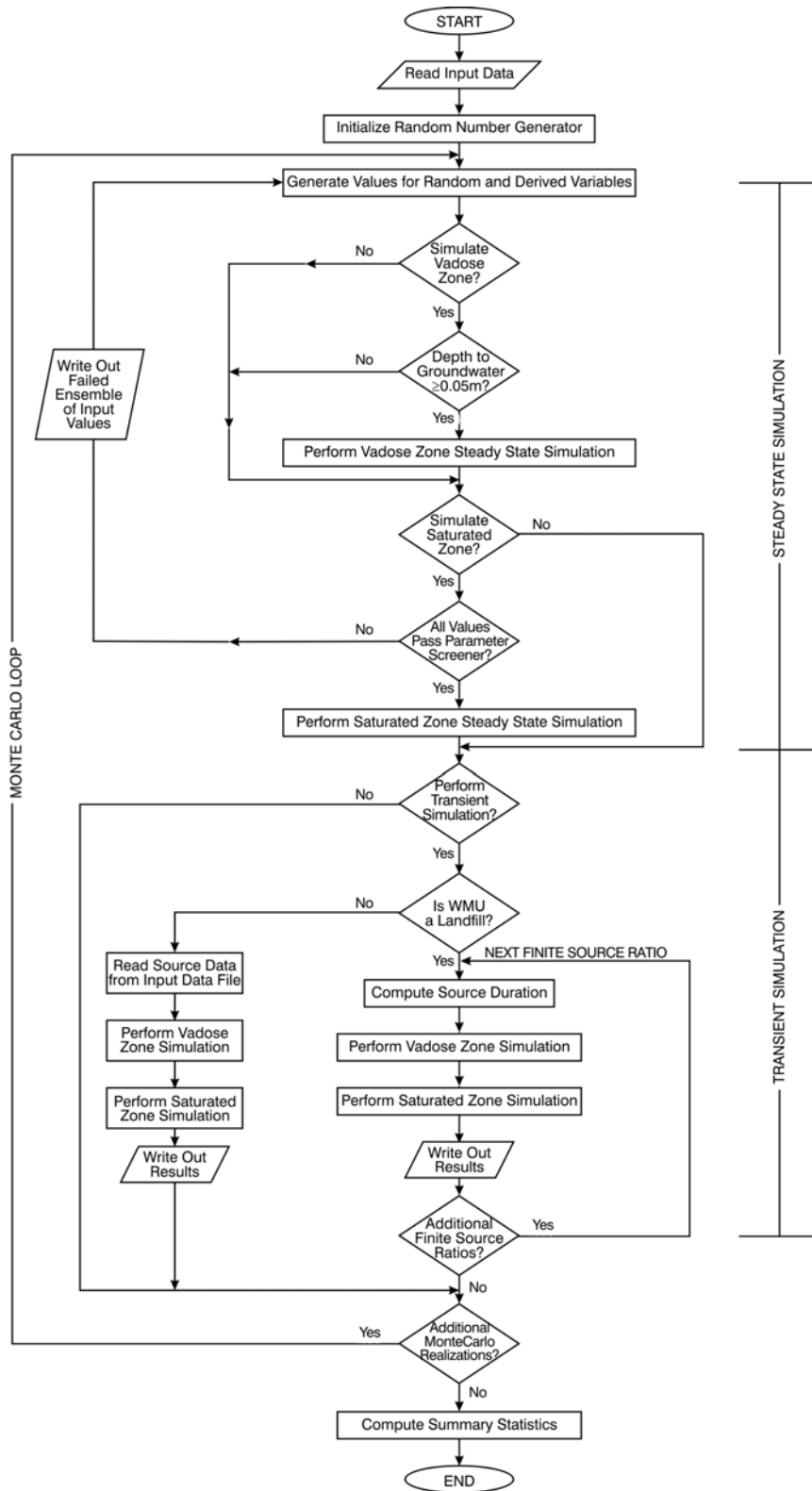


Figure A.1 EPACMTP Code Structure Flowchart

APPENDIX B.1

ANALYTICAL SOLUTION FOR ONE-DIMENSIONAL TRANSPORT OF A STRAIGHT AND BRANCHING CHAIN OF DECAYING SOLUTES

Prepared By:

E. A. Sudicky
Waterloo Centre of Groundwater Research
University of Waterloo
Waterloo, Ontario CANADA N2L 3G1

This page was intentionally left blank.

APPENDIX B.1
**ANALYTICAL SOLUTION FOR ONE-DIMENSIONAL TRANSPORT OF A
STRAIGHT AND BRANCHING CHAIN OF DECAYING SOLUTES**
B.1.1 LIST OF SYMBOLS

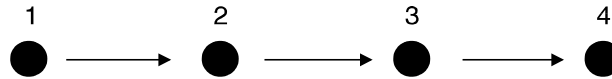
| | | |
|------------------|---|--|
| A | = | Temporary function |
| b_1^- | = | Function defined in Equation B.1.6 |
| b_2^\pm | = | Function defined in Equation B.1.13 |
| b_3^\pm | = | Function defined in Equation B.1.25 |
| c_1 | = | Aqueous concentration of species 1 (mg/L) |
| c_2 | = | Aqueous concentration of species 2 (mg/L) |
| c_3 | = | Aqueous concentration of species 3 (mg/L) |
| c_4 | = | Aqueous concentration of species 4 (mg/L) |
| $\overline{c_1}$ | = | Laplace-transformed aqueous concentration of species 1 (yr-mg/L) |
| $\overline{c_2}$ | = | Laplace-transformed aqueous concentration of species 2 (yr-mg/L) |
| $\overline{c_3}$ | = | Laplace-transformed aqueous concentration of species 3 (yr-mg/L) |
| $\overline{c_4}$ | = | Laplace-transformed aqueous concentration of species 4 (yr-mg/L) |
| c_{p1} | = | Aqueous concentration of species 1 at the source (mg/L) |
| c_{p2} | = | Aqueous concentration of species 2 at the source (mg/L) |
| c_{p3} | = | Aqueous concentration of species 3 at the source (mg/L) |
| c_{p4} | = | Aqueous concentration of species 4 at the source (mg/L) |
| D_x | = | Longitudinal dispersion coefficient (m ² / yr) |
| K_2 | = | Constant defined in Equation B.1.27 |
| L | = | Laplace transformation operator (dimensionless) |
| L^{-1} | = | Inverse Laplace transformation operator (dimensionless) |
| p | = | Laplace transformation parameter (1/ yr) |
| R_1 | = | Retardation factor of species 1 (dimensionless) |
| t | = | Time (yr) |
| v | = | Seepage velocity of ground water (m/ yr) |
| x | = | Spatial coordinate (m) |

Greek Symbols

| | | |
|-------------|---|---|
| β_1 | = | Constant defined in Equation B.1.12b |
| β_2 | = | Constant defined in Equation B.1.24 |
| γ_1 | = | Source decay constant of species 1 (1/yr) |
| γ_2 | = | Source decay constant of species 2 (1/yr) |
| γ_3 | = | Source decay constant of species 3 (1/yr) |
| γ_4 | = | Source decay constant of species 4 (1/yr) |
| λ_1 | = | Decay constant of species 1 (1/yr) |
| λ_2 | = | Decay constant of species 2 (1/yr) |
| λ_3 | = | Decay constant of species 3 (1/yr) |
| λ_4 | = | Decay constant of species 4 (1/yr) |
| ϕ | = | v/ D_x |

- $\omega_1(p)$ = Function of Laplace transform parameter, decay constant, and retardation factor of species 1 defined in Equation B.1.4
 $\omega_2(p)$ = Function of Laplace transform parameter, decay constant, and retardation factor of species 2 defined in Equation B.1.12b
 $\omega_3(p)$ = Function of Laplace transform parameter, decay constant, and retardation factor of species 3 defined in Equation B.1.24
 $\omega_4(p)$ = Function of Laplace transform parameter, decay constant, and retardation factor of species 4

B.1.2 STRAIGHT CHAIN DECAY SOLUTION



Species 1

$$R_1 \frac{\partial c_1}{\partial t} + v \frac{\partial c_1}{\partial x} - D_x \frac{\partial^2 c_1}{\partial x^2} + \lambda_1 R_1 c_1 = 0 \quad (\text{B.1.1})$$

$$c_1(x, 0) = 0 \quad (\text{B.1.2a})$$

$$\frac{\partial c_1}{\partial t}(0, t) + \gamma_1 c_1(0, t) = 0 \quad (\text{B.1.2b})$$

Subject to

$$c_1(0, 0) = c_{p1} \quad (\text{B.1.2c})$$

where c_{p1} is the source concentration

and

$$c_1(\infty, t) = 0 \quad (\text{B.1.2d})$$

Apply the Laplace transform in t defined as:

$$\mathcal{L}[c_1(x, t)] = \bar{c}_1(x, p) = \int_0^{\infty} \bar{c}_1 e^{-pt} dt \quad (\text{B.1.3})$$

to obtain:

$$\frac{d^2 \bar{c}_1}{dx^2} - \frac{v}{D_x} \frac{d\bar{c}_1}{dx} - \frac{1}{D_x} [R_1(p + \lambda_1)] \bar{c}_1 = 0$$

or

$$\frac{d^2 \bar{c}_1}{dx^2} - \phi \frac{d \bar{c}_1}{dx} - \omega_1(\rho) \bar{c}_1 = 0 \quad (\text{B.1.4})$$

$$\bar{c}_1(0, \rho) = c_{p_1} \cdot \frac{1}{\rho + \gamma_1} \quad (\text{B.1.5a})$$

and

$$\bar{c}_1(\infty, \rho) = 0 \quad (\text{B.1.5b})$$

$$\phi = v/D_x$$

The general solution to (B.1.11), subject to (B.1.12a,b) is easily shown to be

$$\bar{c}_1 = \frac{c_{p_1}}{\rho + \gamma_1} \exp(b_1^-(\rho) x) \quad (\text{B.1.6})$$

$$b_1^-(\rho) = \frac{\phi}{2} \left[1 - \left\{ 1 + \frac{4\omega_1(\rho)}{\phi^2} \right\}^{1/2} \right]$$

The task that remains is the inversion of the transforms. Here, we will follow an approach to yield a solution for the Laplace-transformed solution, $\bar{c}_i(x, \rho)$ that will be inverted numerically. We do this because it facilitates the determination of $c_i(x, \rho)$ for $i > 1$. Denoting \mathcal{L}^{-1} as the inverse Laplace transform operator, we can write

$$c_1(x, t) = \mathcal{L}^{-1}[\bar{c}_1(x, \rho)] \quad (\text{B.1.7})$$

This step can be efficiently and accurately performed using the de Hoog et al. (1982) numerical algorithm.

Species 2

$$R_2 \frac{\partial c_2}{\partial t} + v \frac{\partial c_2}{\partial x} - D_x \frac{\partial^2 c_2}{\partial x^2} + \lambda_2 R_2 c_2 - \lambda_1 R_1 c_1 = 0 \quad (\text{B.1.8})$$

$$c_2(x, 0) = 0 \quad (\text{B.1.9a})$$

$$\frac{\partial c_2}{\partial t}(0, t) + \gamma_2 c_2(0, t) - \gamma_1 c_1(0, t) = 0 \quad (\text{B.1.9b})$$

subject to:

$$c_2(0, 0) = c_{p_2} \quad (\text{B.1.9c})$$

$$c_2(\infty, t) = 0 \quad (\text{B.1.9d})$$

Application of the Laplace transform to (B.1.9b) gives:

$$\begin{aligned} \bar{c}_2(0, p) &= \frac{c_{p_2}}{p + \gamma_2} + \frac{\gamma_1}{p + \gamma_2} \bar{c}_1(0, p) \\ &= \frac{c_{p_2}}{p + \gamma_2} + \frac{\gamma_1}{p + \gamma_2} \cdot \frac{c_{p_1}}{p + \gamma_1} \end{aligned} \quad (\text{B.1.10})$$

where (B.1.5a) has been substituted for $\bar{c}_1(0, p)$.

We obtain the following ordinary differential equation describing $\bar{c}_2(x, p)$:

$$\frac{d^2 \bar{c}_2}{dx^2} - \phi \frac{d \bar{c}_2}{dx} - \omega_2(p) \bar{c}_2 = \beta_1 \bar{c}_1 \quad (\text{B.1.11})$$

subject to:

$$\bar{c}_2(0, p) = \frac{c_{p_2}}{p + \gamma_2} + \frac{c_{p_1} \gamma_1}{(p + \gamma_2)(p + \gamma_1)} \quad (\text{B.1.12a})$$

where $\phi = v/D_x$ as before and

$$\bar{c}_2(\infty, p) = 0 \quad (\text{B.1.12b})$$

$$\omega_2(p) = \frac{1}{D_x} [R_2(p + \lambda_2)]$$

$$\beta_1 = -\frac{\lambda_1 R_1}{D_x}$$

The general solution to (B.1.11) is:

$$\begin{aligned} \bar{c}_2 &= A \exp\{b_2^-(p)x\} + B \exp\{b_2^+(p)x\} \\ &+ \frac{\beta_1 c_{p_1}}{p + \gamma_1} \cdot \frac{1}{\omega_1 - \omega_2} \exp\{b_1^-(p)x\} \quad (\text{B.1.13}) \\ &= A \exp\{b_2^- x\} + B \exp\{b_2^+ x\} + \frac{\beta_1}{\omega_1 - \omega_2} \cdot \bar{c}_1(x, p) \\ b_2^\pm &= \frac{\phi}{2} \left[1 \pm \left(\frac{4\omega_2}{\phi^2} \right)^{1/2} \right] \end{aligned}$$

provided that

$$\omega_1 \neq \omega_2 \text{ (i.e., } R_1 \lambda_1 \neq R_2 \lambda_2 \text{)}$$

Requiring that the solution be bounded according to (B.1.12b) implies that $B = 0$. Making use of (B.1.12a) yields:

$$\frac{c_{p_2}}{p + \gamma_2} + \frac{c_{p_1} \gamma_1}{(p + \gamma_1)(p + \gamma_2)} = A + \frac{\beta_1 c_{p_1}}{p + \gamma_1} \cdot \frac{1}{\omega_1 - \omega_2}$$

or

$$A = \frac{c_{p_2}}{(\rho + \gamma_2)} + \frac{c_{p_1} \gamma_1}{(\rho + \gamma_1)(\rho + \gamma_2)} - \frac{c_{p_1} \beta_1}{\rho + \gamma_1} \cdot \frac{1}{\omega_1 - \omega_2} \quad (\text{B.1.14})$$

Thus, substituting for A and B in (B.1,13) gives

$$\begin{aligned} \bar{c}_2 = & \left[\frac{c_{p_2}}{\rho + \gamma_2} + \frac{c_{p_1} \gamma_1}{(\rho + \gamma_2)(\rho + \gamma_1)} \right] \exp b_2^- (\rho, x), \\ & + \frac{c_{p_1}}{\rho + \gamma_1} \cdot \beta_1 \cdot \frac{1}{\omega_1 - \omega_2} [\exp b_1^- (\rho) x - \exp b_2^- (\rho) x] \end{aligned} \quad (\text{B.1.15})$$

or

$$\begin{aligned} \bar{c}_2 = & \left[\frac{c_{p_2}}{\rho + \gamma_2} + \left(\frac{\gamma_1}{\rho + \gamma_2} - \frac{\beta_1}{\omega_1 - \omega_2} \right) \bar{c}_1 (0, \rho) \right] \exp b_2^- x \\ & + \frac{\beta_1}{\omega_1 - \omega_2} \bar{c}_1 (x, \rho) \end{aligned} \quad (\text{B.1.16})$$

provided that

$$\omega_1 \neq \omega_2 \text{ (i.e., } R_1 \lambda_1 \neq R_2 \lambda_2 \text{)}$$

It can be seen that the first term on the right-hand side of (B.1.12a) involving c_{p_2} is of the same form as (B.1.6) for c_1 . If we have the special case that $\omega_1 = \omega_2$ (i.e., $R_1 \lambda_1 = R_2 \lambda_2$), then a modified general solution must be used which yields:

$$\begin{aligned} \bar{c}_2 = & \left[\frac{c_{p_2}}{\rho + \gamma_2} + \frac{c_{p_1} \gamma_1}{(\rho + \gamma_2)(\rho + \gamma_1)} \right] \exp b_2^- (\rho) x \\ & - \frac{x c_{p_1} \beta_1}{(\rho + \gamma_1)(b_2^+ - b_2^-)} \exp b_2^- (\rho) x, \end{aligned} \quad (\text{B.1.17})$$

for the case $\omega_1 = \omega_2$

or

$$\bar{c}_2 = \left[\frac{c_{p_2}}{\rho + \gamma_2} + \frac{\gamma_1}{\rho + \gamma_2} \bar{c}_1(0, \rho) \right] \exp(b_2^- x) - \frac{\beta_1 x}{b_2^+ - b_2^-} \bar{c}_1(x, \rho) \quad (\text{B.1.18})$$

Finally, we can write:

$$c_2(x, t) = \mathcal{L}^{-1} [\bar{c}_2(x, \rho)] \quad (\text{B.1.19})$$

where either (B.1.16) or (B.1.18) is substituted.

Species 3

$$R_3 \frac{\partial c_3}{\partial t} + v \frac{\partial c_3}{\partial x} - D_x \frac{\partial^2 c_3}{\partial x^2} + \lambda_3 R_3 c_3 - \lambda_2 R_2 c_2 = 0 \quad (\text{B.1.20})$$

$$c_3(x, 0) = 0 \quad (\text{B.1.21a})$$

$$\frac{\partial c_3}{\partial t}(0, t) + \gamma_3 c_3(0, t) - \gamma_2 c_2(0, t) = 0 \quad (\text{B.1.21b})$$

Application of the Laplace transform \mathcal{L} to the system (B.1.20) and (B.1.21) leads to

$$\frac{d^2 \bar{c}_3}{dx^2} - \phi \frac{d\bar{c}_3}{dx} - \omega_3(\rho) \bar{c}_3 = \beta_2 \bar{c}_2 \quad (\text{B.1.22})$$

or

$$(\rho + \gamma_3) \bar{c}_3(0, \rho) = c_{p_3} + \gamma_2 \bar{c}_2(0, \rho) \quad (\text{B.1.23})$$

$$\bar{c}_3(0, \rho) = \frac{c_{p_3}}{\rho + \gamma_3} + \frac{\gamma_2}{\rho + \gamma_3} \left(\frac{c_{p_2}}{\rho + \gamma_2} + \frac{c_{p_1} \gamma_1}{(\rho + \gamma_2)(\rho + \gamma_1)} \right) \quad (\text{B.1.24a})$$

$$\bar{c}_3(\infty, \rho) = 0 \quad (\text{B.1.24b})$$

$$\omega_3(\rho) = \frac{1}{D_x} [R_3(\rho + \lambda_3)]$$

$$\beta_2 = -\frac{\lambda_2 R_2}{D_x}$$

The general solution of (B.1.22) after substituting for \bar{c} using (B.1.16) is:

$$\begin{aligned} \bar{c}_3 = & A \exp b_3^-(\rho) x + B \exp b_3^+(\rho) x \\ & + \frac{\beta_2}{\omega_2 - \omega_3} \left[\frac{c_{p_2}}{\rho + \gamma_2} + \left(\frac{\gamma_1}{\rho + \gamma_2} - \frac{\beta_1}{\omega_1 - \omega_2} \right) \bar{c}_1(\rho) \right] \exp b_2^-(\rho) x \\ & + \frac{\beta_1 \beta_2}{(\omega_1 - \omega_2)(\omega_1 - \omega_3)} \bar{c}_1(x, \rho) \end{aligned} \quad (\text{B.1.25})$$

provided that $\omega_2 \neq \omega_3$, $\omega_1 \neq \omega_2$, $\omega_1 \neq \omega_3$

The parameters b_3^- and b_3^+ are defined analogously to those for species 1 or 2 defined earlier except that λ_3 and R_3 are substituted. Boundary condition (B.1.24b) gives $B = 0$ and (B.1.24a) yields:

$$\begin{aligned} A = & \frac{c_{p_3}}{\rho + \gamma_3} + \frac{\gamma_2}{\rho + \gamma_3} \bar{c}_2(0, \rho) - \frac{\beta_2}{\omega_2 - \omega_3} \left[\frac{c_{p_2}}{\rho + \gamma_2} + \left(\frac{\gamma_1}{\rho + \gamma_2} - \frac{\beta_1}{\omega_1 - \omega_2} \right) \bar{c}_1(0, \rho) \right] \\ & - \frac{\beta_1 \beta_2}{(\omega_1 - \omega_2)(\omega_1 - \omega_3)} \bar{c}_1(0, \rho) \end{aligned} \quad (\text{B.1.26})$$

Now, substitute (B.1.26) into (B.1.25) to get:

$$\begin{aligned} \bar{c}_3 = & \left[\frac{c_{p_3}}{\rho + \gamma_3} + \frac{\gamma_2}{\rho + \gamma_3} \bar{c}_2(0, \rho) - \frac{\beta_2}{\omega_2 - \omega_3} \left(\frac{c_{p_2}}{\rho + \gamma_2} + \left\{ \frac{\gamma_1}{\rho + \gamma_2} - \frac{\beta_1}{\omega_1 - \omega_2} \right\} \bar{c}_1(0, \rho) \right) \right. \\ & \left. - \frac{\beta_1 \beta_2}{(\omega_1 - \omega_2)(\omega_1 - \omega_3)} \bar{c}_1(0, \rho) \right] \exp b_3^- x \\ & + \frac{\beta_2}{\omega_2 - \omega_3} \left[\frac{c_{p_2} K_2}{\rho + \gamma_2} + \left(\frac{\gamma_1}{\rho + \gamma_2} - \frac{\beta_1}{\omega_1 - \omega_2} \right) \bar{c}_1(0, \rho) \right] \exp b_2^- x \\ & + \frac{\beta_1 \beta_2}{(\omega_1 - \omega_2)(\omega_1 - \omega_3)} \bar{c}_1(x, \rho) \end{aligned} \quad (\text{B.1.27})$$

$\omega_2 \neq \omega_3, \omega_1 \neq \omega_2, \omega_1 \neq \omega_3$

If on the other hand $\omega_2 = \omega_3$ (i.e., $R_2 \lambda_2 = R_3 \lambda_3$) but $\omega_2 \neq \omega_1$ then we have:

$$\begin{aligned} \bar{c}_3 &= A \exp(b_3^- x) + B \exp(b_3^- x) \\ &- \beta_2 \left[\frac{c_{p_2}}{\rho + \gamma_2} + \left\{ \frac{\gamma_1}{\rho + \gamma_2} - \frac{\beta_1}{\omega_1 - \omega_2} \right\} \bar{c}_1(0, \rho) \right] \left[\frac{1}{b_3^+ - b_3^-} + x \right] \frac{1}{b_3^+ - b_3^-} \exp(b_3^- x) \\ &+ \frac{\beta_1 \beta_2}{(\omega_3 - \omega_1)(\omega_2 - \omega_1)} \bar{c}_1(x, \rho) \end{aligned} \quad (B.1.28)$$

$$\omega_2 = \omega_3 \quad \omega_2 \neq \omega_1 \quad \omega_3 \neq \omega_1$$

Application of the boundary conditions (B.1.23) (or B.1.24a) and (B.1.24b) gives B = 0 and

$$\begin{aligned} A &= \frac{c_{p_3}}{\rho + \gamma_3} + \frac{\gamma_2}{\rho + \gamma_3} \bar{c}_2(0, \rho) + \beta_2 \left[\frac{c_{p_2} \kappa_2}{\rho + \gamma_2} + \left\{ \frac{\gamma_1}{\rho + \gamma_2} - \frac{\beta_1}{\omega_1 - \omega_2} \right\} \bar{c}_1(0, \rho) \right. \\ &\left. \cdot \frac{1}{(b_3^+ - b_3^-)^2} \right] - \frac{\beta_1 \beta_2}{(\omega_3 - \omega_1)(\omega_2 - \omega_1)} \bar{c}_1(0, \rho) \end{aligned} \quad (B.1.29)$$

Substituting (B.1.28) into (B.1.29) for A and letting B = 0 gives:

$$\begin{aligned} \bar{c}_3 &= \left[\frac{c_{p_3}}{\rho + \gamma_3} + \frac{\gamma_2}{\rho + \gamma_3} \bar{c}_2(0, \rho) - \frac{\beta_1 \beta_2}{(\omega_3 - \omega_1)(\omega_2 - \omega_1)} \bar{c}_1(0, \rho) \right] \exp(b_3^- x) \\ &- \frac{\beta_2 x}{b_3^+ - b_3^-} \left[\frac{c_{p_2}}{\rho + \gamma_2} + \left\{ \frac{\gamma_1}{\rho + \gamma_2} - \frac{\beta_1}{\omega_1 - \omega_2} \right\} \bar{c}_1(0, \rho) \right] \exp(b_3^- x) \\ &+ \frac{\beta_1 \beta_2}{(\omega_3 - \omega_1)(\omega_2 - \omega_1)} \bar{c}_1(x, \rho) \end{aligned} \quad (B.1.30a)$$

or

$$\begin{aligned} \bar{c}_3 &= \left[\frac{c_{p_3}}{\rho + \gamma_3} + \frac{\gamma_2}{\rho + \gamma_3} \bar{c}_2(0, \rho) - \frac{\beta_1 \beta_2}{(\omega_3 - \omega_1)(\omega_2 - \omega_1)} \bar{c}_1(0, \rho) \right] \exp(b_3^- x) \\ &- \frac{\beta_2 x}{b_3^+ - b_3^-} \left[\bar{c}_2(x, \rho) - \frac{\beta_1}{\omega_1 - \omega_2} \bar{c}_1(x, \rho) \right] \\ &+ \frac{\beta_1 \beta_2}{(\omega_3 - \omega_1)(\omega_2 - \omega_1)} \bar{c}_1(x, \rho) \end{aligned} \quad (B.1.30b)$$

where

$$\omega_3 = \omega_2, \omega_2 \neq \omega_1, \omega_3 \neq \omega_1$$

where (B.1.16a) is used to express the second term in (B.1.30a). If we have $\omega_3 \neq \omega_1$ but $\omega_2 = \omega_1$, then using (B.1.18a) for \bar{c} in (B.1.22) leads to:

$$\begin{aligned} \bar{c}_3 &= A \exp(b_3^- x) + B \exp(b_3^+ x) + \frac{\beta_2}{\omega_3 - \omega_3} \left[\frac{c_{p_2}}{p + \gamma_2} + \frac{\gamma_1}{p + \gamma_2} \bar{c}_1(0, p) \right] \exp(b_2^- x) \\ &\quad - \frac{\beta_1 \beta_2}{\omega_1 - \omega_3} \cdot \frac{1}{b_2^+ - b_2^-} \left[x - \frac{1}{b_2^- - b_3^+} \right] \bar{c}_1(x, p) \\ &= A \exp(b_3^- x) + B \exp(b_3^+ x) \\ &\quad + \frac{\beta_2}{\omega_2 - \omega_3} \left[\bar{c}_2(x, p) + \frac{\beta_1 \bar{c}_1(x, p)}{(b_2^+ - b_2^-)(b_2^- - b_3^+)} \right] \\ &\quad \omega_2 = \omega_1, \omega_3 \neq \omega_1, \omega_2 \neq \omega_3 \end{aligned} \tag{B.1.31}$$

Application of the boundary conditions yields $B = 0$ and

$$\begin{aligned} A &= \frac{c_{p_3}}{p + \gamma_3} + \frac{\gamma_2}{p + \gamma_3} \bar{c}_2(0, p) - \frac{\beta_2}{\omega_2 - \omega_3} \\ &\quad \times \left[\bar{c}_2(0, p) + \frac{\beta_1 \bar{c}_1(0, p)}{(b_2^+ - b_2^-)(b_2^- - b_3^+)} \right] \end{aligned} \tag{B.1.32}$$

Using (B.1.32) in (B.1.31) gives:

$$\begin{aligned} \bar{c}_3 &= \left[\frac{c_{p_3}}{p + \gamma_3} + \left(\frac{\gamma_2}{p + \gamma_3} - \frac{\beta_2}{\omega_2 - \omega_3} \right) \bar{c}_2(0, p) \right. \\ &\quad \left. - \frac{\beta_2 \beta_1}{\omega_2 - \omega_3} \cdot \frac{1}{(b_2^+ - b_2^-)(b_2^- - b_3^+)} \bar{c}_1(0, p) \right] \exp(b_3^- x) \\ &\quad + \frac{\beta_2}{\omega_2 - \omega_3} \left[\bar{c}_2(x, p) + \frac{\beta_1 \bar{c}_1(x, p)}{(b_2^+ - b_2^-)(b_2^- - b_3^+)} \right] \end{aligned} \tag{B.1.33}$$

where

$$\omega_2 = \omega_1, \omega_3 \neq \omega_1, \omega_2 \neq \omega_3$$

Finally, if $\omega_1 = \omega_2 = \omega_3$:

$$\begin{aligned} \bar{c}_3 &= A \exp(b_3^- x) + B \exp(b_3^+ x) \\ &- \frac{\beta_2}{b_3^+ - b_3^-} \left[\frac{1}{b_3^+ - b_3^-} + x \right] \left[\frac{c_{p_2}}{\rho + \gamma_2} + \frac{\gamma_1}{\rho + \gamma_2} \bar{c}_1(0, \rho) \right] \exp(b_3^- x) \\ &- \frac{\beta_2 \beta_1}{(b_3^+ - b_3^-)^2} \left[\frac{1}{b_3^- - b_3^+} \left(x - \frac{1}{b_3^- - b_3^+} \right) - \frac{x^2}{2} \right] \bar{c}_1(x, \rho) \end{aligned} \quad (\text{B.1.34})$$

Now, making use of the boundary conditions for \bar{c} gives $B = 0$ and

$$\begin{aligned} A &= \frac{c_{p_3}}{\rho + \gamma_3} + \frac{\gamma_2}{\rho + \gamma_3} \bar{c}_2(0, \rho) + \frac{\beta_2}{(b_3^+ - b_3^-)^2} \left[\frac{c_{p_2}}{\rho + \gamma_2} + \frac{\gamma_1}{\rho + \gamma_2} \bar{c}_1(0, \rho) \right] \\ &- \frac{\beta_2 \beta_1}{(b_3^+ - b_3^-)^2} \frac{1}{(b_3^- - b_3^+)^2} \bar{c}_1(0, \rho) \end{aligned} \quad (\text{B.1.35})$$

Finally, substituting for A and B into (B.1.45) gives

$$\begin{aligned} \bar{c}_3 &= \left[\frac{c_{p_3}}{\rho + \gamma_3} + \frac{\gamma_2}{\rho + \gamma_3} \bar{c}_2(0, \rho) \right. \\ &+ \left. \frac{\beta_2}{(b_3^+ - b_3^-)^2} \left\{ \frac{c_{p_2}}{\rho + \gamma_2} + \left(\frac{\gamma_1}{\rho + \gamma_2} - \frac{\beta_1}{(b_3^+ - b_3^-)^2} \right) \bar{c}_1(0, \rho) \right\} \right] \exp(b_3^- x) \\ &- \frac{\beta_2}{b_3^+ - b_3^-} \left[\frac{1}{b_3^+ - b_3^-} + x \right] \left[\frac{c_{p_2}}{\rho + \gamma_2} + \frac{\gamma_1}{\rho + \gamma_2} \bar{c}_2(0, \rho) \right] \exp(b_3^- x) \\ &- \frac{\beta_2 \beta_1}{(b_3^+ - b_3^-)^2} \left[\frac{1}{b_3^- - b_3^+} \left(x - \frac{1}{b_3^- - b_3^+} \right) - \frac{x^2}{2} \right] \bar{c}_1(x, \rho) \end{aligned} \quad (\text{B.1.36})$$

or, upon simplifying (B.1.36):

$$\begin{aligned}
\bar{c}_3 = & \left[\frac{c_{p_3}}{\rho + \gamma_3} + \frac{\gamma_2}{\rho + \gamma_3} \bar{c}_2(0, \rho) - \frac{\beta_2 \beta_1}{(b_3^+ - b_3^-)^4} \bar{c}_1(0, \rho) \right] \exp(b_3^- x) \\
& - \frac{\beta_2}{b_3^+ - b_3^-} \left[x \left(\frac{c_{p_2}}{\rho + \gamma_2} + \frac{\gamma_1}{\rho + \gamma_2} \bar{c}_1(0, \rho) \right) \right] \exp(b_3^- x) \\
& - \frac{\beta_2 \beta_1}{(b_3^+ - b_3^-)^2} \left[\frac{1}{b_3^- - b_3^+} \left(x - \frac{1}{b_3^- - b_3^+} \right) - \frac{x^2}{2} \right] \bar{c}_1(x, \rho)
\end{aligned} \tag{B.1.37}$$

for the case

$$\omega_1 = \omega_2 = \omega_3$$

The inverse transform of \bar{c} is given by substituting either (B.1.27), (B.1.30b), (B.1.33) or (B.1.37) into:

$$c_3(x, t) = \mathcal{L}^{-1} [\bar{c}_3(x, \rho)] \tag{B.1.38}$$

Species 4

$$R_4 \frac{\partial c_4}{\partial t} + v \frac{\partial c_4}{\partial x} - D_x \frac{\partial^2 c_4}{\partial x^2} + \lambda_4 R_4 c_4 - \lambda_3 R_3 c_3 = 0 \tag{B.1.39}$$

subject to:

$$c_4(x, 0) = 0 \tag{B.1.40a}$$

$$\frac{\partial c_4}{\partial t}(0, t) + \gamma_4 c_4(0, t) - \gamma_3 c_3(0, t) = 0 \tag{B.1.40b}$$

$$c_4(0, t) = c_{p_4} \tag{B.1.40c}$$

$$c_4(\infty, t) = 0 \tag{B.1.40d}$$

Application of the Laplace transformation \mathcal{L} to the system (B.1.39) and (B.1.40) yields:

$$\frac{d^2 \bar{c}_4}{dx^2} - \phi \frac{d\bar{c}_4}{dx} - \omega_4(\rho) \bar{c}_4 = \beta_3 \bar{c}_3 \tag{B.1.41}$$

$$\bar{c}_4(0, p) = \frac{c_{p4}}{p + \gamma_4} + \frac{\gamma_3}{p + \gamma_4} \bar{c}_3(0, p) \quad (\text{B.1.41a})$$

$$\bar{c}_4(\infty, p) = 0 \quad (\text{B.1.41b})$$

where:

$$\omega_4(p) = \frac{1}{D_x} [R_4(p + \lambda_4)]$$

$$\beta_3 = - \frac{\lambda_3 R_3}{D_x}$$

Upon substituting (B.1.27) for \bar{c}_3 in (B.1.41) the general solution to (B.1.41) is:

$$\begin{aligned} \bar{c}_4 &= A \exp(b_4^- x) + B \exp(b_4^+ x) \\ &+ \frac{\beta_3}{\omega_3 - \omega_4} \left[\frac{c_{p3}}{p + \gamma_3} + \frac{\gamma_2}{p + \gamma_3} \bar{c}_2(0, p) - \frac{\beta_2}{\omega_2 - \omega_3} \left(\frac{c_{p2}}{p + \gamma_2} + \left\{ \frac{\gamma_1}{p + \gamma_2} - \frac{\beta_1}{\omega_1 - \omega_2} \right\} \right. \right. \\ &\quad \left. \left. \times \bar{c}_1(0, p) - \frac{\beta_1 \beta_2}{(\omega_1 - \omega_2)(\omega_1 - \omega_3)} \bar{c}_1(0, p) \right] \exp(b_3^- x) \quad (\text{B.1.42}) \\ &+ \frac{\beta_2 \beta_3}{(\omega_2 - \omega_3)(\omega_2 - \omega_4)} \left[\frac{c_{p2}}{p + \gamma_2} + \left\{ \frac{\gamma_1}{p + \gamma_2} - \frac{\beta_1}{\omega_1 - \omega_2} \right\} \bar{c}_1(0, \alpha, n, p) \right] \exp(b_2^- x) \\ &+ \frac{\beta_1 \beta_2 \beta_3}{(\omega_1 - \omega_2)(\omega_1 - \omega_3)(\omega_1 - \omega_4)} \bar{c}_1(x, p) \end{aligned}$$

for the case

$$\omega_1 \neq \omega_2 \neq \omega_3 \neq \omega_4$$

Boundary condition (B.1.41b) gives $B = 0$ and (B.1.41a) yields:

$$\begin{aligned}
A = & \frac{c_{p_4}}{\rho + \gamma_4} + \frac{\gamma_3}{\rho + \gamma_4} \bar{c}_3(0, \rho) \\
- & \frac{\beta_3}{\omega_3 - \omega_4} \left[\frac{c_{p_3}}{\rho + \gamma_3} + \frac{\gamma_2}{\rho + \gamma_3} \bar{c}_2(0, \rho) - \frac{\beta_2}{\omega_2 - \omega_3} \left(\frac{c_{p_2}}{\rho + \gamma_2} + \left\{ \frac{\gamma_1}{\rho + \gamma_2} - \frac{\beta_1}{\omega_1 - \omega_2} \right\} \right. \right. \\
& \left. \left. \times \bar{c}_1(0, \rho) \right) - \frac{\beta_1 \beta_2}{(\omega_1 - \omega_2)(\omega_1 - \omega_3)} \bar{c}_1(0, \rho) \right] \\
- & \frac{\beta_2 \beta_3}{(\omega_2 - \omega_3)(\omega_2 - \omega_4)} \left[\frac{c_{p_2}}{\rho + \gamma_2} + \left\{ \frac{\gamma_1}{\rho + \gamma_2} - \frac{\beta_1}{\omega_1 - \omega_2} \right\} \bar{c}_1(0, \rho) \right] \\
- & \frac{\beta_1 \beta_2 \beta_3}{(\omega_1 - \omega_2)(\omega_1 - \omega_3)(\omega_1 - \omega_4)} \bar{c}_1(0, \rho)
\end{aligned} \tag{B.1.43}$$

Substituting (B.1.43) for A into (B.1.42) and letting B = 0 yields the final solution for \bar{c} for the case $\omega_1 \neq \omega_2 \neq \omega_3 \neq \omega_4$. Due to the large number of combinations of special case solutions for $\omega_4 = \omega_3$, etc., these solutions will not be derived here. Finally, using the inversion formula, we can write

$$c_4(x, t) = \mathcal{L}^{-1} \{ \bar{c}_4(x, \rho) \} \tag{B.1.44}$$

Steady-state Solutions

For any species c_i , the steady-state solution follows from the final-value theorem for the Laplace transformation given by:

$$c_i(x) = \lim_{\rho \rightarrow 0} \rho \bar{c}_i(x, \rho) \tag{B.1.45}$$

Note that the contribution of a decaying boundary condition at $x = 0$ for any of the parents leading to c_i is zero, including the contribution of c_{p_i} if it decays also. The limits appearing in (B.1.45) are easily written down.

REFERENCES

de Hoog, F.R., J.H. Knight and A.N. Stokes, An improved method for numerical inversion of Laplace transforms, SIAM J. Sci. Stat. Comput., 3(3), 357-366, 1982.

Churchill, R.V., Operational Mathematics, McGraw-Hill, New York, 1972.

APPENDIX B.2

ANALYTICAL SOLUTION FOR ONE-DIMENSIONAL TRANSPORT OF A SOLUTE WITH NONLINEAR SORPTION

Prepared By:

E. A. Sudicky
Waterloo Centre of Groundwater Research
University of Waterloo
Waterloo, Ontario CANADA N2L 3G1

This page was intentionally left blank.

APPENDIX B.2
ANALYTICAL SOLUTION FOR ONE-DIMENSIONAL TRANSPORT OF A SOLUTE WITH NONLINEAR SORPTION
B.2.1 LIST OF SYMBOLS

| | | |
|----------|---|--|
| C_d | = | Dissolved phase concentration (mg/L) |
| C_i | = | Initial dissolved phase concentration (mg/L) |
| C_o | = | Dissolved phase concentration at boundary (mg/L) |
| C_s | = | Sorbed phase concentration (mg/Kg) |
| D | = | Matrix of dispersion coefficient (m^2/yr) |
| D_u | = | Longitudinal dispersion coefficient in the unsaturated zone (m^2/yr) |
| $f()$ | = | Function |
| $f'()$ | = | Derivative of f with respect to C_d |
| K_d | = | Equilibrium partitioning coefficient (L/Kg) |
| k_1 | = | Freundlich equilibrium partitioning coefficient (L/Kg) ^{1/n} |
| L | = | Domain length (m) |
| M_c | = | Mass flux (mg/L- m/yr) |
| t | = | Time (yr) |
| t_s | = | Starting time of front tracking (yr) |
| t_p | = | Time period during which a constant source is applied at the boundary (yr) |
| V | = | Vector of seepage velocity of ground water (m/ yr) |
| V_u | = | Seepage velocity of ground water in the unsaturated zone (m/ yr) |
| z | = | Spatial coordinate (m) |
| z_{Cd} | = | Front location of concentration C_d (m) |
| z_f | = | Sharp front or sharp tail location (m) |
| z_s | = | Starting front location (m) |

Greek Symbols

| | | |
|-----------------|---|---|
| η | = | Freundlich exponent for equilibrium partitioning coefficient(dimensionless) |
| θ | = | Moisture content (dimensionless) |
| ρ_b | = | Bulk density of soil (g/cm^3) |
| ΔC_d | = | Increment of C_d (mg/L) |
| $\Delta f(C_d)$ | = | Increment of $f(C_d)$ (mg/L) |
| Δt | = | Increment of time (yr) |
| Δz | = | Increment of distance z (m) |

B.2.2 ANALYTICAL SOLUTION

The general advection-dispersion solute transport equation can be written as:

$$\frac{\partial C_d}{\partial t} + \frac{\rho_b}{\theta} \frac{\partial C_s}{\partial t} + \mathbf{V} \cdot \nabla C_d = D \nabla^2 C_d \quad (\text{B.2.2.1})$$

where C_d is the dissolved phase concentration (mg/L), C_s is the sorbed phase concentration (mg/kg), ρ_b is the bulk density of soil, θ is the moisture content, \mathbf{V} is the pore-water velocity vector, and D is the dispersion coefficient. Assuming equilibrium and reversible sorption, the sorbed phase and dissolved phase concentrations are related through:

$$C_s = K_d C_d \quad (\text{B.2.2.2})$$

where K_d is the equilibrium partitioning coefficient (L/kg). Note that when K_d is a function of C_d , as in the metals case, the governing equation (B.2.2.1) becomes nonlinear.

EPACMTP treats flow and transport in the unsaturated zone as one-dimensional in the vertical direction. Then the spatial derivatives in (B.2.2.1) reduce to simpler forms, resulting in the following equation:

$$\frac{\partial C_d}{\partial t} + \frac{\rho_b}{\theta} \frac{\partial C_s}{\partial t} + V_u \frac{\partial C_d}{\partial z} = D_u \frac{\partial^2 C_d}{\partial z^2} \quad (\text{B.2.2.3})$$

where z increases downward from the soil surface, and the subscript u indicates unsaturated zone properties.

The governing equation is supplemented by initial and boundary conditions. Initially, the unsaturated-zone is assumed to be free of contaminant:

$$C_d(z, 0) = 0 \quad (\text{B.2.2.4})$$

The following boundary conditions are used at the source ($z=0$) and the water table ($z=L$):

$$\dot{M}_c = \theta V_u C_d - \theta D_u \frac{\partial C_d}{\partial z} \quad , z = 0 \quad (\text{B.2.2.5})$$

$$\frac{\partial C_d}{\partial z} = 0 \quad , z = L \quad (\text{B.2.2.6})$$

where \dot{M}_c is the specified contaminant mass flux at the source.

An exact analytical solution to (B.2.2.3) in general form is intractable because of the nonlinear adsorption term. In order to solve the problem, some approximations must be resorted to. If the solute transport is advection-dominated, we may ignore the dispersion term in (B.2.2.3). In that case, the transport equation (B.2.2.3) can be written as

$$V_u \frac{\partial C_d}{\partial z} + [1 + f'(C_d)] \frac{\partial C_d}{\partial t} = 0 \quad (\text{B.2.2.10})$$

$$f'(C_d) = \frac{df(C_d)}{dC_d} \quad (\text{B.2.2.11})$$

and $f(C_d)$ is a dimensionless nonlinear function representing the adsorption isotherm.

Alternatively, for nonlinear metals transport, the adsorption function $f(C_d)$ can be defined using tabulated isotherm data, generated by the MINTEQA2 speciation model. The initial and boundary conditions for the one-dimensional transport problem may be expressed as

Initial condition:

$$C_d(z, t = 0) = C_i \quad (z > 0) \quad (\text{B.2.2.12})$$

Boundary conditions:

$$C_d(z = 0, t \leq t_p) = C_o \quad (C_o \neq C_i) \quad (\text{B.2.2.13})$$

and

$$C_d(z = 0, t > t_p) = 0 \quad (\text{B.2.2.14})$$

where C_i is the constant initial concentration of solute; C_o is a constant source concentration of the time period of $t \leq t_p$; and t_p is the time period during which a constant concentration source is applied at the surface boundary.

Equation (B.2.2.10) is a quasi-linear first-order differential equation, which describes traveling of different concentrations at different characteristic speeds given by

$$\left(\frac{dz}{dt} \right)_c = \frac{V_u}{1 + f'(C_d)} \quad (\text{B.2.2.15})$$

The complete solution of concentration can then be obtained by integration of equation (B.2.2.15), subject to the initial and boundary conditions.

Equation (B.2.2.15) indicates that the traveling velocity for a particular concentration, C_d , is constant. Upon integration for a particular concentration, C_d , the penetration position or depth, z_c , of the concentration will be obtained at any time t ($t > t_s$) from

$$\int_{z_s}^{z_c} dz = \int_{t_s}^t \frac{V_u dt}{1 + f'(C_d)}$$

which yields

$$z_{C_d} = \frac{V_u(t - t_s)}{1 + f'(C_d)} + z_s \quad (\text{B.2.2.16})$$

if C_d starts traveling from $z = z_s$ at $t = t_s$.

The above analytical solution is a direct application of chromatographic transport theory to the solute transport problem (Hirasaki, 1981; and Fredrick, 1981). As in the Buckley-Leverett theory for multiphase flow, a shock front may form during the concentration propagation. The occurrence of the shock concentration front depends on the initial and boundary conditions.

In order to use the above frontal advance solution to describe solute transport with nonlinear adsorption effects, one has to recognize the conditions under which a shock front will develop, otherwise, a non-physical solution may be proposed. There are two common situations for the occurrence of the shock front. If the initial concentration is constant, C_i , and a step increase of the concentration, C_o , is injected into the fluid at $z=0$, a shock front will develop under the following two conditions

Situation 1:

$$\left. \begin{array}{l} C_o > C_i \\ \frac{df(C_d)}{dC_d} > 0 \\ \frac{d^2 f(C_d)}{dC_d^2} < 0 \end{array} \right\} \quad (\text{B.2.2.17})$$

Situation 2:

$$\left. \begin{aligned} C_o &< C_i \\ \frac{df(C_d)}{dC_d} &> 0 \\ \frac{d^2 f(C_d)}{dC_d^2} &> 0 \end{aligned} \right\} \quad (\text{B.2.2.18})$$

The two conditions of (B.2.2.17) and (B.2.2.18) can be better understood physically using the Freundlich adsorption isotherm as an example. For a Freundlich isotherm, we have

$$f(C_d) = \frac{\rho_b}{\theta} k_1 C_d^\eta \quad (\text{B.2.2.19})$$

where the coefficient k_1 ($L^{3\eta}/M^\eta$) and η (dimensionless) are nonlinear Freundlich parameters. When the exponent $\eta = 1$, the Freundlich isotherm becomes linear, and the parameter k_1 is then the same as the partition coefficient K_d for a linear adsorption case.

For a case of continuous release of solute with concentration C_o , and constant initial concentration, C_i , in the system, we have

$$\left. \begin{aligned} C_o &> C_i \\ \frac{df(C_d)}{dC_d} &= \frac{\rho_b k_1}{\theta} \eta C_d^{\eta-1} > 0 \\ \frac{d^2 f(C_d)}{dC_d^2} &= \frac{\rho_b k_1}{\theta} \eta (\eta - 1) C_d^{\eta-2} < 0 \\ &\text{for } (0 < \eta < 1) \end{aligned} \right\} \quad (\text{B.2.2.20})$$

When the condition of (B.2.2.17) is satisfied, a shock front for the solute plume will develop during the transport process. Using equation (B.2.2.15), the traveling velocity for a particular concentration, C_d , is

$$\left(\frac{dz}{dt} \right)_{C_d} = \frac{V_u}{1 + \frac{\rho_b k_1}{\theta} \eta C_d^{\eta-1}} \quad \text{for } (0 < \eta < 1) \quad (\text{B.2.2.21})$$

For $C_d \rightarrow 0$, $C_d^{\eta-1} \rightarrow \infty$, and

$$\left(\frac{dz}{dt} \right)_{C_d} \rightarrow 0 \quad (\text{B.2.2.22})$$

For $C_d \rightarrow \infty$, $C_d^{\eta-1} \rightarrow 0$,

$$\left(\frac{dz}{dt} \right)_{C_d} \rightarrow V_u \quad (\text{B.2.2.23})$$

Therefore, the higher the concentration is, the higher the velocity. Physically, this is impossible across the concentration front because of the adsorption effect, and a sharp front will form for the concentration plume. In this case, the velocity of the shock front is described by

$$\left(\frac{\Delta z}{\Delta t} \right)_{\Delta C_d} = \frac{V_u}{1 + \frac{\Delta f(C_d)}{\Delta C_d}} \quad (\text{B.2.2.24})$$

where $\Delta C_d = C_o - C_i$, represents the concentration difference across the front. The penetration depth of the sharp front at time t is given by

$$z_f = \frac{\theta V_u t (C_o - C_i)}{\theta (C_o - C_i) + \rho_b k_1 (C_o^\eta - C_i^\eta)} \quad (\text{B.2.2.25})$$

For a pulse release and the same range of the Freundlich exponent, $0 < \eta < 1$, the condition (B.2.2.20) will not be satisfied at the entrance boundary when $t > t_p$. Consequently, adsorption according to the Freundlich isotherm will result in a sharp leading edge and diffuse trailing of the solute concentration profile when the exponential parameter is in the range of $0 < \eta < 1$.

The second situation for the occurrence of the shock front (condition B.2.2.18) is illustrated using the Freundlich isotherm, $\eta > 1$. This corresponds to a pure water displacement front following a pulse solute injection. Then

$$\left. \begin{aligned}
 C_o &= 0 < C_i \\
 \frac{df(C_d)}{dC_d} &= \frac{\rho_b k}{\theta} \eta C_d^{\eta-1} > 0 \\
 \frac{d^2 f(C_d)}{dC_d^2} &= \frac{\rho_b k}{\theta} \eta (\eta - 1) C_d^{\eta-2} > 0
 \end{aligned} \right\} \quad (\text{B.2.2.26})$$

This satisfies condition (B.2.2.18), resulting in a concentration profile that exhibits a dispersed front and a sharp trail edge (sharp tail). The location of the sharp tail is given by:

$$z_f = \frac{\theta V_u t C_i}{\theta C_i + \rho_b k C_i^\eta} \quad (\text{B.2.2.27})$$

This page was intentionally left blank.

APPENDIX C

ANALYTICAL SOLUTION FOR THREE-DIMENSIONAL STEADY-STATE GROUNDWATER FLOW IN A CONSTANT THICKNESS AQUIFER

Derived by
Dr. Michael Unga

McLaren/Hart

This page intentionally left blank.

APPENDIX C
**ANALYTICAL SOLUTION FOR THREE-DIMENSIONAL
STEADY-STATE GROUNDWATER FLOW IN A CONSTANT
THICKNESS AQUIFER**
Notation

- B Thickness of aquifer (held constant) [L].
- F Net leachate rate under the patch, expressed as a Darcian velocity.
- $\left[\frac{L^3 W}{L^2 T} \right]$ Note that the net infiltration rate at any point is the sum of F and I.
- K_y Hydraulic head [L].
- H_1, H_2 Hydraulic head specified at the upstream ($x=0$) and downstream ($x=L$) boundaries [L]. These are boundary conditions for the x domain.
- I Net regional infiltration rate, expressed as a Darcian velocity $\left[\frac{L^3 W}{L^2 T} \right]$.
- K_x, K_y, K_z Saturated hydraulic conductivity $\left[\frac{L^3 W}{L^2 T} \right]$.
- L Distance between the upstream and downstream specified heads [L].
- x, y, z Spatial coordinates, where z is the vertical dimension, with the aquifer surface specified at $z=0$ and aquifer base as $z=B$ [L].
- x_1, x_2, y_1, y_2 Spatial coordinates defining the areal patch over which flux F is applied [L]. Note that $L \geq x_2 > x_1 \geq 0$ and $y_2 > y_1$.

Steady-state, 3-D flow in an aquifer is defined by Laplace's Equation

$$K_x \frac{\partial^2 H}{\partial x^2} + K_y \frac{\partial^2 H}{\partial y^2} + K_z \frac{\partial^2 H}{\partial z^2} = 0 \left[\frac{L^3 W}{L^3 T} \right] \quad (C.1)$$

with boundary conditions

$$\begin{aligned} H(0, y, z, \infty) &= H_1 \\ H(L, y, z, \infty) &= H_2 \\ \frac{\partial H}{\partial y}(x, \pm\infty, z, \infty) &= 0 \end{aligned} \quad (\text{C.2})$$

$$-K_z \frac{\partial H}{\partial z}(x, y, 0, \infty) = F[U(x-x_1) - U(x-x_2)][U(y-y_1) - U(y-y_2)] + I$$

$$\frac{\partial H}{\partial z}(x, y, B, \infty) = 0$$

where I is the net Darcian infiltration rate of rainfall (uniformly constant), F is the net Darcian infiltration rate of leachate (applied only over the surface patch defined by x_1, x_2, y_1, y_2) and $U(\bullet)$ is the Heaviside unit step function.

A fundamental assumption of the above is that the saturated thickness B remains constant, despite the fact that there is mounding.

Consider the following integral transform for a finite x domain which has two first type boundary conditions:

$$\bar{H}(\beta_m, y, z, \infty) = \sqrt{\frac{2}{L}} \int_{x'=0}^L \sin(\beta_m x') H(x', y, z, \infty) dx' \quad (\text{C.3})$$

and its inversion transform

$$H(x, y, z, \infty) = \sum_{m=1}^{\infty} \sqrt{\frac{2}{L}} \sin(\beta_m x) \bar{H}(\beta_m, y, z, \infty) \quad (\text{C.4})$$

where the eigenvalues β_m are defined by

$$\beta_m = \frac{m\pi}{L} \quad m = 1, 2, \dots \quad (\text{C.5})$$

The integral transform for an infinite y domain is given by:

$$\bar{H}(\beta_m, v, z, \infty) = \int_{y'=-\infty}^{\infty} e^{-iy'} \bar{H}(\beta_m, y', z, \infty) dy' \quad (\text{C.6})$$

and the inversion formula

$$\bar{H}(\beta_m, y, z, \infty) = \frac{1}{2\pi} \int_{v=-\infty}^{\infty} e^{-ivy'} \bar{H}(\beta_m, v, z, \infty) dv \quad (\text{C.7})$$

The integral transform for the finite z domain which has two second type boundary conditions is:

$$\bar{\bar{H}}(\beta_m, v, \psi_n, \infty) = \frac{A_n}{\sqrt{B}} \int_{z'=0}^{\infty} \cos(\psi_n z') \bar{H}(\beta_m, v, z', \infty) dz' \quad (\text{C.8})$$

and the inversion formula

$$\bar{H}(\beta_m, v, z, \infty) = \sum_{n=0}^{\infty} \frac{A_n}{\sqrt{B}} \cos(\psi_n z) \bar{\bar{H}}(\beta_m, v, \psi_n, \infty) \quad (\text{C.9})$$

where the coefficient A_n equals

$$A_n = \begin{cases} 1 & n=0 \\ \sqrt{2} & n=1,2,\dots \end{cases} \quad (\text{C.10})$$

and eigenvalues ψ_n

$$\psi_n = \frac{\pi n}{B} \quad n=0,1,2,\dots \quad (\text{C.11})$$

Remove the x variation in Equation (C.1) by multiplying this equation by

$$\sqrt{\frac{2}{L}} \sin (\beta_m x')$$

integrating the resultant expression with respect to x' from 0 to L , using the transform given by

Equation (C.3) to get:

$$\left\{ K_x \sqrt{\frac{2}{L}} \sin (\beta_m x') \frac{\partial H}{\partial x} \right\}_0^L - \left\{ K_x \beta_m \sqrt{\frac{2}{L}} \cos (\beta_m x) H \right\}_0^L - K_x \beta_m^2 \bar{H} \quad (\text{C.12})$$

$$+ K_y \frac{\partial^2 \bar{H}}{\partial y^2} + K_z \frac{\partial^2 \bar{H}}{\partial z^2} = 0$$

The first term $K_x \sqrt{\frac{2}{L}} \sin (\beta_m x') \frac{\partial H}{\partial x}$ is equates to 0 when integrated from 0 to L .

Substitute the boundary conditions of Equation (C.2) into Equation (C.12) and rearrange to get

$$- K_x \beta_m \sqrt{\frac{2}{L}} [H_2 (-1)^m - H_1] - K_x \beta_m^2 \bar{H} + K_y \frac{\partial^2 \bar{H}}{\partial x^2} + K_z \frac{\partial^2 \bar{H}}{\partial x_2^2} = 0 \quad (\text{C.13})$$

with boundary conditions

$$\frac{\partial \bar{H}}{\partial y} (\beta_m, \pm \infty, z, \infty) = 0$$

$$\frac{\partial \bar{H}}{\partial z} (\beta_m, y, B, \infty) = 0 \quad (\text{C.14})$$

$$- K_z \frac{\partial \bar{H}}{\partial z} (\beta_m, y, 0, \infty) = F \sqrt{\frac{2}{L}} [U(y - y_1) - U(y - y_2)] \int_{x'=x_1}^{x^2} \sin (\beta_m x') dx'$$

$$+ I \sqrt{\frac{2}{L}} \int_{x'=0}^L \sin (\beta_m x') dx'$$

Remove the y variation in Equation (C.13) by multiplying this Equation by $e^{ivy'}$ and then integrating the resultant expression with respect to y' from $\pm\infty$ using the transform given Equation (C.6) to get:

$$-K_x \beta_m \sqrt{\frac{2}{L}} [H_2 (-1)^m - H_1] \int_{-\infty}^{\infty} e^{ivy'} dy' - K_x \beta_m^2 \bar{H} - K_y v^2 \bar{H} + K_z \frac{\partial^2 \bar{H}}{\partial z^2} = 0 \quad (\text{C.15})$$

with boundary conditions

$$\frac{\partial \bar{H}}{\partial z} (\beta_m, v, B, \infty) = 0$$

$$\begin{aligned} K_z \frac{\partial \bar{H}}{\partial z} (\beta_m, v, 0, \infty) &= F \sqrt{\frac{2}{L}} \int_{x=x_1}^{x_2} \sin(\beta_m x') \int_{y=y_1}^{y_2} e^{ivy'} dy' dx' + I \sqrt{\frac{2}{L}} \int_{x'=0}^L \sin(\beta_m x') \\ &\cdot \int_{y'=-\infty}^{\infty} e^{ivy'} dy' dx'. \end{aligned} \quad (\text{C.16})$$

Remove the z variation in Equation (C.15) by multiplying this Equation by

$$\frac{A_n}{\sqrt{B}} \cos(v_n z')$$

and then integrating the resultant expression with respect to z' from 0 to B, using the transform given by Equation (C.8) to get:

$$\begin{aligned} &-K_x \beta_m \frac{A_n}{\sqrt{B}} \sqrt{\frac{2}{L}} [H_2 (-1)^m - H_1] \int_{y'=-\infty}^{\infty} e^{ivy'} \int_{z'=0}^B \cos(\psi_n z') dz' dy' \\ &+ \left\{ K_z \frac{A_n}{\sqrt{B}} \cos(\psi_n z') \frac{\partial \bar{H}}{\partial z} \right\}_0^B + \left\{ K_z \psi_n \frac{A_n}{\sqrt{B}} \sin(\psi_n z) \bar{H} \right\}_0^B \\ &- \bar{H} (K_x \beta_m^2 + K_y v^2 + K_z \psi_n^2) = 0 \end{aligned} \quad (\text{C.17})$$

The third term $K_z \psi_n \frac{A_n}{\sqrt{B}} \sin(\psi_n z) \bar{H}$ equates to 0 when integrated from 0 to L.

Substitute the boundary conditions of Equation (C.16) with Equation (C.17) and solve for

$$\bar{H}(\beta_m, \nu, \psi_n, \infty).$$

$$\bar{H}(\beta_m, \nu, \psi_n, \infty) = - \frac{K_x \beta_m A_n \sqrt{\frac{2}{BL}} [H_2(-1)^m - H_1] \int_{y'=-\infty}^{\infty} e^{-i\nu y'} \cdot \int_{z'=0}^B \cos(\psi_n z') dz' dy'}{(K_x \beta_m^2 + K_y \nu^2 + K_z \psi_n^2)}$$

Return \bar{H} back to H by multiplying Equation (C.18) by the following three variables:

$$\begin{aligned} & \frac{A_n}{\sqrt{B}} \cos(\psi_n z) \\ & + \frac{A_n F \sqrt{\frac{2}{BL}} \int_{y'=y_1}^{y_2} e^{i\nu y'} \int_{x'=x_1}^{x_2} \sin(\beta_m x') dx' dy'}{(K_x \beta_m^2 + K_y \nu^2 + K_z \psi_n^2)} \quad (C.18) \\ & + \frac{A_n I \sqrt{\frac{2}{BL}} \int_{y'=-\infty}^{\infty} e^{i\nu y'} \int_{x'=0}^L \sin(\beta_m x') dx' dy'}{(K_x \beta_m^2 + K_y \nu^2 + K_z \psi_n^2)}. \end{aligned}$$

and sum with respect to n from 0 to ∞ ; $\frac{e^{-i\nu y}}{2\pi}$ and integrate with respect to ν from $\pm\infty$; $\sqrt{\frac{2}{L}} \sin(\beta_m x)$ and sum with respect to m from 1 to ∞ . Upon substitution, Equation (C.18)

reduces to:

$$H(x, y, z, \infty) = \frac{K_x}{LB\pi} \sum_{m=1}^{\infty} \beta_m \sin(\beta_m x) [H_2(-1)^m - H_1] \sum_{n=1}^{\infty} A_n^2 \cos(\psi_n z)$$

$$\cdot \int_{z'=0}^{\infty} \cos(\psi_n z') \int_{y'=-\infty}^{\infty} \cdot \int_{v=-\infty}^{\infty} \frac{e^{-iv(y-y')}}{(K_x \beta_m^2 + K_y v^2 + K_z \psi_n^2)} dv dy' dz' \quad (C.19)$$

$$\frac{F}{BL\pi} \sum_{m=1}^{\infty} \sin(\beta_m x) \sum_{n=0}^{\infty} A_n^2 \cos(\psi_n z) \int_{x'=x_1}^{x_2} \sin(\beta_m x') \int_{y'=-y_1}^{y_2} \cdot \int_{v=-\infty}^{\infty} \frac{e^{-iv(y-y')}}{(K_x \beta_m^2 + K_y v^2 + K_z \psi_n^2)}$$

$$\frac{I}{BL\pi} \sum_{m=1}^{\infty} \sin(\beta_m x') \sum_{m=1}^{\infty} A_n^2 \cos(\psi_n z) \int_{x'=0}^L \sin(\beta_m x') \int_{y'=-\infty}^{\infty} \cdot \int_{v=-\infty}^{\infty} \frac{e^{-iv(y-y')}}{(K_x \beta_m^2 + K_y v^2 + K_z \psi_n^2)}$$

Note the following integral

$$\int_{v=-\infty}^{\infty} \frac{e^{-iv(y-y')}}{(\beta_m^2 K_x + v^2 K_y + \psi_n^2 K_z)} dv = \frac{\pi e^{-|y-y'| \frac{\sqrt{\beta_m^2 K_x + \psi_n^2 K_z}}{K_y}}}{\sqrt{K_y (\beta_m^2 K_x + \psi_n^2 K_z)}} \quad (C.20)$$

Note the following change in variables

$$\begin{array}{ll} n = y - y' & y' \quad \eta \\ d\eta = -dy' & -\infty \quad \infty \\ & y_1 \quad y - y_1 \\ & y^2 \quad y - y_2 \\ & \infty \quad -\infty \end{array} \quad (C.21)$$

Substitute Equations (C.20) and (C.21) into Equation (C.19) and rearrange to get

$$H(x, y, z, \infty) = -\frac{K_x}{LB\sqrt{K_y}} \sum_{m=1}^{\infty} \beta_m \sin(\beta_m x) [H_2(-1)^m - H_1] \sum_{n=0}^{\infty} \frac{A_n^2 \cos(\psi_n z)}{\sqrt{(\beta_m^2 K_x + \psi_n^2 K_z)}}$$

$$\begin{aligned}
& \cdot \int_{z'=0}^B \cos(\psi_n z') \cdot \int_{n=-\infty}^{\infty} \cdot e^{-|\eta| \sqrt{\frac{\beta_m^2 K_x + \psi_n^2 K_z}{K_y}}} d\eta dz' \\
& + \frac{F}{LB\sqrt{K_y}} \sum_{m=1}^{\infty} \sin(\beta_m x) \sum_{n=0}^{\infty} A_n^2 \cos(\psi_n z) \int_{x'=x_1}^{x_2} \frac{\sin(\beta_m x')}{\sqrt{(\beta_m^2 K_x + \psi_n^2 K_z)}} \int_{\eta=y_1-y}^{(y_2-y)} e^{-|\eta| \sqrt{\frac{\beta_m^2 K_x + \psi_n^2 K_z}{K_y}}} d\eta dx' \quad (\text{C.22}) \\
& + \frac{I}{LB\sqrt{K_y}} \sum_{m=1}^{\infty} \sin(\beta_m x) \sum_{n=0}^{\infty} A_n^2 \cos(\psi_n z) \int_{x'=0}^L \frac{\sin(\beta_m x')}{\sqrt{(\beta_m^2 K_x + \psi_n^2 K_z)}} \int_{\eta=-\infty}^{\infty} e^{-|\eta| \sqrt{\frac{\beta_m^2 K_x + \psi_n^2 K_z}{K_y}}} d\eta dx'.
\end{aligned}$$

Note the following integrals:

$$\int_{\eta=-\infty}^{\infty} e^{-a|\eta|} d\eta = 2 \int_{\eta=0}^{\infty} e^{-a\eta} d\eta = \frac{2}{a} \quad (\text{C.23})$$

$$\int_{\eta=y_1-y}^{y_2-y} e^{-a|\eta|} d\eta = [e^{-a|y_1-y|} - 1] \frac{\text{sign}(y_1-y)}{a} - [e^{-a|y_2-y|} - 1] \frac{\text{sign}(y_2-y)}{a} \quad (\text{C.24})$$

$$\text{sign}(\eta) = \begin{cases} 1 & \eta \text{ is positive} \\ 0 & \eta \text{ is zero} \\ -1 & \eta \text{ is negative} \end{cases}$$

The derivative of Equation (C.24) with respect to y is given by

$$\frac{d}{dy} \left\{ \int_{y_1-y}^{y_2-y} e^{-a|\eta|} d\eta \right\} = e^{-a|y_1-y|} - e^{-a|y_2-y|} \quad (\text{C.25})$$

$$\int_{z'=0}^B \cos(\psi_n z') dz' = \frac{(\sin(\psi_n B) - \sin(0))}{\psi_n} = \begin{cases} B & n = 0 \\ 0 & n = 1, 2, \dots \end{cases} \quad (\text{C.26})$$

$$\int_{x'=0}^L \sin(\beta_m x') dx' = \frac{-(\cos(\beta_m L) - \cos(0))}{\beta_m} = \frac{[1 - (-1)^m]}{\beta_m} \quad (\text{C.27})$$

$$\int_{x'=x_1}^{x_2} \sin(\beta_m x') dx' = \frac{-(\cos(\beta_m x_2) - \cos(\beta_m x_1))}{\beta_m} \quad (\text{C.28})$$

Substitute Equations (C.23)-(C.24), (C.26)-(C.28) into Equation (C.22) and rearrange to get

$$\begin{aligned} H(x, y, z, \infty) = & -\frac{2}{L} \sum_{m=1}^{\infty} \frac{\sin(\beta_m x)}{\beta_m} [H_2(-1)^m - H_1] \\ & + \frac{2l}{BL} \sum_{m=1}^{\infty} \frac{\sin(\beta_m x)}{\beta_m} [1 - (-1)^m] \cdot \sum_{n=0}^{\infty} \frac{A_n^2 \cos(\psi_n z)}{(\beta_m^2 K_x + \psi_n^2 K_z)} \\ & + \frac{F}{BL} \sum_{m=1}^{\infty} \frac{\sin(\beta_m x)}{\beta_m} [\cos(\beta_m x_1) - \cos(\beta_m x_2)] \cdot \sum_{n=0}^{\infty} \frac{A_n^2 \cos(\psi_n z)}{(\beta_m^2 K_x + \psi_n^2 K_z)} \\ & \cdot \left\{ [e^{-a|y_1-y|} - 1] \text{sign}(y_1 - y) - [e^{-a|y_2-y|} - 1] \text{sign}(y_2 - y) \right\} \end{aligned} \quad (\text{C.29})$$

where

$$\begin{aligned} a &= \sqrt{\beta_m^2 K_x + \psi_n^2 K_z} \\ A_n &= \begin{cases} 1 & n = 0 \\ \sqrt{2} & n = 1, 2, \dots \end{cases} K_y \\ z: \quad \psi_n &= \frac{n\pi}{B} \quad n = 0, 1, \dots \\ x: \quad \beta_m &= \frac{m\pi}{L} \quad m = 1, 2, \dots \end{aligned}$$

$$\sum_{m=1}^{\infty} \frac{\sin(\beta_m x)}{\beta_m} = \frac{(L-x)}{2} \quad \text{iff } x > 0 \quad (\text{C.30})$$

$$\sum_{m=1}^{\infty} \frac{\sin(\beta_m x)(-1)^m}{\beta_m} = \frac{-x}{2} \quad (\text{C.31})$$

$$\sum_{m=1}^{\infty} \frac{\sin(\beta_m x)}{\beta_m^3} = \frac{L^2 x}{6} - \frac{Lx^2}{4} + \frac{x^3}{12} \quad \text{iff } x > 0 \quad (\text{C.32})$$

$$\sum_{m=1}^{\infty} \frac{\sin(\beta_m x)(-1)^m}{\beta_m^3} = -\frac{L^2 x}{12} + \frac{x^3}{12} \quad (\text{C.33})$$

Substitute Equations (C.30)-(C.33) into Equation (C.29):

$$\begin{aligned} H(x, y, z, \infty) = & H_1 + (H_2 - H_1) \frac{x}{L} + \frac{I}{2K_x B} (Lx - x^2) \\ & + \frac{4I}{LB} \sum_{m=1}^{\infty} \frac{\sin(\beta_m x)}{\beta_m} [1 - (-1)^m] \sum_{n=1}^{\infty} \frac{\cos(\psi_n z)}{(\beta_m^2 K_x + \psi_n^2 K_z)} \\ & + \frac{F}{BL} \sum_{m=1}^{\infty} \frac{\sin(\beta_m x)}{\beta_m} [\cos(\beta_m x_1) - \cos(\beta_m x_2)] \sum_{n=0}^{\infty} \frac{A_n^2 \cos(\psi_n z)}{(\beta_m^2 K_x + \psi_n^2 K_z)} \quad (\text{C.34}) \\ & \cdot \left\{ [e^{-a|y_1-y|} - 1] \text{sign}(y_1 - y) - [e^{-a|y_2-y|} - 1] \text{sign}(y_2 - y) \right\} \end{aligned}$$

where

$$\begin{aligned} A_n &= \begin{cases} 1 & n=0 \\ \sqrt{2} & n=1,2,\dots \end{cases} \\ \psi_n &= n\pi/B \quad n=0,1,\dots \\ \beta_m &= m\pi/L \quad m=1,2,\dots \end{aligned}$$

$$a = \frac{\sqrt{\beta_m^2 K_x + \psi_n^2 K_z}}{K_y}$$

and

$$\sum_{m=1}^{\infty} \frac{\cos(\beta_m x)}{(\beta_m^2 + \alpha^2)} = \frac{L \cosh[\alpha L(1-x/L)]}{2\alpha \sinh[L\alpha]} - \frac{1}{2\alpha^2} \quad (\text{C.35})$$

where $\alpha^2 = \psi_n^2 K_z / K_x$, $\cosh[\cdot]$ is the hyperbolic cosine function, $\sinh[\cdot]$ is the hyperbolic sine function and

$$\sum_{m=1}^{\infty} \frac{\cos(\beta_m x) (-1)^m}{(\beta_m^2 + \alpha^2)} = \frac{L \cosh[\alpha x]}{2\alpha \sinh[L\alpha]} - \frac{1}{2\alpha^2}. \quad (\text{C.36})$$

Integrating Equations (C.35) and (C.36) with respect to x gives the following new infinite series:

$$\sum_{m=1}^{\infty} \frac{\sin(\beta_m x)}{\beta_m (\beta_m^2 + \alpha^2)} = \frac{-L \sinh[\alpha L(1-x/L)]}{2\alpha^2 \sinh[L\alpha]} + \frac{(L-x)}{2\alpha^2} \quad (\text{C.37})$$

$$\sum_{m=1}^{\infty} \frac{\sin(\beta_m x) (-1)^m}{\beta_m (\beta_m^2 + \alpha^2)} = \frac{L \sinh[\alpha x]}{2\alpha^2 \sinh[L\alpha]} - \frac{x}{2\alpha^2}. \quad (\text{C.38})$$

Substitute Equations (C.37) and (C.38) into Equation (C.34).

$$\begin{aligned} H(x, y, z, \infty) = & H_1 + (H_2 - H_1) \frac{x}{L} + \frac{l(Lx - x^2)}{2K_z B} \\ & - \frac{2l}{K_z B} \sum_{n=1}^{\infty} \frac{\cos(\psi_n z)}{\psi_n^2 \sinh(\alpha L)} \left\{ \sinh[\alpha(L-x)] - \sinh(\alpha L) + \sinh(\alpha x) \right\} \\ & - \frac{F}{BL} \sum_{m=1}^{\infty} \frac{\sin(\beta_m)}{\beta_m} [\cos(\beta_m x_2) - \cos(\beta_m x_1)] \cdot \sum_{n=0}^{\infty} \frac{A_n^2 \cos(\psi_n Z)}{(\beta_m^2 K_x + \psi_n^2 K_z)} \quad (\text{C.39}) \end{aligned}$$

$$\cdot \left\{ [e^{-a|y_1-y|} - 1] \text{sign}(y_1 - y) - [e^{-a|y_2-y|} - 1] \text{sign}(y_2 - y) \right\}$$

where

$$a = \frac{\sqrt{\beta_m^2 K_x + \psi_n^2 K_z}}{K_y}$$

$$\alpha = \psi_n \sqrt{K_z/K_x}$$

$$\beta = m\pi/L \quad m = 1, 2, \dots$$

$$\psi_n = n\pi/B \quad n = 0, 1, \dots$$

Note the following infinite series

$$\sum_{n=1}^{\infty} \frac{\sin(\psi_n z)}{\psi_n} = \frac{(B-z)}{2} \quad (\text{C.40})$$

$$\sum_{n=1}^{\infty} \frac{\cos(\psi_n z)}{\psi_n^2} = \frac{B^2}{6} - \frac{Bz}{2} - \frac{z^2}{4} \quad (\text{C.41})$$

$$\sum_{n=1}^{\infty} \frac{\cos(\psi_n z)}{(\beta_m^2 K_x + \psi_n^2 K_z)} = \frac{B \cosh[(B-z)\beta_m \sqrt{K_x/K_z}]}{2\beta_m \sqrt{K_x K_z} \sinh[B\beta_m \sqrt{K_x/K_z}]} - \frac{1}{2\beta_m^2 K_x} \quad (\text{C.42})$$

$$\begin{aligned} \sum_{m=1}^{\infty} \frac{\sin(\beta_m x)}{\beta_m^3} [\cos(\beta_m x_2) - \cos(\beta_m x_1)] &= \frac{x(x_2^2 - x_1^2)}{4} - \frac{Lx(x_2 - x_1)}{2} \\ &+ \frac{L(x - x_1)^2 U(x - x_1)}{4} - \frac{L(x - x_2)^2 U(x - x_2)}{4} \end{aligned} \quad (\text{C.43a})$$

$$\begin{aligned}
\sum_{m=1}^{\infty} \frac{\sin(\beta_m x)}{\beta_m(\beta_m^2 + \alpha^2)} [\cos(\beta_m x_2) - \cos(\beta_m x_1)] &= \frac{L \sinh[\alpha(L - (x + x_1))] - \sinh[\alpha(L - (x + x_2))]}{4\alpha^2 \sinh[\alpha L]} \\
&- \frac{L \sinh[\alpha(L - (x - x_2))]U(x - x_2)}{4\alpha^2 \sinh[\alpha L]} + \frac{L \sinh[\alpha(L - (x_2 - x))]U(x_2 - x)}{4\alpha^2 \sinh[\alpha L]} \\
&+ \frac{L \sinh[\alpha(L - (x - x_1))]U(x - x_1)}{4\alpha^2 \sinh[\alpha L]} - \frac{L \sinh[\alpha(L - (x_1 - x))]U(x_1 - x)}{4\alpha^2 \sinh[\alpha L]} \\
&- \frac{L}{2\alpha^2} [U(x - x_1) - U(x - x_2)]
\end{aligned} \tag{C.43b}$$

Substitute Equations (C.40)-(C.44) into Equation (C.39) and rearrange terms to get the final solution.

The steady-state, 3-D hydraulic head is given by:

$$\begin{aligned}
H(x,y,z,\infty) &= H_1 + (H_2 - H_1) \frac{x}{L} + \frac{l(Lx - x^2)}{2K_x B} + \frac{l}{K_z B} \left[\frac{B^2}{3} - Bz + \frac{z^2}{2} \right] \\
&- \frac{2l}{K_z B} \sum_{n=1}^{\infty} \frac{\cos(\psi_n z)}{\psi_n^2 \sinh(\alpha L)} \left\{ \sinh[\alpha(L - x)] + \sinh(\alpha x) \right\} \\
&+ \frac{F}{2K_x B} [\text{sign}(y_2 - y) - \text{sign}(y_1 - y)] \left[-\frac{x(x_2^2 - x_1^2)}{2L} + x(x_2 - x_1) - \frac{(x - x_1)^2 U(x - x_1)}{2} \right. \\
&\left. + \frac{(x - x_2)^2 U(x - x_2)}{2} \right] \\
&+ \frac{F}{2K_z B} [\text{sign}(y_2 - y) - \text{sign}(y_1 - y)] \left[U(x - x_1) - U(x - x_2) \right] \left[\frac{B^2}{3} - Bz + \frac{z^2}{2} \right] \\
&- \frac{F}{2K_z B} [\text{sign}(y_2 - y) - \text{sign}(y_1 - y)] \sum_{n=1}^{\infty} \frac{\cos(\psi_n z)}{\psi_n^2 \sinh(\alpha L)} \left\{ \sinh[\alpha(L - (x + x_1))] \right. \\
&- \sinh[\alpha(L - (x + x_2))] - \sinh[\alpha(L - (x - x_2))]U(x - x_2) \\
&+ \sinh[\alpha(L - (x_2 - x))]U(x_2 - x) + \sinh[\alpha(L - (x - x_1))]U(x - x_1) \\
&\left. - \sinh[\alpha(L - (x_1 - x))]U(x_1 - x) \right\}
\end{aligned} \tag{C.44}$$

$$\begin{aligned}
& - \frac{F}{LBK_x} \sum_{m=1}^{\infty} \frac{\sin(\beta_m x)}{\beta_m^3} [\cos(\beta_m x_2) - \cos(\beta_m x_1)] \left[e^{-\beta_m \sqrt{\frac{K_x}{K_y}} |y_1 - y|} \cdot \text{sign}(y_1 - y_2) \right. \\
& \quad \left. - e^{-\beta_m \sqrt{\frac{K_x}{K_y}} |y_2 - y|} \cdot \text{sign}(y_2 - y) \right] \\
& + \frac{2F}{LB} \sum_{n=1}^{\infty} \psi_n \sin(\psi_n z) \sum_{m=1}^{\infty} \frac{\sin(\beta_m x)}{\beta_m (\beta_m^2 K_x + \psi_n^2 K_z)} [\cos(\beta_m x_2) - \cos(\beta_m x_1)] \\
& \quad \cdot [e^{-a|y_1 - y|} \cdot \text{sign}(y_1 - y) - e^{-a|y_2 - y|} \cdot \text{sign}(y_2 - y)]
\end{aligned}$$

where

$$\begin{aligned}
\beta_m &= m\pi/L & m &= 1, 2, \dots \\
\psi_n &= n\pi/L & n &= 0, 1, \dots
\end{aligned}$$

$$a = \frac{\sqrt{\beta_m^2 K_x + \psi_n^2 K_z}}{K_y}, \quad \alpha = \psi_n \sqrt{K_z/K_x}$$

The spatial derivatives of the hydraulic head are computed as:

$$\begin{aligned}
\frac{\partial H}{\partial x}(x, y, z, \infty) &= \frac{(H_2 - H_1)}{L} + \frac{l(L - 2x)}{2K_x B} \\
& - \frac{2l}{B\sqrt{K_x K_z}} \sum_{n=1}^{\infty} \frac{\cos(\psi_n z)}{\psi_n \sinh(\alpha L)} \left\{ \cosh[\alpha(L - x)] + \cosh(\alpha x) \right\} \\
& + \frac{F}{2K_x B} [\text{sign}(y_2 - y) - \text{sign}(y_1 - y)] \left[-\frac{x(x_2^2 - x_1^2)}{2L} + (x_2 - x_1) - (x - x_1)U(x - x_1) \right. \\
& \quad \left. + (x - x_2)U(x - x_2) \right] \tag{C.45} \\
& - \frac{F}{2B\sqrt{K_x K_z}} [\text{sign}(y_2 - y) - \text{sign}(y_1 - y)] \sum_{n=1}^{\infty} \frac{\cos(\psi_n z)}{\psi_n \sinh(\alpha L)} [-\cosh[\alpha(L - (x + x_1))] \\
& \quad + \cosh[\alpha(L - (x + x_2))] + \cosh[\alpha(L - (x - x_2))]U(x - x_2) \\
& \quad + \cosh[\alpha(L - (x_2 - x))]U(x_2 - x) - \cosh[\alpha(L - (x - x_1))]U(x - x_1) \\
& \quad - \cosh[\alpha(L - (x_1 - x))]U(x_1 - x)]
\end{aligned}$$

$$-\frac{F}{LBK_x} \sum_{m=1}^{\infty} \frac{\cos(\beta_m x)}{\beta_m^2} [\cos(\beta_m x_2) - \cos(\beta_m x_1)] \left[\begin{aligned} & \text{sign}(y_1 - y) \cdot e^{-\beta_m |y_1 - y| \sqrt{\frac{K_x}{K_y}}} \\ & - \text{sign}(y_2 - y) \cdot e^{-\beta_m |y_2 - y| \sqrt{\frac{K_x}{K_y}}} \end{aligned} \right]$$

$$-\frac{2F}{LB} \sum_{n=1}^{\infty} \cos(\psi_n z) \sum_{m=1}^{\infty} \frac{\sin(\beta_m x)}{\beta_m \sqrt{K_y(\beta_m^2 K_x + \psi_n^2 K_z)}} [\cos(\beta_m x_2) - \cos(\beta_m x_1)] \cdot \left\{ e^{-a|y_1 - y|} - e^{-a|y_2 - y|} \right\}$$

$$\frac{\partial H}{\partial y}(x, y, z, \infty) = -\frac{F}{LB\sqrt{K_x K_y}} \sum_{m=1}^{\infty} \frac{\sin(\beta_m x)}{\beta_m^2} [\cos(\beta_m x_2) - \cos(\beta_m x_1)] \cdot \left[e^{-\beta_m |y_1 - y| \sqrt{\frac{K_x}{K_y}}} - e^{-\beta_m |y_2 - y| \sqrt{\frac{K_x}{K_y}}} \right] \quad (\text{C.46})$$

$$-\frac{2F}{LB} \sum_{n=1}^{\infty} \cos(\psi_n z) \sum_{m=1}^{\infty} \frac{\sin(\beta_m x)}{\beta_m (\beta_m^2 K_x + \psi_n^2 K_z)} [\cos(\beta_m x_2) - \cos(\beta_m x_1)] \cdot \left\{ e^{-a|y_1 - y|} \text{sign}(y_1 - y) - e^{-a|y_2 - y|} \text{sign}(y_2 - y) \right\}$$

$$\begin{aligned}
\frac{\partial H}{\partial z}(x,y,z,\infty) &= \frac{l}{K_z B}(-B+z) + \frac{2l}{K_z B} \sum_{n=1}^{\infty} \frac{\sin(\psi_n z)}{\psi_n \sinh(\alpha L)} \left\{ \sinh[\alpha(L-x)] \right. \\
&+ \sinh(\alpha x) \left. + \frac{F}{2K_z B} [\text{sign}(y_2-y) - \text{sign}(y_1-y)] [U(x-x_1) - U(x-x_2)] [-B+z] \right. \\
&+ \frac{F}{2K_z B} [\text{sign}(y_2-y) - \text{sign}(y_1-y)] \sum_{n=1}^{\infty} \frac{\sin(\psi_n z)}{\psi_n \sinh(\alpha L)} [\sinh[\alpha(L-(x+x_1))] \\
&- \sinh[\alpha(L-(x+x_2))] - \sinh[\alpha(L-(x-x_2))] U(x-x_2) \\
&+ \sinh[\alpha(L-(x_2-x))] U(x_2-x) + \sinh[\alpha(L-(x-x_1))] U(x-x_1) \\
&- \sinh[\alpha(L-(x_1-x))] U(x_1-x) \\
&+ \frac{2F}{LB} \sum_{n=1}^{\infty} \psi_n \sin(\psi_n z) \sum_{m=1}^{\infty} \frac{\sin(\beta_m x)}{\beta_m (\beta_m^2 K_x + \psi_n^2 K_z)} [\cos(\beta_m x_2) - \cos(\beta_m x_1)] \\
&\left. \cdot [e^{-\alpha|y_1-y|} \cdot \text{sign}(y_1-y) - e^{-\alpha|y_2-y|} \cdot \text{sign}(y_2-y)] \right\} \tag{C.47}
\end{aligned}$$

Special 2-D Areal Case

$$K_z \rightarrow 0$$

The 2-D areal groundwater mounding problem can be computed by integrating the partial differential Equation given in Equation (C.1) with respect to z between 0 and B :

$$K_x \frac{\partial^2 \bar{H}}{\partial x^2} B + K_y \frac{\partial^2 \bar{H}}{\partial y^2} B + [K_z \frac{\partial H}{\partial z}] \Big|_0^B = 0 \tag{C.48}$$

where

$$\bar{H}(x,y,\infty) = \int_0^B \frac{H(x,y,z,\infty)}{B} dz \tag{C.49}$$

is the depth averaged head.

Substitute the boundary conditions of Equation (C.2) into Equation (C.48) and then divide through by B:

$$K_x \frac{\partial^2 \bar{H}}{\partial x^2} + K_y \frac{\partial^2 \bar{H}}{\partial y^2} + \frac{I}{B} + \frac{F}{B} [U(x-x_1) - U(x-x_2)][U(y-y_1) - U(y-y_2)] = 0 \quad (\text{C.50})$$

with boundary conditions

$$\begin{aligned} \bar{H}(0, y, \infty) &= H_1 \\ \bar{H}(L, y, \infty) &= H_2 \\ \frac{\partial \bar{H}}{\partial y}(x, \pm\infty, \infty) &= 0 \end{aligned} \quad (\text{C.51})$$

The analytical solution given by Equation (C.44) can also be integrated with respect to z and then divide by B to give the depth averaged head. This corresponds to the solution of Equations (C.50)-(C.51).

Note the following integrals

$$\frac{1}{B} \int_0^B \left(\frac{B^2}{3} - Bz + \frac{z^2}{2} \right) dz = \frac{1}{B} \left[\frac{B^2 z}{3} - \frac{Bz^2}{2} + \frac{z^3}{6} \right] \Big|_0^B = 0 \quad (\text{C.52})$$

$$\frac{1}{B} \int_0^B \cos(\psi_n z) dz = \frac{[\sin(\psi_n B) - \sin(\psi_n 0)]}{B\psi_n} = \begin{cases} 1 & \text{if } \psi_n = 0 \\ 0 & \text{if } \psi_n > 0 \end{cases} \quad (\text{C.53})$$

Substitute Equations (C.52)-(C.53) into Equation (C.44) after integrating Equation (C.44) with respect to z and dividing by B . Also substitute in the infinite series solution given by Equation (C.43a). The 2-D, steady-state hydraulic head is computed as:

$$\begin{aligned}
\bar{H}(x,y,\infty) = & H_1 + (H_2 - H_1)\frac{x}{L} + \frac{I(Lx - x^2)}{2K_x B} \\
& + \frac{F}{2K_x B} [\text{sign}(y_2 - y) - \text{sign}(y_1 - y)] \left[-\frac{x(x_2^2 - x_1^2)}{2L} + x(x_2 - x_1) - \frac{(x - x_1)^2 U(x - x_1)}{2} \right. \\
& \left. + \frac{(x - x_2)^2 U(x - x_2)}{2} \right] - \frac{F}{BLK_x} \sum_{m=1}^{\infty} \frac{\sin(\beta_m x)}{\beta_m^3} [\cos(\beta_m x_2) - \cos(\beta_m x_1)] \quad (C.54) \\
& \left[\text{sign}(y_1 - y) \cdot e^{-\beta_m |y_1 - y| \sqrt{\frac{K_x}{K_y}}} - \text{sign}(y_2 - y) \cdot e^{-\beta_m |y_2 - y| \sqrt{\frac{K_x}{K_y}}} \right]
\end{aligned}$$

where

$$\beta_m = \pi m / L \quad (C.55)$$

and the spatial derivatives of the hydraulic head

$$\begin{aligned}
\frac{\partial \bar{H}}{\partial x}(x,y,\infty) = & \frac{(H_2 - H_1)}{L} + \frac{I(L - 2x)}{2K_x B} \\
& + \frac{F}{2K_x B} [\text{sign}(y_2 - y) - \text{sign}(y_1 - y)] \left[-\frac{(x_2^2 - x_1^2)}{2L} + (x_2 - x_1) - (x - x_1)U(x - x_1) \right. \\
& \left. + (x - x_2)U(x - x_2) \right] \\
& - \frac{F}{BLK_x} \sum_{m=1}^{\infty} \frac{\cos(\beta_m x)}{\beta_m^2} [\cos(\beta_m x_2) - \cos(\beta_m x_1)] \quad (C.56)
\end{aligned}$$

$$\begin{aligned}
& \left[\text{sign}(y_1 - y) \cdot e^{-\beta_m |y_1 - y| \sqrt{\frac{K_x}{K_y}}} - \text{sign}(y_2 - y) \cdot e^{-\beta_m |y_2 - y| \sqrt{\frac{K_x}{K_y}}} \right] \\
\frac{\partial \bar{H}}{\partial y}(x,y,\infty) = & -\frac{F}{BL\sqrt{K_x K_y}} \sum_{m=1}^{\infty} \frac{\sin(\beta_m x)}{\beta_m^2} [\cos(\beta_m x_2) - \cos(\beta_m x_1)] \quad (C.57) \\
& \left[e^{-\beta_m |y_1 - y| \sqrt{\frac{K_x}{K_y}}} - e^{-\beta_m |y_2 - y| \sqrt{\frac{K_x}{K_y}}} \right]
\end{aligned}$$

Special 2-D x, z Cross-Sectional Case

$$\begin{aligned} K_y &\rightarrow 0 \\ y_2 &\rightarrow +\infty \\ y_1 &\rightarrow -\infty \end{aligned}$$

The 2-D cross-sectional groundwater mounding problem for the x, z domain can be computed by setting $K_y = 0$ and $y_2 = +\infty$ and $y_1 = -\infty$ in Equation (C.44):

$$\begin{aligned} \hat{H}(x, z, \infty) = & H_1 + (H_2 - H_1) \frac{x}{L} + \frac{I(Lx - x^2)}{2K_x B} + \frac{I}{K_z B} \left(\frac{B^2}{3} - Bz + \frac{z^2}{2} \right) \\ & - \frac{2I}{K_z B} \sum_{n=1}^{\infty} \frac{\cos(\psi_n z)}{\psi_n^2 \sinh(\alpha L)} \left\{ \sinh[\alpha(L-x)] + \sinh(\alpha x) \right\} \\ & + \frac{F}{K_x B} \left[-\frac{x(x_2^2 - x_1^2)}{2L} + x(x_2 - x_1) - \frac{(x-x_1)^2 U(x-x_1)}{2} + \frac{(x-x_2)^2 U(x-x_2)}{2} \right] \\ & + \frac{F}{K_z B} \left[U(x-x_1) - U(x-x_2) \right] \left[\frac{B^2}{3} - Bz + \frac{z^2}{2} \right] \\ & - \frac{F}{K_z B} \sum_{n=1}^{\infty} \frac{\cos(\psi_n z)}{\psi_n^2 \sinh(\alpha L)} \left\{ \sinh[\alpha(L-(x+x_1))] - \sinh[\alpha(L-(x+x_2))] \right\} \\ & - \sinh[\alpha(L-(x-x_2))] U(x-x_2) + \sinh[\alpha(L-(x_2-x))] U(x_2-x) \\ & + \sinh[\alpha(L-(x-x_1))] U(x-x_1) - \sinh[\alpha(L-(x_1-x))] U(x_1-x) \left. \right\} \end{aligned} \quad (C.58)$$

where

$$\begin{aligned} \beta_m &= m\pi/L \\ \psi_n &= n\pi/B \\ \alpha &= \psi_n \sqrt{K_z/K_x} \end{aligned}$$

$$\begin{aligned}
\frac{\partial \hat{H}}{\partial x}(x,z,\infty) &= \frac{(H_2 - H_1)}{L} + \frac{l(L - 2x)}{2K_x B} \\
&- \frac{2l}{B\sqrt{K_x K_z}} \sum_{n=1}^{\infty} \frac{\cos(\psi_n z)}{\psi_n \sinh(\alpha L)} [-\cosh[\alpha(L-x) + \cosh(\alpha x)] \\
&+ \frac{F}{K_x B} \left[-\frac{(x_2^2 - x_1^2)}{2L} + (x_2 - x_1) - (x - x_1)U(x - x_1) + (x - x_2)U(x - x_2) \right] \quad (C.59) \\
&- \frac{F}{B\sqrt{K_x K_z}} \sum_{n=1}^{\infty} \frac{\cos(\psi_n z)}{\psi_n \sinh(\alpha L)} \left\{ -\cosh[\alpha(L - (x + x_1))] + \cosh[\alpha(L - (x + x_2))] \right. \\
&+ \cosh[\alpha(L - (x - x_2))]U(x - x_2) + \cosh[\alpha(L - (x_2 - x))]U(x - x_2) \\
&\left. - \cosh[\alpha(L - (x - x_1))]U(x - x_1) - \cosh[\alpha(L - (x_1 - x))]U(x_1 - x) \right\}
\end{aligned}$$

$$\begin{aligned}
\frac{\partial \hat{H}}{\partial z}(x,z,\infty) &= \frac{l}{K_z B} (-B + z) + \frac{F}{K_z B} [U(x - x_1) - U(x - x_2)][(-B + z)] \\
&+ \frac{2l}{K_z B} \sum_{n=1}^{\infty} \frac{\sin(\psi_n z)}{\psi_n \sinh(\alpha L)} \left\{ \sinh[\alpha(L - x)] + \sinh(\alpha x) \right\} \\
&+ \frac{F}{K_z B} \sum_{n=1}^{\infty} \frac{\sin(\psi_n z)}{\psi_n \sinh(\alpha L)} \left\{ \sinh[\alpha(L - (x + x_1))] - \sinh[\alpha(L - (x + x_2))] \right. \quad (C.60) \\
&- \sinh[\alpha(L - (x - x_2))]U(x - x_2) + \sinh[\alpha(L - (x_2 - x))]U(x_2 - x) \\
&\left. + \sinh[\alpha(L - (x - x_1))]U(x - x_1) - \sinh[\alpha(L - (x_1 - x))]U(x_1 - x) \right\}
\end{aligned}$$

Special 1-D Longitudinal Case

$$\begin{aligned}
K_y &\rightarrow 0 \\
y_2 &\rightarrow +\infty \\
y_1 &\rightarrow -\infty \\
K_z &\rightarrow 0
\end{aligned}$$

The 1-D longitudinal groundwater mounding problem can be found by setting $K_y = 0$ and $y_2 = +\infty$, $y_1 = -\infty$ in Equation (C.55).

$$H^*(x, \infty) = H_1 + (H_2 - H_1) \frac{x}{L} + \frac{l(Lx - x^2)}{2K_x B} - \frac{2F}{BLK_x} \left[\frac{x(x_2^2 - x_1^2)}{4} - \frac{Lx(x_2 - x_1)}{2} + \frac{L(x - x_1)^2 U(x - x_1)}{4} - \frac{L(x - x_2)^2 U(x - x_2)}{4} \right] \quad (C.61)$$

$$\frac{\partial H^*}{\partial x}(x, \infty) = \frac{(H_2 - H_1)}{L} + \frac{l(L - 2x)}{2K_x B} - \frac{2F}{BLK_x} \left\{ \frac{(x_2^2 - x_1^2)}{4} - \frac{L(x_2 - x_1)}{2} + \frac{L(x - x_1)U(x - x_1)}{2} - \frac{L(x - x_2)U(x - x_2)}{2} \right\} \quad (C.62)$$

Special Depth Averaged Solution

$$h(x, y, \infty) = \frac{\int_{z_1}^{z_2} H(x, y, z, \infty) dz}{\int_{z_1}^{z_2} dz}$$

The 3-D solutions given by Equations (C.44)-(C.47) can be depth averaged by integrating each equation with respect to z from z_1 to z_2 and then dividing through by $z_2 - z_1$ (where $B \geq z_2 > z_1 \geq 0$). The resultant values will represent the average value of the variable over the depth interval z_1 to z_2 . The following new variables are defined as:

$$h(x, y, \infty) = \int_{z_1}^{z_2} \frac{H(x, y, z, \infty)}{(z_2 - z_1)} dz \quad (C.63)$$

$$\frac{\partial h}{\partial x}(x, y, \infty) = \int_{z_1}^{z_2} \frac{\partial H(x, y, z, \infty)}{\partial x} \cdot \frac{1}{(z_2 - z_1)} dz \quad (C.64)$$

$$\frac{\partial h}{\partial y}(x, y, \infty) = \int_{z_1}^{z_2} \frac{\partial H(x, y, z, \infty)}{\partial y} \cdot \frac{1}{(z_2 - z_1)} dz \quad (C.65)$$

$$\frac{\partial h}{\partial z}(x, y, \infty) = \int_{z_1}^{z_2} \frac{\partial H(x, y, z, \infty)}{\partial z} \cdot \frac{1}{(z_2 - z_1)} dz \quad (\text{C.66})$$

Upon integration, Equations (C.44) - (C.47) reduce to:

$$\begin{aligned} h(x, y, \infty) = & H_1 + (H_2 - H_1) \frac{x}{L} + \frac{l(Lx - x^2)}{2K_x B} + \frac{l}{K_z B} \\ & \left(\frac{B^2}{3} - \frac{B(z_2 + z_1)}{2} + \frac{(z_2^2 + z_1 z_2 + z_1^2)}{6} \right) \quad (\text{C.67}) \\ & - \frac{2l}{K_z B} \sum_{n=1}^{\infty} \frac{[\sin(\psi_n z_2) - \sin(\psi_n z_1)]}{(z_2 - z_1) \psi_n^3 \sinh(\alpha L)} [\sinh[\alpha(L - x)] + \sinh(\alpha x)] \\ & + \frac{F}{2K_z B} [\text{sign}(y_2 - y) - \text{sign}(y_1 - y)] [U(x - x_1) - U(x - x_2)] \\ & \left[\frac{B^2}{3} - \frac{B(z_2 + z_1)}{2} + \frac{(z_2^2 + z_1 z_2 + z_1^2)}{6} \right] \\ & - \frac{F}{2K_z B} [\text{sign}(y_2 - y) - \text{sign}(y_1 - y)] \sum_{n=1}^{\infty} \frac{[\sin(\psi_n z_2) - \sin(\psi_n z_1)]}{\psi_n^3 (z_2 - z_1) \sinh(\alpha L)} \left\{ \sinh[\alpha(L - (x + x_1))] \right. \\ & \quad - \sinh[\alpha(L - (x + x_2))] - \sinh[\alpha(L - (x - x_2))] U(x - x_2) \\ & \quad + \sinh[\alpha(L - (x_2 - x))] U(x_2, x) + \sinh[\alpha(L - (x - x_1))] U(x - x_1) \\ & \quad \left. - \sinh[\alpha(L - (x_1 - x))] U(x_1 - x) \right\} \\ & - \frac{F}{LBK_x} \sum_{m=1}^{\infty} \frac{\sin(\beta_m x)}{\beta_m^3} [\cos(\beta_m x_1) - \cos(\beta_m x_2)] \cdot \left[\text{sign}(y_1 - y) \cdot e^{-\beta_m |y_1 - y| \sqrt{\frac{K_x}{K_y}}} \right. \\ & \quad \left. - \text{sign}(y_2 - y) \cdot e^{-\beta_m |y_2 - y| \sqrt{\frac{K_x}{K_y}}} \right] \end{aligned}$$

$$-\frac{2F}{LB} \sum_{n=1}^{\infty} \frac{[\sin(\psi_n z_2) - \sin(\psi_n z_1)]}{\psi_n(z_2 - z_1)} \sum_{m=1}^{\infty} \frac{\sin(\beta_m x)}{\beta_m(\beta_m^2 K_x + \psi_n^2 K_z)} [\cos(\beta_m x_2) - \cos(\beta_m x_1)]$$

$$\cdot [e^{-a|y_1 - y|} \text{sign}(y_1 - y) - e^{-a|y_2 - y|} \text{sign}(y_2 - y)]$$

where

$$\beta_m = m\pi/L$$

$$\psi_n = n\pi/B$$

$$a = \sqrt{\frac{\beta_m^2 K_x + \psi_n^2 K_z}{K_y}}$$

$$\alpha = \psi_n \sqrt{K_z/K_x}$$

$$\frac{\partial h}{\partial x}(x, y, \infty) = \frac{(H_2 - H_1)}{L} + \frac{l(L - 2x)}{2K_x B}$$

$$- \frac{2l}{B\sqrt{K_x K_z}} \sum_{n=1}^{\infty} \frac{[\sin(\psi_n z_2) - \sin(\psi_n z_1)]}{\psi_n^2(z_2 - z_1) \sinh(\alpha L)} \left\{ \cosh[\alpha(L - x)] + \cosh(\alpha x) \right\} \quad (\text{C.68})$$

$$+ \frac{F}{2K_x B} [\text{sign}(y_2 - y) - \text{sign}(y_1 - y)] \left[-\frac{(x_2^2 - x_1^2)}{2L} + (x_2 - x_1) - (x - x_1)U(x - x_1) \right.$$

$$\left. + (x - x_2)U(x - x_2) \right]$$

$$\frac{\partial h}{\partial y}(x, y, \infty) = -\frac{F}{LB\sqrt{K_x K_y}} \sum_{m=1}^{\infty} \frac{\sin(\beta_m x)}{\beta_m^2} [\cos(\beta_m x_2) - \cos(\beta_m x_1)] \quad (\text{C.69})$$

$$\begin{aligned}
& - \frac{2F}{LB} \sum_{n=1}^{\infty} \frac{[\sin(\psi_n z_2) - \sin(\psi_n z_1)]}{\psi_n (z_2 - z_1)} \sum_{m=1}^{\infty} \frac{\cos(\beta_m x)}{(\beta_m^2 K_x + \psi_n^2 K_z)} [\cos(\beta_m x_2) - \cos(\beta_m x_1)] \\
& \quad \cdot \left\{ e^{-a|y_1 - y|} \text{sign}(y_1 - y) - e^{-a|y_2 - y|} \text{sign}(y_2 - y) \right\} \\
& - \frac{F}{LBK_x} \sum_{m=1}^{\infty} \frac{\cos(\beta_m x)}{B_m^2} [\cos(\beta_m x_2)] - \cos(\beta_m x_1) \left[\text{sign}(y_1 - y) \cdot e^{-\beta_m |y_1 - y| \sqrt{\frac{K_x}{K_y}}} \right. \\
& - \left. \text{sign}(y_2 - y) \cdot e^{-\beta_m |y_2 - y| \sqrt{\frac{K_x}{K_y}}} \right] \\
& - \frac{2F}{LB} \sum_{n=1}^{\infty} \frac{[\cos(\psi_n z_2) - \cos(\psi_n z_1)]}{(z_2 - z_1)} \sum_{m=1}^{\infty} \frac{\sin(\beta_m x)}{\beta_m (\beta_m^2 K_x + \psi_n^2 K_z)} [\cos(\beta_m x_2) - \cos(\beta_m x_1)] \\
& \quad \cdot \left\{ e^{-a|y_1 - y|} \cdot \text{sign}(y_1 - y) - e^{-a|y_2 - y|} \cdot \text{sign}(y_2 - y) \right\} \\
& \quad \cdot \left[e^{-\beta_m |y_1 - y| \sqrt{\frac{K_x}{K_y}}} - e^{-\beta_m |y_2 - y| \sqrt{\frac{K_x}{K_y}}} \right] \\
& - \frac{2F}{LB} \sum_{n=1}^{\infty} \frac{[\sin(\psi_n z_2) - \sin(\psi_n z_1)]}{\psi_n (z_2 - z_1)} \sum_{m=1}^{\infty} \frac{\sin(\beta_m x)}{\beta_m \sqrt{K_y} (\beta_m^2 K_x + \psi_n^2 K_z)} \\
& \quad \cdot [\cos(\beta_m x_2) - \cos(\beta_m x_1)] \left\{ e^{-a|y_1 - y|} - e^{-a|y_2 - y|} \right\} \\
& + \frac{F}{2K_x B} [\text{sign}(y_2 - y) - \text{sign}(y_1 - y)] \left[- \frac{x(x_2^2 - x_1^2)}{2L} + x(x_2 - x_1) - \frac{(x - x_1)^2 U(x - x_1)}{2} \right. \\
& \left. + \frac{(x - x_2)^2 U(x - x_2)}{2} \right]
\end{aligned}$$

$$\begin{aligned}
\frac{\partial h}{\partial z}(x, y, \infty) &= \frac{I}{K_z B} \left(-B + \frac{(z_2 + z_1)}{2} \right) \\
&- \frac{2I}{K_z B} \sum_{n=1}^{\infty} \frac{[\cos(\psi_n z_2) - \cos(\psi_n z_1)]}{\psi_n^2 (z_2 - z_1) \sinh(\alpha L)} \left\{ \sinh[\alpha(L-x)] + \sinh(\alpha x) \right\} \\
&+ \frac{F}{2K_z B} [\text{sign}(y_2 - y) - \text{sign}(y_1 - y)] [U(x - x_1) - U(x - x_2)] \left[-B + \frac{(z_2 + z_1)}{2} \right] \\
&- \frac{F}{2K_z B} [\text{sign}(y_2 - y) - \text{sign}(y_1 - y)] \sum_{n=1}^{\infty} \frac{[\cos(\psi_n z_2) - \cos(\psi_n z_1)]}{\psi_n^2 (z_2 - z_1) \sinh(\alpha L)} \\
&\quad \cdot \left\{ \sinh[\alpha(L - (x + x_1))] - \sinh[\alpha(L - (x + x_2))] - \sinh[\alpha(L - (x - x_2))] U(x - x_2) \right. \\
&\quad + \sinh[\alpha(L - (x_2 - x))] U(x_2 - x) + \sinh[\alpha(L - (x - x_1))] U(x - x_1) \\
&\quad \left. - \sinh[\alpha(L - (x_1 - x))] U(x_1 - x) \right\} \\
&- \frac{F}{2B\sqrt{K_x K_z}} [\text{sign}(y_2 - y) - \text{sign}(y_1 - y)] \sum_{n=1}^{\infty} \frac{[\sin(\psi_n z_2) - \sin(\psi_n z_1)]}{\psi_n^2 (z_2 - z_1) \sinh(\alpha L)} \\
&\quad \left\{ \cosh[\alpha(L - (x + x_1))] \cosh[\alpha(L - (x + x_2))] + \cosh[\alpha(L - (x - x_2))] U(x - x_2) \right. \\
&\quad + \cosh[\alpha(L - (x_2 - x))] U(x_2 - x) - \cosh[\alpha(L - (x - x_1))] U(x - x_1) \\
&\quad \left. - \cosh[\alpha(L - (x_1 - x))] U(x_1 - x) \right\}
\end{aligned} \tag{C.70}$$

This page intentionally left blank.

APPENDIX D

VERIFICATION AND VALIDATION OF THE EPA'S COMPOSITE MODEL FOR TRANSFORMATION PRODUCTS (EPACMTP), AND ITS DERIVATIVES

This page intentionally left blank.

TABLE OF CONTENTS

| | Page |
|---|-------------|
| D.1 VERIFICATION HISTORY | D-1 |
| D.1.1 ORD VERIFICATION (1992-1993) | D-1 |
| D.1.2 MODULE-LEVEL VERIFICATION (1993-1994) | D-1 |
| D.1.2.1 Vadose-Zone Module Verification | D-1 |
| D.1.2.2 Aquifer Module Verification | D-3 |
| D.1.2.3 Metals Transport Module | D-6 |
| D.1.3 VERIFICATION OF INDIVIDUAL MODULES AND A COMPOSITE MODEL IN EPACMTP (1997) | D-6 |
| D.1.3.1 Vadose-Zone Module Verification | D-9 |
| D.1.3.2 Aquifer Module Verification | D-9 |
| D.1.3.3 Composite Model Verification | D-9 |
| D.1.4 VERIFICATION OF 3MRA SUBSURFACE FLOW AND TRANSPORT MODULES (1999) | D-12 |
| D.1.4.1 Vadose-Zone Module Verification | D-12 |
| D.1.4.2 Aquifer Module Verification | D-12 |
| D.1.4.3 Pseudo-3D Module Verification | D-15 |
| D.1.5 COMPREHENSIVE VERIFICATION OF THE 3MRA VADOSE-ZONE AND PSEUDO-3D AQUIFER MODULES (2000) | D-15 |
| D.1.5.1 Vadose-Zone Module Verification | D-15 |
| D.1.5.2 Aquifer Module Verification | D-16 |
| D.2 VALIDATION HISTORY | D-16 |
| D.2.1 BORDEN SITE | D-16 |
| D.2.2 LONG ISLAND SITE | D-17 |
| D.2.3 DODGE CITY SITE | D-17 |
| D.2.4 EBOS SITE | D-18 |
| D.3 SUMMARY | D-18 |
| D.4 REFERENCES | D-19 |

LIST OF TABLES

| | Page |
|------------|--|
| Table D.1 | Summary of EPACMTP Verification by the Office of Research and Development, U.S. EPA, and Tetra Tech, Inc. in 1992-1993 (from US EPA, 1992) D-2 |
| Table D.2 | Verification Cases for the Vadose-Zone Module (1993-1994) . . . D-4 |
| Table D.3 | Verification Cases for the Saturated Zone Module (1993-1994) . . D-5 |
| Table D.4 | Verification Cases for Metals Transport in the Vadose-Zone (1993-1994) D-7 |
| Table D.5a | Verification Cases for the Vadose-Zone Module (1997) D-7 |
| Table D.5b | Verification Cases for the Aquifer Module (1997) D-8 |
| Table D.5c | Verification Cases for Composite Module (1997) D-8 |
| Table D.6a | Verification Cases for the 3MRA Vadose-Zone Module (1999) . D-10 |
| Table D.6b | Verification Cases for the 3MRA Aquifer Module (1999) D-11 |
| Table D.6c | Verification Cases for the 3MRA Pseudo-Three Dimensional Aquifer Module (1999) D-11 |
| Table D.7a | Verification Cases for the 3MRA Vadose-Zone Module (2000) . D-13 |
| Table D.7b | Verification Cases for the 3MRA Aquifer Module (2000) D-14 |

APPENDIX D

VERIFICATION AND VALIDATION OF THE EPA'S COMPOSITE MODEL FOR TRANSFORMATION PRODUCTS (EPACMTP), AND ITS DERIVATIVES

D.1 VERIFICATION HISTORY

EPACMTP has been verified extensively by comparing its simulation results against both analytical and numerical solutions. Numerous verification cases were conducted from 1991-2000. A summary of the verification cases is provided in the following subsections. The accompanying Figures for selected test cases are presented in the designated Subappendices.

Subsequent to the verification described below, version 2 of the EPACMTP model (the version of EPACMTP that includes the pseudo-3D aquifer transport option) was tested and verified. The results of this verification are documented in U.S. EPA, 2001.

D.1.1 ORD VERIFICATION (1992-1993)

In 1992, a verification analysis of the newly developed EPACMTP was performed by the Office of Research and Development (ORD) of the US EPA (US EPA, 1992). A list of verification cases in the verification exercise is listed in Table D.1. As shown in the table, two steps of code verification were conducted: a re-verification of the original test problems and data files provided by HydroGeoLogic, Inc. and independent verification using alternative test criteria. Based on the analysis of Tetra Tech, some technical limitations in the EPACMTP code were identified. One of the weaknesses, which occurred in the aquifer module, pertained to potential mass loss of contaminants from the system due to the upstream boundary proximity and conditions in EPACMTP. The code was modified in response to the comments (HydroGeoLogic, Inc., 1993).

D.1.2 MODULE-LEVEL VERIFICATION (1993-1994)

A module-level verification task was performed between 1993-1994 and reported in EPACMTP Background Documents (US EPA, 1996 b, d). Numerous components of EPACMTP's flow and transport sub-modules, in both the vadose and aquifer modules, were verified between 1993-1994 against analytical solutions, and numerical solutions from a number of simulators with similar mathematical frameworks. Details of the verification are presented below.

D.1.2.1 Vadose-Zone Module Verification

The vadose-zone and the aquifer modules were subdivided into the flow and transport sub-modules. The ten verification cases for the vadose-zone module are summarized in Table D.2 and are briefly described below. Excerpts of verification results for the vadose-zone test cases are presented in figures in Subappendix D.A. Reference to the figures in Subappendix D.A is provided in Table D.2. Additional information regarding the test cases and respective verification results may be found in US EPA (1996b). The

Table D.1 Summary of EPACMTP Verification by the Office of Research and Development, U.S. EPA, and Tetra Tech, Inc. in 1992-1993 (from US EPA, 1992)

| Case | Description | Reverification of HGL Tests | Independent Verification |
|------|---|-----------------------------|--------------------------|
| 1 | Steady-state, aquifer flow, single layer | Yes | Yes |
| 2 | Steady-state, vadose-zone transport, two layers | | Yes |
| 3 | Transient vadose-zone transport, single layer - analytical solution | Yes | Yes |
| 4 | Transient vadose-zone transport, single layer - numerical solution | | Yes |
| 5 | Transient vadose-zone transport, single layer, non-conservative solute - numerical solution | | Yes |
| 6 | Transient vadose-zone transport, three layers, non-conservative solute - numerical solution | | Yes |
| 7 | Transient vadose-zone transport, single layer, nonlinear adsorption - numerical solution | Yes | |
| 8 | Multiple species transport; 3-member chain decay; source decay | Yes | |
| 9 | Steady-state, aquifer flow | Yes | Yes |
| 10 | Quasi-3D aquifer transport - numerical solution | Yes | Yes |
| 11 | Non-linear aquifer transport | Yes | Yes |
| 12 | 3-species transport, 2-D (x,y) | Yes | Yes |
| 13 | 7-species transport, 2-D (x,y) | Yes | Yes |
| 14 | Full-3D aquifer flow and transport | Yes | |

vadose-zone module of EPACMTP was originally called FECTUZ. The numerical transport simulation in FECTUZ is no longer part of EPACMTP.

The first three test cases of the vadose-zone module are for the flow sub-module and focus on steady-state flow within layered and non-layered soils. They were verified by comparing the results of the semi-analytical FECTUZ (US EPA, 1989) module against the numerical finite element VADOFT model (Huyakorn, et al., 1987). Test Case 1 evaluated steady-state infiltration in a soil. Test Cases 2 and 3 are similar, both involving steady-state infiltration in a layered soil, whereas Test Case 3 introduced the surface impoundment boundary condition (ponding depth) to the system.

The last seven test cases, summarized in Table D.2, pertain to transport sub-module verification. Test Cases 4 and 5 tested the analytical steady-state transport module and the semi-analytical transport solution, respectively. Test Case 4 involved steady-state transport in a layered soil and verification against the FECTUZ numerical solution, while Test Case 5 evaluated transient transport with verification against both the FECTUZ numerical solution and the HYDRUS code (Kool and van Genuchten, 1991).

Test Cases 6 through 10 utilize the FECTUZ numerical solution to examine transport of a contaminant in a soil column. Case 6 concerns 1-D transport of a conservative solute species and is verified against the analytical solution of Ogata and Banks (1961). Test case 7 considers downward vertical transport of both conservative and non-conservative constituents. The results are compared against the analytical solution given by van Genuchten and Alves (1982). Test Case 8 concerns 1-D transport of a conservative solute species in a layered soil column. Two sub-cases with different dispersivity values were compared with the analytical solutions presented by Shamir and Harlemann (1967) and Hadermann (1980). Test Case 9 considers solute transport with both linear and nonlinear adsorption. This is verified against the MOB1 finite element solution (van Genuchten and Alves, 1982). Test Case 10 examines transport of a 3-member, straight decay chain and is verified against the analytical solution, modified from Hodgkinson and Maul (1985).

D.1.2.2 Aquifer Module Verification

The saturated zone module of EPACMTP was originally developed on a stand alone basis and called CANSAZ-3D. Seven benchmark problems were analyzed to verify the flow and transport solutions in the CANSAZ-3D modules; (Sudicky et al, 1990) and are summarized in Table D.3. Excerpts of verification results for the test cases are presented in Subappendix D.B. Reference to the figures in Subappendix D.B is provided in Table D.3. Additional information regarding the test cases and respective verification results may be found in U.S. EPA (1996b). Test Case 1 was designed to verify the 3-D steady-state groundwater flow solution. For this purpose, the hydraulic head and groundwater flow velocities obtained from CANSAZ-3D were compared against the MNDXYZ analytical solution (Ungs, 1986; Appendix B of U.S. EPA, 1996b). Test Case 2 was designed to compare the analytical and numerical transport solutions for the case of single species transport in a uni-directional steady-state groundwater flow field. Test Case 3 involved two-dimensional transport of a 3-member decay chain. The CANSAZ-3D results for this test problem were verified against the numerical VAM2D code (Huyakorn et al., 1992). Test Case 4 involved verification of CANSAZ-3D against an analytical solution (Sudicky et al., 1991) for a case involving a complex, seven-member branched decay chain. Test Case 5 was designed to verify the nonlinear sorption option. This problem involves 1-D flow and transport with a nonlinear Freundlich isotherm. CANSAZ-3D was verified against the numerical MOB1 (van Genuchten, 1981) and FECTUZ. Test Case 6 involves fully 3-D flow and transport. The CANSAZ-3D solution was compared against results obtained with the 3-D DSTRAM flow and transport code (Huyakorn, et al., 1994). Test Case 7 was designed to evaluate

Table D.2 Verification Cases for the Vadose-Zone Module (1993-1994)

| Case | Description | Verification Method | Excerpts of Verification Results Presented in |
|------|---|--|---|
| 1 | Steady-state infiltration | Semi-analytical FECTUZ module vs. fully numerical finite element VADOFT | Figure D.A.1, Subappendix D.A |
| 2 | Steady-state infiltration in a layered soil | Semi-analytical FECTUZ module vs. fully numerical finite element VADOFT | Figure D.A.2, Subappendix D.A |
| 3 | Steady-state infiltration in a layered soil with a ponding depth | Semi-analytical FECTUZ module vs. fully numerical finite element VADOFT | Figure D.A.3, Subappendix D.A |
| 4 | Steady-state transport in a layered soil | Steady-state analytical solution vs. finite element numerical solution of FECTUZ | Figure D.A.4, Subappendix D.A |
| 5 | 1-D transient transport under pulse input conditions | Semi-analytical solution vs. numerical finite element module of FECTUZ and the HYDRUS code | Figure D.A.5, Subappendix D.A |
| 6 | 1-D transport of a conservative solute species in a saturated soil column of semi-infinite length | Numerical solution of FECTUZ vs. analytical solution of Ogata and Banks (1961) | Figure D.A.6, Subappendix D.A |
| 7 | 1-D transport of a conservative and non-conservative solute species in a saturated soil column of finite length | FECTUZ vs. analytical solution of van Genuchten and Alves (1982) | Figure D.A.7, Subappendix D.A |
| 8 | Transport of a conservative species in a layered soil column | FECTUZ vs. Shamir and Harleman (1967) and Hadermann (1980) | Figures D.A.8 and D.A.9, Subappendix D.A |
| 9 | Transient transport under conditions of nonlinear adsorption with a pulse source | FECTUZ vs. finite difference code MOB1 | Figure D.A.10, Subappendix D.A |
| 10 | Multispecies transport with three member, straight decay chain with a decaying source boundary condition | FECTUZ vs. analytical solution modified from Hodgkinson and Maul (1985) | Figure D.A.11, Subappendix D.A |

Table D.3 Verification Cases for the Saturated Zone Module (1993-1994)

| Case | Description | Verification Method | Excerpts of Verification Results Presented in |
|-------------|--|--|--|
| 1 | Steady-state groundwater flow in a 3-D domain | CANSAZ-3D vs. analytical solution of MNDXYZ | Figure D.B.1, Subappendix D.B |
| 2 | Single species transport in a uni-directional flow field - analytical and numerical transport modules | CANSAZ-3D vs. 3-D analytical solution | Figure D.B.2, Subappendix D.B |
| 3 | 2-D transport of a 3-member decay chain. Steady-state flow and transient solute transport in an unconfined aquifer | CANSAZ-3D vs. VAM2D | Figure D.B.3, Subappendix D.B |
| 4 | 2-D transport of a complex, seven-member branched decay chain with 1-D groundwater flow | CANSAZ-3D vs. Gaussian source analytical solution of Sudicky et al. (1991) | Figure D.B.4, Subappendix D.B |
| 5 | Nonlinear sorption reactions in a 1-D, steady-state flow and transient transport. Pulse source using a Freundlich isotherm | CANSAZ-3D vs. MOB1 and FECTUZ | Figure D.B.5, Subappendix D.B |
| 6 | Steady-state flow and transport modeling of a single conservative species in 3-D aquifer domain | CANSAZ-3D vs. DSTRAM | Figure D.B.6, Subappendix D.B |
| 7 | Steady-state groundwater flow and transient solute transport in 3-D aquifer domain with a horizontal patch source | CANSAZ-3D vs. VAM3D | Figure D.B.7, Subappendix D.B |

the automatic model domain discretization option for a 3-D flow and transport problem and was verified against the numerical VAM3D code (Panday et al., 1993).

D.1.2.3 Metals Transport Module

The major modifications to accommodate metals transport with nonlinear sorption were made to the vadose-zone module, therefore the verification cases are applicable to this module. Five verification test cases are summarized in Table D.4 and excerpts of verification results are presented in Subappendix D.C. Reference to the figures in Subappendix D.C is provided in Table D.4. Additional information regarding the test cases and respective verification results may be found in U.S. EPA (1996d). Test Case 1 involved continuous release of a non-sorbing solute to test the linear adsorption partitioning capabilities. An analytical solution from Ogata (1970) was compared against the EPACMTP results. Test Case 2 involved nonlinear Freundlich adsorption isotherms. The Freundlich isotherm was represented by its closed form. Two different source conditions were utilized: continuous and finite sources. Freundlich exponents greater than and less than one were examined. The results from EPACMTP were compared with those from HYDRUS. Test Case 3 involves transport of lead in a fully saturated soil column. The verification of this case was performed by comparing the computed cumulative mass against the total input mass. Test Case 4 involves 1-D transport of a solute, with Freundlich exponents of less than and greater than one and was verified against HYDRUS.

D.1.3 VERIFICATION OF INDIVIDUAL MODULES AND A COMPOSITE MODEL IN EPACMTP (1997)

In 1997, a testing plan was developed for EPACMTP code verification (US EPA, 1997), in accordance with the ASTM, "Standard Guide for Developing and Evaluating Ground-Water Modeling Codes" (ASTM, 1996). The verification process focused on a single problem geometry, representative of waste disposal scenarios in terms of spatial dimensionality and climatic/hydrogeological conditions. The verification process first subdivided the problem setting into individual hydrogeologic components, assessed their functionality relative to an overall fate and transport problem, and then compared each component to analytical solutions or other codes.

The vadose-zone module, the aquifer module, and the composite model were verified following the ASTM standards. The vadose-zone problem geometry was a 1-D column extending from the land surface to the water table. Boundary conditions for numerical contaminant transport involved a continuous source on the water table beneath the waste management unit. The region of the water table outside the source area received constant recharge from the ground surface. Ten test cases were conducted. These test cases may be subdivided into those for the vadose-zone module, the aquifer module, and the composite model, and are summarized in Tables D.5a, D.5b, and D.5c, respectively.

Table D.4 Verification Cases for Metals Transport in the Vadose-Zone (1993-1994)

| Case | Description | Verification Method | Excerpts of Verification Results Presented in |
|------|---|--|---|
| 1 | Linear adsorption partitioning with continuous release of a non-sorbing solute | Analytical solution (Ogata, 1970) vs. EPACMTP result | Figure D.C.1, Subappendix D.C |
| 2 | Nonlinear adsorption isotherm. The Freundlich isotherm was represented by its closed function form. Freundlich isotherms greater than and less than one were considered for continuous and finite source conditions | EPACMTP vs. HYDRUS | Figures D.C.2 and D.C.3, Subappendix D.C |
| 3 | Transport of lead using MINTEQA2-generated isotherms | Cumulative vs. total input mass | Figure D.C.4, Subappendix D.C |
| 4 | Pulse source and Freundlich exponents of 0.5, 0.8, and 1.5 | Analytic solution vs. HYDRUS | Figure D.C.5, Subappendix D.C |

Table D.5a Verification Cases for the Vadose-Zone Module (1997)

| Case | Description | Verification Method | Excerpts of Verification Results Presented in |
|------|---|--|---|
| 1 | Steady-state variably saturated flow | EPACMTP vs. STAFF3D | Figure D.D.1, Subappendix D.D |
| 2 | Infiltration through a clay liner from a surface impoundment | EPACMTP vs. STAFF3D | Figure D.D.2, Subappendix D.D |
| 3 | Contaminant transport with linear sorption and decay | Numerical EPACMTP vs. analytical EPACMTP | Figure D.D.3, Subappendix D.D |
| 4 | Contaminant transport with branched chain decay and linear sorption | EPACMTP vs. VAM2D | Figure D.D.4, Subappendix D.D |

Table D.5b Verification Cases for the Aquifer Module (1997)

| Case | Description | Verification Method | Excerpts of Verification Results Presented in |
|------|---|--|---|
| 5 | 3-D steady-state groundwater flow | EPACMTP vs. MNDXYZ analytical solution | Figure D.E.1 and D.E.2, Subappendix D.E |
| 6 | 3-D contaminant transport with linear sorption and decay | EPACMTP numerical module vs. EPACMTP analytical module; EPACMTP vs. VAM3DF | Figure D.E.3, Subappendix D.E |
| 7 | 3-D contaminant transport with four species, branched chain decay and linear sorption | EPACMTP vs. STAFF3D | Figure D.E.4, Subappendix D.E |

Table D.5c Verification Cases for Composite Module (1997)

| Case | Description | Verification Method | Excerpts of Verification Results Presented in |
|------|--|---------------------|---|
| 8 | Composite flow and contaminant transport | EPACMTP vs. VAM3DF | Figure D.F.1, Subappendix D.F |
| 9 | Monte Carlo analysis based on composite flow and contaminant transport | EPACMTP vs. VAM3DF | Figure D.F.2, Subappendix D.F |

D.1.3.1 Vadose-Zone Module Verification

The vadose-zone module verification is summarized with four cases in Table D.5a and excerpts of verification results are presented in Subappendix D.D. Reference to the figures in Subappendix D.D is provided in Table D.5a. Additional information regarding the test cases and respective verification results may be found in U.S. EPA (1997). Test Case 1 evaluated steady-state variably saturated flow and Test Case 2 considers infiltration through a clay liner and ponding depth. Test Cases 3 and 4 both considered contaminant transport with linear sorption, but Test Case 3 examined linear decay while Test Case 4 evaluated four species with branched chain decay. Test Cases 1 and 2 were verified against STAFF3D (HydroGeoLogic, Inc., 1995a), Test Case 4 was verified against VAM2D while Test Case 3 compared the steady-state results from numerical and analytical transport modules of EPACMTP.

D.1.3.2 Aquifer Module Verification

The aquifer module verification is summarized with three cases in Table D.5b and excerpts of verification results are shown in Subappendix D.E. Reference to the figures in Subappendix D.E is provided in Table D.5b. Additional information regarding the test cases and respective verification results may be found in U.S. EPA (1997). The 3-D steady-state fully saturated flow module in EPACMTP was verified against the analytical solution MNDXYZ in Test Case 5. Test Cases 6 and 7 examined contaminant transport and were verified against VAM3DF (HydroGeoLogic, Inc., 1995b) and STAFF3D, respectively. Test Case 6 involved transport of a contaminant with linear sorption and decay, while Test Case 7 involved linear sorption and a four species, branched chain decay.

D.1.3.3 Composite Model Verification

The EPACMTP composite model comprises the following fate and transport modules: a vadose-zone module, and a aquifer (saturated zone) module. These modules are connected according to the detailed description in US EPA (1996). The composite model verification is summarized with two test cases in Table D.5c and excerpts of verification results are shown in Subappendix D.F. Reference to the figures in Subappendix D.F is provided in Table D.5c. Additional information regarding the test cases and respective verification results may be found in U.S. EPA (1997). Test Case 8 considered the composite flow and contaminant transport structure. Test Case 9 assessed the sensitivity of the geometric assumptions used to develop EPACMTP. A limited Monte-Carlo analysis was performed to assess the sensitivity of the confined water table assumption to predicting the probability of exceedance at a monitoring well. Both Test Cases 8 and 9 were verified against VAM3DF which is a 3D, variably saturated numerical flow and transport code.

Table D.6a Verification Cases for the 3MRA Vadose-Zone Module (1999)

| Case | Description | Verification Method | Excerpts of Verification Results Presented in |
|-------------|---|--|--|
| 1 | Exponentially depleting conservative source with no sorption or hydrolysis | Vadose-Zone Module vs. EPACMTP | Figure D.G.1, Subappendix D.G |
| 2 | Constant-concentration source pulse with no sorption or hydrolysis | Vadose-Zone Module vs. EPACMTP | Figure D.G.2, Subappendix D.G |
| 3 | Constant-concentration source pulse with sorption and hydrolysis, one species | Vadose-Zone Module vs. EPACMTP | Figure D.G.3, Subappendix D.G |
| 4 | Constant-concentration source pulse with sorption and hydrolysis, and chain decay | Vadose-Zone Module vs. EPACMTP | Figure D.G.4, Subappendix D.G |
| 5 | Metals: (Mercury, and Lead), with constant-concentration source pulse with MINTEQ-based sorption and no hydrolysis | Vadose-Zone Module vs. EPACMTP | Figures D.G.5 and D.G.6, Subappendix D.G |
| 6 | Constant-concentration source pulse with biodegradation, sorption and chain decay | Vadose-Zone Module vs. EPACMTP | Figure D.G.7, Subappendix D.G |
| 7 | 1-D contaminant transport between a top boundary at the bottom of the source zone and the water table with mass loading to the top boundary from the leachate flux from the source module | Vadose-Zone Module vs. MODFLOW-SURFACT | Figure D.G.8, Subappendix D.G |
| 8 | 1-D variable saturated flow between a top boundary at the bottom of the source zone and the water table with mass loading to the top boundary from the leachate flux from the source module | Vadose-Zone Module vs. MODFLOW-SURFACT | Figure D.G.9, Subappendix D.G |

Table D.6b Verification Cases for the 3MRA Aquifer Module (1999)

| Case | Description | Verification Method | Excerpts of Verification Results Presented in |
|------|---|----------------------------|--|
| 1 | Exponentially depleting source with no sorption or hydrolysis | Aquifer Module vs. EPACMTP | Figure D.H.1, Subappendix D.H |
| 2 | Constant-concentration source pulse with no sorption or hydrolysis | Aquifer Module vs. EPACMTP | Figure D.H.2, Subappendix D.H |
| 3 | Constant-concentration source pulse with sorption and hydrolysis, one species | Aquifer Module vs. EPACMTP | Figure D.H.3, Subappendix D.H |
| 4 | Constant-concentration source pulse with sorption and hydrolysis, and two species with chain decay | Aquifer Module vs. EPACMTP | Figures D.H.4 and D.H.5, Subappendix D.H |
| 5 | Metals: (Mercury, and Lead), with constant-concentration source pulse with sorption and no hydrolysis | Aquifer Module vs. EPACMTP | Figure D.H.6, Subappendix D.H |
| 6 | Constant-concentration source pulse with biodegradation, sorption and four species chain decay | Aquifer Module vs. EPACMTP | Figures D.H.7, D.H.8, D.H.9, and H.10, Subappendix D.H |
| 7 | Comparison of Monte Carlo saturated zone simulations | Aquifer Module vs. EPACMTP | Figure D.H.11, Subappendix D.H |

Table D.6c Verification Cases for the 3MRA Pseudo-Three Dimensional Aquifer Module (1999)

| Case | Description | Verification Method | Excerpts of Verification Results Presented in |
|------|--|--|---|
| 1 | Average Groundwater Specific Flow Rate | Aquifer Module vs. Darcy's Law analytical solution | Figure D.I.1, Subappendix D.I |
| 2 | Numerical Component of the Contaminant Transport Sub-module | Aquifer Module vs. analytical solution by Ogata | Figure D.I.2, Subappendix D.I |
| 3 | Analytical-Numerical Component of the Contaminant Transport Sub-module | Aquifer Module vs. analytical solution | Figure D.I.3, Subappendix D.I |

D.1.4 VERIFICATION OF 3MRA SUBSURFACE FLOW AND TRANSPORT MODULES (1999)

In 1999, the flow and transport components for the vadose-zone module and aquifer module were extracted from EPACMTP to provide the groundwater pathway module for the multi-media, multi-pathway, and multiple receptor risk assessment modeling system (3MRA). The basic premise for verification of the vadose-zone and aquifer modules was that EPACMTP had been rigorously verified, so it was sufficient to show that the modules reproduced EPACMTP results. Therefore, both the steady-state flow and transport sub-modules of the aquifer module (US EPA, 1999c) and the flow and transport sub-modules of the vadose-zone module (US EPA, 1999b,c) were compared against the numerical results from EPACMTP to ensure that the extracted modules remained intact. There are two exceptions that will be discussed below. The new saturated zone pseudo-3D module was also developed during this period (US EPA, 1999a).

The eighteen test cases for the vadose-zone, aquifer, and pseudo 3-D modules are summarized in Tables D.6a, D.6b, and D.6c, respectively. The figures are presented in Subappendix D.G through D.I. The vadose-zone problem geometry was a 1-D column extending from the land surface to the water table. Boundary conditions for numerical contaminant transport involved a continuous source on the water table beneath the waste management unit. The region of the water table outside the source area was also considered to be a recharge boundary.

D.1.4.1 Vadose-Zone Module Verification

There are eight vadose-zone module verification cases (Table D.6a). Excerpts of results for the verification cases are presented in Subappendix D.G. Reference to the figures in Subappendix D.G is provided in Table D.6a. Additional information regarding the test cases and respective verification results may be found in U.S. EPA (1999b,c). All of the cases concern contaminant transport. Test Case 1 evaluated an exponentially depleting source. Test Case 2 involved transport of a contaminant with no sorption and no hydrolysis. Test Case 3 examined sorption and hydrolysis with one species, while Test Case 4 involved two species with chain decay. Test Case 5 examined linear and nonlinear metal transport using the MINTEQA2 isotherms. Test Case 6 evaluated biodegradation resulting in chain decay reactions with four species. Test Cases 7 and 8 examined contaminant concentration at a receptor well and pressure heads at each grid node, respectively. In this instance, both Test Case 7 and 8 were verified against MODFLOW-SURFACT (HydroGeoLogic, Inc., 1996), a three-dimensional numerical groundwater flow and transport code.

D.1.4.2 Aquifer Module Verification

There are seven aquifer module verification cases (Table D.6b) with excerpts of verification results presented in Subappendix D.H. Reference to the figures in Subappendix D.H is provided in Table D.6b. Additional information regarding the test cases and respective verification results may be found in U.S. EPA (1999c).

Table D.7a Verification Cases for the 3MRA Vadose-Zone Module (2000)

| Test Area | General Requirements | Number of Verification Cases | Excerpts of Verification Results Presented in |
|-----------|---|------------------------------|---|
| 1 | Verification of reading and screening of source and site- specific input data | 3 | N/A |
| 2 | Verification of pre-simulation processing of input data | 2 | N/A |
| 3 | Verification of the flow component | 1 | N/A |
| 4 | Verification of the non-metals transport component | 5 | Figure D.J.1, Subappendix D.J |
| 5 | Verification of the metals transport component | 4 | Figure D.J.2, Subappendix D.J |
| 6 | Verification of post simulation output | 2 | N/A |
| 7 | Verification of the vadose-zone module's robustness | 13 | N/A |

Table D.7b Verification Cases for the 3MRA Aquifer Module (2000)

| Test Area | General Requirements | Number of Verification Cases | Excerpts of Verification Results Presented in |
|-----------|---|------------------------------|---|
| 1 | Verification of reading and screening of source and site-specific input data | 4 | N/A |
| 2 | Verification of pre-simulation processing of input data | 17 | N/A |
| 3 | Verification of the fractured media component | 3 | N/A |
| 4 | Verification of the heterogeneous saturated media component | 1 | N/A |
| 5 | Verification of reading and screening of chemical-specific, biodegradation, and metal-specific data | 6 | N/A |
| 6 | Verification of numerical grid generation | 4 | N/A |
| 7 | Verification of the flow component | 4 | N/A |
| 8 | Verification of the contaminant fate and transport component | 19 | Figures D.K.1 and D.K.2, Subappendix D.K |
| 9 | Verification of the aquifer module's robustness | 11 | N/A |

Test Case 1 evaluated an exponentially depleting source. Test Case 2 involved transport of a conservative contaminant with no sorption and no hydrolysis. Test Case 3 examined sorption and hydrolysis with one species, while Test Case 4 involved two species with chain decay. Test Case 5 examined linear and nonlinear metal transport using the MINTEQA2 isotherms. Test Case 6 evaluated biodegradation resulting in chain decay reactions with four species. Test Case 7 evaluated the generated Monte Carlo distributions.

D.1.4.3 Pseudo-3D Module Verification

There are three verification cases for the pseudo-3D aquifer module (Table D.6c). Excerpts of verification results are shown in Subappendix D.I. Reference to the figures in Subappendix D.I is provided in Table D.6c. Additional information regarding the test cases and respective verification results may be found in U.S. EPA (1999a,c). Test Case 1 examined the average groundwater specific flow rate determined by the saturated flow sub-module and was verified using Darcy's Law. Test Case 2 examined the numerical component of the contaminant transport sub-module and is verified using the analytical solution by Ogata (1970). Test Case 3 verified the combined analytical-numerical contaminant transport sub-module using verification results of Test Case 2 subject to the analytical portion of the aquifer transport sub-module.

D.1.5 COMPREHENSIVE VERIFICATION OF THE 3MRA VADOSE-ZONE AND PSEUDO-3D AQUIFER MODULES (2000)

In 2000, a comprehensive verification was conducted of all of the components in the extracted aquifer and the vadose-zone modules (US EPA, 2000 a,b). For testing purposes, each component was executed as a stand-alone program outside of the 3MRA Software System environment.

D.1.5.1 Vadose-Zone Module Verification

There are 40 vadose-zone module verification test cases summarized in Table D.7a. Selected figures for Test Areas 4 and 5, the non-metals and metals transport components, are presented in Subappendix D.J. Reference to the figures in Subappendix D.J is provided in Table D.7a. Additional information regarding the test cases and respective verification results may be found in U.S. EPA (2000a). The reading and screening of source and site-specific input data was verified in 3 cases. Verification of the pre-simulation processing of input data was performed with 2 cases. The flow, non-metal transport, and metals transport components were verified with 1, 5 and 4 cases, respectively. The post simulation processing of output data was verified with 2 cases. The robustness testing verified the stability of the simulation when executed with extreme values for selected parameters. The parameters were selected based on the results of a parameter sensitivity analysis (U.S. EPA, 1996e). The vadose-zone module's robustness was verified with 13 cases.

D.1.5.2 Aquifer Module Verification

There are 69 aquifer module verification cases summarized in Table D.7b. Selected figures for Test Area 8, the fate and transport component, are present in Subappendix D.K. Reference to the figures in Subappendix D.K is provided in Table D.7b. Additional information regarding the test cases and respective verification results may be found in U.S. EPA (2000b). The reading and screening of source and site-specific input data was verified in 4 cases. Verification of the pre-simulation processing of input data was performed with 17 cases. The fractured media, and heterogeneous saturated media components were verified with 3, and 1 cases, respectively. The reading and screening of chemical-specific, biodegradation and metal-specific data was verified in 6 tests. The numerical grid generation was verified in 4 cases. The flow component was verified with 4 cases, while the contaminant fate and transport component was verified in 19 cases. The robustness testing verified the stability of the simulation when executed with extreme values for selected parameters. The parameters were selected based on the results of a parameter sensitivity analysis (U.S. EPA, 1996e). The aquifer module's robustness was verified with 11 cases.

D.2 VALIDATION HISTORY

Validation, as defined previously, may be conducted using actual measured field data. It is helpful to assess the validity of simplifying assumptions and the predictive capabilities of EPACMTP against well documented realistic site data. EPACMTP and its predecessors (from which flow and transport components in EPACMTP were derived) have been validated based on actual observations at four sites, although no validation has been performed using the 3MRA vadose-zone and aquifer zone modules. In 1990, EPACMS (CANSAZ) was validated against the data from the Borden Landfill site, along with the data from a second agricultural field site on Long Island, New York (US EPA, 1990). This validation included the combination of the saturated and the vadose-zone modules in EPACMS. In 1993, the composite model was validated against data from a Dodge City, Kansas site (Kool et al., 1994). Then, in 1995 EPACMTP was validated against the data from the EBOS Site 24 in New York (US EPA, 1995). The four validation cases are presented in the following subsections. Note that all the figures that are referenced to in the following subsections are presented in Subappendix D.L.

D.2.1 BORDEN SITE

The Borden landfill is located in Borden, southern Ontario, Canada, and occupies an area of approximately 4 ha (Figure D.L.1). The landfill was operational for 36 years and at its closure was capped with a thin layer of sand. The site overlies 8 to 20 meters of a glaciofluvial sand aquifer, which overlies a confining silty clay deposit. The chloride plume extends about 700 m northward of the landfill and occupies nearly the entire vertical thickness of the aquifer. The waste material was deposited just above the water table, therefore transport did not occur in the vadose-zone.

Generally, the flow and transport parameters and the procedure described by Frind and Hokkanen (1987) were used for the EPACMS simulation. The exception is that Frind and Hokkanen assigned a higher recharge rate to some areas outside of the source area, but this refinement was not utilized for the EPACMS simulation. A curvilinear grid was utilized to describe the aquifer geometry and because EPACMS assumes a constant saturated thickness, the VAM3D-CG code (Huyakorn and Panday, 1989) was used to perform the groundwater flow simulation. Next, the CANSAZ (EPACMTP module) module was used to simulate transient transport. CANSAZ utilized the same finite grid as the groundwater flow simulation, as well as the groundwater velocity distribution from the VAM3D simulation.

The chloride concentrations were compared for the observed values (Figure D.L.2), the CANSAZ simulation values (Figure D.L.3) and the Frind and Hokkanen simulation values (Figure D.L.4). The CANSAZ model accurately predicted the extent of the plume and the overall plume shape compared to both the Frind and Hokkanen model and the field values.

D.2.2 LONG ISLAND SITE

The site is located on the south shore of the North Fork of Long Island, New York (Figure D.L.5). The agricultural site was contaminated with the pesticide aldicarb in the 1970's. The source was a 2.5 ha potato field overlying sandy loam soils with a high infiltration rate. An unconfined aquifer is located approximately 2 meters below the surface.

Both site specific data and monitoring data are limited at this site. The site characterization was obtained from previous studies by INTERA (1980) and Carsel et al. (1985). The EPA Pesticide Root Zone Model (PRZM) (Carsel et al, 1984) was used to predict the 3-year average recharge rate and average aldicarb concentration at the base of the root zone as input for the EPACMS vadose-zone module. The steady-state groundwater flow field was generated using the analytical 2-D solution on EPACMS, followed by a three-year transient aldicarb transport simulation.

The simulated concentrations of aldicarb in groundwater with distance from the source were compared with the observed values (Figure D.L.6). The agreement between the simulated and observed concentrations was quite reasonable, with the relative error decreasing with increasing distance from the source.

D.2.3 DODGE CITY SITE

The Dodge City, Kansas site (Figure D.L.7), located in the Arkansas River valley, is documented by Ourisson et al. (1992). The source is a controlled release of Triasulfuron pesticide (non-conservative) and bromide (conservative) which, over a 2 year period, is transported through the vadose-zone and the aquifer. The site covers an area of approximately 2.3 acres (approximately 1 ha) overlying one meter of sandy loam soil which overlies a sand and gravel unit. The water table is located at a depth of three meters.

The Dodge City site was well characterized, the source was well defined and the monitoring data were available for both soil and groundwater. Site specific values were obtained from Ourisson et al., (1992), Carsel and Parrish (1988), Gelhar et al. (1985), Carsel et al. (1984), and derived values. EPACMTP was used to simulate the flow and transport of both conservative and non-conservative constituents.

The groundwater concentration model predictions were compared against the observed values. The model tended to underestimate bromide concentrations (Figure D.L.8) slightly and overestimate Triasulfuron concentrations (Figure D.L.9). The application of the model to the Kansas field site showed reasonably good agreement between model predictions and groundwater monitoring results.

D.2.4 EBOS SITE

The EPRI research site referred to as EBOS site 24 is a disposal site for a coal tar Manufacturing Gas Plant located in New York state (Figure D.10.). Initially, the coal tar was disposed of in a trench on the site, then over time migrated downward into the aquifer (Figure D.L.11 and D.L.12). The site is characterized by 15 to 30 feet of typical glacial outwash sand deposits overlying a clay confining layer. Napthalene was labeled the constituent of concern, since it was the polyaromatic hydrocarbon (PAH) with the highest concentrations in the coal tar.

The site specific parameters were provided by the Electric Power Research Institute in 1993 and consisted of both known and estimated values. EPACMTP was used to simulate the flow and transport of constituents through the vadose-zone and the aquifer. One point to note was that since the coal tar had moved down into the aquifer, the constituents could be leached out through direct contact with ambient groundwater. In the EPACMTP simulation, it was necessary to leach the constituents out of the waste by infiltration from the vadose-zone.

Napthalene concentrations near the source before (Figure D.L.13) and after (Figure D.L.14) source removal were predicted by EPACMTP. The results from EPACMTP were qualitatively similar to the observed concentration in terms of groundwater concentrations near the source.

D.3 SUMMARY

EPACMTP, its predecessors (EPACMS, CANSAZ, and FECTUZ), and its derivatives (3MRA vadose-zone and aquifer modules) have been verified extensively during the past decade at each of the developmental stages. The model has been verified, in numerous cases, by comparing the simulation results against both analytical and numerical solutions. Additionally, EPACMTP and its predecessors have been validated using actual site data from four different sites. The relevant verification and validation history, discussed in the previous sections of this document, is summarized below.

The preliminary verification of EPACMTP was performed by ORD in 1992. Following the preliminary verification, detailed module-level verification was conducted on the

flow and transport sub-modules of the vadose-zone and the aquifer modules between 1993-1994. The modules were verified against analytical solutions, and numerical solutions from a number of well-documented simulators. In 1997, the EPACMTP code was verified utilizing a testing plan developed according to ASTM standards. The vadose-zone and the aquifer modules, as well as the composite model (based on the sequentially linked vadose-zone and aquifer modules), were verified against analytical and numerical solutions. In 1999, the vadose-zone and aquifer modules were extracted from EPACMTP to be included as part of the multi-media, multi-receptor, and multi-pathway risk assessment (3MRA) software system. The flow and transport sub-modules of both modules were verified against the results from EPACMTP. Additionally, for the 3MRA software system a pseudo-3D aquifer module was developed. An exhaustive verification was conducted of all of the components in the extracted vadose-zone module and the new pseudo-3D aquifer module in 2000. The modules were verified against analytical solutions and EPACMTP results.

EPACMTP and its predecessors have been validated using field data from four unique sites from 1990-1995. These sites include: the Borden site, the Long Island site, the Dodge City site, and the EBOS site 24.

D.4 REFERENCES

- ASTM, 1996. Standard Guide for Developing and Evaluating Ground-Water Modeling Codes. ASTM Subcommittee D-18.21.10, Tracking Number D18.21.92.07, February 9.
- Carsel, R.F., C.N. Smith, L.A. Mulkey, J.D. Dean, and P. Jowise, 1984. User's Manual for the Pesticide Root Zone Model (PRZM): release 1. Environ. Res. Lab., Athens, GA, US EPA, EPA-600/3-84-109.
- Carsel, R.F., L.A. Mulkey, M.N. Lorber, and L.B. Laskin, 1985. The Pesticide Root Zone Model (PRZM): A Procedure for Evaluating Pesticide Leaching Threats to Groundwater. *Ecological Modeling* 30: 4g-6g.
- Carsel, R.F., 1988. Developing Joint Probability Distributions of Soil Water Retention Characteristics. *Water Resources Res.*, 24(5): 755-769.
- Frind, E.O., G.E. Hokkanen, 1987. Simulation of the Borden Plume Using the Alternating Direction Galerkin Technique. *Water Resources Res.*, 23, 918-930.
- Gelhar, L.W., A. Mantoglou, C. Welty, and K.R. Rehfeldt, 1985. A Review of Field-Scale Physical Solute Transport Processes in Saturated and Unsaturated Porous Media. *Electr. Power Res. Inst.*, Palo Alto, CA, EPRI EA-190.
- Hadermann, J., 1980. Radionuclide transport through heterogeneous media, *Nuclear Technology*, v. 47, pp. 311-323.
-

- Hodgkinson, D.P. and P.R. Maul, 1985. One-dimensional Modeling of Radionuclide Migration Through Permeable and Fractured Rock for Arbitrary Length Decay Chains using Numerical Inversion of Laplace Transforms, Rep. AERE-R. 11880, UK Atomic Energy Authority, Oxfordshire, U.K.
- Huyakorn, P.S., and J.E. Buckley, 1987. VADOFT: Finite Element Code for Simulating One-Dimensional Flow and Solute Transport in the Vadose-zone. Technical Report Prepared for the U.S. Environmental Protection Agency, Athens, GA.
- Huyakorn, P.S., and S. Panday, 1989. VAM3D-CG: Variably Saturated Analysis Model in Three Dimensions with Pre-conditioned Gradient Matrix Solvers. HydroGeoLogic, Inc., Herndon, VA.
- Huyakorn, P.S., J.B. Kool, and Y.S. Wu, 1992. VAM2D - Variably Saturated Analysis Model in Two Dimensions. NUREG/CR-5352.
- Huyakorn, P.S., S. Panday, and R. Lingam, 1994. DSTRAM: Density-Dependant Solute Transport Analysis Finite Element Model, version 4.1. User's Manual. HydroGeoLogic, Inc., Herndon, VA.
- HydroGeoLogic, Inc., 1993. Response to Review Comments on EPACMTP Unsaturated Zone and Saturated Zone Modules by TetraTech, Inc. HydroGeoLogic, Inc., 1155 Herndon Parkway, Suite 900, Herndon, VA 20170.
- HydroGeoLogic, Inc., 1995a. STAFF3D: A Three-Dimensional Finite Element Code for Simulating Fluid Flow and Transport of Radionuclides in Fractured Porous Media. Version 3.0. HydroGeoLogic, Inc., 1155 Herndon Parkway, Suite 900, Herndon, VA 20170.
- HydroGeoLogic, Inc., 1995b. VAM3DF: Variably Saturated Analysis Model in Three-Dimensions for the Data Fusion System. Version 1.0. HydroGeoLogic, Inc., 1155 Herndon Parkway, Suite 900, Herndon, VA 20170.
- HydroGeoLogic, Inc., 1996. MS-VMS Software (Version 1.2) Documentation. HydroGeoLogic, Inc., 1155 Herndon Parkway, Suite 900, Herndon, VA 20170.
- INTERA Environmental Consultants, 1980. Mathematical Simulation of Aldicarb Behavior on Long Island. Technical Report, Contract No. 80-6876-02. US EPA, Athens, Georgia.
- Kool, J. B., and M.Th. Van Genuchten, 1991. One-Dimensional Variable Saturated Flow and Transport Model, Including Hysteresis and Root Water Uptake. U.S. Salinity Laboratory, USDA-ARS, Riverside, CA.

-
- Kool, J. B., P.S. Huyakorn, E.A. Sudicky, Z.A. Saleem, 1994. A composite modeling approach for subsurface transport of degrading contaminants from land-disposal sites. *Journal of Contaminant Hydrology*, 17, 69-90.
- National Research Council, 1990. *Groundwater Models: Scientific and Regulatory Applications*. National Academy Press, Washington, DC.
- Ogata, A., and R.B. Banks, 1961. A Solution of the Differential Equation of Longitudinal Dispersion in Porous Media, U.S. Geological Survey Professional Paper No. 411-A.
- Ogata, A., 1970. Theory of Dispersion in a Granular Medium. U.S. Geological Survey Professional Paper No. 411-I, p. 134.
- Ourisson, P.J., 1992. Small Scale Prospective Groundwater Study of Amber on Winterwheat in Kansas, Vol. 1. Ciba Geigy Corp., Agric. Div., Greensboro, NC.
- Panday, S.M., P.S. Huyakorn, R. Therrien, and R.L. Nichols, 1993. Improved three-dimensional finite-element techniques for field simulation of variably saturated flow and transport. *Journal of Contaminant Hydrology*, 12(1), 1-33.
- Shamir, U.Y., and D.R.F. Harlemann, 1967. Dispersion in Layered Porous Media, *J. of the Hydraulics Division, Amer. Soc. Civ. Engr.*, v. 93, Hy5, pp. 237-260.
- Sudicky, E.A., Y.S. Wu, and Z. Saleem, 1991. Semi-Analytical Approach for Simulating Transport of a Seven-Member, Branched Decay Chain in 3D Groundwater Systems, *EPS Trans. AM. Geophys. Union*, p. 135.
- Sudicky, E.A., J.B. Kool and P.S. Huyakorn, 1990. CANSAZ: Combined Analytical-Numerical Model for Simulating Flow and Contaminant Transport in the Saturated Zone. Version 2.0 with Nonlinear Adsorption and Chain Decay Reactions. Technical Report Prepared for US EPA, Office of Solid Waste, Washington, DC, 20460.
- Ungs, M.J., 1986. Steady-state Analytical Solution to the 3-D Groundwater Mounding Problem of an Unconfined Aquifer (MNDXYZ). Prepared for US EPA, Office of Solid Waste, Washington, DC, 20460. Also in Appendix B of U.S.EPA (1996b)
- US EPA, 1989. Unsaturated Zone Flow and Transport Module: Version 2.0 with Nonlinear Sorption and Chain Decay Reactions. US EPA, Office of Solid Waste, Washington, DC, 20460.
- US EPA, 1990. Response to Comments on the CANSAZ Flow and Transport Model for Use in EPACMS by the Science Advisory Board (SAB) of the United States Environmental Protection Agency. US EPA, Office of Solid Waste, Washington, DC, 20460.
-

- US EPA, 1992. Memorandum dated November 6, 1992 from the US EPA Office of Research and Development, Athens, GA, to the US EPA Office of Solid Waste, Washington, DC, 20460.
- US EPA, 1995. Briefing for EPA's Science Advisory Board on EPACMTP, March 8.
- US EPA, 1996a. Background Document for EPACMTP: User's Guide. US EPA, Office of Solid Waste, Washington, DC, 20460.
- US EPA, 1996b. Modeling approach for simulating three-dimensional migration of land disposal leachate with transformation products. Volume I: Background document for the unsaturated zone and saturated zone modules. US EPA, Office of Solid Waste, Washington, DC, 20460.
- US EPA, 1996c. EPA's Composite Model for Leachate Migration with Transformation Products (EPACMTP) Background Document for Finite Source Methodology. US EPA, Office of Solid Waste, Washington, DC, 20460.
- US EPA, 1996d. EPA's Composite Model for Leachate Migration with Transformation Products (EPACMTP) Background Document for Metals: Volume 1. US EPA, Office of Solid Waste, Washington, DC, 20460.
- US EPA, 1996e. Sensitivity Analysis of the EPACMTP Monte Carlo Sampling Techniques and Key Input Parameter Distribution. US EPA, Office of Solid Waste, Washington, DC, 20460.
- US EPA, 1997. Test and Verification of EPA's Composite Model for Leachate Migration with Transformation Products (EPACMTP). US EPA Office of Solid Waste, Washington, DC, 20460.
- US EPA, 1999a. Verification Document for HWIR99 Pseudo-Three Dimensional Aquifer Module. US EPA, Office of Solid Waste, Washington, DC, 20460.
- US EPA, 1999b. Verification Document for HWIR99 Vadose-Zone Module. US EPA, Office of Solid Waste, Washington, DC, 20460.
- US EPA, 1999c. Vadose and Saturated Modules Extracted from EPACMTP for HWIR99. US EPA, Office of Solid Waste, Washington, D.C.
- US EPA, 1999d. Source Modules for Tanks and Surface Impoundments: Background and Implementation for the Multimedia, Multipathway, and Multireceptor Risk Assessment (3MRA) for HWIR99. US EPA, Office of Solid Waste, Washington, D.C.
- US EPA, 1999e. Anaerobic Biodegradation Rates of Organic Chemicals in Groundwater: A Summary of Field and Laboratory Study. US EPA, Office of Solid Waste, Washington, D.C.
-

US EPA, 2000a. Test Plan for HWIR99 Vadose-Zone. US EPA Office of Solid Waste, Washington, DC, 20460.

US EPA, 2000b. Test Plan for HWIR99 Aquifer Module. US EPA Office of Solid Waste, Washington, DC, 20460.

US EPA, 2001. Testing and Verification of EPACMTP Version 2. US EPA Office of Solid Waste, Washington, DC, 20460.

Van der Heijde, P.M.K., 1987. Quality assurance in computer simulations of groundwater contamination. *Environmental Software*, 2(1): 19-28.

Van Genuchten, M.Th., 1981. MOB1: A Numerical Model for the Simulation of Chemical Mobility in Porous Media. Unpublished.

Van Genuchten, M.Th., and W.J. Alves, 1982. Analytical Solutions of the One-Dimensional Convective-Dispersion Solute Transport Equation, U.S. Technical Bulletin No. 1661, p.151.

This page was intentionally left blank.

SUBAPPENDIX D.A
VADOSE-ZONE MODULE VERIFICATION RESULTS
(1993-1994)

This page intentionally left blank.

LIST OF FIGURES

| | | <u>Page</u> |
|---------------|--|-------------|
| Figure D.A.1 | Test Case 1: Predicted Pressure Head Distribution in the Unsaturated Zone. The Solid Line Represents Finite Element Solution, and Data Points Represent Semi-analytical Solution . . . | D.A-1 |
| Figure D.A.2 | Test Case 2: Predicted Saturation Distribution in the Unsaturated Zone. The Solid Line Represents the Finite Element Solution, Data Points Represent the Semi-analytical Solution . . . | D.A-2 |
| Figure D.A.3 | Test Case 3: Predicted Saturation Distribution in the Unsaturated Zone. The Solid Line Represents the Finite Element Solution, and Data Points Represent the Semi-analytical Flow Solution | D.A-3 |
| Figure D.A.4 | Test Case 4: Transport in Layered Soil. The Solid Lines Correspond to the Transient Solution, Evaluated at t=5, 15, 30, and 80 Years. Data Points Represent the Steady-state Solution | D.A-4 |
| Figure D.A.5 | Test Case 5: Comparison of Breakthrough Curves for the Transient Pulse Input Transport Problem. The Solid Line Represents the Solution of the Numerical HYDRUS Code, and the Data Points Represent the Semi-analytical and Numerical Transport Solution of FECTUZ | D.A-5 |
| Figure D.A.6 | Test Case 6: Simulated Concentration Profiles of Solute Transport in a Semi-infinite Soil Column. Solid Lines Represent the Analytical Solution. Data Points Represent the Numerical Solution of FECTUZ | D.A-6 |
| Figure D.A.7 | Test Case 7: Simulated Concentration Profiles of the Problem of Solute Transport in a Soil Column of Finite Length. Sub-case a Involves a Conservative Species, While Sub-case b Involves a Non-conservative Species. The Solid Lines Represent the Analytical Solution, and the Data Points Represent the Numerical Solution of FECTUZ | D.A-7 |
| Figure D.A.8 | Test Case 8, Sub-case 1: Simulated Outflow Breakthrough Curve of the Problem of Solute Transport in a Layered Soil Column. The Dispersivity Values Are 0.076 cm, 0.174 cm, and 0.436 cm for Layers 1, 2, and 3, Respectively. The Solid Line Represents the Analytical Solution While the Data Points Represent the Numerical Solution of FECTUZ | D.A-8 |
| Figure D.A.9 | Test Case 8, Sub-case 2: Simulated Outflow Breakthrough Curve of the Problem of Solute Transport in a Layered Soil Column. The Dispersivity Values Are 0.76 cm, 1.74 cm, and 4.36 cm for Layers 1, 2, and 3, Respectively. The Solid Line Represents the Analytical Solution While the Data Points Represent the Numerical Solution of FECTUZ | D.A-9 |
| Figure D.A.10 | Test Case 9: Comparison Between FECTUZ and MOB1 for Test Case 9, (a) Linear Adsorption and (b) Nonlinear Adsorption. The Solid Line Represents the Finite Element Solution of FECTUZ While the Data Points Represent the Finite Difference Solution of MOB1 | D.A-10 |

LIST OF FIGURES (continued)

| | Page |
|---|-------------|
| Figure D.A.11 Test Case 10: Comparison of the Problem of Transport with a Three-member Decay Chain with (a) First-type and (b) Third-type Decaying Source Boundary Conditions. The Solid Line Represents the Solution by FECTUZ and the Data Points Represent the Analytical Solution | D.A-11 |

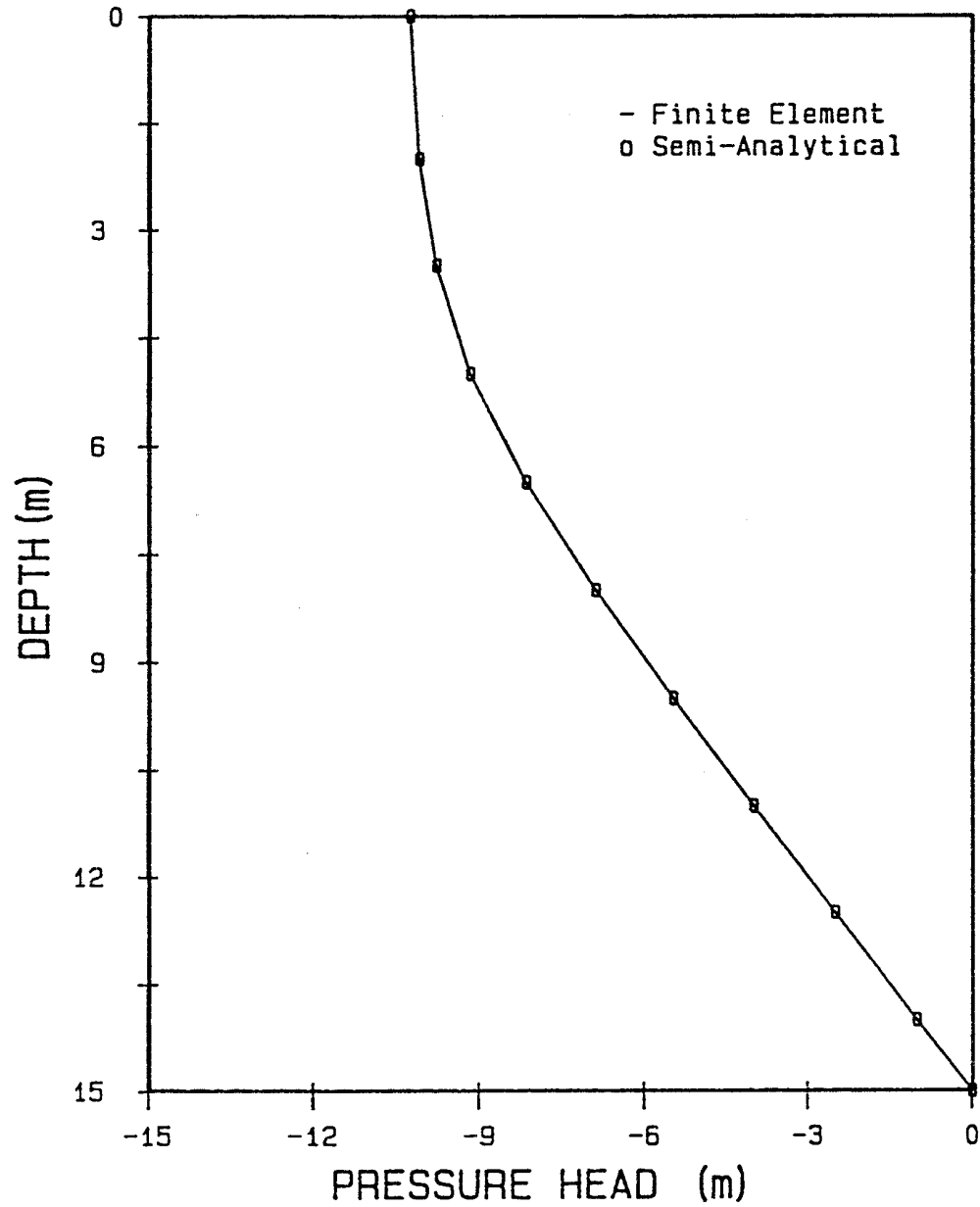


Figure D.A.1 Test Case 1: Predicted Pressure Head Distribution in the Unsaturated Zone. The Solid Line Represents Finite Element Solution, and Data Points Represent Semi-analytical Solution

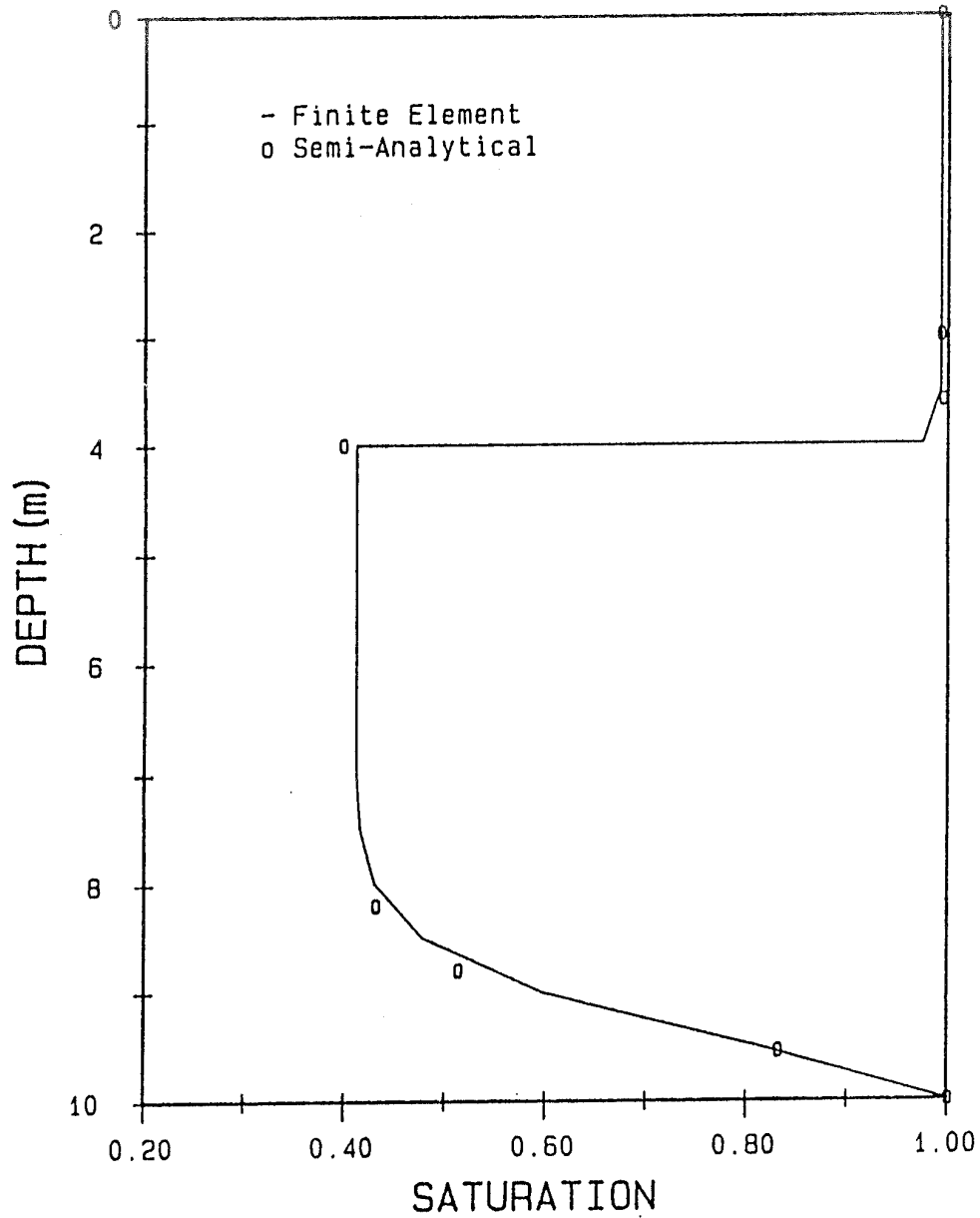


Figure D.A.2 Test Case 2: Predicted Saturation Distribution in the Unsaturated Zone. The Solid Line Represents the Finite Element Solution, Data Points Represent the Semi-analytical Solution

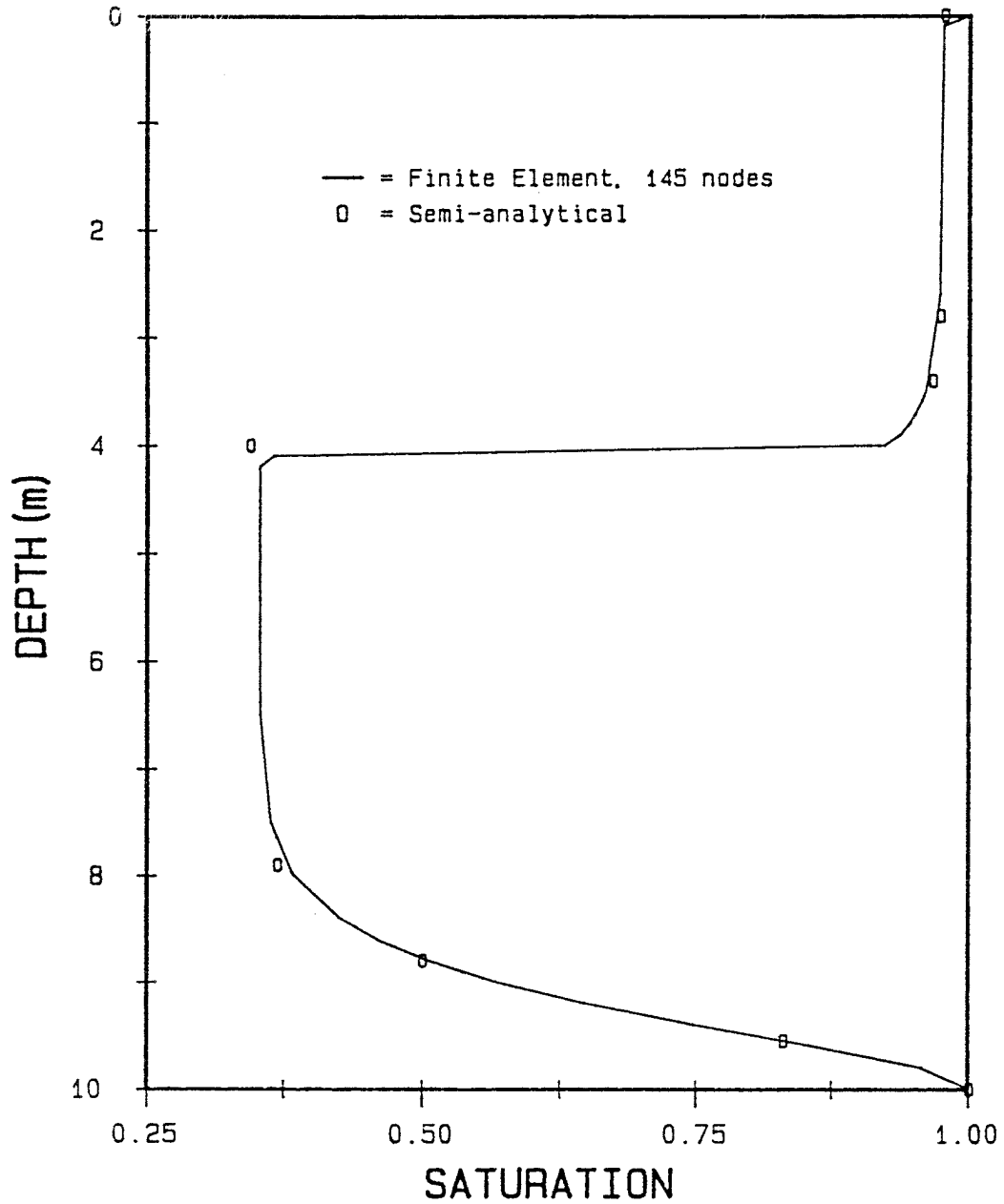


Figure D.A.3 Test Case 3: Predicted Saturation Distribution in the Unsaturated Zone. The Solid Line Represents the Finite Element Solution, and Data Points Represent the Semi-analytical Flow Solution

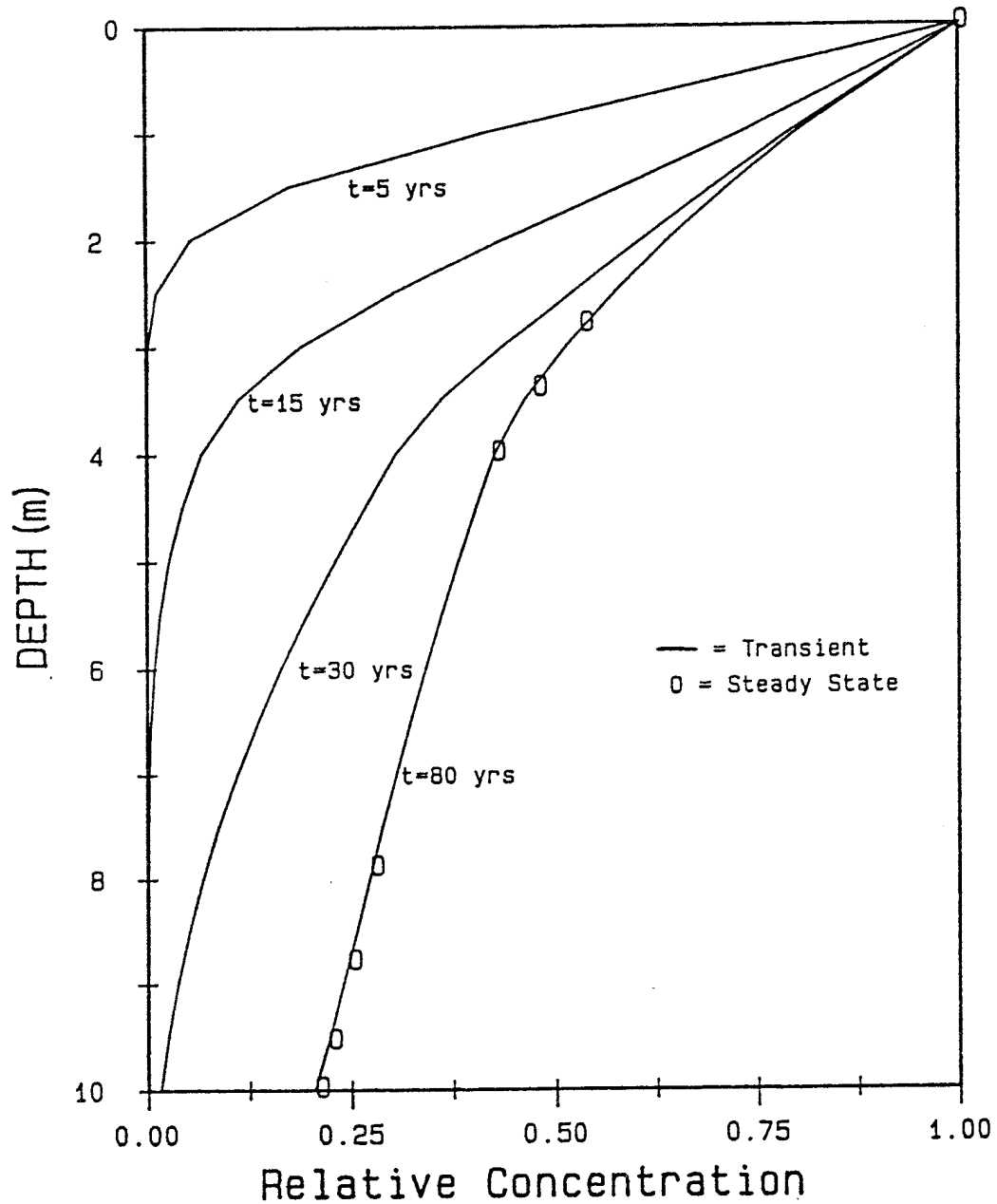


Figure D.A.4 Test Case 4: Transport in Layered Soil. The Solid Lines Correspond to the Transient Solution, Evaluated at $t=5, 15, 30,$ and 80 Years. Data Points Represent the Steady-state Solution

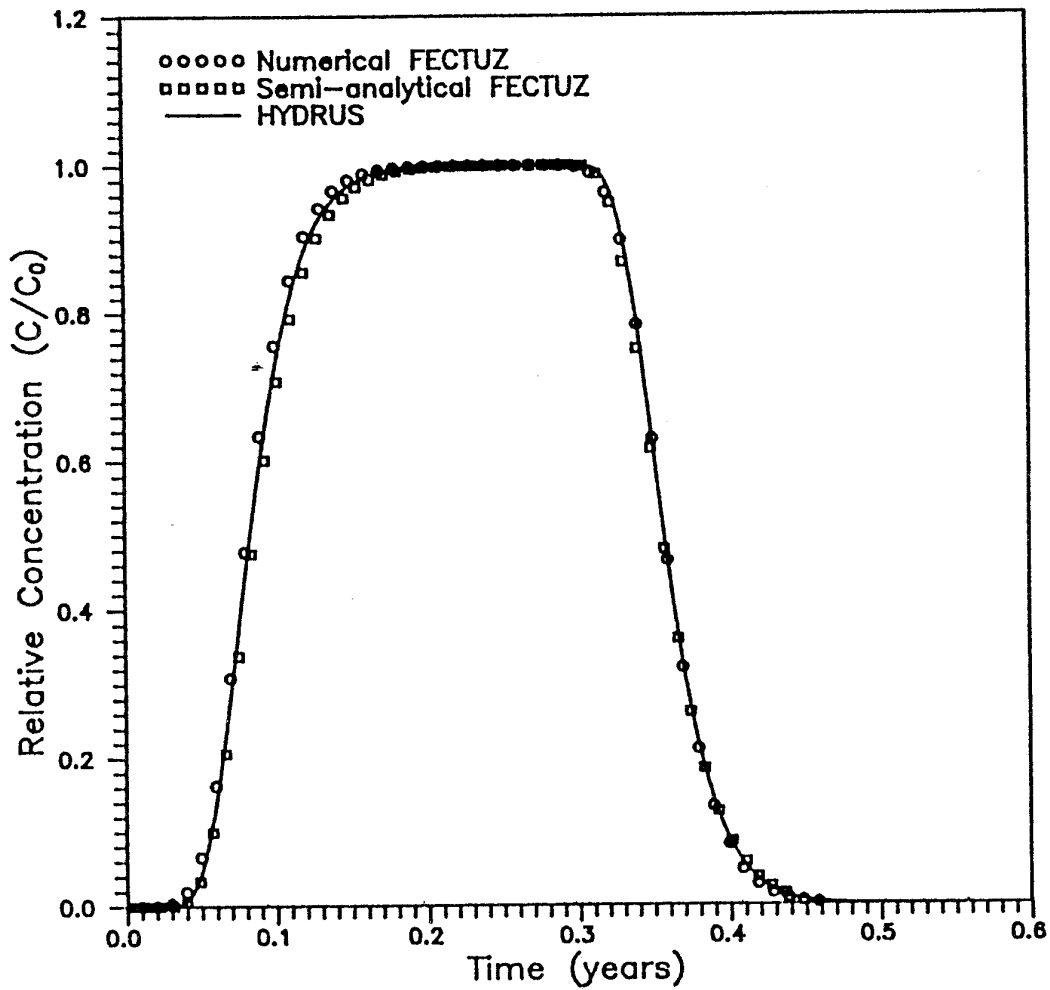


Figure D.A.5 Test Case 5: Comparison of Breakthrough Curves for the Transient Pulse Input Transport Problem. The Solid Line Represents the Solution of the Numerical HYDRUS Code, and the Data Points Represent the Semi-analytical and Numerical Transport Solution of FECTUZ

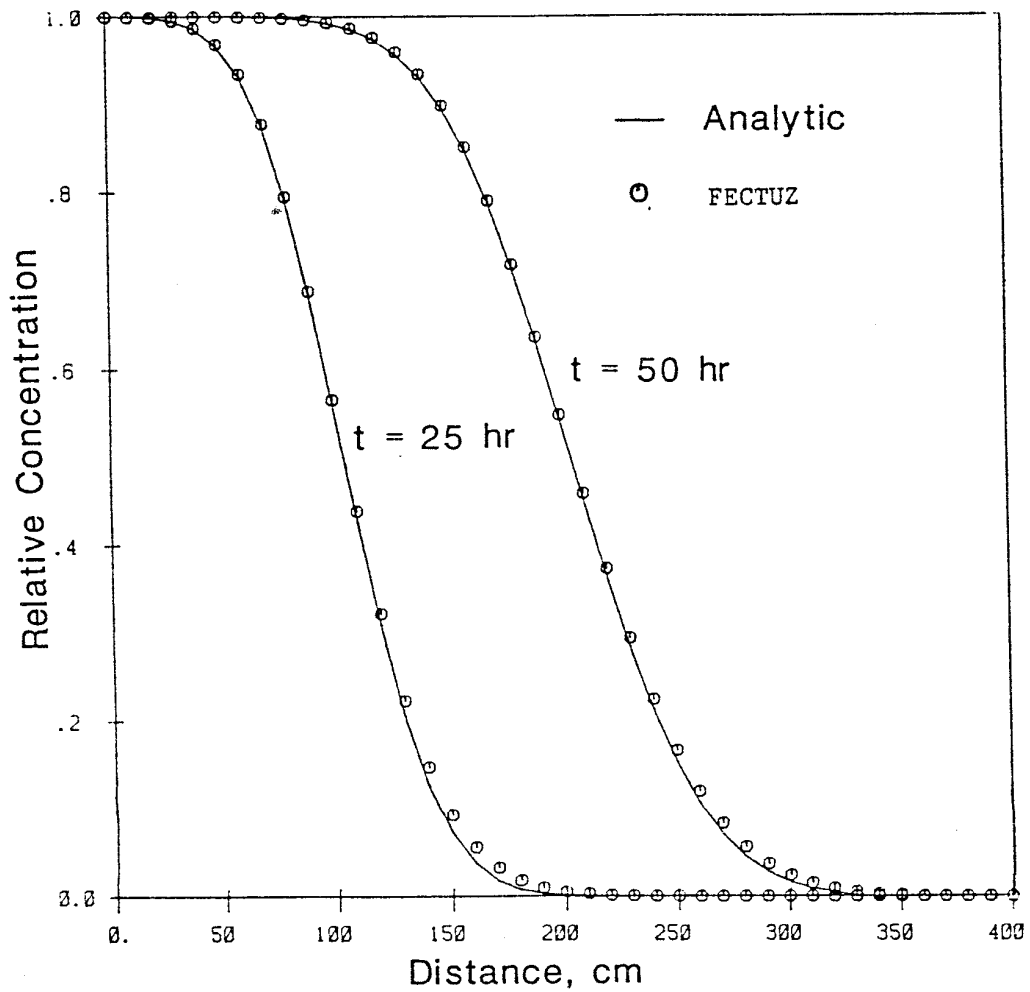


Figure D.A.6 Test Case 6: Simulated Concentration Profiles of Solute Transport in a Semi-infinite Soil Column. Solid Lines Represent the Analytical Solution. Data Points Represent the Numerical Solution of FECTUZ

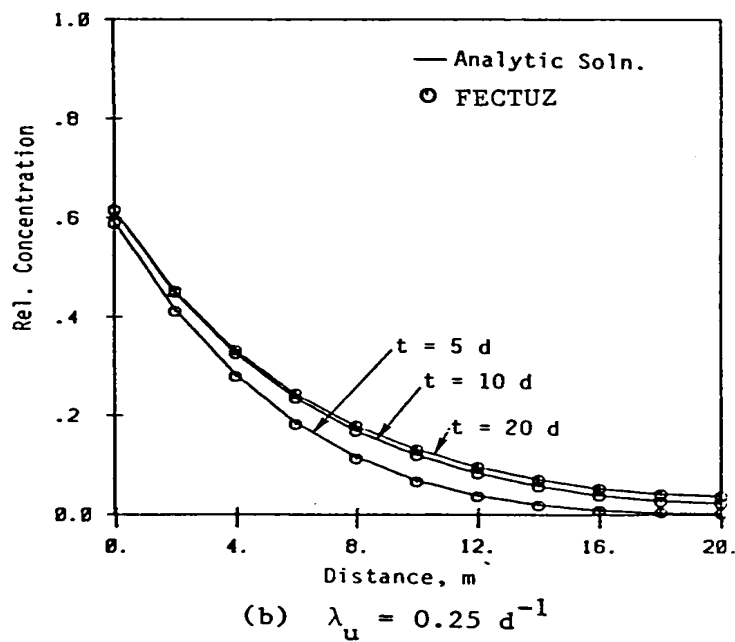
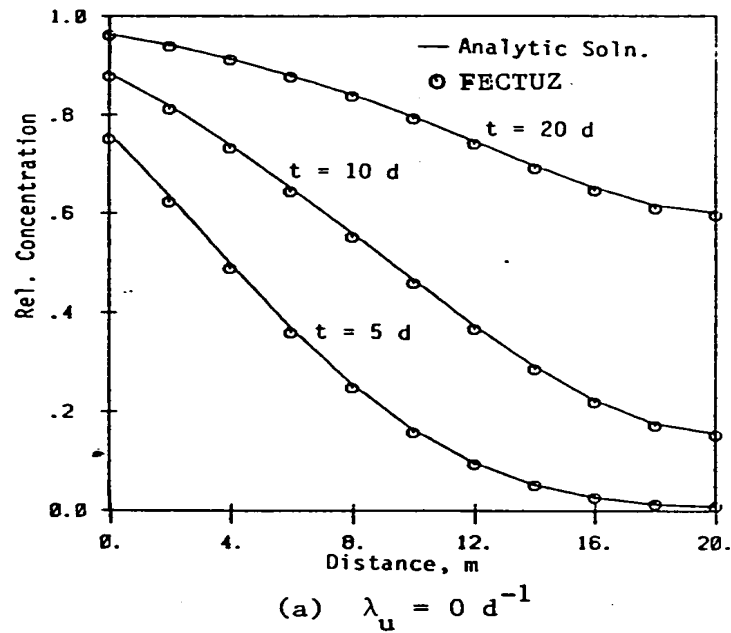


Figure D.A.7 Test Case 7: Simulated Concentration Profiles of the Problem of Solute Transport in a Soil Column of Finite Length. Sub-case a Involves a Conservative Species, While Sub-case b Involves a Non-conservative Species. The Solid Lines Represent the Analytical Solution, and the Data Points Represent the Numerical Solution of FECTUZ

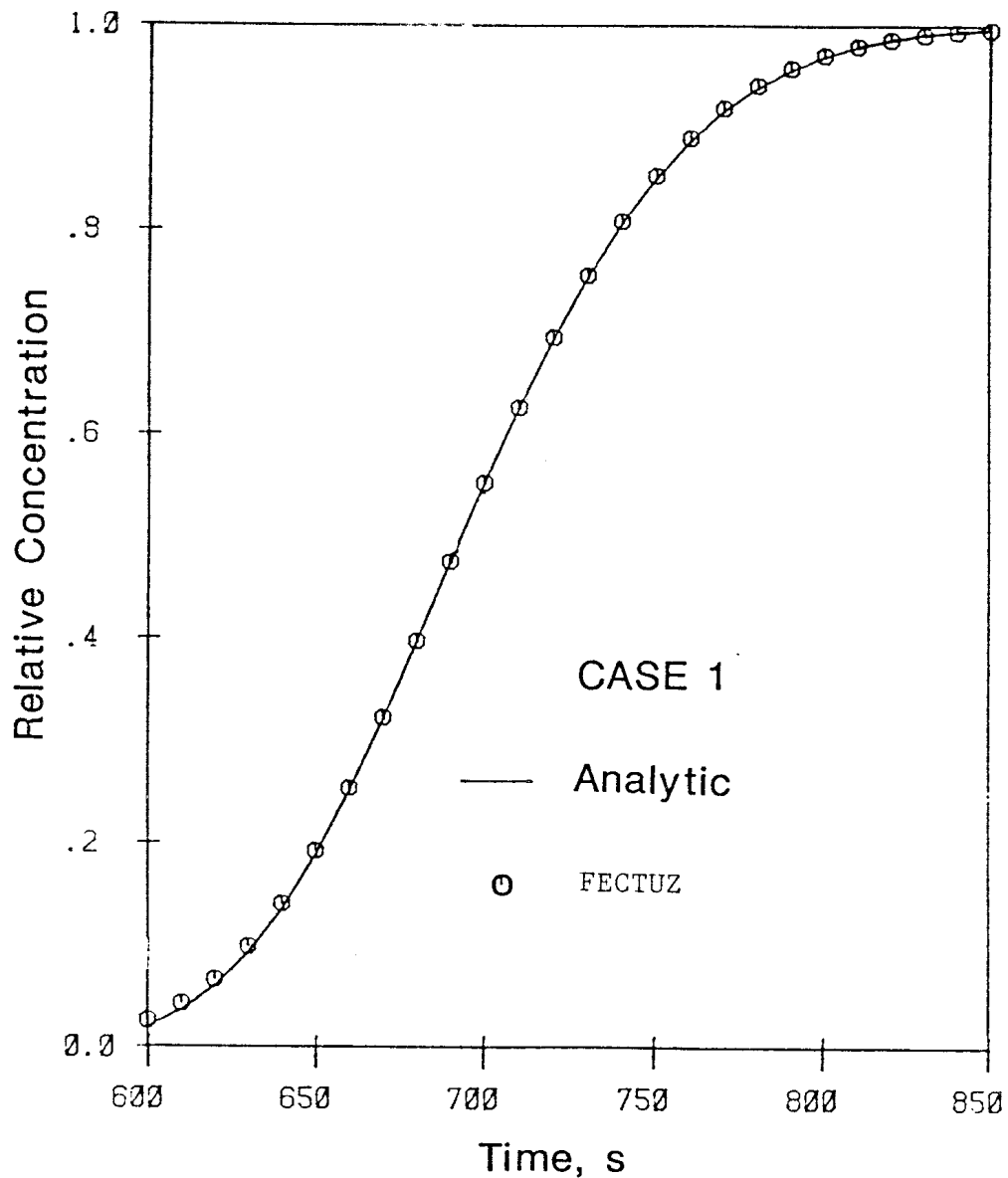


Figure D.A.8 Test Case 8, Sub-case 1: Simulated Outflow Breakthrough Curve of the Problem of Solute Transport in a Layered Soil Column. The Dispersivity Values Are 0.076 cm, 0.174 cm, and 0.436 cm for Layers 1, 2, and 3, Respectively. The Solid Line Represents the Analytical Solution While the Data Points Represent the Numerical Solution of FECTUZ

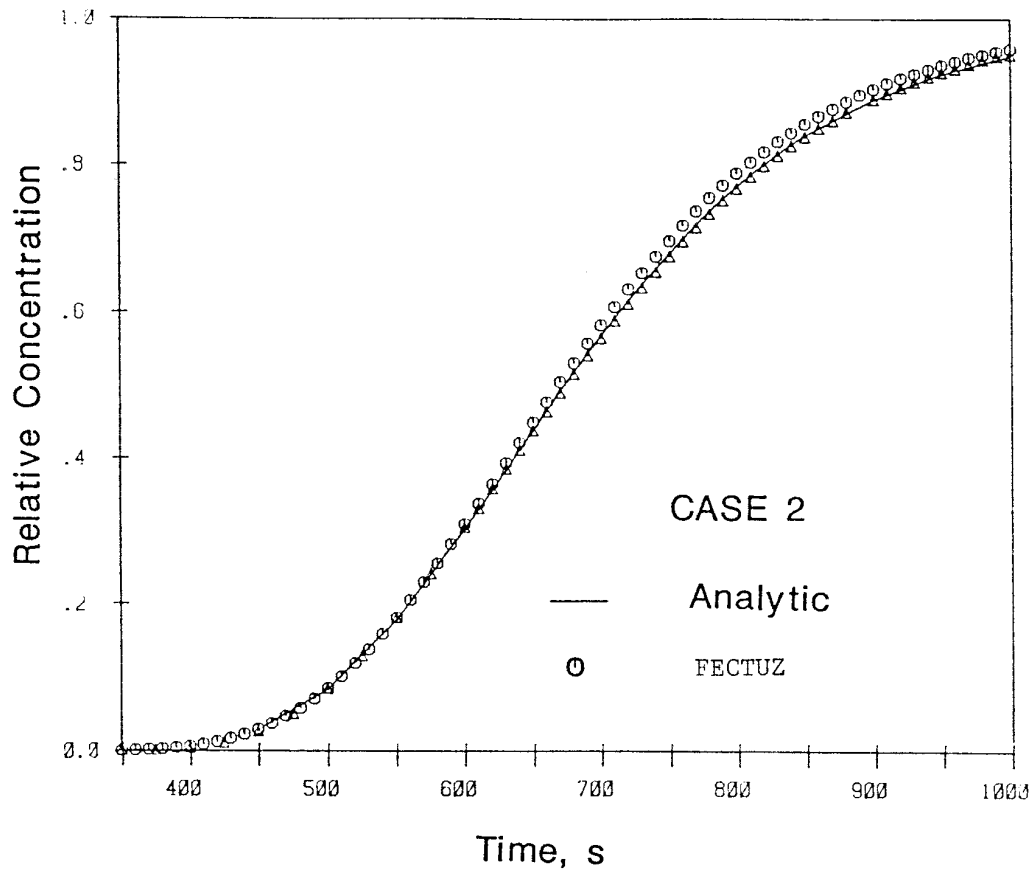
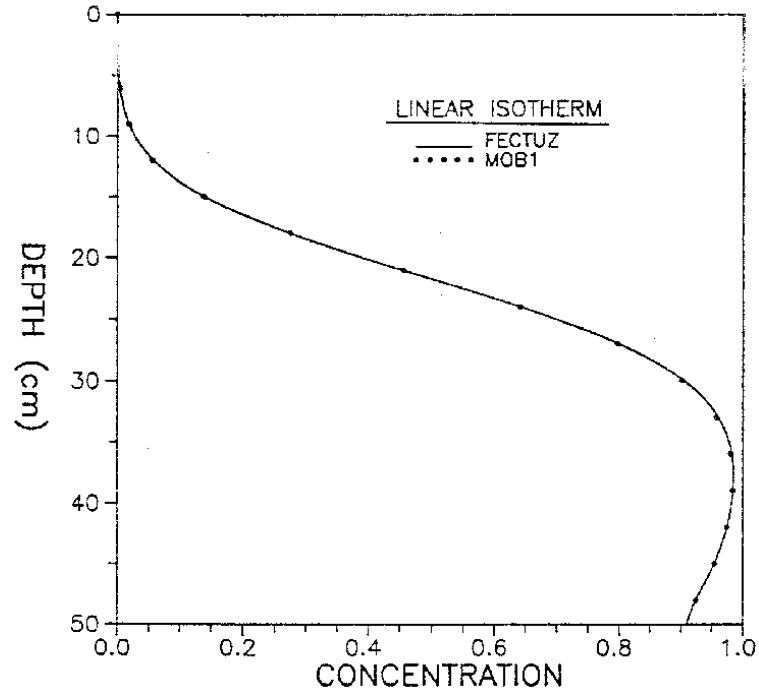
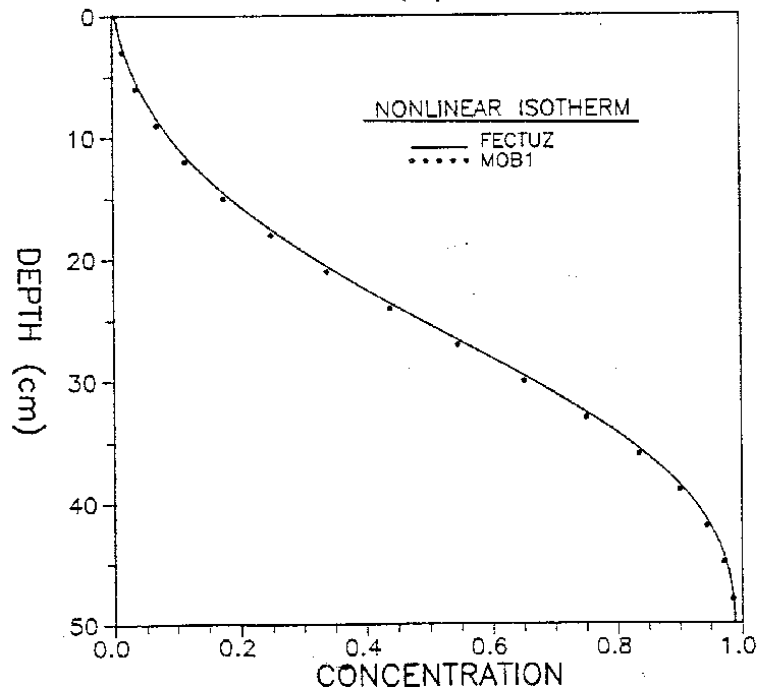


Figure D.A.9 Test Case 8, Sub-case 2: Simulated Outflow Breakthrough Curve of the Problem of Solute Transport in a Layered Soil Column. The Dispersivity Values Are 0.76 cm, 1.74 cm, and 4.36 cm for Layers 1, 2, and 3, Respectively. The Solid Line Represents the Analytical Solution While the Data Points Represent the Numerical Solution of FECTUZ



(a)



(b)

Figure D.A.10 Test Case 9: Comparison Between FECTUZ and MOB1 for Test Case 9, (a) Linear Adsorption and (b) Nonlinear Adsorption. The Solid Line Represents the Finite Element Solution of FECTUZ While the Data Points Represent the Finite Difference Solution of MOB1

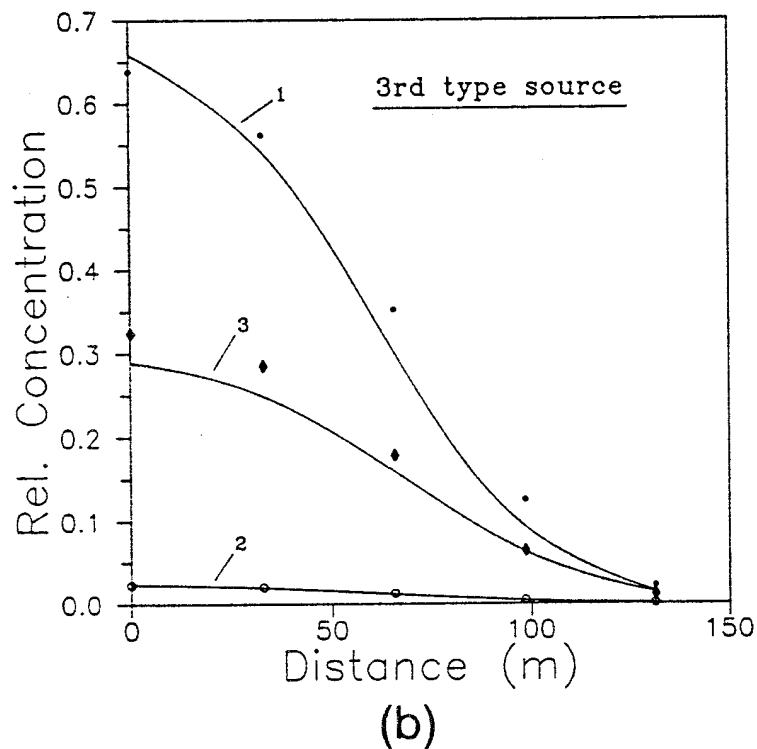
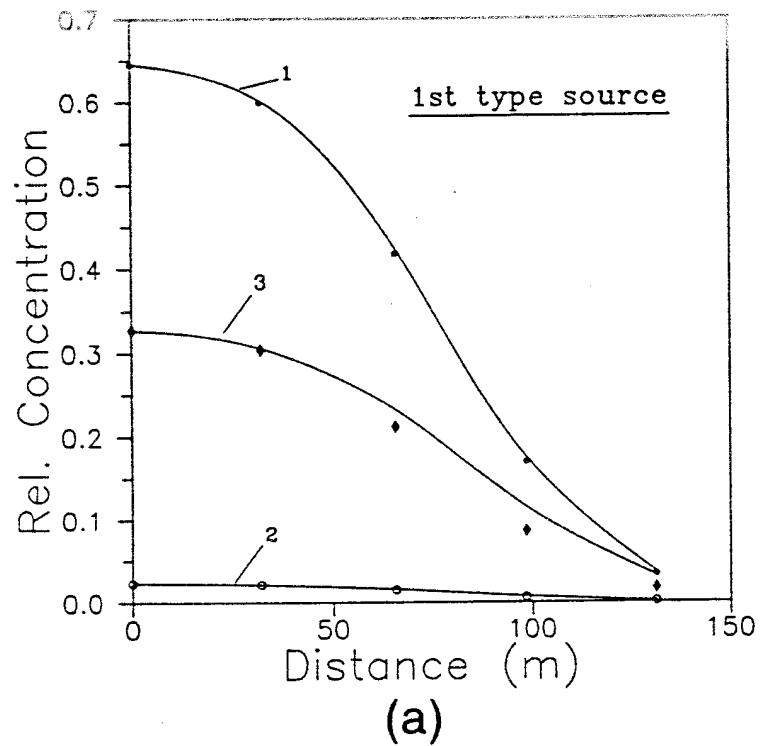


Figure D.A.11 Test Case 10: Comparison of the Problem of Transport with a Three-member Decay Chain with (a) First-type and (b) Third-type Decaying Source Boundary Conditions. The Solid Line Represents the Solution by FECTUZ and the Data Points Represent the Analytical Solution

This page was intentionally left blank.

SUBAPPENDIX D.B

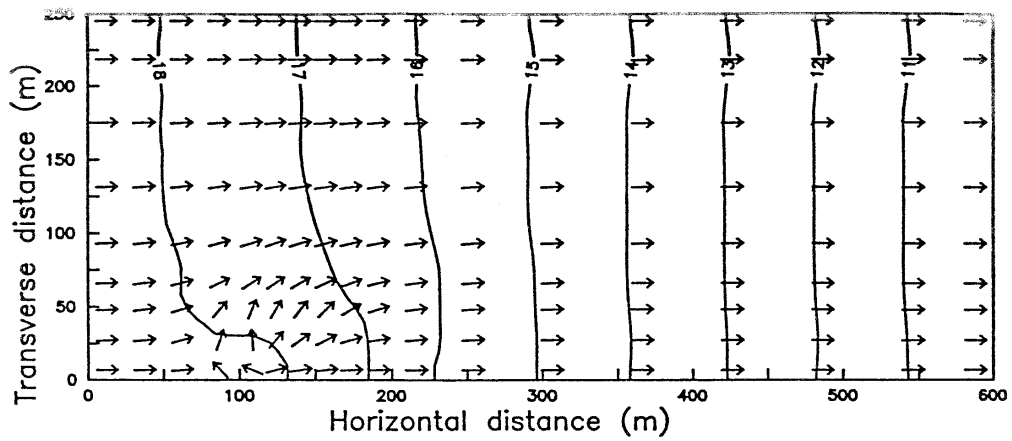
AQUIFER-MODULE VERIFICATION RESULTS (1993-1994)

This page intentionally left blank.

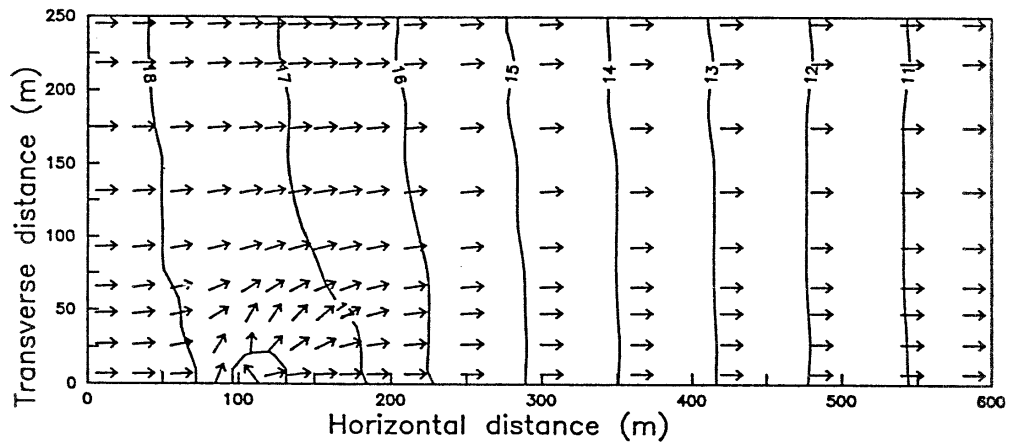
LIST OF FIGURES

| | Page |
|--------------|---|
| Figure D.B.1 | Test Case 1: Comparison of CANSAZ-3D and Analytical 3D Groundwater Flow Solution Showing Hydraulic Heads and Darcy Velocities in the Horizontal Plane at the Top of the Saturated Zone: (A) CANSAZ-3D, (B) Analytical D.B-1 |
| Figure D.B.2 | Test Case 2: Comparison of Predicted Horizontal Transverse Concentration Profiles at X=40 M and X=75 M from the Source D.B-2 |
| Figure D.B.3 | Test Case 3: Comparison of CANSAZ-3D (Solid Contours) and VAM2D (Dashed Contours) D.B-3 |
| Figure D.B.4 | Test Case 4: Comparison Between Analytical Solution (Solid Lines) and CANSAZ-3D (Dashed Lines) for 7-member Decay Chain Problem at T = 200 Yrs D.B-4 |
| Figure D.B.5 | Test Case 5: Predicted Concentration Distributions at T=5 and T=10 Days for the Nonlinear Sorption Option D.B-5 |
| Figure D.B.6 | Test Case 6: Comparison of Steady-state Concentration Contours in the Horizontal Plane at the Top of the Saturated Zone (Z = 15.71 M); Predicted by (A) CANSAZ-3D and (B) DSTRAM D.B-6 |
| Figure D.B.7 | Test Case 7: VAM3D (Dashed Lines) and CANSAZ/EPACMTP (Solid Lines) Predicted Receptor Well Concentrations; A) Y=0, Z=0; B) Y=0, Z=14, C) Y=48, Z=0; D) Y=48, Z=14 D.B-7 |

This page intentionally left blank.



(A)



(B)

**Figure D.B.1 Test Case 1: Comparison of CANSAZ-3D and Analytical 3D Groundwater Flow Solution Showing Hydraulic Heads and Darcy Velocities in the Horizontal Plane at the Top of the Saturated Zone:
(A) CANSAZ-3D, (B) Analytical**

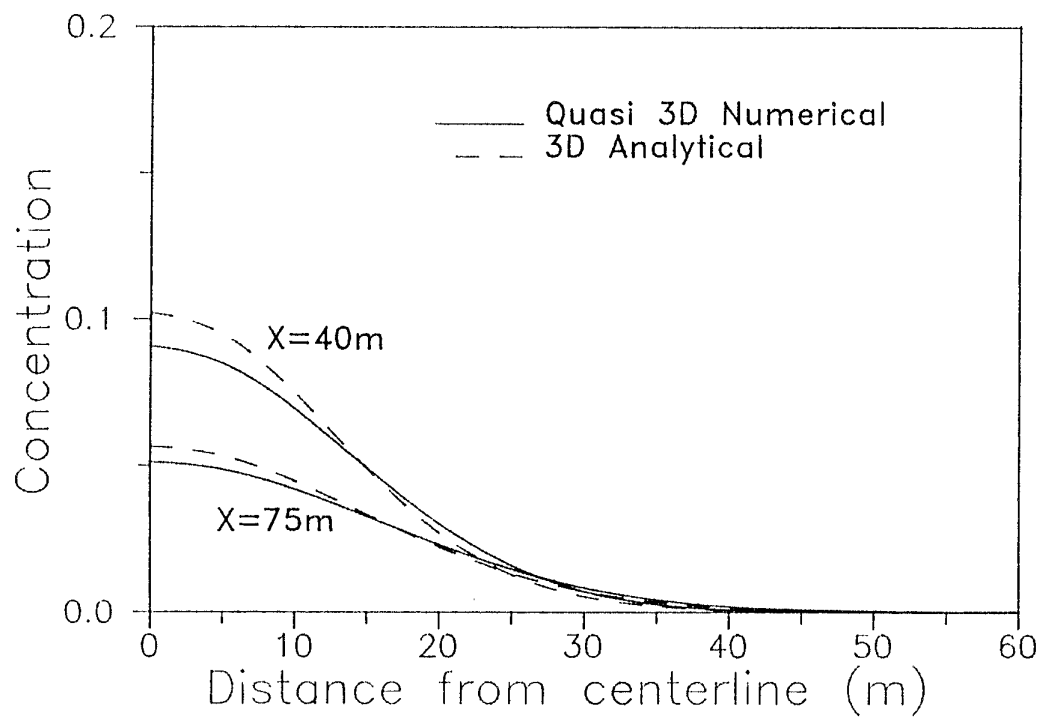


Figure D.B.2 Test Case 2: Comparison of Predicted Horizontal Transverse Concentration Profiles at X=40 M and X=75 M from the Source

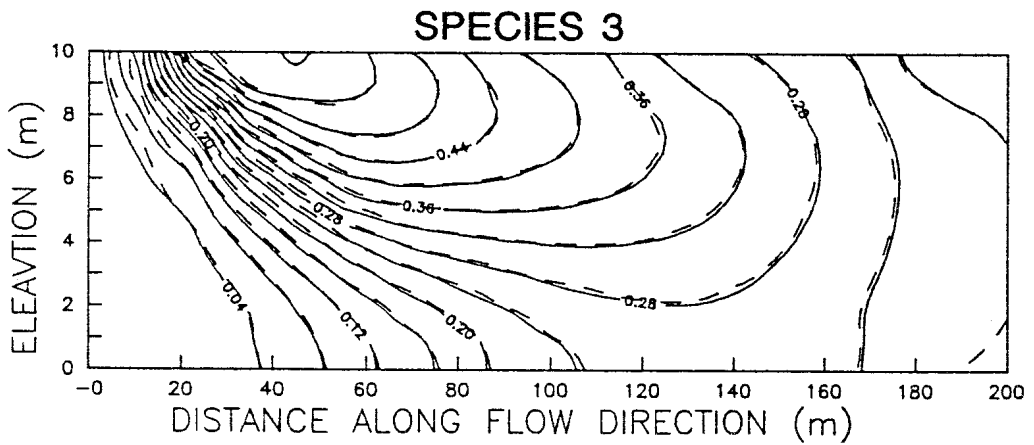
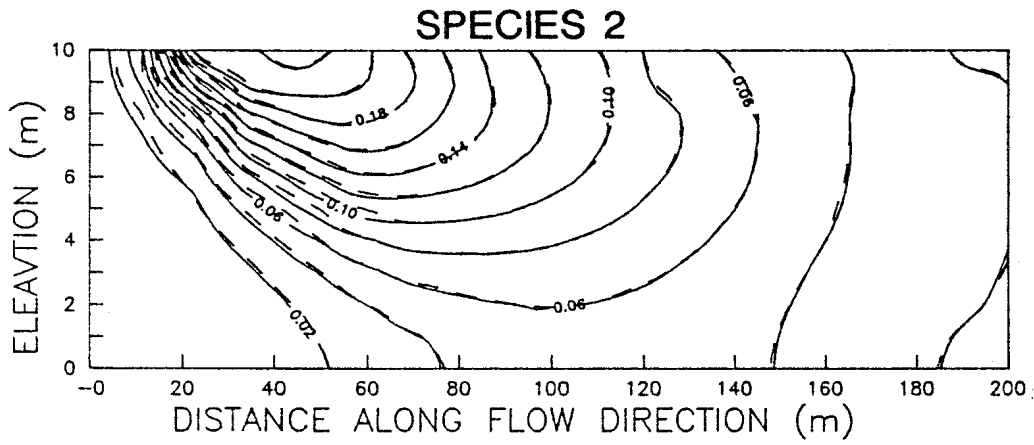
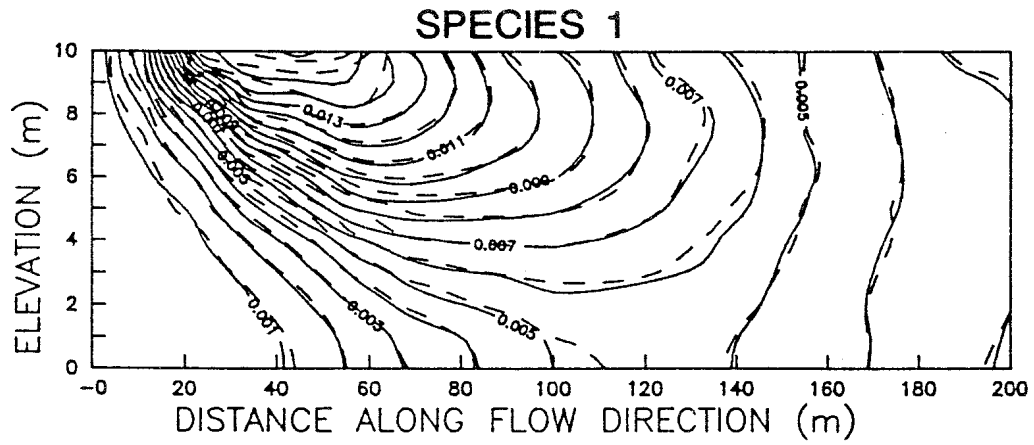


Figure D.B.3 Test Case 3: Comparison of CANSAZ-3D (Solid Contours) and VAM2D (Dashed Contours)

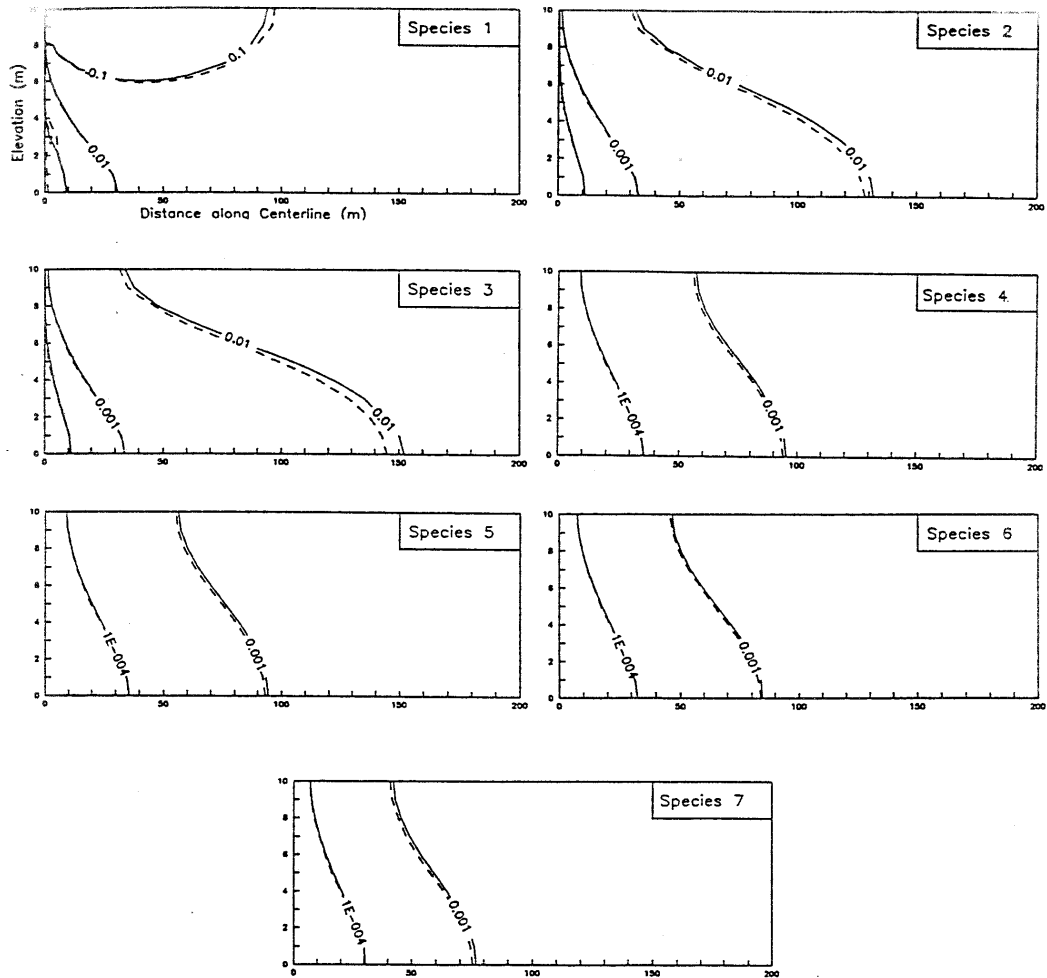


Figure D.B.4 Test Case 4: Comparison Between Analytical Solution (Solid Lines) and CANSAZ-3D (Dashed Lines) for 7-member Decay Chain Problem at T = 200 Yrs

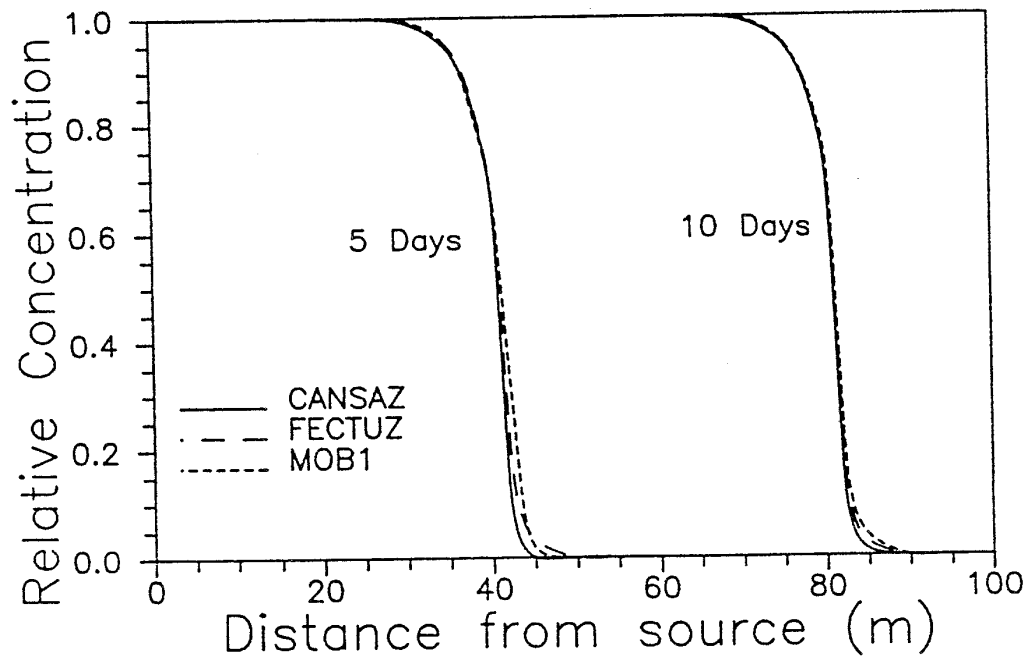
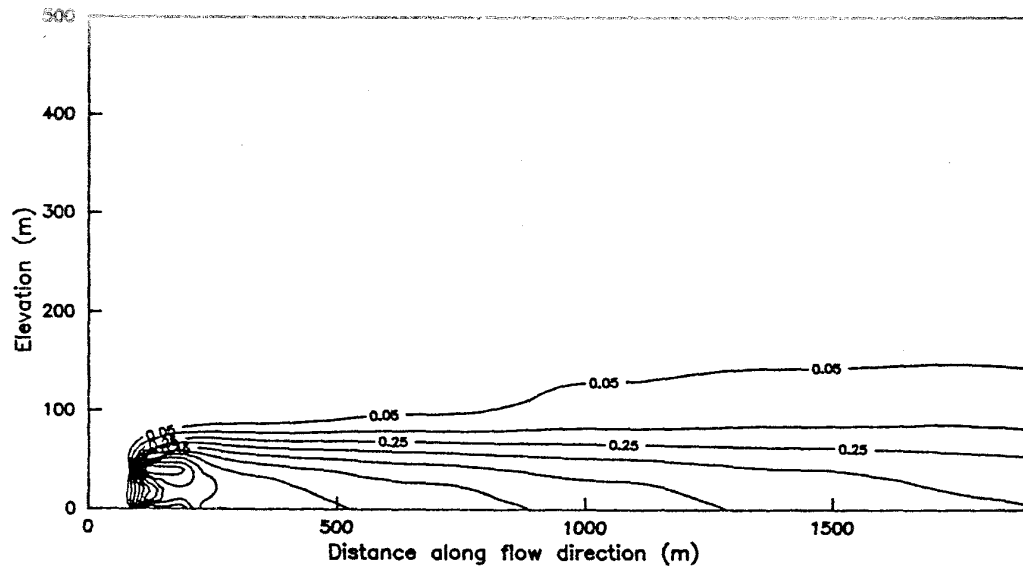
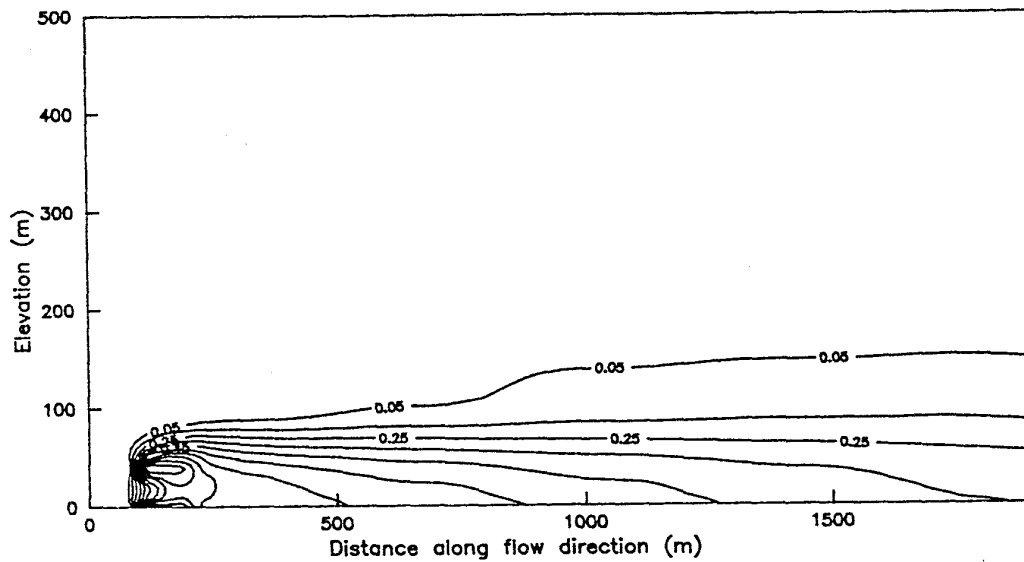


Figure D.B.5 Test Case 5: Predicted Concentration Distributions at T=5 and T=10 Days for the Nonlinear Sorption Option



(A)



(B)

Figure D.B.6 Test Case 6: Comparison of Steady-state Concentration Contours in the Horizontal Plane at the Top of the Saturated Zone (Z = 15.71 M); Predicted by (A) CANSZ-3D and (B) DSTRAM

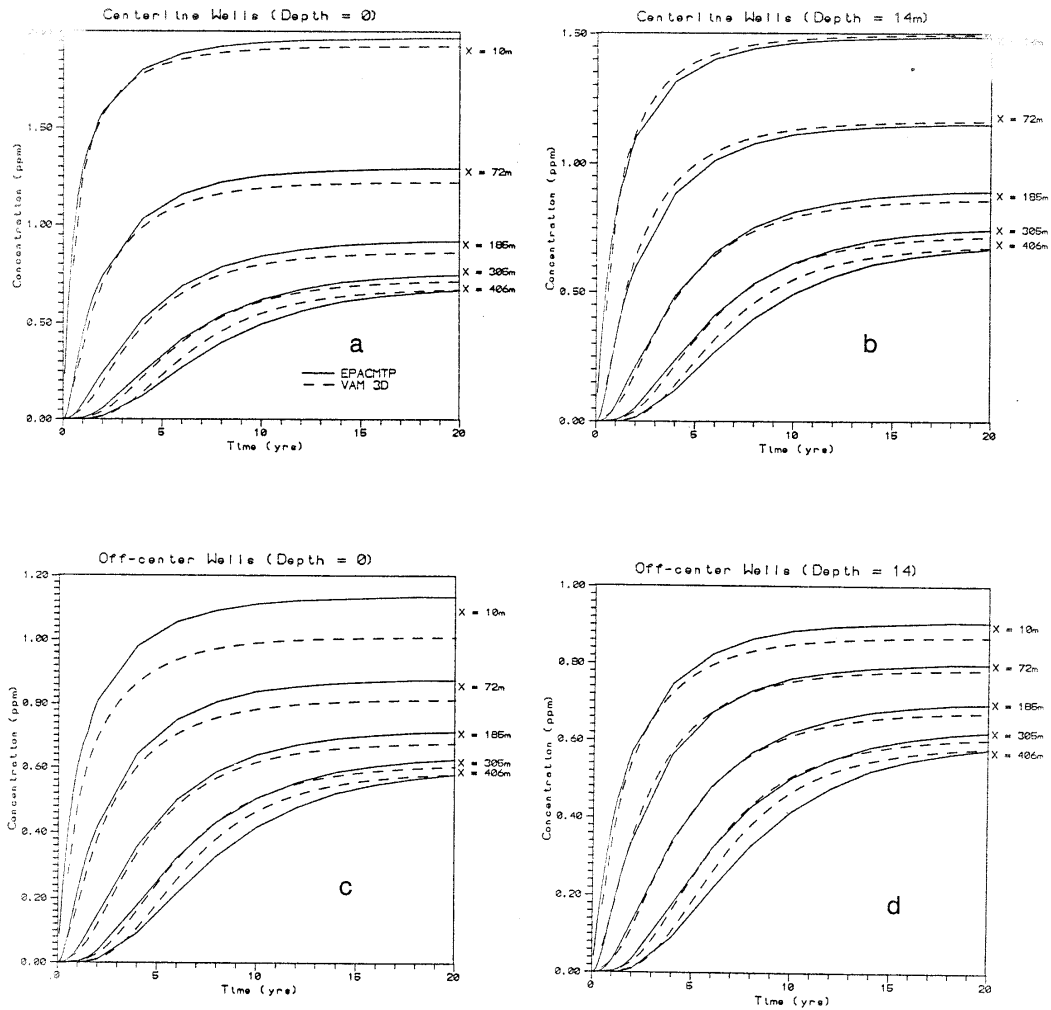


Figure D.B.7 Test Case 7: VAM3D (Dashed Lines) and CANSAZ/EPACHTP (Solid Lines) Predicted Receptor Well Concentrations; A) Y=0, Z=0; B) Y=0, Z=14, C) Y=48, Z=0; D) Y=48, Z=14

This page was intentionally left blank.

SUBAPPENDIX D.C
RESULTS (1993-1994)

This page intentionally left blank.

LIST OF FIGURES

| | Page |
|---|-------------|
| Figure D.C.1 Test Case 1: Comparison of EPACMTP-Metals Result with Analytical Solution for the Unsaturated-zone with Linear Adsorption Isotherm | D.C-1 |
| Figure D.C.2 Test Case 2, Finite Source: Comparison of Unsaturated Zone Concentration Profiles of HYDRUS and EPACMTP-Metals for Nonlinear Adsorption with Freundlich Exponent = 1.5 | D.C-2 |
| Figure D.C.3 Test Case 2, Finite Source: Comparison of Unsaturated Zone Concentration Profiles of HYDRUS and EPACMTP-Metals for Nonlinear Adsorption with Freundlich Exponent = 0.5 | D.C-3 |
| Figure D.C.4 Test Case 3: Cumulative Mass in the Unsaturated Zone and Total Input Mass for Lead Isotherm #3 Corresponding to Low Organic Acids (LOA), Low HFO, Low POM, and High pH Condition | D.C-4 |
| Figure D.C.5 Test Case 4: Comparison of Concentration Profiles for Freundlich Exponent = 0.5 | D.C-5 |

This page intentionally left blank.

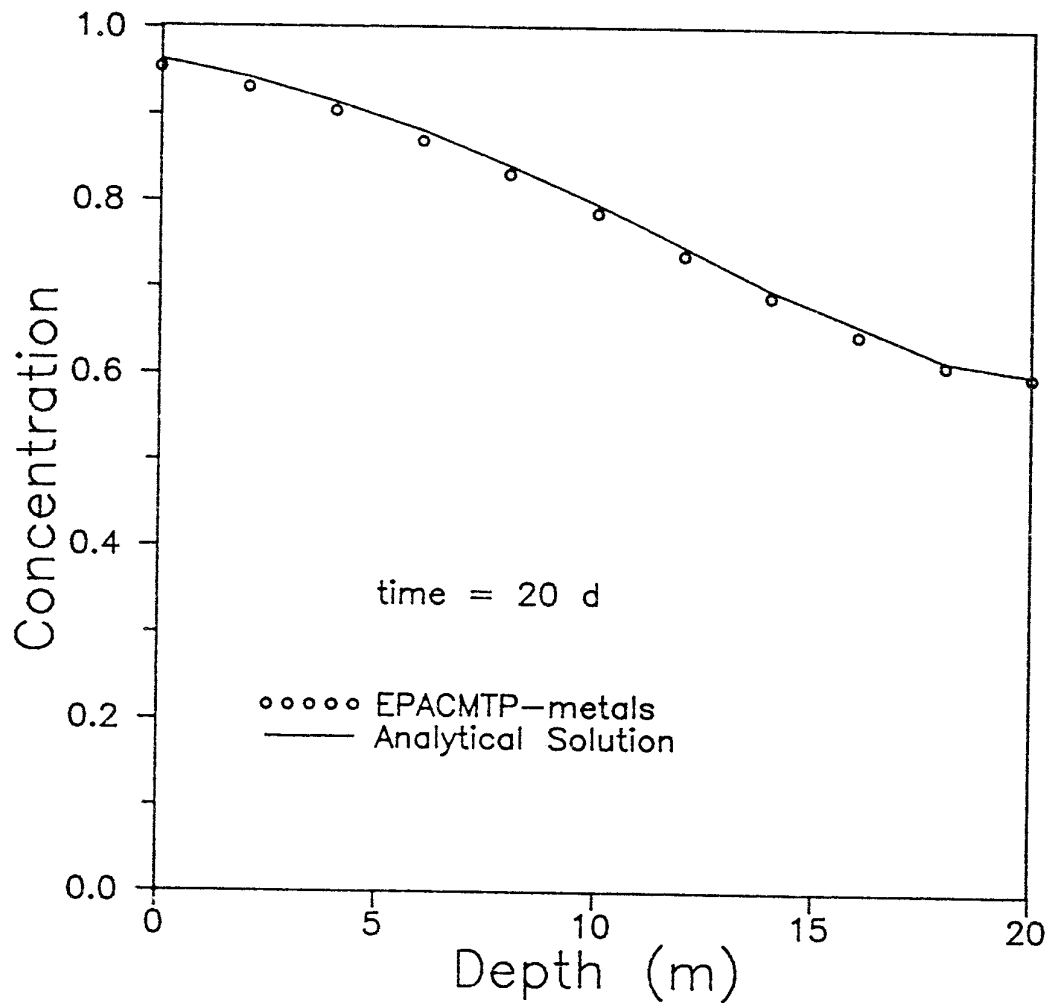


Figure D.C.1 Test Case 1: Comparison of EPACMTP-Metals Result with Analytical Solution for the Unsaturated-zone with Linear Adsorption Isotherm

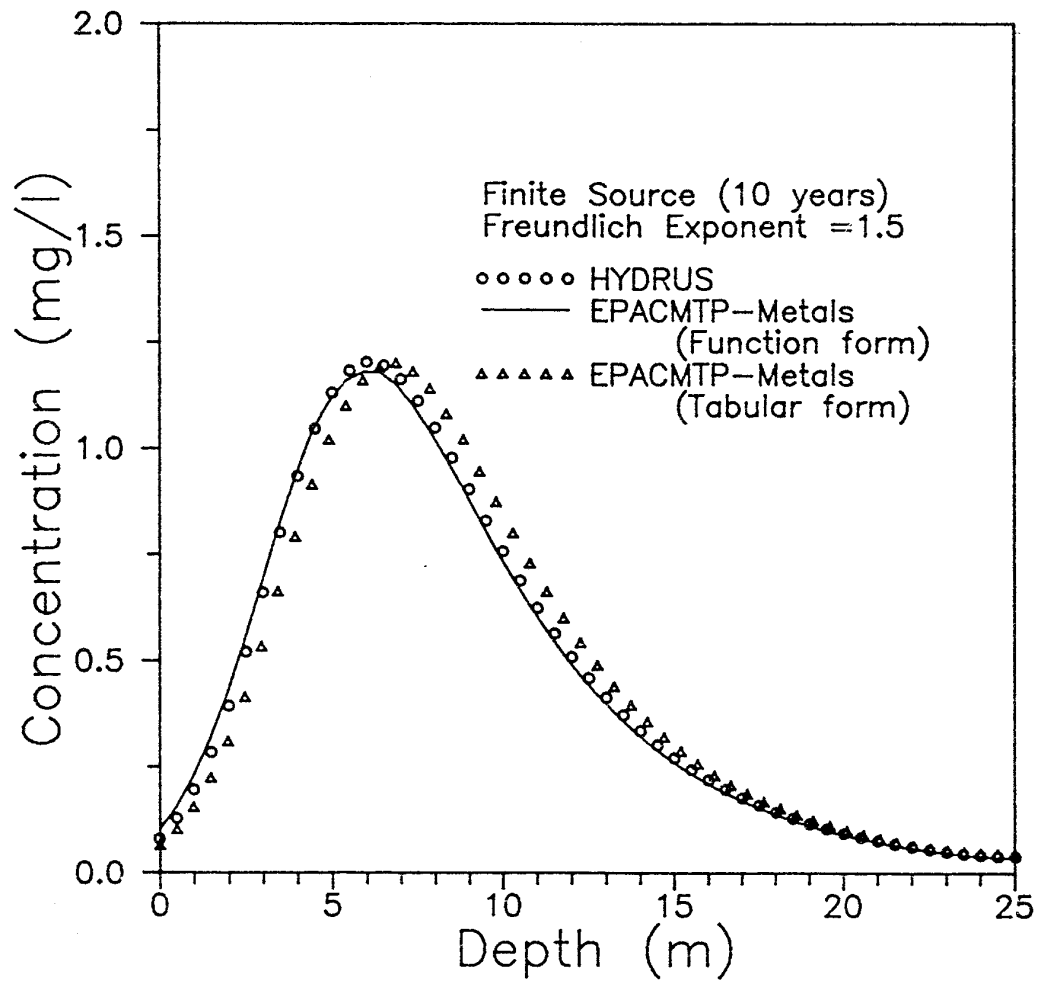


Figure D.C.2 Test Case 2, Finite Source: Comparison of Unsaturated Zone Concentration Profiles of HYDRUS and EPACMTP-Metals for Nonlinear Adsorption with Freundlich Exponent = 1.5

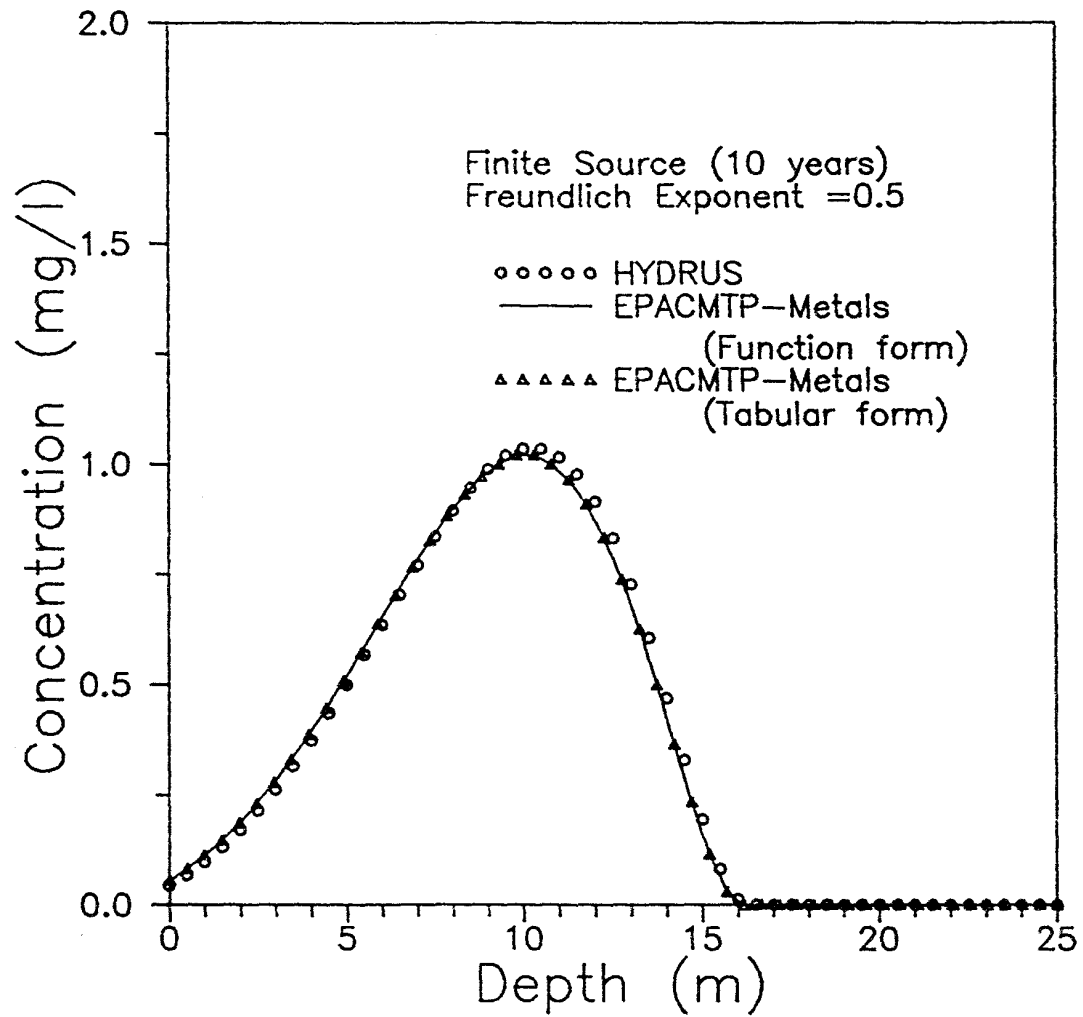


Figure D.C.3 Test Case 2, Finite Source: Comparison of Unsaturated Zone Concentration Profiles of HYDRUS and EPACMTP-Metals for Nonlinear Adsorption with Freundlich Exponent = 0.5

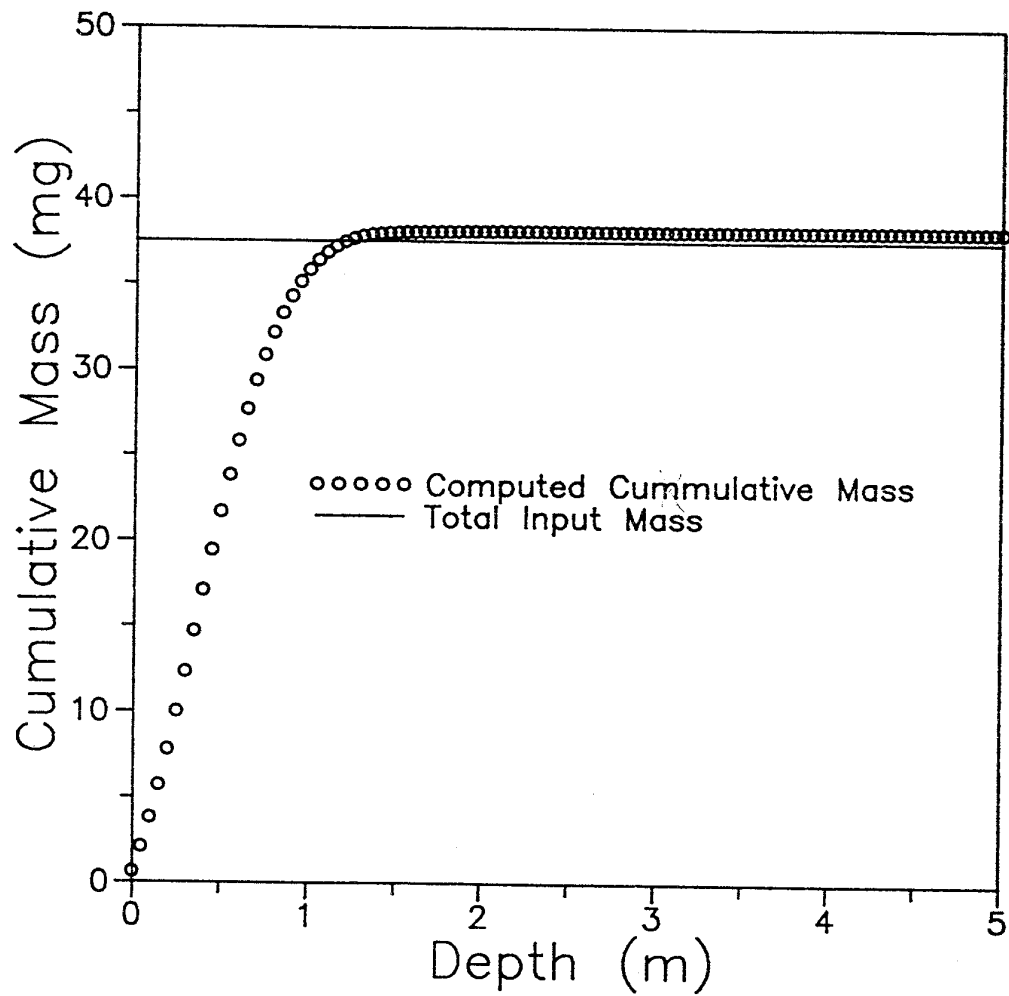


Figure D.C.4 Test Case 3: Cumulative Mass in the Unsaturated Zone and Total Input Mass for Lead Isotherm #3 Corresponding to Low Organic Acids (LOA), Low HFO, Low POM, and High pH Condition

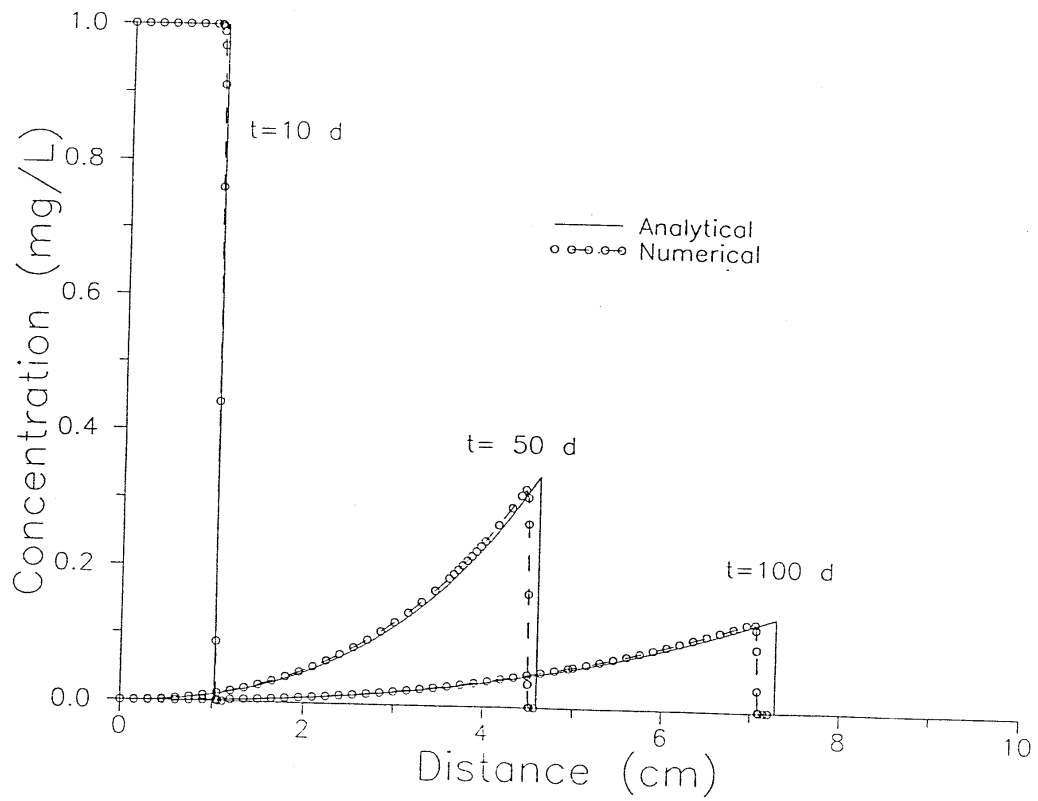


Figure D.C.5 Test Case 4: Comparison of Concentration Profiles for Freundlich Exponent = 0.5

This page was intentionally left blank.

SUBAPPENDIX D.D

VADOSE-ZONE MODULE VERIFICATION RESULTS (1997)

This page intentionally left blank.

LIST OF FIGURES

| | Page |
|--|-------------|
| Figure D.D.1 Test Case 1: Soil Water Saturation Profile, as a Function of Elevation, Where the Water Table Is Located at 5 Meters and Source Infiltration $Q_r = 0.5$ M/y | D.D-1 |
| Figure D.D.2 Test Case 2: Soil Water Saturation Profile, as a Function of Unsaturated Zone Depth for a Surface Impoundment Scenario | D.D-2 |
| Figure D.D.3 Test Case 3: Steady-state Contaminant Concentration Profile, Where the Ground Surface Is Located at 0.0 M and the Water Table Is Located at 5.0 m | D.D-3 |
| Figure D.D.4 Test Case 4: Contaminant Concentration Profiles as a Function of Depth for Four Species Involved in Branched Chain Decay at Time $T=250$ Days. The Ground Surface Is Located at 0.0 M and the Water Table Is Located at 5.0 m | D.D-4 |

This page intentionally left blank.

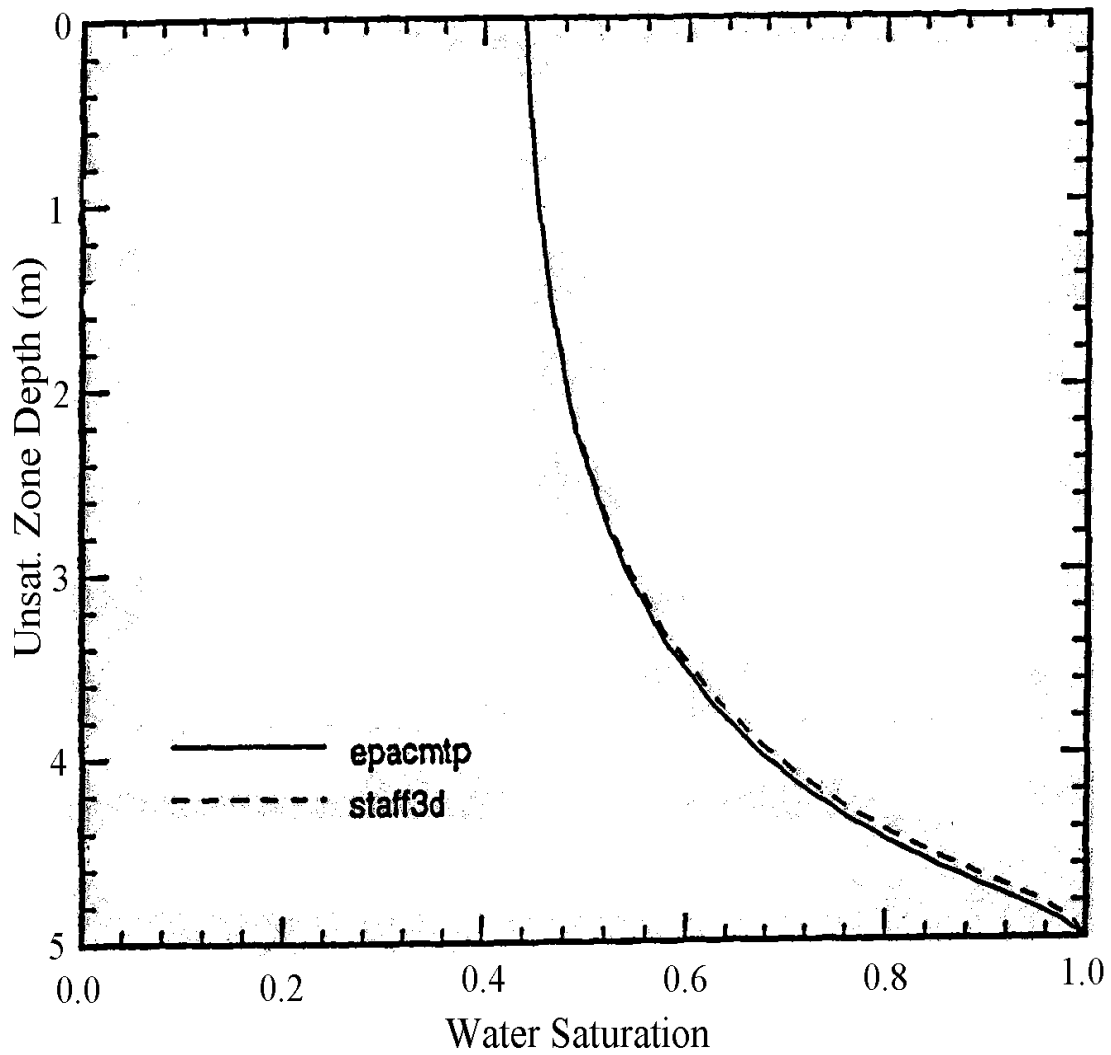


Figure D.D.1 Test Case 1: Soil Water Saturation Profile, as a Function of Elevation, Where the Water Table Is Located at 5 Meters and Source Infiltration $Q_r = 0.5$ M/y

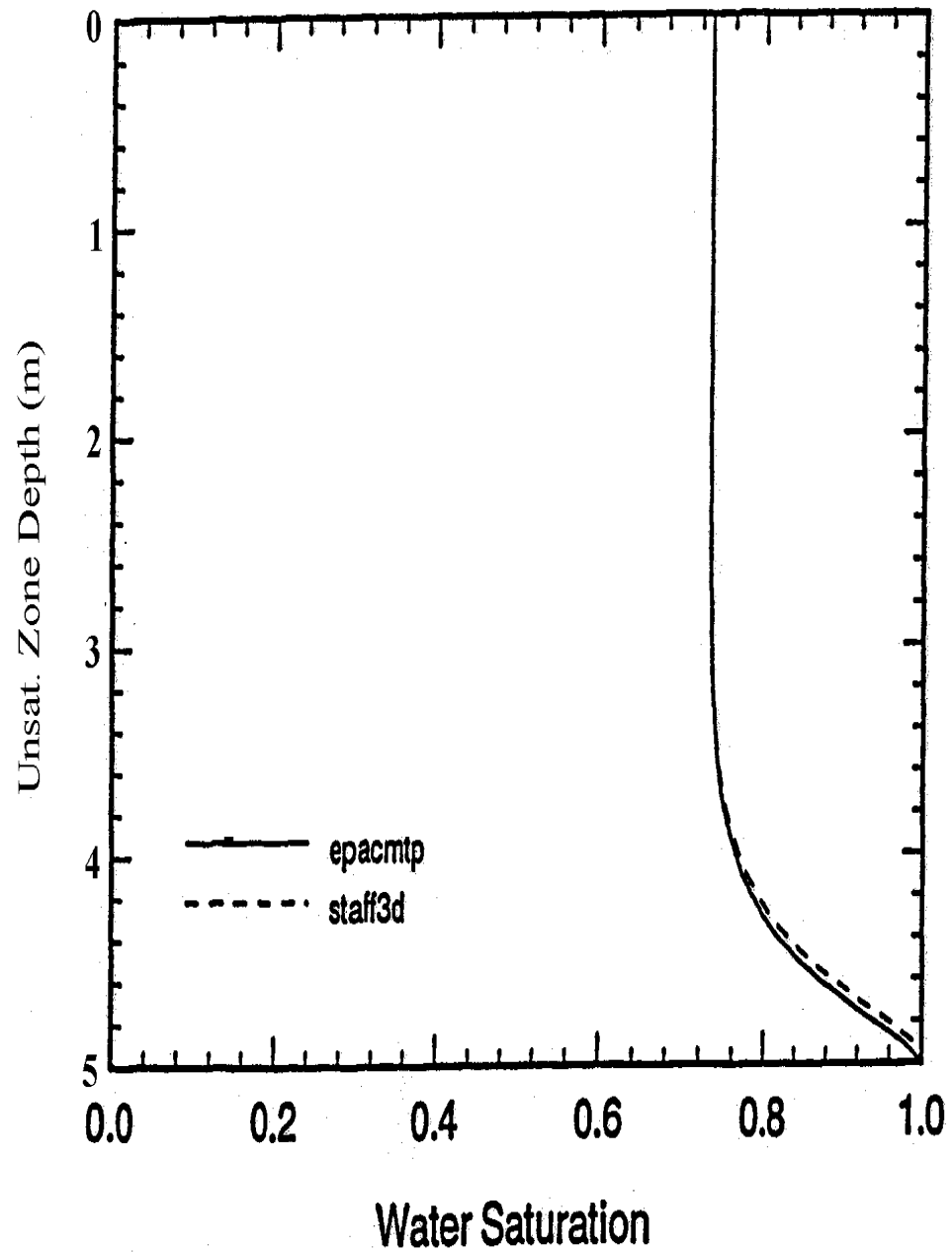


Figure D.D.2 Test Case 2: Soil Water Saturation Profile, as a Function of Unsat. Zone Depth for a Surface Impoundment Scenario

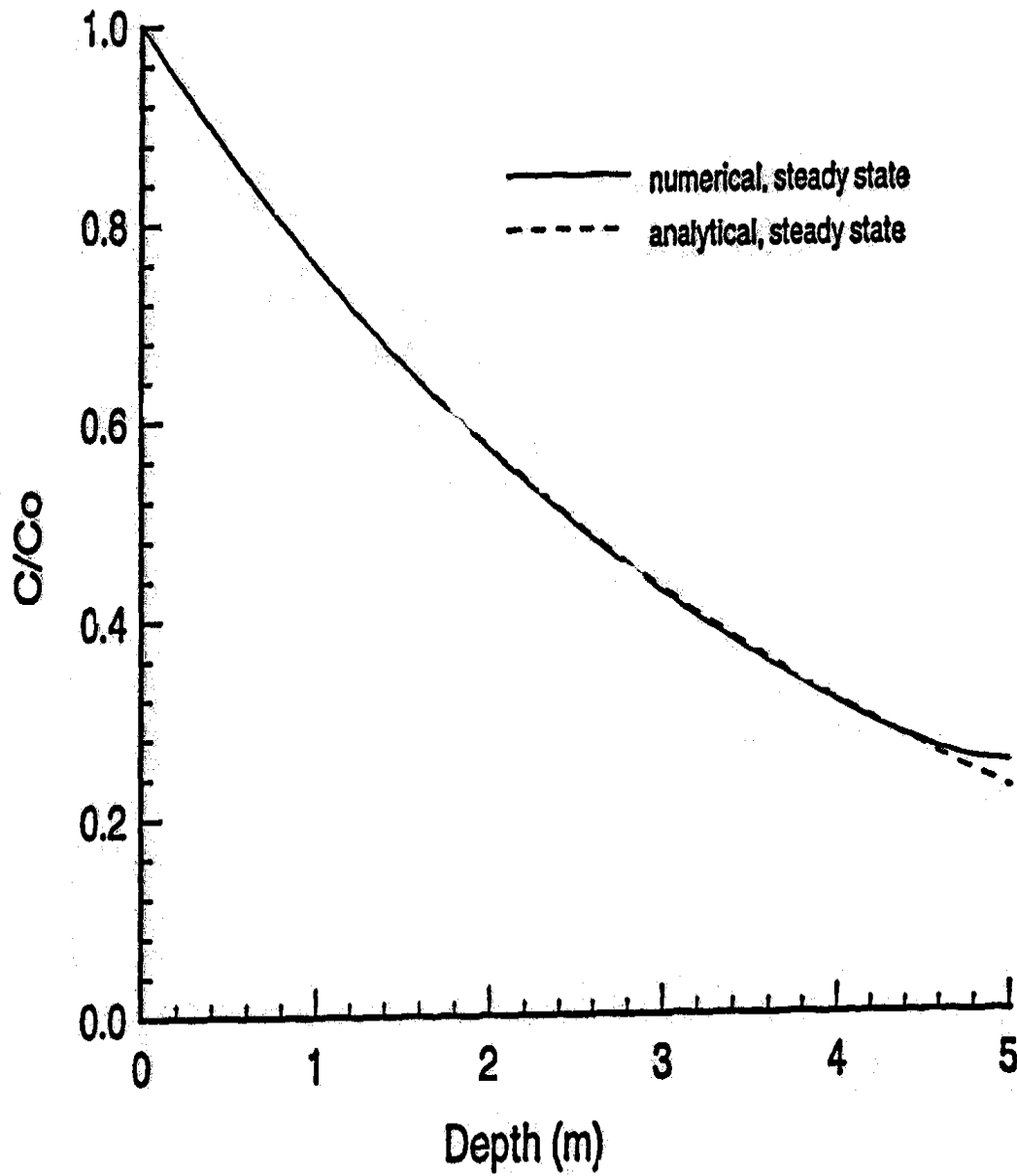


Figure D.D.3 Test Case 3: Steady-state Contaminant Concentration Profile, Where the Ground Surface Is Located at 0.0 M and the Water Table Is Located at 5.0 m

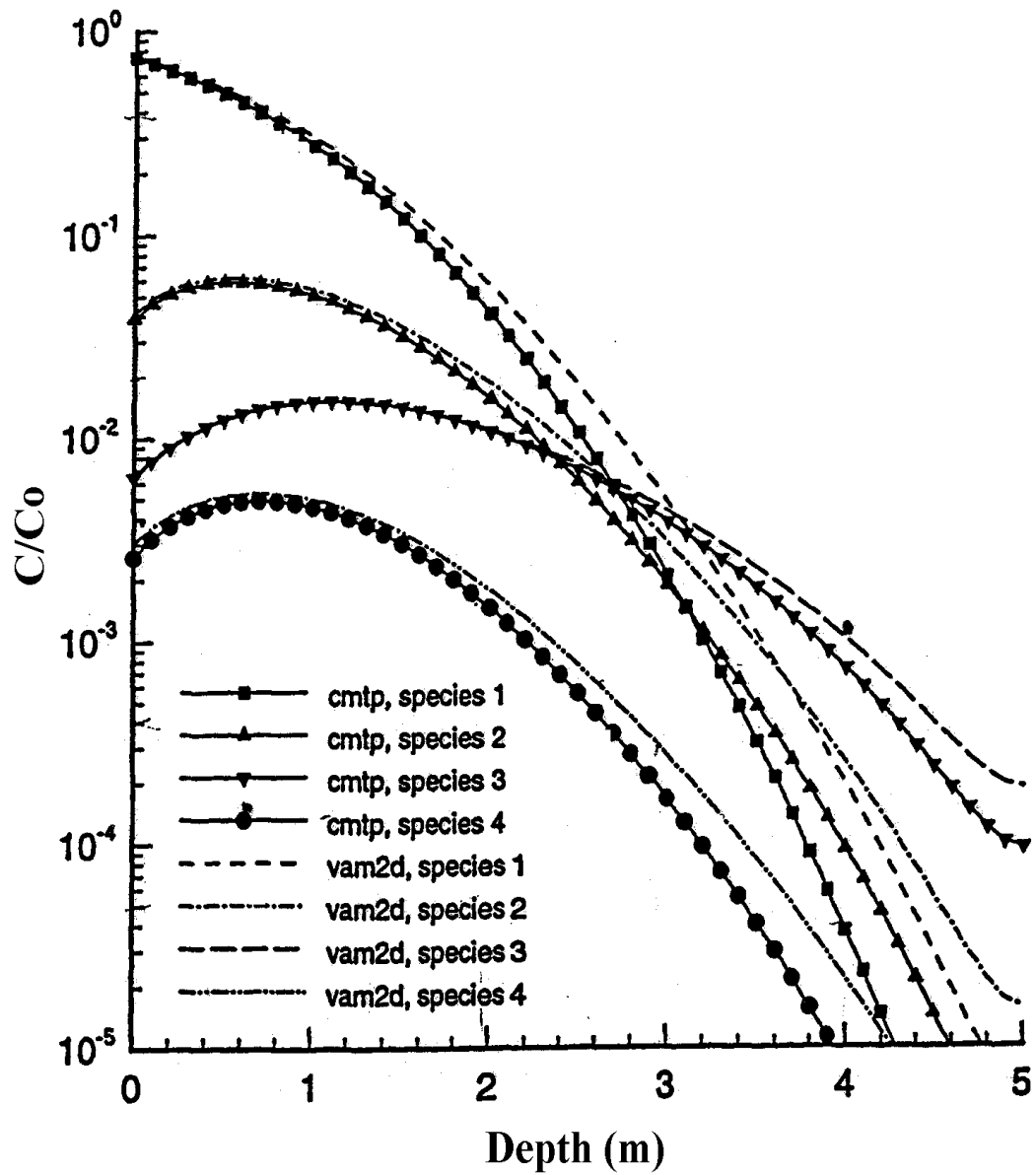


Figure D.D.4 Test Case 4: Contaminant Concentration Profiles as a Function of Depth for Four Species Involved in Branched Chain Decay at Time T=250 Days. The Ground Surface Is Located at 0.0 M and the Water Table Is Located at 5.0 m

SUBAPPENDIX D.E

AQUIFER MODULE VERIFICATION RESULTS (1997)

This page intentionally left blank.

LIST OF FIGURES

| | Page |
|--------------|--|
| Figure D.E.1 | Test Case 5: Steady State Groundwater Flow, Calculated by EPACMTP Distributions of Darcy Velocity Vectors (A) and Hydraulic Head (B) along the Vertical Cross-sectional Views (Z-x); Areal (X-y) Distributions of Darcy Velocity Vector (C) and Hydraulic Head (D) at the Top of the Saturated Zone . . . D.E-1 |
| Figure D.E.2 | Steady State Groundwater Flow Field for Test Case 5 Calculated Using MNDXYZ: Distributions of Darcy Velocity Vectors (A) and Hydraulic Head (B) along the Vertical Cross-sectional Views (X-z); Areal (X-y) Distributions of Darcy Velocity Vectors (C) and Hydraulic Head (D) at the Top of the Saturated Zone D.E-2 |
| Figure D.E.3 | Test Case 6: Concentrations Breakthrough Curves at a Receptor Well Located at the Top of Saturated Zone 100m Downgradient of the Source for Simulations Obtained with EPACMTP Analytical and Numerical (Automatic and Uniform Grid) Solutions and VAM3DF Solution (Uniform Grid) D.E-3 |
| Figure D.E.4 | Test Case 7: Contours of Base-10 Logarithm Concentrations for Species 4 of a Branched Chain Decay Sequence Using EPACMTP at Time T=500 Days along A) the Top of the Saturated Zone and B) on a Cross-section along the Centerline of the Grid. Corresponding Concentration Contours Calculated Using STAFF3D Are Shown along the Same C) Plan and D) Cross-sectional Views D.E-4 |

This page intentionally left blank.

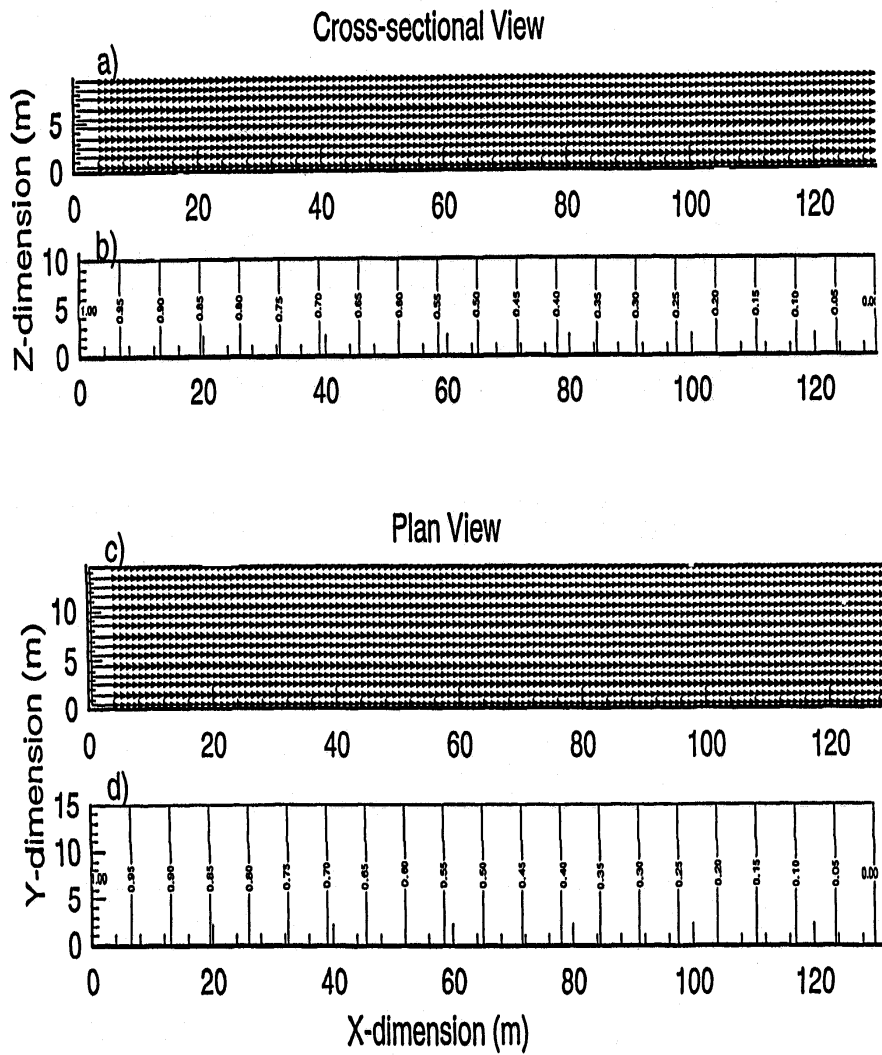


Figure D.E.1 Test Case 5: Steady State Groundwater Flow, Calculated by EPACMTP Distributions of Darcy Velocity Vectors (A) and Hydraulic Head (B) along the Vertical Cross-sectional Views (Z-x); Areal (X-y) Distributions of Darcy Velocity Vector (C) and Hydraulic Head (D) at the Top of the Saturated Zone

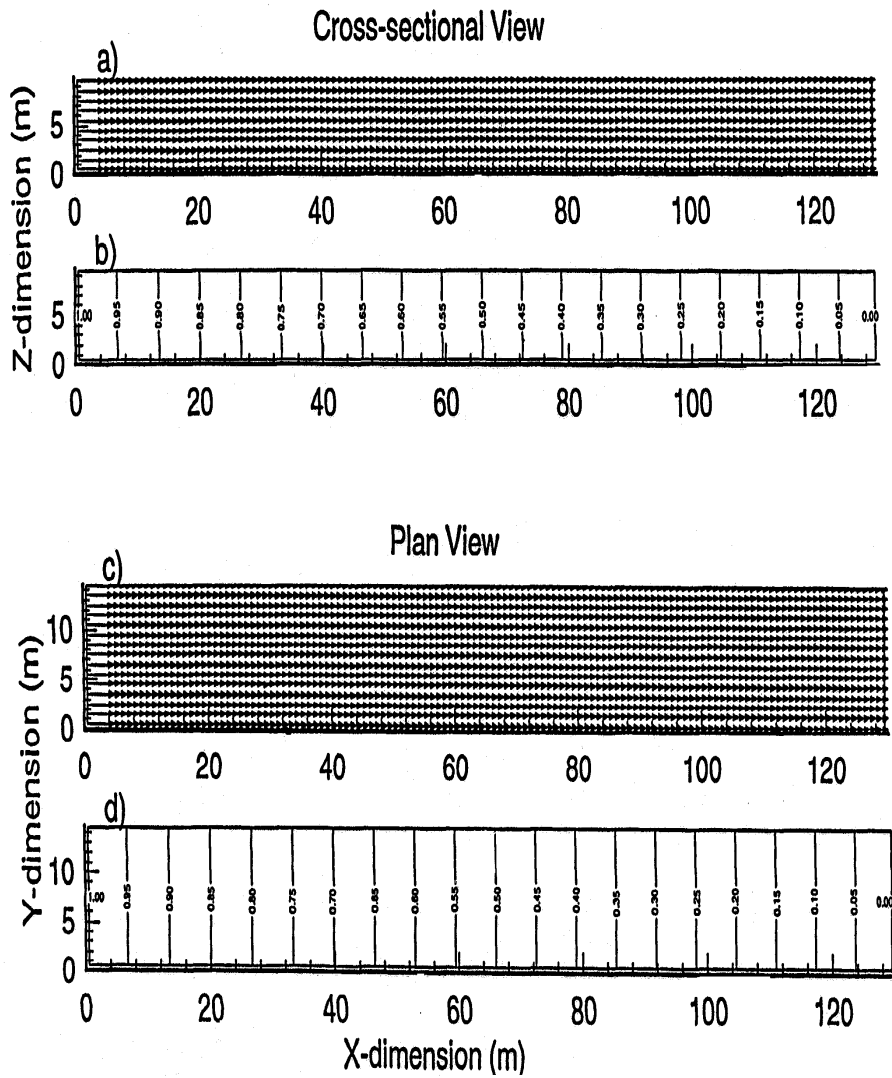


Figure D.E.2 Steady State Groundwater Flow Field for Test Case 5 Calculated Using MNDXYZ: Distributions of Darcy Velocity Vectors (A) and Hydraulic Head (B) along the Vertical Cross-sectional Views (X-z); Areal (X-y) Distributions of Darcy Velocity Vectors (C) and Hydraulic Head (D) at the Top of the Saturated Zone

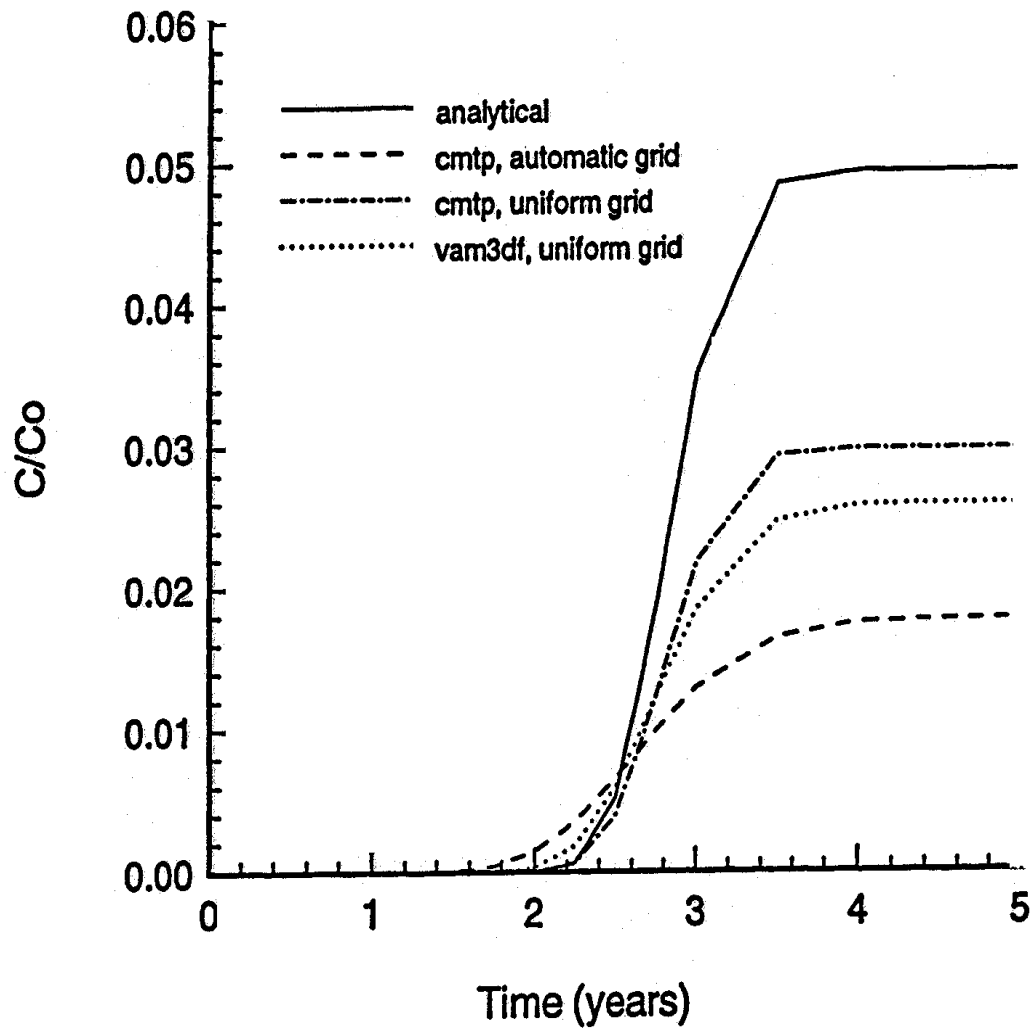


Figure D.E.3 Test Case 6: Concentrations Breakthrough Curves at a Receptor Well Located at the Top of Saturated Zone 100m Downgradient of the Source for Simulations Obtained with EPACMTP Analytical and Numerical (Automatic and Uniform Grid) Solutions and VAM3DF Solution (Uniform Grid)

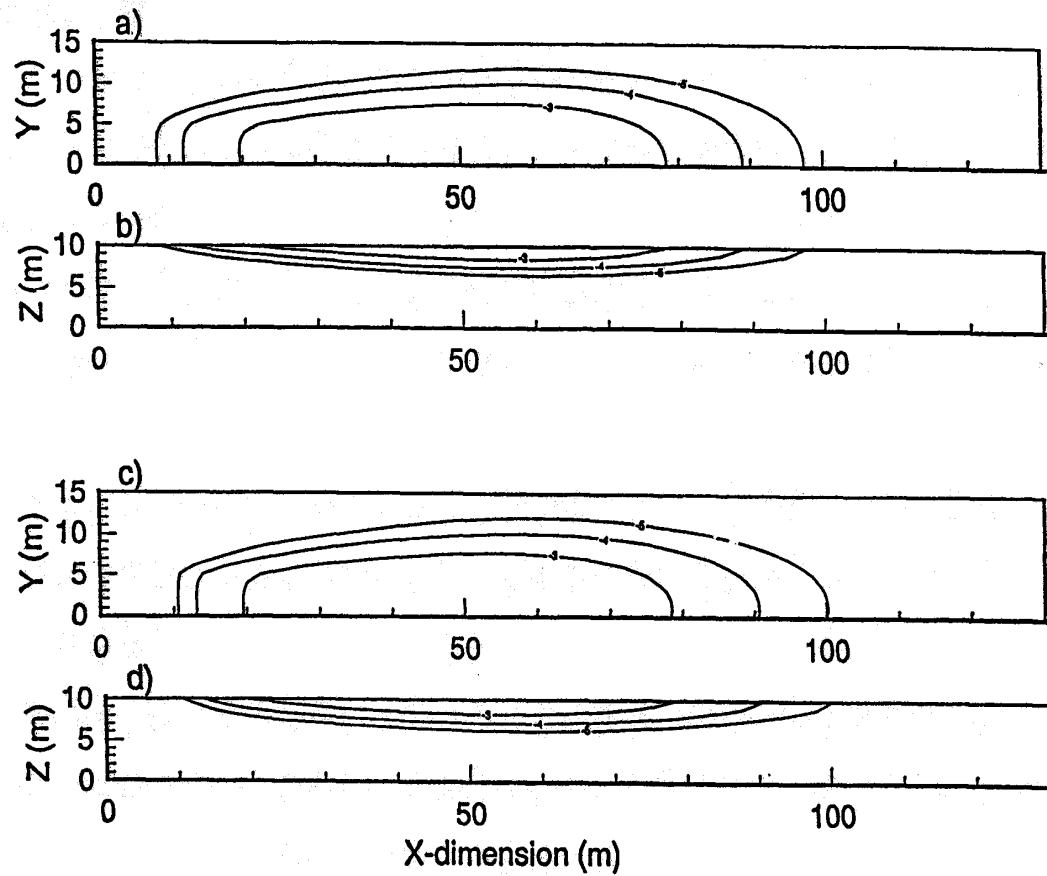


Figure D.E.4 Test Case 7: Contours of Base-10 Logarithm Concentrations for Species 4 of a Branched Chain Decay Sequence Using EPACMTP at Time T=500 Days along A) the Top of the Saturated Zone and B) on a Cross-section along the Centerline of the Grid. Corresponding Concentration Contours Calculated Using STAFF3D Are Shown along the Same C) Plan and D) Cross-sectional Views

SUBAPPENDIX D.F
COMPOSITE MODEL VERIFICATION (1997)

This page intentionally left blank.

LIST OF FIGURES

| | Page |
|--|-------------|
| Figure D.F.1 | |
| Test Case 8: Distribution of Base-10 Logarithm Concentrations Calculated Using EPACMTP at Time T=500 Days along A) the Top of the Saturated Zone (Xy Plane, Z=10.0 M) and B) on a Cross-section along the Centerline of the Grid (Xy Plane, Y=0.0 M). Corresponding Concentration Contours Calculated Using STAFF3D Are Shown along the Same C) Areal and D) Cross-sectional Views | D.F-1 |
| Figure D.F.2 | |
| Test Case 9: Cumulative Probability Curves for Exceeding a Specified Concentration at a Receptor Well Located along the Centerline of the Grid, 100.0 M Downstream of the Source Using A) EPACMTP with a Uniform Grid of 130×15×10 Elements in the Saturated Zone, B) EPACMTP with an Automatic Grid, C) EPACMTP with a Quasi-3d Grid in the Saturated Zone, and D) VAM3DF | D.F-2 |

This page intentionally left blank.

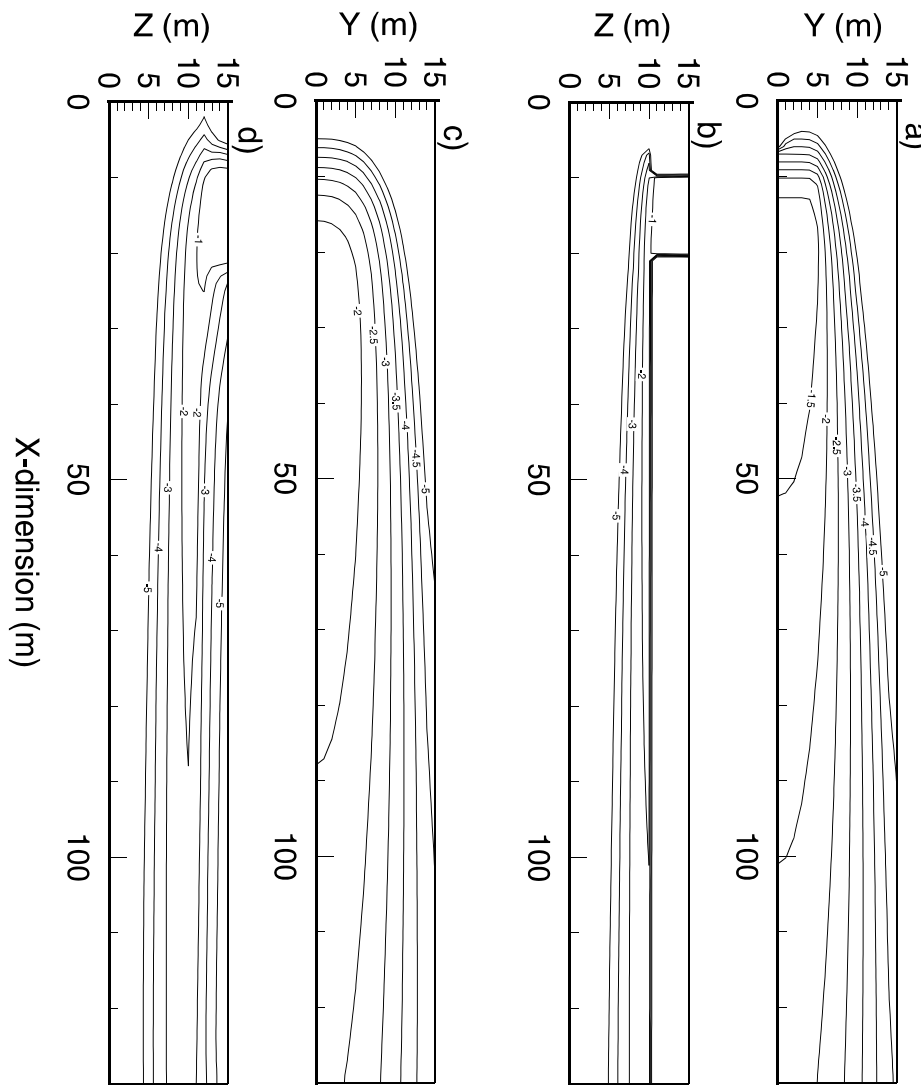


Figure D.F.1 Test Case 8: Distribution of Base-10 Logarithm Concentrations Calculated Using EPACMTP at Time T=500 Days along A) the Top of the Saturated Zone (Xy Plane, Z=10.0 M) and B) on a Cross-section along the Centerline of the Grid (Xy Plane, Y=0.0 M). Corresponding Concentration Contours Calculated Using STAFF3D Are Shown along the Same C) Areal and D) Cross-sectional Views

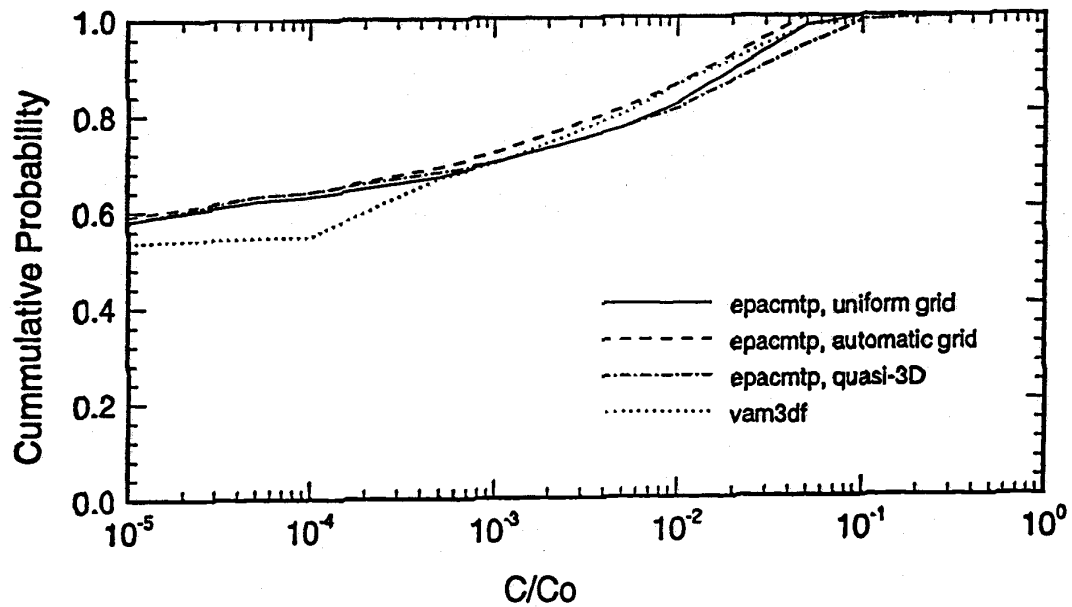


Figure D.F.2 Test Case 9: Cumulative Probability Curves for Exceeding a Specified Concentration at a Receptor Well Located along the Centerline of the Grid, 100.0 M Downstream of the Source Using A) EPACMTP with a Uniform Grid of $130 \times 15 \times 10$ Elements in the Saturated Zone, B) EPACMTP with an Automatic Grid, C) EPACMTP with a Quasi-3d Grid in the Saturated Zone, and D) VAM3DF

SUBAPPENDIX D.G

**3MRA VADOSE-ZONE MODULE VERIFICATION RESULTS
(1997)**

This page intentionally left blank.

LIST OF FIGURES

| | Page |
|--|-------------|
| Figure D.G.1 Test Case 1: Exponentially Depleting Source with No Sorption and No Hydrolysis. Comparison of VZM and EPACMTP | D.G-1 |
| Figure D.G.2 Test Case 2: Constant-Concentration Pulse With No Sorption and No Hydrolysis. Comparison of VZM and EPACMTP | D.G-1 |
| Figure D.G.3 Test Case 3: Constant-Concentration Pulse with Sorption and Hydrolysis. Comparison of VZM and EPACMTP | D.G-2 |
| Figure D.G.4 Test Case 4: Constant-Concentration Pulse with Sorption, Hydrolysis, and Chain Decay. Comparison of VZM and EPACMTP | D.G-2 |
| Figure D.G.5 Test Case 5a: Mercury Transport. Comparison of VZM and EPACMTP | D.G-3 |
| Figure D.G.6 Test Case 5b: Lead Transport. Comparison of VZM and EPACMTP | D.G-3 |
| Figure D.G.7 Test Case 6: Biodegradation Transport. Comparison of VZM and EPACMTP | D.G-4 |
| Figure D.G.8 Test Case 7: Breakthrough Curve at the Water Table for Vadoze Zone Module and Verification Code (MS-VMS) at Site LF0223504 for Benzene (Source was Terminated After Time = 200 Years) | D.G-5 |
| Figure D.G.9 Test Case 8: Pressure Head Profile for the HWIR99 Vadoze Zone Module and Verification Code (MS-VMS) at Site LF0223504 for Benzene | D.G-6 |

This page intentionally left blank.

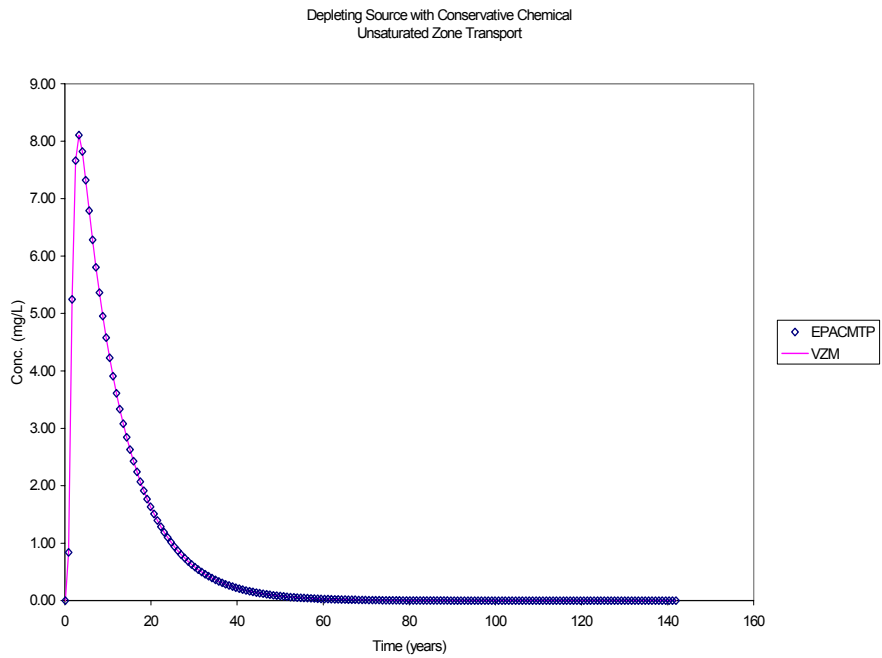


Figure D.G.1 Test Case 1: Exponentially Depleting Source with No Sorption and No Hydrolysis. Comparison of VZM and EPACMTP

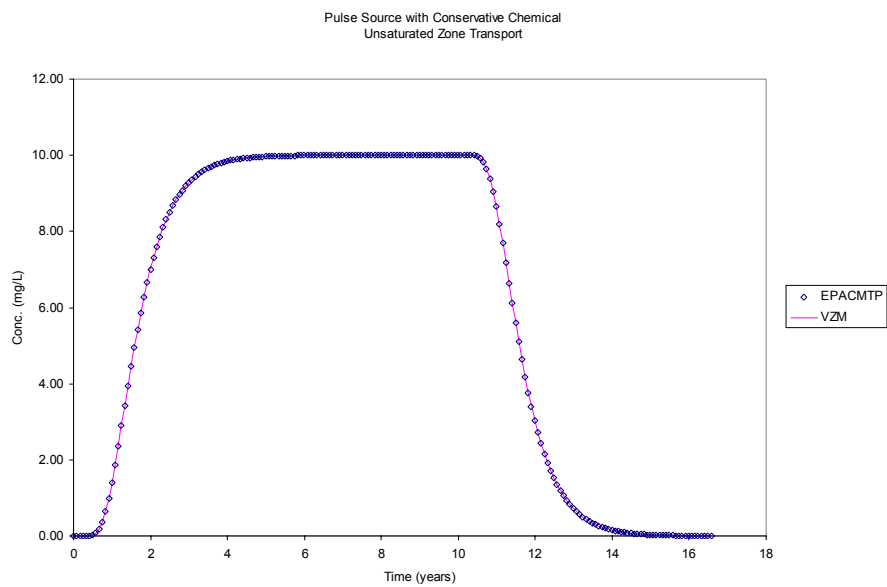


Figure D.G.2 Test Case 2: Constant-Concentration Pulse With No Sorption and No Hydrolysis. Comparison of VZM and EPACMTP

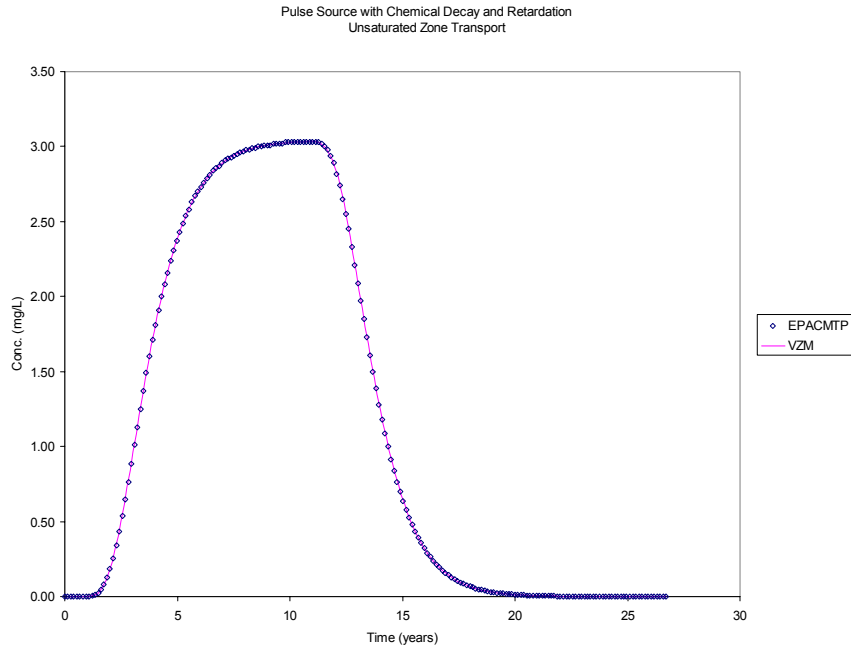


Figure D.G.3 Test Case 3: Constant-Concentration Pulse with Sorption and Hydrolysis. Comparison of VZM and EPACMTP

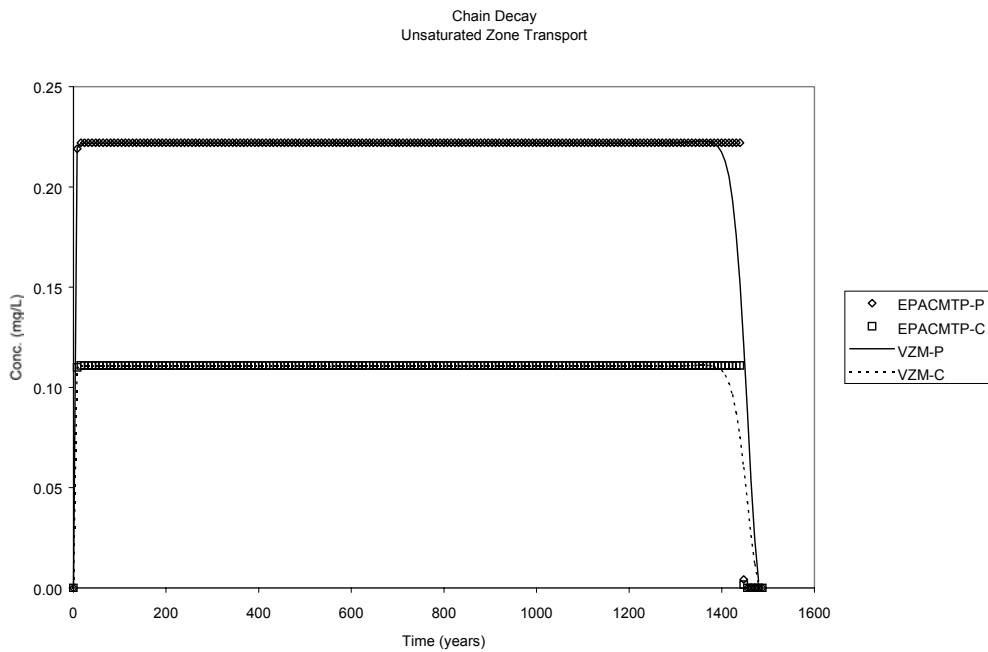


Figure D.G.4 Test Case 4: Constant-Concentration Pulse with Sorption, Hydrolysis, and Chain Decay. Comparison of VZM and EPACMTP

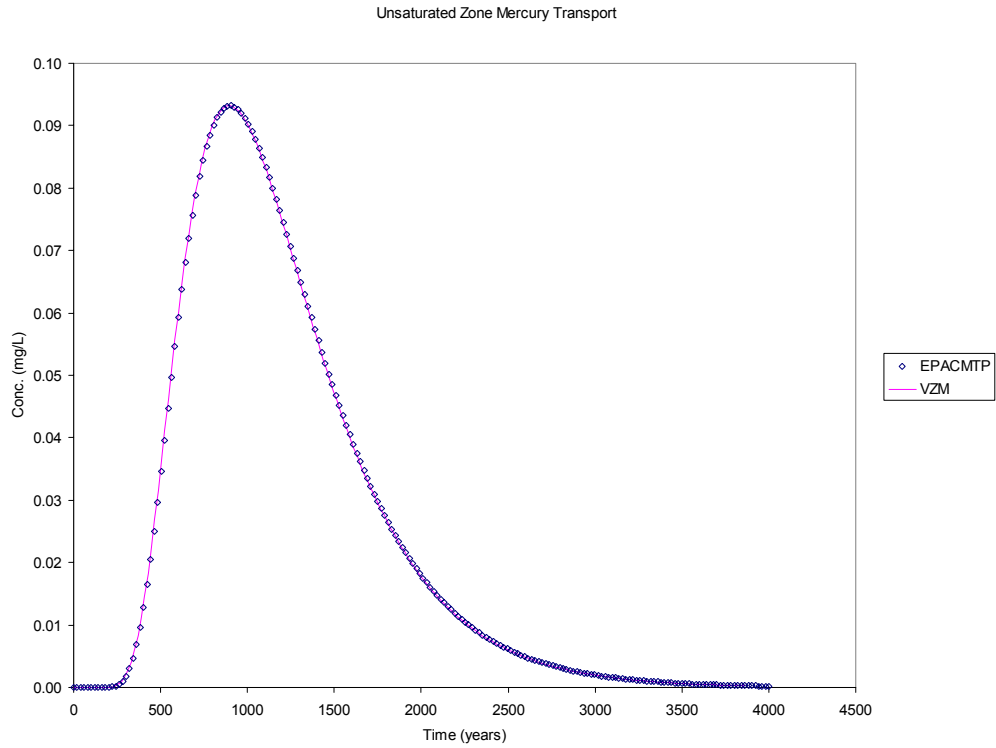


Figure D.G.5 Test Case 5a: Mercury Transport. Comparison of VZM and EPACMTP

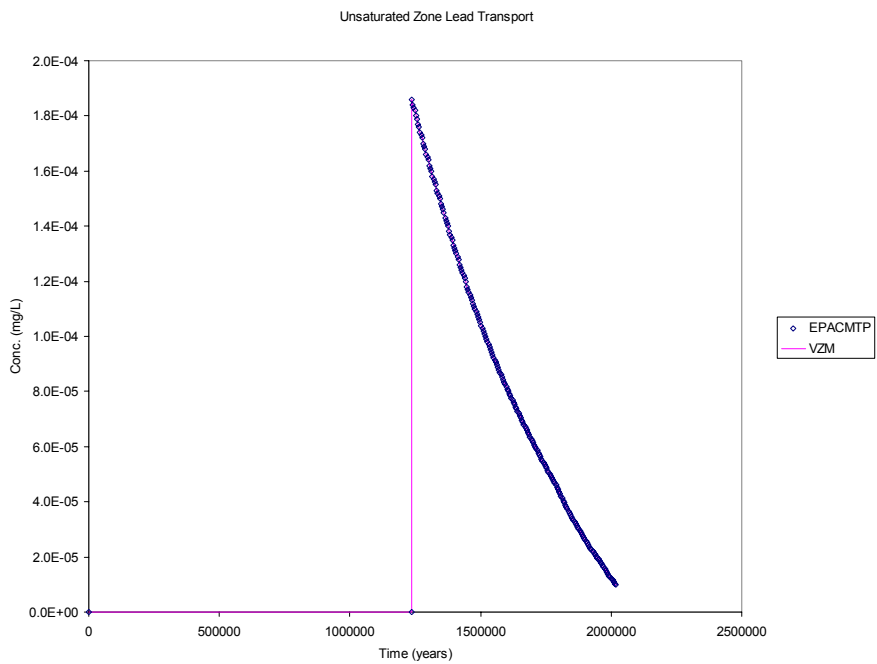


Figure D.G.6 Test Case 5b: Lead Transport. Comparison of VZM and EPACMTP

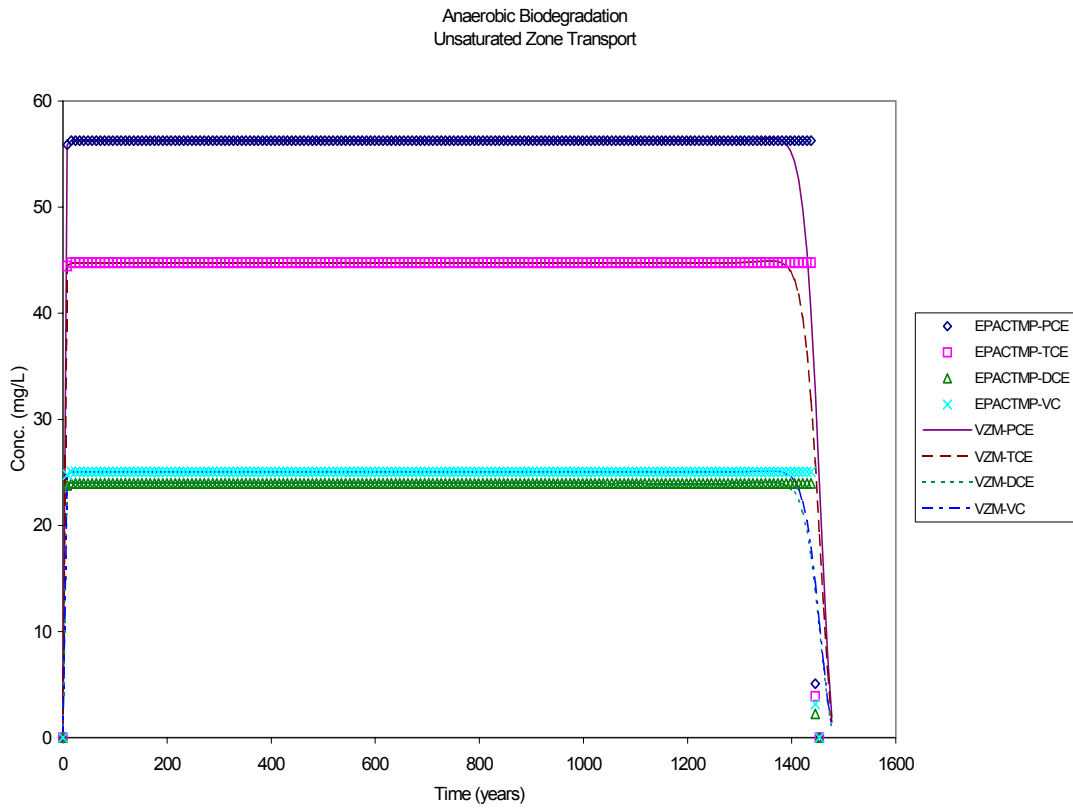


Figure D.G.7 Test Case 6: Biodegradation Transport. Comparison of VZM and EPACMTP

Verification Break Through Curve at the Watertable
for Benzene at LF Site 0223504

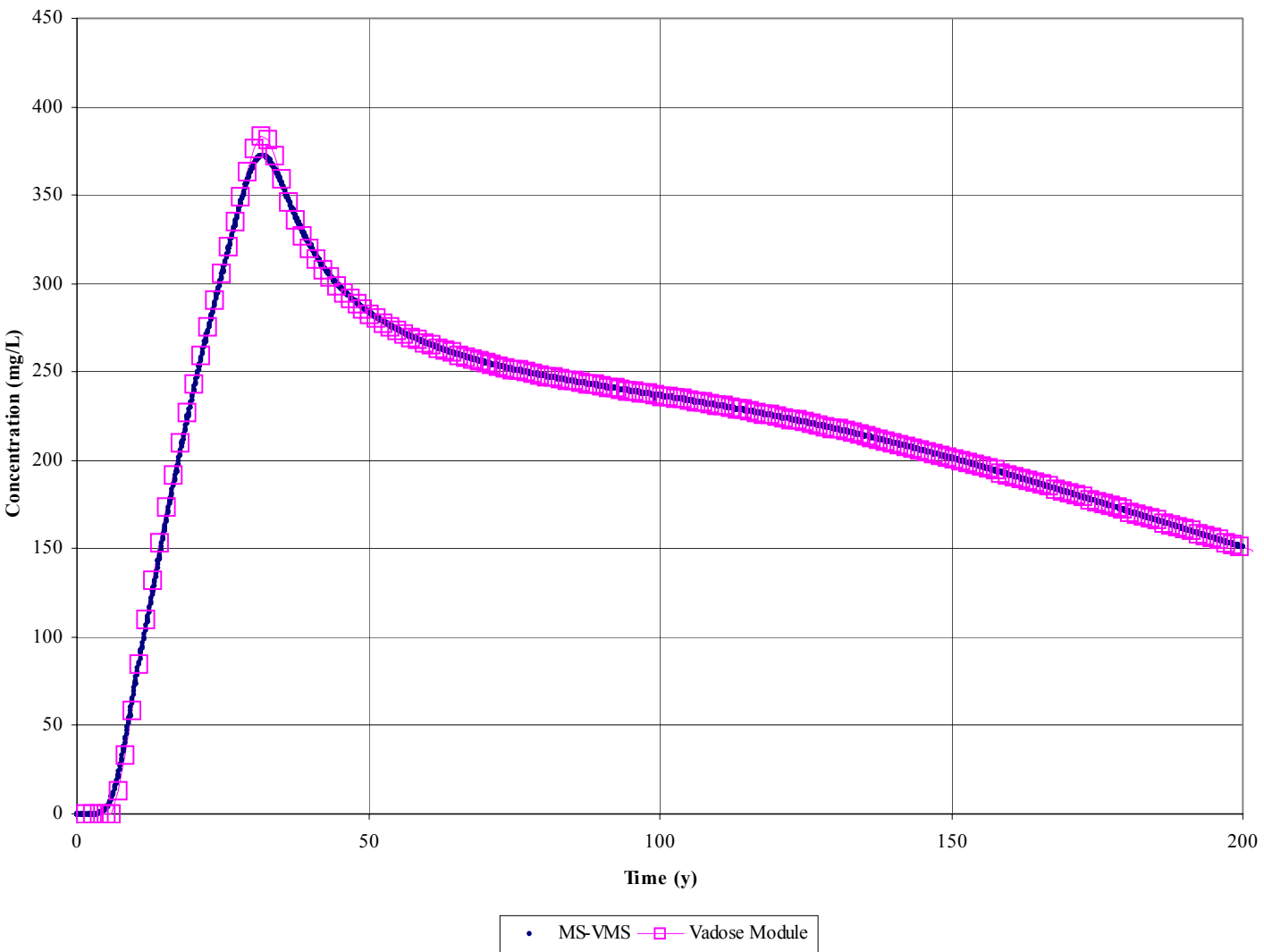


Figure D.G.8 Test Case 7: Breakthrough Curve at the Water Table for Vadose Zone Module and Verification Code (MS-VMS) at Site LF0223504 for Benzene (Source was Terminated After Time = 200 Years)

Verification Pressure Profile for HWIR99 Vadose Zone Module and MS-VMS for Benzene at Site LF0223504

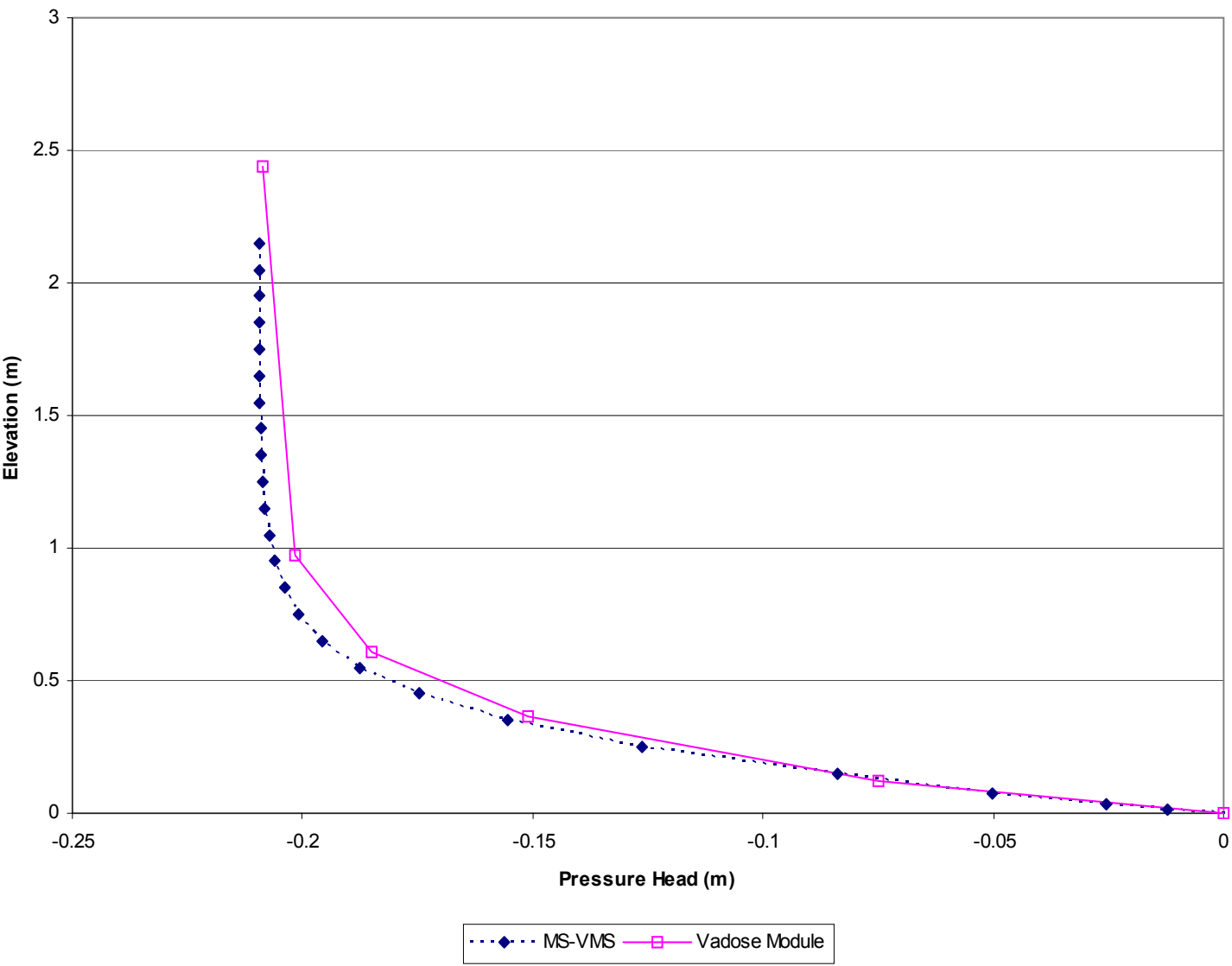


Figure D.G.9 Test Case 8: Pressure Head Profile for the HWIR99 Vadose Zone Module and Verification Code (MS-VMS) at Site LF0223504 for Benzene

SUBAPPENDIX D.H

3MRA ANALYSES MODULE VERIFICATION RESULTS (1997)

This page intentionally left blank.

LIST OF FIGURES

| | Page |
|---------------|---|
| Figure D.H.1 | Test Case 1: Exponentially Depleting Source with No Sorption Nor Hydrolysis. Comparison of SZMs and 3-D EPACMTP D.H-1 |
| Figure D.H.2 | Test Case 2: Constant-concentration Pulse with No Sorption Nor Hydrolysis. Comparison of SZMs and 3-D EPACMTP D.H-1 |
| Figure D.H.3 | Test Case 3: Constant-concentration Pulse with Sorption and Hydrolysis. Comparison of SZMs and 3-D EPACMTP D.H-2 |
| Figure D.H.4 | Test Case 4a: Constant-concentration Pulse with Sorption, Hydrolysis, and Chain Decay. Comparison of SZMs and 3-D EPACMTP, Parent Chemical D.H-2 |
| Figure D.H.5 | Test Case 4b: Constant-concentration Pulse with Sorption, Hydrolysis, and Chain Decay. Comparison of SZMs and 3-D EPACMTP, Daughter Chemical D.H-3 |
| Figure D.H.6 | Test Case 5: Mercury Transport. Comparison of SZMs and 3-D EPACMTP D.H-4 |
| Figure D.H.7 | Test Case 6a: Constant-concentration Pulse with Biodegradation and Chain Decay. Comparison of SZMs and 3-D EPACTMP, Tetrachloroethylene D.H-5 |
| Figure D.H.8 | Test Case 6b: Constant-concentration Pulse with Biodegradation and Chain Decay. Comparison of SZMs and 3-D EPACMTP, Trichloroethylene D.H-6 |
| Figure D.H.9 | Test Case 6c: Constant-concentration Pulse with Biodegradation and Chain Decay. Comparison of SZMs and 3-D EPACMTP, Dichloroethylene D.H-7 |
| Figure D.H.10 | Case 6d: Constant-concentration Pulse with Biodegradation and Chain Decay. Comparison of SZMs and 3-D EPACMTP, Vinyl Chloride D.H-8 |
| Figure D.H.11 | Test Case 7: Monte-Carlo Results for Landfill Waste Management Unit Using HWIR Default Distributions Comparing 3-D EPACMTP and the Pseudo 3-D SZM (SZM-3D1) D.H-9 |

This page intentionally left blank.

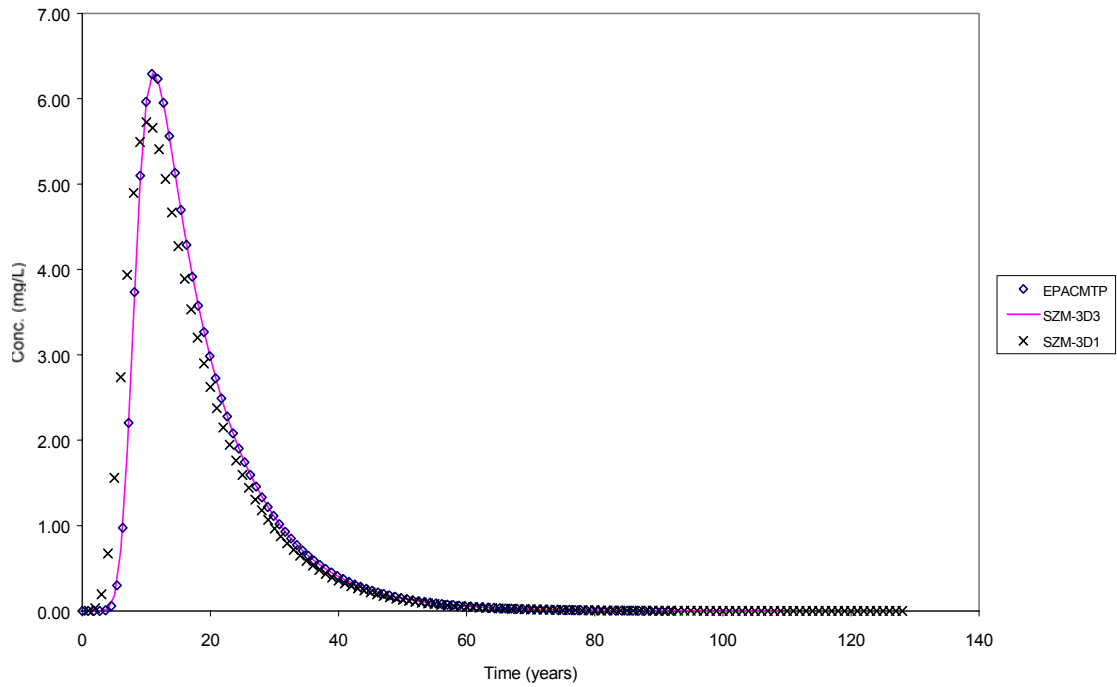


Figure D.H.1 Test Case 1: Exponentially Depleting Source with No Sorption Nor Hydrolysis. Comparison of SZMs and 3-D EPACMTP

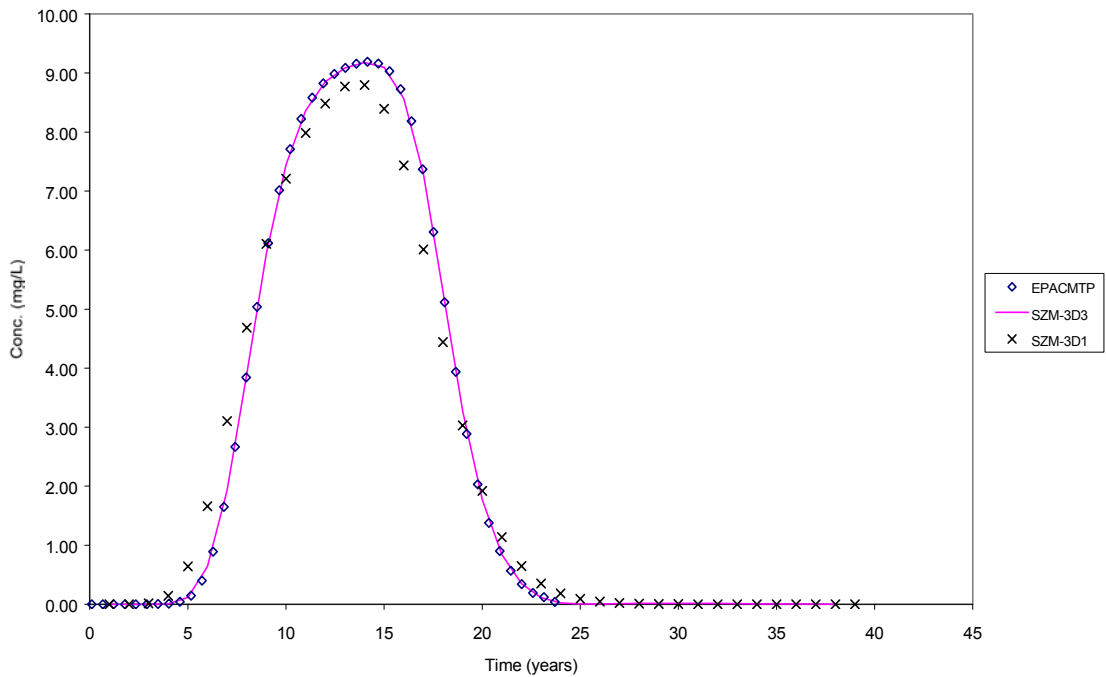


Figure D.H.2 Test Case 2: Constant-concentration Pulse with No Sorption Nor Hydrolysis. Comparison of SZMs and 3-D EPACMTP

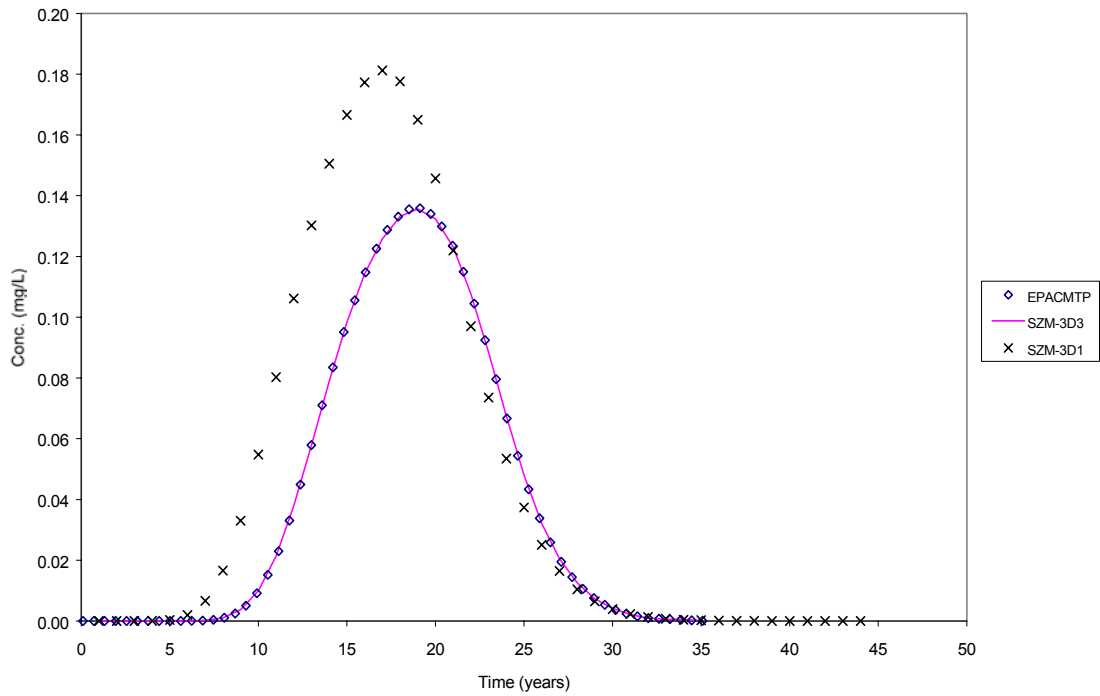


Figure D.H.3 Test Case 3: Constant-concentration Pulse with Sorption and Hydrolysis. Comparison of SZMs and 3-D EPACMTP

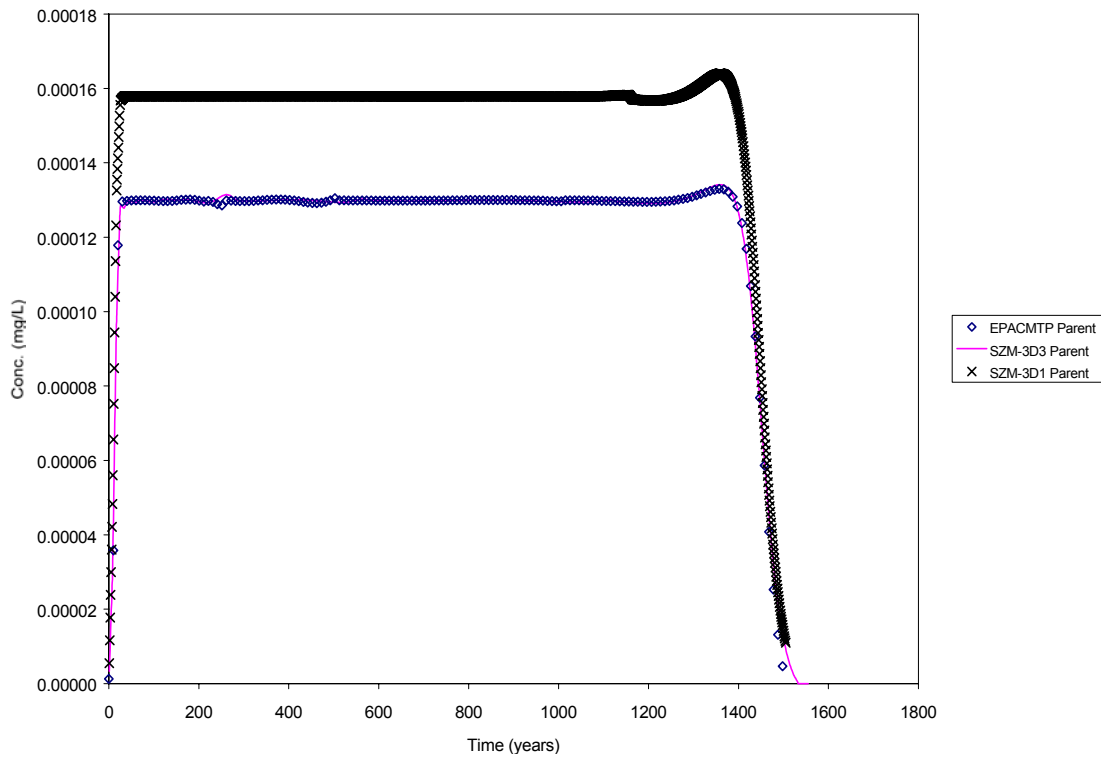


Figure D.H.4 Test Case 4a: Constant-concentration Pulse with Sorption, Hydrolysis, and Chain Decay. Comparison of SZMs and 3-D EPACMTP, Parent Chemical

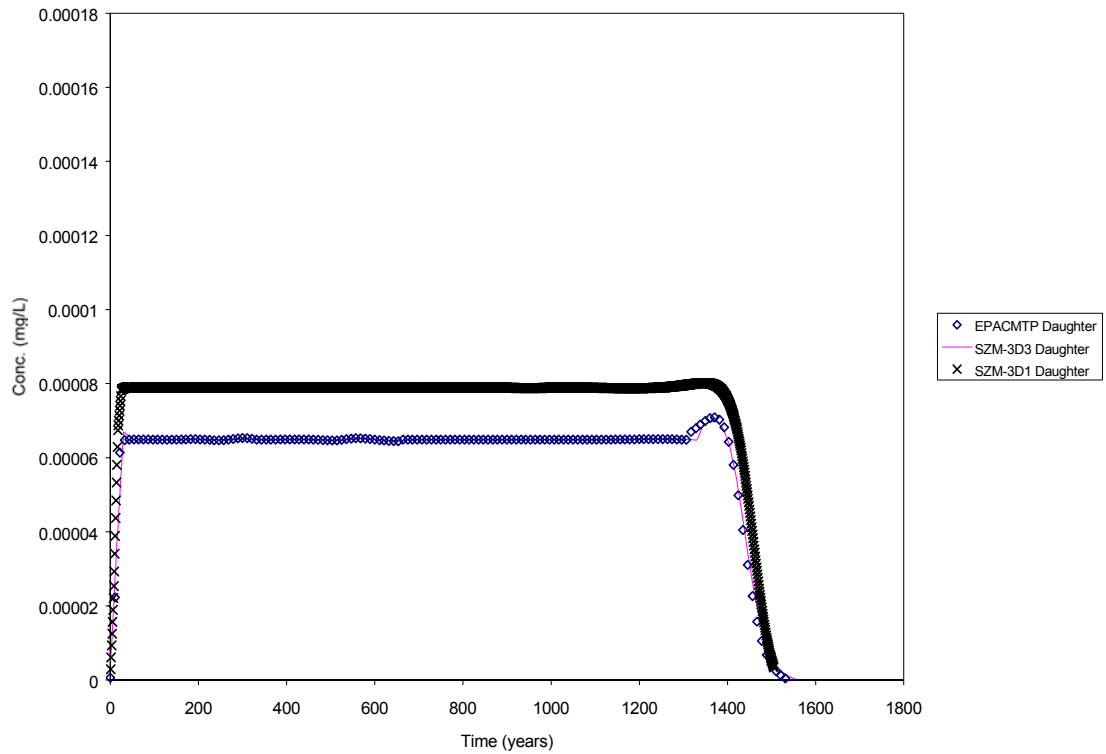


Figure D.H.5 Test Case 4b: Constant-concentration Pulse with Sorption, Hydrolysis, and Chain Decay. Comparison of SZMs and 3-D EPACMTP, Daughter Chemical

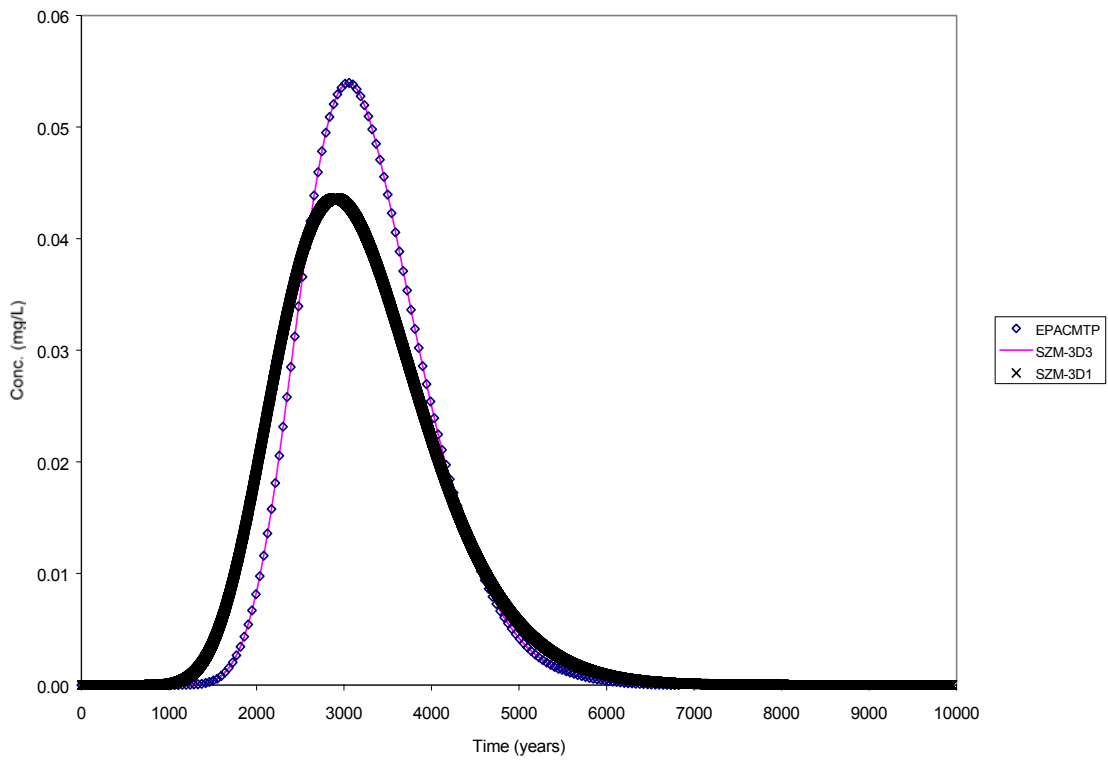


Figure D.H.6 Test Case 5: Mercury Transport. Comparison of SZMs and 3-D EPACMTP

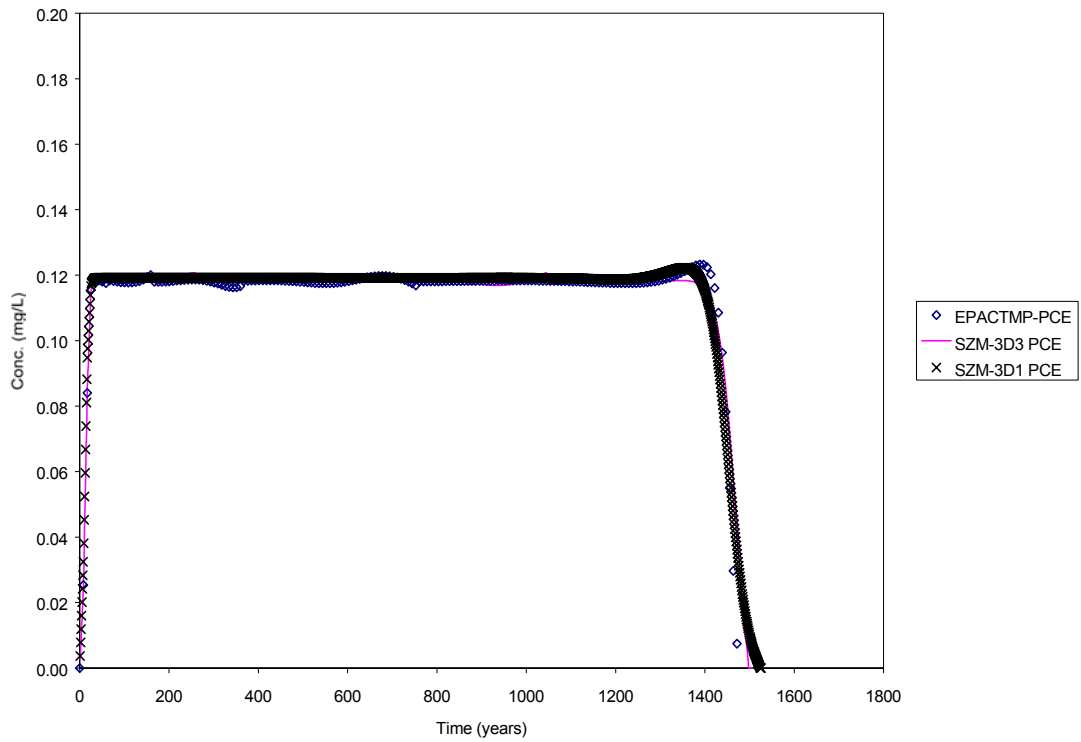


Figure D.H.7 Test Case 6a: Constant-concentration Pulse with Biodegradation and Chain Decay. Comparison of SZMs and 3-D EPACKMP, Tetrachloroethylene

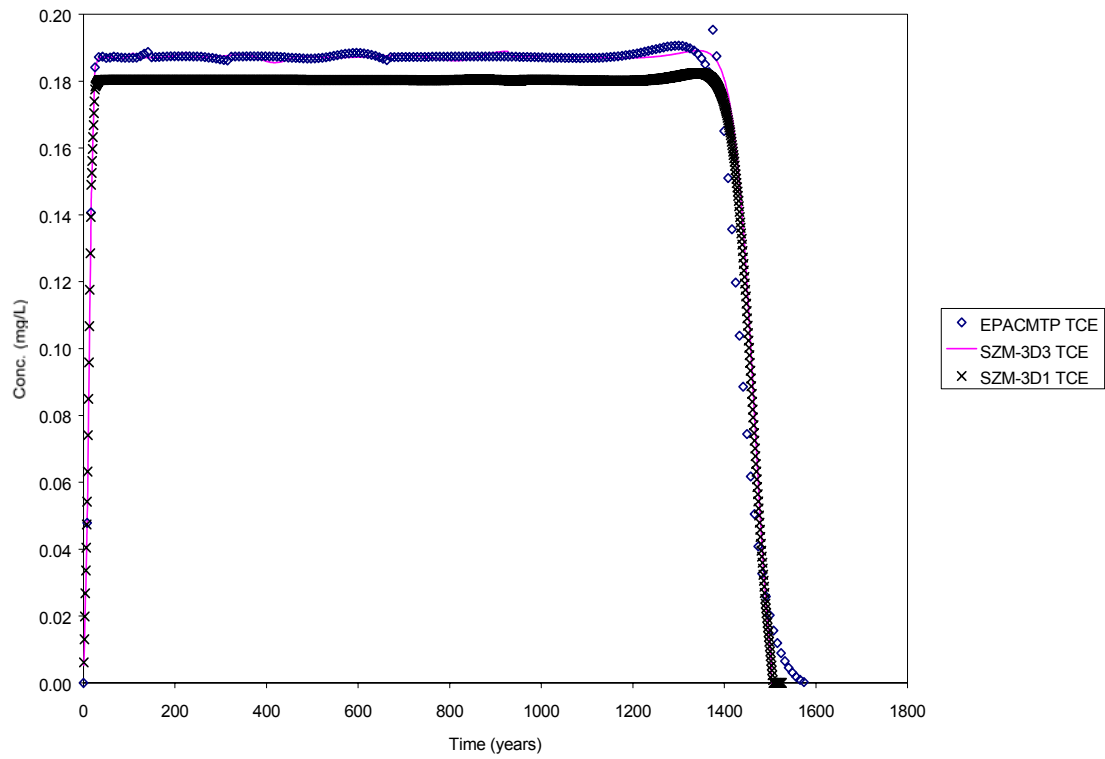


Figure D.H.8 Test Case 6b: Constant-concentration Pulse with Biodegradation and Chain Decay. Comparison of SZMs and 3-D EPACMTP, Trichloroethylene

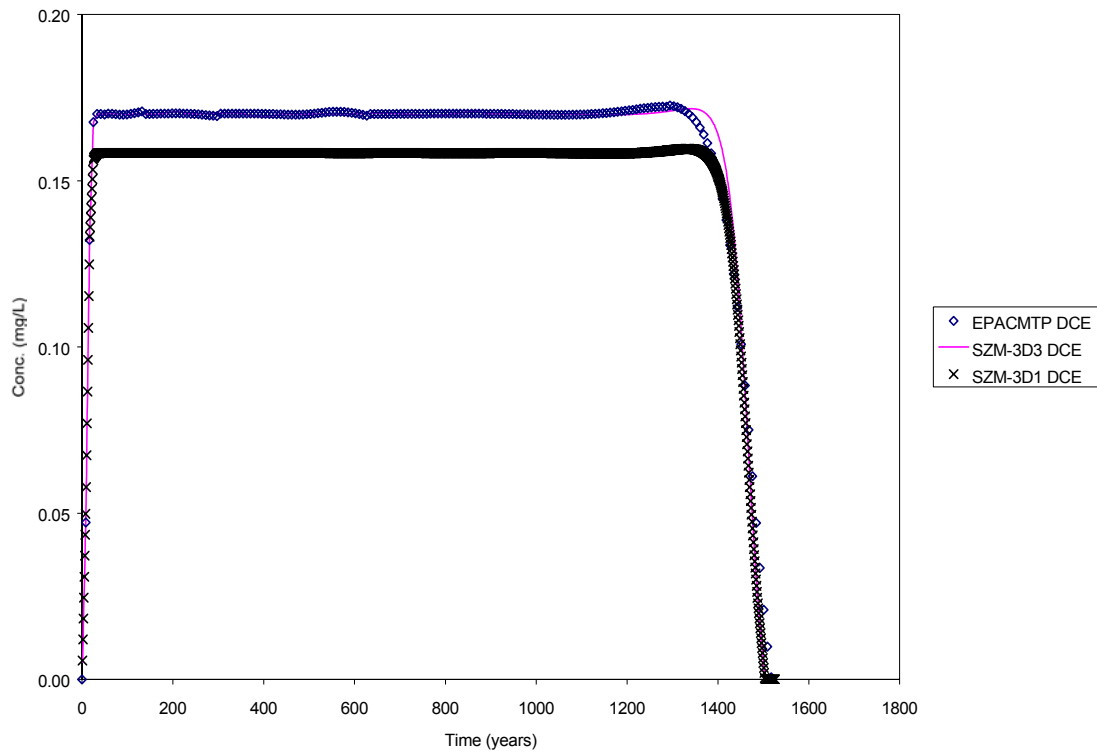


Figure D.H.9 Test Case 6c: Constant-concentration Pulse with Biodegradation and Chain Decay. Comparison of SZMs and 3-D EPACMTP, Dichloroethylene

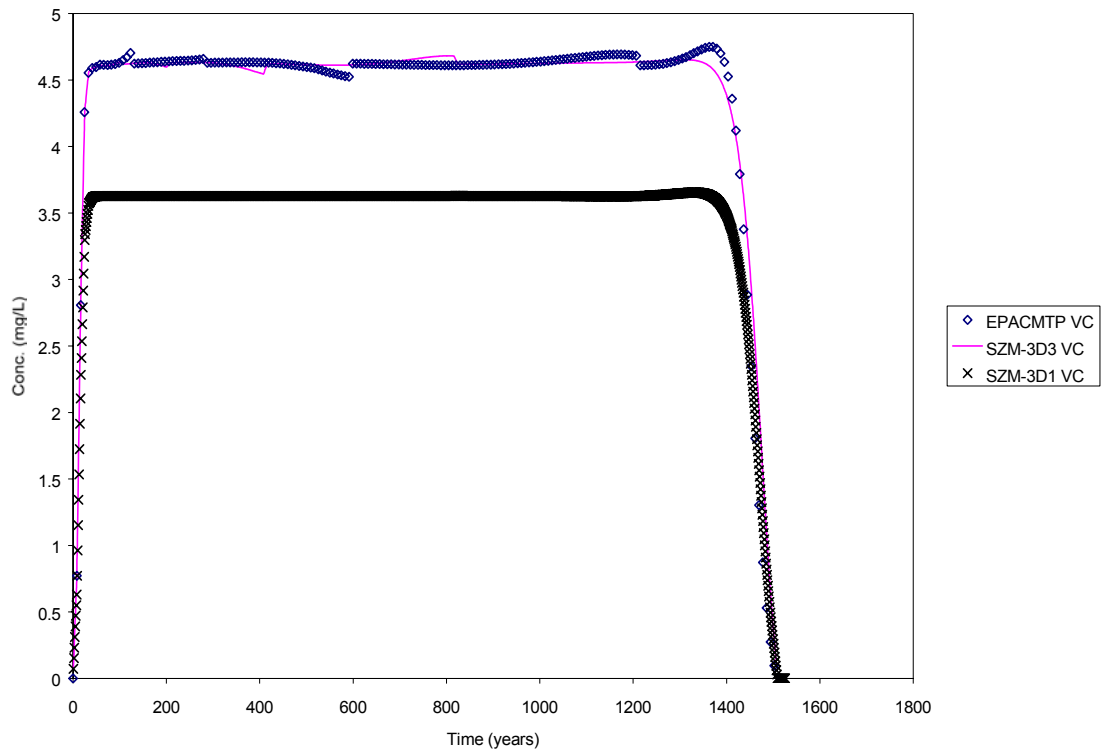


Figure D.H.10 Case 6d: Constant-concentration Pulse with Biodegradation and Chain Decay. Comparison of SZMs and 3-D EPACMTP, Vinyl Chloride

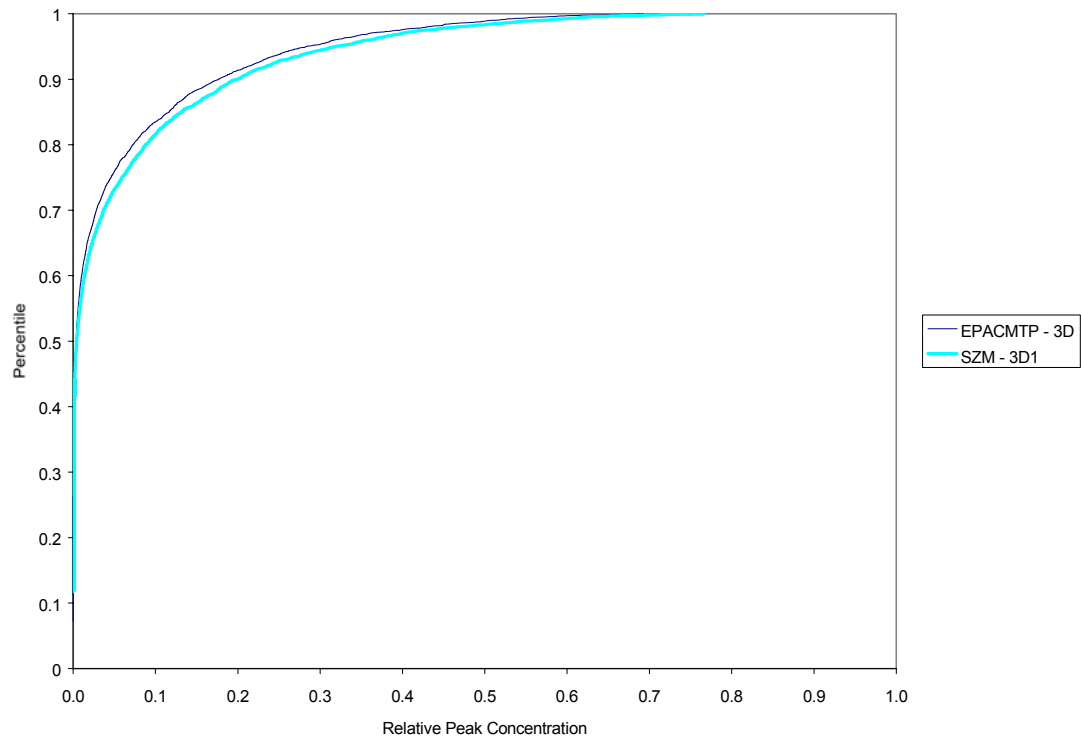


Figure D.H.11 Test Case 7: Monte-Carlo Results for Landfill Waste Management Unit Using HWIR Default Distributions Comparing 3-D EPACMTP and the Pseudo 3-D SZM (SZM-3D1)

This page was intentionally left blank.

SUBAPPENDIX D.I

**3MRA PSEUDO 3-D AQUIFER MODULE VERIFICATION
RESULTS (1999)**

This page intentionally left blank.

LIST OF FIGURES

| | Page |
|--------------|--|
| Figure D.I.1 | Test Case 2: Centerline Breakthrough Curve for HWIR99 and Verification Modules, X = 257, for Well 58 D.I-1 |
| Figure D.I.2 | Test Case 3: Breakthrough Curves for HWIR99 and Verification Modules at Well 81 D.I-2 |

This page intentionally left blank.

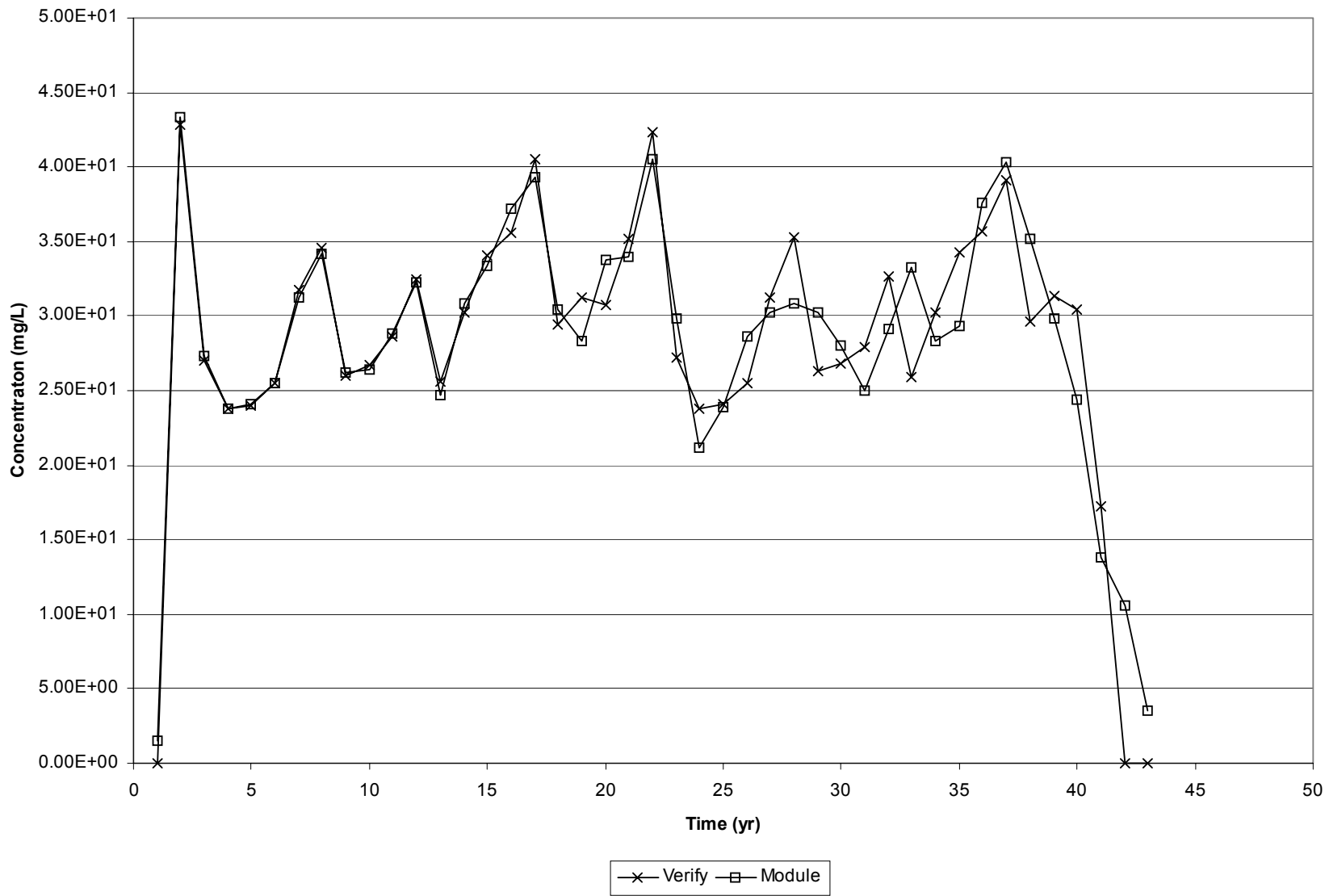


Figure D.I.1 Test Case 2: Centerline Breakthrough Curve for HWIR99 and Verification Modules, X = 257, for Well 58

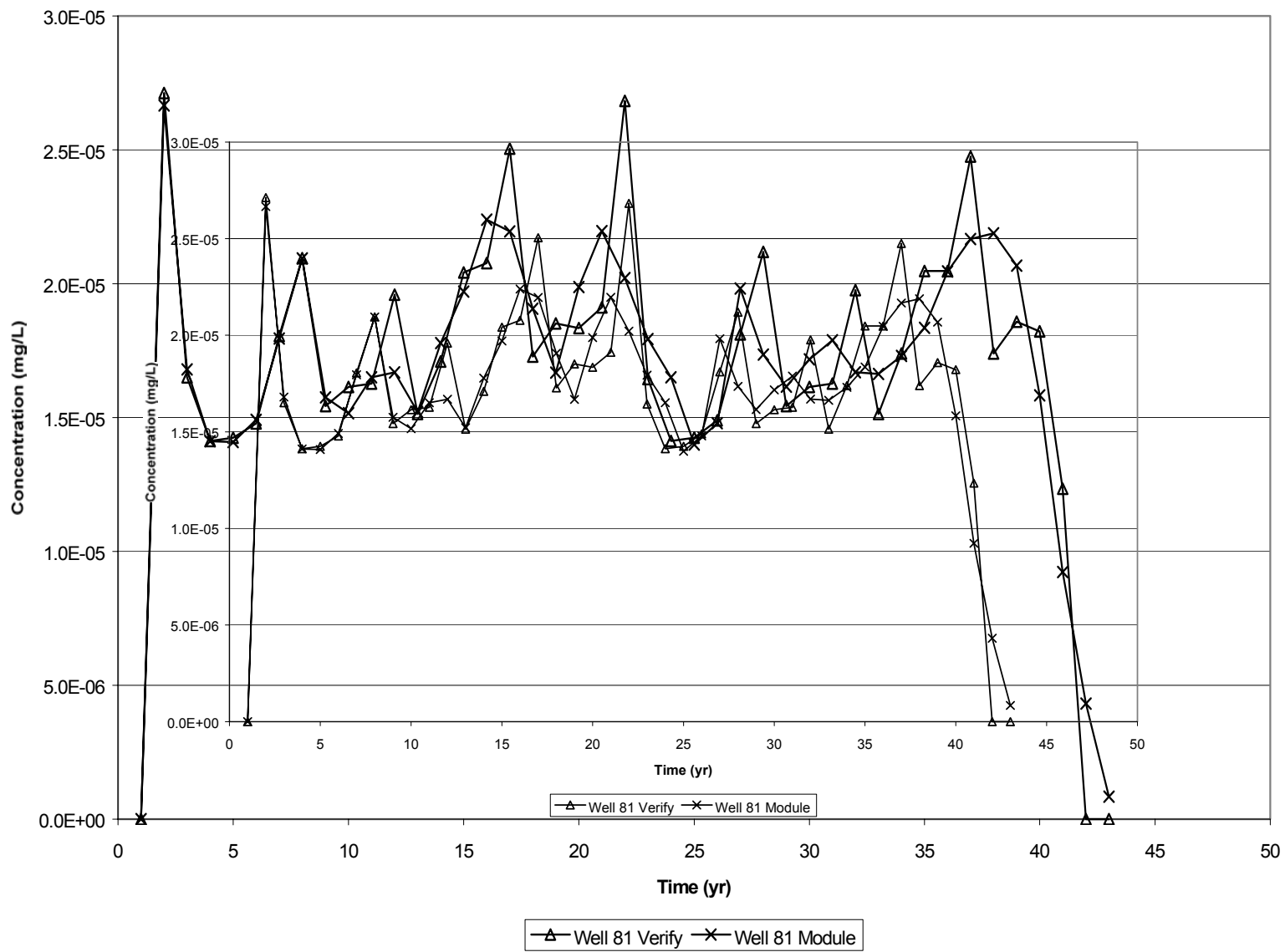


Figure D.I.2 Test Case 3: Breakthrough Curves for HWIR99 and Verification Modules at Well 81

SUBAPPENDIX D.J

**3MRA VADOSE-ZONE MODULE VERIFICATION RESULTS
(2000)**

This page intentionally left blank.

LIST OF FIGURES

| | Page |
|--|-------------|
| Figure D.J.1 Test Area 4: Breakthrough Curve for Conservative Chemical with a Pulse Source, the Non-metals Transport Component of the Vadose-zone Module | D.J-1 |
| Figure D.J.2 Test Area 5: Breakthrough Curve for Metal Transport with Non-Linear Isotherm, the Metals Transport Component for the Vadose-zone Module | D.J-2 |

This page intentionally left blank.

**Breakthrough Curve for Case 6.2
Conservative Chemical, Pulse Source**

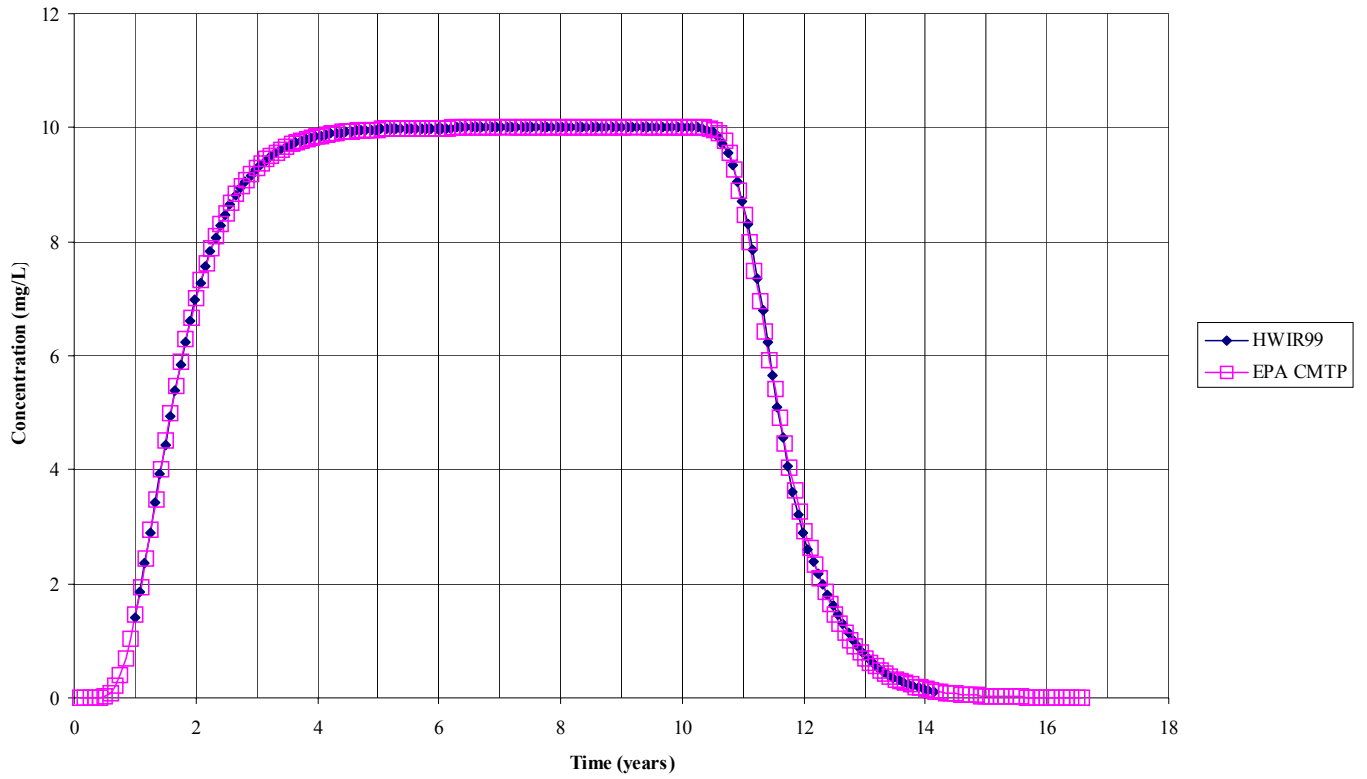


Figure D.J.1 Test Area 4: Breakthrough Curve for Conservative Chemical with a Pulse Source, the Non-metals Transport Component of the Vadose-zone Module

Breakthrough Curve for Case 7.4
Non-Linear Isotherm, Mercury

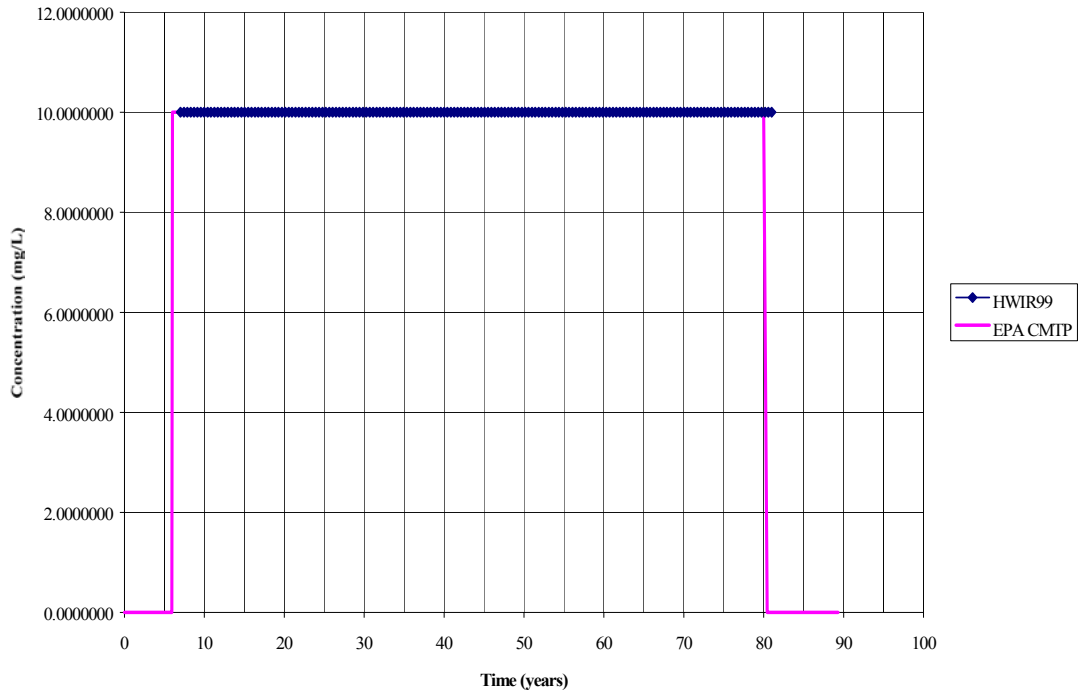


Figure D.J.2 Test Area 5: Breakthrough Curve for Metal Transport with Non-Linear Isotherm, the Metals Transport Component for the Vadose-zone Module

SUBAPPENDIX D.K

3MRA AQUIFER MODULE VERIFICATION RESULTS (2000)

This page intentionally left blank.

LIST OF FIGURES

| | Page |
|---|-------------|
| Figure D.K.1 Test Area 8: Predicted Concentrations at Receptor Well Number 64 by the Aquifer Module and the Analytical Solution . . | D.K-1 |
| Figure D.K.2 Test Area 8: Predicted Concentrations at the Receptor Well by the Aquifer Module and EPACMTP for Straight-chain (Parent to Child) Decay Scenario | D.K-2 |

This page intentionally left blank.

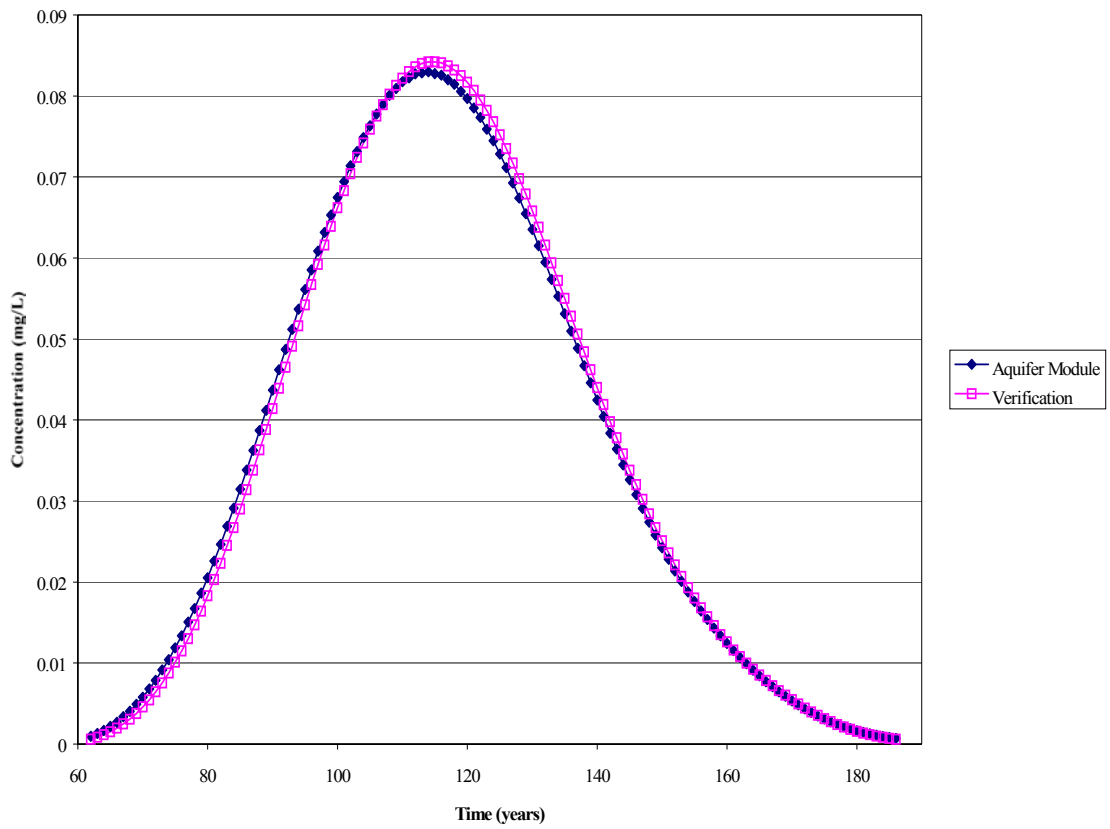


Figure D.K.1 Test Area 8: Predicted Concentrations at Receptor Well Number 64 by the Aquifer Module and the Analytical Solution

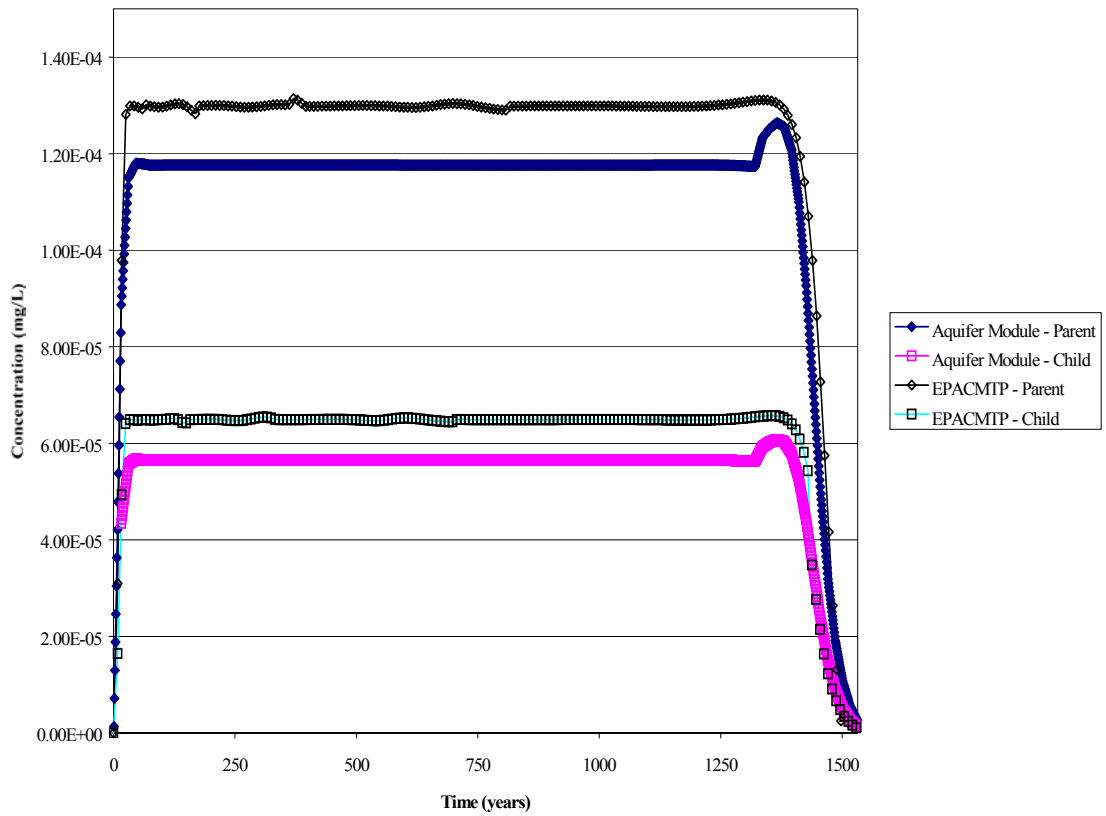


Figure D.K.2 Test Area 8: Predicted Concentrations at the Receptor Well by the Aquifer Module and EPACMTP for Straight-chain (Parent to Child) Decay Scenario

SUBAPPENDIX D.L
EPACMTP VALIDATION RESULTS

This page intentionally left blank.

LIST OF FIGURES

| | Page | |
|---------------|---|--------|
| Figure D.L.1 | Location of the Borden Landfill Showing the Monitoring Network. Cross-section A-A' Is along Longitudinal Plume Axis (From Frind and Hokkanen, 1987) | D.L-1 |
| Figure D.L.2 | Observed Chloride Plume along Cross-section A-A' in August 1979 (From Frind and Hokkanen, 1987) | D.L-2 |
| Figure D.L.3 | The Simulated Chloride Plume Obtained by the CANSAZ Simulation | D.L-3 |
| Figure D.L.4 | The Simulated Chloride Plume Obtained by Frind and Hokkanen, 1987 | D.L-4 |
| Figure D.L.5 | The Plan View of the Long Island Field Site. Groundwater Flow Directions Are Shown with Arrows | D.L-5 |
| Figure D.L.6 | Comparison Between Observed and Predicted Groundwater Aldicarb Concentrations for the Long Island Site in December, 1970 and May, 1980 | D.L-6 |
| Figure D.L.7 | Plan View of Dodge City, Kansas Site Located in the Arkansas River Valley | D.L-7 |
| Figure D.L.8 | Comparison of Predicted and Observed Bromide Breakthrough Curves at the Dodge City, Kansas Site | D.L-8 |
| Figure D.L.9 | Comparison of Predicted and Observed Triasulfuron Breakthrough Curves at the Dodge City, Kansas Site | D.L-9 |
| Figure DL.10 | EBOS Site 24 Layout and Location of Source Area | D.L-10 |
| Figure D.L.11 | EBOS Site 24 Groundwater Sampling Locations | D.L-11 |
| Figure D.L.12 | Changes in the Groundwater Napthalene Plume over Time A) June 1990: Before Source Removal B) October 1992: after Source Removal | D.L-12 |
| Figure D.L.13 | Comparisons Along the Plume Centerline of Groundwater Napthalene Concentrations Before Source Removal | D.L-13 |
| Figure D.L.14 | Comparisons along the Plume Centerline of Groundwater Napthalene Concentrations after Source Removal | D.L-14 |

This page intentionally left blank.

BORDEN LANDFILL SITE

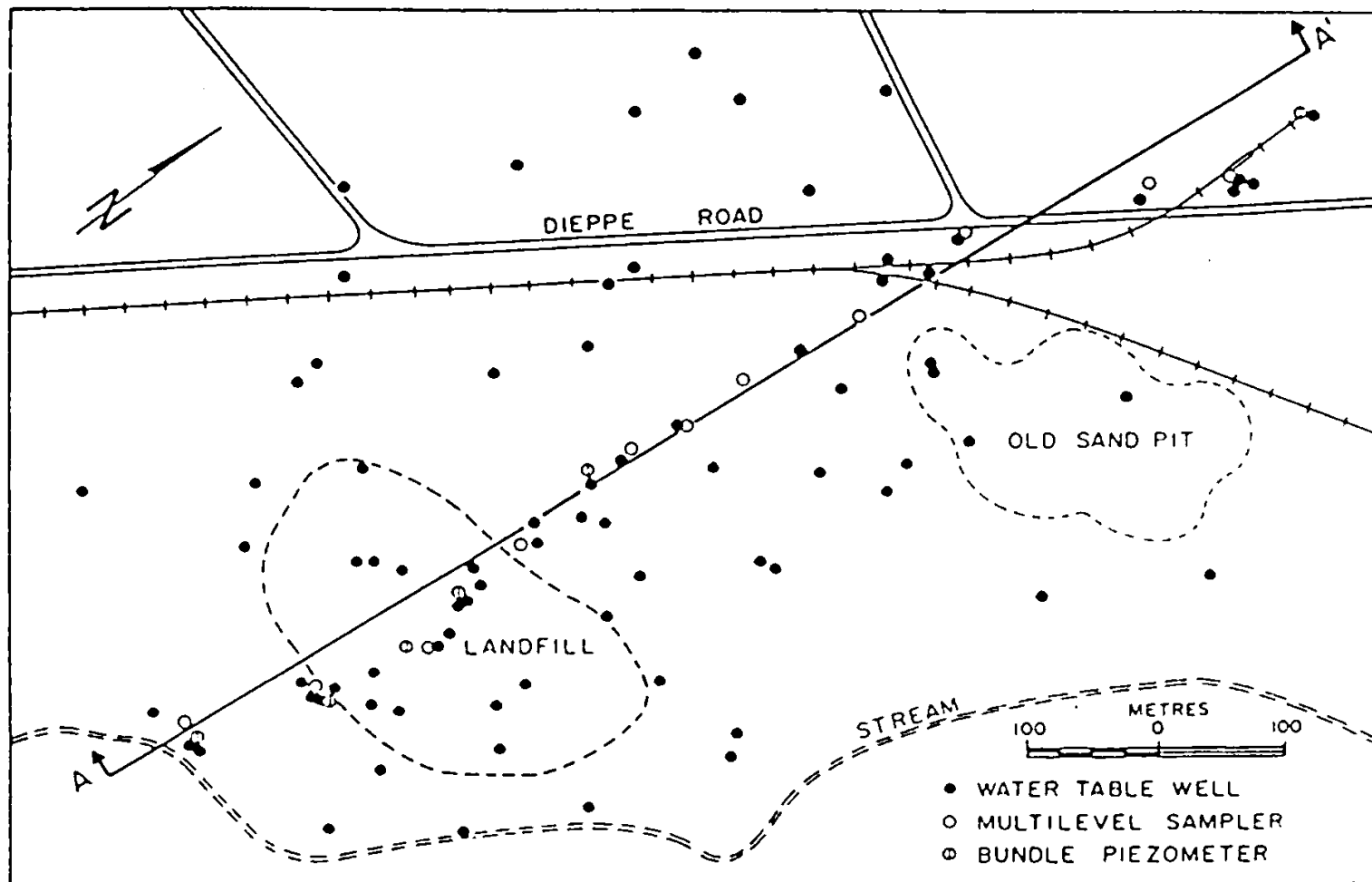


Figure D.L.1 Location of the Borden Landfill Showing the Monitoring Network. Cross-section A-A' Is along Longitudinal Plume Axis (From Frind and Hokkanen, 1987)

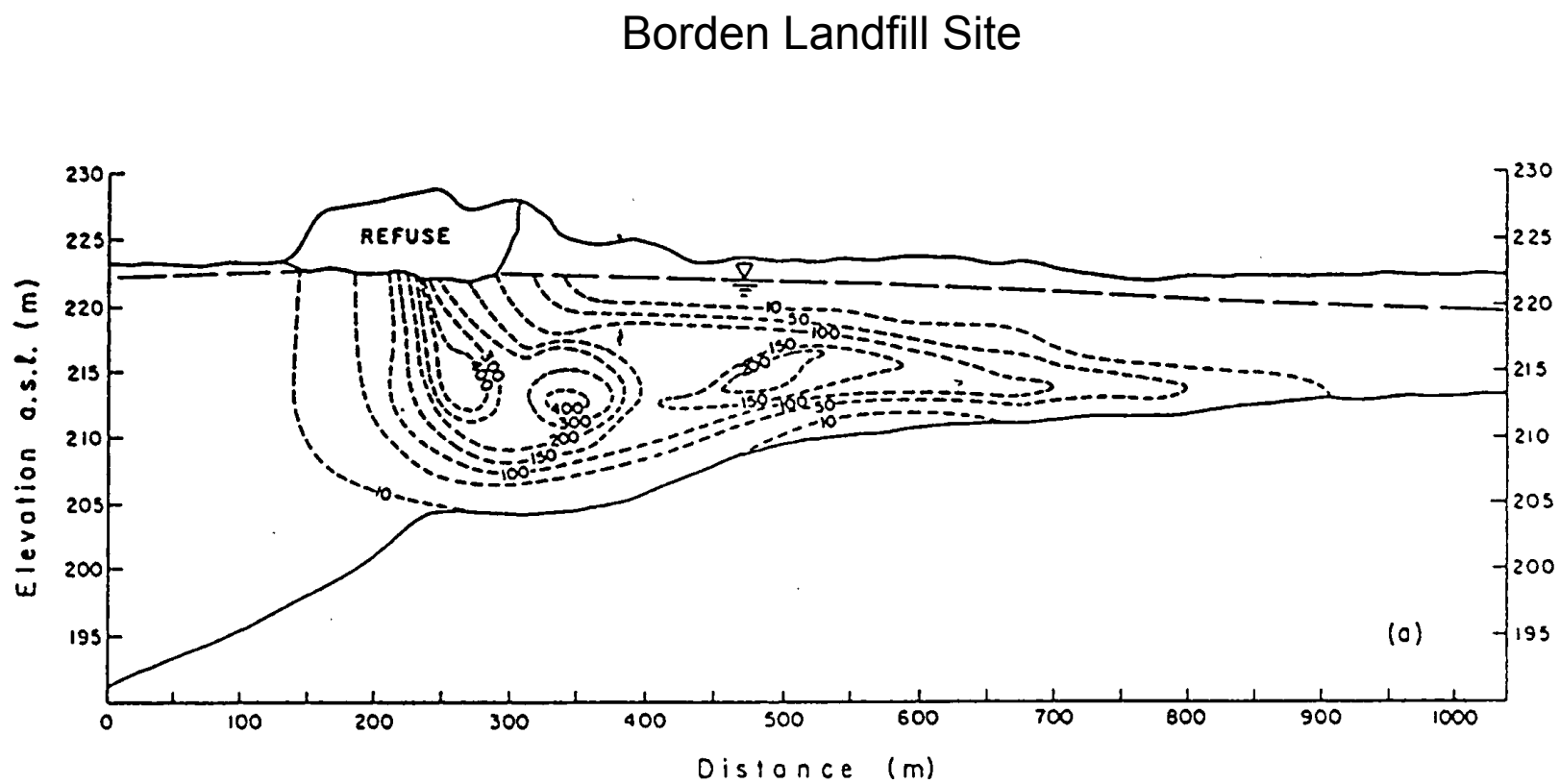


Figure D.L.2 Observed Chloride Plume along Cross-section A-A' in August 1979 (From Frind and Hokkanen, 1987)

BORDEN LANDFILL SITE

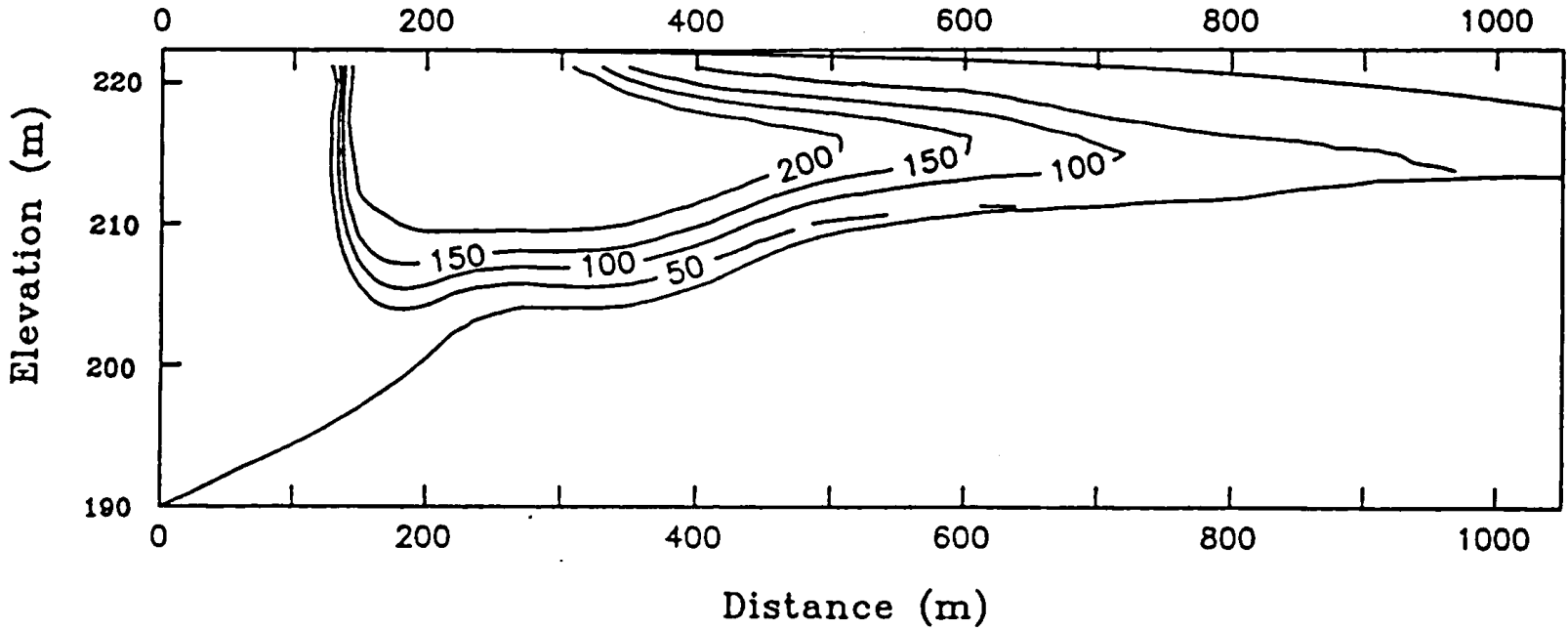


Figure D.L.3 The Simulated Chloride Plume Obtained by the CANSAZ Simulation

BORDEN LANDFILL SITE

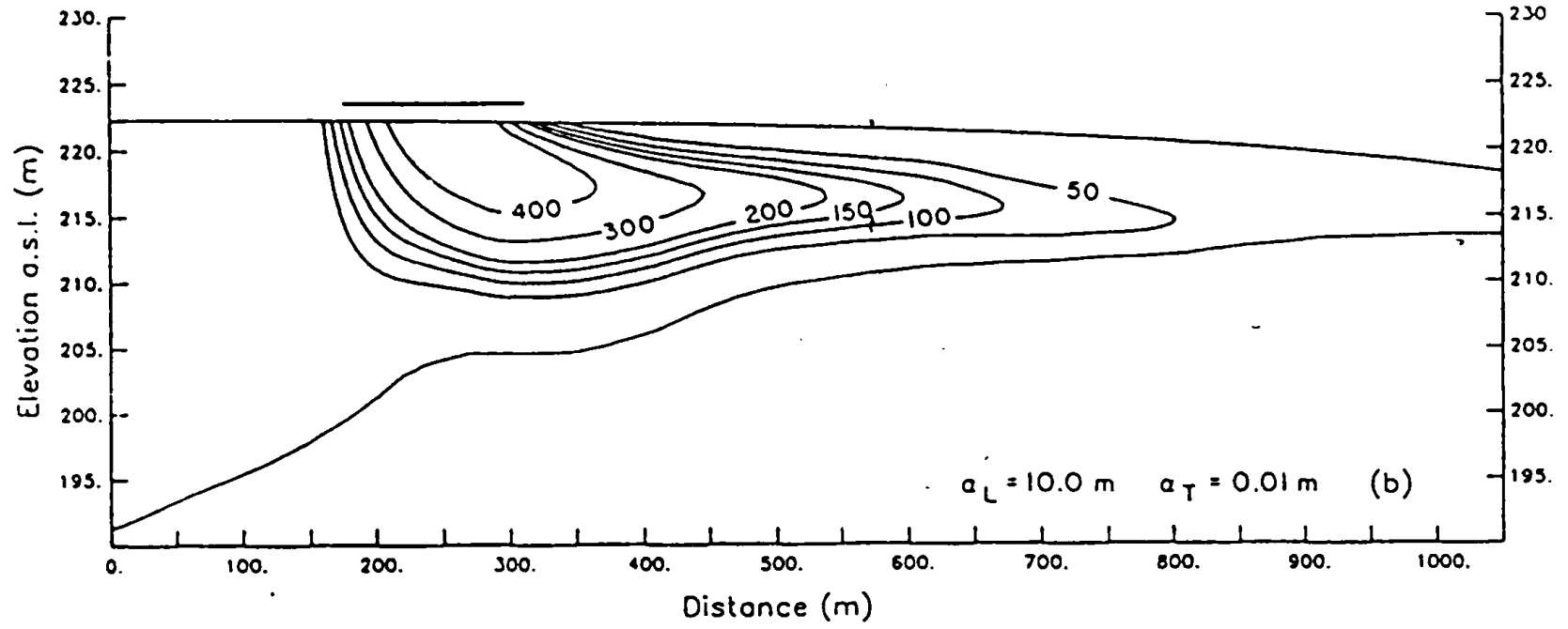


Figure D.L.4 The Simulated Chloride Plume Obtained by Frind and Hokkanen, 1987

PLAN VIEW OF LONG ISLAND FIELD SITE

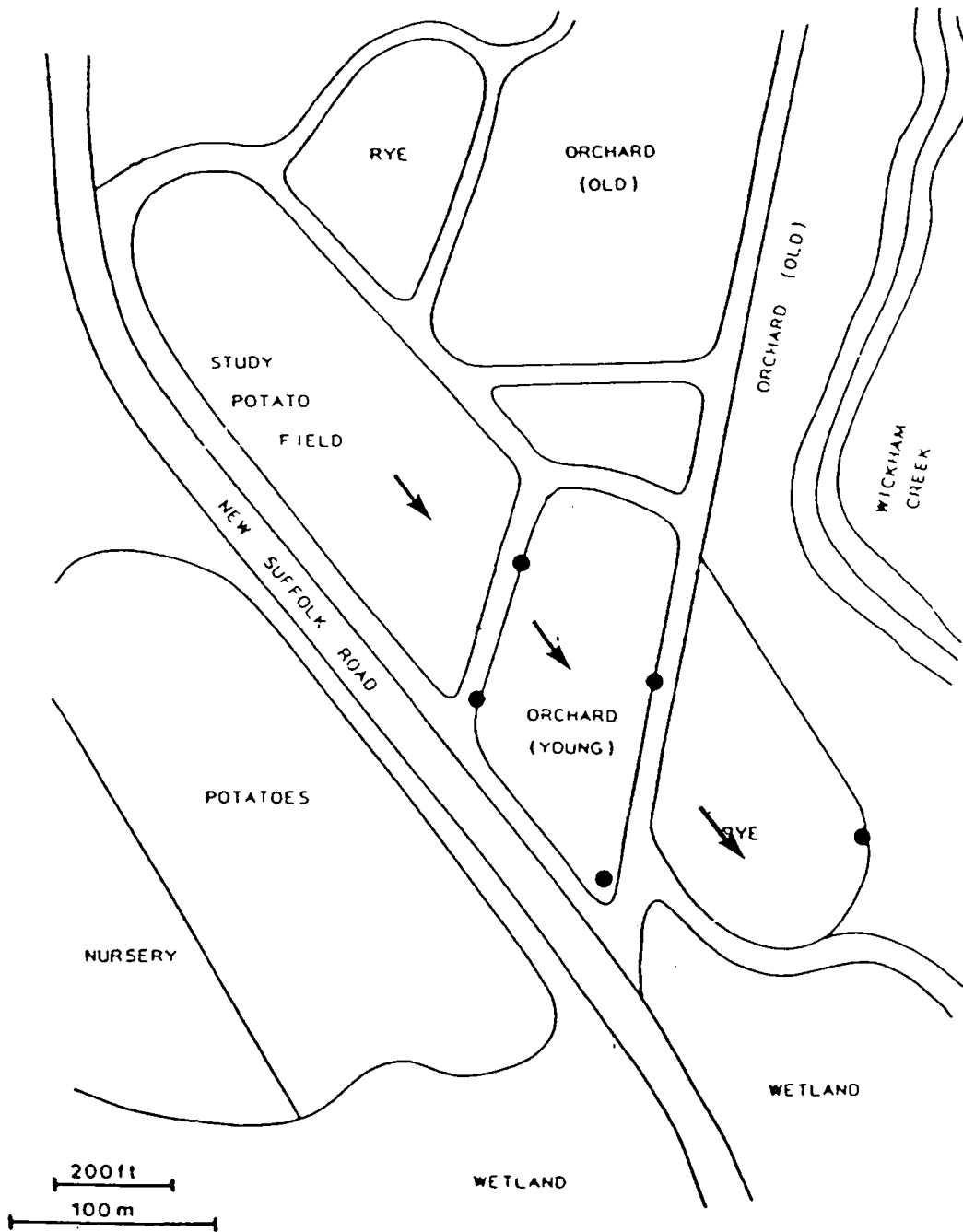


Figure D.L.5 The Plan View of the Long Island Field Site. Groundwater Flow Directions Are Shown with Arrows

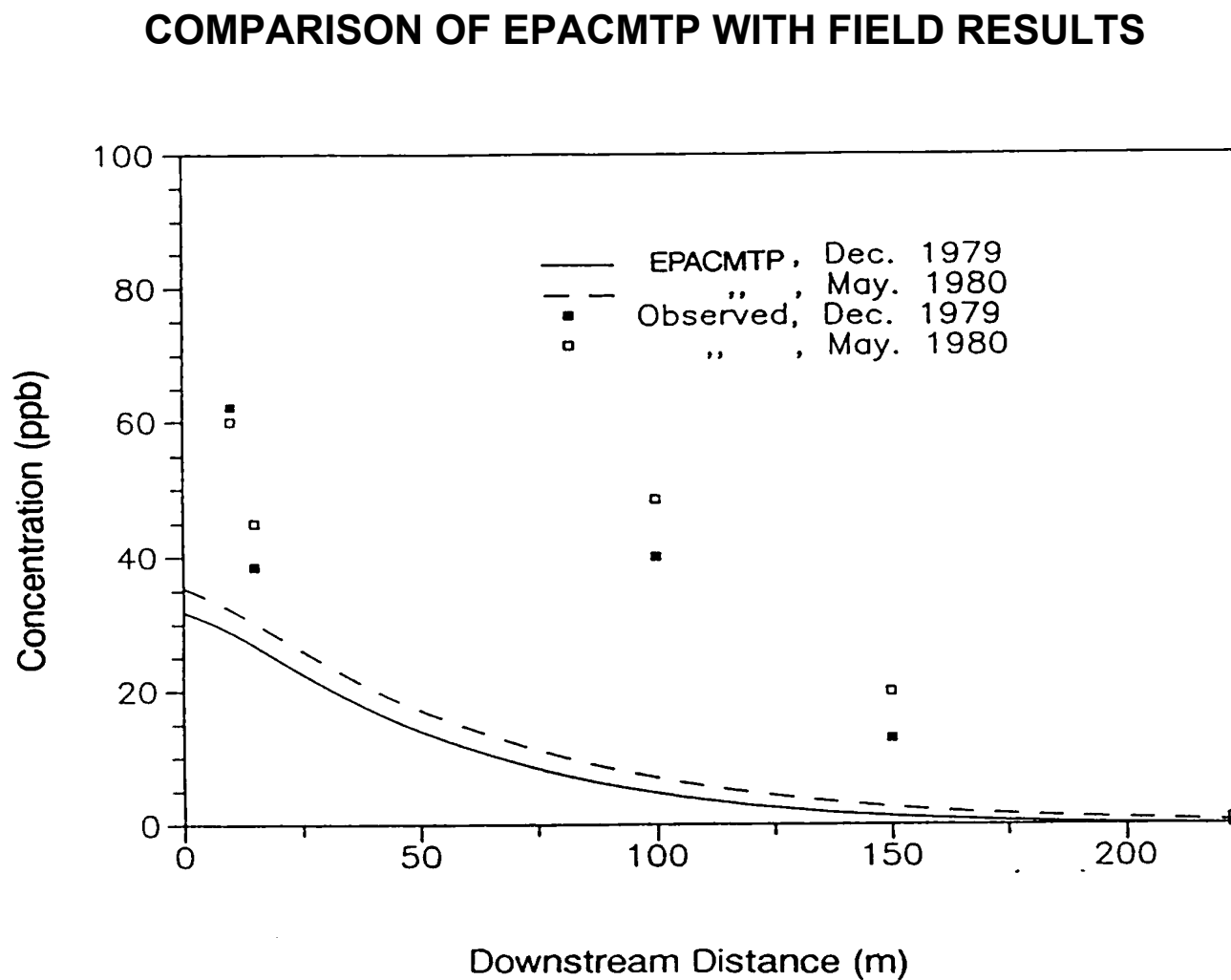


Figure D.L.6 Comparison Between Observed and Predicted Groundwater Aldicarb Concentrations for the Long Island Site in December, 1970 and May, 1980

PLAN VIEW OF THE KANSAS FIELD SITE

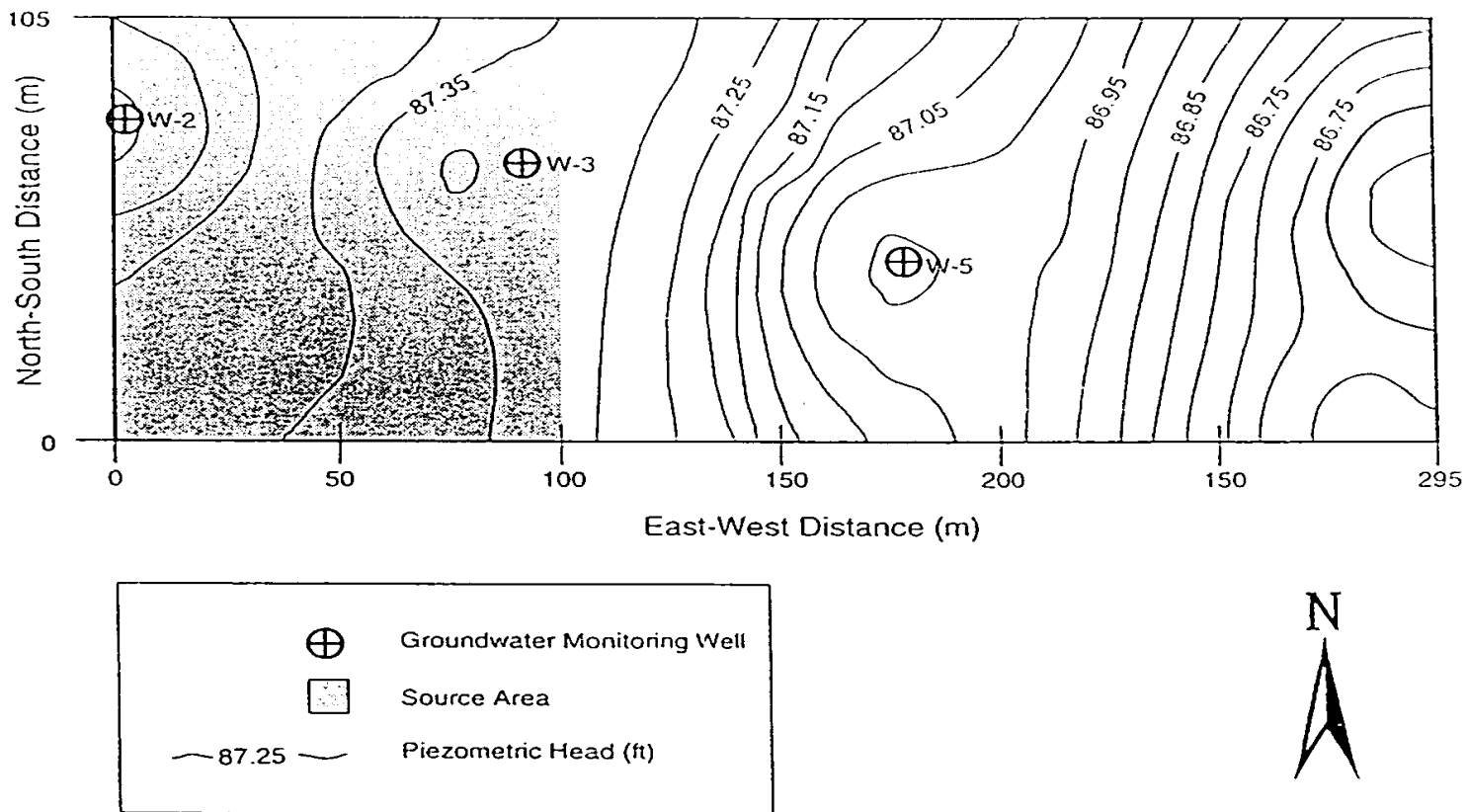


Figure D.L.7 Plan View of Dodge City, Kansas Site Located in the Arkansas River Valley

COMPARISON OF PREDICTED AND OBSERVED BROMIDE BREAKTHROUGH CURVES

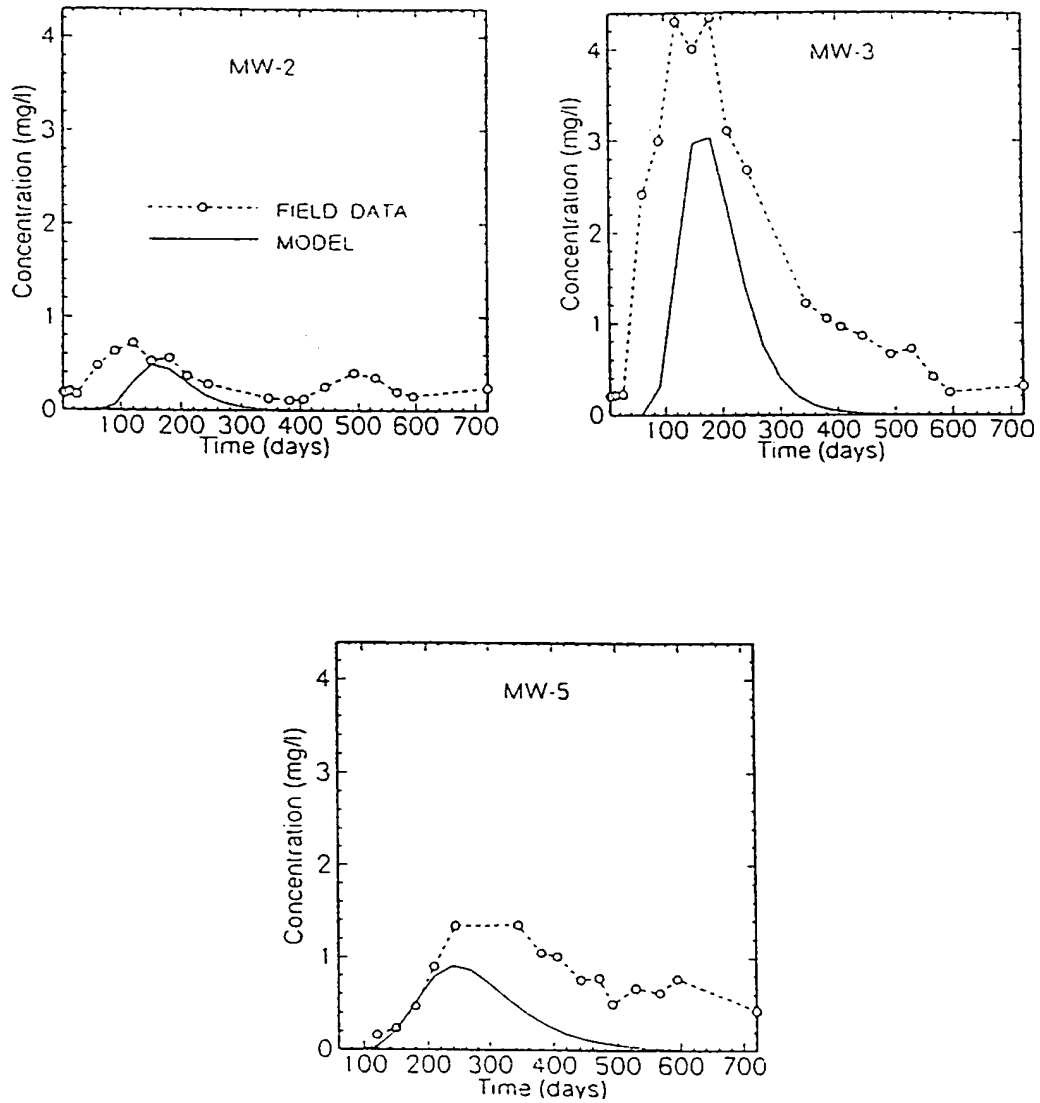


Figure D.L.8 Comparison of Predicted and Observed Bromide Breakthrough Curves at the Dodge City, Kansas Site

COMPARISON OF PREDICTED AND OBSERVED TRIASULFURON BREAKTHROUGH CURVES

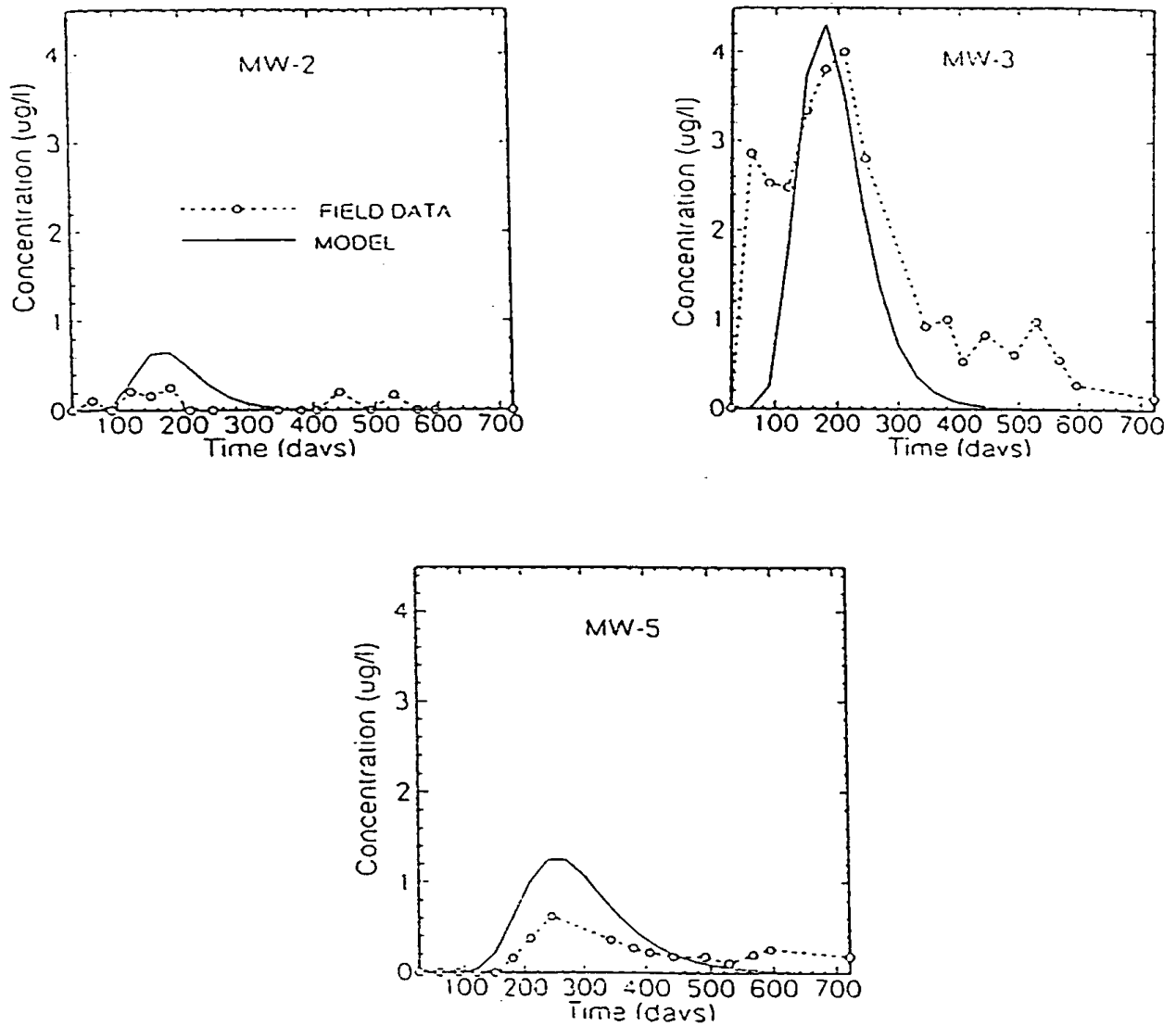


Figure D.L.9 Comparison of Predicted and Observed Triasulfuron Breakthrough Curves at the Dodge City, Kansas Site

EBOS SITE 24 LAYOUT AND LOCATION OF SOURCE AREA

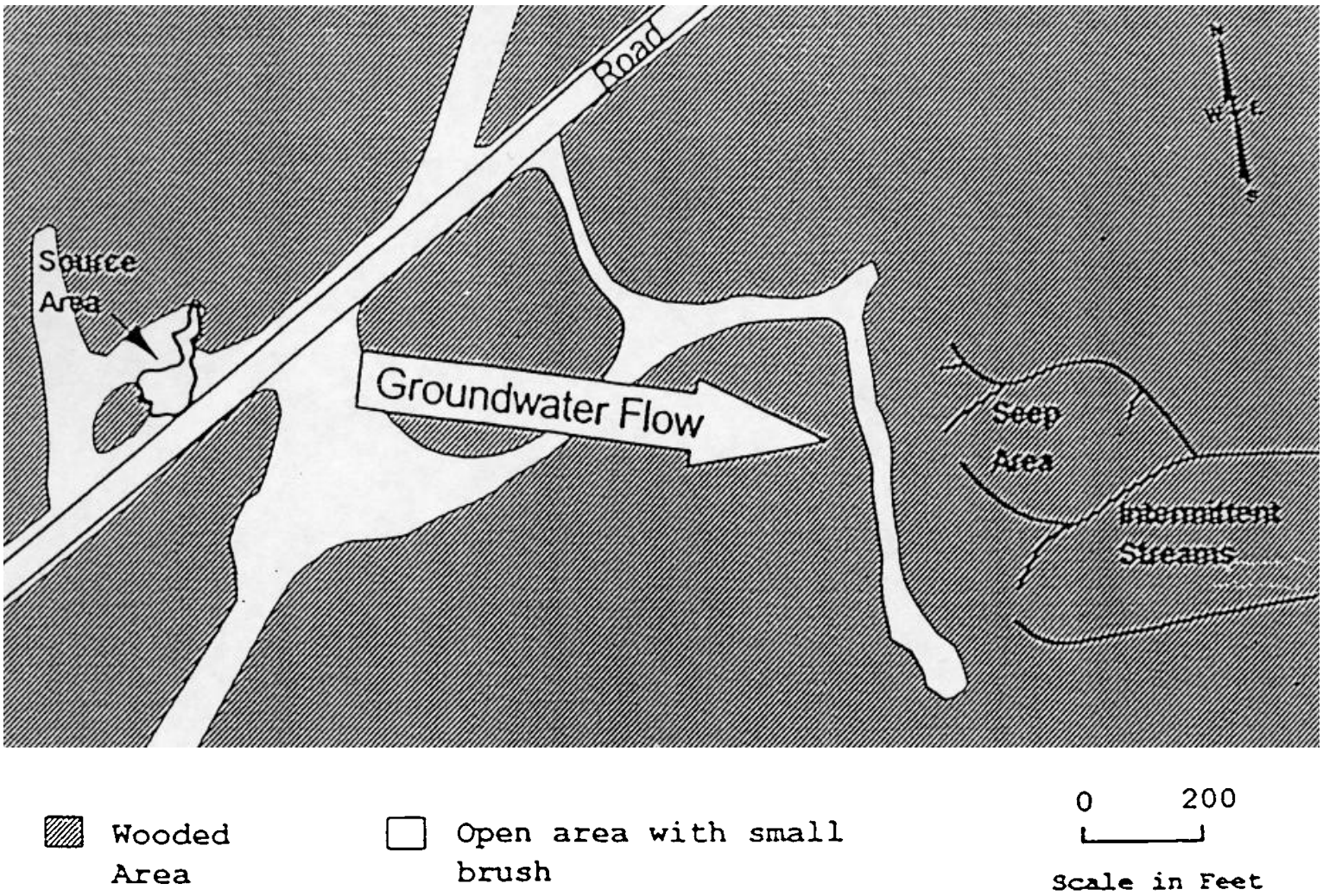


Figure D.L.10 EBOS Site 24 Layout and Location of Source Area

DL-10

Subappendix DL

EPACMTP Validation Results

EBOS SITE 24 GROUNDWATER SAMPLING LOCATIONS

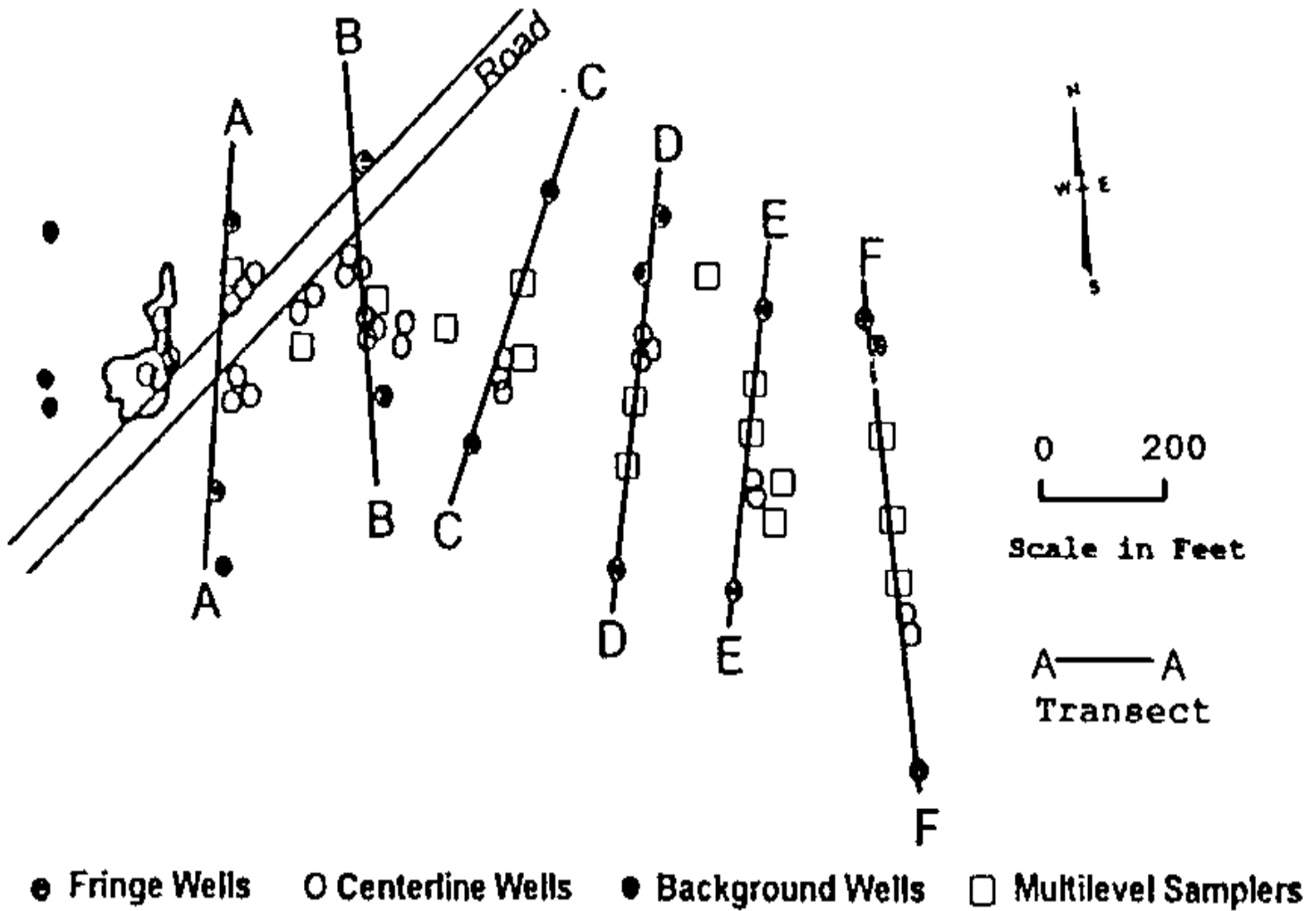
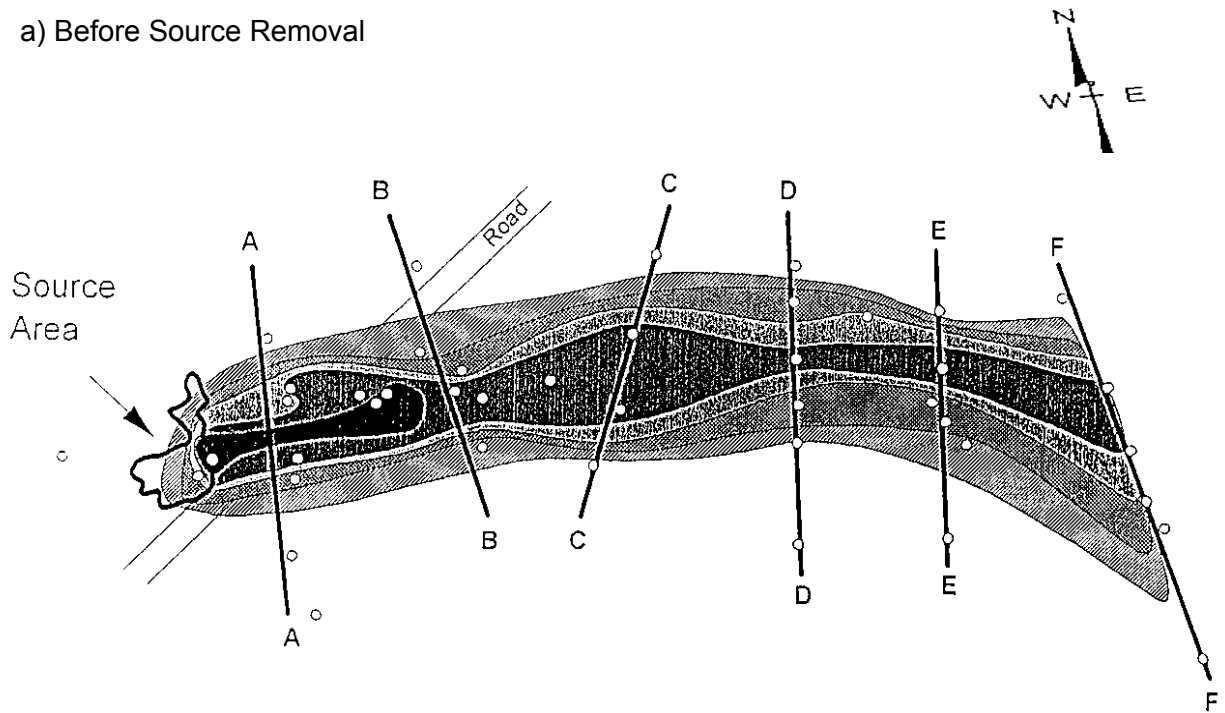


Figure D.L.11 EBOS Site 24 Groundwater Sampling Locations

CHANGES IN GROUNDWATER NAPHTHALENE PLUME OVER TIME

a) Before Source Removal



b) After Source Removal

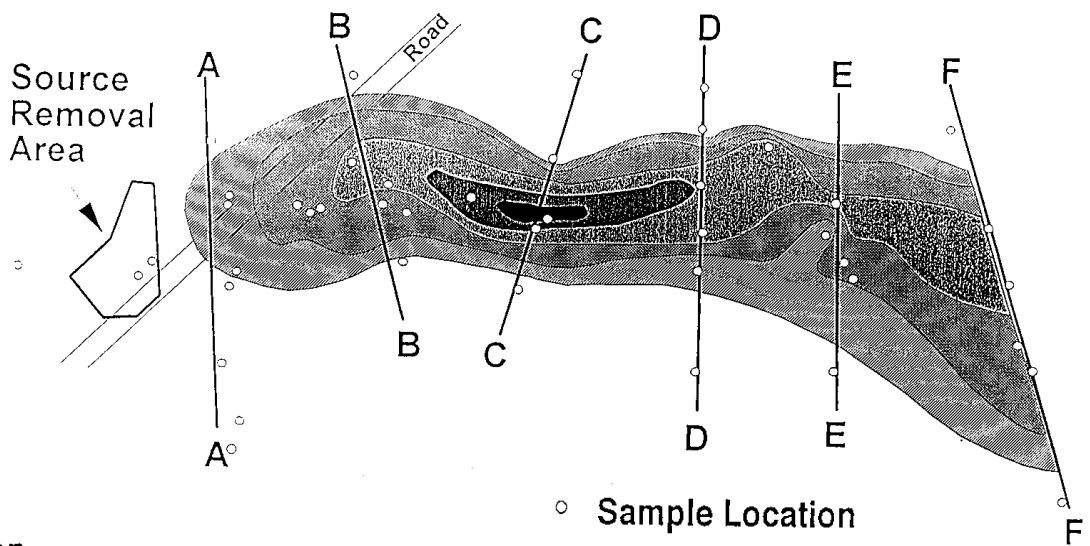


Figure D.L.12 Changes in the Groundwater Naphthalene Plume over Time A) June 1990: Before Source Removal B) October 1992: after Source Removal

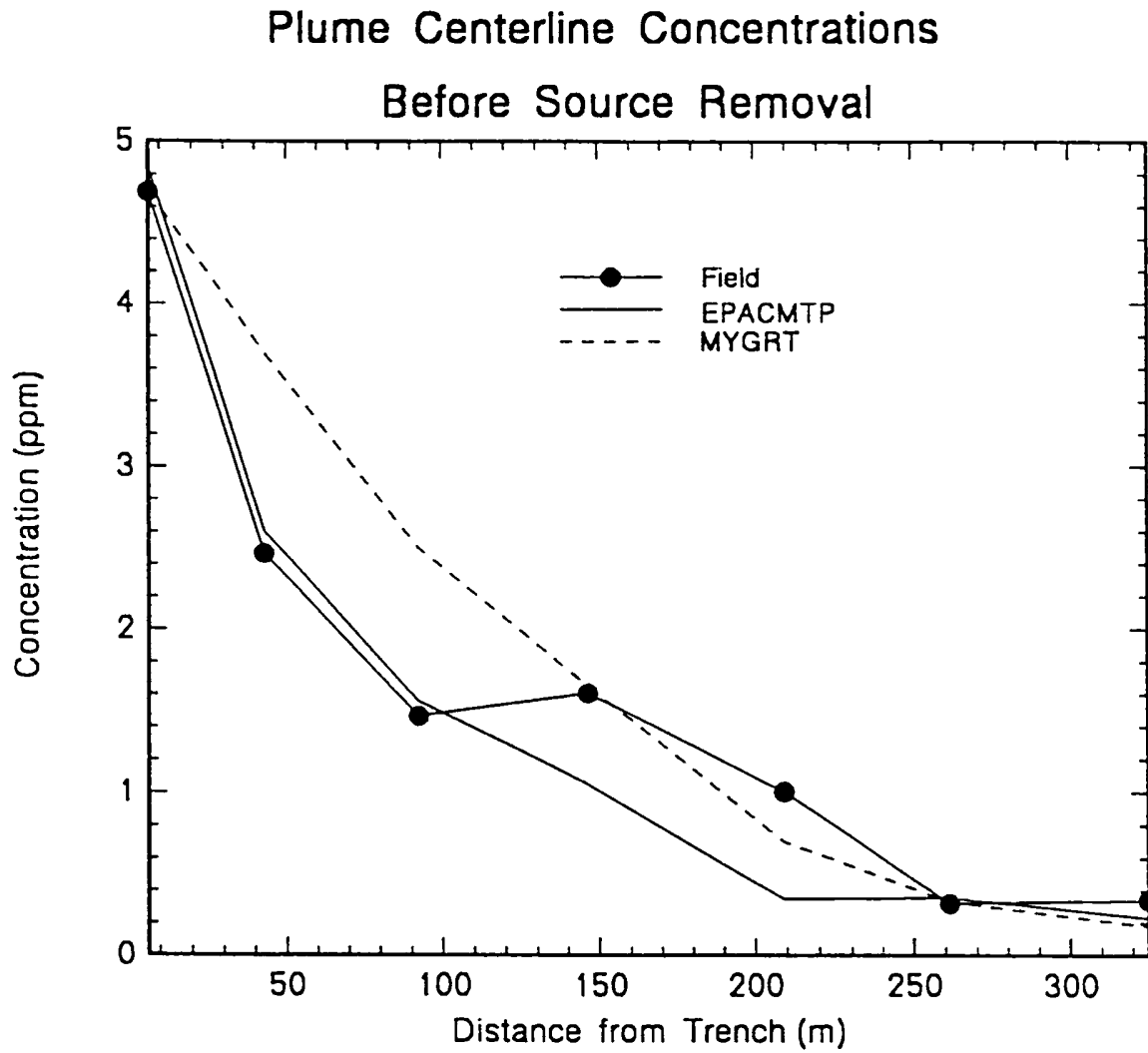


Figure D.L.13 Comparisons Along the Plume Centerline of Groundwater Naphthalene Concentrations Before Source Removal

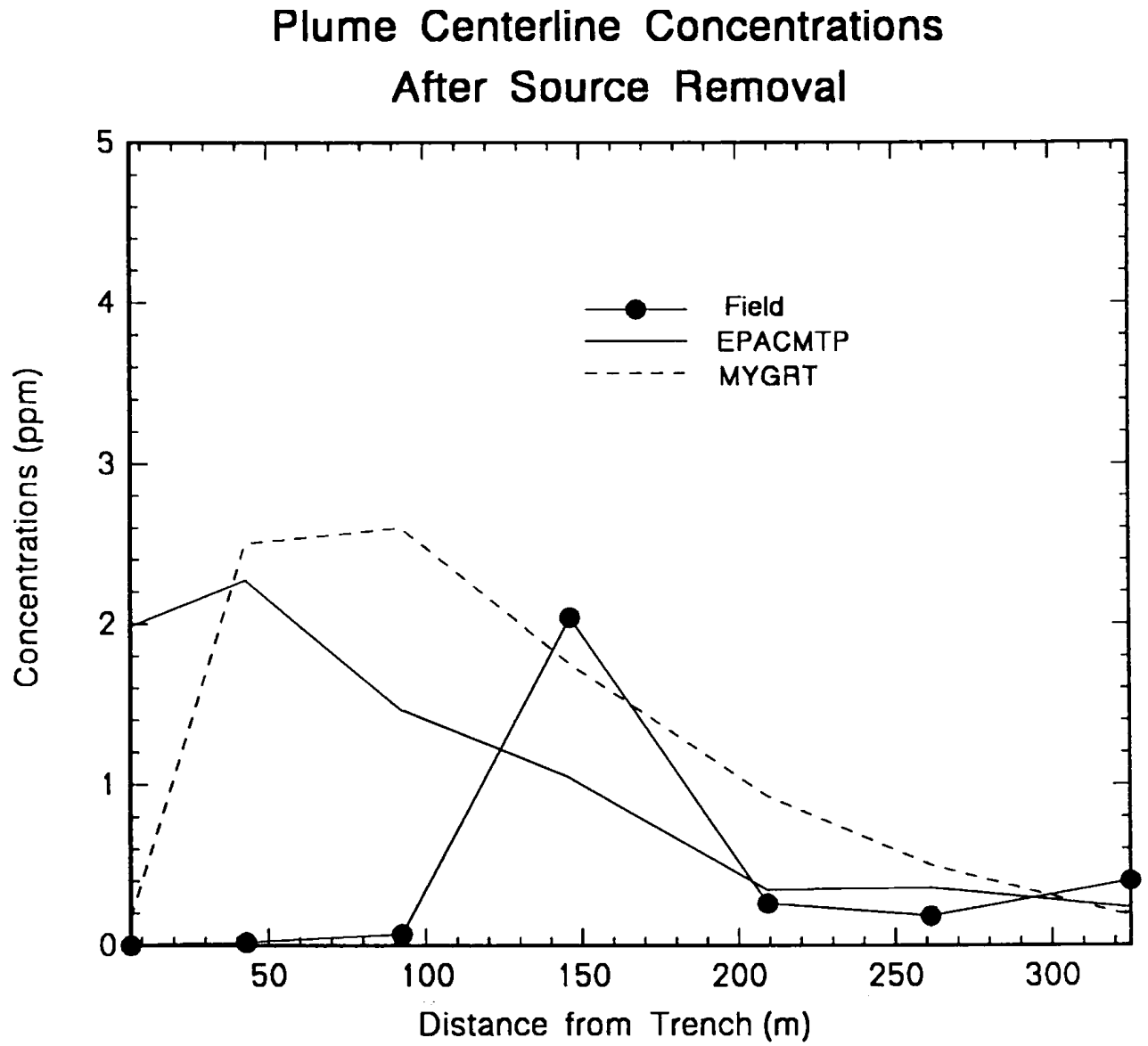


Figure D.L.14 Comparisons along the Plume Centerline of Groundwater Naphthalene Concentrations after Source Removal

APPENDIX E
PARAMETER SCREENING

This page intentionally left blank.

TABLE OF CONTENTS

| | Page |
|--|-------------|
| E.1 INFILTRATION RATE CRITERIA | E-1 |
| E.2 WATER-TABLE-ELEVATION CRITERION | E-2 |
| E.3 AQUIFER TRANSMISSIVITY CRITERION | E-4 |

This page intentionally left blank.

APPENDIX E

PARAMETER SCREENING

Details of the mathematical formulation relating to parameter screening are presented in this appendix. As discussed in Section 4.3.6, the criteria used in parameter screening are:

- Infiltration rate from the waste management unit (WMU)
- Water table elevation due to local recharge and infiltration from the WMU
- Aquifer must be able to support a well with adequate supply for a household

The first criterion is applicable to surface impoundments only. The second and third criteria are applicable to all types of WMU.

E.1 INFILTRATION RATE CRITERIA

For a surface impoundment (SI) that is outseeping (elevation of waste liquid is greater than the water table elevation) and that is hydraulically separated from the water table, the infiltration rate is limited by the following criteria:

- Saturated hydraulic conductivity of the vadose-zone material
- Maximum feasible infiltration rate that does not cause the groundwater mound to rise to the bottom elevation of the SI unit

The first criterion may be written

$$I \leq K_s \tag{E.1}$$

where

| | | |
|----------------|---|--|
| I | = | Infiltration rate from the SI (m/yr) |
| K _s | = | Saturated hydraulic conductivity of the vadose-zone material (m/ yr) |

According to the second criterion, if the calculated infiltration rate from the SI exceeds the rate at which the saturated zone can transport the groundwater, the groundwater level will rise into the unsaturated zone and the assumption of zero pressure head at the base of the SI is violated. This groundwater "mounding" will reduce the effective infiltration rate. The maximum infiltration rate is estimated as

the rate that does not cause the groundwater mound to rise to the bottom elevation of the SI unit. The maximum allowable infiltration rate may be approximated by:

$$I_{Max} \leq \frac{2K_{aqsat}D_{aqsat}(D_{vadose} - H)}{R_0^2 \ln \frac{R_\infty}{R_0}} \quad (E.2)$$

where

| | | |
|--------------|---|---|
| I_{Max} | = | maximum allowable infiltration rate (m/yr) |
| K_{aqsat} | = | hydraulic conductivity of the saturated zone (m/yr) |
| D_{aqsat} | = | depth of the saturated zone (m) |
| D_{vadose} | = | vadose zone thickness (m) |
| H | = | hydraulic head (m) |
| R_0 | = | equivalent source radius (m) |
| R_∞ | = | length between the center of the source and the nearest downgradient boundary where the boundary location has no perceptible effects on the heads near the source (m). The nearest downgradient boundary location is normally the nearest surface water body located along one of the streamlines traversing the surface impoundment. |

The equivalent source radius may be calculated from:

$$R_0 = \sqrt{\frac{A}{\pi}} \quad (E.3)$$

where

| | | |
|-----|---|-------------------------------|
| A | = | source area (m ²) |
|-----|---|-------------------------------|

E.2 WATER-TABLE-ELEVATION CRITERION

Under this criterion, the selected combination of K_{aqsat} , D_{aqsat} , D_{vadose} , and G_{Reg} is rejected when the elevation of water table is above the topographical elevation, i.e.,

$$H(x \text{ at } \frac{dH}{dx} = 0) \geq D_{vadose} + D_{aqsat} \quad (E.4)$$

where

$$\begin{aligned}
 G_{Reg} &= \text{regional hydraulic gradient (m/m)} \\
 &= (H_2 - H_1) / x_L \\
 D_{aqsat} &= \text{depth of the saturated zone (m)} \\
 D_{vadose} &= \text{vadose zone thickness (m)} \\
 H(x) &= \text{the hydraulic head elevation at } x \text{ (m)} \\
 x &= \text{the coordinate from the upgradient end of the domain (m)}
 \end{aligned}$$

$H(x)$ is segmentally defined by the following equations:

For $0 \leq x \leq x_u$

$$H(x) = \frac{-I_r}{2K_x B} x^2 + \left[\frac{I_r - I}{2K_x B} \left(\frac{x_d^2 - x_u^2}{x_L} \right) + \frac{I_r - I}{K_x B} (x_u - x_d) + \frac{I_r}{2K_x B} x_L + \frac{H_2 - H_1}{x_L} \right] x + H_1$$

(E.5)

For $x_u \leq x \leq x_d$

$$I(x) = \frac{-I}{2K_x B} x^2 + \left[\frac{I_r - I}{2K_x B} \left(\frac{x_d^2 - x_u^2}{x_L} \right) - \frac{I_r - I}{K_x B} x_d + \frac{I_r}{2K_x B} x_L + \frac{H_2 - H_1}{x_L} \right] x + \frac{I_r - I}{2K_x B} x_u^2 + I$$

(E.6)

For $x_d \leq x \leq x_L$

$$H(x) = \frac{-I_r}{2K_x B} x^2 + \left[\frac{I_r - I}{2K_x B} \left(\frac{x_d^2 - x_u^2}{x_L} \right) + \frac{I_r}{2K_x B} x_L + \frac{H_2 - H_1}{x_L} \right] x - \frac{I_r - I}{2K_x B} (x_d^2 - x_u^2) + H_1$$

(E.7)

where:

$$\begin{aligned}
 H_1 &= \text{the hydraulic head elevation at } x = x_L \text{ (m)} \\
 H_2 &= \text{the hydraulic head elevation at } x = 0 \text{ (m)} \\
 x_L &= \text{the length of the aquifer system (m)} \\
 B &= \text{the saturated thickness of the system (m)} \\
 x_u &= \text{the upgradient coordinates of the strip source area (m)} \\
 x_d &= \text{the downgradient coordinates of the strip source area (m)} \\
 I_r &= \text{the recharge rate outside the strip source area (m/yr)} \\
 I &= \text{the infiltration rate through the rectangular source area (m)} \\
 K_x &= \text{hydraulic conductivity in the longitudinal direction (m/yr)}
 \end{aligned}$$

E.3 AQUIFER TRANSMISSIVITY CRITERION

In order to ensure that the generated set of hydrogeologic parameters do not represent an aquifer with an unrealistically low transmissivity, an option has been added to the EPACMTP code to perform this check. The LTCHK parameter (in the GP01 record in the EPACMTP data input file) controls whether or not this check is performed. When LTCHK is set to TRUE, the EPACMTP code automatically checks to see if the aquifer can support a well with a sustained pumping rate of 0.35 gpm (or 696 m³/yr) with the maximum drawdown at the well not more than $\frac{3}{8}$ of the saturated thickness. The variables that are used to perform this transmissivity check are recharge rate, saturated thickness, and impact radius. Any combination of hydraulic conductivity, saturated thickness, and recharge rate is permissible if it can sustain a continuous pumping rate of 0.35 gpm with drawdown at the well of less than $\frac{3}{8}$ of the saturated thickness and with an impact radius not greater than 50 m (164 ft). If the generated set of hydrogeologic parameters fails this transmissivity screening, then that set of input values is rejected and a new data set is generated. The pumping rate of 0.35 gpm was chosen because it is approximately the maximum water usage for a four-person household.

APPENDIX F

GROUND-WATER-TO-SURFACE-WATER MASS FLUX

This page intentionally left blank.

APPENDIX F

GROUND-WATER-TO-SURFACE-WATER MASS FLUX

A groundwater to surface water pathway is included in the analysis by calculating the total contaminant mass flux at a given downgradient location selected to represent the intersection of the contaminant plume with a surface water body. It is assumed that the surface water body fully penetrates the aquifer and the plume fully intersects the water body. The total contaminant mass flux in mg/year is calculated by multiplying the groundwater flux with the net contaminant mass across the entire plume cross section:

$$M_{flux} = i \cdot K_H \cdot C_{net} \quad (F.1)$$

where

- C_{net} = net contaminant mass in plume cross-section perpendicular to groundwater flow direction in mg/meter
 i = hydraulic gradient
 K_H = hydraulic conductivity in m/year

The net contaminant mass is calculated from the plume-center concentration, vertically and transversely integrated. The concentration as a function of transverse distance is approximately given by (Domenico and Schwartz, 1990),

$$C(y) = \frac{C_{zo}}{2} \left[\operatorname{erf} \left(\frac{y + \frac{ys}{2}}{2\sqrt{\alpha_T x}} \right) - \operatorname{erf} \left(\frac{y - \frac{ys}{2}}{2\sqrt{\alpha_T x}} \right) \right] \quad (F.2)$$

where

- C_{zo} = vertically integrated concentration at plume center in $\frac{mg \cdot m}{l}$
 ys = source width (m)
 α_T = transverse dispersivity (m)
 x = downgradient distance from source (m)

The net contaminant mass is determined by integrating $C(y)$ from the plume centerline to the plume boundary:

$$C_{net} = F \cdot C_{zo} \int_{y=0}^{y_{plume}} \left[\operatorname{erf} \left(\frac{y + \frac{ys}{2}}{2\sqrt{\alpha_T x}} \right) - \operatorname{erf} \left(\frac{y - \frac{ys}{2}}{2\sqrt{\alpha_T x}} \right) \right] dy \quad (\text{F.3})$$

where

$$y_{plume} = \frac{ys}{2} + 3\sqrt{\alpha_T x}$$

$$F = 1000 \frac{\ell}{m^3} \text{ (conversion factor)}$$

The integral in Equation (F.3) was evaluated numerically using Simpson's 3/8 rule (Burden and Faires, 1989) because a closed form solution is not available:

$$\int_{y_0}^{y_4} f(y) dy \approx \frac{2h}{45} [7f(y_0) + 32f(y_1) + 12f(y_2) + 32f(y_3) + 7f(y_4)] \quad (\text{F.4})$$

where

$$h = \text{interval between } y_0 \text{ and } y_1, y_1 \text{ and } y_2, \text{ etc.}$$

REFERENCES

- Burden, R.L. and J.D. Faires, 1989. *Numerical Analysis*. PWS Publishing Company, Boston. 729 pp.
- Domenico, A.J., and F.W. Schwartz, 1990. *Physical and Chemical Hydrogeology*. John Wiley & Sons, Inc., New York. 820 pp.

APPENDIX G

MINTEQA2-BASED METALS ISOTHERMS

This page intentionally left blank.

TABLE OF CONTENTS

| | Page |
|--|-------------|
| G.1 INTRODUCTION | G-1 |
| G.2 MINTEQA2 MODELING | G-2 |
| G.2.1 Input Parameters | G-3 |
| G.2.2 Metals of Interest | G-8 |
| G.2.3 Modeling Methods and Results | G-8 |
| G.2.4 MINTEQA2 Modeling Assumptions and Limitations | G-12 |
| G.3 INCORPORATION OF MINTEQA2 ADSORPTION ISOTHERMS IN EPACMTP | G-14 |
| G.3.1 Incorporation of MINTEQA2 Isotherms | G-14 |
| G.3.2 Precipitation Effects | G-15 |
| G.3.3 Variable Soil Moisture Content | G-16 |
| G.3.4 Linearization of MINTEQA2 Adsorption Isotherm | G-17 |
| G.4 IMPLEMENTATION OF EPACMTP FOR METALS | G-17 |
| G.4.1 Additional Input Data for Metals | G-18 |
| G.4.1.1 Control Parameters | G-18 |
| G.4.1.2 Metal Specific Data | G-18 |
| G.4.2 Evaluation of Approaches for Handling Metals Isotherms | G-19 |
| G.4.3 Determination of Isotherm Monotonicity | G-20 |
| G.4.4 Application of Isotherm Monotonicity | G-21 |
| G.4.5 Selection of Sorption Coefficient for Saturated Zone | G-22 |
| G.4.6 References | G-23 |

LIST OF FIGURES

| | Page |
|------------|---|
| Figure G.1 | MINTEQA2 Computes the Equilibrium Distribution of Metal G-2 |
| Figure G.2 | Cr(VI) Isotherms Illustrating Influence of pH G-10 |
| Figure G.3 | Pb Isotherms Illustrating Influence of FeOx Sorbent Concentration G-11 |
| Figure G.4 | Pb Isotherms Illustrating Influence of POM/DOM Concentration G-11 |
| Figure G.5 | Cu Isotherms Illustrating Influence of LOM Concentration G-12 |

LIST OF TABLES

| | Page |
|------------|---|
| Table G.1 | Composition Of Representative Ground Waters G-4 |
| Table G.2 | Concentration Levels For Goethite Sorbent G-5 |
| Table G.3 | Model Parameters For The Goethite Sorbent G-5 |
| Table G.4 | POM and DOM Concentration Levels G-6 |
| Table G.5 | Site Concentrations For POM And DOM Components In MINTEQA2 G-7 |
| Table G.6 | Model Concentrations Of Representative Leachate Acids G-7 |
| Table G.7 | Atomic weight of metals (CRC, 1970) G-15 |
| Table G.8 | Additional Control Parameters for Metals Simulation G-18 |
| Table G.9 | Additional Input Parameters for Metals Specific (MT) Group . . . G-19 |
| Table G.10 | METAL_ID and Corresponding Metal Species G-19 |

APPENDIX G

MINTEQA2-BASED METALS ISOTHERMS

G.1 INTRODUCTION

This appendix describes the development of concentration-dependent metal partition coefficients for use in EPACMTP. In the subsurface, metal contaminants undergo reactions with ligands in the pore water and with surface sites on the solid aquifer or soil matrix material. Reactions in which the metal is bound to the solid matrix are referred to as sorption reactions, and metal that is bound to the solid is said to be sorbed. The ratio of the concentration of metal sorbed to the concentration in the mobile aqueous phase at equilibrium is referred to as the partition coefficient (K_d). During contaminant transport, sorption to the solid matrix results in retardation of the contaminant front. Thus, groundwater fate and transport models such as EPACMTP include the contaminant partition coefficient in the calculation of the overall retardation factor (the ratio of the average linear particle velocity to the velocity of that portion of the plume where the contaminant is at 50 percent dilution) for a given chemical constituent. Use of K_d in EPACMTP transport modeling requires the assumption that local equilibrium between the solutes and the sorbents is attained. This implies that the rate of sorption reactions is fast relative to advective-dispersive transport of the contaminant and that the sorption.

Among the options incorporated in EPACMTP for modeling the fate and transport of metals is the option of using non-linear sorption isotherms in the form of tabulated sorption data (see Section 3.3.3.4 for other available options for modeling the sorption of metals). These isotherms reflect the tendency of K_d to decrease as the total metal concentration in the system increases. The non-linear isotherms available for use in EPACMTP are specified in terms of the dissolved metal concentration and the corresponding sorbed concentration at a series of total metal concentrations. The isotherms were calculated using the geochemical speciation model, MINTEQA2. For a particular metal, K_d values in a soil or aquifer are dependent upon the metal concentration and various geochemical characteristics of the soil or aquifer and the associated pore water. Geochemical parameters that have the greatest influence on the magnitude of K_d include the pH of the system and the nature and concentration of sorbents associated with the soil or aquifer matrix. In the subsurface beneath a waste disposal facility, the concentration of leachate constituents may also influence K_d . Although the dependence of metal partitioning on the total metal concentration and on pH and other geochemical characteristics is apparent from partitioning studies reported in the scientific literature, K_d values for many metals are not available for the range of metal concentrations or geochemical conditions needed in risk assessment modeling. For this reason, the U.S. EPA has chosen to use an equilibrium speciation model, MINTEQA2, to estimate partition coefficients in a number of recent risk assessments that required modeling the groundwater fate and transport of metals. The use of a speciation model like MINTEQA2 allows K_d values to be estimated for a range of total metal concentrations in various model systems designed to depict natural variability in those geochemical characteristics that most influence metal partitioning.

G.2 MINTEQA2 MODELING

From input data consisting of total concentrations of inorganic chemicals, MINTEQA2 calculates the fraction of a contaminant metal that is dissolved, adsorbed, and precipitated at equilibrium (see Figure G.1). The total concentrations of major and minor ions, trace metals and other chemicals are specified in terms of key species known as components. MINTEQA2 automatically includes an extensive database of solution species and solid phase species representing reaction products of two or more of the components. The model does not automatically include sorption reactions, but these can be included in the calculations if supplied by the user. When sorption reactions are included, the dimensionless partition coefficient can be calculated from the ratio of the sorbed metal concentration to the dissolved metal concentration at equilibrium. The dimensionless partition coefficient can be converted to K_d with units of liters per kilogram (L/kg) by normalizing by the mass of soil (in kilograms) with which one liter of porewater is equilibrated (the phase ratio). An isotherm is then generated by estimating the equilibrium metal distribution between sorbed and dissolved fractions is estimated for a series of total metal concentrations.

Progress in accounting for sorption in equilibrium calculations over the past decade has resulted in the development of coherent databases of sorption reactions for particular sorbents. These databases include acid-base sorption reactions and reactions for major ions in aquatic systems (Ca, Mg, SO_4 , etc.). Including such reactions along with those representing sorption of trace metals makes it possible to estimate sorption in systems of varying pH and composition. Examples of coherent databases of sorption reactions include that for the hydrous ferric oxide surface presented by Dzombak and Morel (1990) and a similar database for goethite presented by Mathur (1995).

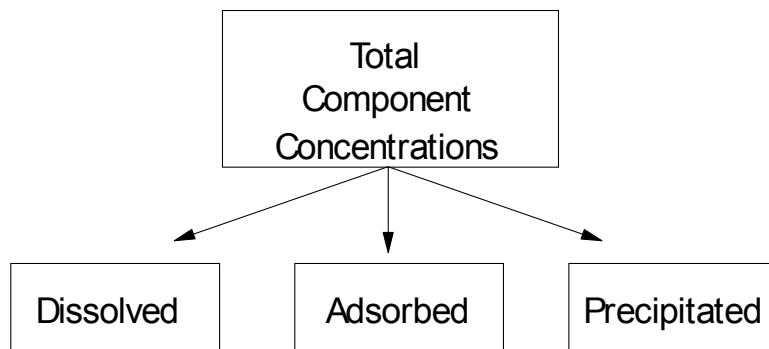


Figure G.1 MINTEQA2 Computes the Equilibrium Distribution of Metal

G.2.1 Input Parameters

We accounted for the expected natural variability in K_d for a particular metal in the MINTEQA2 modeling by including variability in five important input parameters upon which K_d depends. These five input parameters, also called the geochemical master variables, are:

- groundwater compositional-type (carbonate or non-carbonate)
- groundwater pH
- concentration of adsorbents (ferric oxide (goethite) and particulate natural organic matter (POM))
- concentration of dissolved natural organic matter (DOM)
- dissolved concentration of representative anthropogenic (leachate) organic acids (LOA) (derived from leachate infiltrating from the base of the WMU)

Two groundwater compositional types were modeled, one with composition representative of a carbonate-terrain system and one representative of a non-carbonate system. The two groundwater compositional types are correlated with the hydrogeologic environment parameter in EPACMTP (see Section 4.2.3.1 of the *IWEM Technical Background Document*). The carbonate type corresponds to the “solution limestone” hydrogeologic environment setting. The other eleven hydrogeologic settings in EPACMTP are represented by the non-carbonate groundwater type. For each groundwater type, a representative, charge-balanced groundwater chemistry specified in terms of major ion concentrations and natural pH was selected from the literature. The carbonate system was represented by a sample reported in a limestone aquifer. This groundwater had a natural pH of 7.5 and was saturated with respect to calcite. The non-carbonate system was represented by a sample reported from an unconsolidated sand and gravel aquifer with a natural pH of 7.4. An unconsolidated sand and gravel aquifer was selected to represent the non-carbonate compositional type because it is the most frequently occurring of the twelve hydrogeologic environments in HGDB database (see Section 4.2.3.1 of the *IWEM Technical Background Document*). The composition of both the carbonate and non-carbonate representative ground-water samples is shown in Table G.1.

Table G.1 Composition Of Representative Ground Waters

| Constituent Chemical | Concentrations (mg/L) | |
|----------------------|--------------------------|----------------------------|
| | Carbonate Ground water | Non-carbonate Ground water |
| Ca | 55 | 49 |
| Mg | 28 | 13 |
| SO ₄ | 20 | 27 |
| HCO ₃ | 265 | 384 |
| Na | 3.1 | 105 |
| Cl | 10 | 34 |
| K | 1.5 | 3.0 |
| NO ₃ | --- | 7.8 |
| F | --- | 0.3 |
| SiO ₂ | --- | 21 |
| pH | 7.5 | 7.4 |
| Temp | 18 C | 14 C |
| Other | Equilibrium with calcite | --- |

Two types of adsorbents were represented in modeling the K_d values: ferric oxide (FeOx) and particulate organic matter (POM). Mineralogically, the ferric oxide was assumed to be goethite (FeOOH). A database of sorption reactions for goethite reported by Mathur (1995) was used with the diffuse-layer sorption model in MINTEQA2 to represent the interactions of protons and metals with the goethite surface. The concentration of sorption sites used in the model runs was based on a measurement of ferric iron extractable from soil samples using hydroxylamine hydrochloride as reported in EPRI (1986). This method of Fe extraction is intended to provide a measure of the exposed amorphous hydrous oxide of Fe present as mineral coatings and discrete particles and available for surface reaction with pore water. The variability in FeOx content represented by the variability in extractable Fe from these samples was included in the modeling by selecting low, medium and high FeOx concentrations corresponding to the 17th, 50th and 83rd percentiles of the sample measurements. The specific surface area and site density used in the diffuse-layer model were as prescribed by Mathur. These values along with the molar concentration of FeOx sorbing sites are shown in Table G.3. Although the same distribution of extractable ferric oxide sorbent was used in the saturated and unsaturated zones, the actual concentration of sorbing sites corresponding to the low, medium, and high FeOx settings in MINTEQA2 was different in the two zones because the phase ratio was different (4.57 kg/L in the unsaturated zone; 3.56 kg/L in the saturated zone). The extractable Fe weight percentages used in the modeling are shown in Table G.2.

Table G.2 Concentration Levels For Goethite Sorbent

| Concentration Level | Weight Percent Fe (extractable) | FeOOH Sorbent Concentration (g/L) |
|-------------------------|---------------------------------|-----------------------------------|
| <i>Unsaturated zone</i> | | |
| Low | 0.0182 | 1.325 |
| Medium | 0.0729 | 5.309 |
| High | 0.1190 | 8.667 |
| <i>Saturated zone</i> | | |
| Low | 0.0182 | 1.032 |
| Medium | 0.0729 | 4.136 |
| High | 0.1190 | 6.751 |

Table G.3 Model Parameters For The Goethite Sorbent

| Parameter | Model Value |
|---|------------------------|
| Specific surface area (m ² /g) | 60 |
| Site density (moles of sites per mole Fe) | 0.018 |
| <i>Unsaturated zone: Site concentration (mol/L)</i> | |
| Low | 2.680x10 ⁻⁴ |
| Medium | 1.074x10 ⁻³ |
| High | 1.753x10 ⁻³ |
| <i>Saturated zone: Site concentration (mol/L)</i> | |
| Low | 2.087x10 ⁻⁴ |
| Medium | 8.365x10 ⁻⁴ |
| High | 1.365x10 ⁻³ |

The concentration of the second adsorbent, POM, was obtained from existing organic matter distributions that were developed for use in the EPACMTP model. In the unsaturated zone, low, medium, and high concentrations for components representing particulate organic matter in the MINTEQA2 model runs were based on the distribution of solid organic matter in EPACMTP for the silt loam soil type. (The silt loam soil type is intermediate in weight percent organic matter in comparison with the other two EPACMTP soil types and is also the most frequently occurring soil type among the three.) The low, medium, and high POM concentrations used in the saturated zone MINTEQA2 model runs was obtained from the EPACMTP organic matter distribution for the saturated zone. For both the FeOx and POM adsorbents, the amount of sorbent included in the MINTEQA2 modeling was scaled to

correspond with the phase ratio in the unsaturated zone (4.57 kg/L) and saturated zones (3.56 kg/L).

A dissolved organic matter (DOM) distribution for the saturated zone was obtained from the U.S. EPA STORET database. This distribution was used to provide low, medium, and high DOM concentrations for the MINTEQA2 model runs. The low, medium, and high DOM values were used exclusively with the low, medium, and high values, respectively, of POM. In the unsaturated zone, there was no direct measurement of DOM available. The ratio of POM to DOM in the unsaturated zone was assumed to be the same as that in the saturated zone. This ratio, 194.6, was applied to the low, medium, and high weight percent POM values of the unsaturated zone to obtain DOM concentrations at the low, medium, and high levels. In MINTEQA2 the POM and DOM components were modeled using the Gaussian distribution model. This model includes a database of metal-DOM reactions (Susetyo et al., 1991). Metal reactions with POM were assumed to be identical in their mean binding constants with the DOM reactions. The weight percent POM and concentration (mg/L) of both POM and DOM is shown in Table G.4 for all three concentration levels in both zones.

Table G.4 POM and DOM Concentration Levels

| | POM wt% | POM Concentration (mg/L) | DOM Concentration (mg/L) |
|-------------------------|---------|--------------------------|--------------------------|
| <i>Unsaturated zone</i> | | | |
| Low | 0.034 | 1553.8 | 6.6 |
| Medium | 0.105 | 4798.5 | 20.4 |
| High | 0.325 | 14852.5 | 63.20 |
| <i>Saturated zone</i> | | | |
| Low | 0.020 | 712.0 | 3.00 |
| Medium | 0.074 | 2634.4 | 14.40 |
| High | 0.275 | 9790.0 | 69.38 |

For both POM and DOM, a site density of 1.2×10^{-6} moles of sites per mg organic matter was assumed. The site concentrations for organic matter in both zones are listed in Table G.5

Table G.5 Site Concentrations For POM And DOM Components In MINTEQA2

| | POM Site Concentration (mol/L) | DOM Site Concentration (mol/L) |
|-------------------------|---------------------------------------|---------------------------------------|
| <i>Unsaturated zone</i> | | |
| Low | 1.865×10^{-3} | 7.896×10^{-6} |
| Medium | 5.758×10^{-3} | 2.439×10^{-5} |
| High | 1.782×10^{-2} | 7.548×10^{-5} |
| <i>Saturated zone</i> | | |
| Low | 8.544×10^{-4} | 3.600×10^{-6} |
| Medium | 3.161×10^{-3} | 1.728×10^{-5} |
| High | 1.175×10^{-2} | 8.326×10^{-5} |

Leachate exiting a WMU may contain elevated concentrations of anthropogenic leachate organic acids. This organic matter may consist of various compounds including organic acids that represent primary disposed waste or that result from the breakdown of more complex organic substances. Many organic acids found in landfill leachate have significant metal-complexing capacity that may influence metal mobility. In an effort to incorporate in the K_d modeling the solubilizing effect of organic acids, representative carboxylic acids were included in the MINTEQA2 modeling at three concentration levels. An analysis of total organic carbon (TOC) in landfill leachate by Gintautas et al. (1993) was used to select and quantify the organic acids. The low, medium, and high values for the representative acids in the modeling were based on the lowest, the average, and the highest measured TOC among the six landfill leachates analyzed; these values are presented below in Table G.6.

Table G.6 Model Concentrations Of Representative Leachate Acids

| Concentration Level | Acetic acid (mg/L) | Propionic acid (mg/L) | Butyric acid (mg/L) |
|----------------------------|---------------------------|------------------------------|----------------------------|
| <i>Unsaturated zone</i> | | | |
| Low | 24.80 | 14.61 | 15.68 |
| Medium | 111.00 | 64.30 | 67.94 |
| High | 274.60 | 158.60 | 169.00 |
| <i>Saturated zone</i> | | | |
| Low | 3.54 | 2.09 | 2.24 |
| Medium | 15.86 | 9.19 | 9.71 |
| High | 39.23 | 22.66 | 24.14 |

G.2.2 Metals of Interest

The metal contaminants whose partition coefficients have been estimated using MINTEQA2 include arsenic (As), antimony (Sb), barium (Ba), beryllium (Be), cadmium (Cd), cobalt (Co), copper (Cu), chromium (Cr), fluoride (F), mercury (Hg), manganese (Mn), molybdenum (Mo), lead (Pb), nickel (Ni), selenium (Se), silver (Ag), thallium (Tl), vanadium (V), and zinc (Zn).

Several of these metals occur naturally in more than one oxidation state. The modeling described here is restricted to the oxidation states that are most likely to occur in waste systems or most likely to be mobile in ground-water waste systems. For arsenic, chromium, and selenium, partition coefficients were estimated for two oxidation states. These were: As(III) and As(V), Cr(III) and Cr(VI), and Se(IV) and Se(VI). For antimony, molybdenum, thallium, and vanadium, only one oxidation state was modeled although multiple oxidation states occur. For all four of these metals, the choice of which state to model was dictated by practical aspects such as availability of sorption reactions and by subjective assessment of the appropriate oxidation state. The oxidation states modeled were Sb(V) (there were no sorption reactions available for Sb(III)), Mo(VI) (molybdate seems the most relevant form from literature reports), thallium (I) (this form is more frequently cited in the literature as having environmental implications), and V(V) (vanadate; sorption reactions were not available for other forms).

G.2.3 Modeling Methods and Results

The MINTEQA2 modeling was conducted separately for each metal in three steps for the unsaturated zone; these steps were then repeated for the saturated zone:

- Sorbents were pre-equilibrated with groundwaters: Each of nine possible combinations of the two FeOx and POM sorbent concentrations (low FeOx, low POM; low FeOx, medium POM; etc.) were equilibrated with each of the two groundwater types (carbonate and non-carbonate). Because the sorbents adsorb some groundwater constituents (calcium, magnesium, sulfate, fluoride), the input total concentrations of these constituents were adjusted so that their equilibrium dissolved concentrations in the model were equal to their original (reported) groundwater dissolved concentrations. This step was conducted at the natural pH of each groundwater, and calcite was imposed as an equilibrium mineral for the carbonate groundwater type. Small additions of inert ions were added to maintain charge balance.
- The pre-equilibrated systems were titrated to new target pH's: Each of the nine pre-equilibrated systems for each groundwater type were titrated with NaOH to raise the pH or with HNO₃ to lower the pH. Nine target pH's spanning the range 4.5 to 8.2 were used for the non-carbonate groundwater. Three target pH's spanning the range 7.0 to 8.0 were used for the carbonate groundwater. Titration with acid or base to adjust the pH allowed charge balance to be maintained.

- Leachate organic acids and the contaminant metal were added: Each of the eighty-one pre-equilibrated, pH-adjusted systems of the non-carbonate groundwater and the twenty-seven pre-equilibrated, pH-adjusted systems of the carbonate groundwater were equilibrated with three concentrations of leachate organic acids. The equilibrium pH was not imposed in MINTEQA2; pH was calculated and reflected the acid and metal additions. The contaminant metal was added as a metal salt (e.g., PbNO_3) at a series of forty-four total concentrations spanning the range 0.001 mg/L to 10,000 mg/L of metal. Equilibrium composition and K_d was calculated at each of the forty-four total metal concentrations to produce an isotherm of sorbed metal versus metal concentration. The isotherm can also be expressed as K_d versus metal concentration.

For each metal, the modeling resulted in 243 isotherms for the non-carbonate ground water for the unsaturated zone and 81 isotherms for the carbonate ground water for the unsaturated zone. The same number of isotherms was produced for each ground water type for the saturated zone. Each isotherm corresponds to a particular setting of FeOx sorbent concentration, POM sorbent (and associated DOM) concentration, leachate acid concentration, and pH. In Monte Carlo or site-specific mode, EPACMTP selects the appropriate isotherm based on the conditions being modeled. As detailed in Section G.2.2, isotherms were produced for Ag, As(III), As(V), Ba, Be, Cd, Co, Cr(III), Cr(VI), Cu, F, Hg, Mn(II), Mo(V), Ni, Pb, Sb(V), Se(IV), Se(VI), Tl(I), V(V), and Zn.

Example isotherms for Cr(VI) are shown in Figure G.2. This figure shows K_d versus total Cr(VI) concentration for the non-carbonate ground water saturated zone at various pH values. The isotherms plotted are for the medium concentration level of FeOx and POM sorbents and the low concentration level of leachate organic matter. Because chromate behaves as an anion in ground water, its adsorption is enhanced at low pH relative to high pH. This behavior is reversed for metals that behave as cations.

Figure G.3 shows the impact of FeOx concentration level on the K_d values of lead. As expected, sorption is enhanced at the higher FeOx concentrations resulting in larger K_d values. The example shown is for the unsaturated zone of the carbonate ground water with the low concentration levels of POM and leachate organic acids. The pH corresponds to the lowest setting for the carbonate systems: 7.0.

The impact of varying the POM concentration level differs among the various metals. The effect of POM concentration level also depends on the pH. The variable impact of POM is due to two factors: the absence of organic matter reactions for anionic metals and the concurrent influence of DOM for those metals for which organic matter reactions are included. In the MINTEQA2 modeling procedure used here, increasing the POM sorbent concentration is always accompanied by a proportional increase in the DOM concentration. The overall impact on the amount of metal sorbed depends on the relative competition among all constituents in the systems for these two substances. The “winner” of this relative competition (POM or DOM) shifts with pH because both substances undergo acid-base reactions. Figure G.4 shows

the impact of varying the POM/DOM concentration level on lead sorption for the non-carbonate ground water unsaturated zone with medium FeOx concentration level and low leachate organic matter concentration level at pH 6.3.

The influence of the leachate organic matter concentration level is illustrated in Figure G.5 for copper sorption. The LOM level is represented in the model by particular concentrations of three representative leachate organic acids. The acids exert two modes of influence on metal sorption: (1) they lower the pH, reducing sorption of cations and enhancing sorption of anions; (2) for those metals that complex these acids, metal sorption is reduced through competition. The latter effect is generally restricted to metals that behave as cations. The results shown in Figure G.5 correspond to high concentration levels of FeOx and POM sorbents in the unsaturated zone for the carbonate ground water. The pH is 7.0.

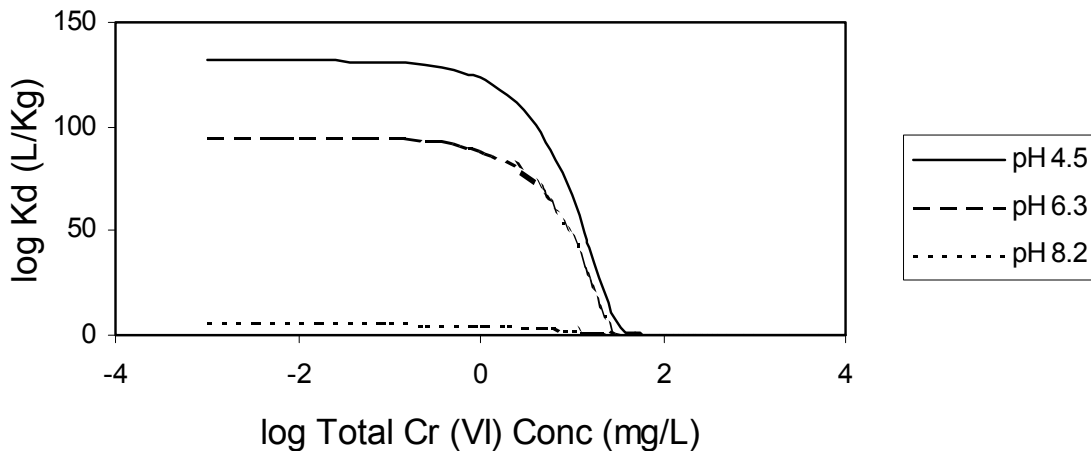


Figure G.2 Cr(VI) Isotherms Illustrating Influence of pH

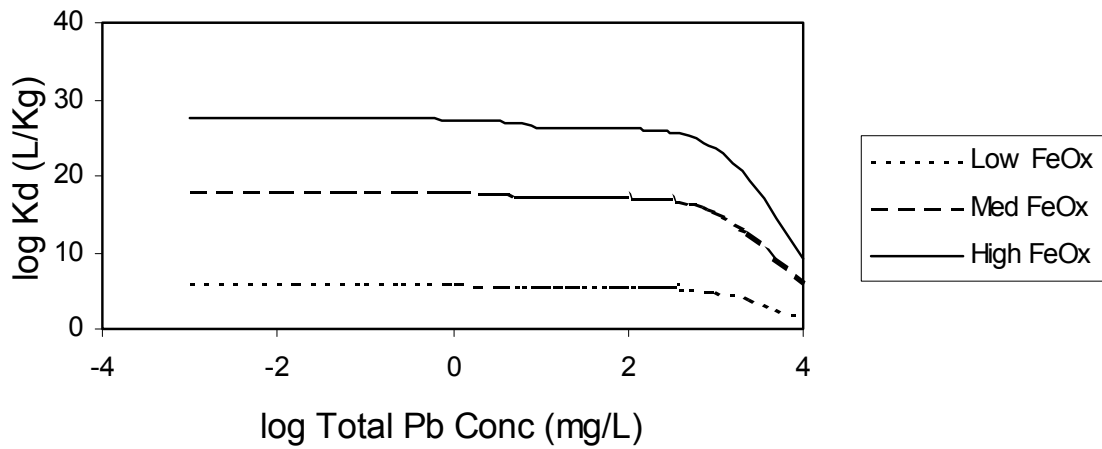


Figure G.3 Pb Isotherms Illustrating Influence of FeOx Sorbent Concentration

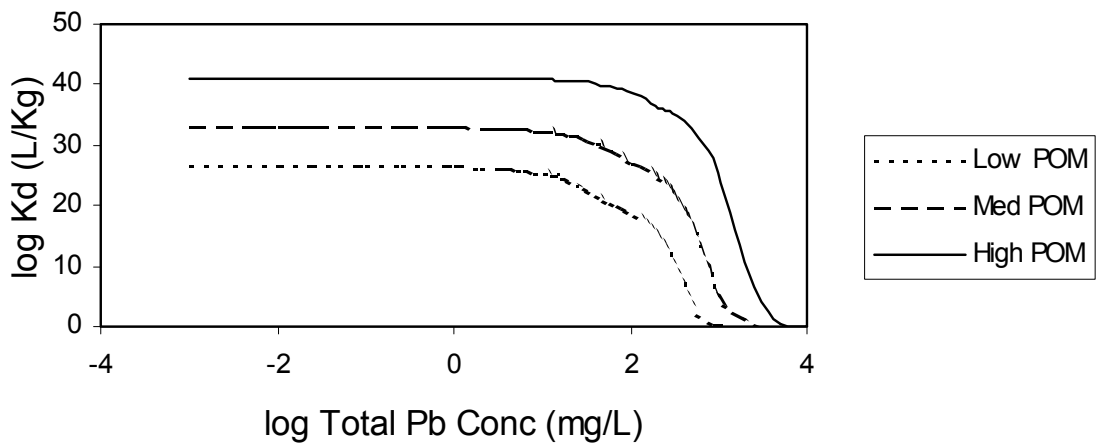


Figure G.4 Pb Isotherms Illustrating Influence of POM/DOM Concentration

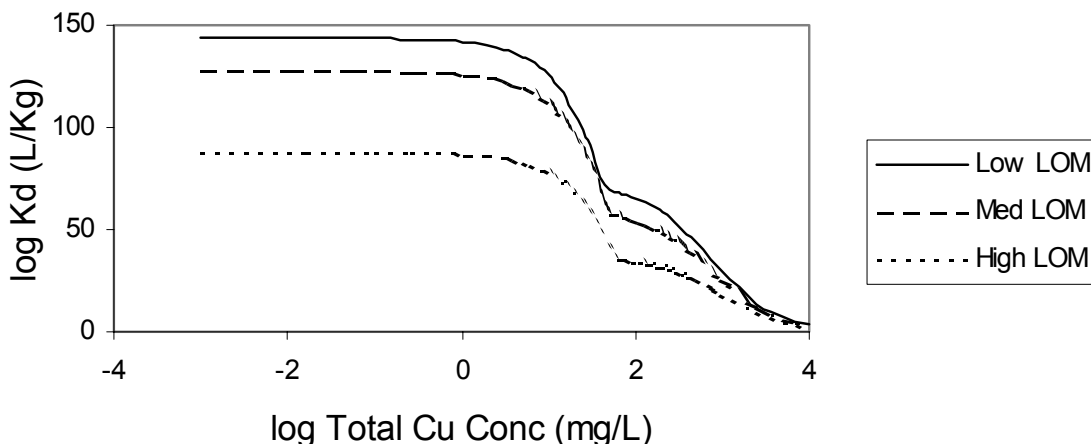


Figure G.5 Cu Isotherms Illustrating Influence of LOM Concentration

G.2.4 MINTEQA2 Modeling Assumptions and Limitations

There are many assumptions inherent in the use of a speciation model to estimate partition coefficients. Some of these must be acknowledged to result in limitations on the utility of the model results. Undoubtedly, the modeling results are more accurate for some metals than for others. The assumptions and limitations inherent in using the MINTEQA2 speciation model to estimate sorption isotherms for metals are summarized below. Although the impact of potential error in the estimated K_d values is apparent from some of these limitations, for many issues listed here, it appears impossible to quantify their effect on the modeled K_d values.

Issues concerning the characterization of the groundwater chemistry include:

- The categorization of all ground waters into two types, carbonate and non-carbonate, is quite broad.
- Although the pre-equilibration step is helpful in more realistically establishing appropriate major ion concentrations, it is somewhat artificial in the sense that sorbents are not correlated with ground water.
- Both ground waters were artificially adjusted to different pH's of interest by titrating with an acid or base. The degree to which this procedure can result in model ground-water compositions that adequately represent true variability in factors that impact K_d is unknown.

Issues concerning the characterization of the adsorbent include:

- Only two sorbents are represented in the model systems. Other sorbents are important in some circumstances including clays, hydrous aluminum and manganese oxides, calcite, and silica.
- The ferric oxide was accounted in the modeling as goethite. Other ferric oxides may be important in ground water, including hydrous ferric oxide (HFO).
- The data used to quantify the FeOx and POM sorbents (and the DOM) is sparse. The degree to which the true variability in concentration levels of these sorbents has been captured in the modeling is unknown.
- There is no provision in the modeling to account for occlusion of sorbents (formation of coatings over other surfaces).
- The ferric oxide (goethite) sorbent is included in all model runs, implying that it is ubiquitous. However, there are natural ground-water conditions that preclude the formation of ferric oxide precipitates (low pH and low E_h).
- The Gaussian model for estimating metal interactions with organic matter was developed for dissolved organic matter. It has not been tested for estimating the degree of metal sorption onto POM.

Issues concerning the characterization of the leachate include:

- The concentration levels for leachate organic matter were based on a limited sampling from six municipal landfills.
- Other leachate constituents may be present at elevated concentrations, but these are not accounted for. Some of these (e.g., Ca, Mg, SO_4 , Cl, etc.) may reduce the amount of metal sorption by competing for adsorption sites (especially Ca) or by complexing metals so that a greater fraction is retained in solution (especially SO_4 and Cl).
- Leachate from highly alkaline wastes was not included in the modeling. Highly alkaline leachates may result in elevation of the ground-water pH above the upper bound for which isotherms have been computed. Sorption tends to increase with pH for many metals up to about pH 8 to 9. Above this level, formation of metal hydroxy solution species may inhibit sorption for some metals.
- The metal was introduced as a metal salt. The metal species was chosen to avoid impact on the pH, but some pH effect is unavoidable.

-
- Methylated forms of metal were not accounted for in this modeling. Mercury and arsenic are known to undergo methylation in the environment.

Other modeling issues include:

- The system redox potential was not explicitly defined in the modeling. All species that might undergo oxidation-reduction reactions were constrained to remain in the form in which they were entered in the model.
- All contaminant metals were introduced separately and individually in the modeling. The possible simultaneous presence of multiple metals is unaccounted for.

G.3 INCORPORATION OF MINTEQA2 ADSORPTION ISOTHERMS IN EPACMTP

Monte Carlo modeling of metals transport using the MINTEQA2-derived adsorption isotherms requires, for each Monte Carlo realization, selecting one of the available isotherms for each metal species, for both the unsaturated and saturated zones. The selection of the appropriate adsorption isotherm for each Monte Carlo realization depends on the values of the five geochemical master variables, as discussed in Section G.2.1. These values of the geochemical master variables are generated randomly from given distributions. This section describes how EPACMTP selects and prepares adsorption isotherms for use in the transport simulations and how the option to linearize the nonlinear MINTEQA2-generated isotherms works; additional technical details are provided in Section 3.3.3 of the *EPACMTP Parameters and Data Background Document*.

G.3.1 Incorporation of MINTEQA2 Isotherms

In the Monte Carlo transport simulations, for each realization a value is generated for each of the five geochemical master variables according to the specified distributions. Each generated value is then compared to contiguous ranges of values. This set of rangewise classifications is then used to choose the appropriate adsorption isotherm from the matrix of master variables to be used for that realization. Note that isotherms are selected independently for the unsaturated and saturated zones; that is, this process is performed once for the unsaturated zone and then repeated for the saturated zone.

The isotherm curves generated by running the MINTEQA2 model are provided to EPACMTP in tabular form. The table of values consists of a set of dissolved concentration and associated distribution coefficient (K_d) pairs for each isotherm. For each metal, the modeling resulted in 243 isotherms for the non-carbonate ground water for the unsaturated zone and 81 isotherms for the carbonate ground water for the unsaturated zone. The same number of isotherms was produced for each ground water type for the saturated zone. Each isotherm is indexed to the particular values of the five geochemical variables used in its generation by

MINTEQA2, and to the zone (unsaturated or saturated) to which it applies. Note that the unit of concentration used in MINTEQA2, and hence presented in the isotherms, is mol liter⁻¹, while EPACMTP uses mg liter⁻¹. EPACMTP converts isotherm units to mg liter⁻¹ using the atomic weights shown in Table 4.3.

Table G.7 Atomic weight of metals (CRC, 1970)

| Metals | Atomic Weight |
|------------------|---------------|
| Ba ²⁺ | 137.34 |
| Cd ²⁺ | 112.40 |
| Cr ³⁺ | 51.995 |
| Hg ²⁺ | 200.59 |
| Ni ²⁺ | 58.71 |
| Pb ²⁺ | 207.19 |
| Ag ⁺⁴ | 107.89 |
| Zn ⁺² | 65.38 |
| Cu ⁺² | 63.55 |
| V ⁺⁴ | 50.94 |

G.3.2 Precipitation Effects

In the EPACMTP Monte Carlo transport simulations, the effect of adsorption is incorporated through a partition coefficient K_d , defined as the ratio of the metal bound on the soil (C_s , expressed in mass of metal per mass soil) to dissolved phase concentration (C_d , expressed in mass of metal per volume of solution). In EPACMTP, K_d has the units liter kg⁻¹. The K_d values computed from the MINTEQA2 output are dimensionless, because in that model, the equilibrium mass of metal in each phase (dissolved, sorbed, and precipitated) is expressed relative to a liter of solution. Here, the sorbed metal should be regarded as the mass of metal that has been *sorbed from the liter of solution*. Hence, dimensionless K_d , called K_d' , can be expressed:

$$K_d' = \frac{C_s}{C_d} \quad (\text{G.1})$$

where C_s and C_d have, as in MINTEQA2, the same units. (Conversion of K_d' to K_d is discussed in Section G.3.3.) Because the output from the MINTEQA2 model simulations includes the equilibrium mass of metal in each of the three phases: dissolved, adsorbed, and precipitated (C_p), the effect of precipitation can, in principle, be incorporated into the transport simulations by defining K_d' (which becomes K_d after units conversion in the transport model) as the ratio of immobile concentration ($C_s + C_p$) to mobile concentration (C_d). However, if K_d' is defined in this way, rather than as in (4.1), the form of the isotherm relating dissolved concentration and K_d is no longer monotonic. The K_d initially will decrease with increasing metal concentration, but when the solubility product is exceeded and precipitation occurs, K_d will begin to increase. The slope of the K_d curve may change again as total metal

concentration increases if the anion with which the metal is co-precipitating becomes depleted. In the Monte Carlo transport analysis, EPACMTP uses a robust and computationally efficient analytical solution technique for the unsaturated zone simulations (see Section 3.3.5.3). This solution method requires a monotonic isotherm; it cannot accommodate the non-monotonic isotherms that result when precipitation is included. Therefore, precipitation is not included in the EPACMTP transport analysis. This is justified somewhat by the fact that precipitation, when it does occur, is restricted to the high end of the concentration range for the metals simulated using MINTEQA2. At lower concentrations, precipitation does not occur. Also, to include precipitation would require making assumptions about the availability of the anion(s) with which the metal is precipitating. Ignoring precipitation in the transport simulations will, for those cases where it does occur in the MINTEQA2 simulations, lead to a more conservative model outcome.

G.3.3 Variable Soil Moisture Content

The partition coefficient needed in the EPACMTP transport simulations has units of volume per mass (liters kg⁻¹), but the K_d' values provided by MINTEQA2 are dimensionless. As mentioned in the preceding section, this is simply because the sorbed mass in MINTEQA2 is expressed in terms of mass of metal sorbed *from* a liter of the solution rather than mass of metal sorbed *onto* the mass of soil with which one liter is equilibrated. The partition coefficient can be transformed to the units appropriate for the transport model (i.e., liters kg⁻¹) by normalizing the MINTEQA2 sorbed concentration (in mg liter⁻¹) by the phase ratio (the mass of soil with which one liter is equilibrated, given in kg liter⁻¹). As explained in Chapter 3, the phase ratio was always 4.57 kg liter⁻¹ in the unsaturated zone and 3.56 kg liter⁻¹ in the saturated zone. These values were determined from the median values of water content (θ) and soil dry bulk density (ρ_b) from EPACMTP distributions for these parameters. The phase ratio (a) is used in calculating the concentration of HFO and POM adsorption sites specified in the MINTEQA2 model runs. It follows that the dimensionless K_d' values should be normalized by 4.57 and 3.56 kg liter⁻¹, respectively, for the unsaturated and saturated zones to provide the input K_d for EPACMTP:

$$K_d = \frac{K_d'}{a} = K_d' \frac{\theta^M}{\rho_b^M} \quad (\text{G.2})$$

where θ^M and ρ_b^M are the median water content and dry bulk density. In the subsequent EPACMTP calculations, sorption is incorporated through the retardation factor R , defined as:

$$R = 1 + \frac{\rho_b}{\theta} K_d \quad (\text{G.3})$$

where θ and ρ_b are selected from their corresponding distributions for each particular Monte Carlo realization.

G.3.4 Linearization of MINTEQA2 Adsorption Isotherm

Although EPACMTP can be run using nonlinear adsorption in both the unsaturated and saturated zones in the deterministic case (in other words, for a single set of hydrogeological parameters), the computer processing time required for a Monte Carlo analysis that includes nonlinear adsorption in both zones is prohibitive. For that reason, a technique was developed that calculates a single value of K_d from a nonlinear isotherm. This "linearized" single K_d value can then be used as a linear partition coefficient in the model, which decreases computer processing time dramatically. Obviously, when the original nonlinear isotherm from which the linear K_d is calculated is almost linear to begin with, the impact of reducing it to a linear K_d is small. Conversely, the error associated with using a linear approximation is increased for highly nonlinear isotherms.

In EPACMTP, two methods are provided for approximating a linear isotherm from a nonlinear isotherm. In the first method, a concentration-interval weighted approach is used to compute a single K_d from the nonlinear K_d versus C_d curve. In effect, the technique simply calculates an average K_d over the range of dissolved metal concentration represented by the isotherm. Concentration-interval weighting is used to account for the fact that the dissolved concentration values are not evenly spaced on the isotherm. This option is provided for use in the unsaturated zone. In the second method (for use in the saturated zone), the K_d corresponding to the peak water table metal concentration is used for linear partitioning. The procedure involves the following steps: First, a saturated zone isotherm is specified by Monte Carlo selection of values for the four geochemical master variables. Then, the peak dissolved metal concentration at the water table is determined, and the K_d corresponding to this dissolved concentration is obtained from the isotherm by interpolation. If the peak concentration at the water table is lower than the minimum dissolved concentration given by the isotherm, the K_d value corresponding to the minimum concentration is used. Likewise, if the peak concentration is higher than the maximum concentration on the isotherm, the K_d corresponding to the isotherm maximum is used.

The specific options used in EPACMTP pertaining to linearizing isotherms and further discussion of the implications of linearized isotherms is presented in Section 3.3.3 of the EPACMTP Parameters/Data Background Document.

G.4 IMPLEMENTATION OF EPACMTP FOR METALS

The EPACMTP computer code was modified to include capabilities to simulate fate and transport of metals. Most of the existing algorithms in the EPACMTP model are applicable to the simulation of metals. However, significant modifications were necessary to simulate metals adsorption with nonlinear sorption isotherms. Additional modifications were made to the data input module and the Monte Carlo module for assigning values to each model parameter.

G.4.1 Additional Input Data for Metals

Several input parameters were added to EPACMTP for metal simulations. A control parameter (a FORTRAN logical variable) was added to indicate if the contaminant of interest is a metal species. Additional parameters, specifying the type of adsorption isotherm to be used and the distributions of the geochemical waste variables were also included.

G.4.1.1 Control Parameters

The following parameters were added to the General Parameter (GP01) record.

Table G.8 Additional Control Parameters for Metals Simulation

| Variable | Type | Column | Descriptions |
|----------|---------|--------|---|
| IF-METAL | logical | 41-45 | Enter 'T' for metals simulations and 'F' otherwise. |
| KDEVAL | integer | 46-50 | Isotherm type; (required only when IF_METAL='T') =1 for pH-dependent linear isotherm =2 for linearized MINTEQA2 isotherm =3 for nonlinear MINTEQA2 isotherm |

Note that the KDEVAL=1 option is available only for the five metals: As^{III}, Cr^{VI}, Se^{VI}, Sb^V, T1. The other two options are available for the ten metals: Ag, Ba, Cd, Cr^{III}, Cu, Hg, Ni, Pb, V and Zn. It is possible that certain other metals may be assumed to behave like one of the above metals (e.g., K_d results for Be may be assumed to be the same as for Ba; As^{III} results may be assumed to apply to As^V, etc.).

G.4.1.2 Metal Specific Data

A separate data group was added to specify additional parameters for metals simulations. This data group is identified in the input data file with the code 'MT'. The first variable in this group specifies the identification number for the metal species to be simulated. The remaining variables specify the distributions of the geochemical master variables for the unsaturated and saturated zones.

Table G.9 Additional Input Parameters for Metals Specific (MT) Group

| Variable No. | Description |
|--------------|---|
| 1 | Metal identification number (1-12, Table 5.3) |
| 2 | pH for both unsaturated and saturated zones |
| 3 | HFO for both unsaturated and saturated zones |
| 4 | Leachate organic acids for unsaturated zone |
| 5 | POM for unsaturated zone |
| 6 | POM for saturated zone |

Each metal species is identified using a numerical code, which is shown in Table 5.3. The table also shows the isotherm selection options available for the different metal species.

Table G.10 METAL_ID and Corresponding Metal Species

| METAL ID | 1 | 2 | 3 | 4 | 5 | 6 | 7 | 8 | 9 | 10 | 13 | 14 | 15 | 16 | 17 |
|------------------|---------|----|-------------------|----|----|----|----|----|----|----|-------------------|------------------|------------------|----|-----------------|
| Metal species | Ba | Cd | Cr ^{III} | Hg | Ni | Pb | Ag | Zn | Cu | V | As ^{III} | Cr ^{VI} | Se ^{VI} | Tl | Sb ^V |
| KDEVAL available | 2 and 3 | | | | | | | | | | 1 | | | | |

The remaining parameters in the metals group specify distributions of the geochemical master variables for the unsaturated and saturated zones. The distributions of the parameters were presented in Section G. of the EPACMTP Parameters/Data Background Document. Note that the distributions of pH and natural organic matter (NOM) are also required for degrading chemicals (organics) as part of the unsaturated zone and saturated zone data groups. However, they are duplicated in the metal-specific data input group to emphasize the dependence of metals on these parameters. For the HWIR analyses of industrial waste management units, the leachate organic matter is always assigned a value of low.

G.4.2 Evaluation of Approaches for Handling Metals Isotherms

The partitioning of metals between aqueous and soil components through adsorption is generally a nonlinear function of metal concentration. However, including nonlinear adsorption in metals transport simulations in a Monte Carlo framework places great demands on computer processing resources. In fact, accounting for nonlinear adsorption in both the unsaturated and saturated zone simulations is not feasible. In the unsaturated zone, several different adsorption schemes for metals transport are included in EPACMTP, including a coefficient for linear partitioning calculated by the model by linearizing the MINTEQA2 isotherms as described earlier and a nonlinear partitioning isotherm developed using MINTEQA2. These two options were compared for modeling adsorption in the unsaturated zone and the results were evaluated in terms of model response and computational efficiency, leading to the following conclusions:

- Linearization of the adsorption isotherm to produce a linear partition coefficient and subsequent use of the analytical unsaturated zone transport solution (option 2) is computationally efficient, but produces significantly different water table concentrations than using nonlinear adsorption (option 3). Option 2 should only be used for unsaturated zone transport when the concentration range being modeled corresponds to a segment of the isotherm that is approximately linear (relatively low concentrations).
- The use of nonlinear adsorption with the numerical unsaturated zone transport solution can lead to convergence problems in the model, especially if the isotherm has a high degree of nonlinearity. In that case, the transport time step must be made very small to insure convergence, but this leads to long computer simulation times.
- The use of nonlinear adsorption with the analytical unsaturated zone transport solution is both fast and accurate. Only minor differences were found between this solution technique and the numerical technique, which includes dispersion. The nonlinearity of the isotherm itself creates a contaminant profile with a sharp front and a long (dispersed) tail. For typical MINTEQA2 isotherms, this effect was found to be more pronounced than for cases involving hydrodynamic dispersion alone.

For saturated zone transport, a linear partition coefficient must always be used in EPACMTP, regardless of the unsaturated zone adsorption option selection. Linear partitioning must be used because including nonlinear partitioning in the saturated zone requires a numerical solution, which in turn requires small time steps to insure convergence. This places an insupportable demand on computational resources, given the Monte Carlo framework of the problem to be solved. Further, there is some justification for its use in that, at low concentration ranges, most of the MINTEQA2 adsorption isotherms are linear. Also, the maximum saturated zone metal concentrations are expected to be lower than the leachate concentrations of metal leaving the waste disposal unit due to adsorption in the unsaturated zone and initial dilution in the groundwater. This provides some logical basis for the use of linear partitioning in the saturated zone. EPACMTP determines the K_d value to be used in the saturated zone from the selected MINTEQA2 isotherm after the unsaturated zone simulation has been completed. This permits the saturated zone K_d to be determined as a function of the peak metal concentration exiting the unsaturated zone. The method is described in Section G.4.5.

G.4.3 Determination of Isotherm Monotonicity

A new approach for determining the monotonicity of any tabular metal sorption isotherm utilizes the frequency of upward and downward changes in adjacent tabulated values of the distribution coefficient, K_d , with respect to the dissolved concentration, C , as well as the magnitude of these changes. This approach improves upon the current approach in the EPACMTP which identifies the overall trend of an isotherm as increasing if the frequency of upward changes in tabulated

values of K_d is greater than downward changes in K_d , or visa versa. In addition, all tabulated values of the selected isotherm are used in the current approach regardless of the maximum concentration entering the unsaturated zone, C_{max} . Therefore, trends may be establish without regard to the range of constituent concentrations in the media.

The proposed approach calculates the incremental changes in area under the plotted isotherm (the logarithm of K_d plotted as a function of the logarithm of C) for all concentrations less than or equal to C_{max} . If the sum of upward changes in area is greater than the sum of downward changes, the isotherm is assumed to be monotonically increasing over the range $[C_{min}, C_{max}]$, where C_{min} is the minimum concentration represented by the isotherm. If the sum of upward changes in area is less than the sum of downward changes, the isotherm is assumed to be monotonically decreasing over the range $[C_{min}, C_{max}]$.

The sum of incremental upward changes in area, A^+ , is expressed as

$$A^+ = \sum \delta C_i \times \delta K_{d_i}, \quad i \in \delta K_{d_i} > 0 \quad (G.4)$$

where the i^{th} incremental changes in concentration, δC_i , and distribution coefficient, δK_{d_i} , are calculated as

$$\begin{aligned} \delta K_{d_i} &= \log(K_{d_{i+1}}) - \log(K_{d_i}) = \log\left(\frac{K_{d_{i+1}}}{K_{d_i}}\right) \\ \delta C_i &= \log(C_{i+1}) - \log(C_i) = \log\left(\frac{C_{i+1}}{C_i}\right), \end{aligned} \quad (G.5)$$

for all tabulated pairs (C, K_d) for all C less than or equal to C_{max} . The sum of incremental downward changes in area, A^- , is expressed as

$$A^- = \sum |\delta C_i \times \delta K_{d_i}|, \quad i \in \delta K_{d_i} < 0 \quad (G.6)$$

If A^+ is greater than A^- , the trend of the isotherm is assumed to be monotonically increasing. Conversely, if A^+ is less than A^- , the trend of the isotherm is assumed to be monotonically decreasing.

G.4.4 Application of Isotherm Monotonicity

A modification of the existing approach for enforcing the assumption of monotonicity on tabular metal sorption isotherms in the EPACMTP ensures a more conservative application of these nonlinear isotherms. The approach utilizes enhancements made in the determination of an isotherm's trend to smooth the raw data into a monotonically increasing or decreasing isotherm.

For the case of an isotherm that is determined to have a downward trend over the concentration range [Cmin, Cmax], where Cmin is the minimum dissolved concentration represented in the isotherm and Cmax is the maximum dissolved concentration entering the unsaturated zone, the filtered isotherm is

$$Kd_i = \min(Kd_{i-1}, Kd_i), \quad i = 2, N, \quad (G.7)$$

where N is the number of tabulated pairs (C, Kd) for all C less than or equal to Cmax. For the case of an isotherm determined to have an upward trend over the concentration range [Cmin, Cmax], the filtered isotherm is

$$Kd_i = \min(Kd_i, Kd_{i+1}), \quad i = N-1, 1. \quad (G.8)$$

G.4.5 Selection of Sorption Coefficient for Saturated Zone

The new search algorithm for a distribution coefficient for the saturated zone (Kd_{SAT}) determines the most conservative value for Kd_{SAT} within the range of Kd's in the tabulated isotherm corresponding to dissolved concentrations that are less than or equal to the diluted maximum observed water table concentration. The resulting value of Kd_{SAT} is independent of the isotherm used, original or monotonic.

Given:

| | |
|--------------------|---|
| $C_{MAX_{Dilute}}$ | Diluted maximum observed concentration at the watertable |
| C | Array of dissolved concentration in tabular isotherm |
| Kd | Array of distribution coefficients corresponding to concentrations in C |
| N | Number of (Kd, C) pairs in tabular isotherm |

Result:

Kd_{SAT} Distribution coefficient for saturated zone simulation

Algorithm:

```

KdSAT = Kd(1)
i = 1
While C(i) < CMAXDilute & i <= N
    KdSAT = min(Kd(i), KdSAT)
    i = i + 1
End

```

G.4.6 References

- Dobbs, J.C., W. Susetyo, L.A. Carreira, and L.V. Azarraga, 1989. Competitive binding of protons and metal ions in humic substances by lanthanide ion probe spectroscopy. *Analytical Chemistry*, 61:1519-1524.
- Dzombak, D.A. and F.M.M. Morel, 1990. *Surface Complexation Modeling: Hydrous Ferric Oxide*. John Wiley & Sons, New York, 393p.
- EPRI, 1986. Physicochemical Measurements of Soils at Solid Waste Disposal Sites. Electric Power Research Institute, prepared by Battelle, Pacific Northwest Laboratories, Richland, WA, EPRI EA-4417.
- Freeze, R.A. and J.A. Cherry, 1979. *Groundwater*. Prentice-Hall, Inc., New Jersey, 604p.
- Gintautas, P.A., K.A. Huyck, S.R. Daniel, and D.L. Macalady, 1993. Metal-Organic Interactions in Subtitle D Landfill Leachates and Associated Groundwaters, in *Metals in Groundwaters*, H.E. Allen, E.M. Perdue, and D.S. Brown, eds. Lewis Publishers, Ann Arbor, MI.
- Hem, J.D., 1977. Reactions of metal ions at surfaces of metal oxides. *Geochimica et Cosmochimica Acta*, 41:527-538.
- Mathur, S. S., 1995. Development of a Database for Ion Sorption on Goethite Using Surface Complexation Modeling. Master's Thesis, Department of Civil and Environmental Engineering, Carnegie Mellon University, Pittsburgh, PA.
- Susetyo, W., L.A. Carreira, L.V. Azarraga, and D.M. Grimm, 1991. Fluorescence techniques for metal-humic interactions. *Fresenius Jour. Analytical Chemistry*, 339:624-635.
- Tipping, E., 1994. WHAM— A chemical equilibrium model and computer code for waters, sediments, and soils incorporating a discrete site/electrostatic model of ion binding by humic substances. *Computers and Geosciences*, 20:973-1023.
- White, D.E., J.D. Hem, and G.A. Waring, 1963. *Data of Geochemistry*. U.S. Geological Survey Professional Paper 440-F, U.S. Government Printing Office, Washington, DC.

This page was intentionally left blank.